Assessment of the Technical Issues relating to Significant Amounts of EHV Underground Cable in the All-island Electricity Transmission System

Public Report

November 2009

Tokyo Electric Power Company

Contract CA209:

Assessment of the Technical Issues relating to Significant Amounts of EHV Underground Cable in the All-island Electricity Transmission System

Public Report

November 2009

Tokyo Electric Power Company

Executive Summary

Executive Summary

TEPCO has carried out the following studies in order to evaluate the effect of cable installations on the NIE/EirGrid network:

Part 1: Evaluation of the potential impact on the all-island transmission system of significant lengths of EHV underground cable, either individually or in aggregate

Part 2: Feasibility study on the 400 kV Woodland – Kingscourt – Turleenan line as AC EHV underground cables for the entire length

Part 3: Feasibility study of the 400 kV Woodland – Kingscourt – Turleenan line as mixed OHL / underground cable

For Part 1, the 400 kV Kilkenny – Cahir – Aghada line was selected as the focus of the study except for the series resonance overvoltage analysis.   The series resonance overvoltage analysis in Part 1 focused on the 400 kV Woodland – Kingscourt – Turleenan line as in Part 2 and 3.   For each part of the study, the reactive power compensation analysis, the temporary overvoltage analysis, and the slow-front overvoltage analysis were conducted.   Further, the lightning overvoltage analysis was conducted additionally for Part 3.

[Part 1]

First, the results of the reactive power compensation analysis led to the necessity of having to achieve compensation rates close to 100 % in order to ensure the safe operation of the network. The following compensation patterns all yielded satisfactory voltage profiles under different operating conditions:

Kilkenny – Cahir line

Kilkenny	Cahir	Compensation Rate
100 MVA × 4	80 MVA × 4	99.5 %

Cahir – Aghada line

Cahir	Reactor Station	Aghada	Compensation Rate
100 MVA × 4	80 MVA × 7	80 MVA × 5	100.7 %

The temporary overvoltage analysis was performed based on the compensation pattern determined by the reactive power compensation analysis. Resonance overvoltages and overvoltages caused by load shedding were studied with different cable lengths as well as under different network conditions.

The highest series resonance overvoltage was found in the Woodland 220 kV network. It was found to be lower than the standard short-duration power-frequency withstand voltage (395 or 460 kV, r.m.s.) specified in IEC 71-1.

The parallel resonance overvoltage was studied with transformer energisation. The observed overvoltage was much higher than the withstand voltage of a typical 400 kV surge arrester.

Load sheddings also yielded a very high overvoltage. However, such overvoltage is not a concern with regards to the safe operation of the network as it can be evaluated using SIWV (1050 kV) due to its fast decaying properties. The overvoltage caused by load shedding was also studied with lower compensation rates. The overvoltage exceeded SIWV when the compensation rate was 50 %.

		Highest overvoltage (peak)	Withstand voltage for evaluation
Series resonance		549.0 kV (3.06 pu)	360, 395, 460 kV (r.m.s.) (2.83, 3.11, 3.62 pu)
Parallel resonance	No load	881.5 kV (2.70 pu)	370 kV (r.m.s.) (1.60 pu) for 10 seconds
	With load	634.5 kV (1.94 pu)	
Load shedding		651.3 kV (1.99 pu)	1050 kV (peak)

$$1\,\text{pu} = 400 \text{ or } 220\,\text{kV} \times \frac{\sqrt{2}}{\sqrt{3}}\,(\text{peak}),\ 400 \text{ or } 220\,\text{kV} \times \frac{1}{\sqrt{3}}\,(\text{r.m.s.})$$

No significant overvoltage was found in the slow-front overvoltage analysis as shown below.

	Highest overvoltage (peak)	Withstand voltage (peak) for evaluation
Line energisation	564.2 kV (1.72 pu)	1050 kV
Ground fault and fault clearing	692.7 kV (2.12 pu)	

The voltage stability/variation and black-start capability were also studied in Part 1. In the assumed cable installation scenario and the black-start procedure, it was found that the black-start generator at Cathleen's Fall station had to be operated with a terminal voltage lower than 40 % in

order to avoid a steady-state overvoltage. In addition, parallel resonance frequency was found at 100 Hz at some steps, which required careful consideration. Transformer energisation at these steps is not recommended.

[Part 2]

As a result of the transmission capacity calculation, the following cable types were selected for the 400 kV Woodland – Kingscourt – Turleenan line:

- Al 1400 mm^2 for double circuit

- Cu 2500 mm^2 for single circuit

The results of the reactive power compensation analysis determined the necessity of achieving close to 100% compensation rates in order to ensure the safe operation of the network. The following compensation patterns yielded satisfactory voltage profiles under different operating conditions:

Woodland – Kingscourt line (for each circuit)

	Woodland	Kingscourt	Compensation Rate
Double circuit	150 MVA × 2	120 MVA × 2	100.1 %
Single circuit	200 MVA × 2	150 MVA × 2	100.1 %

Kingscourt – Turleenan line (for each circuit)

	Kingscourt	Reactor Station	Turleenan	Compensation Rate
Double circuit	100 MVA × 2	120 MVA × 3	100 MVA × 2	99.7 %
Single circuit	150 MVA × 2	150 MVA × 2	150 MVA × 2	91.0 %

The temporary overvoltage analysis was performed based on the compensation pattern determined by the reactive power compensation analysis. Resonance overvoltages and overvoltages caused by load shedding were studied under different network conditions.

The severest parallel resonance overvoltage was found with transformer energisation. The observed overvoltage was higher than the withstand voltage of a typical 400 kV surge arrester. From a manufacturer's standpoint, it is possible to develop a surge arrester with higher withstand voltages, for example 1.8 pu for 10 seconds. In this sense, the observed overvoltage is not at a level which would affect the feasibility of the 400 kV Woodland – Kingscourt – Turleenan line.

Load sheddings also yielded very high overvoltages. However, as observed in the Part 1 studies, in terms of the safe operation of the network, an overvoltage is not a concern because it can be evaluated by SIWV (1050 kV) due to its rapid decaying properties.

	Highest overvoltage (peak)	Withstand voltage for evaluation
Parallel resonance	541.7 kV (1.66 pu)	370 kV (r.m.s.) (1.60 pu) for 10 seconds
Load shedding	606.6 kV (1.86 pu)	1050 kV (peak)

No significant overvoltage was found in the slow-front overvoltage analysis as shown below.

	Highest overvoltage (peak)	Withstand voltage (peak) for evaluation
Line energisation	607.0 kV (1.86 pu)	1050 kV
Ground fault and fault clearing	593.0 kV (1.82 pu)	

[Part 3]

As a mixed OHL / underground cable line, the following combinations were studied for the 400 kV Kingscourt – Turleenan line. For the underground cable sections, the cable types used were assumed to be Al 1400 mm^2 – 2 cct.

- Cable section 30 %, OHL section 70 %

- Cable section: 60 %, OHL section: 40 %

The OHL section of the line was assumed to be single circuit. In addition, the 400 kV Woodland – Kingscourt line was assumed to be a single circuit OHL.

Generally, the compensation rate must be limited to around 70 – 80 % for mixed OHL / underground cable lines, due to the consideration of the resonance overvoltage in an opened phase. As a result of the reactive power compensation analysis, together with the open phase resonance analysis, the following compensation patterns were found to be appropriate under different operating conditions:

Kingscourt – Turleenan line (for each circuit)

	Kingscourt	Turleenan	Compensation Rate
30 % cable	100 MVA × 2	100 MVA × 2	81.7 %
60 % cable	200 MVA × 2	200 MVA × 2	85.7 %

The temporary overvoltage analysis was performed based on the compensation pattern determined by the reactive power compensation analysis.   Resonance overvoltage and overvoltage caused by load shedding were studied under different network conditions.

No significant overvoltage was found in the parallel resonance overvoltage analysis.   As in Part 1 and 2 studies, load sheddings yielded very high overvoltages, but this is not a concern for the safe operation of the network as it can be evaluated by SIWV (1050 kV) due to its rapid decaying properties.

	Highest overvoltage (peak)	Withstand voltage for evaluation
Parallel resonance	500.5 kV (1.53 pu)	370 kV (r.m.s.) (1.60 pu) for 10 seconds
Load shedding	771.0 kV (2.36 pu)	1050 kV (peak)

No significant overvoltage was found in the slow-front overvoltage analysis as shown below.

	Highest overvoltage (peak)	Withstand voltage (peak) for evaluation
Single phase autoreclose	523.0 kV (1.60 pu)	1050 kV
Three phase autoreclose	631.0 kV (1.93 pu)	

The lightning overvoltage analysis was additionally conducted in Part 3 in order to evaluate the overvoltage in the metallic sheath.   In order to maintain the sheath overvoltage lower than 60 kV at the connection between the OHL and the cable, grounding resistance at the gantry must be lower than 2 Ω.

Conclusion

The results of this thorough study concluded that with regards to the long cable network an attention must be paid to lower frequency phenomena such as temporary and steady-state overvoltages. The slow-front overvoltage is not a concern for the safe operation of the network because of the decay in the cable and large capacitance of the cable. For example, dominant frequency components contained in the energisation overvoltage is not determined by the propagation time of the overvoltage as is often discussed in the textbooks that deal with surge analysis. They are rather determined by parallel resonance frequencies and are often very low due to the compensation.

Severe overvoltages were found in the parallel resonance overvoltage analysis in studies Part 1 and 2. Both of them exceeded the withstand overvoltage of a typical 400 kV surge arrester. The magnitude of the overvoltage found in Part 1 is at a level in which there is no solution except operational countermeasures. In contrast, manufacturers will be able to develop a surge arrester that can withstand the overvoltages found in Part 2. It will, however, lead to higher protective levels ensured by the surge arrester, which may affect the insulation design of other equipment. These additional costs need to be evaluated by manufacturers. Finally, it will of course affect the total insulation coordination studied by the utilities.

In Part 1, the overvoltage that exceeded SIWV was found also in the load shedding analysis when a lower compensation ratio was adopted. Overall, Part 1 studies exhibited severer results compared to Part 2 or 3 studies. It is mainly due to the weak system around Aghada, Cahir, and Kilkenny, which limited the propagation of the overvoltage. Another contributing factor was the fact that Part 1 studies had more freedom in terms of choosing study parameters.

Generally speaking, temporary overvoltages, such as the resonance overvoltages and the overvoltages caused by load shedding are low probability phenomenon. Only certain, particular network operating conditions can yield such a severe overvoltage that they would lead to equipment failure. Evaluating a low-probability high-consequence risk is difficult but must be done when installing cables. The risks may be avoided via carefully prepared operational countermeasures, but unfortunately it will be a major burden for system analysts.

Table of contents

Part 1: Evaluations of the potential impact on the all-island transmission system of significant lengths of EHV underground cable, either individually or in aggregate introduction

Part 2: Feasibility study on the 400 kV Woodland – Kingscourt – Turleenan line as AC EHV underground cables for the entire length

Part 3: Feasibility study on the 400 kV Woodland – Kingscourt – Turleenan line as mixed OHL / underground cable circuits

Appendix: Figures from the series resonance overvoltage analysis in Part 1

Chapter 1 Introduction

1.1 Background

As climate change being an important issue for most countries and regions, renewable electricity targets are set for the introduction of renewable generation in order to reduce carbon emissions. Due to the availability of natural resources, Northern Ireland and the Republic of Ireland set ambitious targets to contribute to the climate change mitigation.

However, accommodating upwards of 8,000 MW of renewable generation in the NIE / EirGrid transmission system requires the creation of a new interconnector between NIE and EirGrid.   The cross-border power transfer between NIE and EirGrid has to be enhanced by the new 400 kV interconnector while maintaining the system security in the loss of the existing 275 kV interconnector.

In order to achieve this goal, NIE and EirGrid are cooperative to study various options for the new 400 kV interconnector.   Especially, the difficulty in obtaining wayleaves for overhead lines and environmental concerns make it necessary for NIE and EirGrid to consider underground options either for the entire length or as mixed OHL / underground cable.

It should be noted that the purpose of this study is purely technical evaluations under various options and parameters, and it does not reflect the view of NIE and EirGrid to OHL or underground cable options.
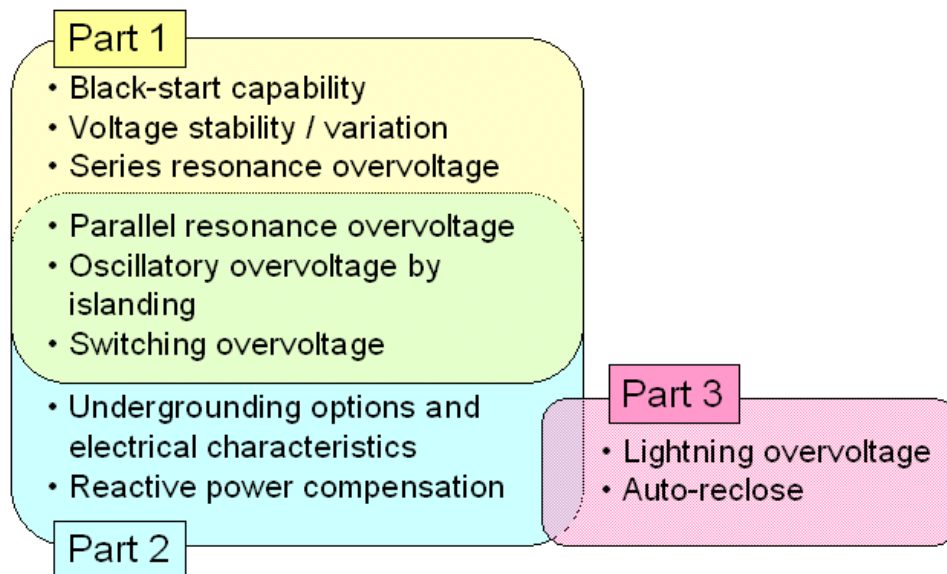
1.2 Scope of Works

The scope of this study is divided into the following three parts:

Part 1: Evaluation of the potential impact on the all-island transmission system of significant lengths of EHV underground cable, either individually or in aggregate

Part 2: Feasibility study on the 400 kV Woodland – Kingscourt – Turleenan line as AC EHV underground cables for the entire length

Part 3: Feasibility study of the 400 kV Woodland – Kingscourt – Turleenan line as mixed OHL / underground cable

The insulation levels of equipment, such as cable, GIS, transformers, measurement transformers, surge arresters, and shunt reactors are evaluated against the specifications of the NIE and EirGrid.   When any problems or violations are found, necessary countermeasures are

proposed and their effectiveness is evaluated.

For each part of the study, the following items shown in the figure below need to be studied. The series resonance overvoltage analysis was initially included in Part 2, but later excluded since it was found out that the target network for Part 2 did not have enough 275 / 220 kV cables (capacitance) to cause series resonance.   The methodologies for each analysis are explained in Section 1.3.

Part 1
- Black-start capability
- Voltage stability / variation
- Series resonance overvoltage

- Parallel resonance overvoltage
- Oscillatory overvoltage by islanding
- Switching overvoltage

- Undergrounding options and electrical characteristics
- Reactive power compensation

Part 2

Part 3
- Lightning overvoltage
- Auto-reclose

1.3 Methodology

1.3.1   Underground Options and Electrical Characteristics (Part 2)

The proposed Woodland – Kingscourt – Turleenan line is required to carry 1500 MW in either direction.   In addition, the circuits are allowed to be fully loaded only under contingency conditions.   Based on these conditions, TEPCO studied the appropriate XLPE cable options, such as the cable size, the number of circuits, and electrical characteristics.   The best cable option that this study yielded was selected as the foundation for subsequent analyses.

1.3.2   Reactive Power Compensation (Part 2)

An appropriate reactive power compensation scheme, in terms of location and amount, was studied for the two EHV underground cables.   For a long EHV underground cable, shunt reactors are often connected directly to the cable, considering:

- Temporary overvoltage when one end of the cable is opened, and

- Voltage variation when the cable is energised

These conditions were studied in off-peak demand based on the powerflow calculation in PSS/E to determine a location to install the shunt reactors.   If no concerns are raised with regards to the powerflow calculation results, the shunt reactors can be connected to the substation buses, which yield higher flexibility in the areas of voltage and reactive power control.   Shunt reactors could be installed to the secondary or tertiary buses of a substation as a cheaper option.   However, shunt reactors may not be used during a transformer outage when they are installed to the tertiary bus of the substation.

The appropriate amount of shunt reactors was determined from the voltage profile in off-peak demand.   The voltage profile along the length of the cables as well as the voltage profile of the 400 kV network was studied.   The voltage profile was evaluated with all shunt reactors in service and one unit out of service for different loading conditions.

The necessity of shunt reactor stations (or switching stations) along the length of the cables was determined from the following:

- Impact on the necessary amount of shunt reactors

- Active power loss in the cables

For Part 1, the reactive power compensation analysis is not a focus of the study.   As discussed in Chapter 2, however, a large number of 400 / 275 / 220 kV new / uprated / replaced OHLs were replaced by underground cables in Part 1.   As such, it was also necessary for Part 1 to

carry out the reactive power compensation analysis in order to obtain a reasonable power flow data after introducing a large amount of cable.

1.3.3　Series Resonance Overvoltage (Part 1)

If the frequency of the switching overvoltage of the 400kV line matches the series resonance frequency of the lower voltage system,(the 275/220kV system), it may cause a large series resonance overvoltage.　TEPCO had experienced a transformer failure due to an overvoltage caused by series resonance during a test energisation.

For the series resonance overvoltage analysis, it is necessary to model a 400 kV and 275/220 kV system around the Woodland S/S, Kingscourt S/S, and Turleenan S/S in EMTP.

Before the time domain simulations, the series resonance frequencies of the Woodland, Kingscourt, and Turleenan network were found from the results of frequency scan.　Different resonance frequencies can be found under different network conditions.　The frequency components contained in the overvoltages caused by the energisation of the Woodland – Kingscourt – Turleenan cable were found via the Fourier analysis.　The series resonance overvoltage analysis was conducted under the following two conditions:

(a) Normal condition where all the 400/275 kV and 400/220 kV transformers and the 275 kV and 220 kV lines around the Woodland, Kingscourt, and Turleenan are in service

(b) Assumed severest condition where the frequency contained in the energisation overvoltage is closest to the resonance frequency

1.3.4　Parallel Resonance (Part 1, 2, and 3)

The parallel resonance condition is likely to appear when equivalent source impedance is large; that is, when an EHV underground cable has significant length and is installed in a weak part of the all-island transmission system.

Before the time domain simulations, the parallel resonance frequencies seen from Kilkenny, Cahir, or Aghada were found by frequency scan in Part 1.　For Parts 2 and 3, the parallel resonance frequencies seen from Woodland, Kingscourt, and Turleenan were studied.

Depending on the results of frequency scan, switching operations were selected to cause an overvoltage near the parallel resonance frequency.　When the parallel resonance frequency is close to 100 Hz, transformer inrush was selected as the severest case.　The parallel resonance overvoltage was finally evaluated based on the results of the time domain simulations with the selected switching operations.

1.3.5   Oscillatory Overvoltage Caused by the System Islanding (Part 1 and 2)

Depending on the network configuration, a part of the transmission system can be separated from the main grid after clearing a bus fault.   When this islanded system includes generators, sustained temporary overvoltage can be caused after the system islanding.   In addition, the fault clearing overvoltage is superimposed on it, posing a severe stress on the cable and other equipment. According to its theoretical definition, the longer a cable is, the stronger is its tendency to cause a larger overvoltage.

The oscillatory overvoltage analysis was performed in EMTP, with a 400 kV bus fault in Kilkenny S/S, Cahir S/S, or in Aghada S/S in Part 1.   For Part 2, a 400 kV bus fault was placed in Woodland S/S, Kingscourt S/S, and Turleenan S/S.   One end of the cable is tripped by this fault, which may cause a subsequent severe oscillatory overvoltage.

1.3.6   Overvoltage caused by Line Energisation (Part 1 and 2)

The energisation of the Kilkenny – Cahir cable (Part 1) and the Woodland – Kingscourt – Turleenan cable (Part 2) was studied in EMTP.   Line energisations were simulated two hundred times using statistical switches, in order to investigate slow-front overvoltages caused by different switching timings.   The slow-front overvoltage (2% value) was evaluated against SIWV of equipment.

In the analysis, it was assumed that the time between the line outage and line energisation is long enough to discharge each cable.   Hence, residual voltage in the cable was not taken into account in line energisations.

1.3.7   Ground Fault and Fault Clearing Overvoltage (Part 1 and 2)

The slow-front overvoltage caused by ground fault and fault clearing was studied with different fault timings.   The slow-front overvoltage (2% value) was evaluated against SIWV of equipment.   The conditions of this analysis are:

Fault point: Seven points in each 400 kV cable route

(Kilkenny – Cahir for Part 1, Woodland – Kingscourt – Turleenan for Part 2)

Fault type: Single line to ground fault (core to sheath) in Phase A

Fault timing: 0° – 180° (10° step)

1.3.8   Black-start capability (Part 1)

In the restoration of the bulk power system, sustained power frequency overvoltages may be caused by charging current.   When the restoration has to be realized through an EHV underground cable with significant length, black-start generators are required to have sufficient under-excitation capability, depending on the compensation rate of the cable charging capacity.

Besides the sustained power frequency overvoltages, a harmonic resonance overvoltage can be caused in the restoration of the bulk power system.   The highest concern is the second harmonic current injection as in the parallel resonance overvoltage analysis.   In the restoration through the network largely composed of OHTLs, it is generally possible to avoid the resonance condition by connecting generators and loads and/or undergoing other operational measures.   For the network largely composed of EHV underground cables, careful assessment is of utmost importance when establishing restoration procedures.   In this case, it is not possible to establish general restoration procedures given that these procedures must be specific especially in terms of the on-line generators, connected loads, and energised lines including shunt reactors.   As such, TEPCO has studied two examples of the restoration procedure to show the harmonic resonance overvoltage analysis in the restoration process.

1.3.9   Voltage stability and variation (Part 1)

Underground cables have smaller impedance compared with OHTLs, when equal transmission capacity is acquired by the introduction of either underground cables or OHLs.   In addition, the reactive power support can be available from the underground cable as long as an appropriate reactive power compensation scheme is selected.

The loss of the cable may cause a voltage stability problem, however, only when the compensation rate is low, either by design or due to an outage of a shunt reactor.   In this case, the loss of the cable leads to the loss of reactive power supply, which can pose a severer condition than the loss of OHLs.

The loss of the Kilkenny – Cahir line and the loss of the Woodland – Kingscourt – Turleenan line were studied in order to find their effects on voltage stability and variation.

1.3.10 Lightning overvoltage (Part 3)

When a cable section is terminating in a substation, it is sometimes not necessary to install a surge arrester connected to the cable.   In order to evaluate the necessity of the surge arrester, the lightning overvoltage analysis is often performed.   This analysis is not necessary in Part 3, since it is assumed that a cable section is an intermediate section not terminating in one of the terminal substations.

Here, the lightning overvoltage analysis was carried out in order to evaluate the overvoltage in a metallic sheath.   When lightning strikes a ground wire near the connection between the overhead line and the underground cable, lightning current that flows into earth through a tower or a gantry may cause a very high overvoltage in the metallic sheath.   The level of the overvoltage highly depends on the tower footing resistance at the connection between the overhead line and the underground cable, and it is important to have as low impedance as possible, which is similar to substation mesh.   When a very high overvoltage is observed, it is necessary to evaluate the energy absorption capability of SVLs (sheath voltage limiters).

1.3.11 Overvoltage caused by autoreclose (Part 3)

It is possible to apply high-speed autoreclose for the mixed overhead line / underground cable, when a fault section detection system is installed to distinguish whether a fault is in the cable section or not.   An example of the fault section detection system in TEPCO is shown in Fig. 1.1. When a fault location is detected to be in the cable section, the fault section detection system sends out a signal to block high-speed autoreclose.
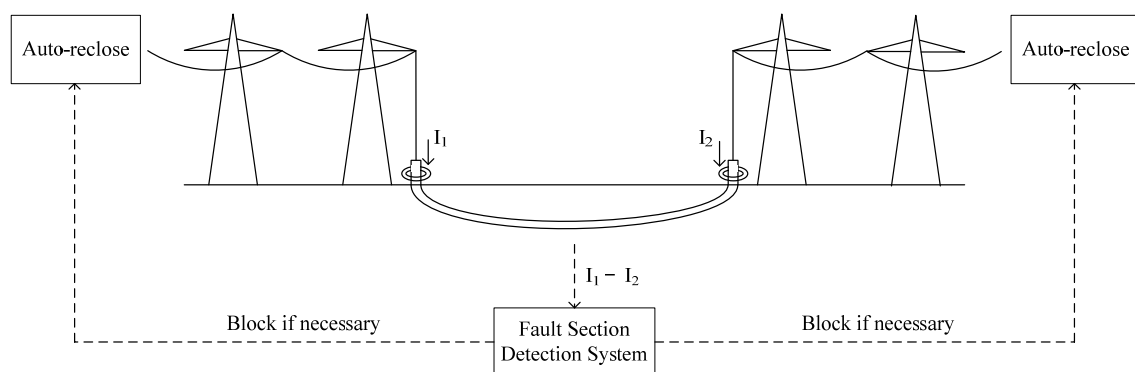
Fig. 1.1 Fault section detection system for a mixed overhead line / underground cable.

The conditions for autoreclose are different in the following two points compared to the line energisation studied in Part 2:

(a) The cable is re-energised before the cable is discharged, and

(b) When single phase autoreclose is applied, only a faulted phase (single phase) can be opened and re-energised.

The energisation overvoltage analysis performed in Part 2 was repeated under different conditions as described in (a) and (b). In the same way, as in Part 2, line energisations were simulated two hundred times using statistical switches in order to investigate slow-front overvoltages caused by different switching timings. The slow-front overvoltage (2% value) was evaluated against SIWV of equipment.

Chapter 2 Planned Transmission System in 2020

2.1 Power Flow Data in 2020

The feasibility study was performed based on the planned transmission system in the year 2020. For Part 1, the following points were modified from the original plan provided from the NIE/EirGrid. All modified lines are shown from Table 2-1 to Table 2-6:

- The Woodland – Kingscourt – Turleenan line was changed from an OHL to a double circuit underground cable;

- New/Rep 400 kV OHLs were replaced by a 400kV single circuit underground cables;

- Some of the new 275kV OHLs were replaced by 275 kV single or double circuit underground cables;

- New/Upr/Rep 220 kV OHLs were replaced by 220 kV single circuit underground cables;

- New/Upr 110 kV OHLs were replaced by 110 kV single circuit underground cables.

For Parts 2 and 3, the following two points were modified from the original plan provided from the NIE/EirGrid:

- The Woodland – Kingscourt – Turleenan line was changed from the OHL to the underground cable for the feasibility study;

- The Woodland – Maynooth – Dunstown line was changed from the 400 kV OHL to 220 kV OHL in order to keep the 400 kV system close to the current one.

As a result, in the planned transmission system in the year 2020, the Woodland – Kingscourt – Turleenan line is the only 400 kV cable line in Parts 2 and 3, except the submarine cable (Moneypoint – Tarbert). No 275 kV cable lines exist in the NIE network.

The power flow diagram of the planned transmission system for the year 2020 in summer off-peak demand is shown in Fig. 2.1 (Part 1) and Fig. 2.2 (Part 2 and 3).

2.1.1   400 kV Woodland – Kingscourt – Turleenan line

Impedance data of the 400 kV Woodland – Kingscourt - Turleenan line were derived based on 400 kV Al 1400 mm^2 XLPE cables, which ensures the transmission capacity of 750 MVA/cct.

Table 2-1 400 kV Woodland – Kingscourt – Turleenan Line

kV	Original Plan	Modified Plan	From Bus		To Bus	
400 kV	OHL	Cable 2cct	3774	KINGSCOURT	5464	WOODLAND
	OHL	Cable 2cct	3774	KINGSCOURT	90140	TURL

2.1.2   Standard 400 kV cables used to replace new 400 kV OHLs

Impedance data of standard 400 kV cables were derived based on 400 kV Cu 2500mm^2 XLPE cables.

Table 2-2 Standard 400 kV Cables Used to Replace New 400 kV OHLs

kV	Original Plan	Modified Plan	From Bus		To Bus	
400 kV	OHL	Cable 1cct	1044	AGHADA	1724	CAHIR
	OHL	Cable 1cct	1124	ARKLOW	2744	GREAT_ISL
	OHL	Cable 1cct	1724	CAHIR	3264	KILKENNY
	OHL	Cable 1cct	2524	FLAGFORD	3774	KINGSCOURT
	OHL	Cable 1cct	3344	KELLIS	3554	LAOIS
	OHL	Cable 1cct	2204	DUNSTOWN	3854	MAYNOOTH
	OHL	Cable 1cct	3854	MAYNOOTH	5464	WOODLAND

2.1.3   275 kV cables used to replace new 275 kV OHLs

Impedance data of 275 kV cables were derived based on Cu 1600 mm^2 XLPE cables.

Table 2-3 275 kV Cables Used to Replace New 275 kV OHLs

KV	Original Plan	Modified Plan	From Bus		To Bus		Id
275 kV	OHL	Cable 2cct	87520	OMAH	90120	TURL	1
	OHL	Cable 2cct	87520	OMAH	90120	TURL	2
	OHL	Cable 2cct	87520	OMAH	89520	STRABANE	1
	OHL	Cable 2cct	75520	COOLKEER	89520	STRABANE	1

2.1.4 220 kV cables used to replace new/upr/rep 220 kV OHLs

Impedance data of 220kV cables were derived from those of the Carrickmines − Irishtown cable.

Table 2-4 220 kV Cables Used to Replace New/Upr/Rep 220 kV OHLs

KV	Original Plan	Modified Plan	From Bus		To Bus		Id
220 kV	OHL	cable 1cct	2002	CULLENAG	2742	GREAT IS	1
	OHL	cable 1cct	3282	KILLONAN	5492	WMD_220	1
	OHL	cable 1cct	2202	DUNSTOWN	3342	KELLIS	1
	OHL	cable 1cct	1122	ARKLOW	1742	CARRICKM	1
	OHL	cable 1cct	1642	CASHLA	4522	PROSPECT	1
	OHL	cable 1cct	4942	SHANNONB	5492	WMD_220	1
	OHL	cable 1cct	4522	PROSPECT	5142	TARBERT	1
	OHL	cable 1cct	2042	CORDUFF	5462	WOODLAND	1
	OHL	cable 1cct	2042	CORDUFF	5462	WOODLAND	2
	OHL	cable 1cct	3852	MAYNOOTH	4952	KINNEGAD	1
	OHL	cable 1cct	4942	SHANNONB	4952	KINNEGAD	1
	OHL	cable 1cct	2532	FINNSTOW	3852	MAYNOOTH	2
	OHL	cable 1cct	1432	BALLYRAGGET	3262	KILKENNY	1
	OHL	cable 1cct	1432	BALLYRAGGET	3552	LAOIS	1

Impedance data of the following 220 kV cables were derived from those of the Carrickmines − Irishtown cable but with increased phase spacing of 850 mm.

Table 2-5 220 kV Cables (Increased spacing) Used to Replace New/Upr/Rep 220 kV OHLs

kV	Original Plan	Modified Plan	From Bus		To Bus		Id
220 kV	OHL	cable 1cct	1402	BELLACOR	2522	FLAGFORD	1
	OHL	cable 1cct	5142	TARBERT	9992	NEW_TRIEN	2
	OHL	cable 1cct	1072	AGHADA4	3202	KNOCKRAH	1
	OHL	cable 1cct	3522	LOUTH	5462	WOODLAND	1
	OHL	cable 1cct	2742	GREAT IS	3642	LODGEWOO	1
	OHL	cable 1cct	2842	GORMAN	3842	MAYNOOTH	1
	OHL	cable 1cct	3522	LOUTH	3772	KINGSCOURT	1

	OHL	cable 1cct	1122	ARKLOW	3642	LODGEWOO	1
	OHL	cable 1cct	2522	FLAGFORD	3772	KINGSCOURT	1
	OHL	cable 1cct	2842	GORMAN	3522	LOUTH	1
	OHL	cable 1cct	1602	CLASHAVO	3202	KNOCKRAH	1
	OHL	cable 1cct	5142	TARBERT	9992	NEW_TRIEN	1
	OHL	cable 1cct	1122	ARKLOW	2032	CHARLESLAND	1
	OHL	cable 1cct	1742	CARRICKM	2032	CHARLESLAND	1

2.1.5　110 kV cables used to replace new/upr/rep 110 kV OHLs

Impedance data of the 110 kV cables were derived from those of the Artane - Fin_urba cable.

Table 2-6 110 kV Cables Used to Replace New/Upr/Rep 110 kV OHLs

kV	Original Plan	Modified Plan	From Bus		To Bus		Id
110 kV	OHL	cable 1cct	1121	ARKLOW	1301	BALLYBEG	1
	OHL	cable 1cct	1281	BALLYLIC	1601	CLASHAVO	1
	OHL	cable 1cct	1601	CLASHAVO	3881	MACROOM	2
	OHL	cable 1cct	1611	CLONKEEN	3301	KNOCKERA	2
	OHL	cable 1cct	3221	KILBARRY	3881	MACROOM	1
	OHL	cable 1cct	3521	LOUTH	4061	MULLAGHA	2
	OHL	cable 1cct	3551	LAOIS	4481	PORTLAOI	2
	OHL	cable 1cct	3551	LAOIS	4481	PORTLAOI	3
	OHL	cable 1cct	3581	LETTERKE	5191	TIEVEBRA	1
	OHL	cable 1cct	3581	LETTERKE	5361	TRILLICK	1
	OHL	cable 1cct	1721	CAHIR	2161	DOON	1
	OHL	cable 1cct	1221	ATHY	1901	CARLOW	1
	OHL	cable 1cct	1221	ATHY	3551	LAOIS	1
	OHL	cable 1cct	1181	ARVA	1861	CARICKON	1
	OHL	cable 1cct	4981	SLIGO	5041	SRANANAG	1
	OHL	cable 1cct	4981	SLIGO	5041	SRANANAG	2
	OHL	cable 1cct	2001	CULLENAG	5441	WATERFOR	1
	OHL	cable 1cct	1361	BALLYDIN	2161	DOON	1
	OHL	cable 1cct	1361	BALLYDIN	2001	CULLENAG	1
	OHL	cable 1cct	3401	KILLOTER	5441	WATERFOR	1
	OHL	cable 1cct	2741	GREAT IS	5441	WATERFOR	1

	OHL	cable 1cct	1481	BUTLERST	3401	KILLOTER	1
	OHL	cable 1cct	2741	GREAT IS	5501	WEXFORD	1
	OHL	cable 1cct	2741	GREAT IS	5441	WATERFOR	2
	OHL	cable 1cct	1661	CASTLEBA	1821	CLOON	1
	OHL	cable 1cct	2521	FLAGFORD	5341	TONROE	1
	OHL	cable 1cct	1661	CASTLEBA	2281	DALTON	1
	OHL	cable 1cct	2741	GREAT IS	3441	KILMURRY	1
	OHL	cable 1cct	2521	FLAGFORD	3501	LANESBOR	1
	OHL	cable 1cct	1541	BANOGE	1841	CRANE	1
	OHL	cable 1cct	1901	CARLOW	3341	KELLIS	1
	OHL	cable 1cct	1901	CARLOW	3341	KELLIS	2
	OHL	cable 1cct	1481	BUTLERST	2001	CULLENAG	1
	OHL	cable 1cct	1121	ARKLOW	1541	BANOGE	1
	OHL	cable 1cct	1641	CASHLA	2361	ENNIS	1
	OHL	cable 1cct	1621	COOLROE	3061	INISCARR	1
	OHL	cable 1cct	1661	CASTLEBA	5341	TONROE	1
	OHL	cable 1cct	1981	CORRACLA	2821	GORTAWEE	1
	OHL	cable 1cct	3261	KILKENNY	3441	KILMURRY	1
	OHL	cable 1cct	5301	THURLES	31019	IKERIN T	1
	OHL	cable 1cct	4941	SHANNONB	31019	IKERIN T	1
	OHL	cable 1cct	1981	CORRACLA	79016	ENNK_PST	1
	OHL	cable 1cct	2521	FLAGFORD	4981	SLIGO	1
	OHL	cable 1cct	1021	ARDNACRU	2121	DRUMLINE	1
	OHL	cable 1cct	4941	SHANNONB	22419	DALLOW T	1
	OHL	cable 1cct	1021	ARDNACRU	2361	ENNIS	1
	OHL	cable 1cct	3261	KILKENNY	3341	KELLIS	1
	OHL	cable 1cct	5141	TARBERT	5281	TRALEE	1
	OHL	cable 1cct	1701	CATH_FAL	1981	CORRACLA	1
	OHL	cable 1cct	1841	CRANE	5501	WEXFORD	1
	OHL	cable 1cct	4481	PORTLAOI	22419	DALLOW T	1
	OHL	cable 1cct	3201	KNOCKRAH	3221	KILBARRY	1
	OHL	cable 1cct	2181	DRYBRIDG	3521	LOUTH	1
	OHL	cable 1cct	3281	KILLONAN	3541	LIMERICK	2
	OHL	cable 1cct	3501	LANESBOR	4001	MULLINGA	1
	OHL	cable 1cct	1141	ATHLONE	4941	SHANNONB	1

	OHL	cable 1cct	1141	ATHLONE	3501	LANESBOR	1
	OHL	cable 1cct	1181	ARVA	4961	SHANKILL	1
	OHL	cable 1cct	1841	CRANE	3641	LODGEWOO	1
	OHL	cable 1cct	3521	LOUTH	3821	MEATH HI	1
	OHL	cable 1cct	1861	CARICKON	10619	ARIGNA_T	1
	OHL	cable 1cct	1141	ATHLONE	4941	SHANNONB	2
	OHL	cable 1cct	3221	KILBARRY	3961	MARINA	1
	OHL	cable 1cct	1631	CORDERRY	10619	ARIGNA_T	1
	OHL	cable 1cct	2841	GORMAN	4501	PLATIN	1
	OHL	cable 1cct	1701	CATH_FAL	5041	SRANANAG	1
	OHL	cable 1cct	1701	CATH_FAL	5041	SRANANAG	2
	OHL	cable 1cct	1701	CATH_FAL	1761	CLIFF	1
	OHL	cable 1cct	2181	DRYBRIDG	2841	GORMAN	1
	OHL	cable 1cct	1881	CHARLEVI	4021	MALLOW	1
	OHL	cable 1cct	3281	KILLONAN	3541	LIMERICK	1
	OHL	cable 1cct	3201	KNOCKRAH	3221	KILBARRY	2
	OHL	cable 1cct	3221	KILBARRY	3961	MARINA	2
	OHL	cable 1cct	3551	LAOIS	4481	PORTLAOI	1
	OHL	cable 1cct	1241	BALLYCUM	3541	LIMERICK	1
	OHL	cable 1cct	1241	BALLYCUM	3901	MONETEEN	1
	OHL	cable 1cct	5361	TRILLICK	75510	COOL1-	1
	OHL	cable 1cct	3581	LETTERKE	89510	STRABANE	2
	OHL	cable 1cct	3581	LETTERKE	89510	STRABANE	1
	OHL	cable 1cct	75010	COLE1-	81510	KELS1-	1
	OHL	cable 1cct	79010	ENNISKIL	87510	OMAH1-	1
	OHL	cable 1cct	79010	ENNISKIL	87510	OMAH1-	2
	OHL	cable 1cct	87510	OMAH1-	89510	STRABANE	1
	OHL	cable 1cct	87510	OMAH1-	89510	STRABANE	2
	OHL	cable 1cct	1901	CARLOW	3341	KELLIS	2
	OHL	cable 1cct	1481	BUTLERST	2001	CULLENAG	1
	OHL	cable 1cct	1121	ARKLOW	1541	BANOGE	1
	OHL	cable 1cct	1641	CASHLA	2361	ENNIS	1
	OHL	cable 1cct	1621	COOLROE	3061	INISCARR	1
	OHL	cable 1cct	1661	CASTLEBA	5341	TONROE	1
	OHL	cable 1cct	1981	CORRACLA	2821	GORTAWEE	1

	OHL	cable 1cct	3261	KILKENNY	3441	KILMURRY	1
	OHL	cable 1cct	5301	THURLES	31019	IKERIN T	1
	OHL	cable 1cct	4941	SHANNONB	31019	IKERIN T	1
	OHL	cable 1cct	1981	CORRACLA	79016	ENNK_PST	1
	OHL	cable 1cct	2521	FLAGFORD	4981	SLIGO	1
	OHL	cable 1cct	1021	ARDNACRU	2121	DRUMLINE	1
	OHL	cable 1cct	4941	SHANNONB	22419	DALLOW T	1
	OHL	cable 1cct	1021	ARDNACRU	2361	ENNIS	1
	OHL	cable 1cct	3261	KILKENNY	3341	KELLIS	1
	OHL	cable 1cct	5141	TARBERT	5281	TRALEE	1
	OHL	cable 1cct	1701	CATH_FAL	1981	CORRACLA	1
	OHL	cable 1cct	1841	CRANE	5501	WEXFORD	1
	OHL	cable 1cct	4481	PORTLAOI	22419	DALLOW T	1
	OHL	cable 1cct	3201	KNOCKRAH	3221	KILBARRY	1
	OHL	cable 1cct	2181	DRYBRIDG	3521	LOUTH	1
	OHL	cable 1cct	3281	KILLONAN	3541	LIMERICK	2
	OHL	cable 1cct	3501	LANESBOR	4001	MULLINGA	1
	OHL	cable 1cct	1141	ATHLONE	4941	SHANNONB	1
	OHL	cable 1cct	1141	ATHLONE	3501	LANESBOR	1
	OHL	cable 1cct	1181	ARVA	4961	SHANKILL	1
	OHL	cable 1cct	1841	CRANE	3641	LODGEWOO	1
	OHL	cable 1cct	3521	LOUTH	3821	MEATH HI	1
	OHL	cable 1cct	1861	CARICKON	10619	ARIGNA_T	1
	OHL	cable 1cct	1141	ATHLONE	4941	SHANNONB	2
	OHL	cable 1cct	1141	ATHLONE	3501	LANESBOR	1
	OHL	cable 1cct	1181	ARVA	4961	SHANKILL	1
	OHL	cable 1cct	1841	CRANE	3641	LODGEWOO	1
	OHL	cable 1cct	3521	LOUTH	3821	MEATH HI	1
	OHL	cable 1cct	1861	CARICKON	10619	ARIGNA_T	1
	OHL	cable 1cct	1141	ATHLONE	4941	SHANNONB	2
	OHL	cable 1cct	3221	KILBARRY	3961	MARINA	1
	OHL	cable 1cct	1631	CORDERRY	10619	ARIGNA_T	1
	OHL	cable 1cct	2841	GORMAN	4501	PLATIN	1
	OHL	cable 1cct	1701	CATH_FAL	5041	SRANANAG	1
	OHL	cable 1cct	1701	CATH_FAL	5041	SRANANAG	2

	OHL	cable 1cct	1701	CATH_FAL	1761	CLIFF	1
	OHL	cable 1cct	2181	DRYBRIDG	2841	GORMAN	1
	OHL	cable 1cct	1881	CHARLEVI	4021	MALLOW	1
	OHL	cable 1cct	3281	KILLONAN	3541	LIMERICK	1
	OHL	cable 1cct	3201	KNOCKRAH	3221	KILBARRY	2
	OHL	cable 1cct	3221	KILBARRY	3961	MARINA	2
	OHL	cable 1cct	3551	LAOIS	4481	PORTLAOI	1
	OHL	cable 1cct	1241	BALLYCUM	3541	LIMERICK	1
	OHL	cable 1cct	1241	BALLYCUM	3901	MONETEEN	1
	OHL	cable 1cct	5361	TRILLICK	75510	COOL1-	1
	OHL	cable 1cct	3581	LETTERKE	89510	STRABANE	2
	OHL	cable 1cct	3581	LETTERKE	89510	STRABANE	1
	OHL	cable 1cct	75010	COLE1-	81510	KELS1-	1
	OHL	cable 1cct	79010	ENNISKIL	87510	OMAH1-	1
	OHL	cable 1cct	79010	ENNISKIL	87510	OMAH1-	2
	OHL	cable 1cct	87510	OMAH1-	89510	STRABANE	1
	OHL	cable 1cct	87510	OMAH1-	89510	STRABANE	2

Planned Transmission System 2020 for Part 1

LEGEND

⎯⎯	400 kV Lines
⎯⎯	275 kV Lines
⎯⎯	220 kV Lines
- - -	400 kV Cables
- - -	275 kV Cables
- - -	220 kV Cables
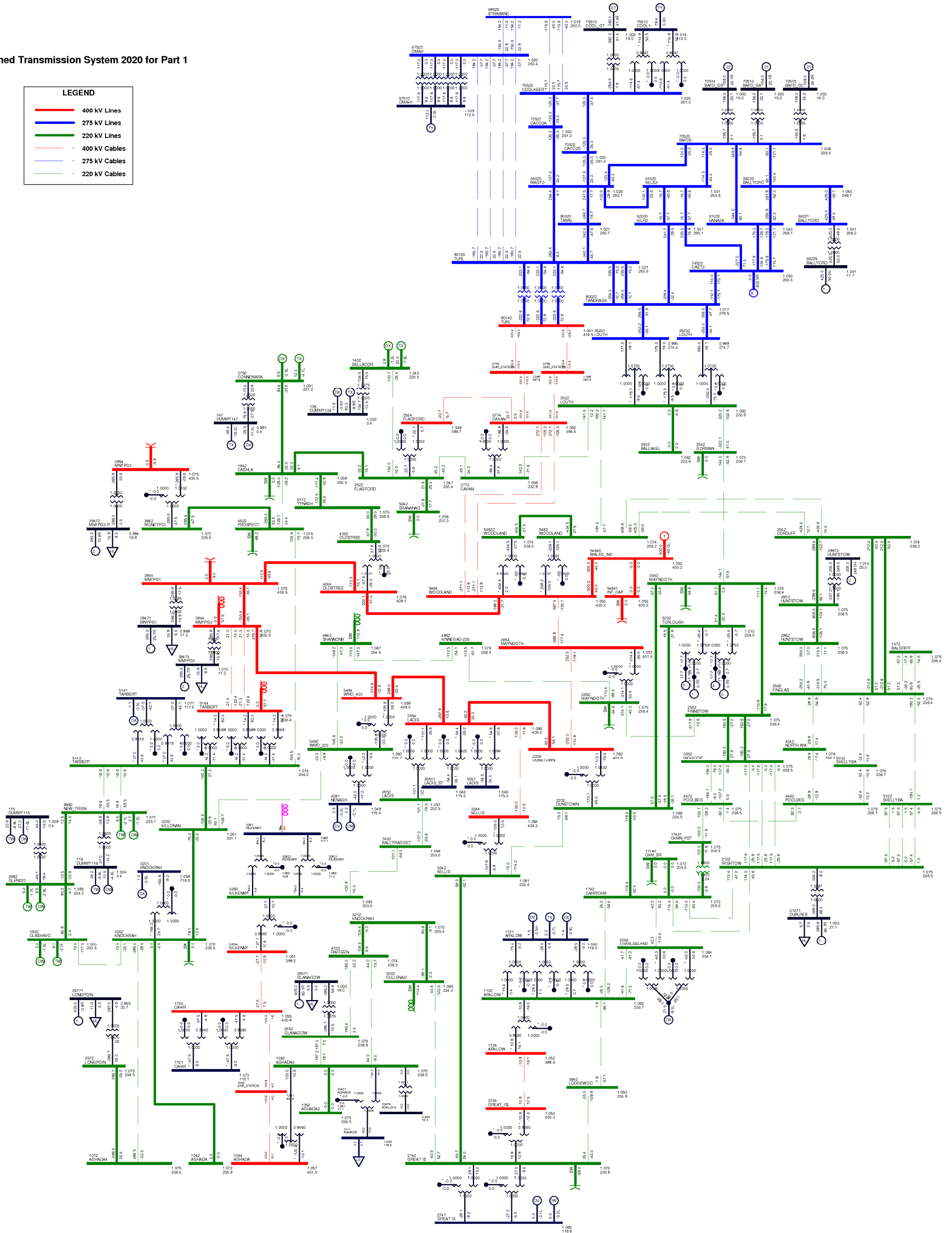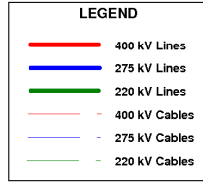
Fig. 2.1 Power flow diagram of the modified planned transmission system in the year 2020 in summer off-peak demand (Part 1).

Planned Transmission System 2020
for the Feasibility Study of
the Woodland - Kingscourt - Turleenan Cable

LEGEND
━━━ 400 kV Lines
━━━ 275 kV Lines
━━━ 220 kV Lines
╌╌╌ 400 kV Cables
╌╌╌ 220 kV Cables
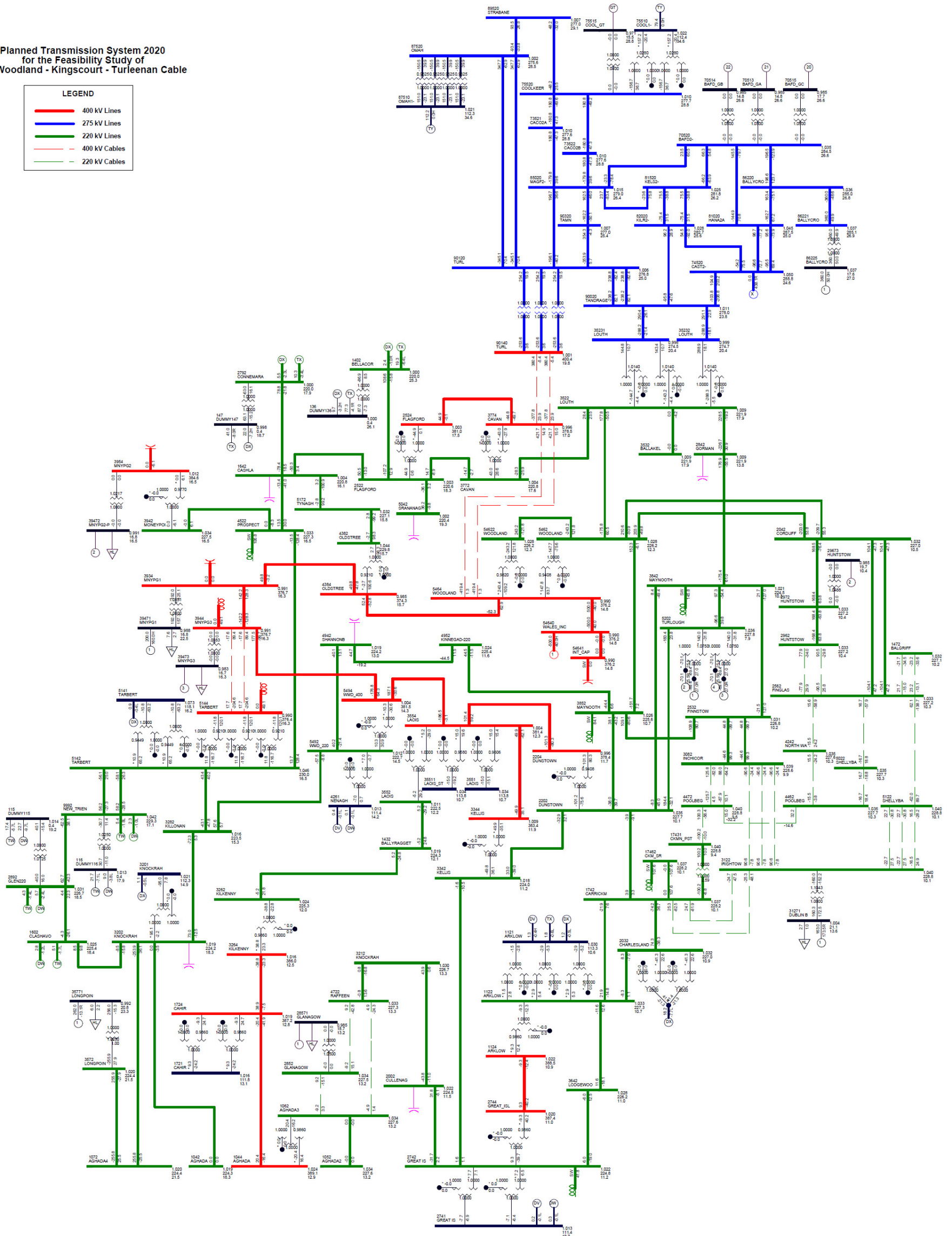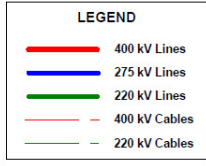
Fig. 2.2 Power flow diagram of the modified planned transmission system in the year 2020 in summer off-peak demand (Part 2 and 3).

Chapter 3 Selection of the Cable

3.1 Examples of EHV XLPE Cables

The Woodland – Kingscourt – Turleenan line is required to carry 1500 MVA as a continuous rating, in order to facilitate further power transactions between NI and RoI and thus to allow for further connections of renewable generators to the all-island transmission system.

Table 3-1 shows examples of the EHV XLPE directly buried cables with their transmission capacities.   It can be seen that it is difficult to secure 1500 MVA/cct if the cable is directly buried. A large conductor size with favorable ground conditions will be required.

Note that EHV cables in Vienna and Milan are a part of the mixed OHL/cable line.   Both of them connect the double circuit cable to a single circuit OHL to balance the transmission capacity in the cable section and the OHL section.

Table 3-1 Examples of EHV XLPE Directly Buried Cables

Location	Year	Voltage [kV]	Length [km]	Conductor Size [mm2]	CKT	Transmission Capacity (Winter) [MVA/cct]
Copenhagen	1997	400	22	1600	1	**900**
	1999		12		1	**(800)**
Jutland (Denmark)	2004	400	14 (4.5+2.5+7)	1200	2	**500**
Vienna	2005	400	5.2	1200	2	**620** **(1030 with cooling)**
Milan	2006	380	8.4	2000	2	**1050**

Table 3-2 Examples of EHV XLPE Cables in a Tunnel

Location	Year	Voltage [kV]	Length [km]	Conductor Size [mm2]	CKT	Transmission Capacity (Winter) [MVA/cct]
Berlin	1998	400	6.3	1600	2	**1100**
	2000		5.5		2	**1100**
Tokyo	2000	500	39.8	2500	2	**900 – 1200**
Madrid	2004	400	12.8	2500	2	**1720**
London	2005	400	20	2500	1	**1600**

Table 3-2 shows examples of EHV XLPE cables laid in a tunnel with their transmission capacities.   As shown in the table, transmission capacity of 1500 MVA/cct has been achieved in Madrid and London.

In Berlin, Madrid, and London, cables are laid with 500 – 600 mm space between phases. Because of this phase spacing, these EHV cables occupy a large proportion of the space in a tunnel. This will make it difficult for tunnel installation to achieve a cost advantage over directly buried cables.

3.2 Transmission Capacity Calculation

3.2.1 Woodland – Kingscourt – Turleenan line

In order to find a cable type and layout which assures transmission capacity of 1500 MVA, transmission capacity calculation was conducted based on IEC 60287.   Since the load factor was specified as unity as the severest assumption, the cyclic rating was not calculated. (IEC 60853 was not used.)

Based on the results of the transmission capacity calculation, the following cable types and layouts were selected for further study.   In the table, double circuit was selected as base case, upon which all subsequent conditions will be studied.   Single circuit was selected as optional; only designated severe cases will be studied with Single circuit.

Table 3-3 Selected Cable Types and Layouts

	Double circuit	Single circuit
Conductor	Al 1400 mm^2	Cu 2500 mm^2
Buried formation	Flat	Flat
Phase spacing	500 mm	700 mm

In choosing the cable types and layouts shown in Table 3-3, transmission capacity was calculated for the various cable types and phase spacings.   Fig. 3.1 shows the result of the transmission capacity calculation for double circuit.   With phase spacing of 500 mm, Al 1400 mm^2 is a reasonable choice in order to assure transmission capacity of 1500 MVA.
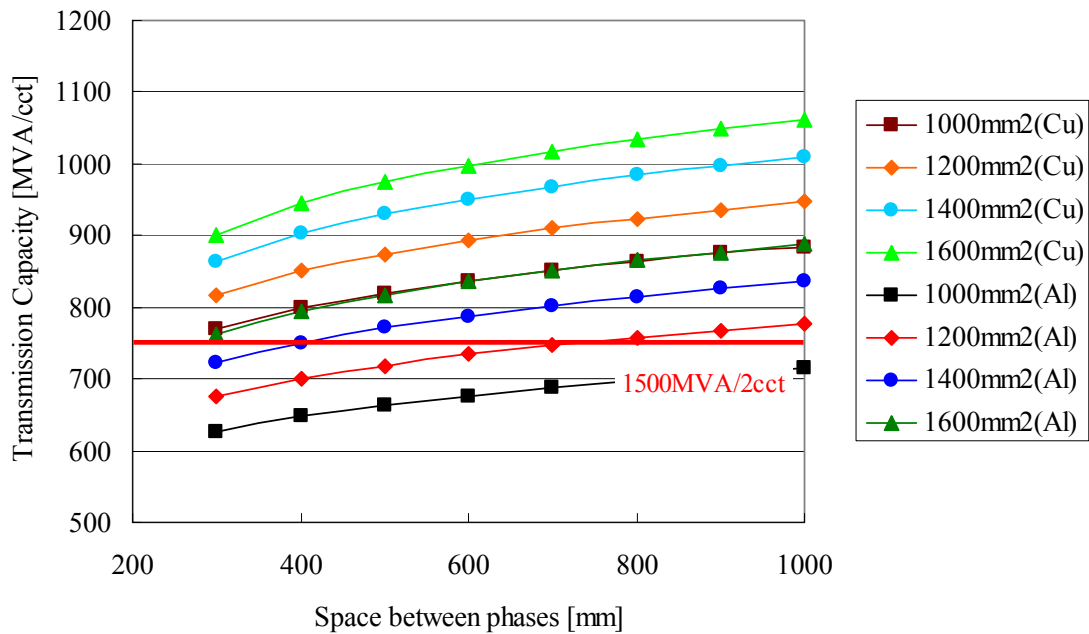
Fig. 3.1 Result of the transmission capacity calculation for double circuit.

Fig. 3.2 shows the result of the transmission capacity calculation for single circuit.   It can be seen that the conductor size of 3000 mm^2 is necessary in order to achieve 1500 MVA/cct.   Since XLPE cables with a conductor size of 3000 mm^2 are still under development, however, Cu 2500 mm^2 was selected for the study of severe cases.
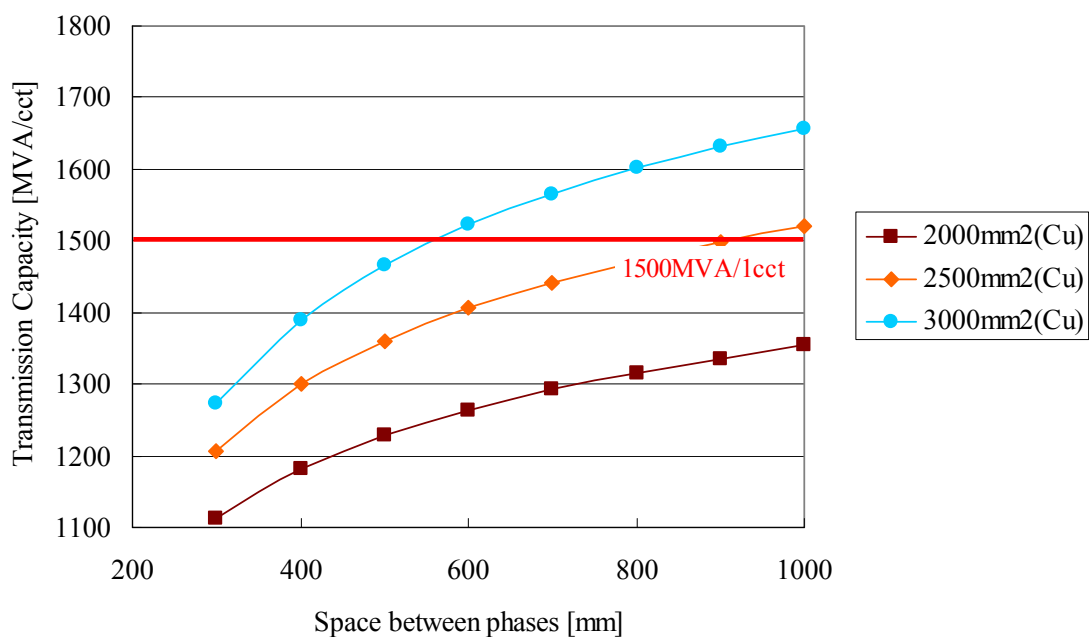
Fig. 3.2 Result of the transmission capacity calculation for single circuit.

Even though the single circuit option was studied, it does not reflect the intention of TEPCO to recommend the single circuit option.   It needs to be noted that this line will be the longest EHV cable line if it is built as the cable line for the whole length.   Considering relatively poor performance of the XLPE cables and their accessories [1], the double circuit option should be preferred to secure the required reliability.   However, the reliability of XLPE technology requires careful assessment since the preferred joint type is in the process of transition from the extruded mold joint to the pre-molded joint.

[1] CIGRE Working Group B1.10, TB 379, April 2009, "Update of Service Experience of HV Underground and Submarine Cable Systems"

The key assumptions adopted in the transmission capacity calculation were provided from the NIE/EirGrid as follows:

Maximum soil temperature:	15 deg C
Soil thermal resistivity:	1.2 K.m/W
Buried depth:	1.3 m (from ground surface to the cable axis)
Load factor:	1.0
Skin effect coefficient:	1.0 (most pessimistic assumption, for double circuit)
	0.25[2] (copper enamelled wire, for single circuit)
Proximity effect coefficient:	0.8 (most pessimistic assumption, for double circuit)
	0.15[2] (copper enamelled wire, for single circuit)

[2] These values are given in the CIGRE Working Group B1.03, TB 272, June 2005, "Large Cross-sections and Composite Screens Design".

3.2.2   Standard 400 kV Cable

Standard 400 kV cables were used to replace the new 400 kV OHLs as shown in Table 2-2. Their required transmission capacity is 1424 MVA.   Referring to Fig. 3.2, the following cable types and layouts were selected in order to secure 1424 MVA/cct.

Table 3-4 Selected Cable Type and Layout for the Standard 400 kV Cable

	Standard 400 kV Cable
Conductor	Cu 2500 mm^2
Number of circuit	1
Buried formation	Flat
Phase spacing	700 mm

3.2.3 Standard 275 kV Cable

Standard 275 kV cables were used to replace new 275 kV OHLs as shown in Table 2-3. Their required transmission capacity is 710 MVA or 1207 MVA. The transmission capacity calculation was performed in order to determine the cable type and layout. Fig. 3.3 shows the result of the calculation. The conditions of the calculation were set to equal to those of the Woodland – Kingscourt – Turleenan line (double circuit).
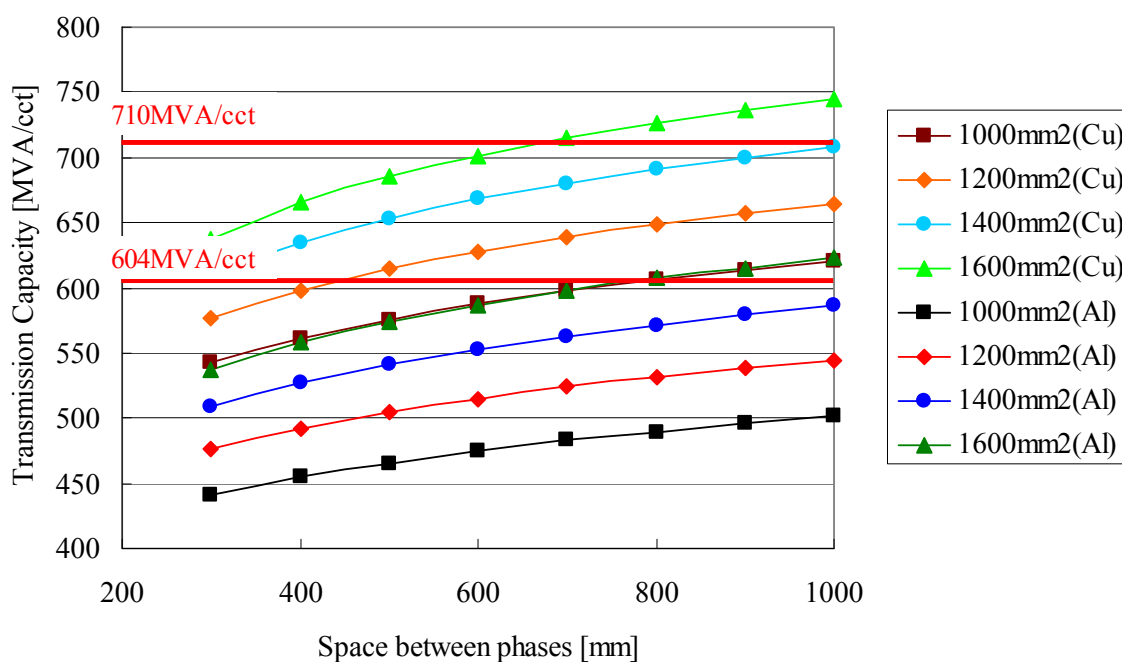
Fig. 3.3 Result of the transmission capacity calculation for the standard 275 kV cable.

Based on the results of the calculation, the following cable types and layouts were selected to replace the new 275 kV OHLs.

Table 3-5 Selected Cable Type and Layout for the Standard 275 kV Cable

	1207 MVA route	710 MVA route
Conductor	Cu 1200 mm^2	Cu 1600 mm^2
Number of circuit	2	1
Buried formation	Flat	Flat
Phase spacing	600 mm	800 mm

3.3 Impedance Calculation

Impedance and susceptance of 400 kV and 275 kV cables were derived from the following equations:

$$R_p = R \times (1 + \lambda) \quad [\Omega/\text{km}]$$

$$X_p = \frac{\omega \mu_0}{2\pi}(\frac{1}{4} + \ln\frac{GMR}{r_c}) \quad [\Omega/\text{m}]$$

$$= 0.2\omega(\frac{1}{4} + \ln\frac{\sqrt[3]{s \cdot s \cdot (2s)}}{r_c}) \times 10^{-3} \quad [\Omega/\text{km}]$$

$$= \omega(0.05 + 0.2\ln\frac{2s\sqrt[3]{2}}{d_c}) \times 10^{-3} \quad [\Omega/\text{km}]$$

$$B_p = \omega\frac{2\pi\varepsilon_r\varepsilon_0}{\ln(\frac{d_{in}}{d_{c0}})} \times 10^{-6} \quad [\text{mho}/\text{km}]$$

, where

R: a.c. resistance of conductor at the maximum operating temperature

λ: loss factor for sheath

s: phase spacing of the cable

d_c: diameter of conductor

ε_r: relative permittivity of insulation (2.4)

ε_0: permittivity of free space (0.008854 μF/km)]

d_{in}: diameter of insulation

d_{c0}: diameter of conductor including conductor screen

Here, R and λ have to be obtained through transmission capacity calculation.

The data applied to the impedance calculation is shown in Table 3-6. Diameters of the 400 kV cables were obtained from Nexan's specifications. The insulation thickness of the standard 275 kV cable (18.7 mm) were converted from the insulation thickness of 400 kV cables (25.4 mm) using the proportion of LIWV.

25.4 mm × (1050 kV / 1425 kV) = 18.7 mm

Table 3-6 Input Data for Impedance Calculation

	Woodland – Turleenan line		Standard 400 kV Cable	Standard 275 kV Cable	
Conductor	Al 1400 mm^2	Cu 2500 mm^2	Cu 2500 mm^2	Cu 1200 mm^2	Cu 1600 mm^2
Buried formation	Flat	Flat	Flat	Flat	Flat
s [mm]	500	700	700	600	800
d_c [mm]	45.0	65.2	65.2	41.7	48.2
d_{c0} [mm]	48.0	68.2	68.2	44.7	51.2
d_{in} [mm]	98.8	119.0	119.0	82.1	88.6
R [Ω/m]	3.001×10^{-5}	9.722×10^{-6}	9.722×10^{-6}	2.292×10^{-5}	1.880×10^{-5}
λ	0.05070	0.08324	0.08324	0.04152	0.03972

Based on the results of the calculation, impedance and capacitance of the cables were determined as follows:

Table 3-7 Impedance and Capacitance of the Selected Cables

	Woodland – Turleenan line		Standard 400 kV Cable	Standard 275 kV Cable	
	Al 1400 mm^2	Cu 2500 mm^2	Cu 2500 mm^2	Cu 1200 mm^2	Cu 1600 mm^2
R_p [Ω/km]	0.03153	0.01053	0.01053	0.02387	0.01955
X_p [Ω/km]	0.2251	0.2229	0.2229	0.2413	0.2503
C [μF/km]	0.1850	0.2398	0.2398	0.2196	0.2435

Part 1

Part 1:

Evaluation of the Potential Impact on the All-island Transmission System of Significant Length of EHV Underground Cable, Either Individually or in Aggregate Introduction

Table of contents

Chapter 1 Introduction

The objective of Part 1 is to evaluate the potential impact on the all-island transmission system of significant lengths of EHV underground cables.   In order to fulfill this objective, the following studies were performed:

(1) Transmission Capacity Calculation

(2) Impedance and Admittance Calculation

(3) Reactive Power Compensation Analysis

(4) Overvoltage Analysis

(5) Voltage Stability and Variation Analysis

(6) Black-start Studies

Here, (1) and (2) have already been conducted as a common study for Part 1, 2, and 3 and are not included in this Part 1 report.   Using cable information, such as cable size, type, layout, and impedance / admittance, found in (1) and (2), the remaining studies (3) – (6) were conducted as Part 1 studies.

The purpose of (3) is to find shunt reactors that should be installed together with the 400 kV cable.   The best combination in terms of the number of shunt reactors, shunt reactor size, and location was found from (3).

The studies (4) – (6) are to look into the potential adverse effects caused by significant lengths of EHV underground cables.   Temporary overvoltage analysis in the study (4) addresses the most important concern due to significant lengths of EHV underground cables.   In order to set the most severe condition in (4), the 400 kV Kilkenny – Cahir – Aghada line was selected as the focus of the study except for the series resonance overvoltage analysis.   The 400 kV Kilkenny – Cahir – Aghada line was selected since it was the longest 400 kV line in the weakest part of the network in the planned transmission system for the year 2020.   The series resonance overvoltage analysis focused on the 400 kV Woodland – Kingscourt – Turleenan line because of possible large cable capacitance generated in the 220 kV Woodland / Kingscourt network and the 275 kV Turleenan network.

Although the objective of Part 1 to evaluate the potential impact on the all-island transmission system of significant lengths of EHV underground cables, it is not possible to evaluate all possible scenarios or to choose one *severest* case.   The study instead focused on the reasonable worst-case scenario in terms of the feasibility.   For the installation of a particular cable line, more work has to be done for the cable line.

Chapter 2 Reactive Power Compensation

2.1 Considerations in Reactive Power Compensation

Shunt reactors are often installed with long cable lengths to compensate for the reactive power generated with these cables.   A compensation rate of close to 100% is preferable as the cable installation does not change the voltage profile of the network.   However it may lead to a severe zero-miss phenomenon.   The effect of the compensation rate is summarized in Table 2-1.

Table 2-1 Effect of Compensation Rate

Analyses	Close to 100%	Away from 100%
Reactive power compensation	Preferable	Generally not preferable (depends on typical operating conditions)
Zero-miss phenomenon	Not preferable (but can be avoided by a special relay)	Preferable
Oscillatory overvoltage	Preferable	Not preferable

Zero-miss phenomenon and associated equipment failure can be avoided by installing the special relay or operational countermeasures.   If it is permissible to adopt thes relays or countermeasures, it is preferable to have a compensation rate close to 100%.

Additionally, the location of shunt reactors must be taken into consideration.   Shunt reactors are connected directly to the cable, to the substation bus, or to the tertiary side of a transformer. The advantages and disadvantages of these options are described in Table 2-2.

Table 2-2 Installed Location of Shunt Reactors

Connection	Advantage	Disadvantage
Directly connected to the cable	- Can limit the overvoltage when one side of the cable is opened	- Cannot be used for voltage control when the cable is not-in-service (some exceptions exist.)
Substation bus or tertiary side of a transformer	- Can be shared by multiple cable routes - Cheaper (tertiary side)	- May cause reactive power imbalance during switching operations

For extended cable systems such as the 400 kV Woodland – Kingscourt – Turleenan line, shunt reactors should be directly connected to the cables to control overvoltage when one side of the cable is opened.

2.2 Maximum Unit Size of 400 kV Shunt Reactors

In Part 1, the 400 kV Kilkenny – Cahir – Aghada line was selected to be the focus of the study except for the series resonance overvoltage analysis. The Kilkenny – Cahir – Aghada line was considered to have the most critical conditions due to the long length of the line and small fault current level around the line. For the series resonance analysis, the 400 kV Woodland – Kingscourt – Turleenan line was selected to be the focus of the study since it was necessary to have a large amount of cables on the secondary side in order to have low series resonance frequency.

In this chapter in Part 1, the reactive power compensation of the 400 kV Kilkenny – Cahir – Aghada line was studied. The reactive power compensation analysis of the 400 kV Woodland – Kingscourt – Turleenan line is described in Chapter 1 of the Part 2 report.

First, the maximum unit size of 400 kV shunt reactors have been determined from a voltage variation when one unit of these shunt reactors was switched. The following voltage variation is allowed in the operation of the all-island transmission system.

> Under normal operating conditions: 3 %   (11.4 kV)
>
> Under contingencies: 10 %   (38.0 kV)

Note that the power flow data provided from the NIE/EirGrid uses a nominal voltage of 380 kV. In this report, however, all the values are calculated based on the nominal voltage 400 kV (equivalent to 1 pu).

The voltage variation increases under lower load conditions. Power flow data during summer off-peak demand was selected to allow the analysis of this voltage variation. Shunt reactors of different sizes were switched on and off at the Kilkenny 400 kV bus. Fig. 2-1 shows the voltage variation at the buses near Kilkenny 400 kV.
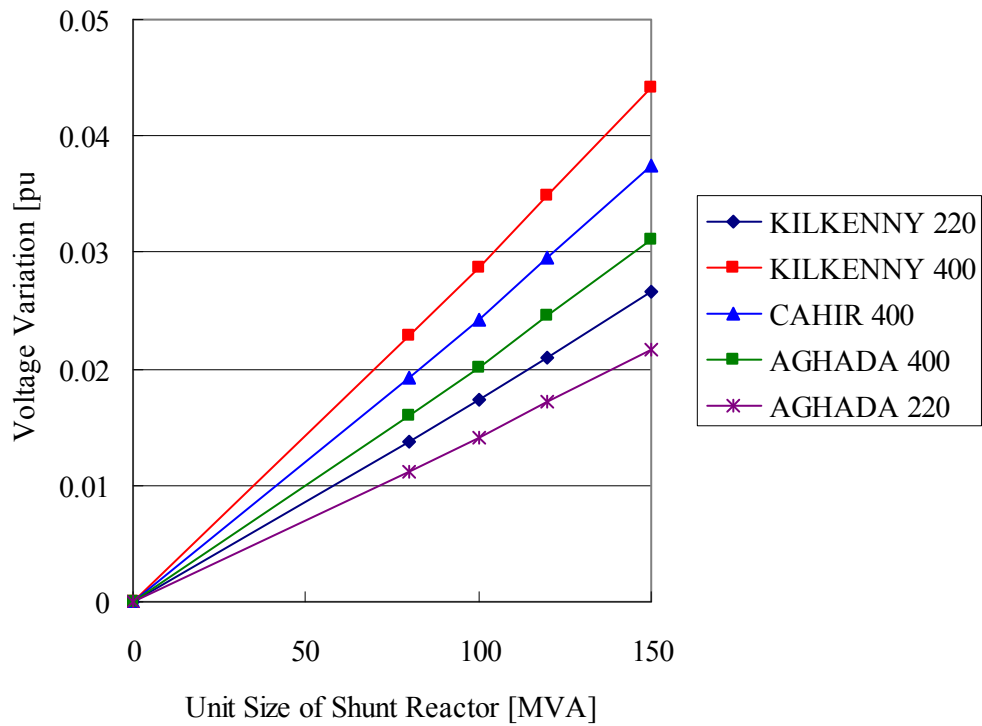
Fig. 2-1 Voltage variation with shunt reactor switchings at the Kilkenny 400 kV bus.

From Fig. 2-1, it can be seen that the maximum unit size which can be installed to the Kilkenny 400 kV bus is 100 MVA.   The same limitation can be applied when the shunt reactor is directly connected to the cable near the Kilkenny 400 kV bus.

The same analysis was performed with shunt reactors connected to the Cahir 400 kV bus. The result of the analysis is shown in Fig. 2-2.
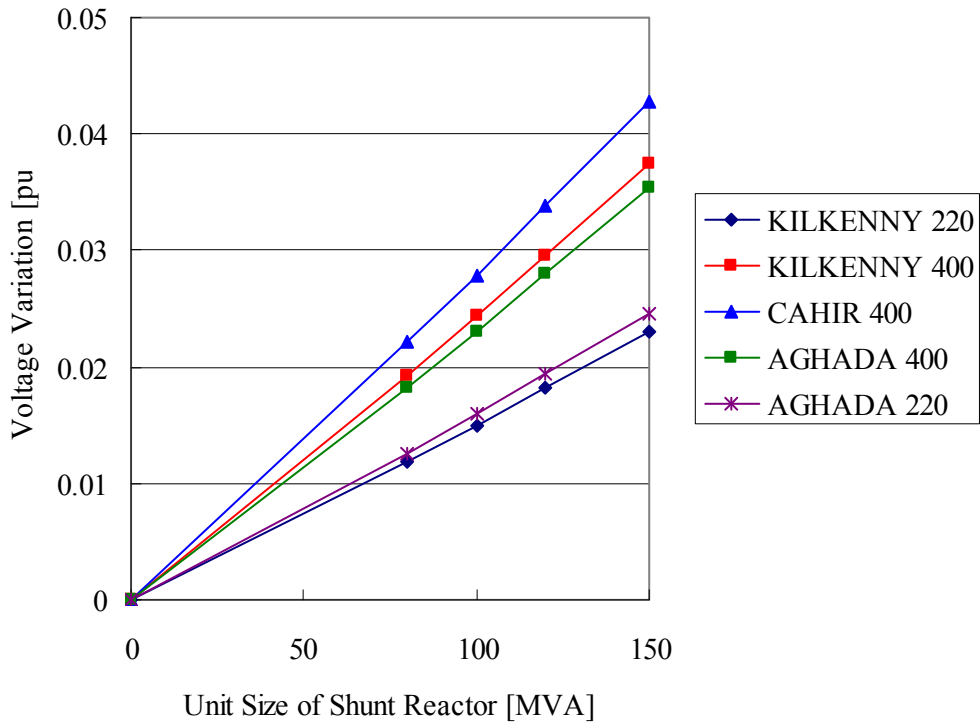
Fig. 2-2 Voltage variation with shunt reactor switchings at the Cahir 400 kV bus.

It can be seen that the maximum unit size which can be installed to the Cahir 400 kV bus is 100 MVA. The same limitation can be applied when the shunt reactor is directly connected to the cable near the Cahir 400 kV bus.
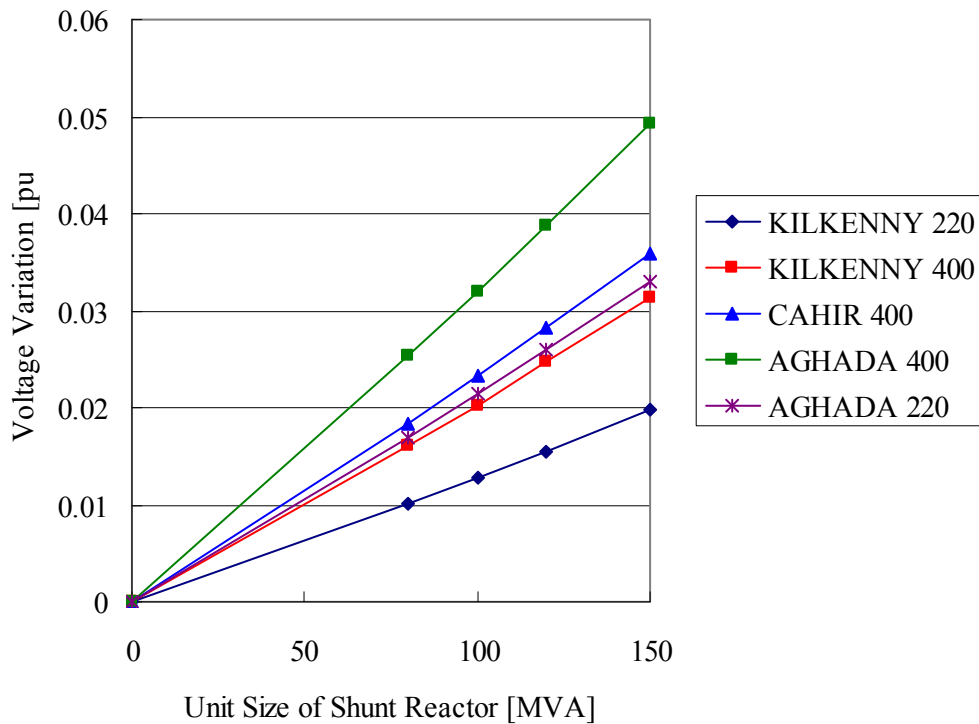
Fig. 2-3 Voltage variation with shunt reactor switchings at the Aghada 400 kV bus.

Fig. 2-3 shows the result of the same analysis for the Aghada 400 kV bus. The 400 kV bus voltage of Aghada is less stable than that of Cahir. It can be seen that the maximum unit size which can be installed to the Cahir 400 kV bus is 80 MVA. The same limitation can be applied when the shunt reactor is directly connected to the cable near the Aghada 400 kV bus.
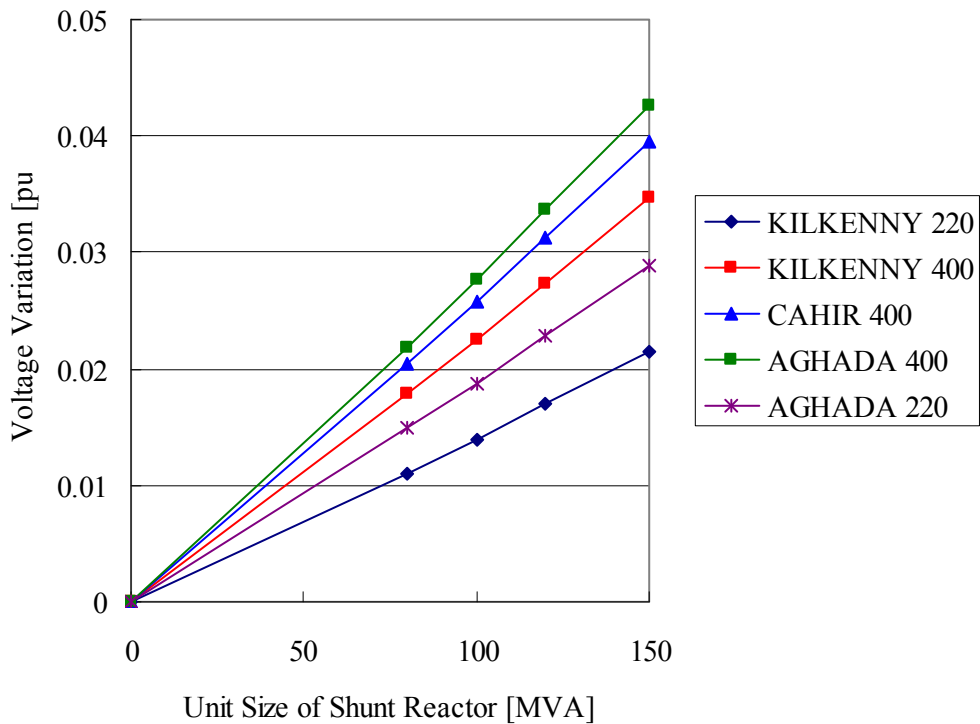
Fig. 2-4 Voltage variation with shunt reactor switchings at the shunt station.

Fig. 2-4 shows the voltage variation when a 400 kV shunt reactor is switched on/off at a shunt reactor station located at the center of the 400 kV Cahir – Aghada line. It can be seen that the maximum unit size which can be installed at the shunt reactor station is 100 MVA.

2.3 Proposed Compensation Patterns

Charging capacity of the Kilkenny – Cahir – Aghada line is:

Kilkenny – Cahir: 723.3 MVA @ 400 kV

Cahir – Aghada: 1350.2 MVA @ 400 kV

Based on the maximum unit size found in the previous section, the following reactive power compensation patterns were proposed:

Table 2-3 Proposed Compensation Patterns

For the 400 kV Kilkenny – Cahir cable:

Locations	Case A
Kilkenny Cahir	100 MVA × 4 80 MVA × 4
Compensation Rate [%]	99.5

For the 400 kV Cahir – Aghada cable:

Locations	Case B1	Case B2	Case B3
Cahir Station Aghada	100 MVA × 4 80 MVA × 8 80 MVA × 4	100 MVA × 4 80 MVA × 7 80 MVA × 5	80 MVA × 4 80 MVA × 8 80 MVA × 5
Compensation Rate [%]	100.7	100.7	100.7

Case B1,B2 and B3 consider the shunt reactor station at the center of the Cahir – Aghada line.

2.4 Voltage Profile under Normal Operating Conditions

From the reactive power compensation analysis, a simple power flow data for the Kilkenny – Cahir – Aghada line was constructed. In this simple model, both the Kilkenny – Cahir line and the Cahir – Aghada line were divided into six sections of equal length, in order to observe the voltage profile along the line and to model shunt reactor stations.

The following conditions were assumed in the power flow data:

- The 400 kV bus voltages of Kilkenny and Aghada are maintained below 410 kV. As the most severe condition, these bus voltages are fixed to 410 kV.

The power flow model created for the reactive power compensation analysis is shown in Fig. 2-5.
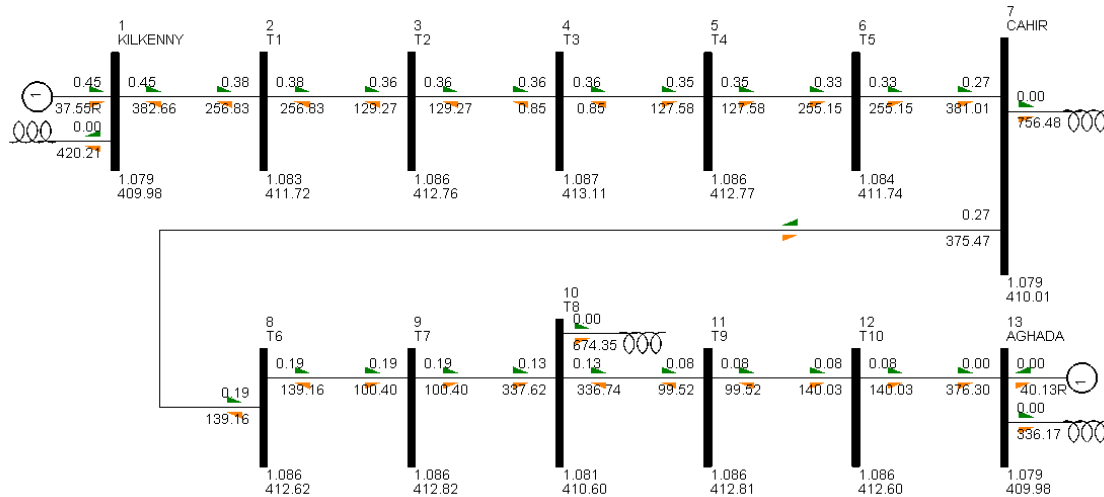
Fig. 2-5 Power flow model for the reactive power compensation analysis.

Using this power flow model, the voltage profile along the line was initially considered with all the equipment in service. The analysis was performed under no load conditions.

The results of the analysis are shown in Fig. 2-6. The voltage rise at the center of the line peaks at 4 kV. Considering the highest voltage (420 kV) of equipment, all compensation patterns have a satisfactory voltage profile.
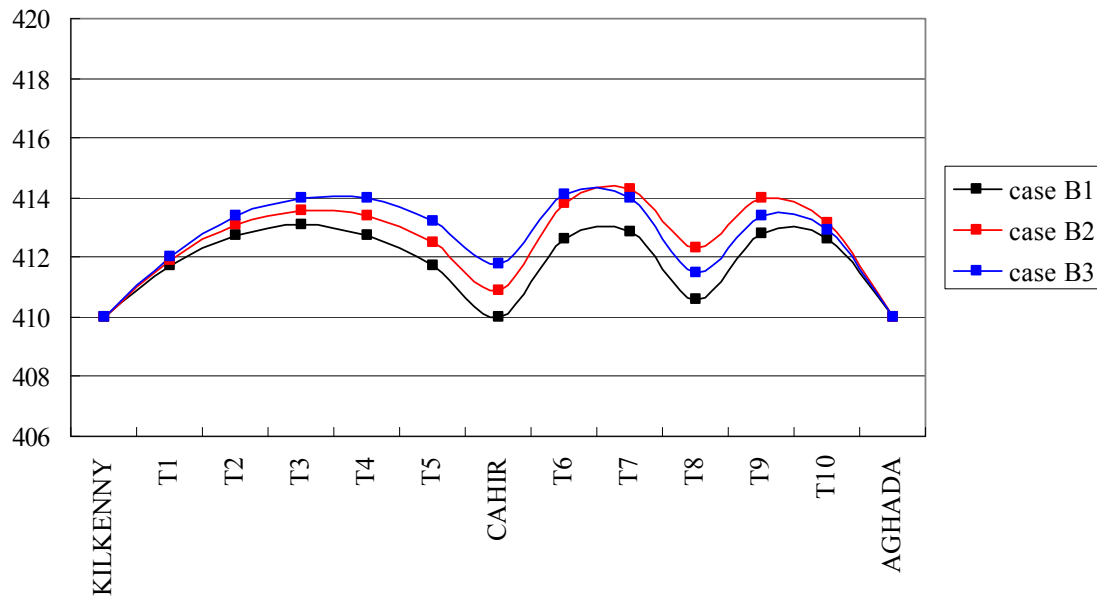
Fig. 2-6 Voltage profile in the normal operating condition (no load).

2.5 Ferranti Phenomenon

When one end of the line is opened due to a switching operation or a bus fault, the voltage at the open terminal may rise due to charging current.   Although equipment failure caused by this overvoltage can be prevented by opening the other end of the line, this overvoltage can be overlooked since the voltage at the open terminal is not monitored.   From a planning standpoint, it is recommended to maintain the voltage at the open terminal below 420 kV in order to relieve operational concerns.

2.5.1 Shunt Reactors Connected to the Line

First, the voltage profile when all shunt reactors were directly connected to the line was studied.   When connected to the line, shunt reactors can be used to suppress the open terminal voltage.

Fig. 2-7 shows the voltage profile when the Aghada terminal is opened.   The different compensation patterns Case B1 – B3 were studied for the Cahir – Aghada line.   The compensation pattern of the Cahir – Aghada line was fixed to Case B3, and the Kilkenny 400 kV bus voltage was fixed at 410 kV.   It appears that all compensation patterns have a satisfactory voltage profile.
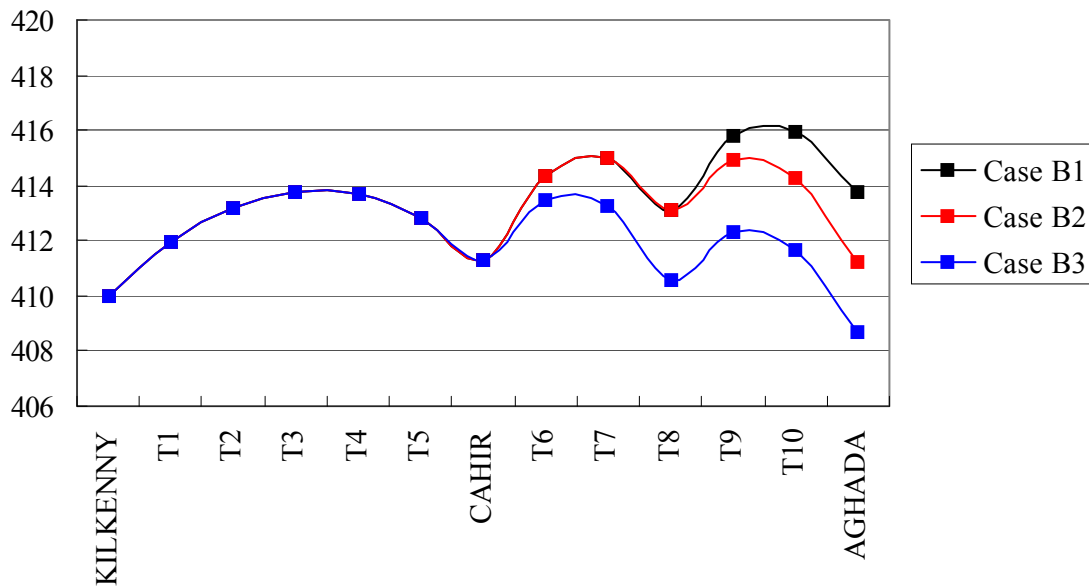
Fig. 2-7 Voltage profile when the Aghada terminal is opened.

Fig. 2-8 shows the voltage profile when the Kilkenny terminal is opened. The different compensation patterns Case B1 – B3 were studied for the Cahir – Aghada line. The Aghada 400 kV bus voltage was fixed at 410 kV. It can be seen that all compensation patterns have a satisfactory voltage profile.
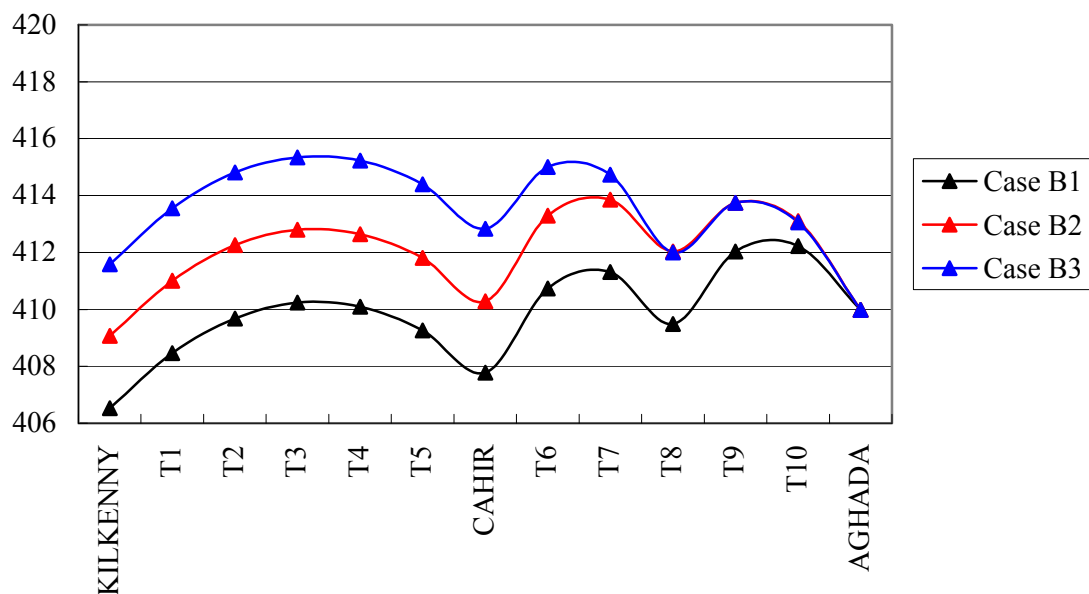
Fig. 2-8 Voltage profile when the Kilkenny terminal is opened.

2.5.2   Shunt Reactors Connected to the Bus

Shunt reactors connected to the bus is often preferred, compared to those connected to the line, because of increased flexibility for wider use as voltage and reactive power control equipment. When considering the Ferranti phenomenon, bus-connected shunt reactors present more severe conditions as they can not be used to suppress open terminal voltage.

When shunt reactors are connected to the line, they will suppress the open terminal voltage as long as they are available.   When line-connected shunt reactors are not available, for example due to maintenance outage, the condition becomes similar to bus-connected shunt reactors.

Fig. 2-9 shows the voltage profile when the Aghada terminal is opened.   All conditions are identical to those in Section 2.5.1, but 1 unit of the shunt reactors at the Aghada open terminal has been disconnected.   It can be seen from the figure that Case B3 has a satisfactory voltage profile. In Cases B1 and B2, the voltage along the Cahir – Aghada line exceeds 420 kV, but the voltage rise from Cahir is within 10 kV.   If the Cahir 400 kV bus voltage is maintained below 410 kV, the open terminal voltage will be maintained below 420 kV.
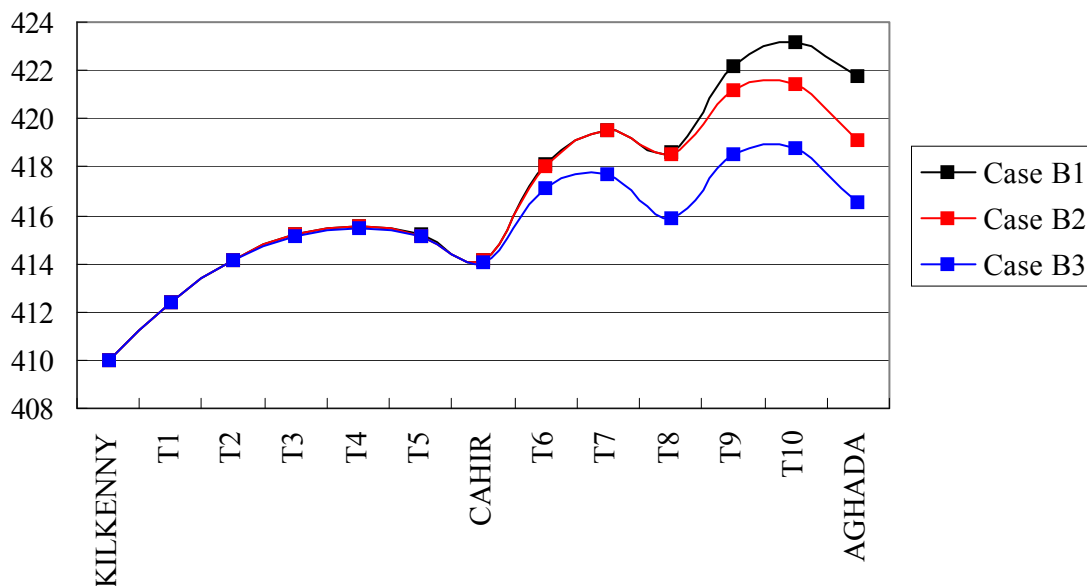
Fig. 2-9 Voltage profile when the Aghada terminal is opened without one unit of shunt reactors.

Fig. 2-10 shows the voltage profile when the Kilkenny terminal is opened.   All conditions are identical to those in Section 2.5.1, but one unit of shunt reactors at the Kilkenny open terminal has been disconnected.   It can be seen from the figure that Case B1 has a satisfactory voltage profile. In Cases B2 and B3, the voltage along the Kilkenny – Cahir line exceeds 420 kV, but the voltage rise from Cahir is within 10 kV.   If the Cahir 400 kV bus voltage is maintained below 410 kV, the open terminal voltage will be maintained below 420 kV.
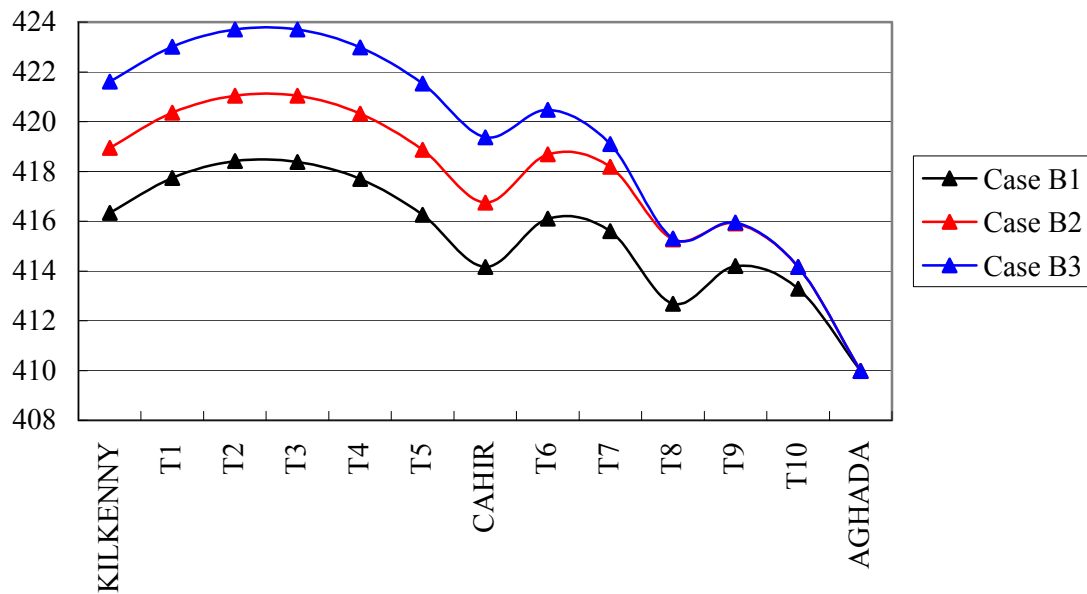
Fig. 2-10 Voltage profile when the Kilkenny terminal is opened without one unit of shunt reactors.

2.6 Conclusion

As a result of the reactive power compensation analysis, compensation patterns A and B2 were selected for further analysis.

Locations	Case A
Kilkenny Cahir	100 MVA × 4 80 MVA × 4
Compensation Rate [%]	99.5

For the 400 kV Cahir – Aghada cable, Cases B1-B3 have a satisfactory voltage profile when all shunt reactors are connected to the line. When one unit of shunt reactors at the open terminal are disconnected, the open terminal voltage exceeds 420 kV in all compensation patterns, but the voltage rise from Cahir is within 10 kV.   If the Cahir 400 kV bus voltage is maintained below 410 kV, the open terminal voltage will be maintained below 420 kV.

Case B2 is selected because of its more preferable voltage profile when one unit of shunt reactors at the open terminal has been disconnected.

Locations	Case B1	Case B2	Case B3
Cahir Station Aghada	100 MVA × 4 80 MVA × 8 80 MVA × 4	100 MVA × 4 80 MVA × 7 80 MVA × 5	80 MVA × 4 80 MVA × 8 80 MVA × 5
Compensation Rate [%]	100.7	100.7	100.7

Note: If it is not necessary to switch these shunt reactors for the voltage and reactive power control, it is possible to choose a shunt reactor of larger unit size.   For example in Case B2, it is possible to install two units of 200 MVA shunt reactors in Cahir instead of four units of 100 MVA.   The compensation pattern in Case B2 was selected without the consideration of the requirements for the voltage and reactive power control, since it is not included in the scope of this study and the difference can have only small effects on the simulation results.

When a shunt reactor with large unit size is selected, an outage of this shunt reactor will significantly lower the compensation rate of the cable line, which may prohibit the use of the line during the outage.

Chapter 3 Model Setup

3.1 Modeled Area for This Project

In Part 1, the 400 kV Kilkenny – Cahir – Aghada line was selected to be the focus of the study except for the series resonance overvoltage analysis as mentioned in Chapter 1.   The figure below shows an example of the model created by ATP-Draw.
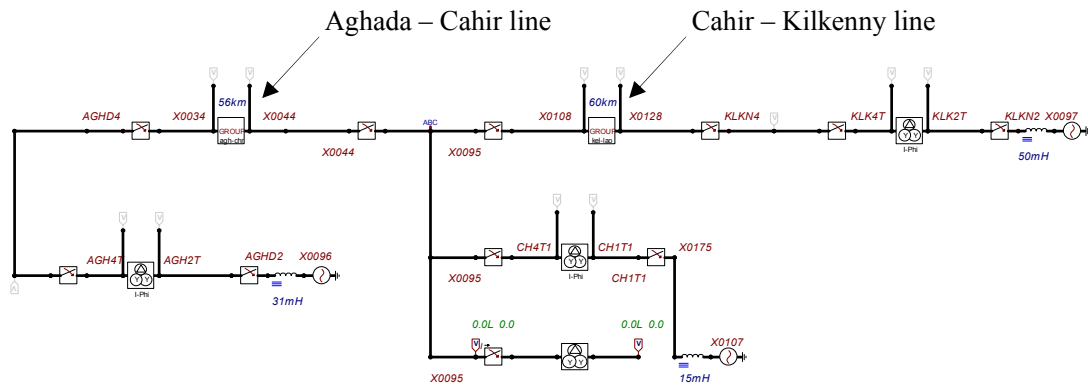
Fig. 3-1 Simulation model for the temporary overvoltage and slow-front overvoltage analysis.

For the series resonance analysis, the 400 kV Woodland – Kingscourt – Turleenan line was selected to be the focus of the study.   Since the Part 2 study focused on the 400 kV Woodland – Kingscourt – Turleenan line, simulation models for the series resonance analysis were introduced in the Part 2 report.

For the series resonance overvoltage analysis, it is necessary to model the 275 kV and 220 kV network.   The 275 kV and 220 kV networks around Woodland, Kingscourt, and Turleenan were included in the model by distributed parameter models, whose input data were derived from PSS/E powerflow data.

3.2 Transformers

Model parameters of the Kingscourt 400/220 kV transformer were provided from NIE/EirGrid. These parameters are shown in Table 3-1.　Aghada and Kilkenny 400/220 kV transformers in the RoI were assumed to have the same parameters as the Kingscourt 400/220 kV transformer.

Model parameters of the Cahir 400/110 kV transformer were derived from PSS/E power flow data.

Table 3-1 Model Parameters of the Kingscourt 400/220 kV Transformer

Transformer	Kingscourt ABB 500MVA		
Voltage rating	HV	LV	TV
kV line-line	400	220	21
MVA Rating	500	500	80
Vector Config	Y auto	Y auto	delta
S/C Impedances	HV-LV	HV-TV	LV - TV
% on 500MVA base	13.46	39.5	18.63
S/C Loss kW	653	218	163
Core loss @ 1.0pu (kW)		250	
Capacitances	pF		
HV-LV	2500		
LV-TV	2200		
HV-Earth	1100		
LV-Earth	400		
TV-Earth	8900		

For leakage inductances in Table 3-1, percent impedances were converted to mH by the following calculations.

$$(x_{\%1\text{-}2},\ x_{\%1\text{-}3},\ x_{\%2\text{-}3}) \rightarrow (x_{\%1},\ x_{\%2},\ x_{\%3})$$

$$x_{\%1} = \frac{x_{\%1-2} + x_{\%1-3} - x_{\%2-3}}{2}$$

$$x_{\%2} = \frac{x_{\%1-2} + x_{2-3} - x_{\%1-3}}{2}$$

$$x_{\%3} = \frac{x_{\%1-3} + x_{\%2-3} - x_{\%1-2}}{2}$$

$$(x_{\%1},\ x_{\%2},\ x_{\%3}) \rightarrow (x_1,\ x_2,\ x_3)$$

$$x_1 = \frac{x_{\%1}}{100} \times \frac{(400\text{kV})^2}{100\text{MVA}} \times \frac{1}{2\pi \times 50} \times 1000 \quad [\text{mH}]$$

$$x_2 = \frac{x_{\%2}}{100} \times \frac{(275 \text{ or } 220\text{kV})^2}{100\text{MVA}} \times \frac{1}{2\pi \times 50} \times 1000 \quad [\text{mH}]$$

$$x_3 = \frac{x_{\%3}}{100} \times \frac{(33 \text{ or } 21\text{kV})^2}{100\text{MVA}} \times \frac{1}{2\pi \times 50} \times 1000 \quad [\text{mH}]$$

Internal resistance and leakage inductance of these transformers were obtained as follows:

Substations	R1 [Ω]	X1 [mH]	R2 [Ω]	X2 [mH]	R3 [Ω]	X3 [mH]
Aghada Kilkenny	0.3719	137.10	0.1793	0.001	0.035430	1.8812
Cahir	0.0001	273.49	0.0581	4.814	0.002481	0.0790

Saturation characteristic of a 400/275/13 kV 750 MVA transformer in National Grid was provided from NIE/EirGrid as shown in Table 3-2. The same saturation characteristic was assumed for the Cahir 400/110 kV transformer.

Table 3-2 Saturation Characteristic of the 400 kV Transformer (defined in tertiary)

I [A]	Phi [Wb-T]
51.63578	2.30940
55.07817	5.35781
58.52055	9.79186
61.96294	21.70836
65.40533	61.43004
68.84771	187.06140
72.29010	424.92960
82.61725	6267.24695

For transformer inrush studies, the magnetizing branch hysteresis curve was derived from the saturation characteristic in Table 3-2 using the subroutine HYSDAT. The lower half of the obtained hysteresis curve is shown in Table 3-3.

Table 3-3 Hysteresis Curve of the 400 kV Transformer (defined in primary)

I [A]	Phi [Wb-T]
-29.4000	-1424.49
-3.6750	-1349.38
2.2050	-1243.19
5.1450	-966.929
9.9225	837.430
15.4350	1105.06
26.4600	1269.09
48.8775	1381.33
117.6000	1467.66
161.7000	1476.29

3.3 Shunt Reactors

3.3.1   400 kV Shunt Reactor

Shunt reactors were connected to both ends of the 400 kV cables or 400 kV buses, in order to compensate charging capacity of the cables.   Only for the Kingscourt – Turleenan line and the Kilkenny – Aghada line, shunt reactors were also connected to the center of the line.   Shunt reactors for the Kilkenny – Cahir – Aghada line were modeled based on the result of the analysis in Chapter 1.   400 kV shunt reactors in the simulation model are shown in Table 3-4.

Table 3-4 400 kV Shunt Reactors in the Simulation Model

From Bus		To Bus		Length [km]	From [MVA]	Centre [MVA]	To [MVA]
3774	KINGSCOURT	5464	WOODLAND	58	120× 2	-	150× 2
3774	KINGSCOURT	5464	WOODLAND	58	120× 2	-	150× 2
3774	KINGSCOURT	90140	TURL	82	100× 2	120× 3	100× 2
3774	KINGSCOURT	90140	TURL	82	100× 2	120× 3	100× 2
1044	AGHADA	1724	CAHIR	112	80× 5	80× 7	100× 4
1124	ARKLOW	2744	GREAT_ISL	60	180× 2	-	180× 2
1724	CAHIR	3264	KILKENNY	60	80× 4	-	100× 4
2524	FLAGFORD	3774	CAVAN	60	180× 2	-	180× 2
3344	KELLIS	3554	LAOIS	60	180× 2	-	180× 2
2204	DUNSTOWN	3854	MAYNOOTH	30.55	180× 1	-	180× 1
3854	MAYNOOTH	5464	WOODLAND	22.5	150× 1	-	150× 1

When 400 kV shunt reactors are close to *the point of interest*, they are modeled with the saturation characteristic.   Otherwise, they are modeled as linear inductances.

3.3.2   275 kV Shunt Reactor

Shunt reactors were connected to both ends of 275 kV cables in order to compensate charging capacity of the cables.   Shunt reactors connected to the 275 kV cables in the simulation model are shown in Table 3-5.

Table 3-5 Shunt Reactors Connected to Both Ends of 275 kV Cables in the Simulation Model

From Bus		To Bus		Length[km]	From [MVA]	To [MVA]
87520	OMAH	90120	TURL	42	100	100
87520	OMAH	90120	TURL	42	100	100
87520	OMAH	90120	TURL	42	100	100
87520	OMAH	90120	TURL	42	100	100
87520	OMAH	89520	STRABANE	60	160	160
87520	OMAH	89520	STRABANE	60	160	160
75520	COOLKEER	89520	STRABANE	25	60	60
75520	COOLKEER	89520	STRABANE	25	60	60

Shunt reactors were connected to 275 kV buses in order to compensate charging capacity of the short 110 kV cables.   Shunt reactors connected to 275 kV buses in the simulation model are shown in Table 3-6.

Table 3-6 Shunt Reactors connected to 275 kV buses in the Simulation Model

kV	Bus number	Bus name	Shunt reactor [MVA]	
			Winter_peak_ wind_maximum	Summer_ off_peak
	75520	COOLKEER	100	100
275	87520	OMAH	100	100
	89520	STRABANE	100	100

3.3.3   220 kV Shunt Reactor

Shunt reactors were connected to both ends of long 220 kV cables in order to compensate charging capacity of the cables.   Shunt reactors connected to the 220 kV cables in the simulation model are shown in Table 3-7.

Table 3-7 Shunt Reactors Connected to Both Ends of 220 kV Cables in the Simulation Model

From Bus		To Bus		Length [km]	From [MVA]	To [MVA]
1402	BELLACOR	2522	FLAGFORD	123	160	160
1642	CASHLA	4522	PROSPECT	90	120	120
4942	SHANNONB	5492	WMD_220	70	100	100
2522	FLAGFORD	3772	CAVAN	90	120	120

Shunt reactors were connected to 220 kV buses in order to compensate charging capacity of the 110 kV and short 220 kV cables.   Shunt reactors were connected to the 220 kV buses in order to meet the following conditions:

- Voltage profile of the 220 kV network in the modified data is nearly equal to that of the original data.

- Unit size of shunt reactor is greater than 100 MVA.

Shunt reactors connected to 220 kV buses in the simulation model are shown in Table 3-8.

Table 3-8 Shunt Reactors Connected to 220 kV Buses in the Simulation Model

KV	Bus number	Bus name	Shunt reactor [MVA]	
			Winter peak wind_maximum	Summer off_peak
220	1122	ARKLOW	250	250
	1432	BALLYRAGGET	100	100
	1602	CLASHAVO	100	100
	1642	CASHLA	-	150
	2002	CULLENAG	100	100
	2032	CHARLESLAND	100	100
	2042	CORDUFF	100	100
	2202	DUNSTOWN	100	100
	2522	FLAGFORD	100	100
	2742	GREAT IS	-	100
	2842	GORMAN	-	200
	3202	KNOCKRAH	-	100
	3282	KILLONAN	100	100
	3342	KELLIS	100	100
	3522	LOUTH	200	200
	3552	LAOIS	100	100
	3642	LODGEWOO	150	150
	4942	SHANNONB	100	100
	4952	KINNEGAD-220	100	200
	5042	SRANANAG	-	100
	5142	TARBERT	100	100
	5462	WOODLAND	-	100
	9992	NEW_TRIEN	100	100

Note: Other sections of this capter have been removed from this public report.

Chapter 4 Temporary Overvoltage Analysis

For long EHV cables, temporary overvoltages are of highest concerns in terms of the safe operation after the installation. Highest temporary overvoltages are often higher than highest slow-front overvoltages.

Due to the large capacitance associated with the long EHV cable and the inductance of shunt reactors for the reactive power compensation, the following temporary overvoltages require a close attention for the network with long EHV cables. The theoretical backgrounds relating the large capacitance and the inductance to these temporary overvoltages are given in the beginning of each section:

(1) Series resonance overvoltage

(2) Parallel resonance overvoltage

(3) Oscillatory overvoltage caused by the system islanding

For equipment whose highest voltage is lower than or equal to 245 kV, the standard short-duration power-frequency withstand voltage is specified in IEC 71-1. The series resonance overvoltage analysis in the Woodland and Kingston 220 kV network evaluates the overvoltage level against the standard short-duration power-frequency withstand voltage.

For equipment whose highest voltage is higher than 245 kV, the standard short-duration power-frequency withstand voltage is not specified in IEC, but it is specified by a utility or a manufacturer. Surge arresters are generally the weakest among different equipment. The temporary overvoltages have to be evaluated against typical withstand voltage and energy absorption capability of surge arresters. Note that the temporary overvoltages may be evaluated with SIWV depending on their decay time.

4.1 Series Resonance Overvoltage

For the series resonance overvoltage analysis, it is necessary to model its 275/220 kV network. The 275/220 kV networks of target substations were included in the model by distributed parameter models, whose input data were derived from PSS/E powerflow data.

Series resonance caused by the energisation of each route from both directions was studied. The switching scenarios are shown below.   Before the time domain analysis, frequency scan was performed for the energised line as well as the combination of 400/275/220 kV transformers and the 275/220 kV network.   The frequency of the overvoltage caused by the energisation and the resonance frequency of the 275/220 kV network can be found from the result of frequency scan, and it is possible to assess the chance of having series resonance.   After the frequency scan, the series resonance overvoltage analysis was conducted under the following two conditions with time-domain simulation:

(1) Normal condition where all 400/275/220 kV transformers and 275/220 kV lines in Woodland, Kingscourt, and Turleenan are in service

(2) Assumed most severe condition where the frequency of the overvoltage is closest to the resonance frequency of the 275/220 kV network
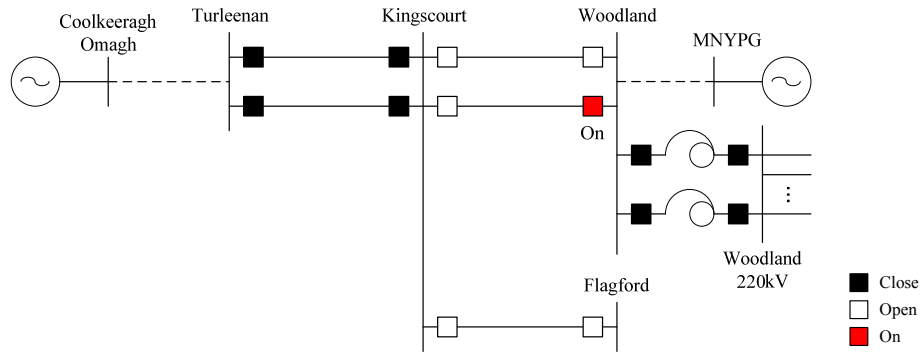
Woodland 220 kV system
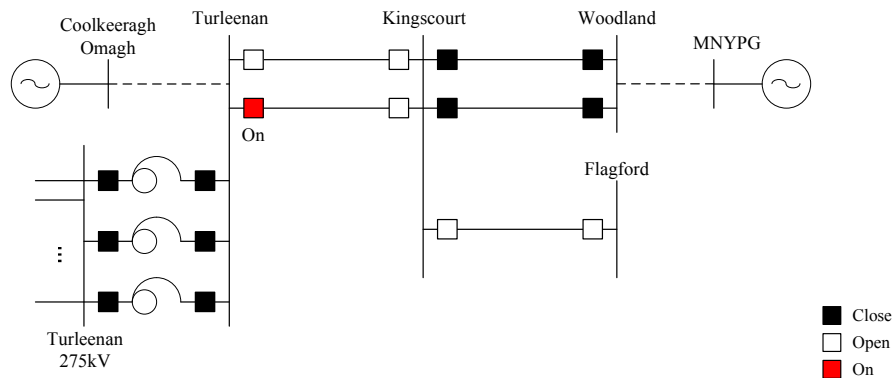
Turleenan 275 kV
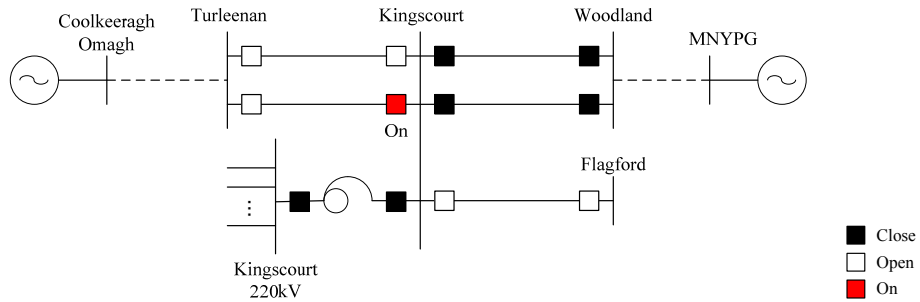
Kingscourt 220 kV system (Closing of Turleenan side)
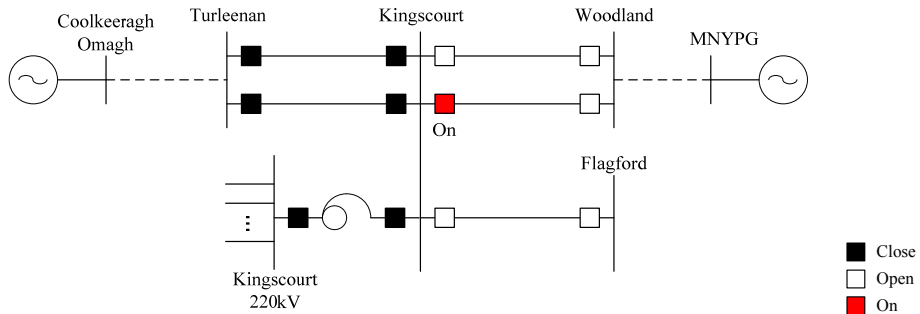
Kingscourt 220 kV system (Closing of Woodland side)

Fig. 4-1 Switching scenarios for the series resonance overvoltage analysis.

Frequency scans of the system were performed to obtain the characteristics of the system in the configurations shown in Fig. 4-1.   The current source of 1 A from 10 Hz to 2000 Hz was injected into the system.

Fig. 4-2 shows an example of a frequency scan model.   In order to study the series resonance overvoltage in the Woodland 220 kV network, 1 A current was injected from the Woodland 400 kV bus.
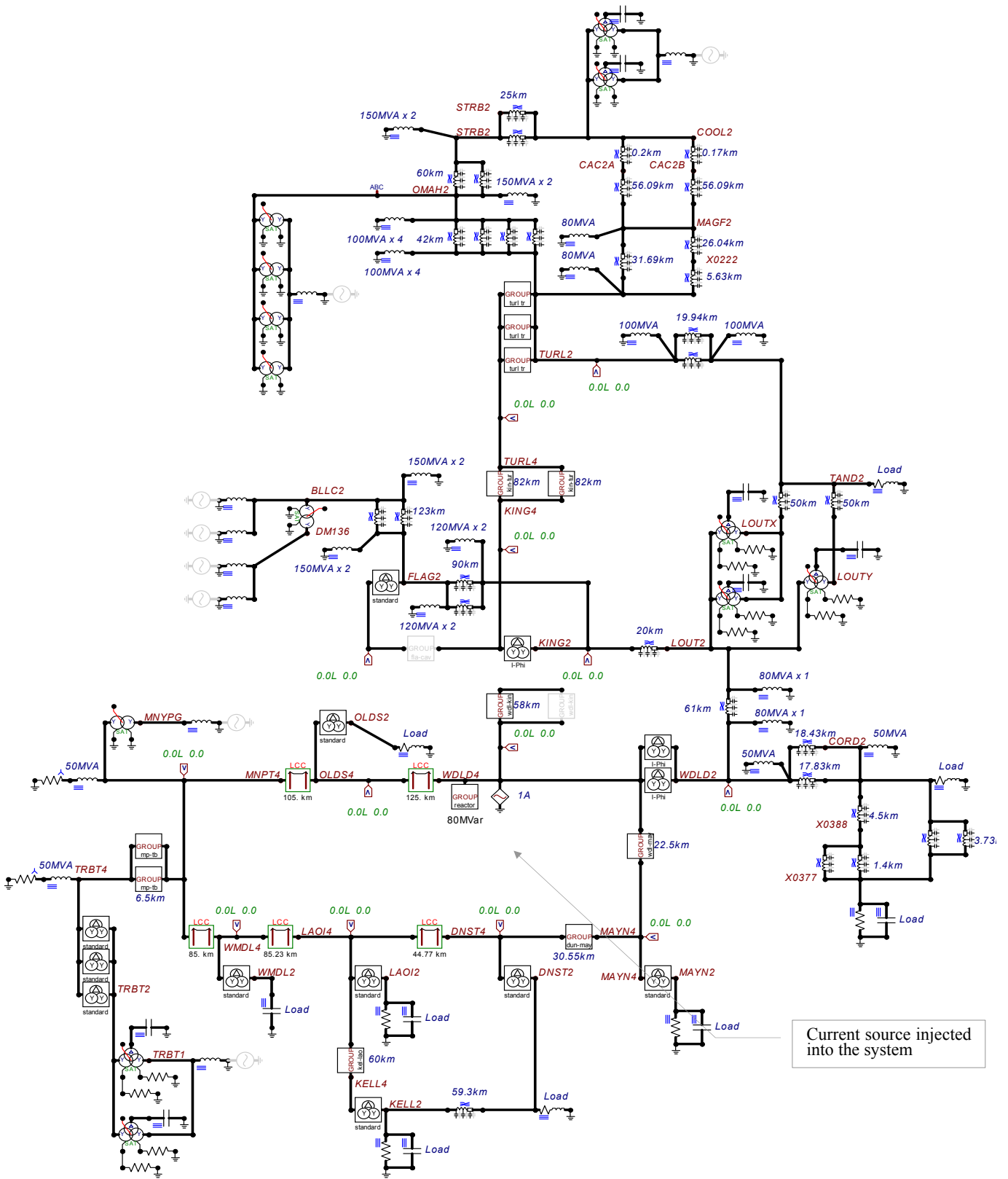
Fig. 4-2 Example of an ATP Draw model for frequency scan of the system.

4.1.1 Resonance overvoltage in the Woodland 220 kV system

(1) Normal condition

[Frequency scan]

The following figure shows the system configuration for the series resonance overvoltage analysis in the Woodland 220 kV system caused by the energisation of the 400 kV Woodland – Kingscourt line from the Woodland S/S. The target frequency applied to the cable model (Bergeron model) was decided from its length, which is from Dunstown S/S to Kingscourt S/S. Since the total length is about 111 km (58 + 22.5 + 30.55), the target frequency is

$$f = \frac{1}{4}\frac{1.7 \times 10^8\,\text{m/s}}{(58000 + 22500 + 30550)\,\text{m}} \approx 380\,\text{Hz}$$
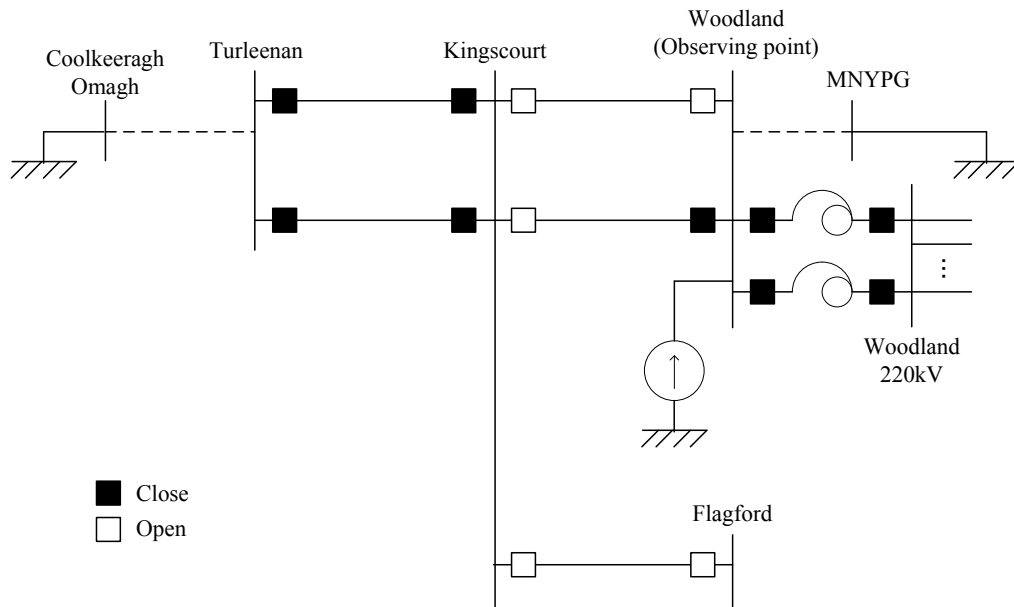
Fig. 4-3 System configuration for the series resonance overvoltage analysis in the Woodland 220 kV system.

Fig. 4-4 shows the result of frequency scan.   The vertical axis of the figure shows voltages observed at the Woodland 400 kV, which is equal to the equivalent impedance of the network seen from the Woodland 400 kV bus because the injected current is 1 Amp.
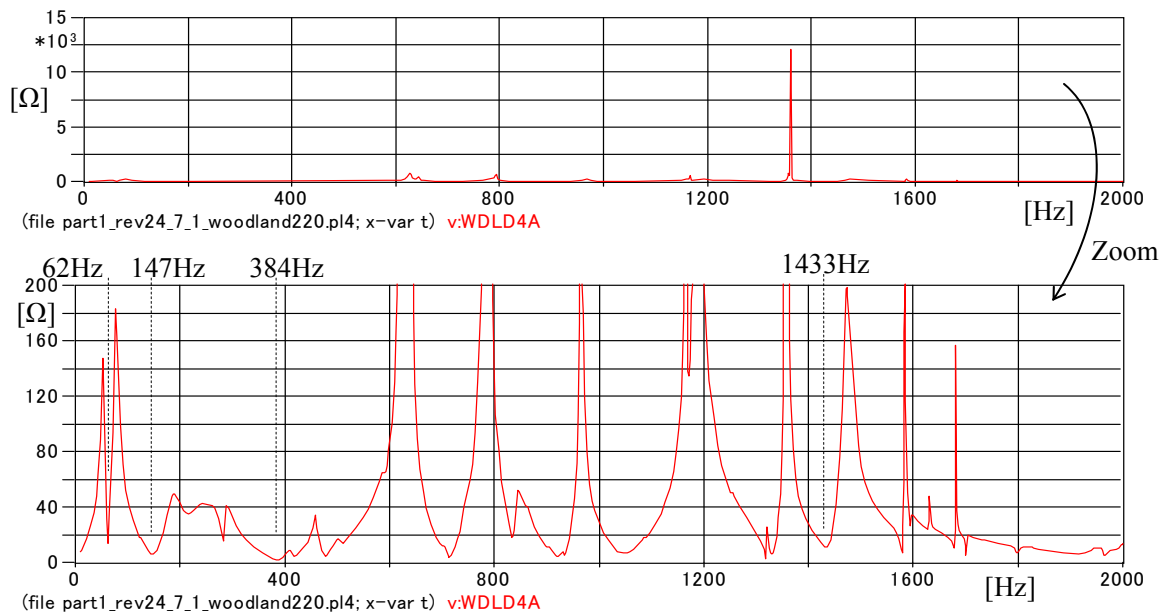
Fig. 4-4 Frequency scan at the Woodland 400 kV bus.

It can be seen from Fig. 4-4 that the series resonance overvoltage might occur since one of series resonance frequencies found in Fig. 4-4 (384 Hz) is close to target frequency of the 400 kV cable (380Hz).

At the same time, the voltage of the Woodland 220 kV bus can also be observed under the same frequency scan conditions. Fig. 4-5 shows the result of frequency scan at Woodland 220 kV bus and 400 kV bus.
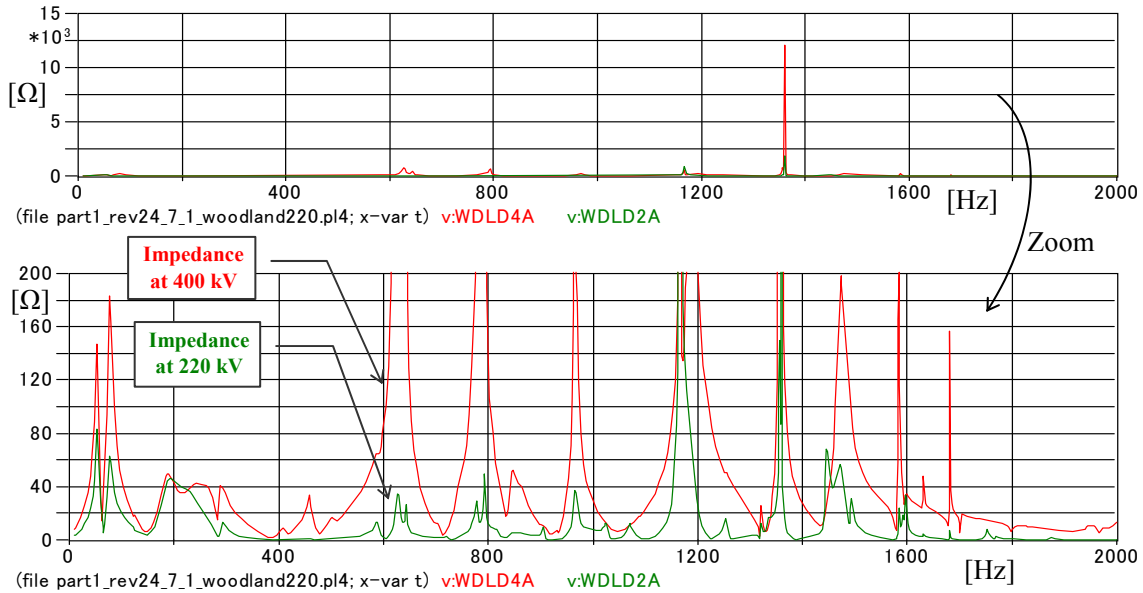
Fig. 4-5 Frequency scan at the Woodland 400 kV bus and 220 kV bus.

From the result shown above, the ratio of the 220 kV bus voltage to the 400 kV bus voltage, which is called the amplification ratio, can be derived as shown in Fig. 4-6.
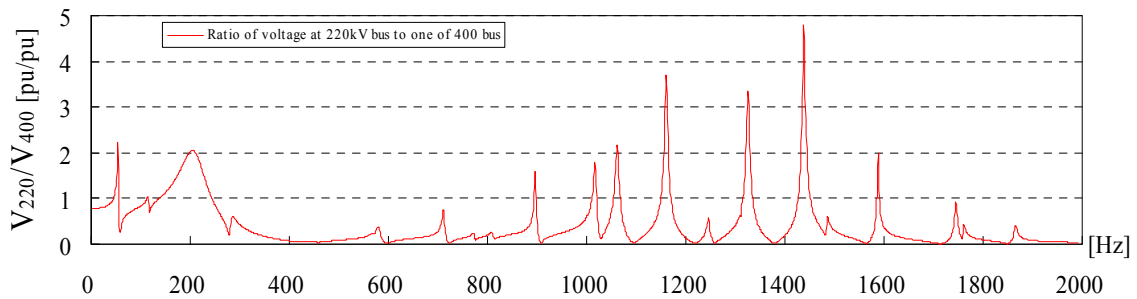
Fig. 4-6 Amplification ratio at Woodland.

At series resonance frequencies, impedance in Fig. 4-4 is close to zero and the amplification ratio in Fig. 4-6 is large. Since the amplification ratio at 380 Hz is not so large in Fig. 4-6, the series resonance overvoltage does not seem to occur at 380 Hz under this condition.

[Time domain simulation for the normal condition]

Time domain simulation was conducted for the normal operating condition. Fig. 4-7 and Fig. 4-8 show voltage waveforms when the Woodland – Kingscourt line is energised from the Woodland side as shown in Fig. 4-3. It did not cause high overvoltage due to series resonance, because the amplification ratio of the 220 kV bus voltage to the 400 kV bus voltage is very small as shown in Fig. 4-6.

(Phase to earth)
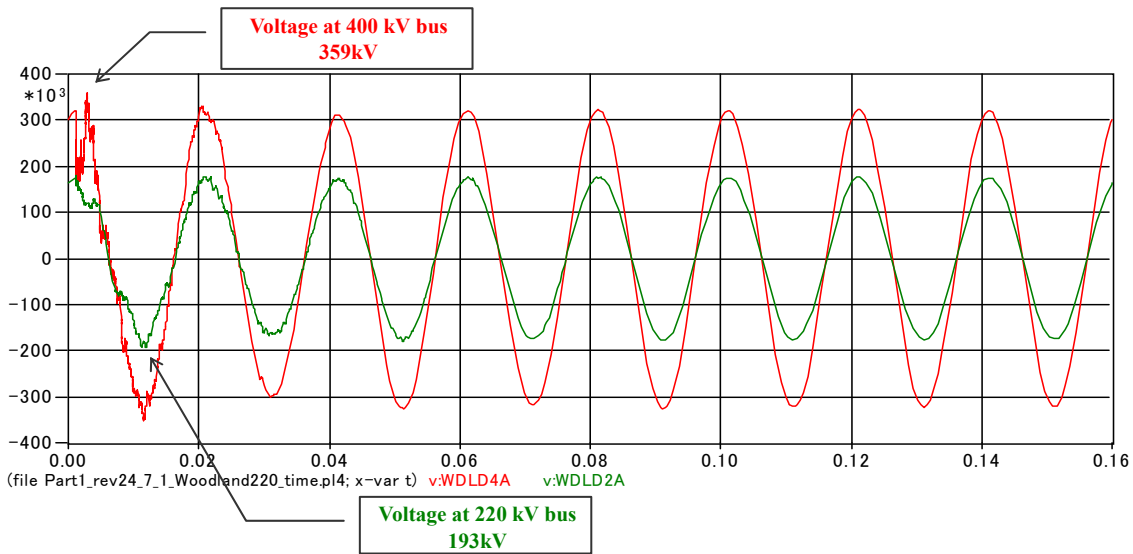
Fig. 4-7 Waveforms of the switching overvoltage at Woodland 400 kV and 220 kV buses (phase to earth).
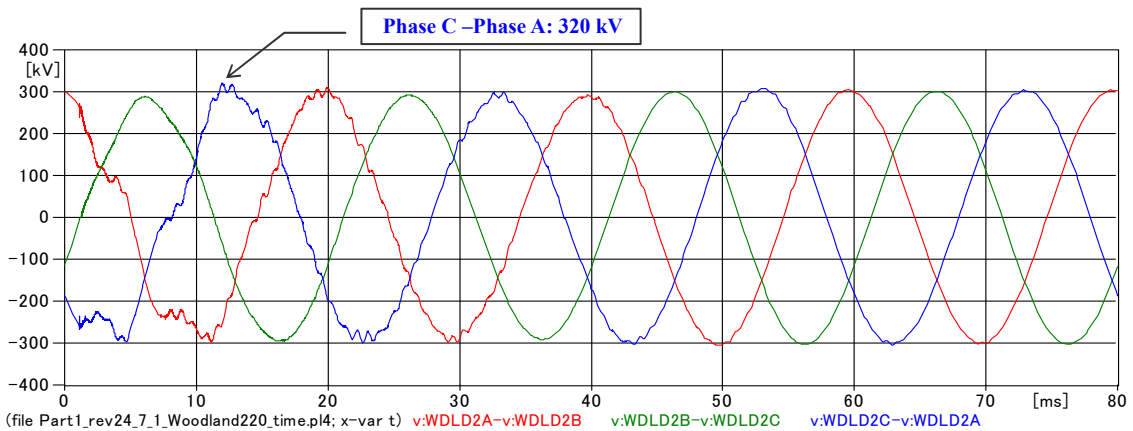
(Phase to Phase)

Fig. 4-8 Waveforms of the switching overvoltage at the Woodland 220 kV bus (phase to phase).

Fig. 4-9 and Fig. 4-10 respectively show frequency component spectrums derived from the voltage waveforms at Woodland 400 kV and 220 kV buses. The frequency components in the figures were calculated for one cycle immediately after line energisation. Comparing Fig. 4-9 to Fig. 4-10, the amplification ratio around 200Hz is relatively large, but in a higher frequency range, the amplification ratio is small.

MC's PlotXY – Fourier chart(s). Copying date: 2009/02/27
File Part1_rev24_7_1_Woodland220_time.pl4 Variable v:WDLD4A [|pu of harm. 1|]
Initial Time: 1.200E–03 Final Time: 0.0212
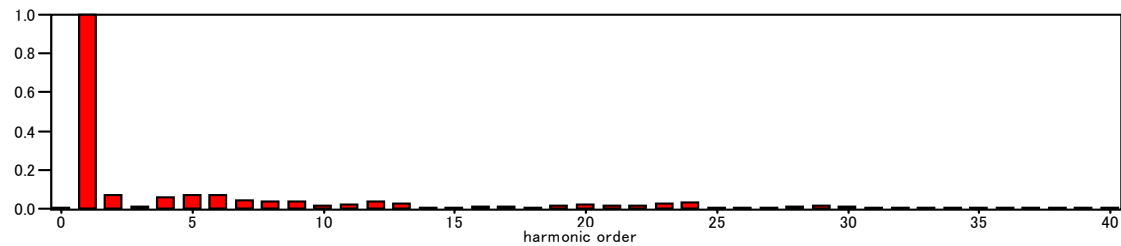
Fig. 4-9 Frequency component spectrum of the voltage waveform at the Woodland 400 kV bus.

MC's PlotXY – Fourier chart(s). Copying date: 2009/02/27
File Part1_rev24_7_1_Woodland220_time.pl4 Variable v:WDLD2A [|pu of harm. 1|]
Initial Time: 1.200E–03 Final Time: 0.0212
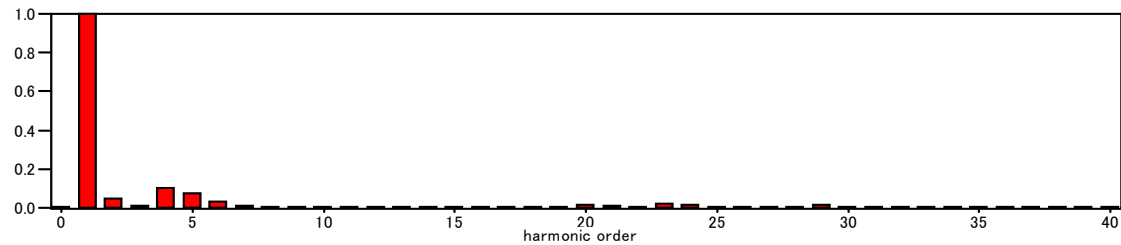
Fig. 4-10 Frequency component spectrum of the voltage waveform at the Woodland 220 kV bus.

(2) Assumed most severe condition:

(2) –1 Series resonance frequency 200 Hz

[Frequency scan]

From Fig. 4-5 and Fig. 4-6, it can be seen that the Woodland 220 kV system is under the series resonance condition at around 200 Hz. The assumed most severe condition can be caused when the overvoltage caused by the energisation of the 400 kV Woodland – Kingscourt line contains a large 200 Hz component.

The overvoltage caused by the line energisation generally contains frequency components that are determined by parallel resonance frequencies and propagation time (τ) in addition to 50 Hz. It is possible to adjust $1/4\tau$ to series resonance frequency, but it is not possible to match one of parallel resonance frequencies to series resonance frequency. Hence, in order to generate a 200 Hz component by line energisation, it is necessary to adjust the length of the 400 kV Woodland – Kingscourt line to satisfy the equation $1/4\tau = 200$ Hz.

In order to satisfy the equation, the total length of the 400 kV Dunstown – Maynooth – Woodland – Kingscourt cable line must be equal to

$$\frac{1}{4}\frac{1.7\times 10^{8}\,\text{m/s}}{200\,\text{Hz}} \approx 212500\text{ m}$$

The system configuration for the calculation is shown in Fig. 4-11. Target frequency of the cable models was set to 200 Hz.
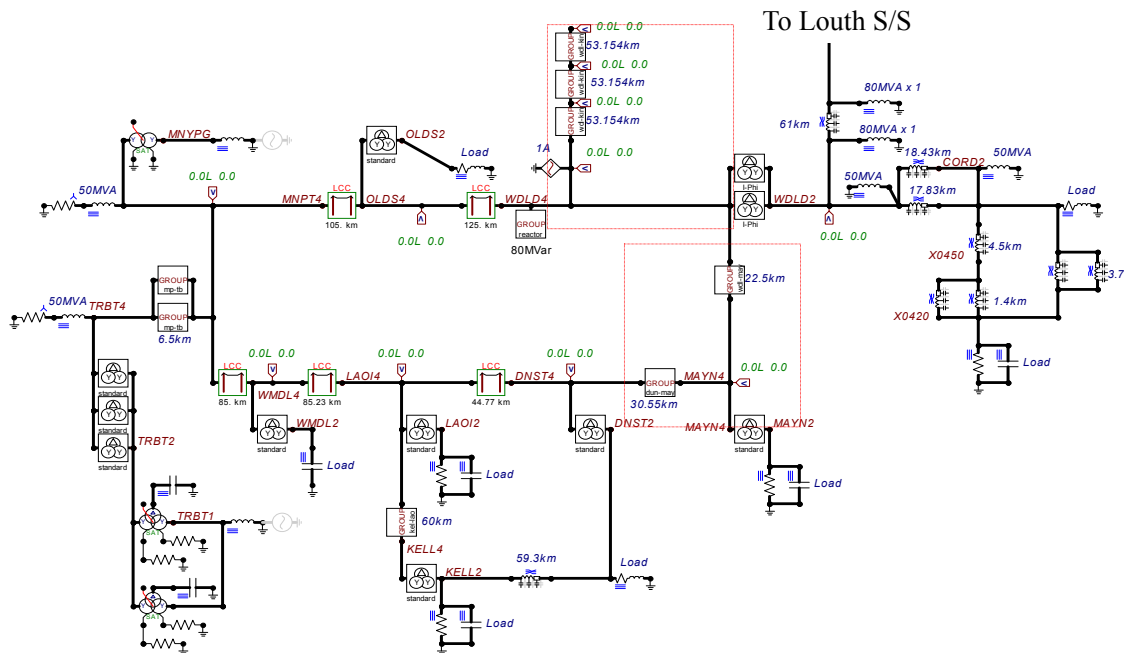
Fig. 4-11 System configuration for frequency scan.

Fig. 4-12 shows the result of frequency scan at the Woodland 220 kV and 400 kV bus.
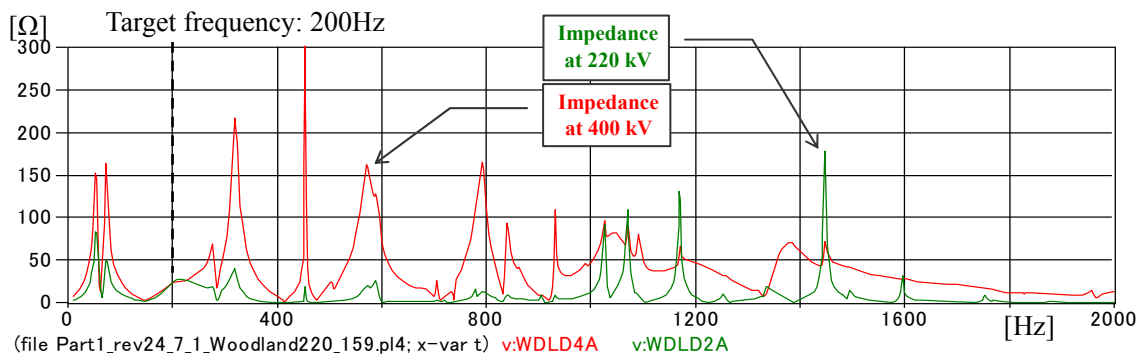
Fig. 4-12 Frequency scan at Woodland 400 kV bus and 220 kV.

[Time domain simulation]

Fig. 4-13 and Fig. 4-14 show the waveform of the overvoltage when the 400 kV Woodland – Kingscourt line is energised from the Woodland side as shown in Fig. 4-3.   It did not cause severe series resonance overvoltage.

(Phase to earth)
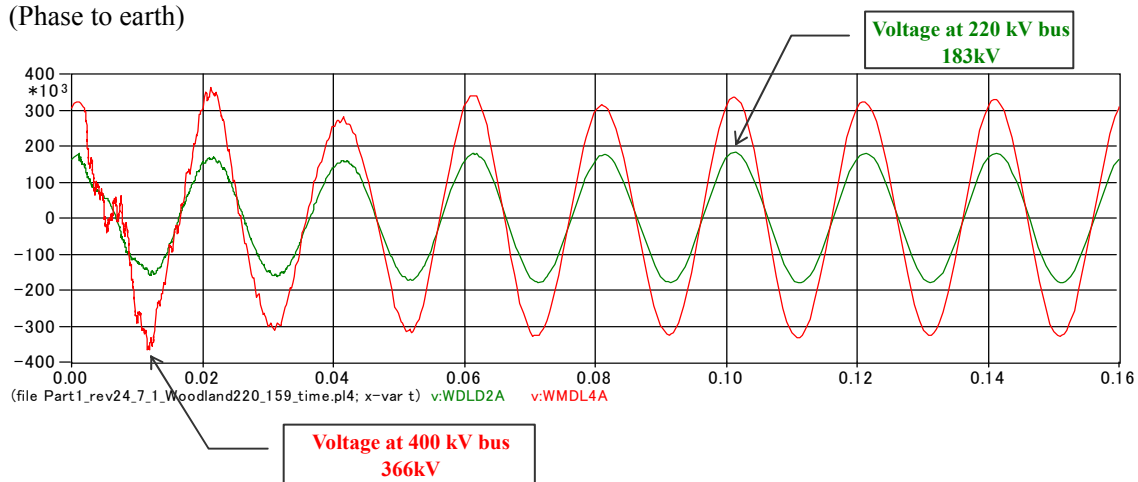
Fig. 4-13 Waveform of the overvoltage at the Woodland 400 kV and 220 kV buses.
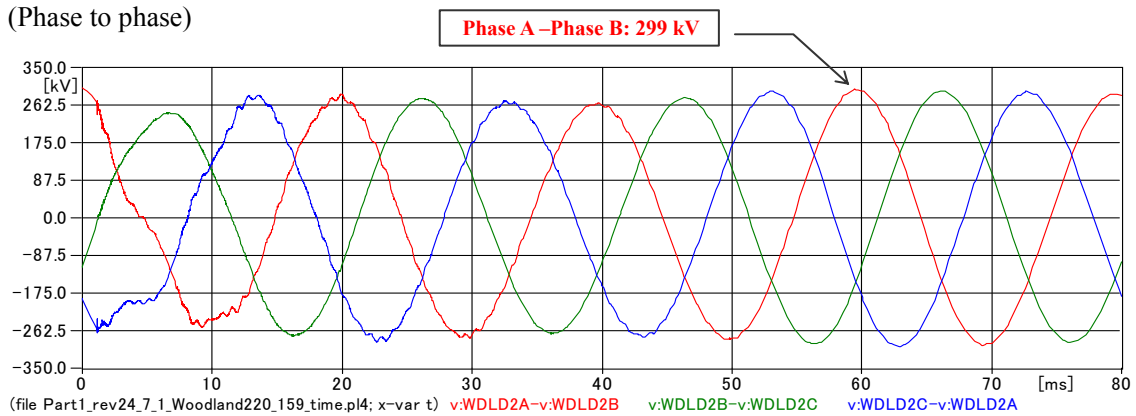
(Phase to phase)

Fig. 4-14 Waveforms of the switching overvoltage at the Woodland 220 kV bus (phase to phase).

Fig. 4-15 and Fig. 4-16 respectively show frequency component spectrums derived from the voltage waveforms at the Woodland 400 kV and 220 kV buses.
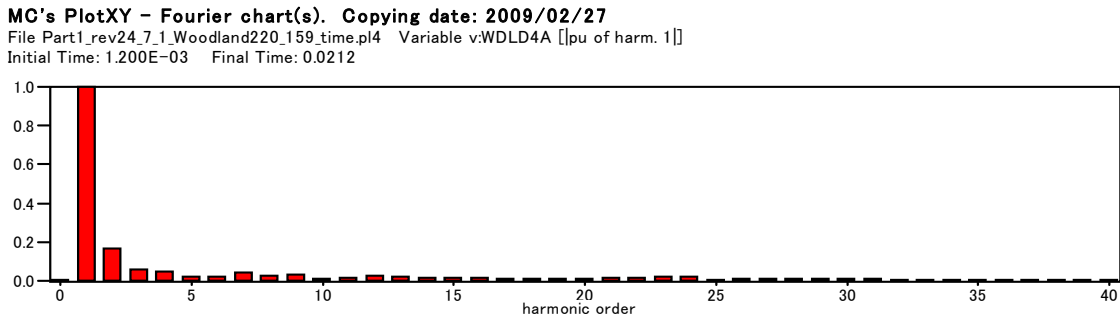
Fig. 4-15 Frequency component spectrum of the switching waveform at the Woodland 400 kV bus.
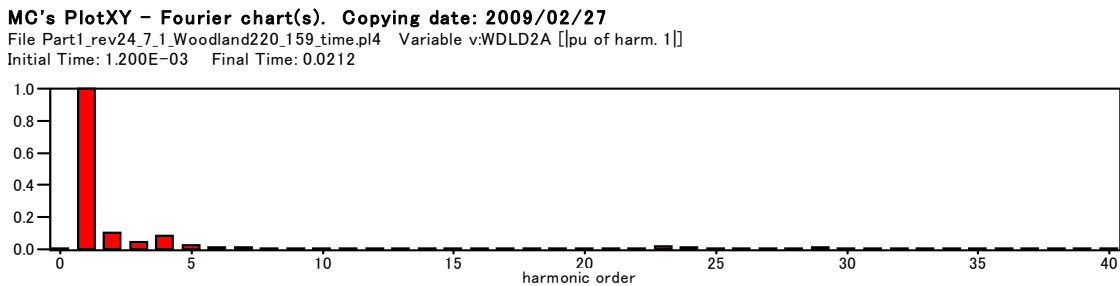
Fig. 4-16 Frequency component spectrum of the switching waveform at the Woodland 220 kV bus.

Comparing Fig. 4-15 to Fig. 4-16, it can be found that the 200 Hz component is slightly amplified from the Woodland 400 kV bus to the Woodland 220 kV bus. However, the magnitude of 200 Hz component is very small in both the Woodland 400 kV and 220 kV buses. It is expected that the frequency components contained in the energisation overvoltage were highly damped due to the long length of the 400 kV Dunstown – Maynooth – Woodland – Kingscourt line.

(2) –2 Series resonance frequency 1430 Hz

[Frequency scan]

In Fig. 4-6, the largest amplification ratio was found at around 1430 Hz.   Here, the total length of the 400 kV Woodland – Kingscourt line was adjusted to satisfy the equation $1/4\tau$ = 1430 Hz.   The calculated total length is

$$\frac{1}{4}\frac{1.7\times10^{8}\,\text{m/s}}{1430\,\text{Hz}} \approx 29700\,\text{m}$$

Compensation rate of the cable was set to be approximately equal to the original length as shown in Table 4-1.

Table 4-1 Compensation of Compensation Rates

Length	58 km (Original)		29.7 km	
Charging capacity	539.2 MVA/cct		276.1 MVA/cct	
Reactor	Woodland	Kingscourt	Woodland	Kingscourt
	300 MVA (150 * 2)	240 MVA (120 * 2)	150 MVA (150 * 1)	120 MVA (120 * 1)
	Total	540 MVA	Total	270 MVA
Compensation rate	100.1%		97.8%	

The system configuration for frequency scan is shown in Fig. 4-17.   The 400 kV Woodland – Maynooth line is assumed to be out of service to satisfy $1/4\tau$ = 1430 Hz.
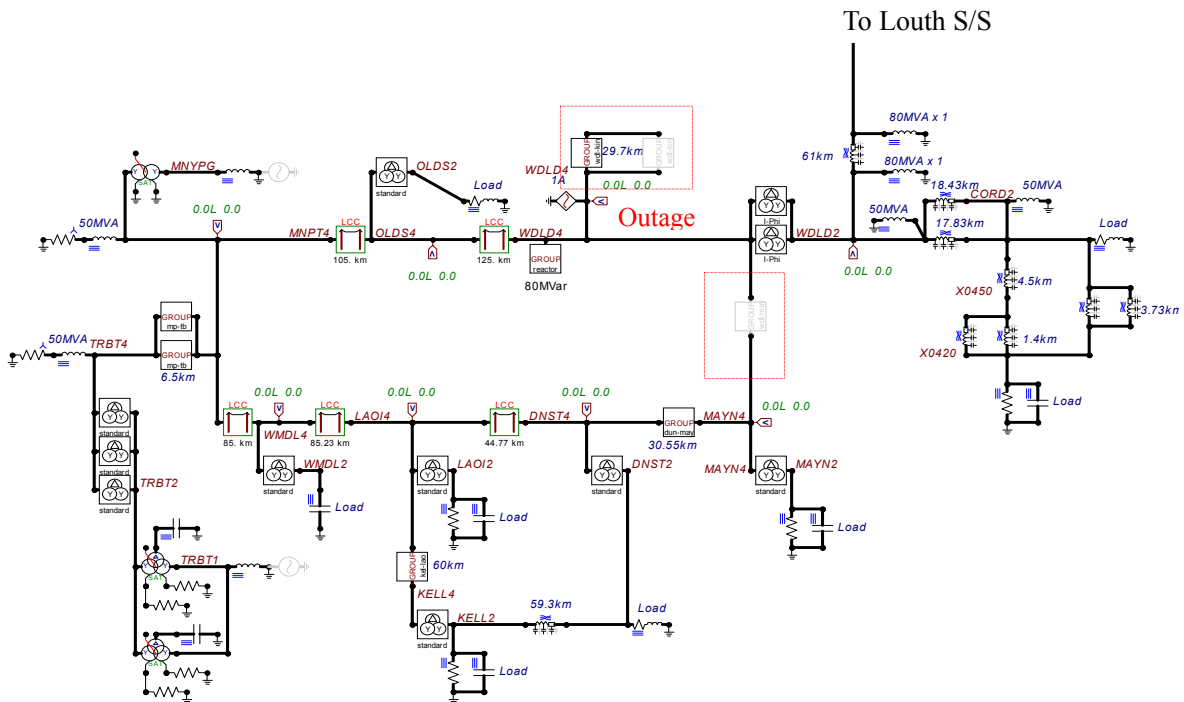
Fig. 4-17 System configuration for a frequency scan.

Fig. 4-18 shows the result of frequency scan at the Woodland 220 kV and 400 kV bus. It appears that the series resonance condition is not severe at 1430 Hz.
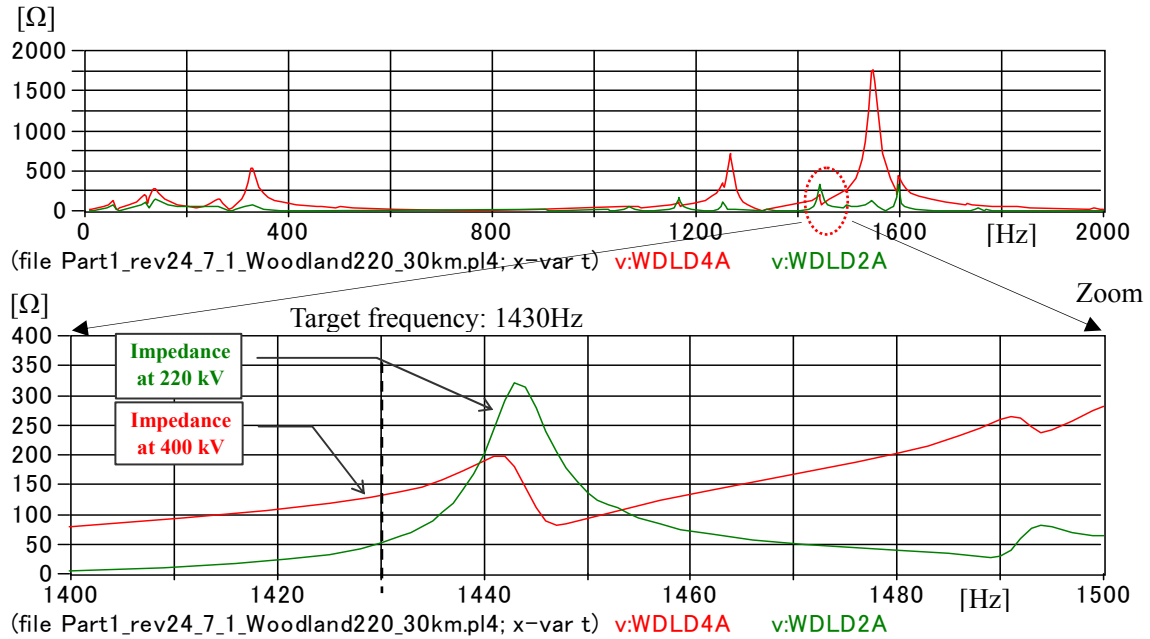
Fig. 4-18 Frequency scan at the Woodland 400 kV and 220 kV bus.

Fig. 4-19 shows the comparison of 400 kV Woodland bus voltages with the original and its modified line length. The figure illustrates why the series resonance condition at 1430 Hz is not very severe in Fig. 4-18. As can be seen from the figure, the frequency response has changed due to an outage of the 400 kV Woodland – Maynooth line and the change of the 400 kV Woodland – Kingscourt line length.
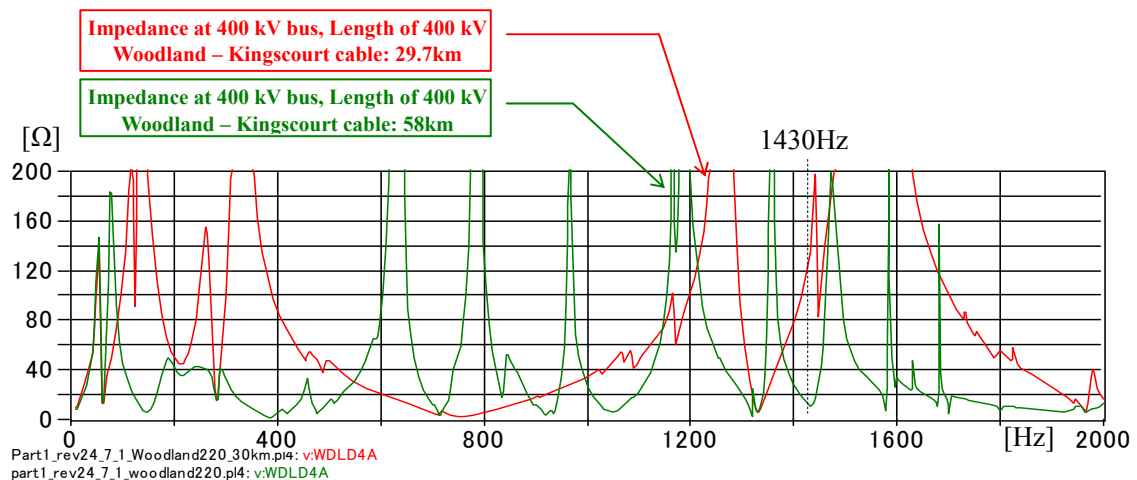
Fig. 4-19 Comparison of different conditions with respect to 400 kV cable length.

(3) Simplified system

The study in *(2) Assumed most severe condition* shows the difficulty of matching series resonance frequency to the dominant frequency in the overvoltage intentionally.   In order to search for the most severe condition, parametric studies were performed in (4) and (5).   For the parametric studies, the system has to be simplified so that the effect of the changes can be theoretically understood.   For this objective, the following changes were introduced to the normal conditions:

- It was assumed that all the Woodland 220 kV system was fed from other substations except the 220 kV Woodland – Louth line.

- The Woodland 220 kV system was separated from the Louth 220 kV system.

- The 400 kV Woodland – Maynooth line was out of service.

The loads at Corduff and Finglas were removed together from the simulation model due to this simplification, which will lead to a severe condition.
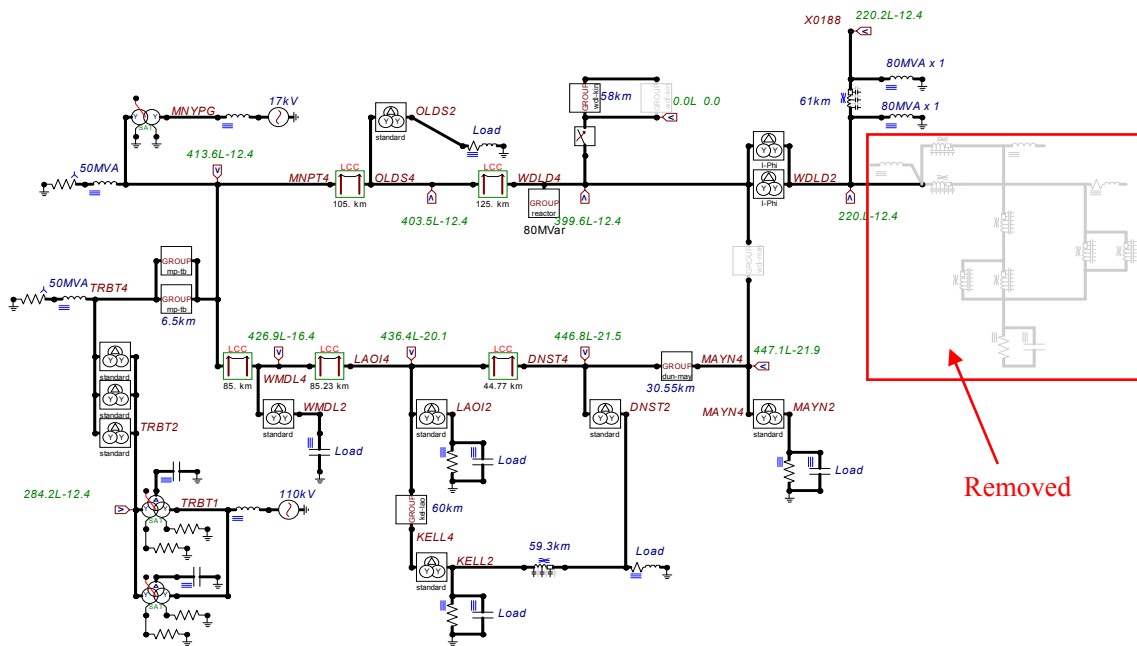
Fig. 4-20 Simplified system configuration for parametric studies.

(4) Parametric studies – 220 kV Woodland – Louth cable

In the simplified system created in (3), frequency scans and time domain simulations were performed with different lengths of the 220 kV Woodland – Louth line. For the time domain simulations, the energisation of the 400 kV Woodland – Kingscourt line was studied.

The change of the 220 kV Woodland – Louth line length shifts series resonance frequencies, which may match with the dominant frequencies contained in the overvoltage.

Table 4-2 Length of the 220 kV Woodland – Louth Cable

	220 kV Woodland – Louth cable		Notes
	Length	Number of circuits	
Case (4)-0	61.0 km	1	Base case
Case (4)-1	7.625 km	1	(Length of the base case) /8
Case (4)-2	12 km	1	
Case (4)-3	15.25 km	1	(Length of the base case) /4
Case (4)-4	30.5 km	1	(Length of the base case) /2
Case (4)-5	91.5 km	1	(Length of the base case) * 1.5
Case (4)-6	122.0 km	1	(Length of the base case) * 2
Case (4)-7	183.0 km	1	(Length of the base case) * 3
Case (4)-8	244.0 km	1	(Length of the base case) * 4

Table 4-3, Fig. 4-21 and Fig. 4-22 summarize the results of the analysis. All the figures obtained in the parametric study are shown in Appendix 1.

Table 4-3 Overvoltage Observed at the Woodland 220 kV Bus and the 220 kV Cable Open End

	220kV cable length	Phase to the Earth				Phase to Phase	
		Voltage at the 220kV bus		Voltage at the 220kV cable open end		Voltage at the 220kV bus	
Case (4)-1	7.63 km (61km/8)	319 kV	1.78 p.u.	326 kV	1.81 p.u.	513 kV	2.86 p.u.
Case (4)-2	12 km	304 kV	1.69 p.u.	312 kV	1.74 p.u.	489 kV	2.72 p.u.
Case (4)-3	15.3 km (61km/4)	321 kV	1.79 p.u.	328 kV	1.83 p.u.	522 kV	2.91 p.u.
Case (4)-4	30.5 km (61km/2)	354 kV	1.97 p.u.	375 kV	2.09 p.u.	549 kV	3.06 p.u.
Case (4)-0	61 km	278 kV	1.55 p.u.	332 kV	1.85 p.u.	471 kV	2.62 p.u.
Case (4)-5	91.5 km (61km*1.5)	257 kV	1.43 p.u.	350 kV	1.95 p.u.	429 kV	2.39 p.u.
Case (4)-6	122 km (61km*2)	235 kV	1.31 p.u.	311 kV	1.73 p.u.	385 kV	2.14 p.u.
Case (4)-7	183 km (61km*3)	212 kV	1.18 p.u.	331 kV	1.84 p.u.	415 kV	2.31 p.u.
Case (4)-8	244 km (61km*4)	234 kV	1.30 p.u.	309 kV	1.72 p.u.	416 kV	2.32 p.u.

$$1\text{p.u.}= 220\text{kV} * \frac{\sqrt{2}}{\sqrt{3}}$$

(Phase to earth)
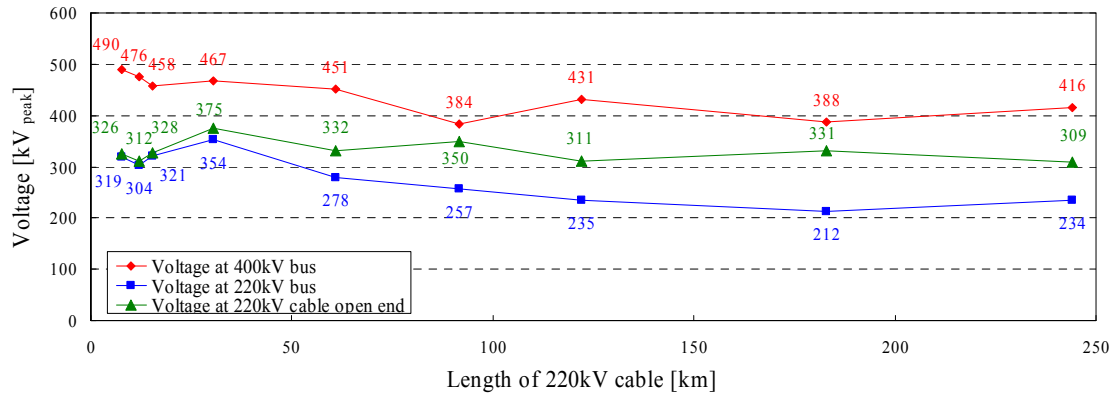
Fig. 4-21 Overvoltage observed at the Woodland 400 kV and 220 kV buses and 220 kV cable open end (phase to earth).
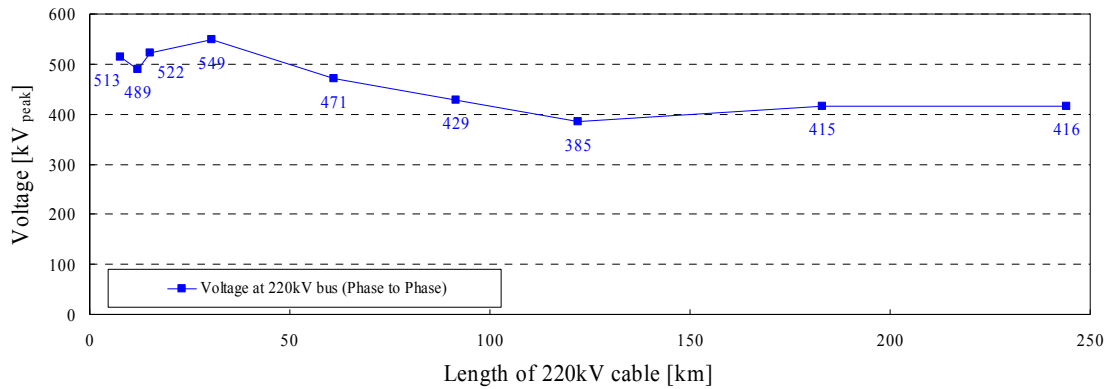
(Phase to phase)

Fig. 4-22 Overvoltage observed at the Woodland 220 kV bus (phase to phase).

(5) Parametric studies – 400 kV Woodland – Kingscourt cable

In the simplified system created in (3), frequency scans and time domain simulations were performed with different lengths of the 400 kV Woodland – Kingscourt line.   For the time domain simulations, the energisation of the 400 kV Woodland – Kingscourt line was studied.

The change of the 220 kV Woodland – Kingscourt line length shifts dominant frequencies contained in the energisation overvoltage, which may match with series resonance frequencies. The compensation rates of the 400 kV cable were kept around 100 % with different lengths of the cable as shown in Table 4-4.

Table 4-4 Length of the 400 kV Woodland – Kingscourt Line

	400kV cable	Target frequency	Charging capacity	Reactor for 400kV cable Woodland	Kingscourt	Compensation rate
(5)- 1	141.7 km	300 Hz	1,317 MVA	750 MVA	600 MVA	102.5%
(5)- 2	106.3 km	400 Hz	988 MVA	600 MVA	360 MVA	97.2%
(5)- 3	85.0 km	500 Hz	790 MVA	450 MVA	360 MVA	102.5%
(5)- 4	70.8 km	600 Hz	659 MVA	300 MVA	360 MVA	100.2%
(5)- 5	60.7 km	700 Hz	564 MVA	300 MVA	300 MVA	106.3%
(5)- 6	47.2 km	900 Hz	439 MVA	300 MVA	120 MVA	95.7%
(5)- 7	38.6 km	1100 Hz	359 MVA	240 MVA	120 MVA	100.2%
(5)- 8	26.6 km	1600 Hz	247 MVA	120 MVA	120 MVA	97.2%
(5)- 9	22.4 km	1900 Hz	208 MVA	120 MVA	120 MVA	115.4%

Charging capacity: 9.3 MVA/cct/km

Table 4-5, Fig. 4-23 and Fig. 4-24 summarize the result of the analysis.   All the figures obtained in the parametric study are shown in Appendix 2.

Table 4-5 Overvoltage Observed at the Woodland 220 kV Bus and the 220 kV Cable Open End

	400kV cable length	Target frequency	Phase to the Earth Voltage at the 220kV bus		Voltage at the 220kV cable open end		Phase to Phase Voltage at the 220kV bus	
(5)-1	141.7 km	300 Hz	225 kV	1.25 p.u.	243 kV	1.35 p.u.	362 kV	2.02 p.u.
(5)-2	106.3 km	400 Hz	258 kV	1.44 p.u.	279 kV	1.55 p.u.	421 kV	2.34 p.u.
(5)-3	85.0 km	500 Hz	260 kV	1.45 p.u.	326 kV	1.81 p.u.	443 kV	2.47 p.u.
(5)-4	70.8 km	600 Hz	278 kV	1.55 p.u.	285 kV	1.59 p.u.	502 kV	2.79 p.u.
(5)-5	60.7 km	700 Hz	264 kV	1.47 p.u.	322 kV	1.79 p.u.	478 kV	2.66 p.u.
(5)-6	47.2 km	900 Hz	263 kV	1.46 p.u.	305 kV	1.70 p.u.	469 kV	2.61 p.u.
(5)-7	38.6 km	1100 Hz	277 kV	1.54 p.u.	318 kV	1.77 p.u.	465 kV	2.59 p.u.
(5)-8	26.6 km	1600 Hz	267 kV	1.49 p.u.	344 kV	1.92 p.u.	443 kV	2.47 p.u.
(5)-9	22.4 km	1900 Hz	279 kV	1.55 p.u.	341 kV	1.90 p.u.	441 kV	2.46 p.u.

$$1 \text{p.u.} = 220 \text{kV} * \frac{\sqrt{2}}{\sqrt{3}}$$

(Phase to earth)
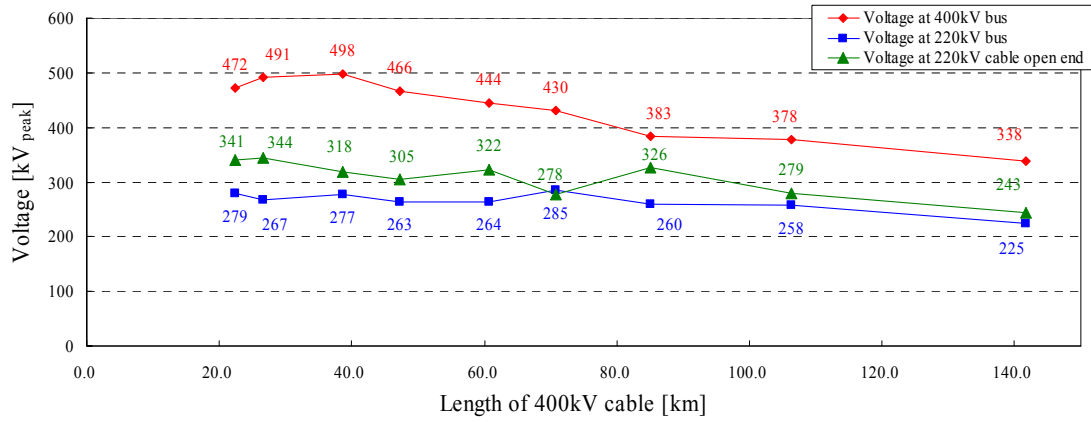
Fig. 4-23 Overvoltage observed at the Woodland 400 kV and 220 kV buses and 220 kV cable open end (phase to earth).
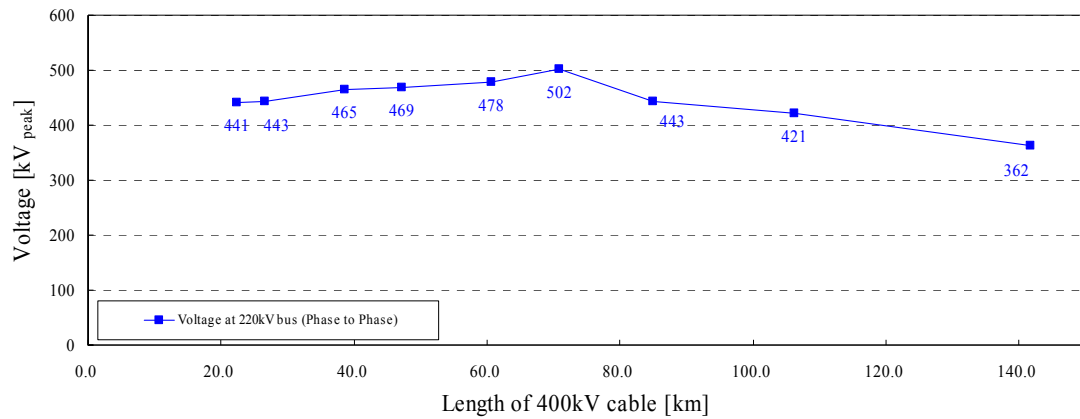
(Phase to phase)

Fig. 4-24 Overvoltage observed at the Woodland 220 kV bus (phase to phase).

4.1.2　Resonance overvoltage in the Turleenan 275 kV system

Fig. 4-25 shows the system configuration for the series resonance overvoltage analysis in the Turleenan 275 kV system caused by the energisation of the 400 kV Kingscourt – Turleenan line from the Turleenan S/S.
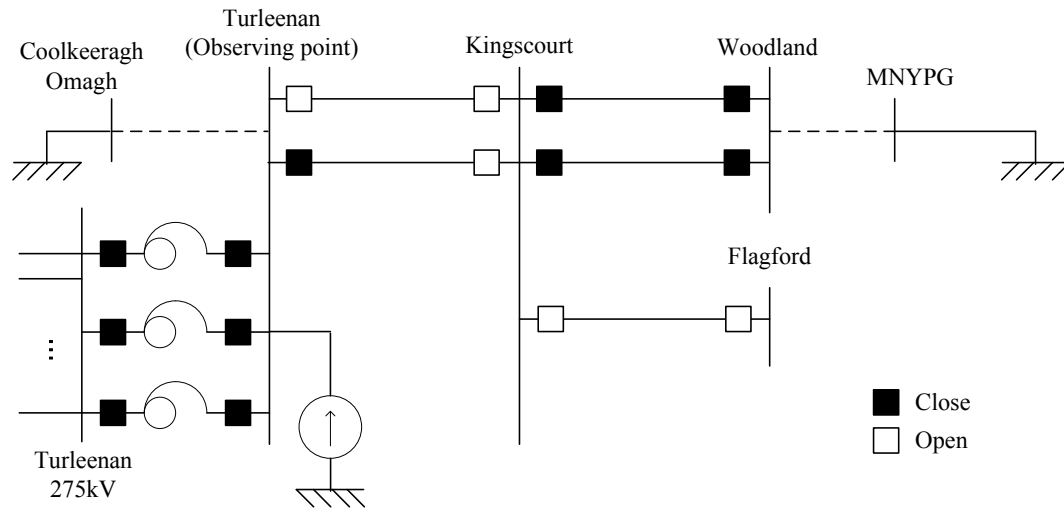
Fig. 4-25 System configuration for series resonance overvoltage in Turleenan 275 kV system.

Fig. 4-26 shows a result of frequency scan.　The vertical axis of the figure shows voltages observed at the Turleenan 400 kV, which is equal to the equivalent impedance of the network seen from the Turleenan 400 kV bus because the injected current is 1 Amp.
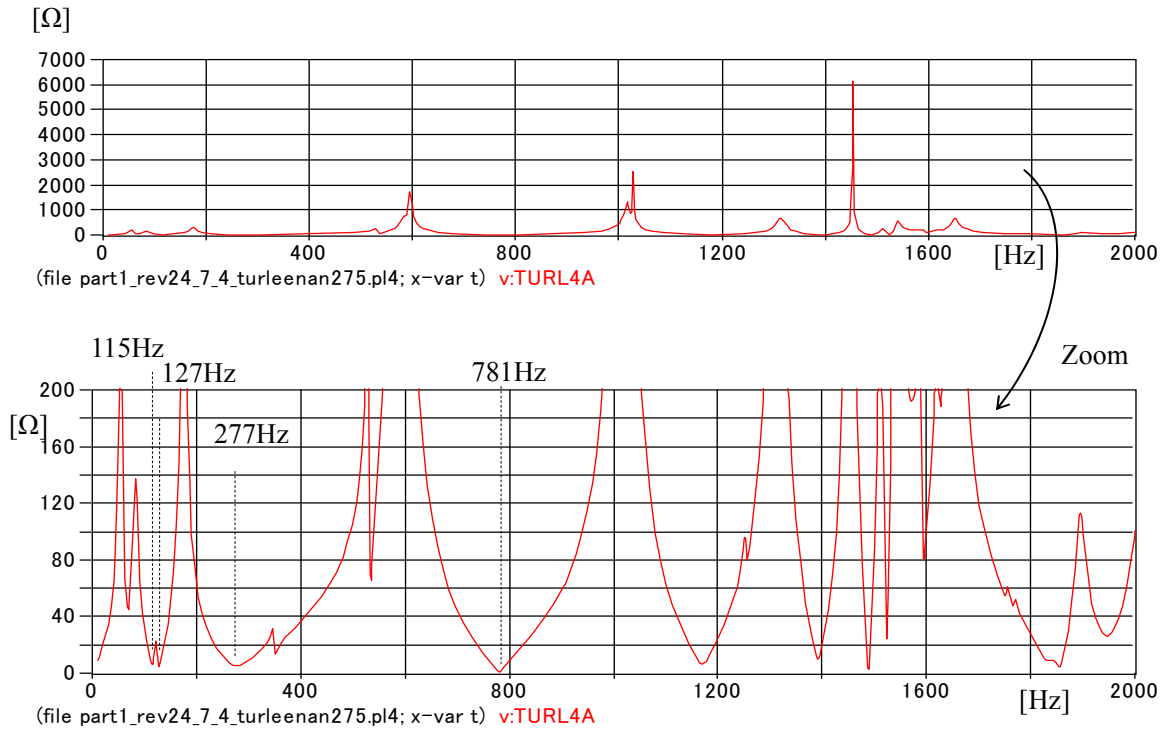
Fig. 4-26 Frequency scan at Turleenan 400 kV bus in the normal condition.

Fig. 4-27 shows the result of frequency scan at the Turleenan 400 kV and 275 kV buses, and the amplification ratio from Turleenan 400 kV to 275 kV bus voltage is shown in Fig. 4-28.
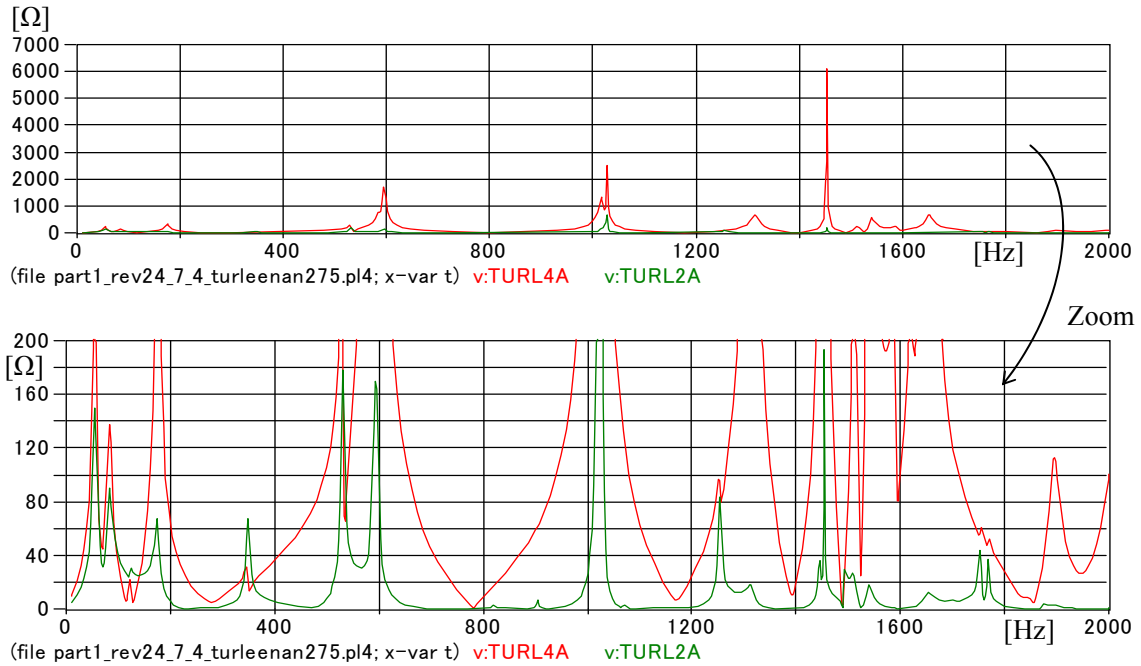
Fig. 4-27 Frequency scan at Turleenan 400 kV and 275 kV bus in the normal condition.
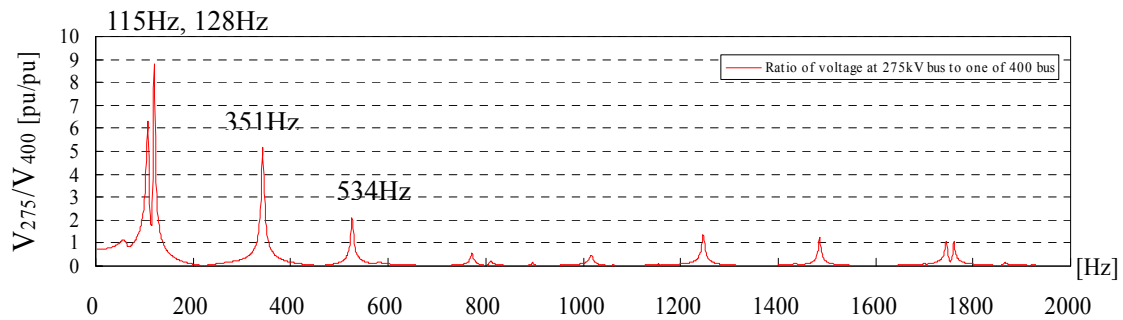
Fig. 4-28 Amplification ratio at Turleenan.

Series resonance frequencies were found at 115 Hz, 128 Hz, 351 Hz, and 534 Hz.

[Time domain simulations in the normal condition]

The energisation of the 400 kV Kingscourt – Turleenan line was studied under normal conditions. Fig. 4-29 and Fig. 4-30 show the overvoltage in the Turleenan 400 kV and 275 kV buses. It was found that the energisation of the 400 kV Kingscourt – Turleenan line did not cause high overvoltage due to series resonance.
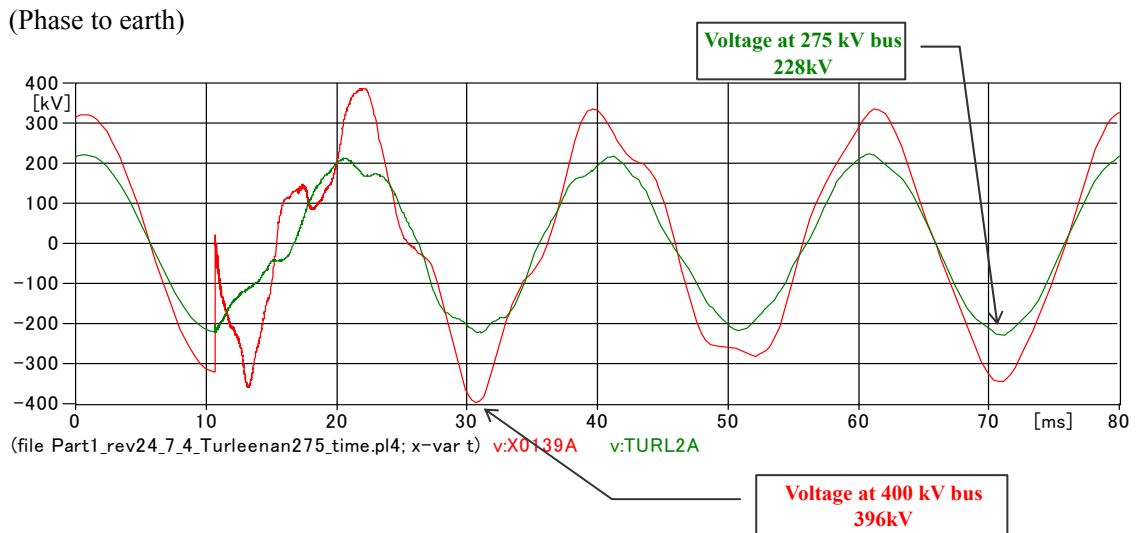
(Phase to earth)

Fig. 4-29 Waveforms of the overvoltage at Turleenan 400 kV and 275 kV buses (phase to earth).
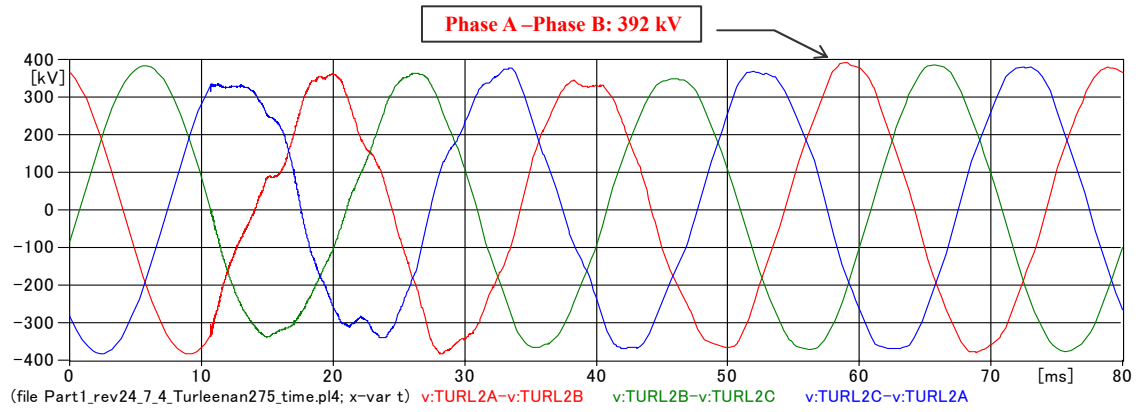
(Phase to phase)

Fig. 4-30 Waveforms of the overvoltage at the Turleenan 275 kV bus (phase to phase).

The Fourier transforms of the waveforms for 100 ms yield frequency components by 10 Hz step. Fig. 4-31 and Fig. 4-32 respectively show frequency components contained in the voltage waveform at the Turleenan 400 kV and 275 kV buses.
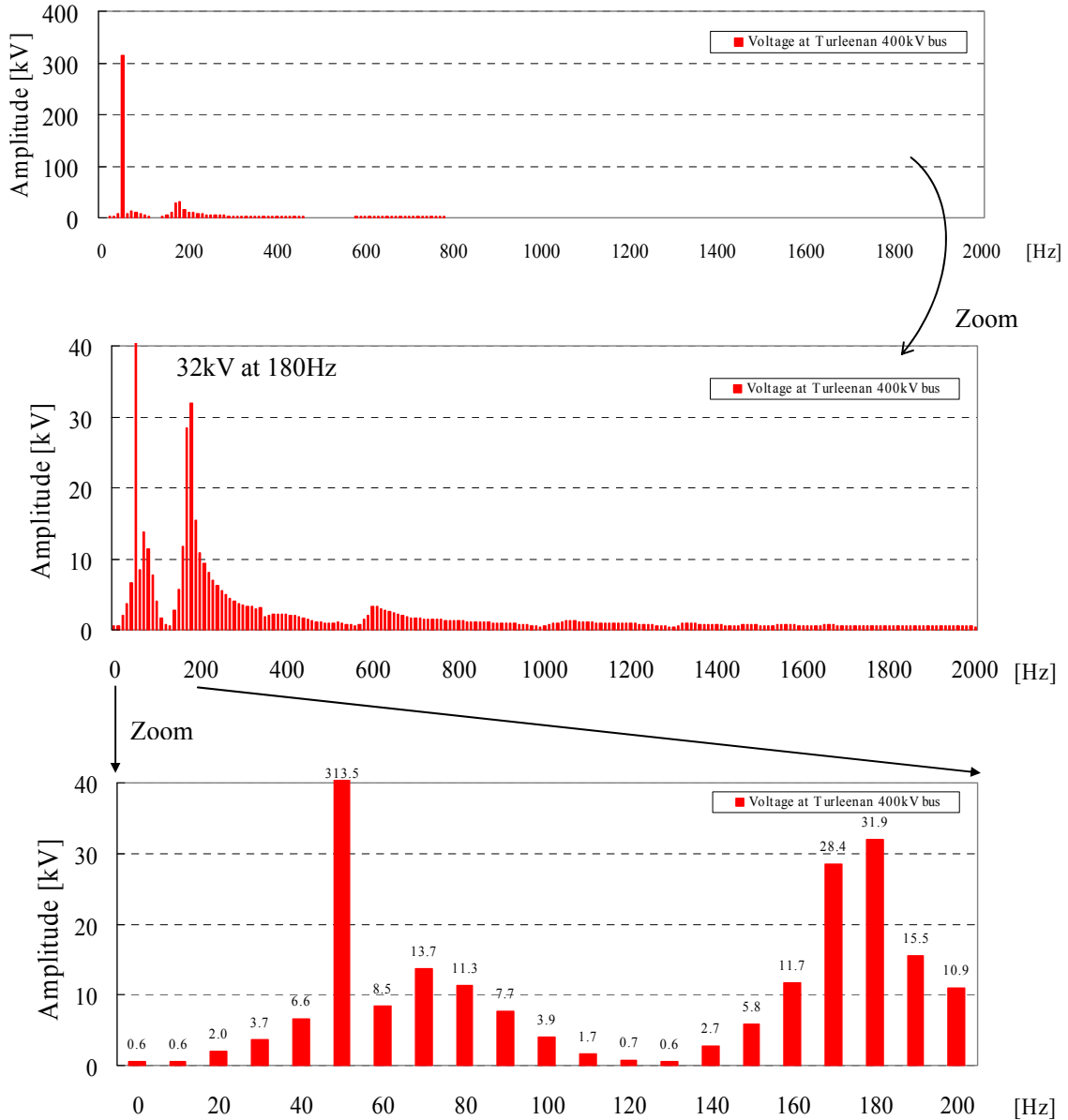
Fig. 4-31 Frequency components in the waveform at the Turleenan 400 kV bus.
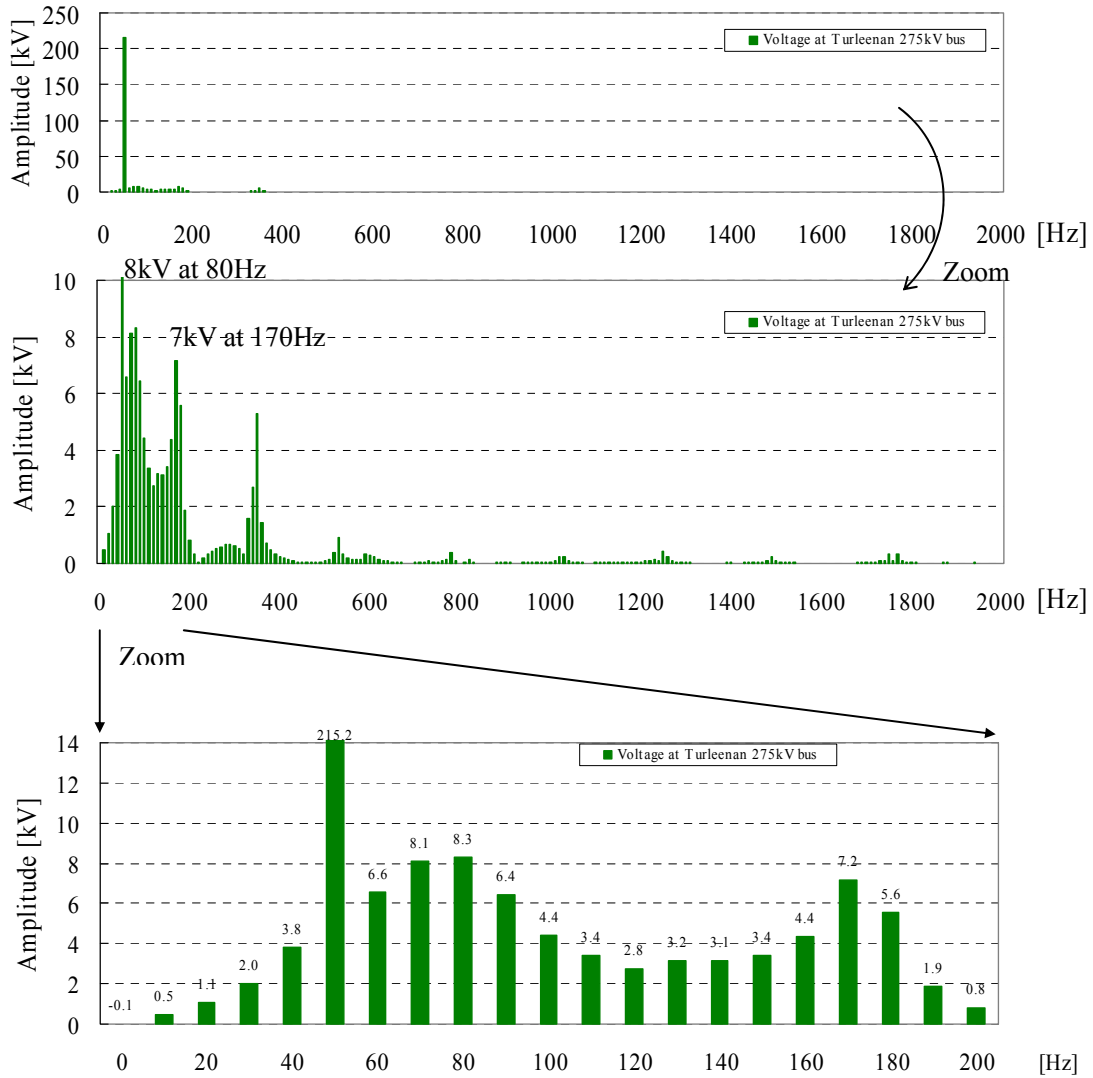
Fig. 4-32 Frequency components in the waveform at the Turleenan 275 kV bus.

The amplification ratio from the Turleenan 400 kV bus to the 275 kV bus can be derived from Fig. 4-31 and Fig. 4-32.   The obtained amplification ratio is shown in Fig. 4-33.
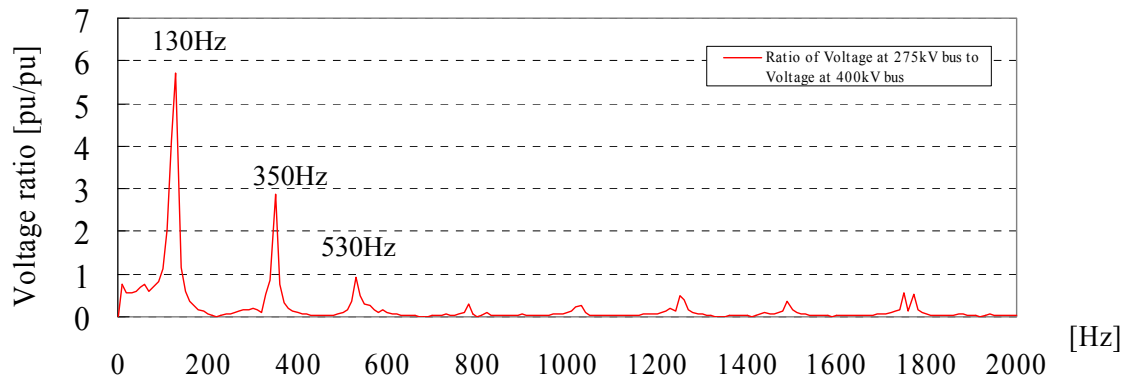
Fig. 4-33 Amplification ratio of voltage from the Turleenan 400 kV bus to the 275 kV bus.

Results from the frequency scan showed that series resonance frequencies were found at 115 Hz, 128 Hz, 351 Hz, and 534 Hz as shown in Fig. 4-28.   Results from the time domain simulation showed that series resonance frequencies were found at 130 Hz, 350 Hz, and 530 Hz as depicted in Fig. 4-33.   It is apparent that series resonance frequencies found by two different approaches closely match with each other.

As a result, the parametric study of the Turleenan 275 kV system could not find a severe series resonance condition.   Instead, the study came across a parallel resonance condition, which is not described in this public report, at 50 Hz, and it should be avoided while operating the network. Fortunately, the condition assumed for parallel resonance was extreme which may be realized only during a black-start operation.   The result shows the necessity of studying parallel resonance when establishing a black-start procedure in the NIE network.

4.1.3 Resonance overvoltage in the Kingscourt 220 kV system by the energisation of the Kingscourt – Turleenan line

Fig. 4-34 shows the system configuration for the series resonance overvoltage analysis in the Kingscourt 220 kV system caused by the energisation of the 400 kV Kingscourt – Turleenan line from the Kingscourt S/S.
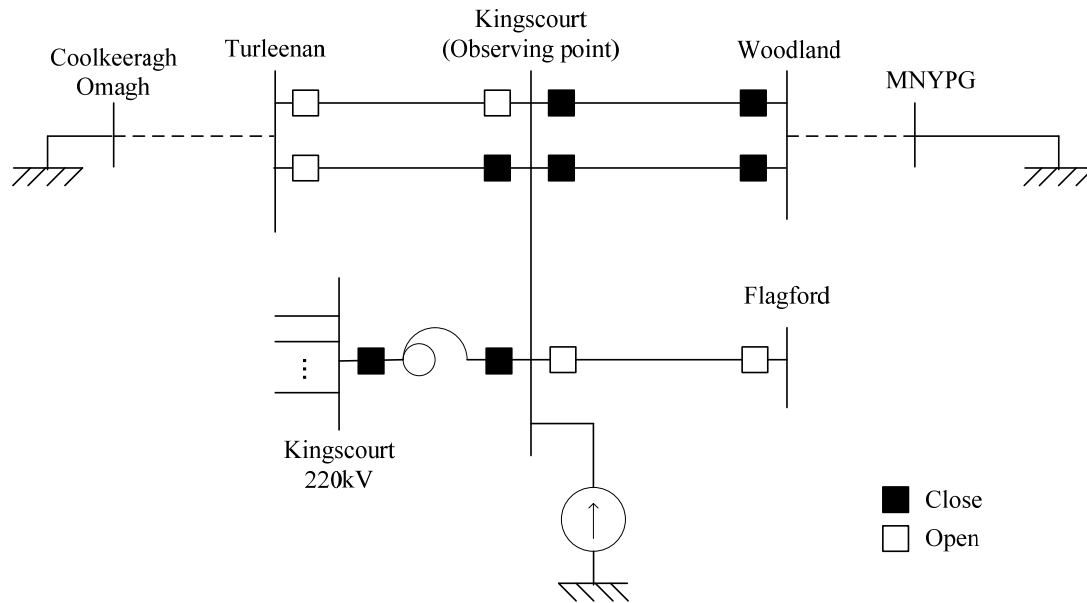
Fig. 4-34 System configuration for the series resonance overvoltage analysis in Kingscourt 220 kV system.

Target frequency of the 400 kV cable is calculated considering the total cable length from Dunstown to Turleenan.

$$f = \frac{1}{4} \frac{1.7 \times 10^8 \, \text{m/s}}{(30{,}550 + 22{,}500 + 58{,}000 + 82{,}000)\text{m}} \approx 220 \, \text{Hz}$$

Fig. 4-35 shows the result of frequency scan under normal conditions.   The vertical axis of the figure shows the voltages observed at the Kingscourt 400 kV bus, which is equal to the magnitude of impedance of the network seen from the Kingscourt 400 kV bus.
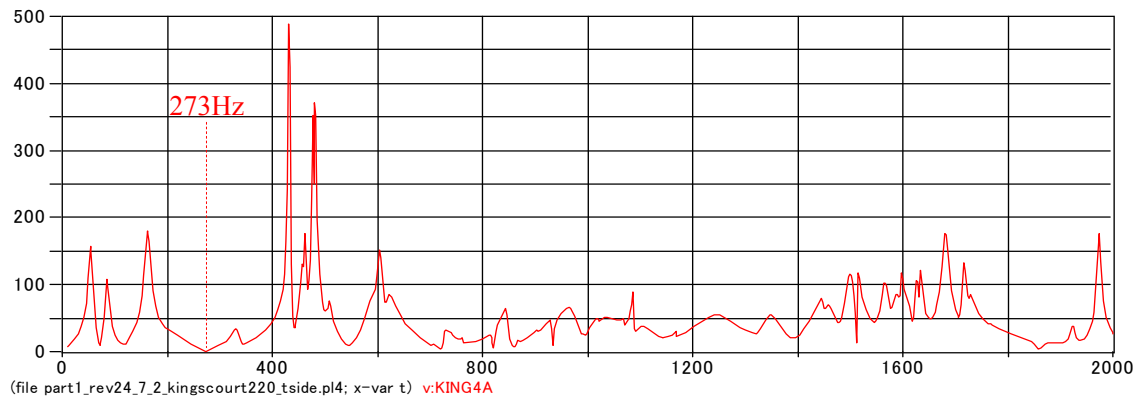
Fig. 4-35 Frequency scan at Kingscourt in the normal condition.

Fig. 4-36 shows the result of frequency scan at the Kingscourt 220 kV and 400 kV buses, and Fig. 4-37 shows the amplification ratio from the Kingscourt 400 kV bus to the 220 kV bus.
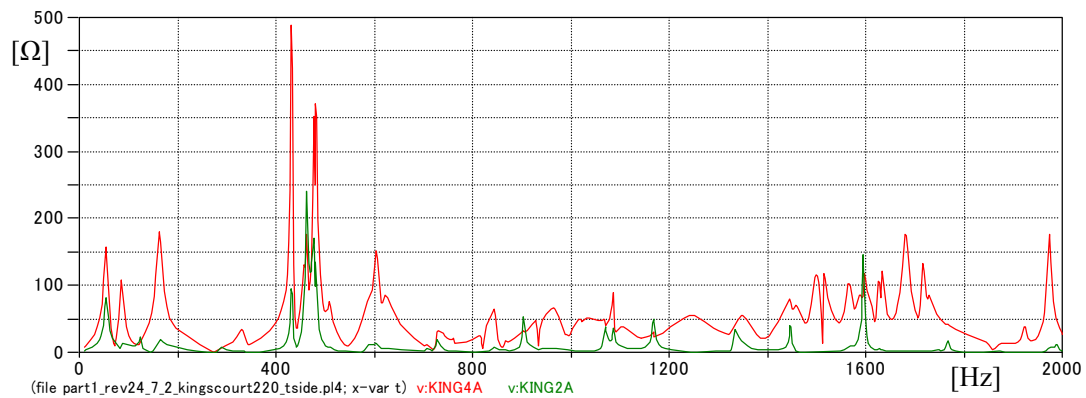
Fig. 4-36 Frequency scan at the Kingscourt 400 kV and 220 kV buses in the normal condition.
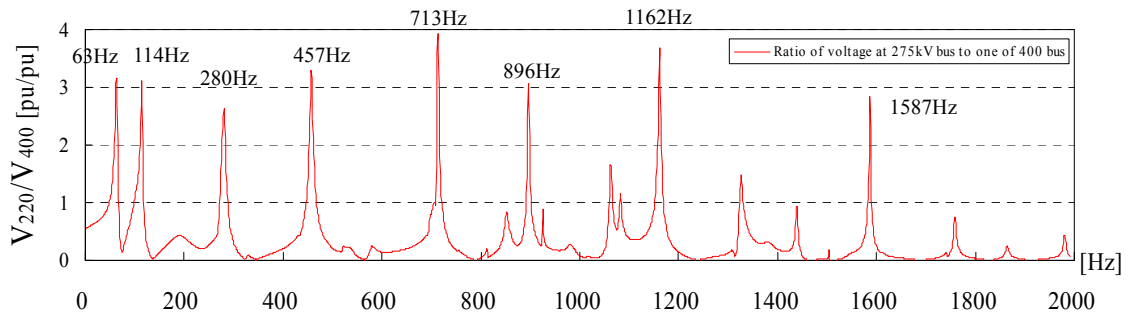
Fig. 4-37 Amplification ratio at Kingscourt.

Series resonance frequency was not found at $1/4\tau = 220$ Hz.

Fig. 4-38 and Fig. 4-39 show the results of the time domain simulation under normal conditions.

(Phase to earth)

(file Part1_rev24_7_1_Kingscourt220_Tside_time.pl4; x-var t) v:X0325A   v:KING2A
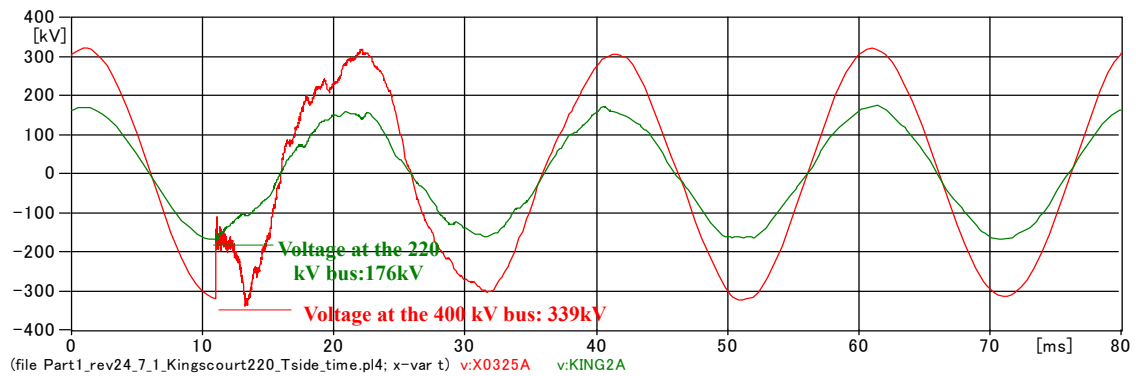
Fig. 4-38 Waveforms of the overvoltage at the Kingscourt 400 kV and 220 kV buses (phase to earth).

(Phase to phase)

(file Part1_rev24_7_1_Kingscourt220_Tside_time.pl4; x-var t) v:KING2A-v:KING2B   v:KING2B-v:KING2C   v:KING2C-v:KING2A
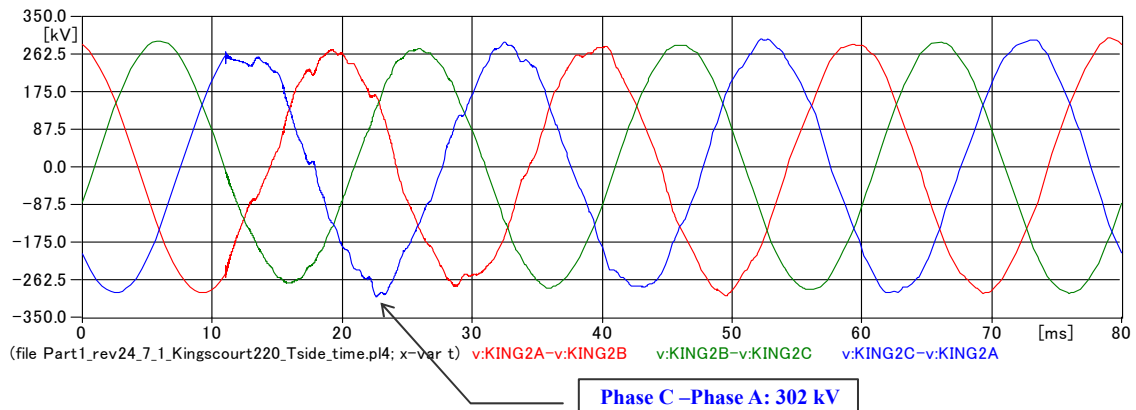
Fig. 4-39 Waveforms of the overvoltage at the 220 kV buses bus (phase to phase).

Fig. 4-40 and Fig. 4-41 respectively show frequency component spectrums derived from the voltage waveforms at the Kingscourt 400 kV and 220 kV buses.   The frequency components were calculated for one cycle immediately after the line energisation.

From these figures, it can be seen that harmonic components contained in the energisation overvoltage are very low.   In addition, since $1/4\tau$ does not match series resonance frequencies, severe resonance overvoltage was not observed in the simulation result.

MC's PlotXY – Fourier chart(s). Copying date: 2009/03/03
File Part1_rev24_7_1_Kingscourt220_Tside_time.pl4   Variable v:X0325A [|pu of harm. 1|]
Initial Time: 0.01102   Final Time: 0.03102
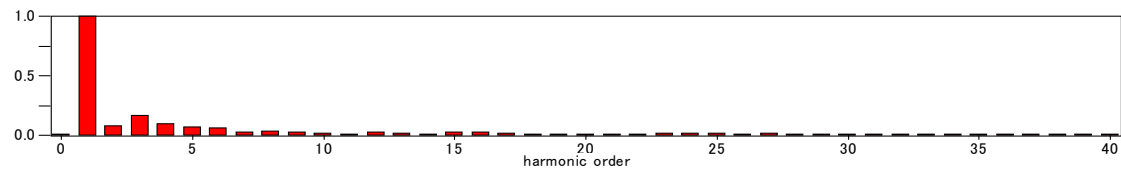
Fig. 4-40 Frequency component spectrum of the switching waveform at the Kingscourt 400 kV bus

MC's PlotXY – Fourier chart(s). Copying date: 2009/03/03
File Part1_rev24_7_1_Kingscourt220_Tside_time.pl4   Variable v:KING2A [|pu of harm. 1|]
Initial Time: 0.01102   Final Time: 0.03102
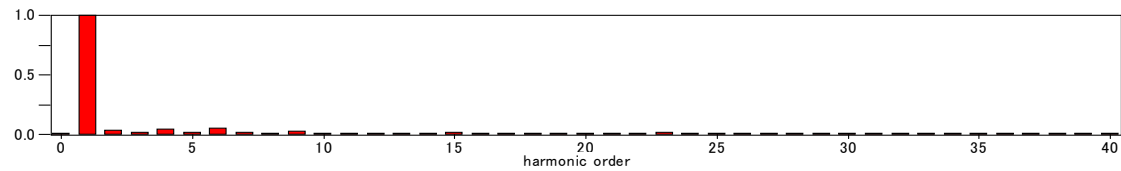
Fig. 4-41 Frequency component spectrum of the switching waveform at the Kingscourt 220 kV bus

4.1.4   Resonance overvoltage in the Kingscourt 220 kV system by the energisation of the Woodland – Kingscourt line

Fig. 4-42 shows the system configuration for the series resonance overvoltage analysis in the Kingscourt 220 kV system caused by the energisation of the 400 kV Woodland – Kingscourt line from the Kingscourt S/S.
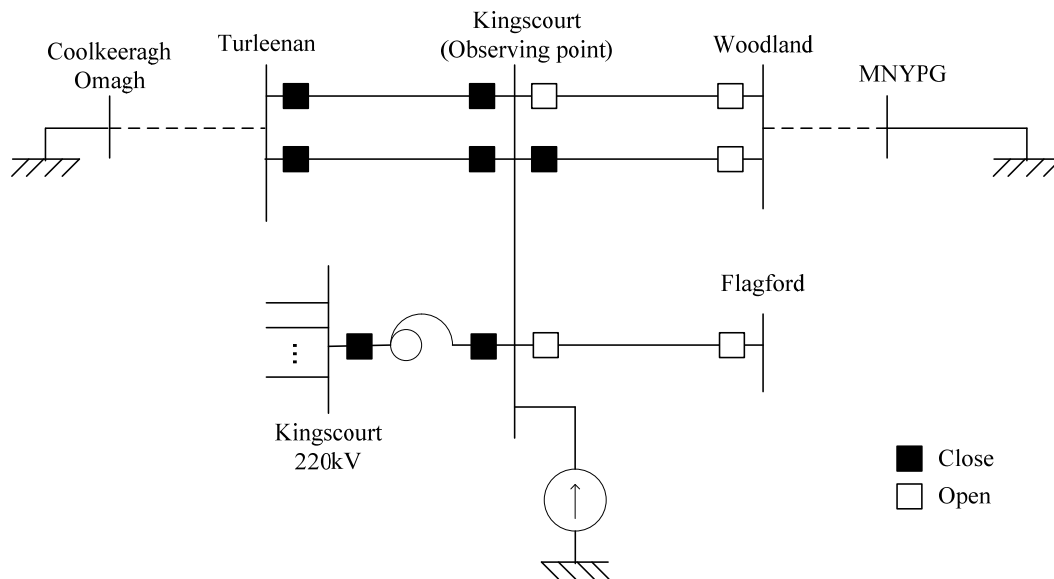
Fig. 4-42 System configuration for the series resonance overvoltage analysis in the Kingscourt 220 kV system.

Target frequency of the 400 kV cable is calculated considering the total cable length from Woodland to Turleenan.

$$f = \frac{1}{4} \frac{1.7 \times 10^8 \, \text{m/s}}{(58,000 + 82,000)\text{m}} \approx 300 \, \text{Hz}$$

Fig. 4-43 shows the result of frequency scan under normal conditions. The vertical axis of the figure shows the voltages observed at the Kingscourt 400 kV bus, which is equal to the magnitude of impedance of the network seen from the Kingscourt 400 kV bus.
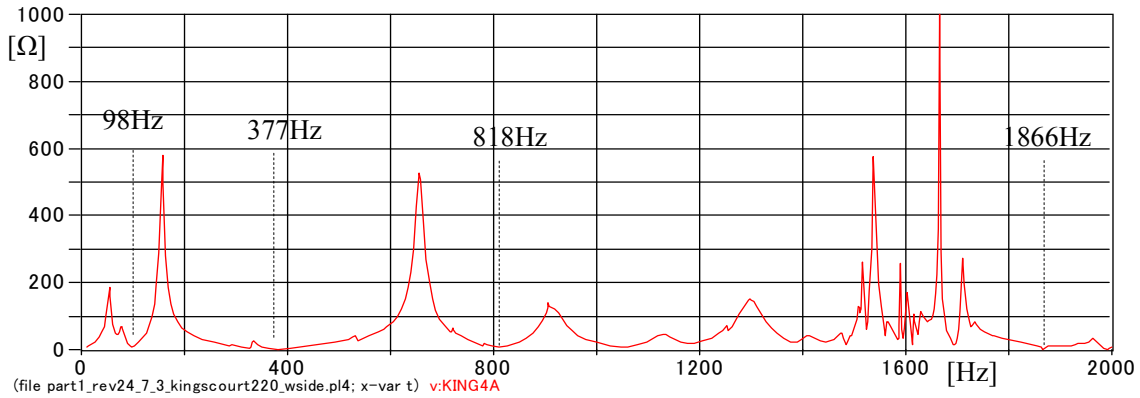
Fig. 4-43 Frequency scan at Kingscourt.

Fig. 4-44 shows the result of frequency scan at the Kingscourt 220 kV and 400 kV buses, and Fig. 4-45 shows the amplification ratio from the Kingscourt 400 kV bus to the 220 kV bus.
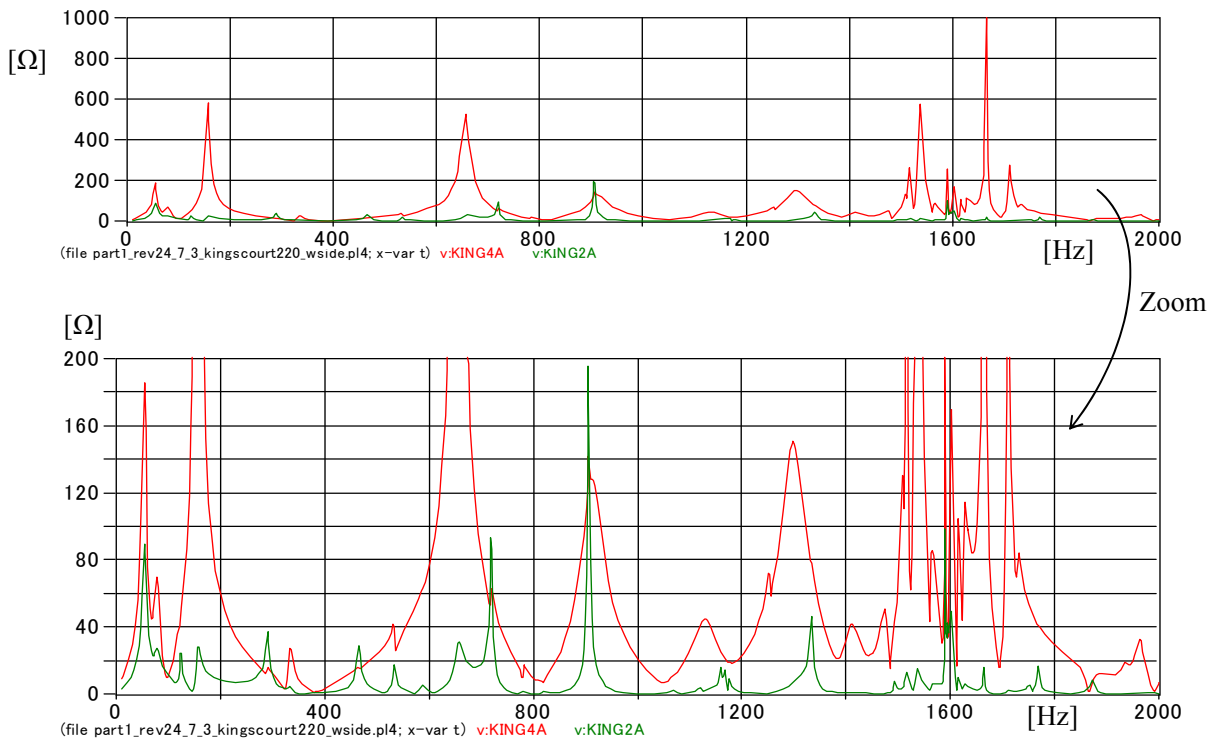
Fig. 4-44 Frequency scan at the Kingscourt 400 kV and 220 kV buses under normal conditions.
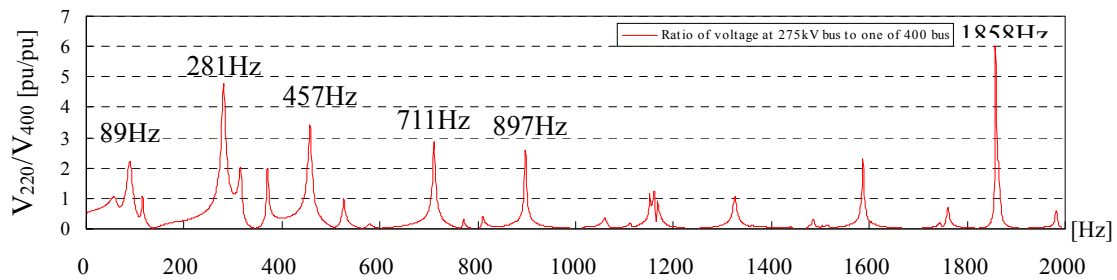
Fig. 4-45 Amplification ratio at Kingscourt.

Series resonance frequency was not found at $1/4\tau = 300$ Hz.

Fig. 4-46 and Fig. 4-47 show the result of the time domain simulation under normal conditions. As in the analysis in Section 3.1.3, harmonic components contained in the energisation overvoltage are very low. Additionally, since $1/4\tau$ does not match series resonance frequencies, severe resonance overvoltage was not observed in the simulation result.

(Phase to earth)
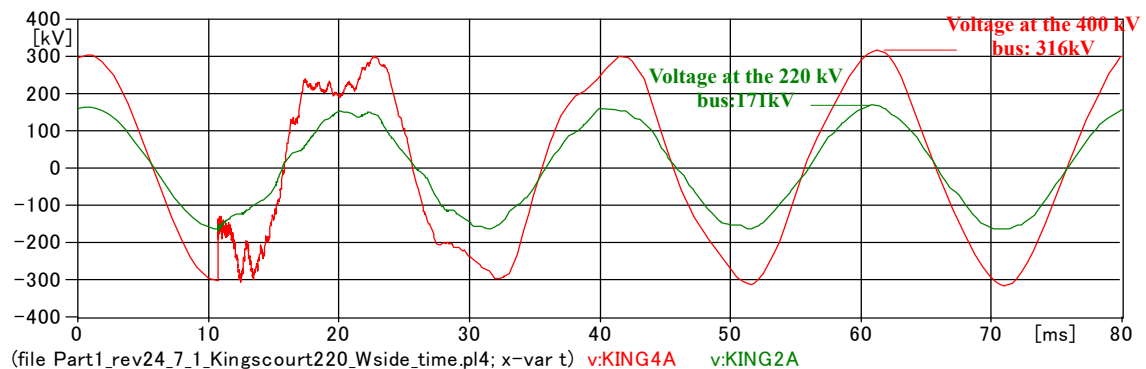
Fig. 4-46 Waveforms of the overvoltage at the Kingscourt 400 kV and 220kV buses (phase to earth).
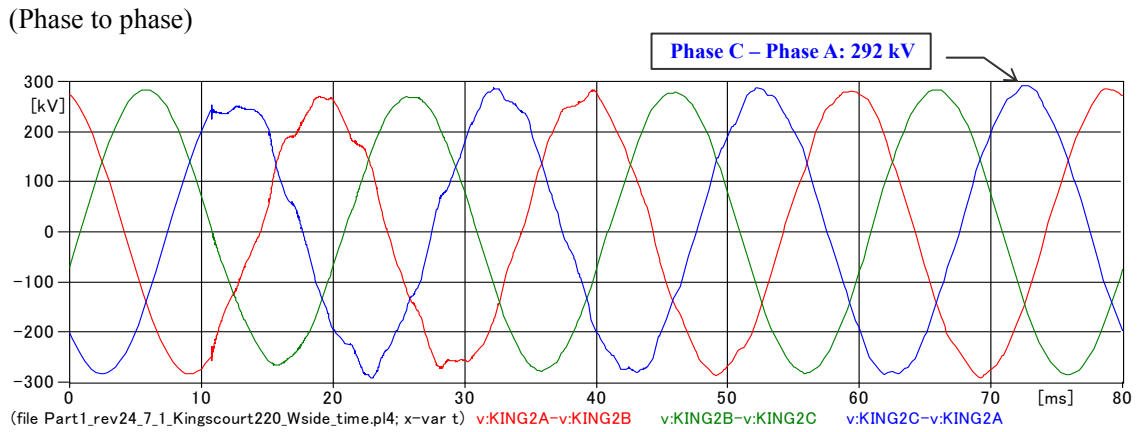
(Phase to phase)

Fig. 4-47 Waveforms of the overvoltage at the Kingscourt 220kV bus (phase to phase).

4.2 Parallel Resonance Overvoltage

In EHV systems, the highest concern in terms of parallel resonance is the second harmonic current injection due to transformer inrush.   Parallel resonance frequencies will be found from the results of frequency scan in EMTP.

When the EHV underground cable has significant length, the switching overvoltage caused by its energisation can have very low frequency components for switching overvoltage.   For example, an energisation of EHV underground cable of a length of around 100 km may largely contain third to fifth harmonics.   Therefore, parallel resonance frequencies higher than 100 Hz (second harmonic) will also be searched for in frequency scan.
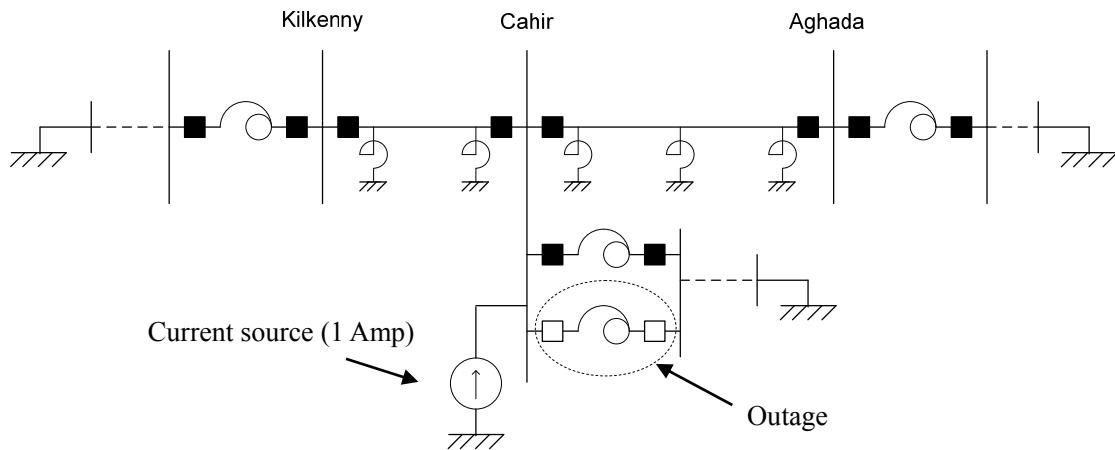
Parallel resonance frequency seen from the Cahir substation for the study of overvoltage caused by transformer inrush current
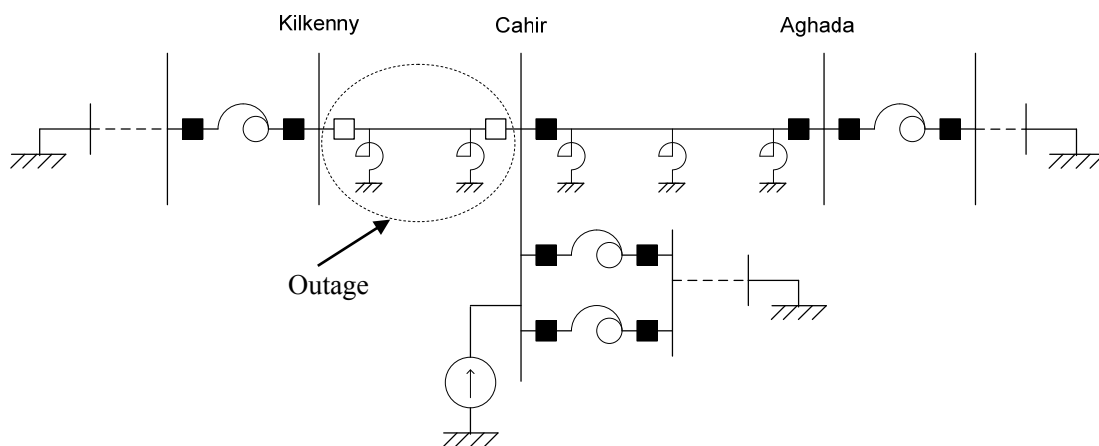
Parallel resonance frequency seen from the Cahir substation for the study of overvoltage caused by underground cable energisation

Fig. 4-48 Frequency scan for the parallel resonance overvoltage analysis.

4.2.1　Fault current level

In the parallel resonance analysis, an effect of the fault current level (source impedance) at Kilkenny 220 kV, Cahir 110 kV, and Aghada 220 kV buses was studied as one of the parameters. First, the fault current calculation was performed at these buses to find the reasonable range for this parameter.　Here, power flow data for the planned transmission system in 2020 were used for the calculation.

The result of the calculation is shown in Table 4-6.　Since it is necessary to find the fault current level in the 220 kV and 110 kV network, fault current that flows from the 400 kV network is not included in the calculation result.　In the table, values of source impedance that correspond to the fault current levels are shown in parentheses.

Table 4-6 Fault Current Levels at Kilkenny, Cahir, and Aghada LV Side Buses

	Original data			Modified data
	Summer off-peak	Winter peak with maximum wind	Normal winter peak	Winter peak with maximum wind
Kilkenny 220 kV	4.38 kA (92.37 mH)	4.65 kA (86.98 mH)	4.80 kA (84.22 mH)	7.16 kA (56.50 mH)
Cahir 110 kV	8.90 kA (22.71 mH)	9.20 kA (21.96 mH)	9.44 kA (21.42 mH)	12.40 kA (16.30 mH)
Aghada 220 kV	5.57 kA (72.52 mH)	9.46 kA (42.75 mH)	11.93 kA (33.89 mH)	9.87 kA (40.97 mH)

Actual generators are not included in the simulation model, and fault current levels were adjusted by adding dummy sources with different source impedance values.　Based on the fault current calculation result, the source impedance values were varied as shown in the ranges below.

Table 4-7 Assumed Range of Source Impedance Values

Kilkenny 220 kV	50 – 100 mH
Cahir 110 kV	15 – 25 mH
Aghada 220 kV	20 – 90 mH

4.2.2   Overvoltage caused by transformer inrush current

Overvoltage caused by transformer inrush current will be studied with the switching scenario shown in Fig. 4-49.
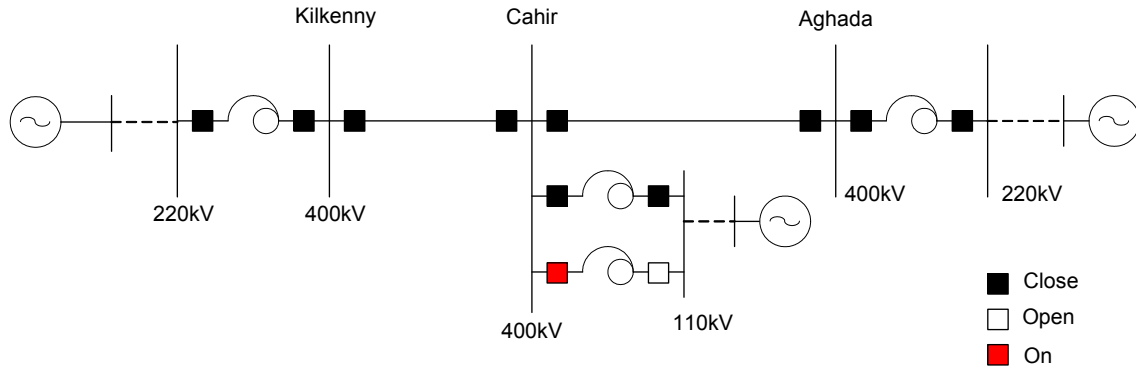
Fig. 4-49 Switching scenario for the overvoltage caused by transformer inrush current.

4.2.3   Parallel resonance frequency seen from Cahir 400 kV

Parallel resonance frequency of the network seen from Cahir 400 kV was found by frequency scan using the simulation model in Fig. 4-50.
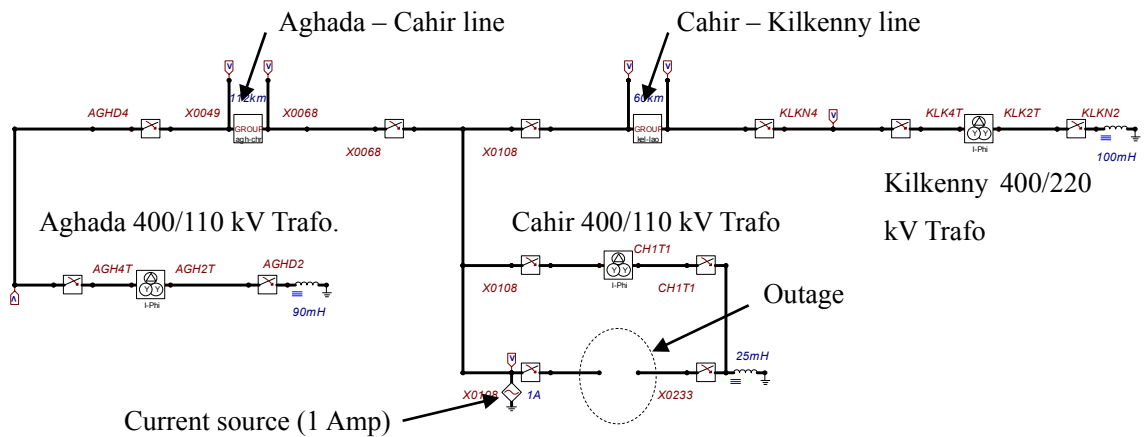
Fig. 4-50 Frequency scan for the parallel resonance overvoltage analysis.

In the first example, the largest source impedance (lowest fault current level) in Table 4-7 was set to Kilkenny 220 kV, Cahir 110 kV, and Aghada 220 kV buses.   The result of this frequency scan is shown in Fig. 4-51.   The highest peak was found at 75 Hz, and the other high peaks were not the level which required careful consideration.
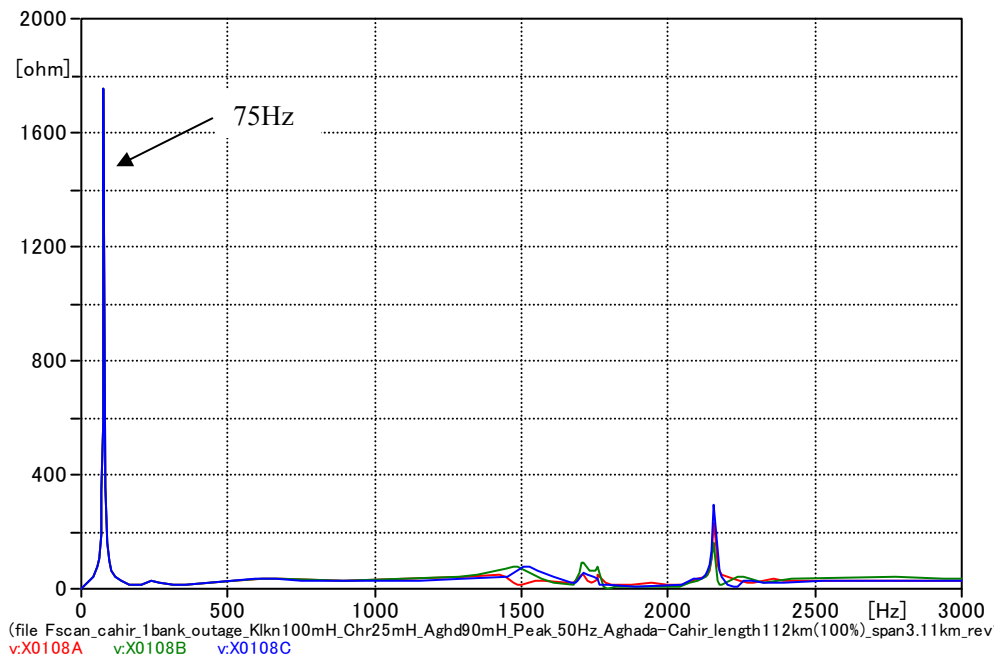
Fig. 4-51 Parallel resonance frequency of the network seen from Cahir 400 kV.

In deriving parallel resonance frequencies in Fig. 4-51, 220 and 110 kV cable capacitances were not considered. In order to study the effect of 220 kV cable capacitances, frequency scan was repeated with different shunt capacitances connected to the Aghada 220 kV bus.
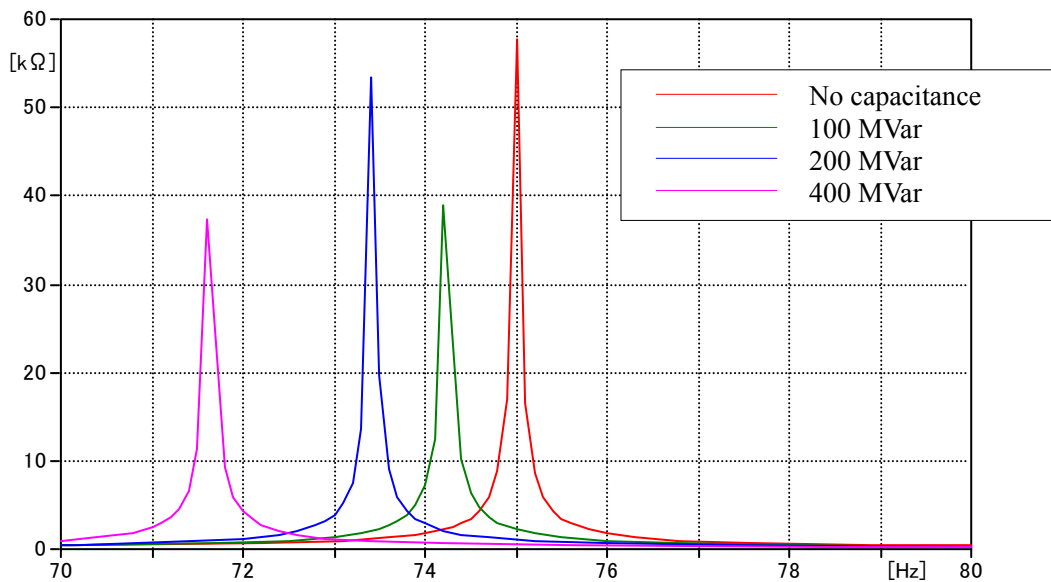
Fig. 4-52 Effect of shunt capacitance connected to the Aghada 220 kV bus.

As can be seen from Fig. 4-52, parallel resonance frequency goes away from 100 Hz when 220 kV cable capacitances are considered, which makes it difficult to have parallel resonance

frequency at 100 Hz. In addition, equivalent impedance of the network at parallel resonance frequency does not rise due to the connection of shunt capacitance.

In order to find an effect of the source impedance, the source impedance connected to Kilkenny 220 kV bus was reduced from 100 mH to 75 mH or 50mH, the source impedance connected to Cahir 110 kV bus was reduced from 25 mH to 10 mH or 15 mH, the source impedance connected to Aghada 220 kV bus was reduced from 90 mH to 55 mH or 20 mH.

Table 4-8 Effect of Source Impedance

Kilkenny 220 kV	Cahir 110 kV	Aghada 220 kV	Parallel resonance frequency [Hz]	Difference [Hz]
100 mH			75.0	-
75 mH	25 mH	90 mH	76.5	+1.5
50 mH			78.7	+3.7
	25 mH		75.0	-
100 mH	20 mH	90 mH	75.6	+0.6
	15 mH		76.4	+1.4
		90 mH	75.0	-
100 mH	25 mH	55 mH	77.8	+2.8
		20 mH	83.0	+8.0
50 mH	15 mH	20 mH	88.0	+13.0

Table 4-8 shows the effect of the source impedance. By changing the source impedance from the largest values to the smallest values, parallel resonance frequency was shifted by 13.0 Hz. The result of frequency scan is shown in Fig. 4-53. It can be seen that the magnitude of impedance at parallel resonance significantly decreases for smaller source impedance (a higher fault current level).
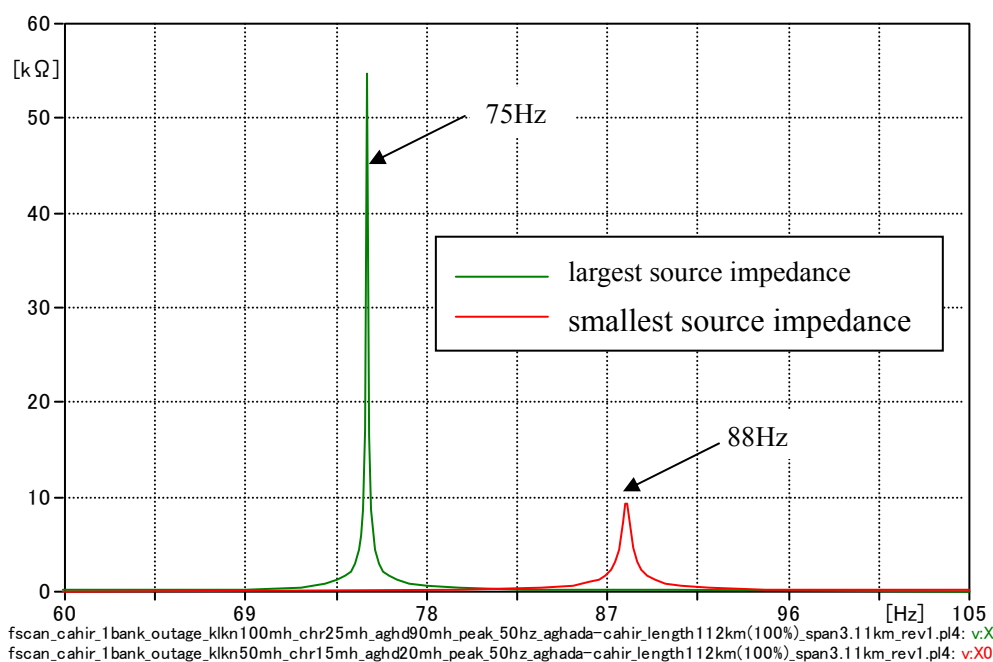
Fig. 4-53 Effect of the source impedance on parallel resonance frequency of the network seen from Cahir 400 kV.

Then, in order to find the effect of the cable length, the length of the 400 kV Aghada – Cahir line was varied from 50 % to 200 % by 25 % steps. In this analysis, the compensation rate of cables was maintained at the same values as that of the original cable length.

Table 4-9 Effect of the Length of 400 kV Aghada-Cahir Cable.

Length [km]	Span length [km]	Number of major cross bonding sections	Shunt reactor [MVA]	Parallel resonance frequency [Hz]	Difference [Hz]
57 (50%)	3.111	6	680	85.4	+10.4
84 (75%)	2.333	12	1020	79.4	+4.4
112 (100%)	3.111	12	1360	75.0	-
140 (125%)	2.333	20	1700	71.7	-3.3
168 (150%)	2.333	24	2040	68.9	-6.1
196 (175%)	2.333	28	2380	66.7	-8.3
224 (200%)	2.333	32	2720	64.8	-10.2

Table 4-9 shows the effect of the cable length.   By increasing the cable length from 100 % to 200 %, parallel resonance frequency was increased by 10.2 Hz.   By decreasing the cable length from 100 % to 50 %, parallel resonance frequency was decreased by 10.4 Hz.

The result of frequency scan is shown in Fig. 4-54.   It can be seen that the magnitude of impedance at parallel resonance frequency significantly decreases for longer cable length because the impedance of the shunt reactor is smaller for the larger capacity of the shunt reactor.

fscan_cahir_1bank_outage_klkn100mh_chr25mh_aghd90mh_peak_50hz_aghada-cahir_length112km(100%)_span3.11km_rev1.pl4: v:X
fscan_cahir_1bank_outage_peak_50hz_aghada-cahir_length56km(50%)_span3.11km_rev1.pl4: v:X0094A
fscan_cahir_1bank_outage_peak_50hz_aghada-cahir_length224km(200%)_span3.11km_rev1.pl4: v:X0142A
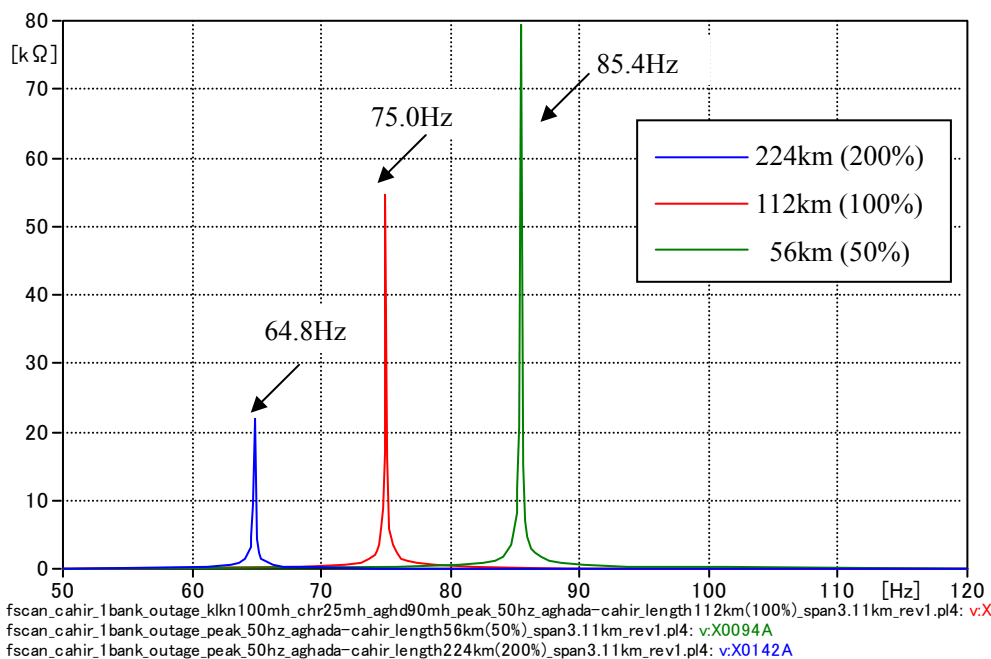
Fig. 4-54 Effect of the length of the 400 kV Aghada – Cahir line.

Then, in order to find an effect of the compensation rate of the Aghada – Cahir line, the compensation rate was varied from 71.1 % to 130.4 % by changing the unit number of shunt reactors.

Table 4-10 Effect of the Compensation Rate of 400 kV Aghada-Cahir Cable.

Cable length	Shunt reactor [MVA]	Compensation Rate [%]	Parallel Resonance Frequency [Hz]	Difference [Hz]
56 km	480	71.1	83.4	-2.0
	580	85.9	84.4	-1.0
	680	100.7	85.4	-
	780	115.5	86.4	+1.0
	880	130.4	87.4	+2.0

	960	71.1	71.9	-3.1
	1160	85.9	73.5	-1.5
112 km	1360	100.7	75.0	-
	1560	115.5	76.5	+1.5
	1760	130.4	77.9	+2.9
	1920	71.1	60.8	-4.0
	2320	85.9	62.9	-1.9
224 km	2720	100.7	64.8	-
	3120	115.5	66.6	+1.8
	3520	130.4	68.2	+3.4

Table 4-10 shows the effect of the compensation rate. When cable length was 112 km, by decreasing the compensation rate from 100.7 % to 71.1 %, parallel resonance frequency was decreased by 3.1 Hz. In contrast, by increasing the compensation rate from 100.7 % to 130.4 %, parallel resonance frequency was increased by 2.9 Hz.

In order to yield parallel resonance frequency at 100 Hz, the length of the 400 kV Aghada – Cahir line and source impedance at Kilkenny 220 kV bus, Cahir 110 kV bus and Aghada 220 kV bus were adjusted. The values of the cable length and source impedance are shown in Table 4-11, together with the magnitude of impedance at parallel resonance frequency.

Table 4-11 Magnitude of impedance at parallel resonance frequency (Cahir)

Cable length [km]	Source impedance [mH]			Compensation rate [%]	Magnitude of impedance
	Kilkenny 220 kV	Cahir 110 kV	Aghada 220 kV		
56 (50%)	50	15	31	100.7	19631 Ω

Then, the time domain simulation was carried out with the assumed most severe condition. Transformer energisation was simulated at switch timings between 10 ms and 30 ms by 0.56 ms steps in order to find the most critical switch timing. The step of 0.56 ms corresponds to the step of 10 degrees in the phase angle. The result of the analysis is summarized in Table 4-12.

In the simulation, residual flux (+85% in Phase A, -85% in Phase B and no residual flux in Phase C) was included in the model. It is very pessimistic, but 80 – 85 % is a typical assumption in Japan.

Table 4-12 Highest Overvoltage for Different Switch Timings

Switch timing		Highest overvoltage [kV]			Switch timing		Highest overvoltage [kV]		
[ms]	[deg]	Phase A	Phase B	Phase C	[ms]	[deg]	Phase A	Phase B	Phase C
10.00	-	589.7	440.9	589.1	20.00	+180	643.3	**871.7**	557.7
10.56	+10	558.0	439.5	622.7	20.56	+190	611.2	629.8	497.0
11.11	+20	521.8	445.5	641.0	21.11	+200	509.1	427.5	473.9
11.67	+30	493.1	457.2	670.7	21.67	+210	340.2	340.0	361.4
12.22	+40	480.6	470.3	710.4	22.22	+220	333.2	334.5	335.8
12.78	+50	472.7	483.0	745.7	22.78	+230	333.2	333.4	334.4
13.33	+60	474.7	498.0	772.7	23.33	+240	333.2	333.4	334.4
13.89	+70	467.6	503.5	**777.5**	23.89	+250	333.2	333.4	334.8
14.44	+80	450.6	495.6	728.0	24.44	+260	334.5	337.1	342.4
15.00	+90	438.2	498.6	664.4	25.00	+270	384.2	401.1	506.8
15.56	+100	434.4	498.5	617.4	25.56	+280	512.5	427.4	561.9
16.11	+110	435.4	545.5	612.1	26.11	+290	725.2	481.0	584.2
16.67	+120	439.3	600.7	586.7	26.67	+300	844.3	565.3	632.3
17.22	+130	447.7	656.7	528.9	27.22	+310	**881.5**	563.5	649.5
17.78	+140	486.0	734.0	522.8	27.78	+320	863.1	557.0	626.8
18.33	+150	538.4	802.4	548.5	28.33	+330	808.7	529.7	591.0
18.89	+160	576.2	839.7	581.9	28.89	+340	730.5	495.4	573.3
19.44	+170	600.9	867.3	597.6	29.44	+350	633.2	446.7	558.4
					30.00	+360	589.7	440.9	589.4

As can be seen from Table 4-12, the highest overvoltage occurred in Phase A. The voltage of the Cahir 400 kV bus and inrush current into the Cahir 400/110 kV transformer for the switch timing 27.22 ms are shown in Fig. 4-55 and Fig. 4-56.
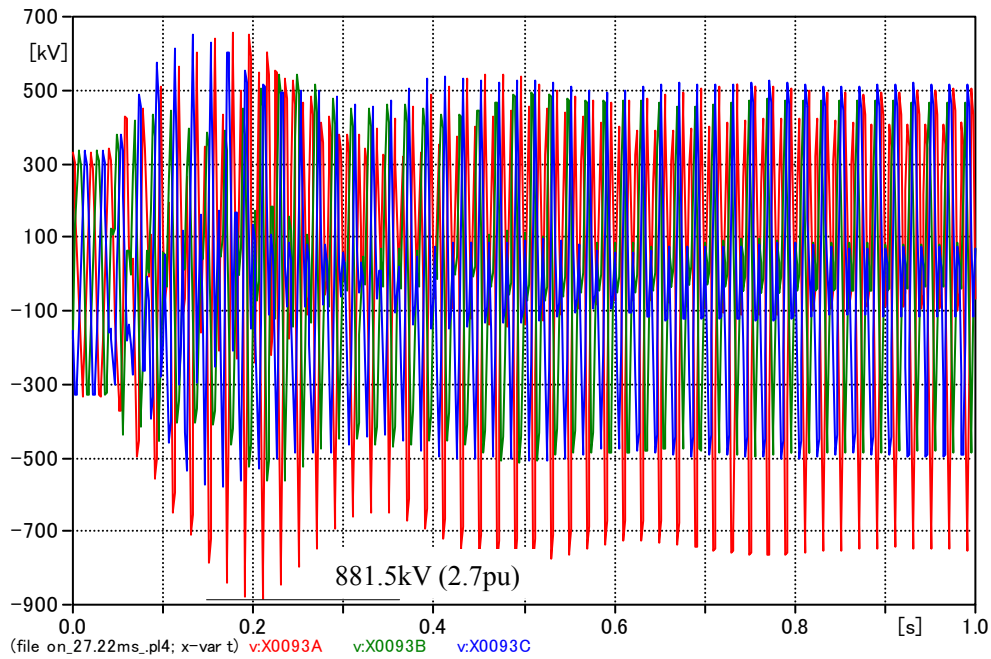
Fig. 4-55 Cahir 400 kV bus voltage in transformer inrush.
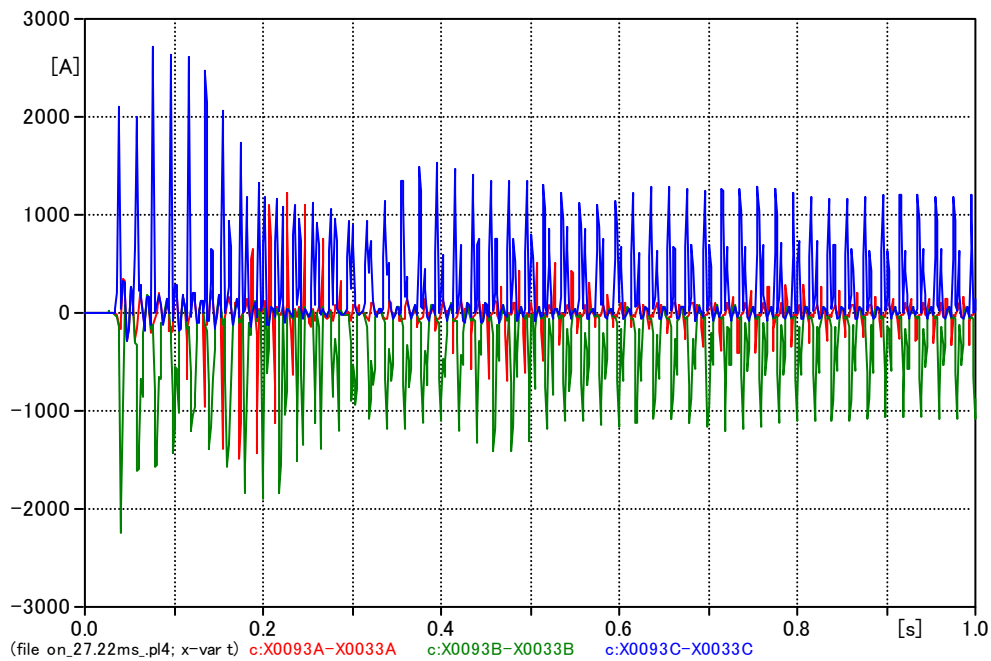
Fig. 4-56 Inrush current into the Cahir 400/110 kV transformer.

Since the observed overvoltage was very high for a temporary overvoltage, it is necessary to evaluate the energy absorption capability of the surge arrester located at the Cahir 400 kV bus. As a result of the analysis as shown in Fig. 4-57 and Fig. 4-58, it was confirmed that the energy absorption exceeded the capability of the surge arrester.
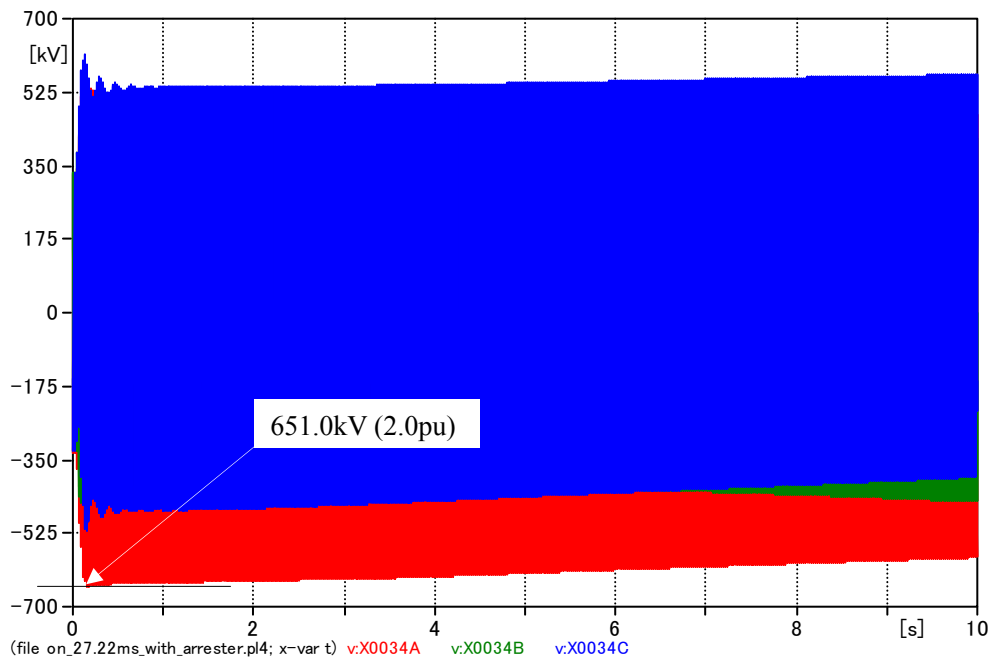
Fig. 4-57 Cahir 400 kV bus voltage in transformer inrush with a surge arrester.
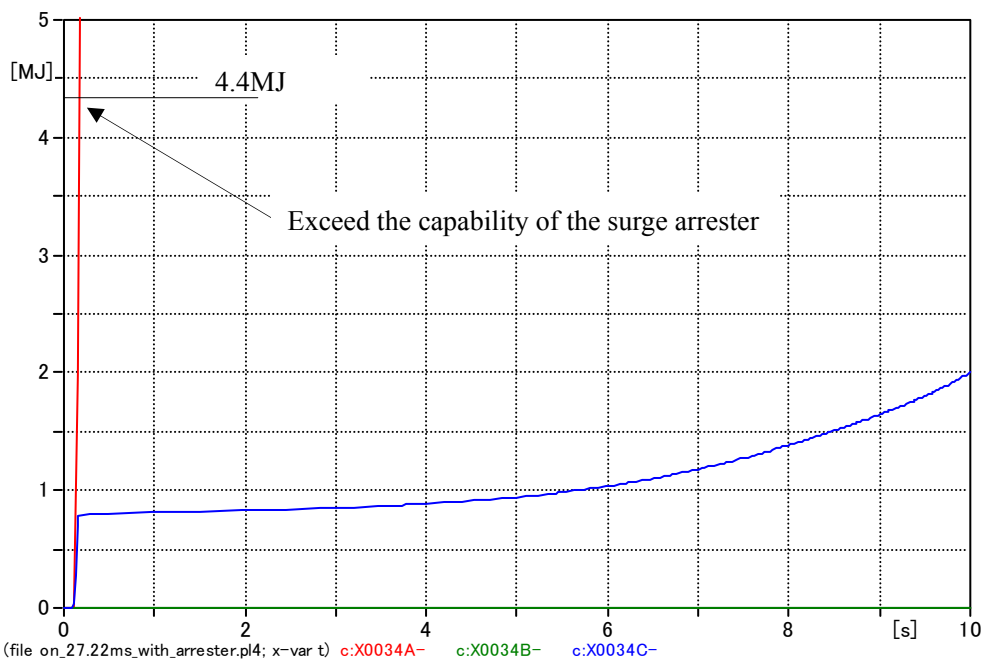
Fig. 4-58 Energy absorbed by the surge arrester.

The result of the analysis was evaluated against the energy absorption capability of the surge arrester with line discharge class 3, but the evaluation is assumed to be almost equivalent for the Class 4 or 5 surge arresters.

4.2.4 Effect of hysteresis curve

Saturation characteristic of a 400/275/13 kV 750 MVA transformer in the National Grid was provided from the NIE/EirGrid. The same saturation characteristic was assumed for the Cahir 400/110 kV transformer.

Table 4-13 Saturation Characteristic of the 400 kV Transformer (defined in primary)

I [A]	Phi [Wb-T]	Pu
0.04333	917.29	0.88
0.10053	978.44	0.94
0.18373	1039.60	1.00
0.40733	1100.75	1.06
1.15267	1161.90	1.12
3.51000	1223.05	1.18
7.97333	1284.21	1.24
117.59789	1467.66	1.41

For transformer inrush studies, the magnetizing branch hysteresis curve was derived from the saturation characteristics in Table 4-13 using the subroutine HYSDAT. The lower half of the obtained hysteresis curve is shown in Table 4-14. The analysis with the original hysteresis curve is a severe assumption because of the larger inrush current.

Table 4-14 Hysteresis Curve of the 400 kV Transformer (defined in primary)

Original data		Another data	
Derived from the characteristic at 1.41pu		Derived from the characteristic at 1.24pu	
I [A]	Phi [Wb-T]	I [A]	Phi [Wb-T]
-29.4000	-1424.49	-1.9933	-1246.439
-3.6750	-1349.38	-0.2492	-1180.72
2.2050	-1243.19	0.1495	-1087.80
5.1450	-966.929	0.3488	-846.07
9.9225	837.430	0.6727	732.76
15.4350	1105.06	1.0465	966.93
26.4600	1269.09	1.7940	1110.46
48.8775	1381.33	3.3139	1208.67
117.6000	1467.66	7.9733	1284.21
161.7000	1476.29	10.9633	1291.76

In order to find an effect of the hysteresis curve of the transformer, the same analysis was performed with another hysteresis curve in Table 4-14. The results of this analysis are summarized in Table 4-15.

Table 4-15 Highest Overvoltage for Different Switch Timings

Switch timing		Highest over voltage [kV]			Switch timing		Highest over voltage [kV]		
[ms]	[deg]	Phase A	Phase B	Phase C	[ms]	[deg]	Phase A	Phase B	Phase C
10.00	-	**549.9**	453.7	572.4	20.00	+180	504.3	438.0	460.8
10.56	+10	546.4	454.9	562.4	20.56	+190	459.1	415.6	450.4
11.11	+20	532.0	461.4	544.6	21.11	+200	402.9	390.8	430.3
11.67	+30	506.4	472.8	515.6	21.67	+210	351.0	365.6	402.3
12.22	+40	470.3	490.1	474.7	22.22	+220	345.8	341.7	365.5
12.78	+50	429.5	511.7	429.9	22.78	+230	333.2	333.4	334.4
13.33	+60	392.2	527.8	446.4	23.33	+240	333.2	333.4	334.4
13.89	+70	388.2	531.5	449.2	23.89	+250	333.2	333.4	334.4
14.44	+80	387.3	548.3	473.8	24.44	+260	341.2	335.6	348.9
15.00	+90	400.7	577.5	528.8	25.00	+270	361.6	361.3	387.8
15.56	+100	410.5	**590.4**	548.4	25.56	+280	385.8	396.8	419.9
16.11	+110	426.6	587.8	554.8	26.11	+290	409.4	432.0	455.3
16.67	+120	451.5	571.1	551.0	26.67	+300	430.3	456.3	493.0
17.22	+130	482.0	551.6	540.1	27.22	+310	446.1	464.0	518.7
17.78	+140	510.8	526.9	519.6	27.78	+320	454.7	461.6	531.2
18.33	+150	532.7	500.1	495.3	28.33	+330	462.2	453.0	537.8
18.89	+160	540.8	464.4	480.9	28.89	+340	514.1	452.8	560.9
19.44	+170	529.4	451.4	470.6	29.44	+350	542.7	456.0	**573.2**
					30.00	+360	**549.9**	453.7	572.4

As can be seen from Table 4-15, the highest overvoltage occurred in Phase B. The voltage of the Cahir 400 kV bus and inrush current into the Cahir 400/110 kV transformer for the switch timing 15.56 ms are shown in Fig. 4-59 and Fig. 4-60.
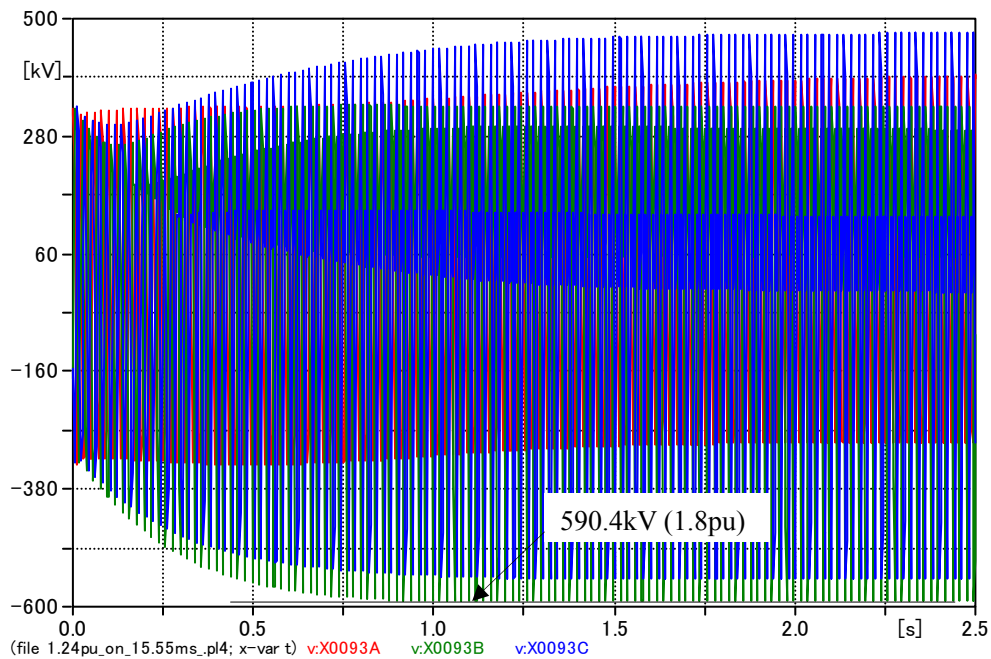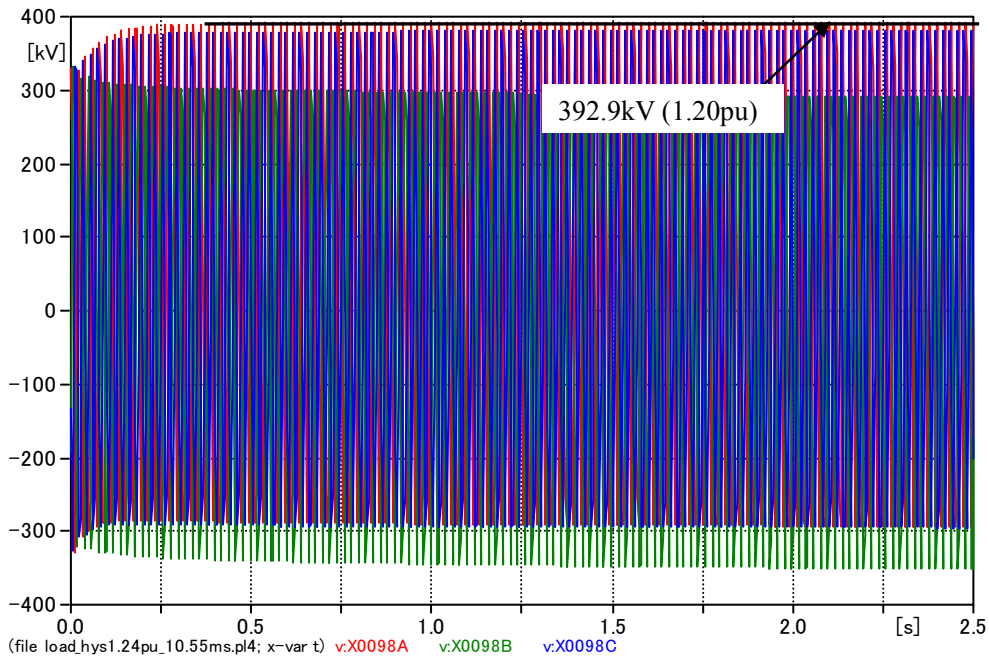
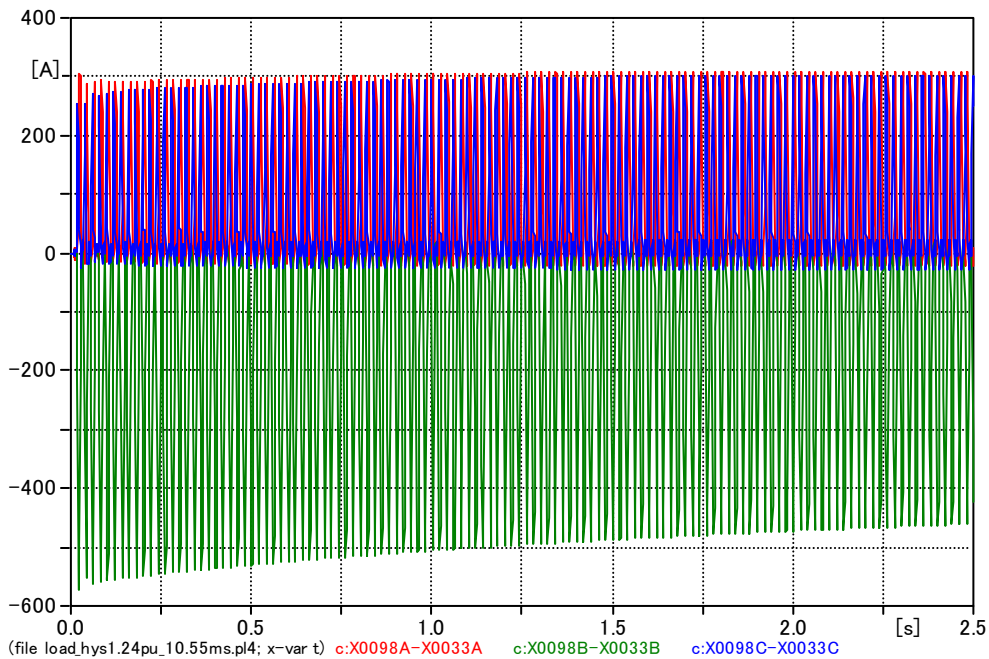**Fig. 4-59 Cahir 400 kV bus voltage in transformer inrush.**
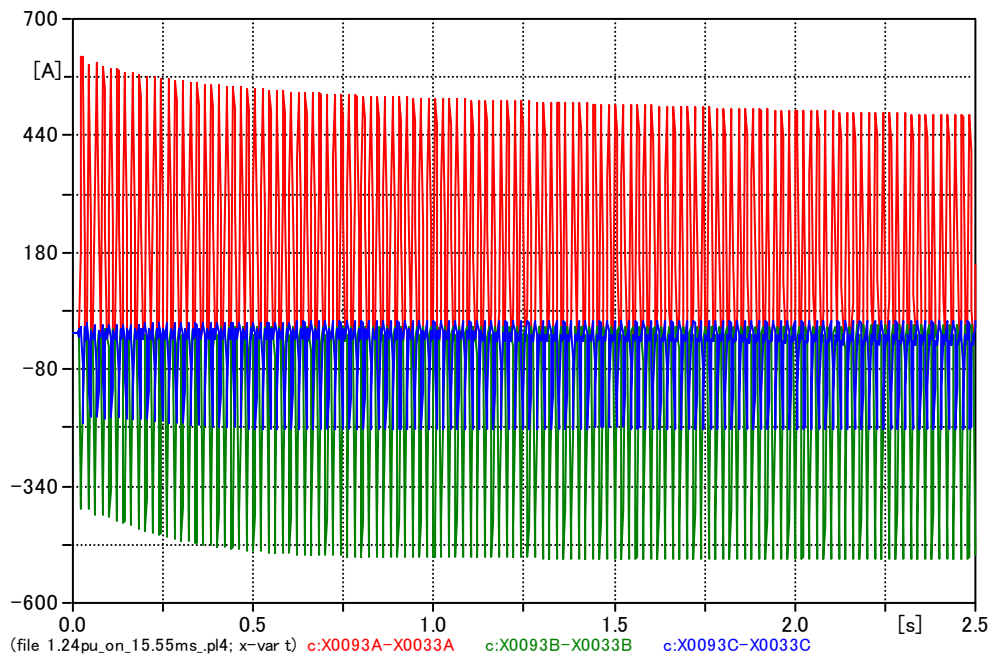
Fig. 4-60 Inrush current into the Cahir 400/110 kV transformer.

Since the observed overvoltage was very high for a temporary overvoltage, it is necessary to evaluate the energy absorption capability of the surge arrester located at the Cahir 400 kV bus.   As a result of the analysis as shown in Fig. 4-61 and Fig. 4-62, it was confirmed that the energy absorption exceeded the capability of the surge arrester.
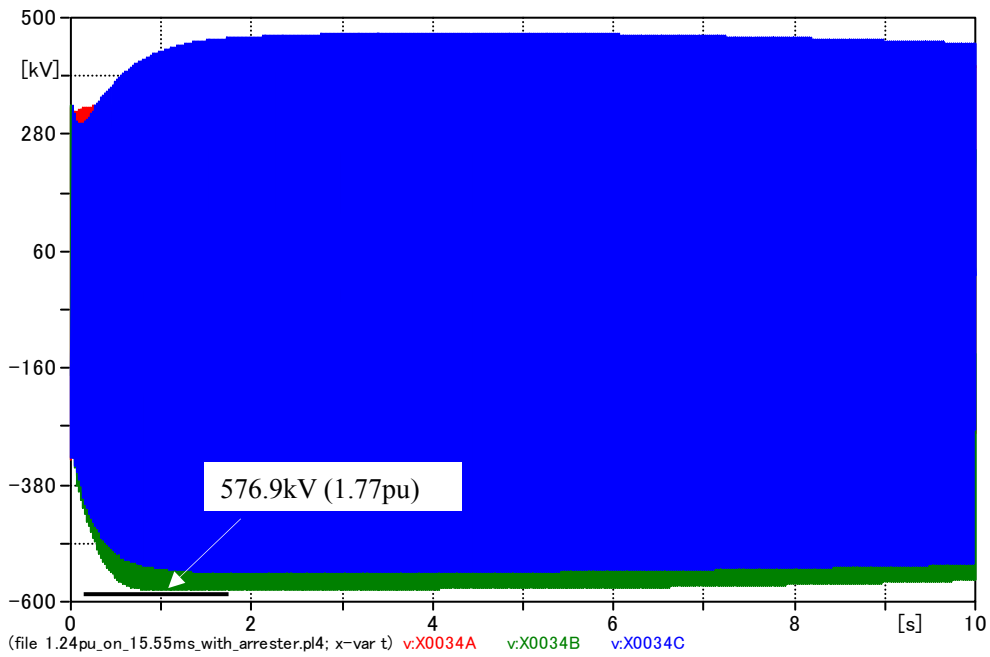
Fig. 4-61 Cahir 400 kV bus voltage in transformer inrush with a surge arrester.
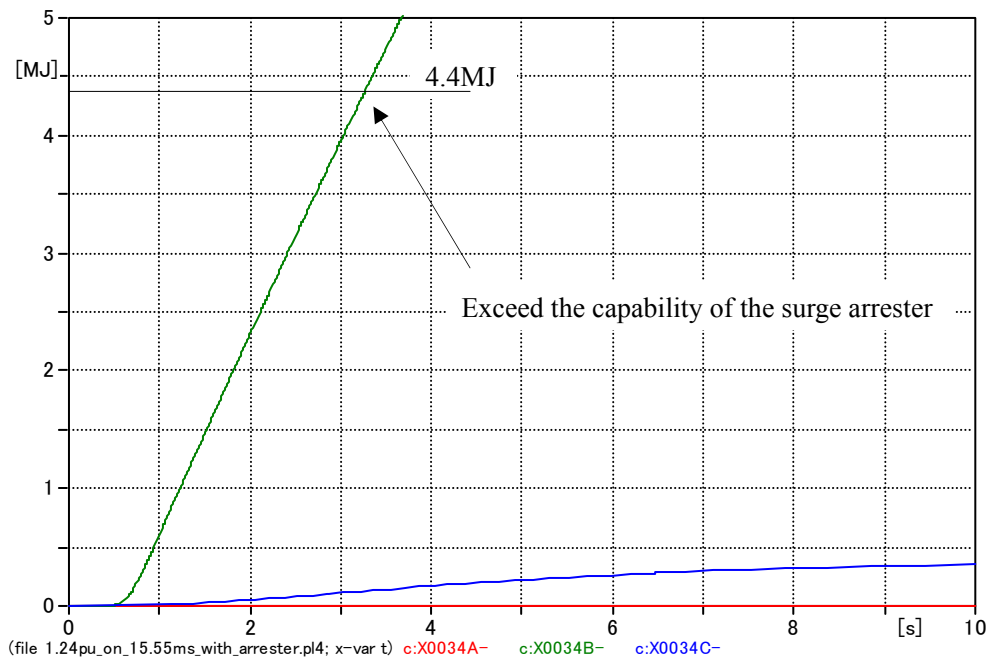
Fig. 4-62 Energy absorbed by the surge arrester.

4.2.5   Effect of loads

As the most severe condition, the simulation model for the transient overvoltage analysis around the Kilkenny – Cahir – Aghada line was built without load models, which is a typical assumption when building a small model for the transient overvoltage analysis.   In order to find an effect of the load models, the same analysis was performed with load models.
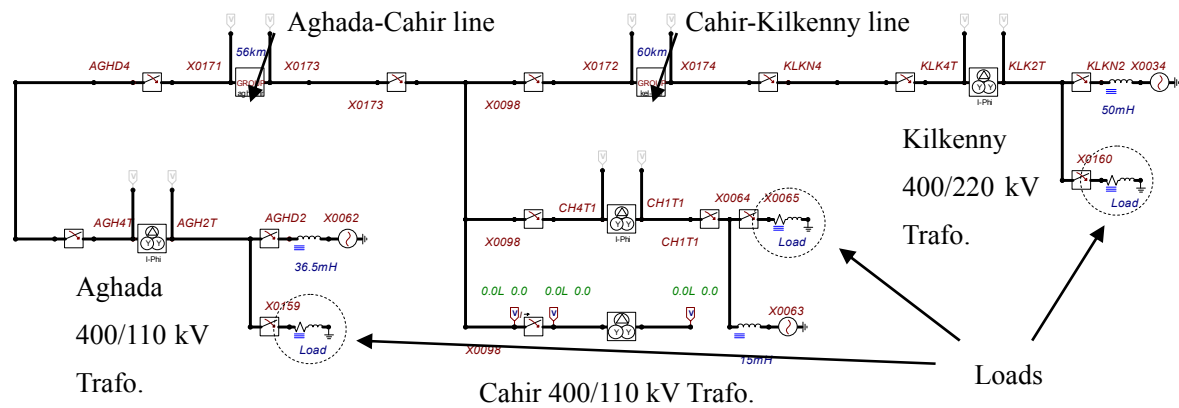
Fig. 4-63 Load models added to the ATP-Draw data.

The load models connected to the Kilkenny, Cahir, and Aghada LV side buses are shown in Table 4-22.   These load models are based on power flow data in summer off-peak demand for the planned transmission system in 2020.

Table 4-16 Loads at Kilkenny, Cahir, and Aghada LV Side Buses

	P [MW]	Q [MVar]	R[ohm]	X [mH]	Area Number	Area Name
Kilkenny 220 kV	181.0	41.8	253.9	186.7	6	SE
Cahir 110 kV	205.5	59.5	54.3	50.0	5	CAHIR NETW
Aghada 220 kV	308.4	88.3	145.0	132.1	3	CORK KERRY

The parallel resonance frequency of the network seen from Cahir 400 kV was changed by connecting the load models.   In order to yield parallel resonance frequency at 100 Hz, values of source impedance at Kilkenny 220 kV bus, Cahir 110 kV bus and Aghada 220 kV bus were adjusted.   The values of the source impedance and the magnitude of impedance at parallel resonance frequency are shown in Table 4-17.

Table 4-17 Magnitude of Impedance at Parallel Resonance Frequency (Cahir)

Cable length [km]	Source impedance [mH]			Compensation rate [%]	Magnitude of impedance
	Kilkenny 220 kV	Cahir 110 kV	Aghada 220 kV		
56 (50%)	50	15	36.5	100.7	1604Ω

As can be seen from Table 4-17, the magnitude of impedance was significantly decreased from 19631 Ω in Table 4-11 to 1604 Ω by the addition of the load models.

Next, time domain simulation was carried out with the load models. The result of the analysis is summarized in Table 4-18.

Table 4-18 Highest Overvoltage for Different Switch Timings

Switch timing		Highest over voltage [kV]			Switch timing		Highest over voltage [kV]		
[ms]	[deg]	Phase A	Phase B	Phase C	[ms]	[deg]	Phase A	Phase B	Phase C
10.00	-	495.8	415.2	491.5	20.00	+180	505.9	591.3	422.6
10.56	+10	492.7	420.6	514.5	20.56	+190	491.1	508.2	427.8
11.11	+20	482.6	429.4	528.3	21.11	+200	451.8	419.6	419.9
11.67	+30	452.7	439.1	537.3	21.67	+210	377.8	356.1	404.0
12.22	+40	428.7	449.0	555.3	22.22	+220	333.8	332.3	351.2
12.78	+50	426.3	459.0	577.2	22.78	+230	330.5	330.8	331.4
13.33	+60	419.3	469.7	599.2	23.33	+240	330.5	330.8	331.4
13.89	+70	414.0	475.9	**612.4**	23.89	+250	330.5	330.8	331.4
14.44	+80	412.9	476.2	608.9	24.44	+260	330.5	330.8	331.4
15.00	+90	404.6	467.5	574.0	25.00	+270	331.3	331.1	338.7
15.56	+100	403.9	463.7	533.5	25.56	+280	352.2	356.8	405.3
16.11	+110	408.7	471.8	509.7	26.11	+290	397.2	393.8	442.6
16.67	+120	414.7	493.1	510.2	26.67	+300	496.0	416.5	475.4
17.22	+130	423.9	528.8	485.8	27.22	+310	572.0	424.6	506.0
17.78	+140	437.1	559.6	462.0	27.78	+320	617.5	428.2	511.2
18.33	+150	471.0	588.4	452.9	28.33	+330	**634.5**	424.6	506.4
18.89	+160	500.1	614.7	455.2	28.89	+340	615.3	413.3	495.6
19.44	+170	506.5	**621.2**	445.1	29.44	+350	552.2	414.1	485.3
					30.00	+360	495.7	415.3	491.9

As can be seen from Table 4-18, the highest overvoltage occurred in Phase A.   The voltage of the Cahir 400 kV bus and inrush current into the Cahir 400/110 kV transformer for the switch timing 28.33 ms are shown in Fig. 4-64 and Fig. 4-65.
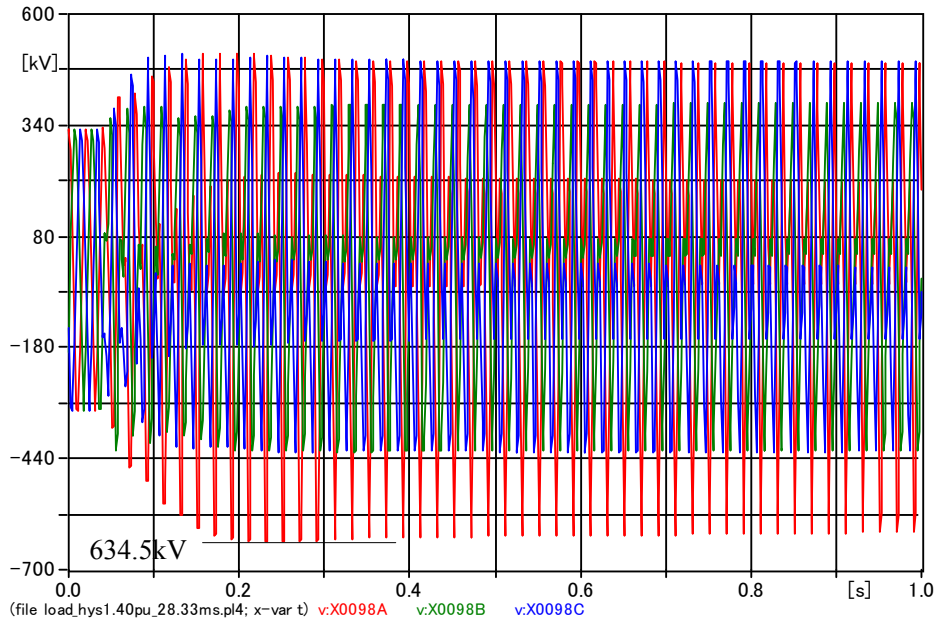
Fig. 4-64 Cahir 400 kV bus voltage in transformer inrush.
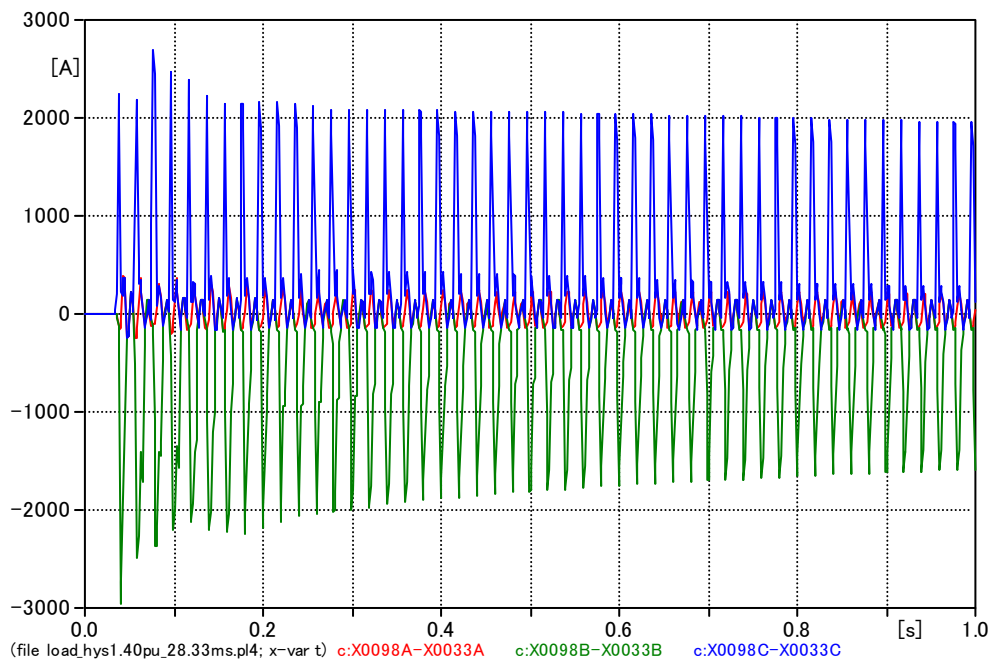
Fig. 4-65 Inrush current into the Cahir 400/110 kV transformer.

Since the observed overvoltage was very high for temporary overvoltage, it is necessary to evaluate the energy absorption capability of the surge arrester located at the Cahir 400 kV bus. As a result of the analysis shown in Fig. 4-66 and Fig. 4-67, it was confirmed that the energy absorption exceeded the capability of the surge arrester.
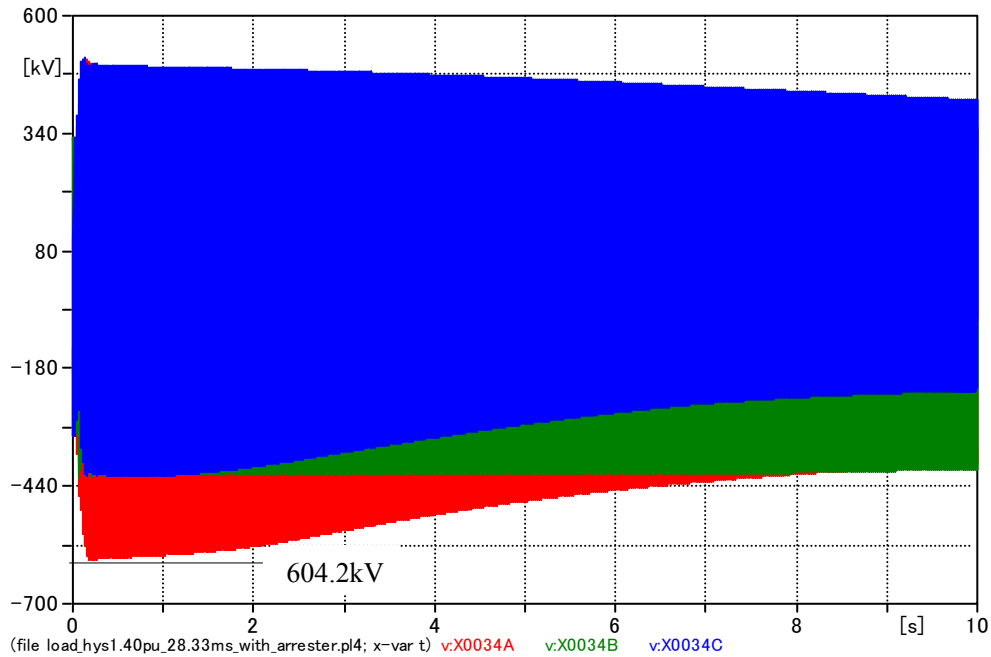
Fig. 4-66 Cahir 400 kV bus voltage in transformer inrush with a surge arrester.
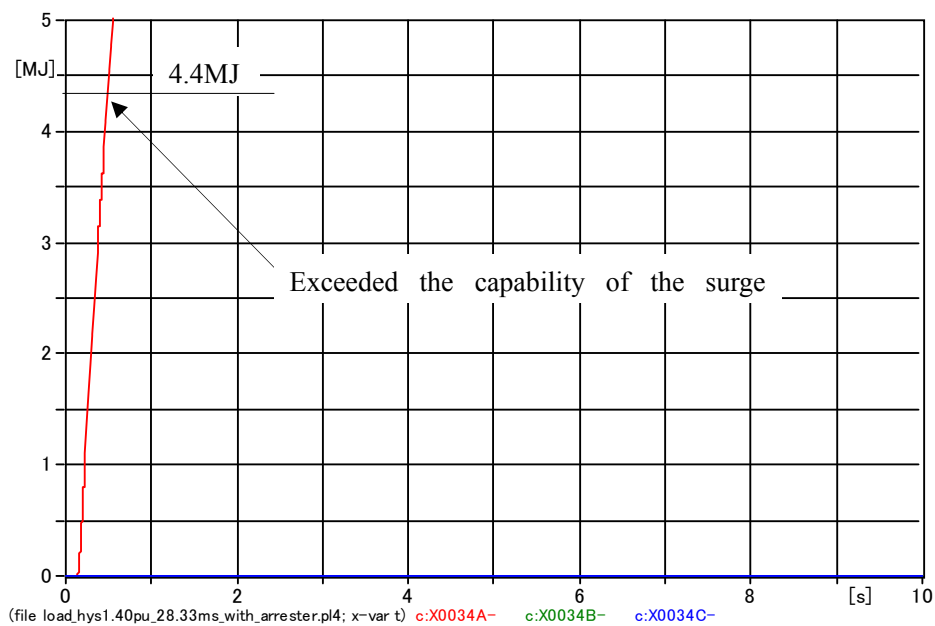
Fig. 4-67 Energy absorbed by the surge arrester.

Finally, the same analysis was performed with another hysteresis curve in Table 4-14. The results of the analysis are summarized in Table 4-19.

Table 4-19 Highest Overvoltage for Different Switch Timings

Switch timing		Highest over voltage [kV]			Switch timing		Highest over voltage [kV]		
[ms]	[deg]	Phase A	Phase B	Phase C	[ms]	[deg]	Phase A	Phase B	Phase C
10.00	-	388.6	358.8	380.7	20.00	+180	356.3	345.5	364.4
10.56	+10	**392.9**	356.3	380.2	20.56	+190	346.4	340.0	359.6
11.11	+20	392.3	355.2	375.8	21.11	+200	338.0	335.2	352.2
11.67	+30	388.0	356.2	366.8	21.67	+210	331.9	331.6	342.4
12.22	+40	380.6	359.1	354.4	22.22	+220	330.5	330.8	332.0
12.78	+50	371.1	363.6	339.9	22.78	+230	330.5	330.8	331.4
13.33	+60	363.3	367.1	350.5	23.33	+240	330.5	330.8	331.4
13.89	+70	362.3	367.8	351.2	23.89	+250	330.5	330.8	331.4
14.44	+80	361.1	370.2	354.9	24.44	+260	333.5	332.6	339.8
15.00	+90	356.0	377.4	369.4	25.00	+270	337.9	340.8	348.1
15.56	+100	353.4	383.6	381.6	25.56	+280	342.0	350.0	354.5
16.11	+110	353.2	**387.4**	389.6	26.11	+290	346.0	358.9	359.2
16.67	+120	355.2	384.3	**392.4**	26.67	+300	349.1	367.2	362.7
17.22	+130	359.0	376.0	390.9	27.22	+310	351.1	371.6	365.3
17.78	+140	363.0	364.7	386.7	27.78	+320	353.8	372.0	367.6
18.33	+150	366.3	352.7	381.2	28.33	+330	366.2	366.4	372.5
18.89	+160	370.6	345.4	374.7	28.89	+340	379.0	361.8	377.3
19.44	+170	370.7	352.5	369.1	29.44	+350	388.6	358.8	380.7
					30.00	+360	356.3	345.5	364.4

As can be seen from Table 4-19 the highest overvoltage occurred in Phase A, but it significantly decreases from the effects of hysteresis curve and loads. The voltage of the Cahir 400 kV bus and inrush current into the Cahir 400/110 kV transformer for the switch timing 10.56 ms are shown in Fig. 4-68 and Fig. 4-69.

Fig. 4-68 Cahir 400 kV bus voltage in transformer inrush.

Fig. 4-69 Inrush current into the Cahir 400/110 kV transformer.

Since the observed overvoltage was not high for a temporary overvoltage, it is not necessary to evaluate the energy absorption capability of the surge arrester located at the Cahir 400 kV bus.

4.2.6 Overvoltage caused by line energisation

Overvoltage caused by line energisation was studied with the switching scenario shown in Fig. 4-70.
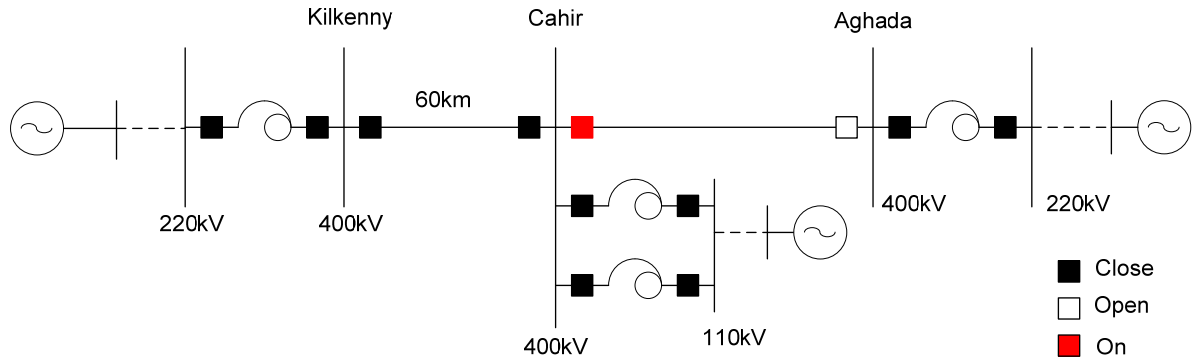
Fig. 4-70 Switching scenario for the overvoltage caused by line energisation.

4.2.7 Parallel resonance frequency seen from Cahir 400 kV

Parallel resonance frequency of the network seen from Cahir 400 kV was found by frequency scan using the simulation model in Fig. 4-71.
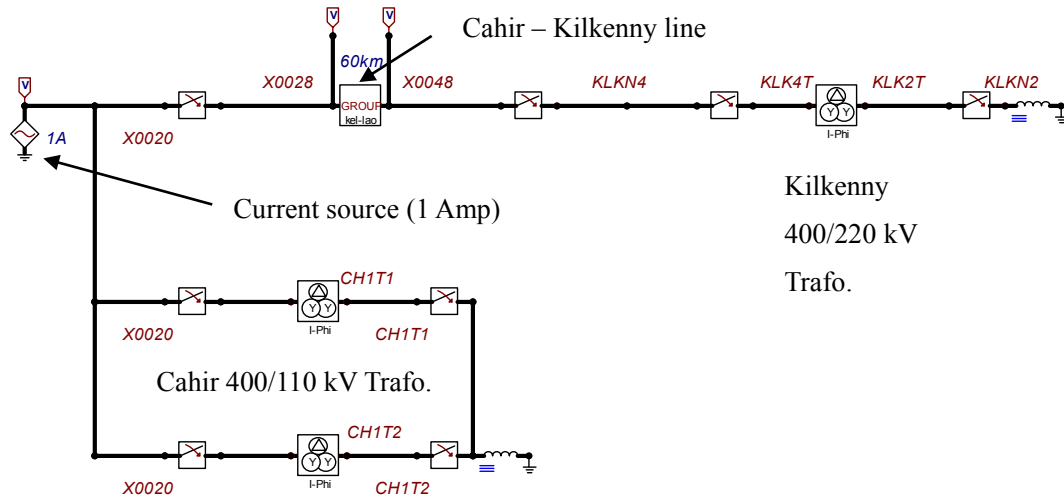
Fig. 4-71 Frequency scan for the parallel resonance overvoltage analysis.

In the first example, the largest source impedance (lowest fault current level) in Table 4-23 was set to Kilkenny 220 kV, Cahir 110 kV, and Aghada 220 kV buses. The result of frequency scan is shown in Fig. 4-72. The highest peak was found at 94.9 Hz, and other high peaks were not the level which required careful consideration.

(file Fscan_Peak_Cahir400kVbus_Chr25mH_Klkn100mH_50Hz_CHR_rev1.pl4; x-var t) v:X0020A v:X0020B v:X0020C
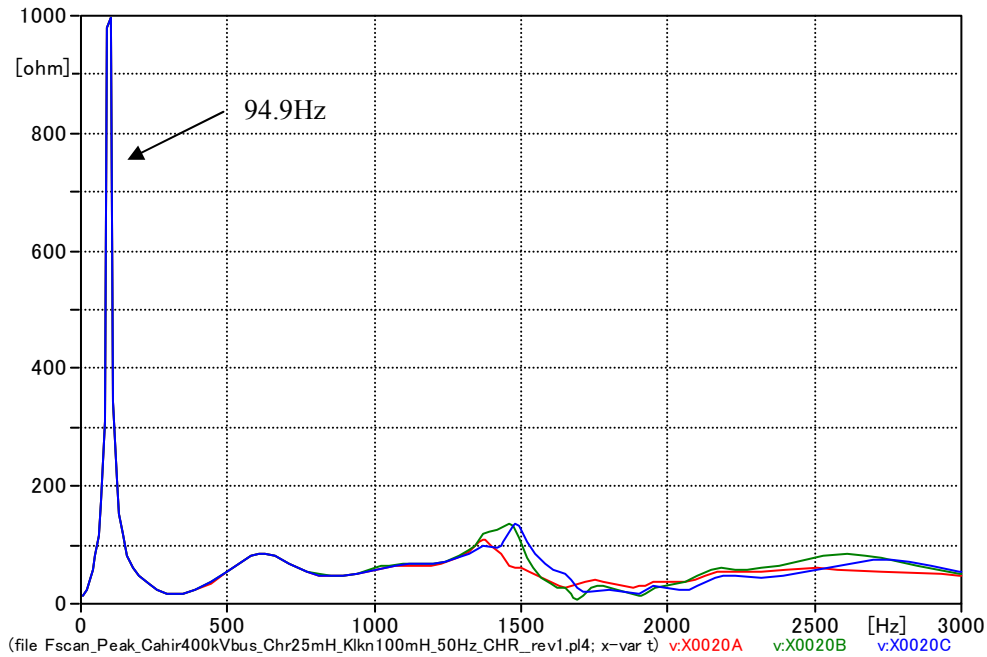
Fig. 4-72 Parallel resonance frequency of the network seen from Cahir 400 kV.

In order to find an effect of the source impedance, the source impedance connected to Kilkenny 220 kV bus was reduced from 100 mH to 75 mH or 50mH, the source impedance connected to Cahir 110 kV bus was reduced from 25 mH to 10 mH or 15mH.

Table 4-20 Effect of Source Impedance

Kilkenny 220 kV	Cahir 110 kV	Parallel resonance frequency [Hz]	Difference [Hz]
100 mH		94.9	-
75 mH	25 mH	98.7	+3.8
50 mH		104.0	+9.1
	25 mH	94.9	-
100 mH	20 mH	97.5	+2.6
	15 mH	100.8	+5.9
50 mH	15 mH	109.4	+14.5

Table 4-20 shows the effect of the source impedance.   By changing the source impedance from the largest values to the smallest values, parallel resonance frequency was shifted by 14.5 Hz

As can be seen from Table 4-20, it is possible to shift parallel resonance frequency to only 100 Hz within the reasonable range of source impedance value at Kilkenny 220 kV and Cahir 110 kV buses.

In this switching scenario shown in Fig. 4-70, the overvoltage is reflected at both ends of the Kilkenny – Cahir – Aghada line.   The reflection does not occur at Cahir 400 kV since the characteristic impedance of the Kilkenny – Cahir line and the Cahir – Aghada line is equal. Theoretical dominant frequency in the 400 kV Cahir – Aghada line energisation is shown in Table 4-21.   In this calculation, propagation velocity was assumed to be 170 m/μs, and the length of the 400 kV Kilkenny – Cahir line was assumed to be 60 km.

Table 4-21 Theoretical Dominant Frequency in the Line Energisation

	50 %	75 %	100 %	125 %	150 %	175 %	200 %
Cahir – Aghada [km]	56	84	112	140	168	196	224
Kilkenny – Aghada [km]	116	144	172	200	228	256	284
Dominant frequency [Hz]	366.4	295.1	247.1	212.5	186.4	166.0	149.6

In order to find an effect of the cable length, line energisation was simulated with three different cable lengths – 56 km (green), 112 km (blue), and 228 km (red).   The switch in front of the voltage source was closed at a voltage peak of Phase A to energise the line.   In this analysis, the compensation rate of cables was maintained at the same value as that of the original cable length.

The voltage at the Cahir 400 kV bus is shown in Fig. 4-73.

energisation_56km(50%)_peak_cahir400kvbus_chr25mh_klkn100mh_50hz_chr_rev1.pl4: v:X0152A
energisation_224km(200%)_peak_cahir400kvbus_chr25mh_klkn100mh_50hz_chr_rev1.pl4: v:X0428A
energisation_peak_cahir400kvbus_chr25mh_klkn100mh_50hz_chr_rev1.pl4: v:X0216A
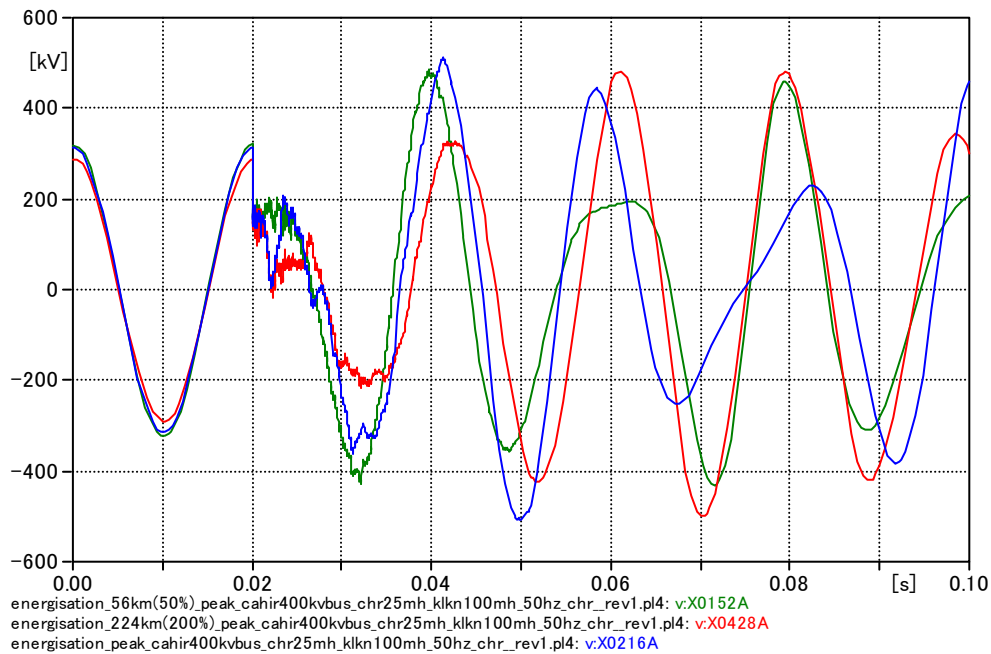
Fig. 4-73 Cahir 400 kV bus voltage in line energisation.

The result of Fourier transform of each curve in Fig. 4-73 is shown in Fig. 4-74. The dominant frequencies in the case of cable length 56 km, 112 km, and 224 km are found to be around 340 Hz, 240 Hz, and 150 Hz respectively. This corresponds to the theoretical dominant frequency calculated.

As can be seen from this result, it is not possible to shift the dominant frequency to 100 Hz within the reasonable range of the length of the 400 kV Aghada – Cahir line.
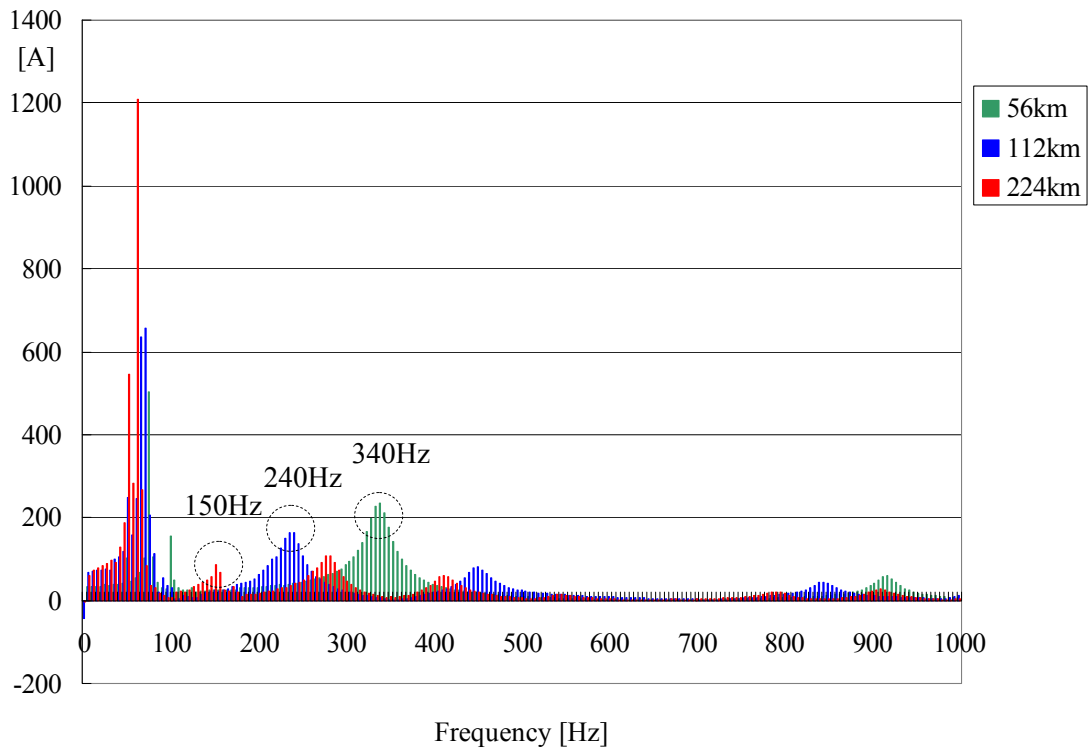
Fig. 4-74 Fourier transform of the line energisation overvoltage.

In summary, it was found that parallel resonance could cause a very high overvoltage that exceeded the withstand voltage of a typical 400 kV surge arrester. The overvoltage occurs in transformer inrush, depending on the network conditions. If the 400 kV Aghada – Cahir – Kilkenny line is built as an underground cable line as studied in this section, careful consideration is necessary before energising a transformer at Aghada, Cahir, and Kilkenny.

4.3 Overvoltage Caused by the System Islanding

When one end of the cable is opened after a three phase fault (load shedding), the oscillatory overvoltage can be caused by the superimposition of overvoltage of two different frequencies.

Resonance frequencies can be calculated by a simple method shown below.   Fig. 4-75 shows impedance and admittance data of the 400 kV Cahir – Kilkenny line and the Kilkenny 400/220 kV transformer.   Impedance and admittance data in this figure is extracted from the PSS/E data set. Xb is assumed to be source impedance and resistances are neglected in the figure.
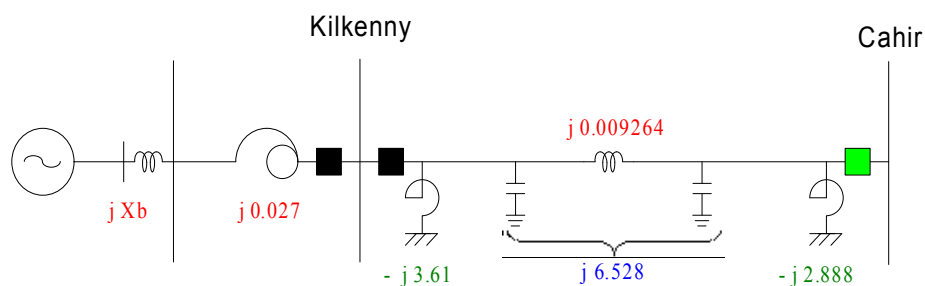
Fig. 4-75 Impedance and admittance of the 400 kV Kilkenny – Cahir line and the Kilkenny 400/220 kV transformer.

The following equations explain that X_0, Y, X can be calculated from data in Fig. 4-75.

$$X_0 = 0.027 + 0.009264 + Xb$$
$$X = (3.61 + 2.888)^{-1} = 0.15389$$
$$Y = 6.528$$

where Xb is a source impedance behind the 220 kV Kilkenny bus.   Resonance frequencies were calculated with the source between 0.02 pu and 0.08 pu using the following equation, and calculated resonance frequencies are shown in Fig. 4-76.

$$\frac{\omega_0}{\omega} = \sqrt{\frac{1}{YX_0} + \frac{1}{YX}}$$

Source impedances behind the 220 kV Kilkenny bus were given by short circuit calculations in PSS/E under the summer off-peak demand and the winter peak demand with maximum windpower.
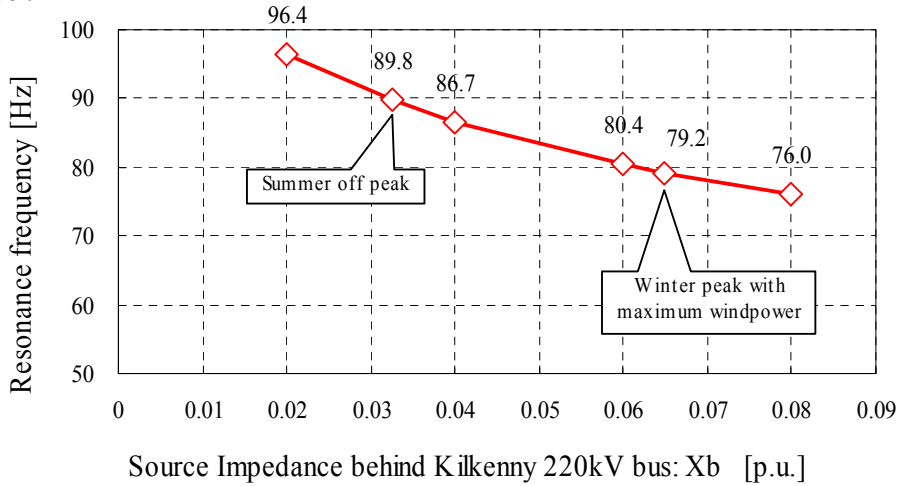
Fig. 4-76 Calculated resonance frequencies.

Fig. 4-77 and Fig. 4-78 show overvoltages in the 400 kV Kilkenny – Cahir line caused by islanding under the summer off-peak demand and the winter peak demand with maximum windpower. The overvoltage decays within one second.

(file offpeak_case3_50_chr.pl4; x-var t) v:CK021A   v:CK021B   v:CK021C
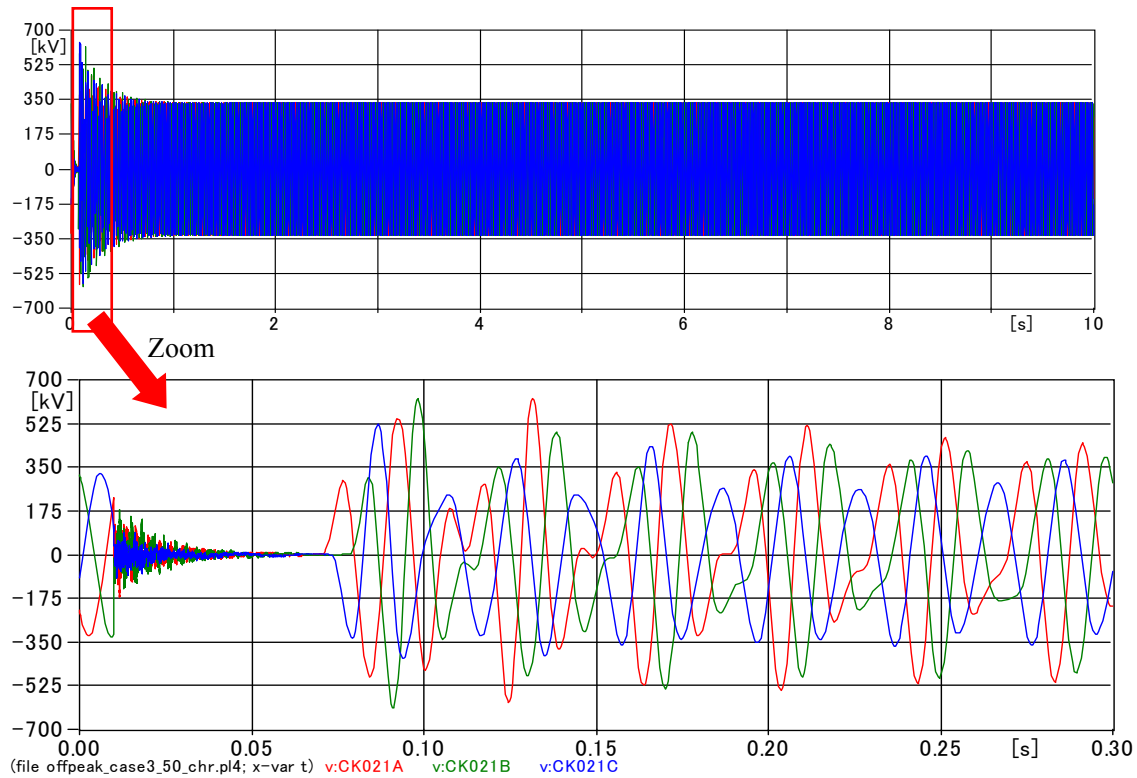
Fig. 4-77 Overvoltage caused by islanding under the summer off-peak demand.
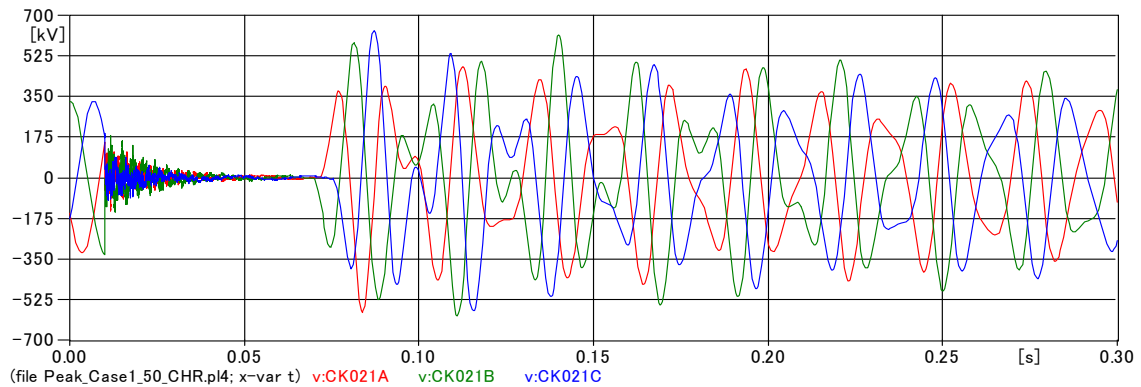
Fig. 4-78 Overvoltage caused by islanding under the off-peak condition with full windpower.

Those voltage waveforms were decomposed into their frequency components as shown in Fig. 4-79.   The phase in which the highest voltage was observed was chosen for each Fourier analysis.
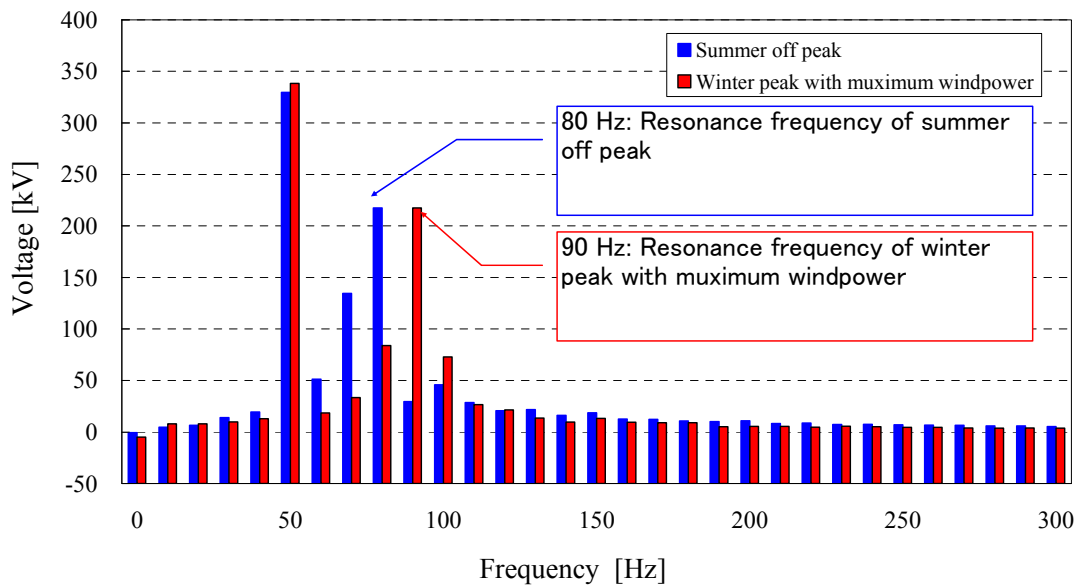
Fig. 4-79 Frequency components contained in the overvoltage.

Spectrums in the summer off-peak demand and the winter peak demand with maximum windpower respectively have peaks at 80 Hz and 90 Hz, as well as at 50 Hz.   The results match with calculated resonance frequencies shown in Fig. 4-76.

The voltage waveforms just after the fault clearance were used to derive frequency components in Fig. 4-79. Fig. 4-80 shows the decay of non-fundamental frequency components. As can be seen from Fig. 4-80, it is difficult to observe non-fundamental frequency components after one second.
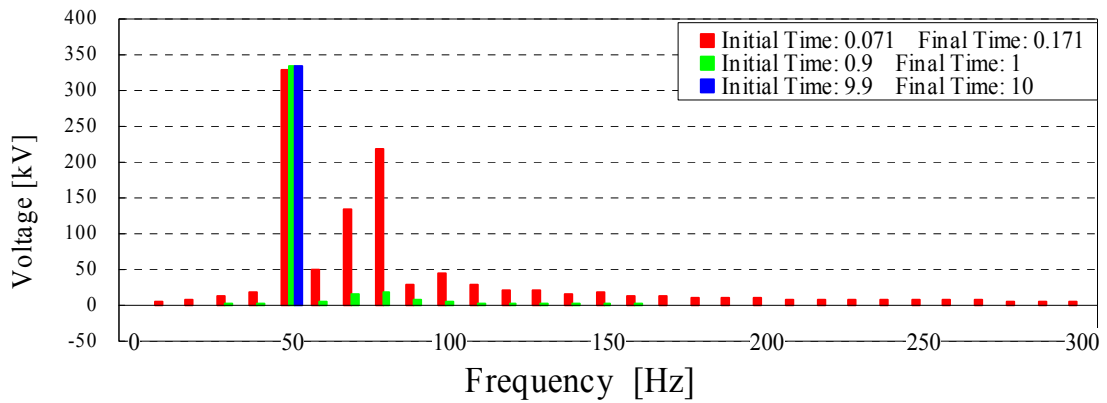
Summer off peak
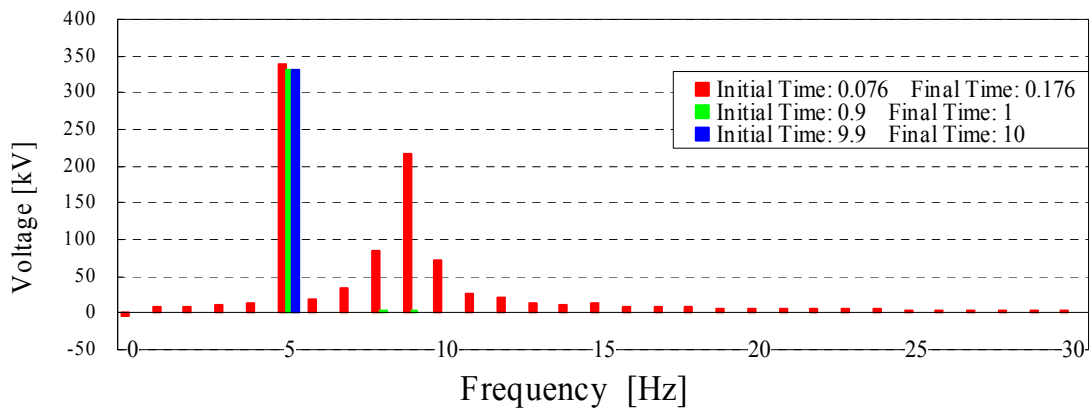
Winter peak with maximum windpower

Fig. 4-80 Decay of non-fundamental frequency components.

Overvoltage caused by load shedding will be studied with the switching scenario shown Fig. 4-81 and Fig.4-82. A three phase fault in the 400 kV bus in Woodland, Kingscourt and Turleenan, and subsequent trippings of cable lines will be assumed in the switching scenario. A sudden trip of cable lines without loads could possibly cause a large overvoltage. In general, larger impedance and admittance from an equivalent source yield a more severe condition.
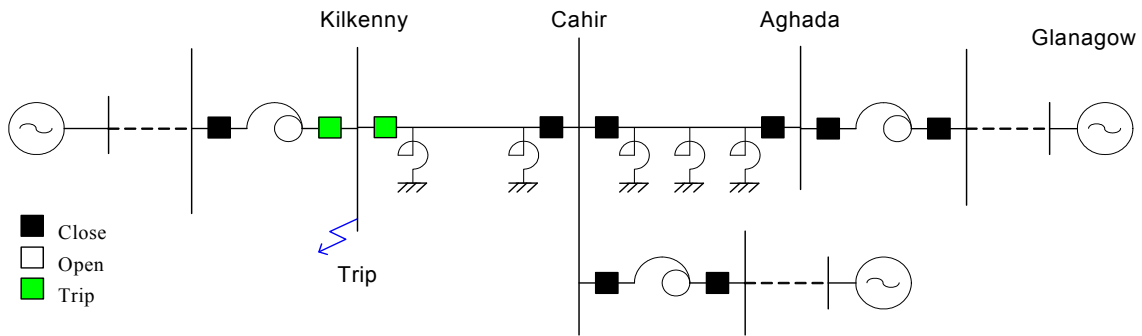
Fig. 4-81 Switching scenarios for the overvoltage caused by the system islanding - Three phase fault at Kilkenny 400 kV bus.
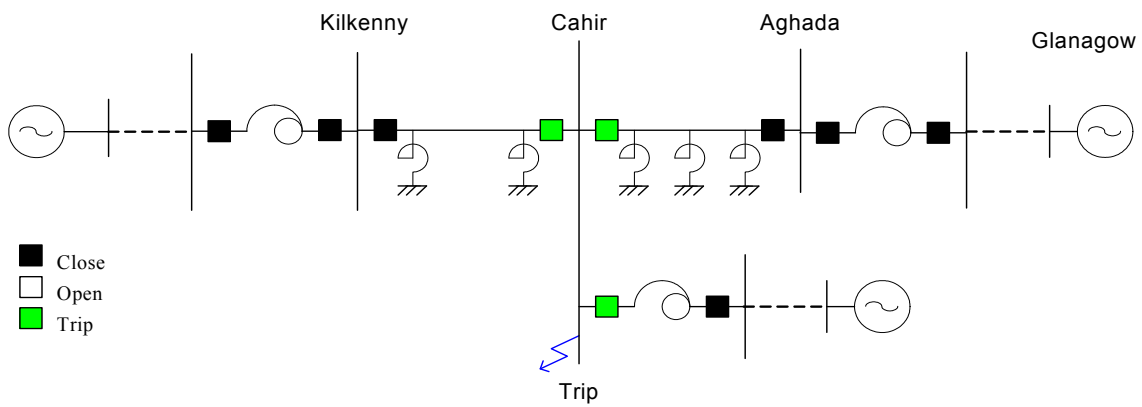
Fig.4-82 Switching scenarios for the overvoltage caused by the system islanding - Three phase fault at Cahir 400 kV bus.

Basically, source impedance values in Fig. 4-81 and Fig.4-82 are assumed to be in the ranges shown in the following table.

Table 4-22 Assumed Range of Source Impedance Values

Kilkenny 220 kV	50 – 100	mH
Cahir 110 kV	15 – 25	mH
Aghada 220 kV	20 – 90	mH

4.3.1 Effect of source impedance on an oscillatory overvoltage

First, the following three cases were carried out with regard to source impedances in each scenario as shown in Fig. 4-81 and Fig.4-82.

Table 4-23 Assumed Sets of Source Impedance Values

	Kilkenny 220 kV	Cahir 110 kV	Aghada 220 kV
Case 1	50 mH	15 mH	20 mH
Case 2	75 mH	20 mH	55 mH
Case 3	100 mH	25 mH	90 mH

The results of the analysis are summarized in Table 4-24.

Table 4-24 Overvoltage Caused by Load Shedding

	Fault point	Overvoltage	
Case 1	Kilkenny	592.1 kV (1.81 pu)	
	Cahir	646.3 kV (1.98 pu)	on the Kilkenny-islanding system
Case 2	Kilkenny	631.9 kV (1.93 pu)	
	Cahir	638.9 kV (1.96 pu)	on the Aghada-islanding system
Case 3	Kilkenny	623.3 kV (1.91 pu)	
	Cahir	651.3 kV (1.99 pu)	on the Aghada-islanding system

$$(1 \text{ pu} = 400 \text{ kV} \times \frac{\sqrt{2}}{\sqrt{3}} = 326.60 \text{ kV})$$

The highest overvoltage was observed in Case 3.   The following figure shows the result of the analysis with Case 3.
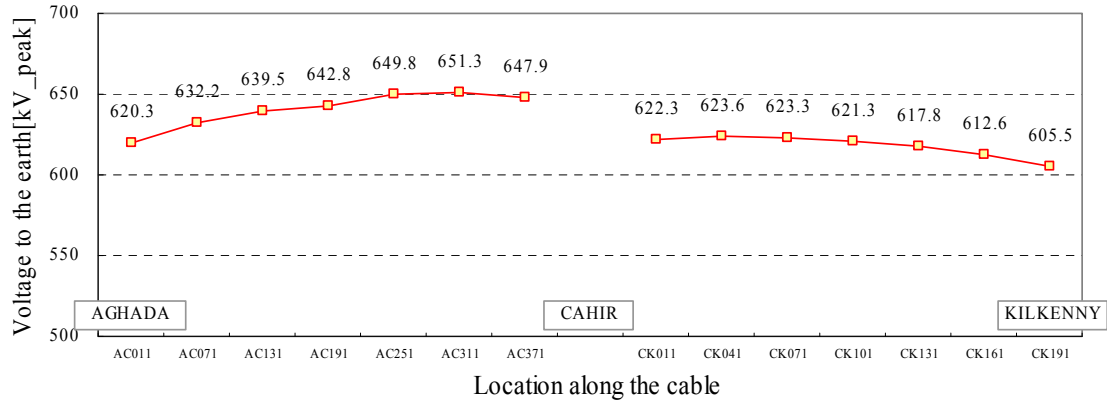
Fig. 4-83 Voltage profile of the overvoltage caused by system islanding in Case 3.
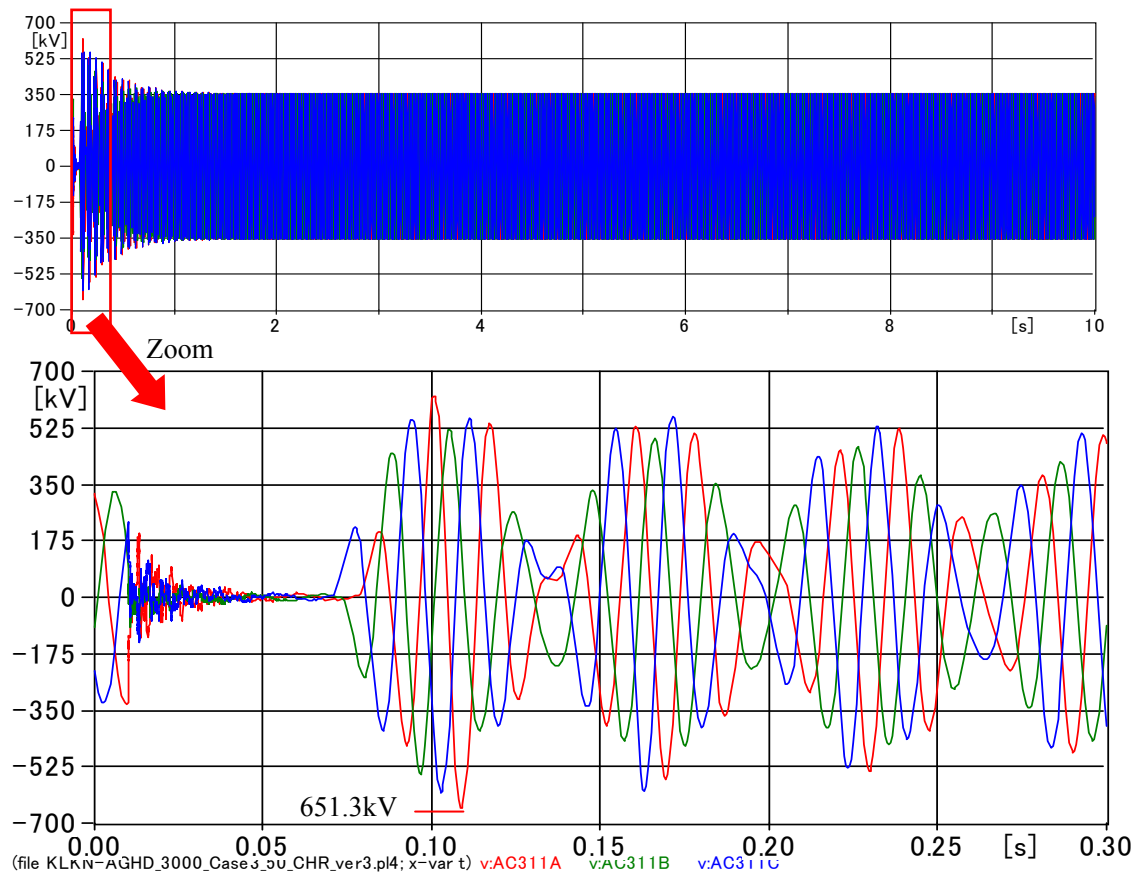
Fig. 4-84 Waveform of the overvoltage caused by system islanding in Case 3.

The overvoltage in Case 3 was observed in the islanded system including the 400 kV Cahir – Kilkenny line as shown in Fig. 4-85.
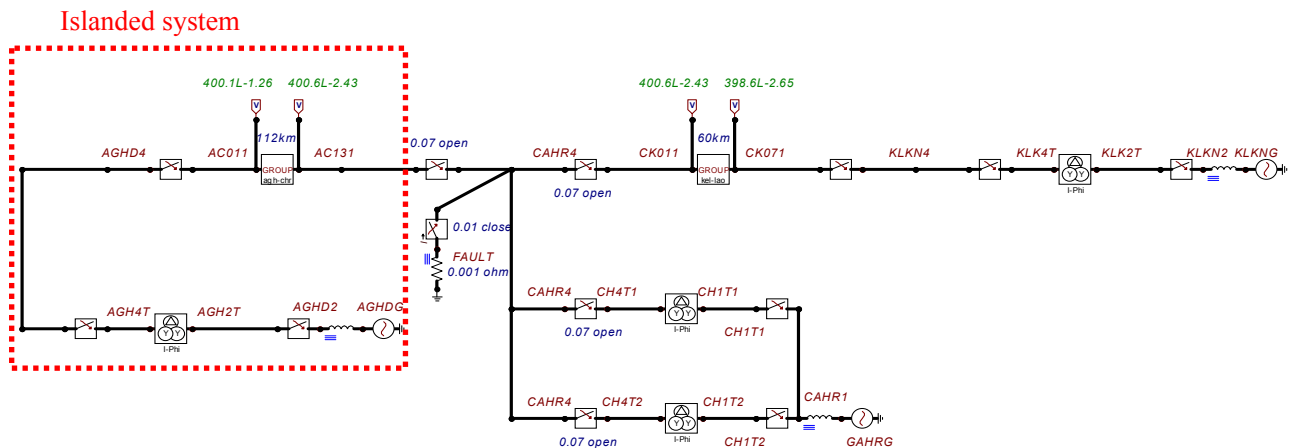
Fig. 4-85 Islanded system which causes oscillatory overvoltage shown in Fig. 4-84.

4.3.2   Effect of compensation rate of the cable

In this section, oscillatory overvoltage caused by islanding was studied with different compensation rates of the cable.   The switching scenario as shown in Fig.4-82 was studied because the scenario in Fig.4-82 caused higher overvoltage than the one in Fig. 4-81.

From the results of simulations shown in the previous section, the focus of the study is on the 400 kV Aghada – Cahir line together with a dummy voltage source connected to the Aghada 220 kV bus.   Source impedance of the dummy source was set to Case 1 shown in Table 4-23.

Time domain simulations were carried out with each compensation rate shown in Table 4-25. In order to keep the conditions as equal as possible (excluding the compensation rate of the 400 kV Aghada – Cahir line), the total compensation rate of the 400 kV Kilkenny – Cahir line and the Cahir – Aghada line was not changed in the study as shown in Table 4-25.

Table 4-25 Compensation rate of 400 kV Kilkenny – Cahir – Aghada Line

Locations	Case B2 (Base case)	Case B4	Case B5
Kilkenny Cahir	100MVA×4 80MVA×4	100MVA×5 80MVA×7	100MVA×6 80MVA×10
Compensation rate of Kilkenny – Cahir line	99.5 [%]	146.6 [%]	193.6 [%]
Cahir Reactor staion Aghada	100MVA×4 80MVA×7 80MVA×5	100MVA×3 80MVA×6 80MVA×3	100MVA×2 80MVA×4 80MVA×2
Compensation rate of Cahir - Aghada line	100.7 [%]	75.5 [%]	50.4 [%]

The results of the analysis are summarized in Table 4-26.　As can be seen from the table, a lower compensation rate yields a higher overvoltage.

Table 4-26 Overvoltage Caused by Load Shedding – Effect of Compensation Rate

	Fault point	Overvoltage	Compensation rate
Case B2	Cahir	651.3　kV　(　1.99　p.u.)	99.5%
Case B4	Cahir	805.2　kV　(　2.47　p.u.)	75.5%
Case B5	Cahir	1058.0　kV　(　3.24　p.u.)	50.4%

The results of the analyses with Case B4 and Case B5 are shown in the following figures.
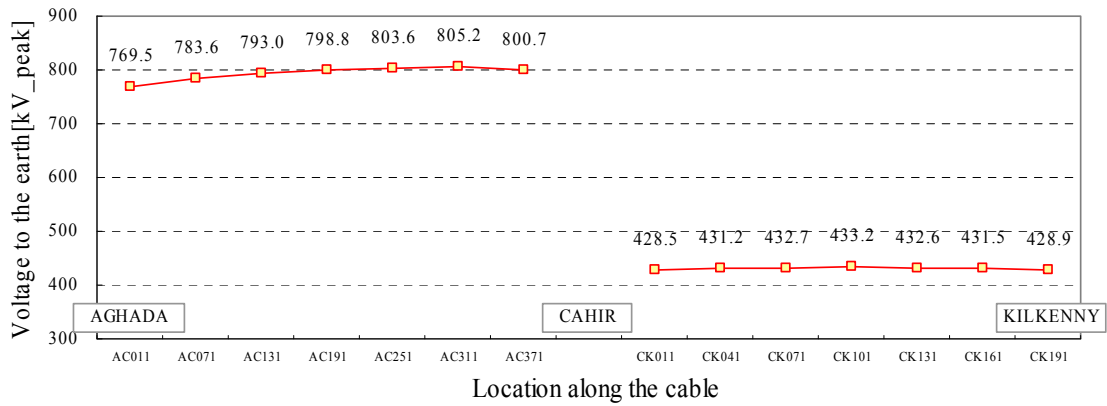
Fig. 4-86 Overvoltage caused by system islanding in Case B4 (approx. 75% compensation).

(file KLKN-AGHD_3000_Case3_50_CHR_75p_ver4.pl4; x-var t) v:AC311A   v:AC311B   v:AC311C
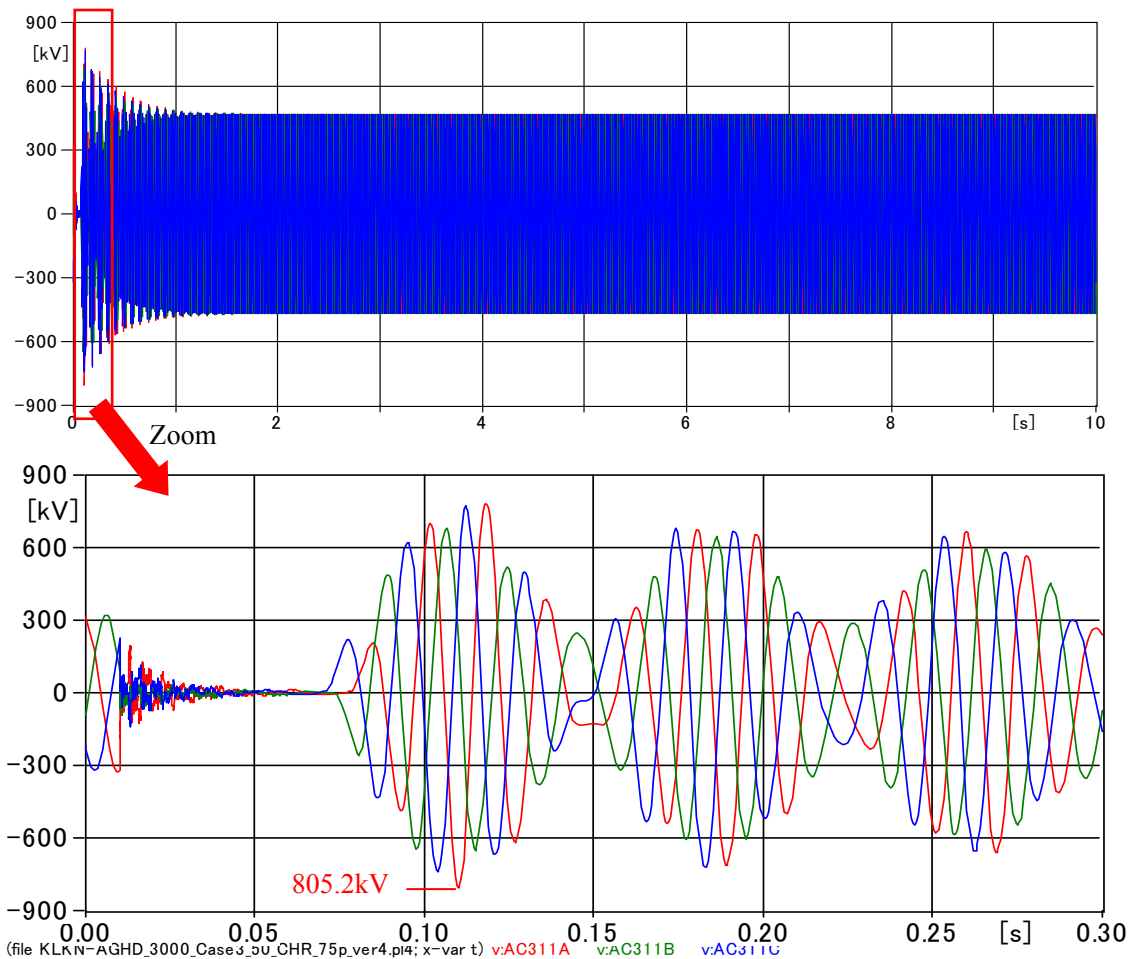
Fig. 4-87 Waveform of the highest overvoltage in Case B4 (approx. 75% compensation).

4-72
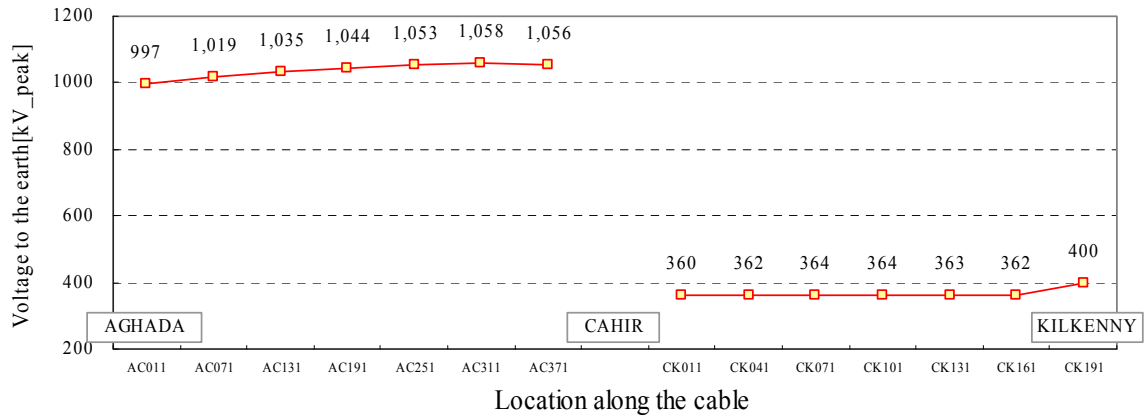
Fig. 4-88 Overvoltage caused by system islanding in Case B5 (approx. 50% compensation).
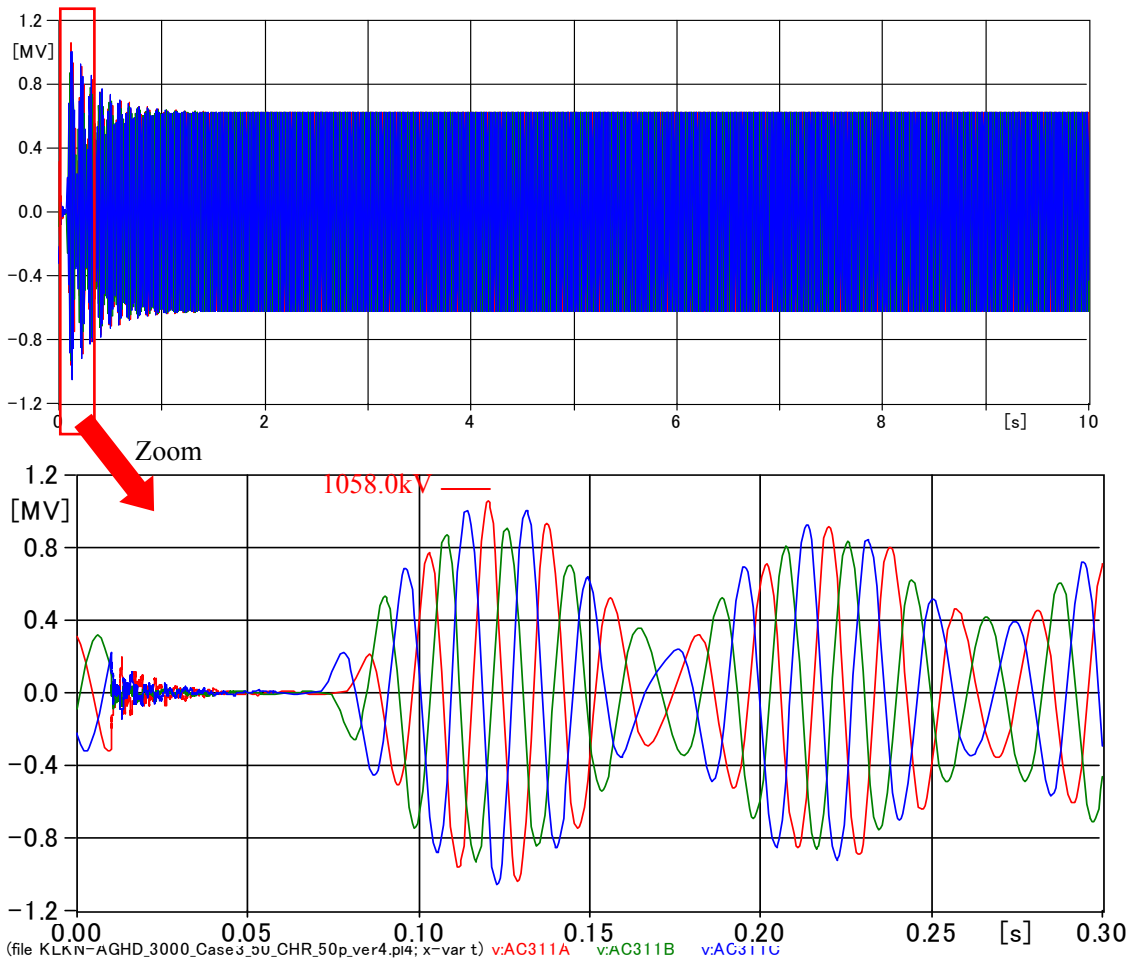
Fig. 4-89 Waveform of the highest overvoltage in Case B5 (approx. 50% compensation).

4.3.3　　Effect of the surge arrester

If surge arresters are connected to the Aghada 400 kV bus, the overvoltage can be mitigated to some extent.　 Fig. 4-90 shows an example of the configuration considering surge arresters.
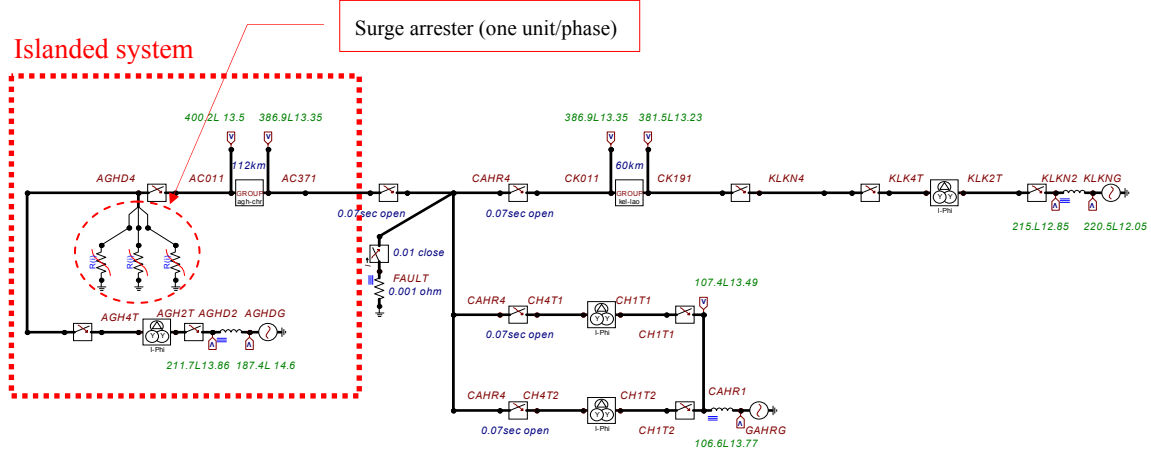
Fig. 4-90 System configuration considering surge arresters.

The results of the analysis considering surge arresters at Aghada S/S with Case B2 (approx. 100 % compensation) is shown in Fig. 4-91 and Fig. 4-92.

[Case B2, approx. 100% compensation]
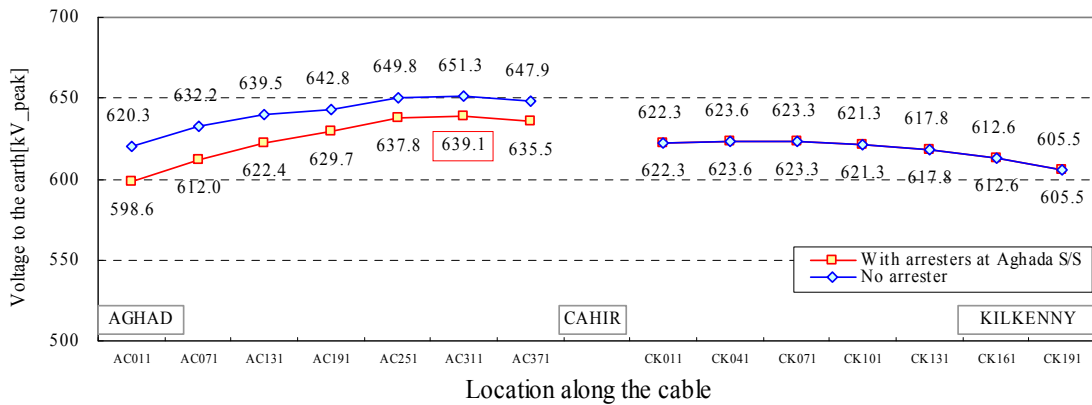
Fig. 4-91 Overvoltage caused by system islanding with and without arresters in Case B2 (approx. 100% compensation).
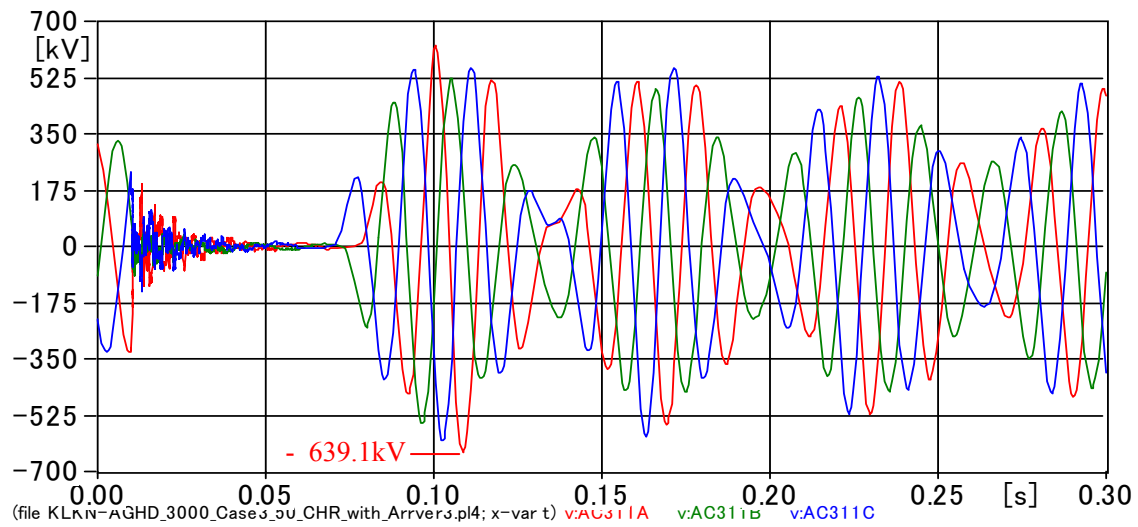
Fig. 4-92 Waveform of the highest overvoltage with arresters at Aghada S/S in Case B2

(approx. 100% compensation).

Energy absorbed by surge arresters at Aghada 400 kV bus was shown in Fig. 4-93. Since energy absorption capability of the surge arrester is 4.4 MJ (= 13 kJ/kV × 336 kV) for thermal stress, absorbed energy shown below is far less than its capability.
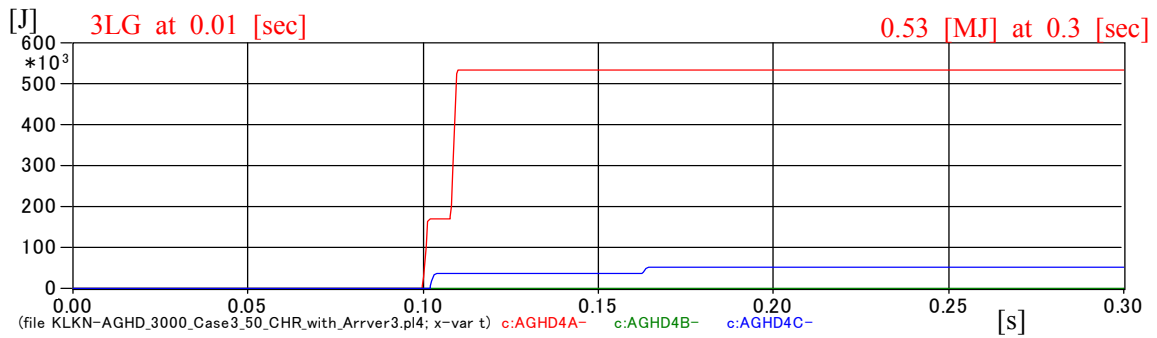
Fig. 4-93 Absorbed energy by surge arresters in Case B2.

The results of the analysis considering surge arresters at Aghada S/S with Case B4 (approx. 75 % compensation) is shown in Fig. 4-94 and Fig. 4-95.

[Case B4, approx. 75% compensation]
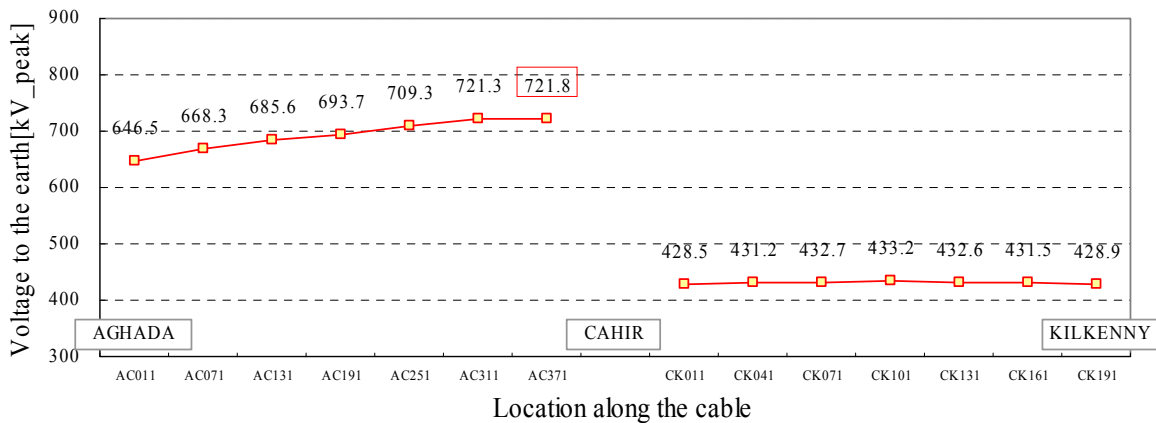
Fig. 4-94 Overvoltage caused by system islanding with arresters in Case B4 (approx. 75% compensation).
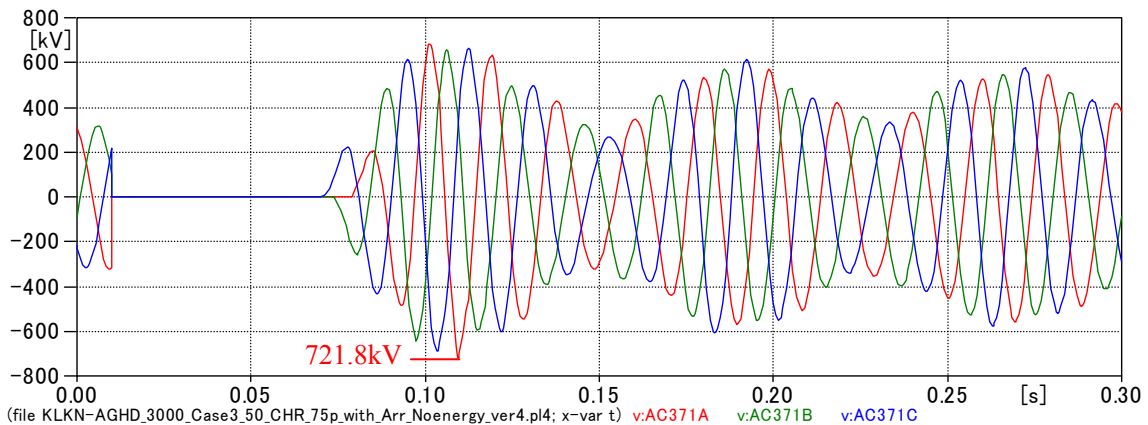
Fig. 4-95 Waveform of the highest overvoltage in Case B4 (approx. 75% compensation).

Energy absorbed by arresters at Aghada 400 kV bus is shown in Fig. 4-96.   Absorbed energy by one of arresters was 4.2 [MJ], which was very close to its energy absorption capability (If the capability is 4.4 [MJ]).

3LG at 0.01 [sec]   4.2 [MJ] at 0.12 [sec]
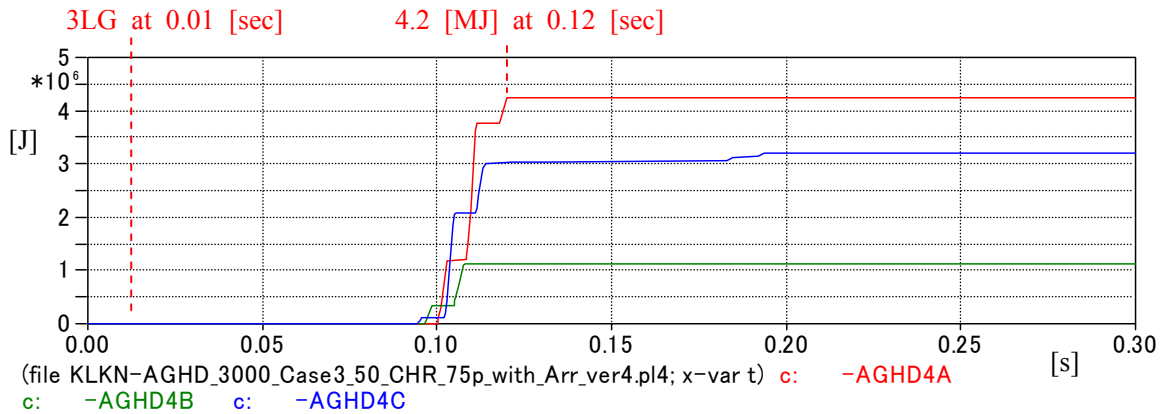
Fig. 4-96 Absorbed energy by surge arresters in Case B4

Countermeasures might as well be adopted to prevent the arrester from thermal breakdown. However, the most secure countermeasure is to keep the compensation rate for the long (112km, in this case) cable at about 100%.

The results of the analysis considering surge arresters at Aghada S/S with Case B5 (approx. 50 % compensation) is shown in Fig. 4-97 and Fig. 4-98.

[Case B5, approx. 50% compensation]
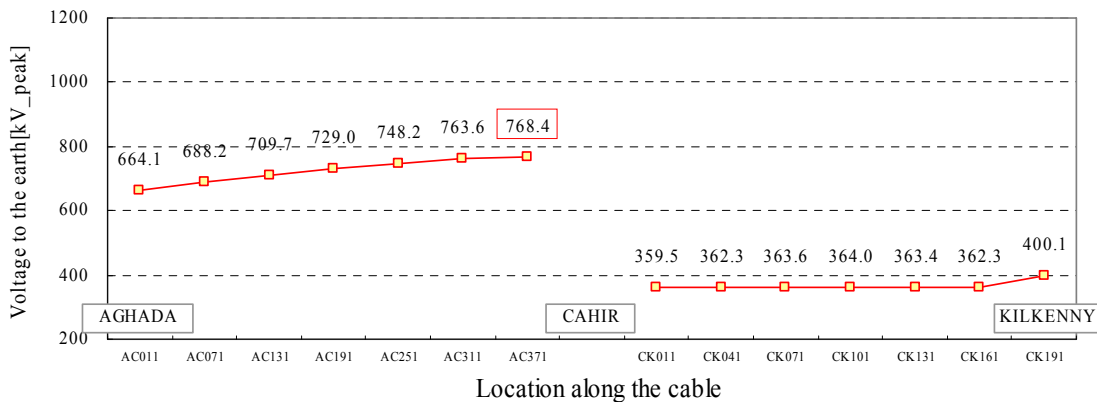
Fig. 4-97 Overvoltage caused by system islanding with arresters in Case B5 (approx. 50% compensation).
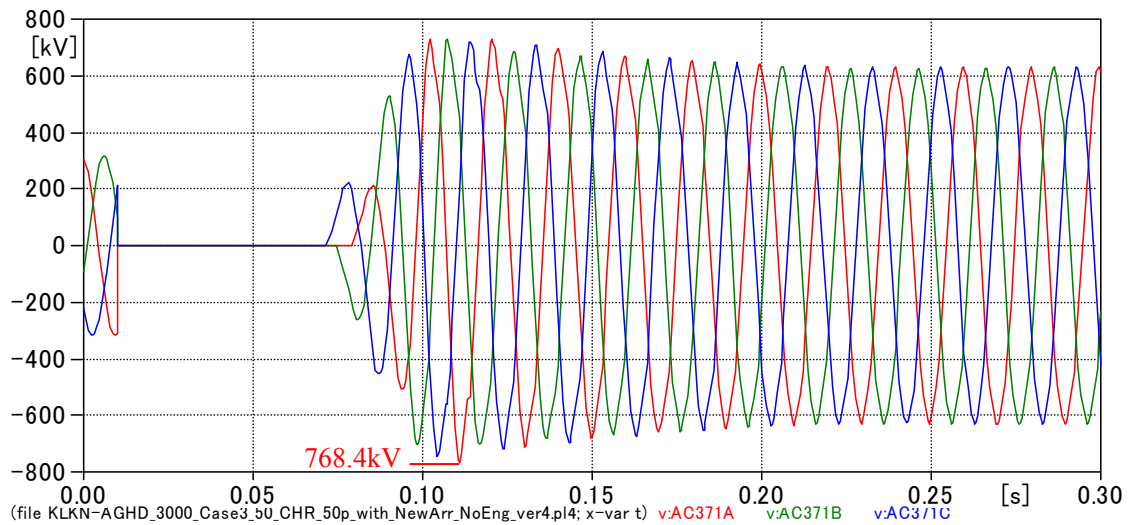
Fig. 4-98 Waveform of the highest overvoltage in Case B5 (approx. 50% compensation).

Energy absorbed by arresters at Aghada 400 kV bus are shown in Fig. 4-99. Energy absorbed by one of arresters exceeded its limit (4.4 [MJ]) in less than one cycle after overvoltage occurred.
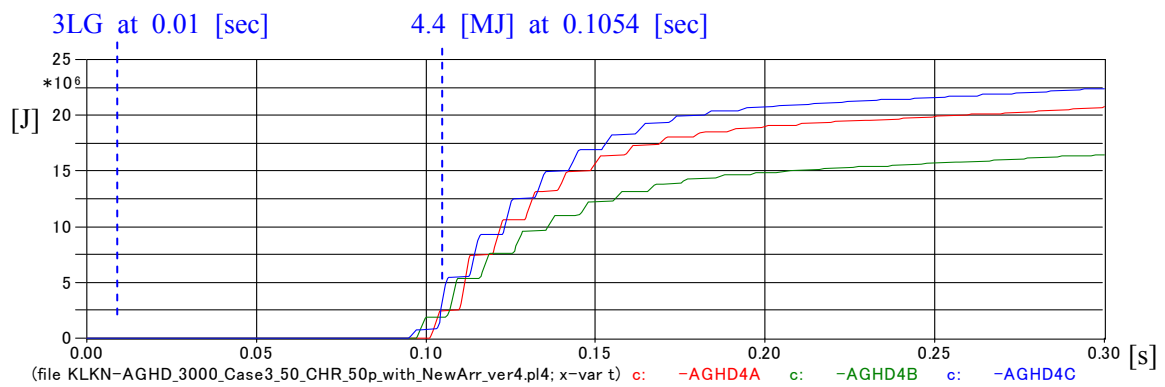
Fig. 4-99 Absorbed energy by surge arresters in Case B5.

4.3.4   Effect of the cable length

In this section, oscillatory overvoltage caused by islanding was calculated with different lengths of the cable.   The switching scenario that led to islanding was assumed to be the one shown in Fig.4-82.   Compensation rates were assumed to be about 100 % as shown in Table 4-27.

Table 4-27 Length of 400 kV Cahir – Aghada Line and Compensation Rates

	Length of 400 kV Cahir – Aghada line	Shunt reactors [MVA]			Compensation rate
		Aghada	Station[*1]	Cahir	
Base case	112 km	400	560	400	100.7 %
50 % case	56 km	400	---	300	103.7 %
150 % case	168 km	560	880	600	100.7 %

*1 Shunt reactor station

[50 % case] Length of Cahir - Aghada cable: 56 km

Fig. 4-100 and Fig. 4-101 show the result of the analysis when the length of the 400 kV Cahir – Aghada cable is 56 km, or half of the base case.
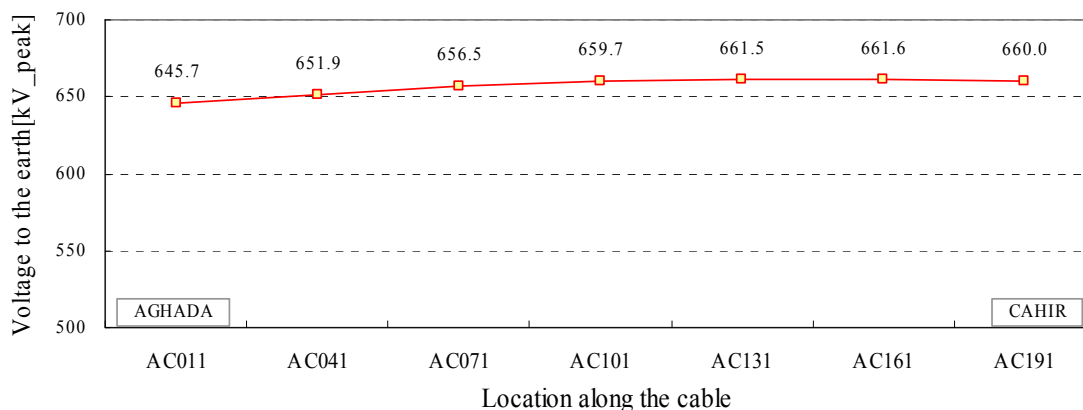
Fig. 4-100 Overvoltage caused by system islanding with 50 % cable length.
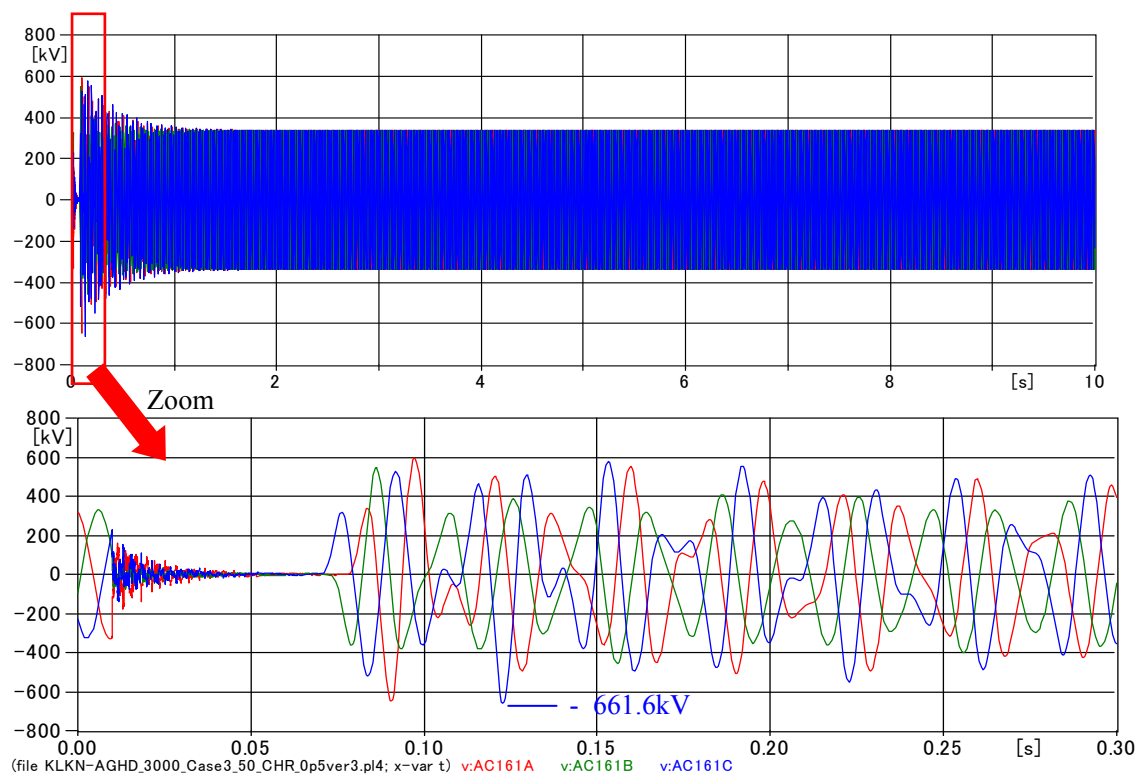
Fig. 4-101 Waveform of the highest overvoltage with a 50 % cable length.

[150 % case] Length of Cahir - Aghada cable: 168 km

Fig. 4-102 and Fig. 4-103 show the result of the analysis when the length of the 400 kV Cahir – Aghada cable is 168 km.
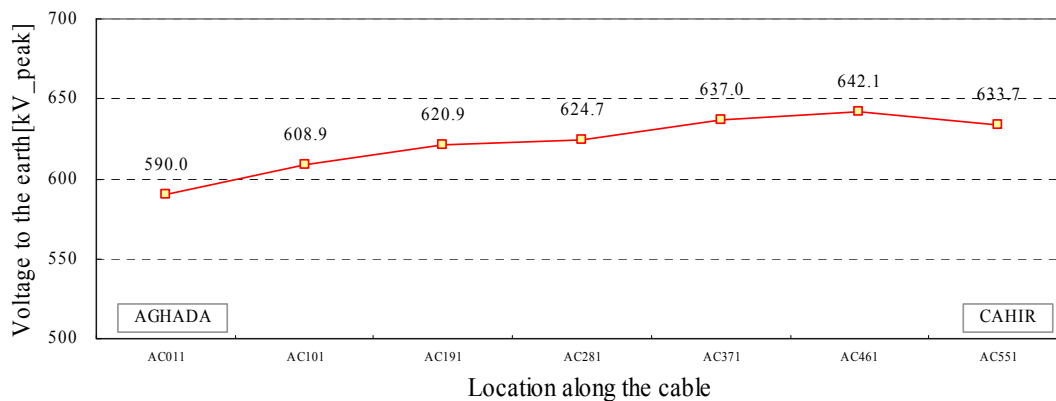
Fig. 4-102 Overvoltage caused by System Islanding with 150 % cable length.
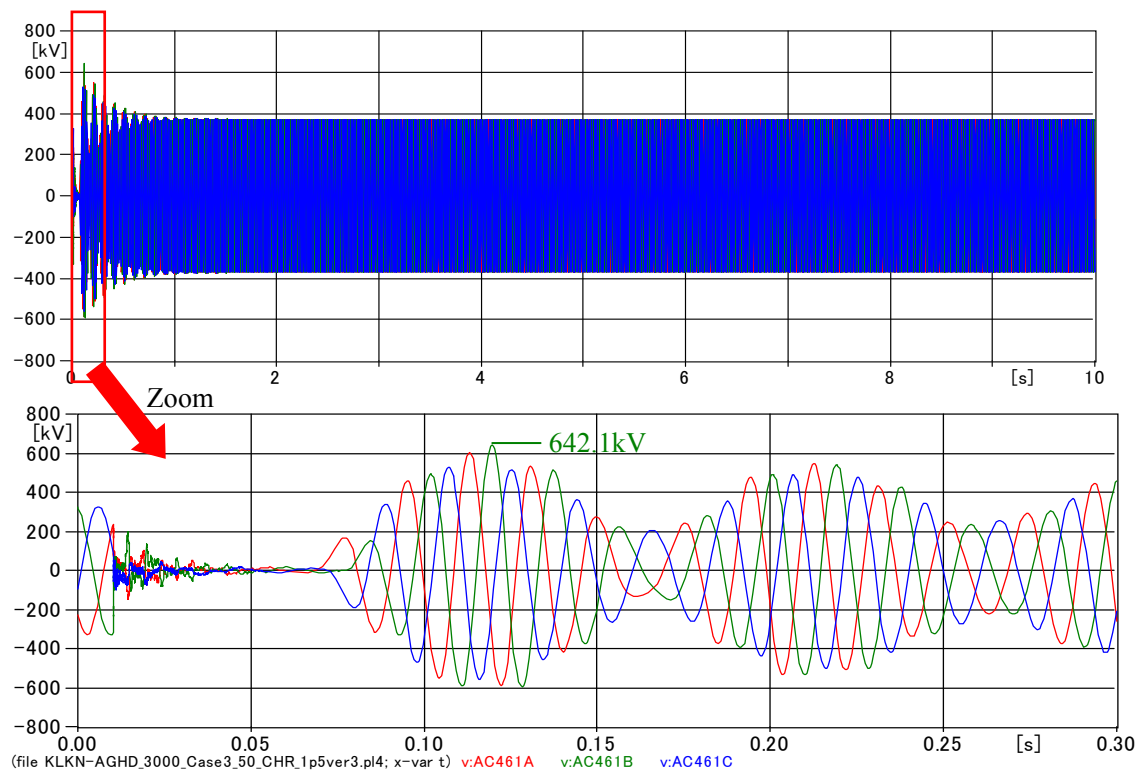
Fig. 4-103 Waveform of the highest overvoltage with 150% cable length.

The effect of the cable length is summarized in Table 4-28.　As can be seen from the table, the effect of the cable length is relatively small.

Table 4-28 Effect of the 400 kV cable length

	Length of 400 kV Cahir – Aghada cable	Maximum voltage
Base case	112 km	651.3　kV　(　2.0　p.u.)
50 % case	56 km	661.6　kV　(　2.0　p.u.)
150 % case	168 km	642.1　kV　(　2.0　p.u.)

Fig. 4-104 shows the frequency component spectrum derived from waveforms shown in Fig. 4-101 and Fig. 4-103.
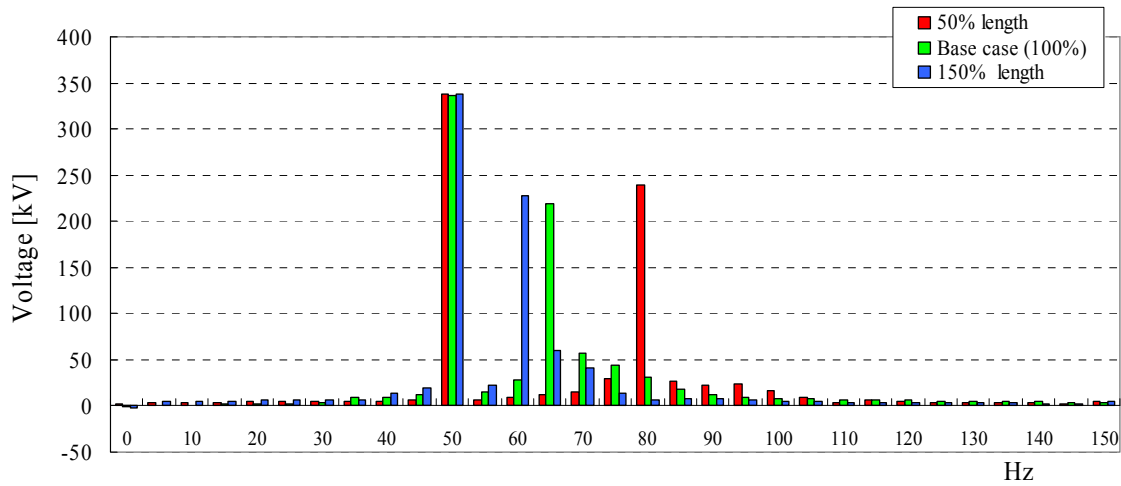
Fig. 4-104 Frequency component spectrum derived from voltage waveforms with different cable length.

In summary, it was found that load sheddings could cause a very high overvoltage that exceeded the withstand voltage of a typical 400 kV surge arrester. However, such overvoltage is not a concern with regards to the safe operation of the network as it can be evaluated using a SIWV (1050 kV) due to its fast decaying properties.

The overvoltage caused by load shedding was also studied using lower compensation rates. The overvoltage exceeded SIWV when the compensation rate was 50 %. In addition, the energy absorbed by the surge arrester exceeded its capability with the compensation rate 50 %. It is strongly recommended to adopt a compensation rate close to 100 % when the 400 kV Aghada – Cahir – Kilkenny line is built as an underground cable line as studied in this section.

4.4 Conclusion

The temporary overvoltage analysis was performed based on the compensation pattern determined by the reactive power compensation analysis. Resonance overvoltages and overvoltages caused by load shedding were studied with different cable lengths as well as under different network conditions.

The highest series resonance overvoltage was found in the Woodland 220 kV network. It was found to be lower than the standard short-duration power-frequency withstand voltage (395 or 460 kV, r.m.s.) specified in IEC 71-1.

The parallel resonance overvoltage was studied with transformer energisation. The observed overvoltage was much higher than the withstand voltage of a typical 400 kV surge arrester. If the 400 kV Aghada – Cahir – Kilkenny line is built as an underground cable line as studied in this section, careful study is necessary before energising a transformer at Aghada, Cahir, and Kilkenny. It is recommended to consider the application of the point-on-wave switching for the transformer energisation. It has not found its application yet, but the technology itself is already established.

Load sheddings also yielded a very high overvoltage. However, such overvoltage is not a concern with regards to the safe operation of the network as it can be evaluated using SIWV (1050 kV) due to its fast decaying properties. The overvoltage caused by load shedding was also studied with lower compensation rates. The overvoltage exceeded SIWV when the compensation rate was 50 %.

Table 4-29 Summary of the Temporary Overvoltage Analysis

		Highest overvoltage (peak)	Withstand voltage for evaluation
Series resonance		549.0 kV (3.06 pu)	360, 395, 460 kV (r.m.s.) (2.83, 3.11, 3.62 pu)
Parallel resonance	No load	881.5 kV (2.70 pu)	370 kV (r.m.s.) (1.60 pu) for 10 seconds
	With load	634.5 kV (1.94 pu)	
Load shedding		651.3 kV (1.99 pu)	1050 kV (peak)

$$1\,\mathrm{pu} = 400 \text{ or } 220\,\mathrm{kV} \times \frac{\sqrt{2}}{\sqrt{3}} \text{ (peak)}, 400 \text{ or } 220\,\mathrm{kV} \times \frac{1}{\sqrt{3}} \text{ (r.m.s.)}$$

Chapter 5 Slow-front Overvoltage Analysis

Generally, the overvoltage caused by energisation, de-energisation, fault clearance, and other switching events is lower for longer cables due to the decay of the overvoltage along the length of the cable. The overvoltage in the cable is caused by the superimposition of overvoltages reflected at the both ends of the cable. When the cable has a significant length, the overvoltage would decay enough by the time it reaches at one end of the cable.

TEPCO has studied switching overvoltages of various lengths of EHV cables, including the 500 kV 39.5 km cable and the 400 kV 106 km cable. The studies did not show any concerns on the switching overvoltage, particularly due to the significant lengths of the cables.

With this in mind, however, it is a typical practice to study slow-front overvoltages for the installation of EHV cables. Slow-front overvoltage caused by line energisation, ground fault, and fault clearing was studied in this chapter for reference. The results of the analysis were evaluated with SIWV (1050 kV: phase to earth, peak) of 400 kV equipment in NIE and EirGrid.

5.1 Overvoltage Caused by Line Energisation

Overvoltage caused by line energisations was studied by the switching scenarios shown in Fig. 5-1. When one circuit is energised, other circuits are assumed to be out of service as shown in the figure. This assumption yields the most severe condition for line energisation since the overvoltage cannot propagate into other circuits.

It was assumed that the time between the line outage and line energisation was long enough to discharge each cable. The decay time of the residual voltage mainly depends on the X/R ratio of shunt reactors, and lower X/R ratio means faster decay of the residual voltage. For the typical X/R ratio of the 400 kV shunt reactors, it can take several minutes to discharge a cable. Considering this decay time and normal operation practices, it is a common practice to ignore the residual voltage in the line energisation overvoltage analysis. In addition, the cable will be discharged through VTs instead of shunt reactors when shunt reactors are not connected to the cable. In this case, the cable will be discharged within 100 ms.

Line energisations were simulated two hundred times using the statistical switch, in order to investigate slow-front overvoltages caused by different switching timings.
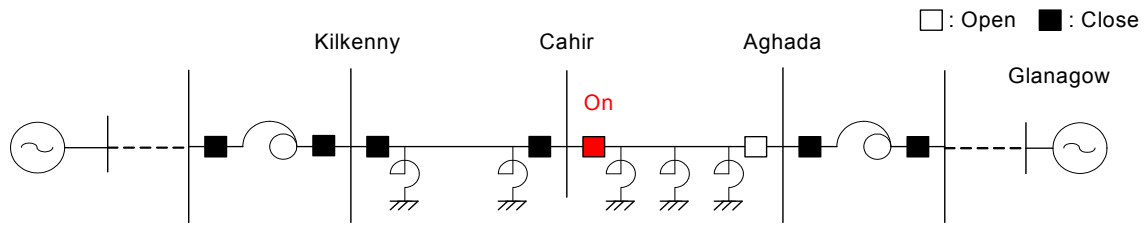
Fig. 5-1 Switching scenarios for the overvoltage caused by line energisation.

5.1.1 Overvoltage caused by line energization in the base case

Before simulating the energisation of the 400 kV Cahir – Aghada line, steady state power flow calculations were conducted under the conditions shown in Fig. 5-2. Source voltages were adjusted to set the highest voltage along the cable to around 400 kV.
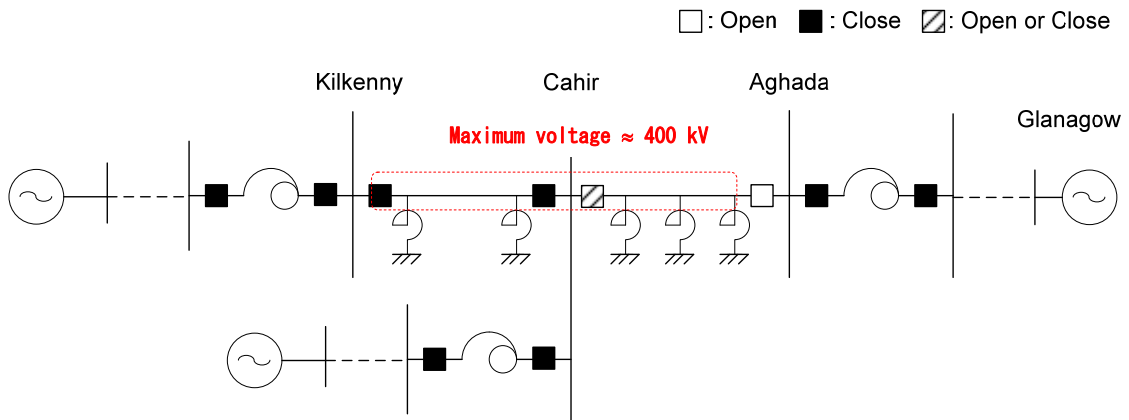
Fig. 5-2 Steady state power flow calculation before simulating line energizations.

Node names are illustrated in Fig. 5-3.
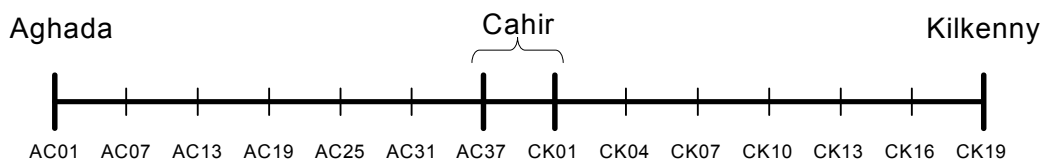
Fig. 5-3 Node names.

Fig. 5-4 shows the profile of the overvoltage along the 400 kV Aghada – Cahir – Kilkenny line. The 2 % value in the figure corresponds to the fourth highest overvoltage observed in 200 times repeated simulations.
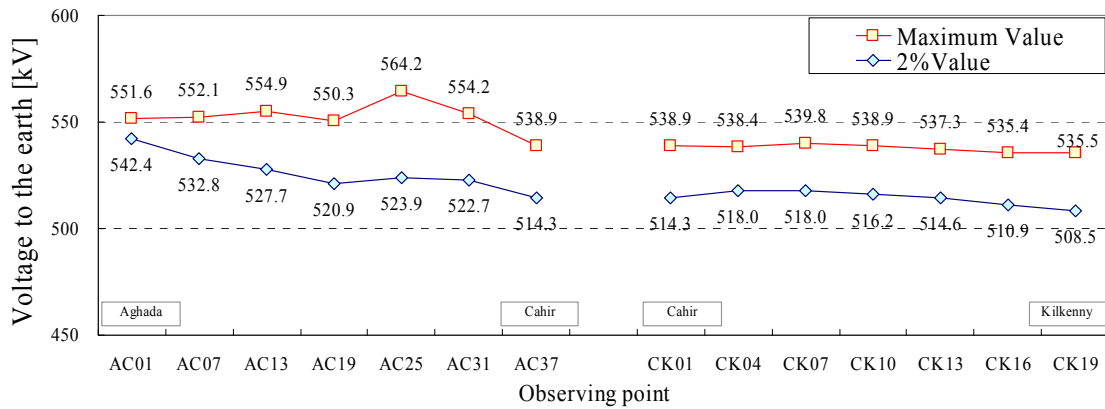
Fig. 5-4 The maximum and 2% overvoltage profile in line energisation.

Table 5-1 Maximum Overvoltage along Aghada – Cahir – Kilkenny Line

	Aghada - Cahir		Node	Cahir - Kilkenny		Node
	Voltage		Node	Voltage		Node
Max	564.2kV	(1.72 p.u.)	AC25	539.8kV	(1.65 p.u.)	CK07
2%	542.4kV	(1.66 p.u.)	AC01	518.0kV	(1.59 p.u.)	CK04, CK07

Fig. 5-5 shows the voltage waveform at the Aghada end of the Aghada – Cahir line when the 2 % value 542.4 kV (1.66 pu) was observed in Phase C.
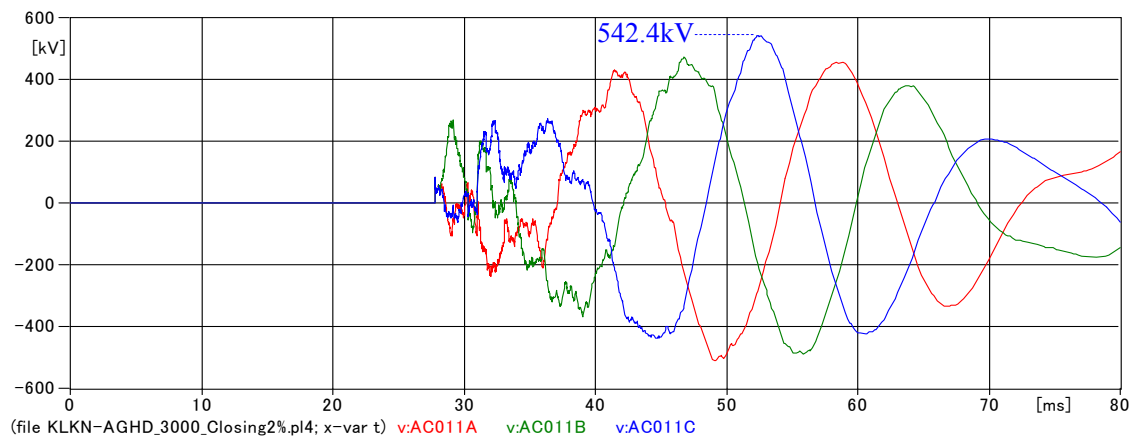
Fig. 5-5 Voltage waveform at the Aghada end of the Aghada - Cahir line

5.1.2   Effect of line length to overvoltage caused by line energization

The slow-front overvoltage caused by line energization was studied with different lengths of the 400 kV Cahir – Aghada line as shown in Table 5-2.   The target frequency of the cable model (Bergeron model) was adjusted for each case, considering the total cable length between Kilkenny and Aghada.

Table 5-2 Length of 400 kV Cahir – Aghada Line and Target Frequency of the Cable Model

	Length [*1]	f $_{Target}$	Reactor compensation [MVA]			Compensation rate
			Aghada	Station [*2]	Cahir	
Base case	112 km	250 Hz	400	560	400	100.7 %
50 % case	56 km	366 Hz	400	---	300	103.7 %
150 % case	168 km	186 Hz	560	880	600	100.7 %

*1 Length of 400 kV Cahir – Aghada line

*2 Shunt reactor station

[50 % case] Length of Cahir – Aghada cable: 56 km

Node names are illustrated in Fig. 5-6.
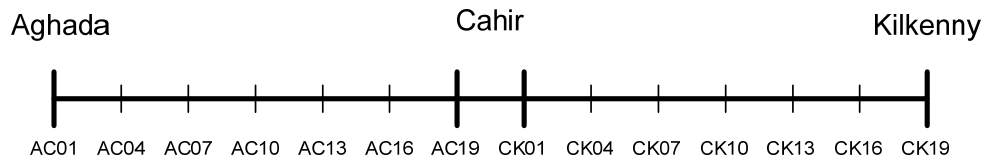
Fig. 5-6 Node names.

Fig. 5-7 and Table 5-3 show the result of a simulation repeated 200 times.
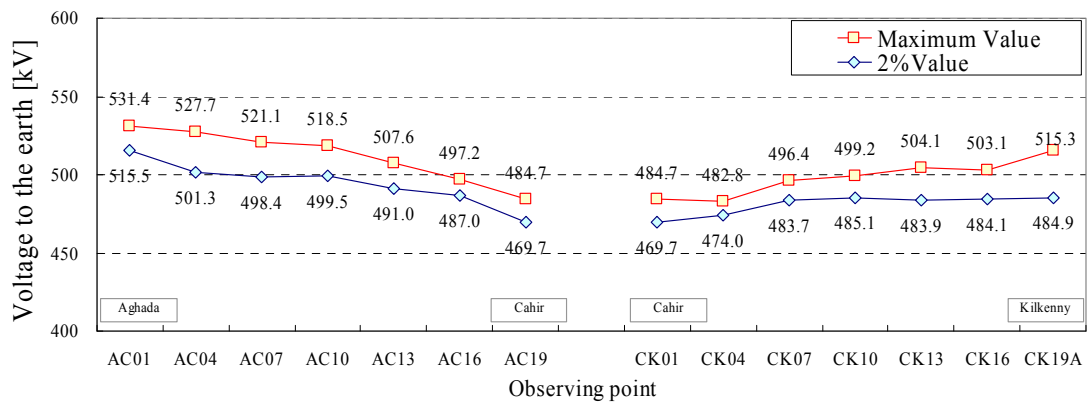
Fig. 5-7 Profile of the maximum and 2 % value in line energization for a 50 % case.

Table 5-3 Maximum Overvoltage along the Aghada – Cahir – Kilkenny Line for 50 % Case

	Aghada – Cahir		Node	Cahir – Kilkenny		Node
	Voltage		Node	Voltage		Node
Max	531.4 kV	(1.63 pu)	AC01	515.3 kV	(1.58 pu)	CK19
2 %	515.5 kV	(1.58 pu)	AC01	485.1 kV	(1.49 pu)	CK10

Fig. 5-8 shows the voltage waveform at the Aghada end of the Aghada – Cahir line when the 2 % value 515.5 kV (1.58 pu) was observed in Phase C.
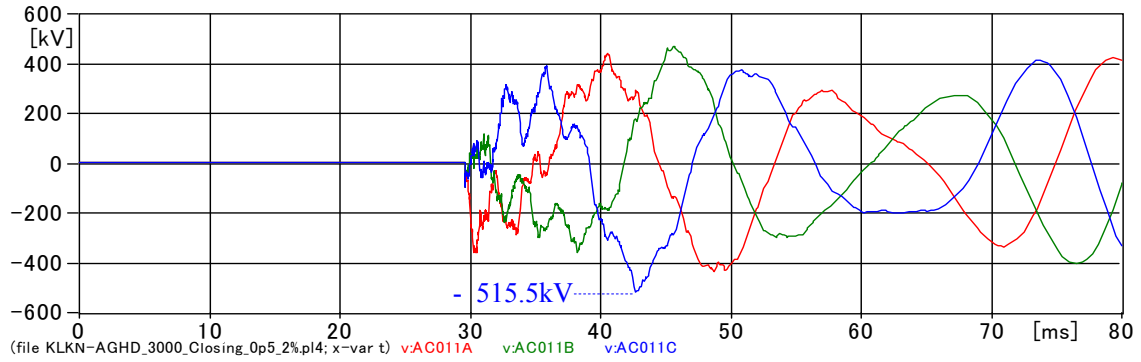
Fig. 5-8 Voltage waveform at the Aghada end of the Aghada - Cahir line for 50 % case.

[150 % case] Length of Cahir - Aghada cable: 186 km

Node names are illustrated in Fig. 5-9.
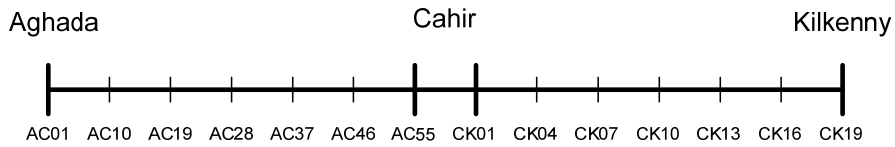
Fig. 5-9 Node names.

Fig. 5-10 and Table 5-4 show the result of 200 times repeated simulations.
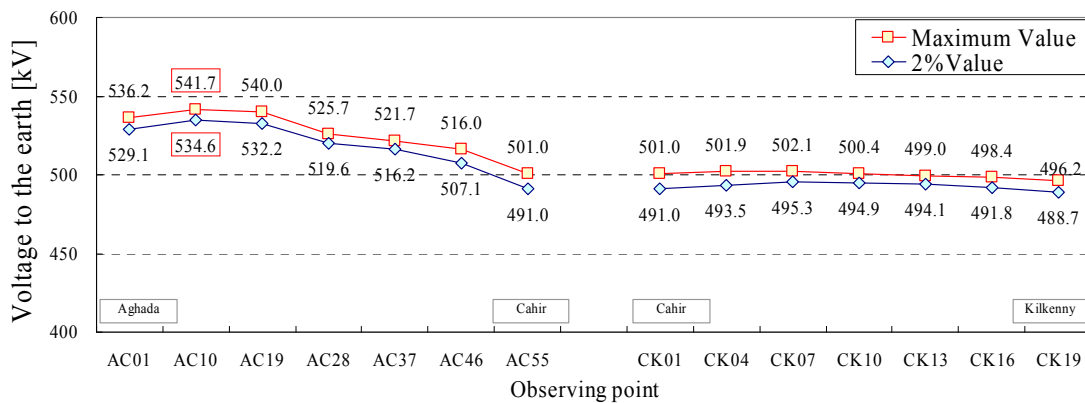
Fig. 5-10 Profile of the maximum and 2 % value in line energization for 150 % case.

Table 5-4 Maximum Overvoltage along the Aghada – Cahir – Kilkenny Line for 150 % Case

	Aghada - Cahir			Cahir - Kilkenny		
	Voltage		Node	Voltage		Node
Max	541.7kV	(1.66 p.u.)	AC10	502.1kV	(1.57 p.u.)	CK07
2%	534.6kV	(1.64 p.u.)	AC10	495.3kV	(1.52 p.u.)	CK07

Fig. 5-8 shows the voltage waveform at the Aghada end of the Aghada – Cahir line when the 2 % value 534.6 kV (1.64 pu) was observed in Phase A.
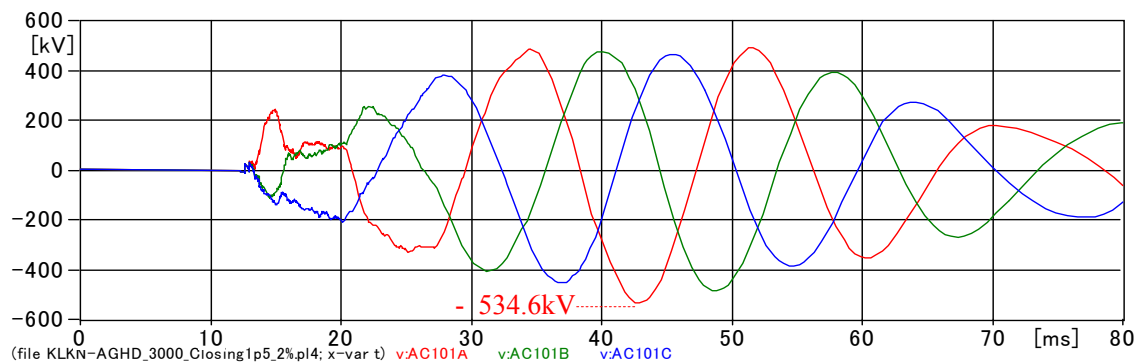
Fig. 5-11 2% overvoltage waveform at Aghada end of the 400 kV Aghada - Cahir cable when length of 400 kV Aghada – Cahir cable is 150%

Fig. 5-12 summarizes the maximum and 2% values for different cable lengths. The observed overvoltages were much lower than SIWV in all simulated cases, which is typical for long cable systems.
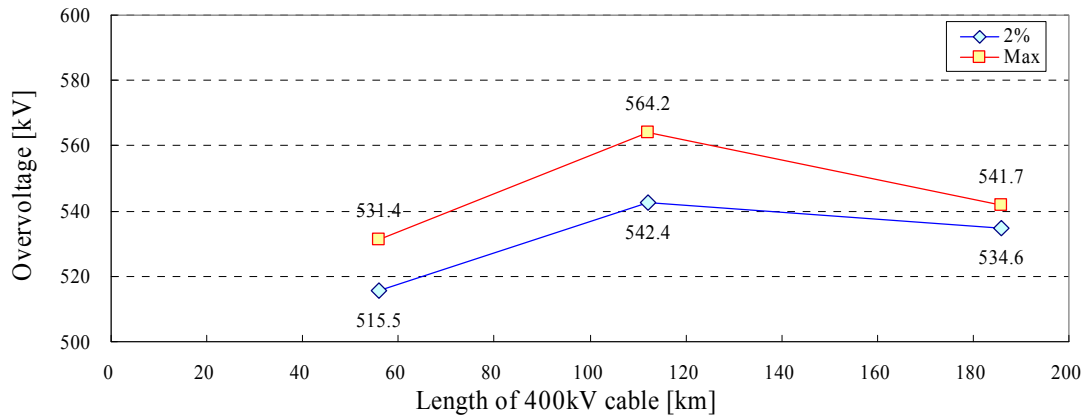
Fig. 5-12 The maximum and 2% values for different cable lengths.

5.2 Ground Fault and Fault Clearing Overvoltage

5.2.1   Ground fault and fault clearing overvoltage on the base case

The slow-front overvoltage caused by the ground fault and fault clearing was studied with different fault timings.   The conditions of the analysis are:

Fault point: Seven points in 400 kV Cahir – Kilkenny cable route

Fault type: Single line to ground fault (core to sheath) in Phase A

Fault timing: 0° – 170° (10° step – 18 fault timings)

Fig. 5-13 illustrates the switching scenario for the ground fault and fault clearing overvoltage analysis.
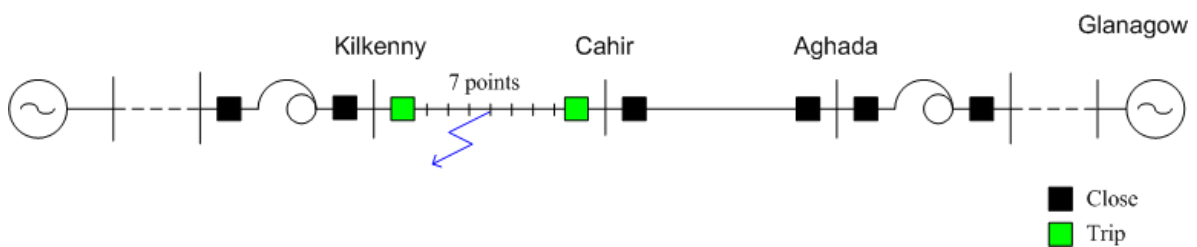
Fig. 5-13 Switching scenarios for the ground fault and fault clearing overvoltage analysis.

For this analysis, target frequency of all Bergeron models was set to 250 Hz in consideration of the length of the 400 kV Kilkenny – Cahir – Aghada line.   Source impedances were chosen from short circuit calculation results in summer off-peak demand.

Since the system including 400 kV Cahir – Aghada line is isolated from the main grid after the tripping of the Kilkenny – Cahir line, the overvoltage in the 400 kV Cahir – Aghada line is similar to the one caused by load shedding.   In general, a smaller model, as in the isolated system, yields a larger overvoltage due to its lower attenuation and smaller number of propagation routes for the overvoltage.

Fig. 5-14 shows the profile of an overvoltage along the 400 kV Aghada – Cahir – Kilkenny line.　In this analysis, the simulation was repeated 126 times for each case (= 7 fault points × 18 fault timings).　Hence, a 2 % value corresponds to the seventh largest value (126 simulations × 3 phases × 0.02) in the simulation at each observation point.
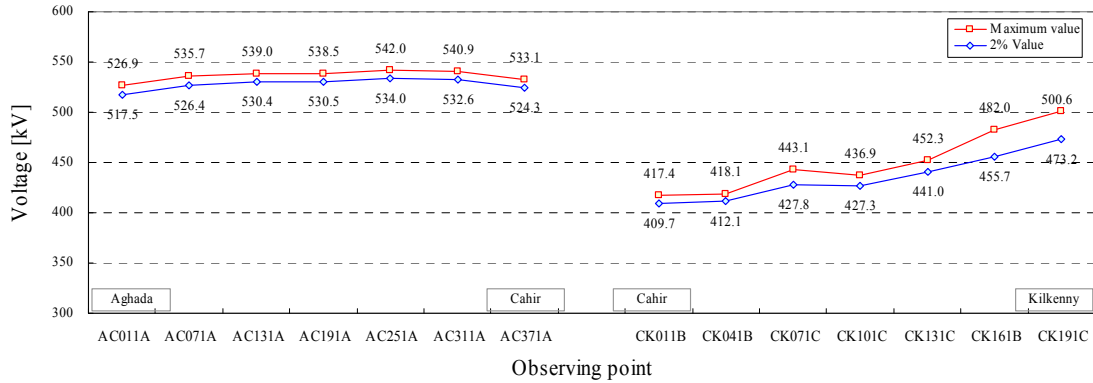
Fig. 5-14 Result of the ground fault and fault clearing analysis.

The maximum value was 542.0 kV (1.66 pu), and the 2 % value was 534.0 kV (1.63 pu), which were both lower than SIWV.

The 2 % value at the 400 kV Kilkenny bus was observed when the fault occurred at the Cahir end of the 400 kV Cahir – Kilkenny line at a phase angle of 60°.　Fig. 5-15 shows the voltage waveform at this location when the 2 % value was observed.
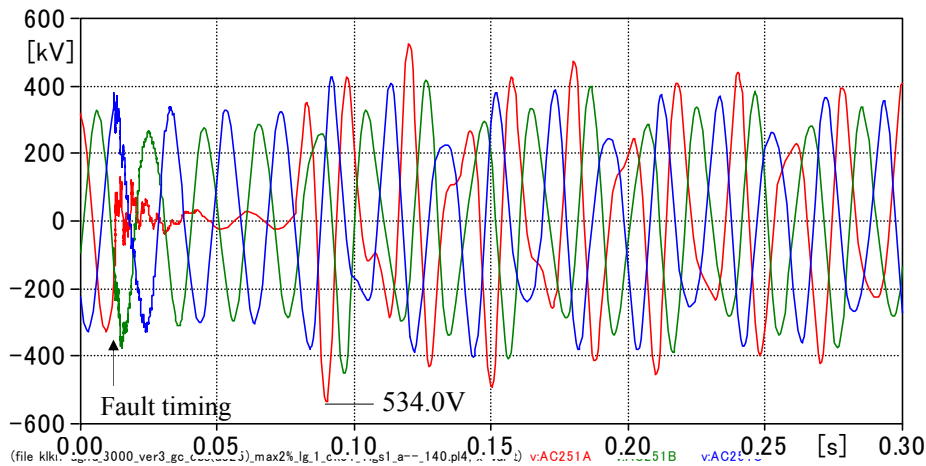
Fig. 5-15 Overvoltage after the fault clearing of the 400 kV Aghada – Cahir line

The highest overvoltage between Kilkenny and Cahir (500.6 kV) was observed at the Kilkenny 400 kV bus.   The overvoltage was caused by the fault in the Cahir 400 kV bus.
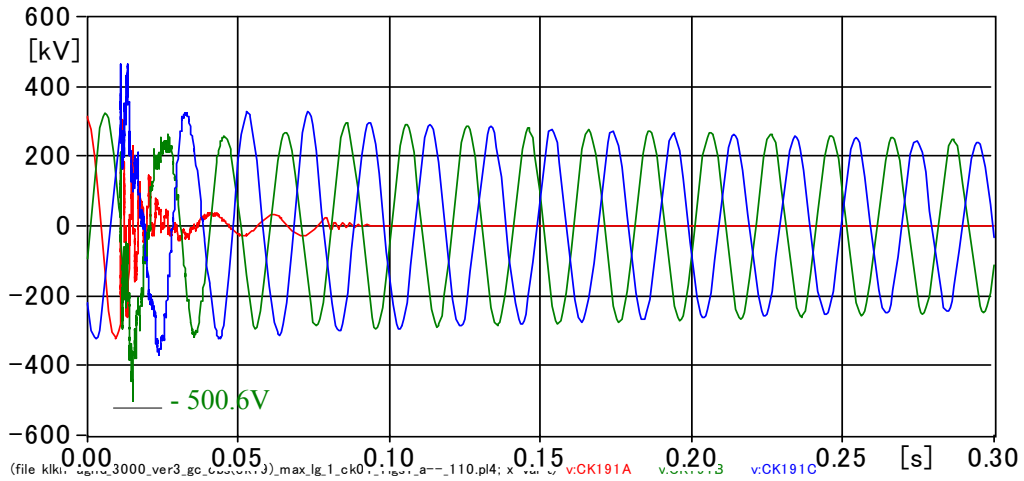
Fig. 5-16 The highest overvoltage in the Kilkenny 400 kV bus.

5.2.2   Effect of the cable length

In this section, the ground fault and fault clearing overvoltage was studied with different lengths of the 400 kV Cahir – Aghada line as shown in Table 5-5.

Table 5-5 Length of 400 kV Cahir – Aghada Line

	Length of Cahir – Aghada line.
Base case	112 km
150 % case	168 km
50 % case	56 km

The results of the analyses are shown in Fig. 5-17, Fig. 5-18, and Table 5-6.
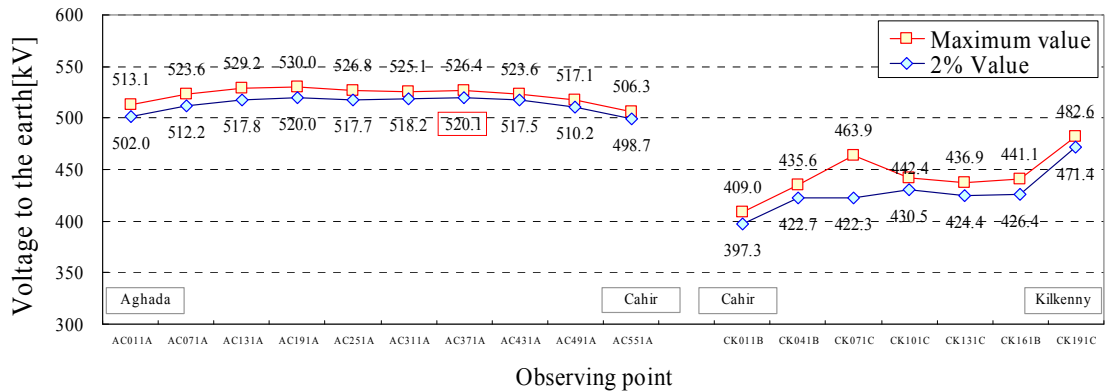
Fig. 5-17 Result of the ground fault and fault clearing analysis for 50 % case
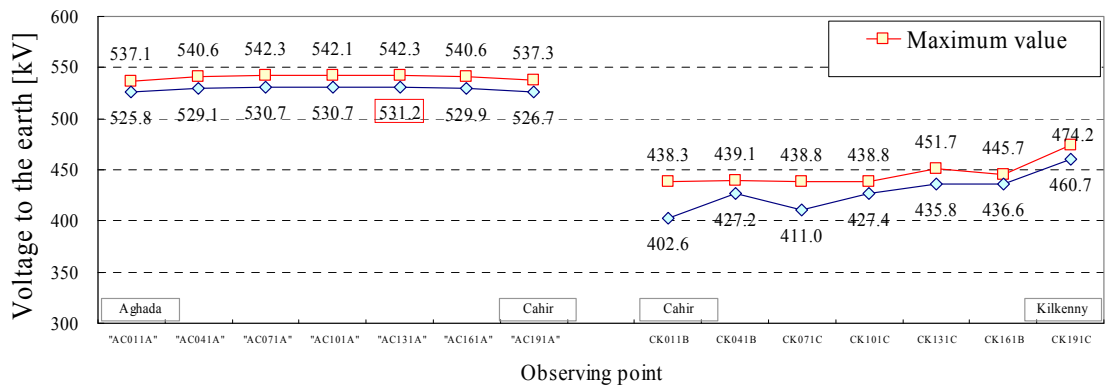
Fig. 5-18 Result of the ground fault and fault clearing analysis for 150 % case

Table 5-6 Effect of Cable Length to the Ground Fault and Fault Clearing Overvoltage

	Overvoltage	
	Maximum	2%
50 % case	542.3 kV (1.66 pu)	531.2 kV (1.63 pu)
Base case	542.0 kV (1.66 pu)	534.0 kV (1.63 pu)
150 % case	526.4 kV (1.61 pu)	520.1 kV (1.59 pu)

The following figures show the waveform of the overvoltages in a 50 % case and a 150 % case when the 2 % values were observed.
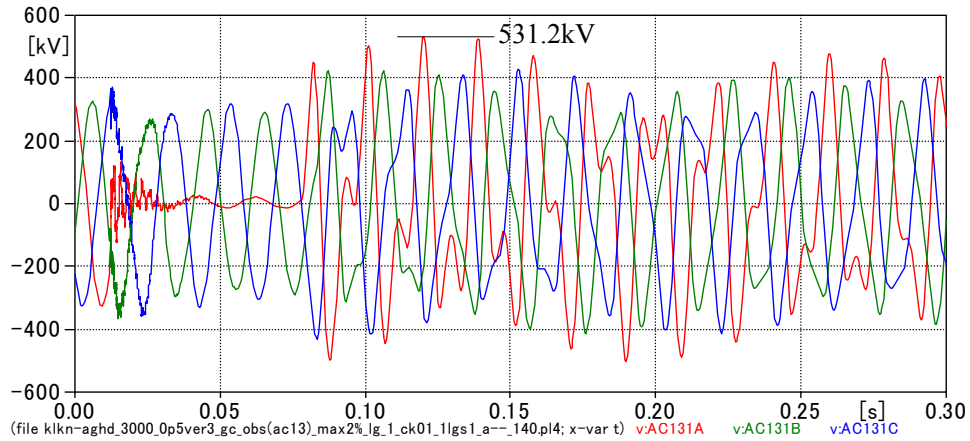
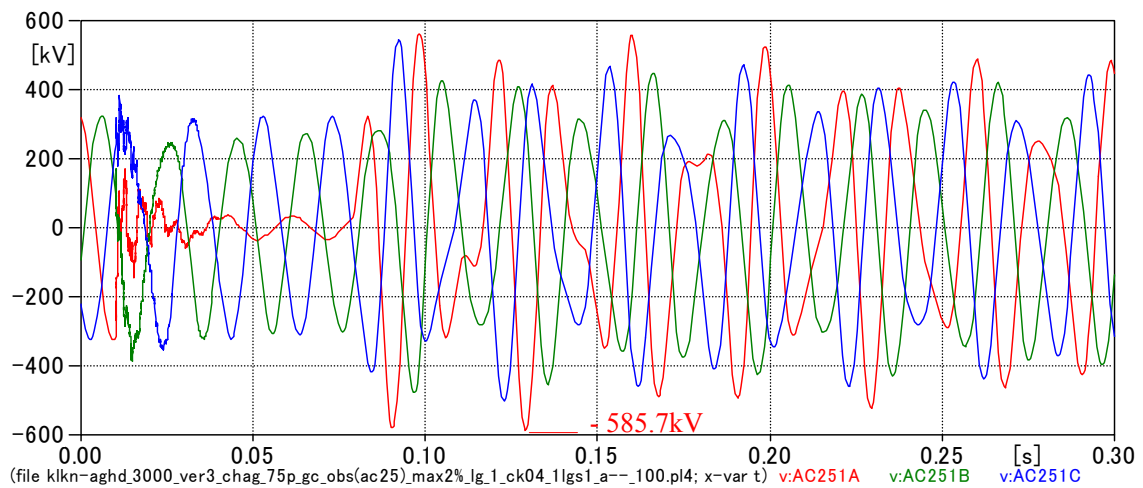**Fig. 5-19 Overvoltage in the 400 kV Aghada – Cahir line in 50 % case.**
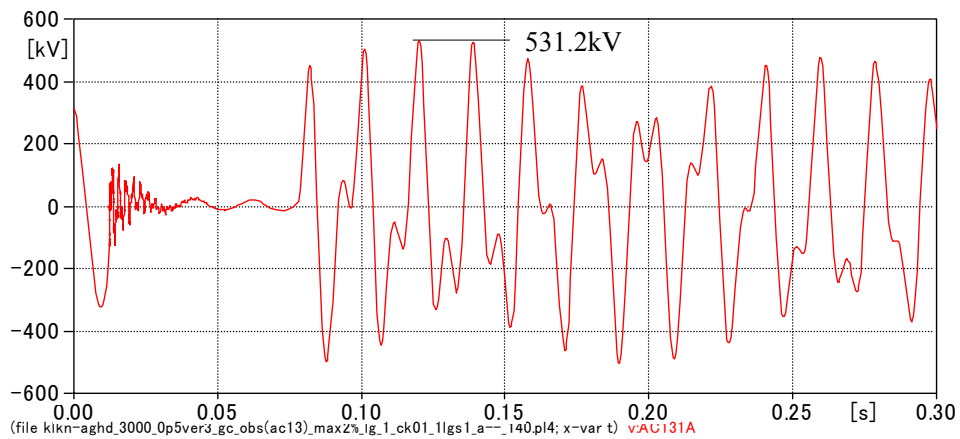
Fig. 5-20 Overvoltage in the 400 kV Aghada – Cahir line in 50 % case (Phase A).
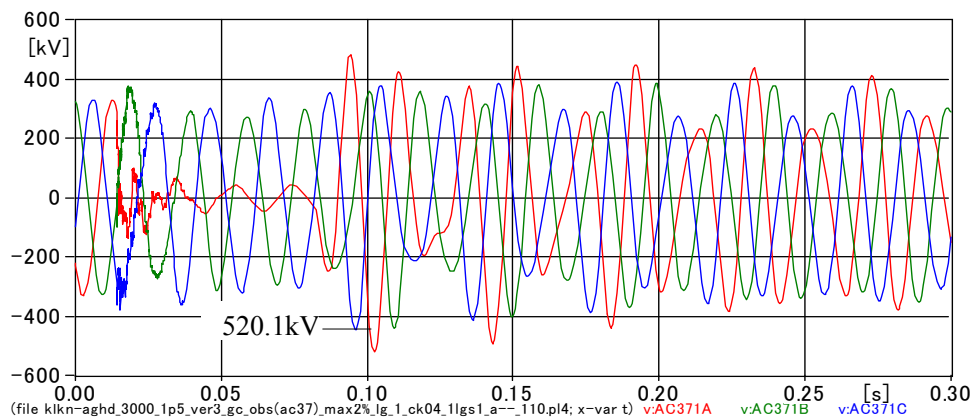
Fig. 5-21 Overvoltage in the 400 kV Aghada – Cahir line in 150 % case.
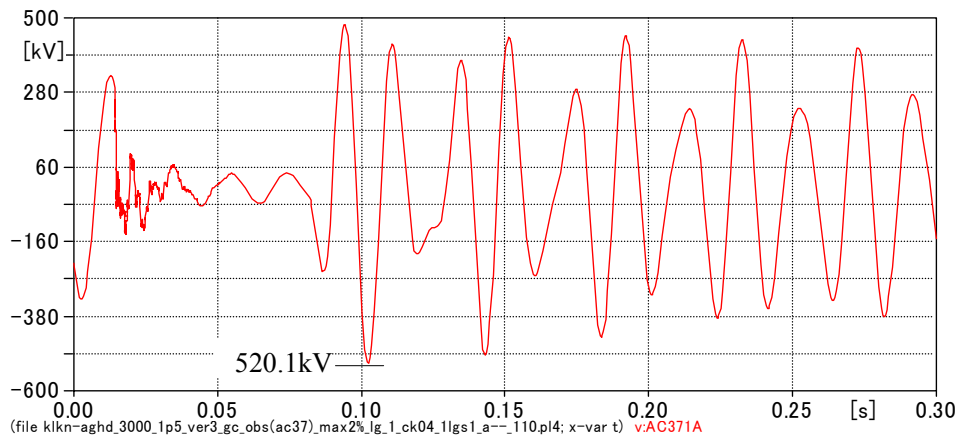
Fig. 5-22 Overvoltage in the 400 kV Aghada – Cahir line in 150 % case (Phase A).

The waveform of the overvoltage in Phase A (faulted phase) in the Base case is extracted from Fig. 5-15 as shown in Fig. 5-23.
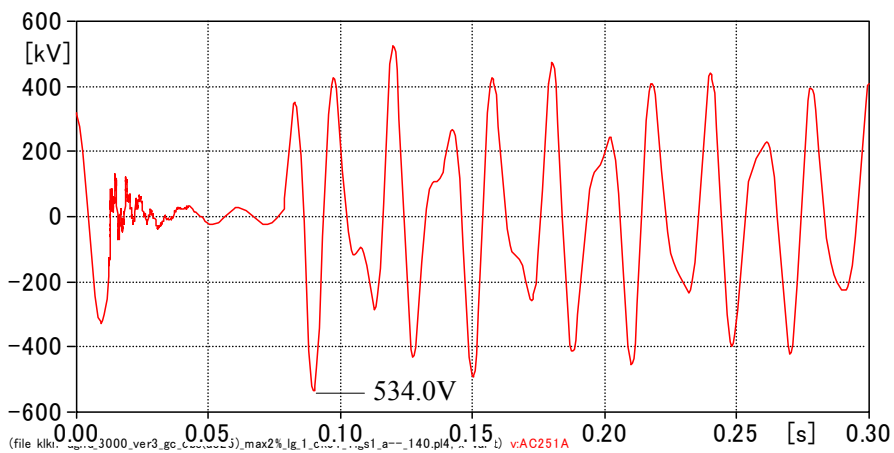
Fig. 5-23 Overvoltage in the 400 kV Aghada – Cahir line in Base case (Phase A).

Fig. 5-24 shows the result of the Fourier transform performed to the waveforms in Fig. 5-20, Fig. 5-22, and Fig. 5-23.
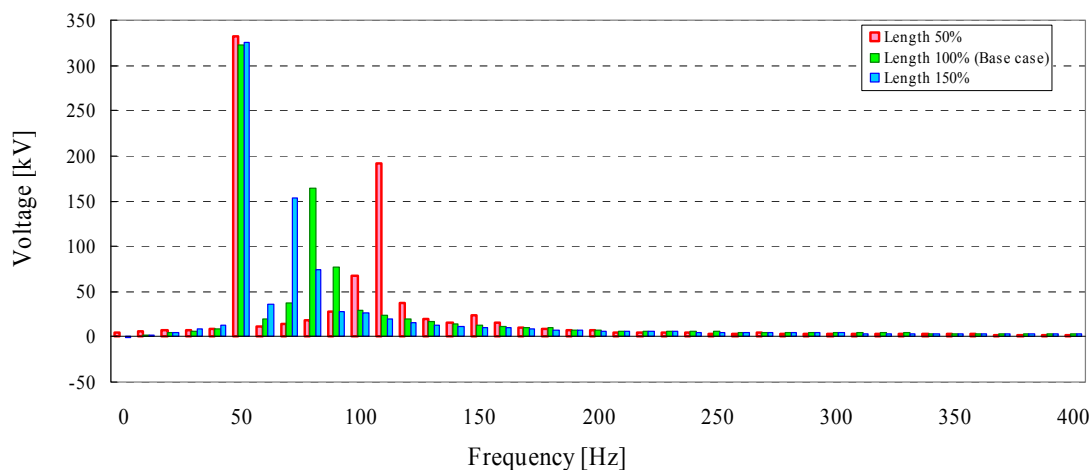
Fig. 5-24 Frequency spectrum of the overvoltage for different lengths of the Aghada – Cahir line.

5.2.3   Effect of the compensation rate

In this section, the ground fault and fault clearing overvoltage was studied with different compensation rates as shown in Table 5-7 and Fig. 5-25 – Fig. 5-27.

Table 5-7 Compensation Rate of the 400 kV Kilkenny – Cahir – Aghada Line

Locations	Case B2 (Base case)	Case B4	Case B5
Kilkenny Cahir	100MVA×4 80MVA×4	100MVA×5 80MVA×7	100MVA×6 80MVA×10
Compensation rate of Kilkenny – Cahir line	99.5 [%]	146.6 [%]	193.6 [%]
Cahir Reactor station Aghada	100MVA×4 80MVA×7 80MVA×5	100MVA×3 80MVA×6 80MVA×3	100MVA×2 80MVA×4 80MVA×2
Compensation rate of Cahir - Aghada line	100.7 [%]	75.5 [%]	50.4 [%]

Fig. 5-25 Compensation of 400 kV Kilkenny – Cahir – Aghada line in Case B2 (Base case).
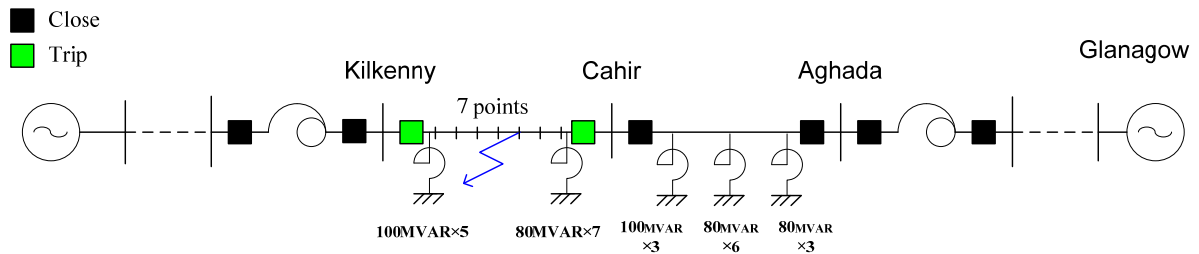
Fig. 5-26 Compensation of 400 kV Kilkenny – Cahir – Aghada line in Case B4 (approx. 75 % compensation).
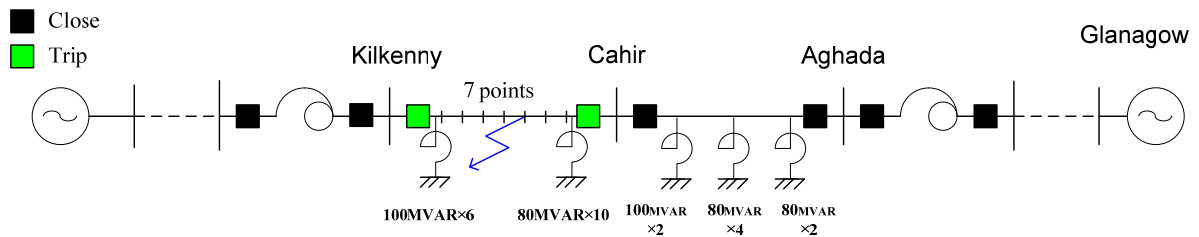
Fig. 5-27 Compensation of 400 kV Kilkenny – Cahir – Aghada line in Case B5 (approx. 50 % compensation).

For this analysis, source impedances were decided from short circuit calculation results under summer off-peak demand.

The profile of the overvoltage in Cases B4 and B5 are shown in Fig. 5-28 and Fig. 5-29.
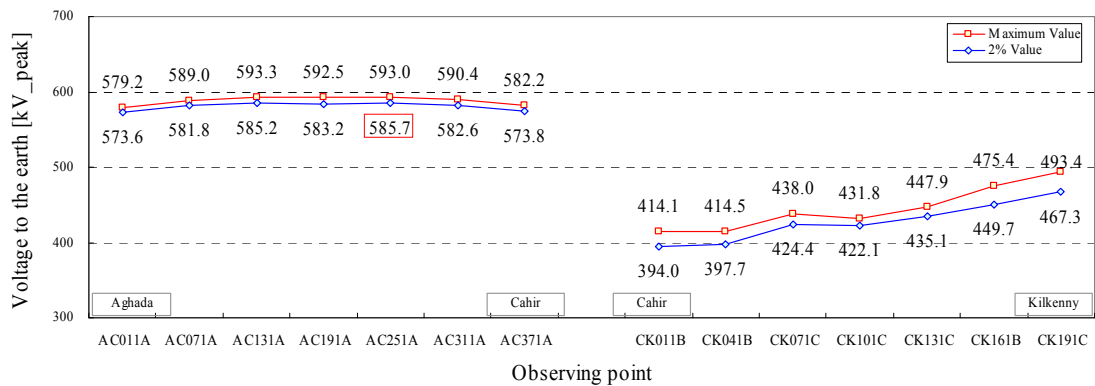
Fig. 5-28 Result of the ground fault and fault clearing analysis in Case B4 (approx. 75 % compensation).
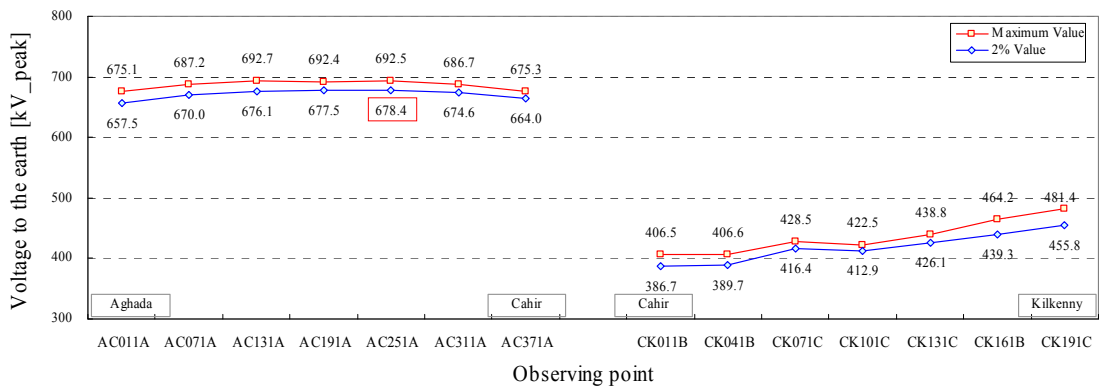
Fig. 5-29 Result of the ground fault and fault clearing analysis in Case B5 (approx. 50 % compensation).

Effects of the compensation rates are summarized in Table 5-8.   A lower compensation rate yields higher overvoltage, but the observed overvoltage was much lower than SIWV.

Table 5-8 Effect of Compensation Rate

	Over voltage	
	Maximum	2 %
Case B2 (approx. 100 % compensation)	542.3 kV (1.66 pu)	531.2 kV (1.63 pu)
Case B4 (approx. 75 % compensation)	593.3 kV (1.82 pu)	585.7 kV (1.79 pu)
Case B5 (approx. 50 % compensation)	692.7 kV (2.12 pu)	678.4 kV (2.08 p.u.)

Fig. 5-30 and Fig. 5-31 show the waveforms of the ground fault and fault clearing overvoltage when the 2 % value was observed in Cases B4 and B5.

(file klkn-aghd_3000_ver3_chag_75p_gc_obs(ac25)_max2%_lg_1_ck04_1lgs1_a--_100.pl4; x-var t)   v:AC251A   v:AC251B   v:AC251C

Fig. 5-30 Overvoltage in the 400 kV Aghada – Cahir line in Case B4 (approx. 75% compensation).

(file klkn-aghd_3000_ver3_chag_50p_gc_obs(ac25)_max2%_lg_1_ck07_1lgs1_a--_100.pl4; x-var t)   v:AC251A   v:AC251B   v:AC251C
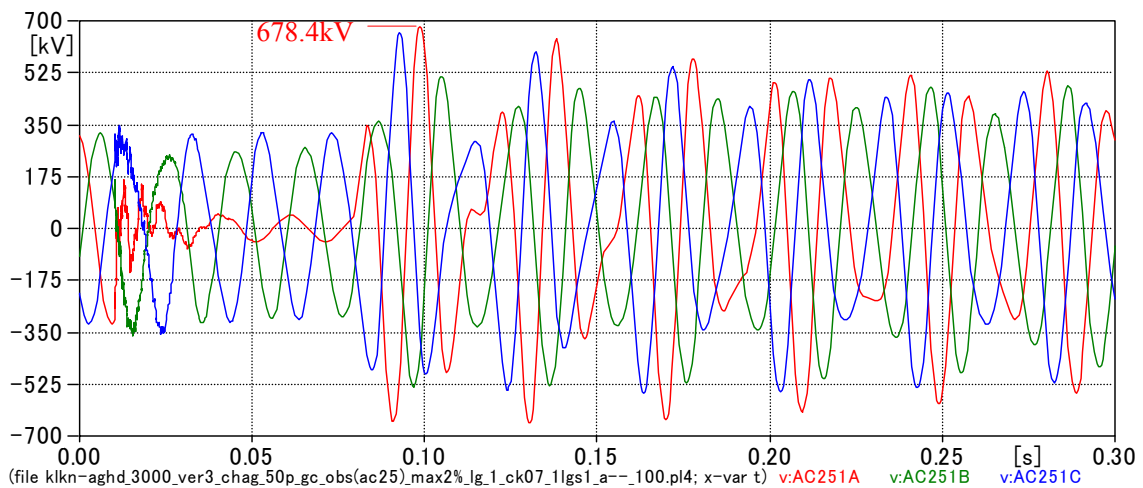
Fig. 5-31 Overvoltage in the 400 kV Aghada – Cahir line in Case B5 (approx. 50% compensation).

5.2.4   Effect of source impedance

The effect of source impedance to the ground fault and fault clearing overvoltage was studied with the source impedance values shown in Table 5-9.

Table 5-9 Assumed Sets of Source Impedance Values

	Kilkenny 220 kV	Cahir 110 kV	Aghada 220 kV
Case 1	50 mH	15 mH	20 mH
Case 2	75 mH	20 mH	55 mH
Case 3	100 mH	25 mH	90 mH

Results of the analysis in Case 1, Case 2 and Case 3 are shown in Fig. 5-32 – Fig. 5-34.
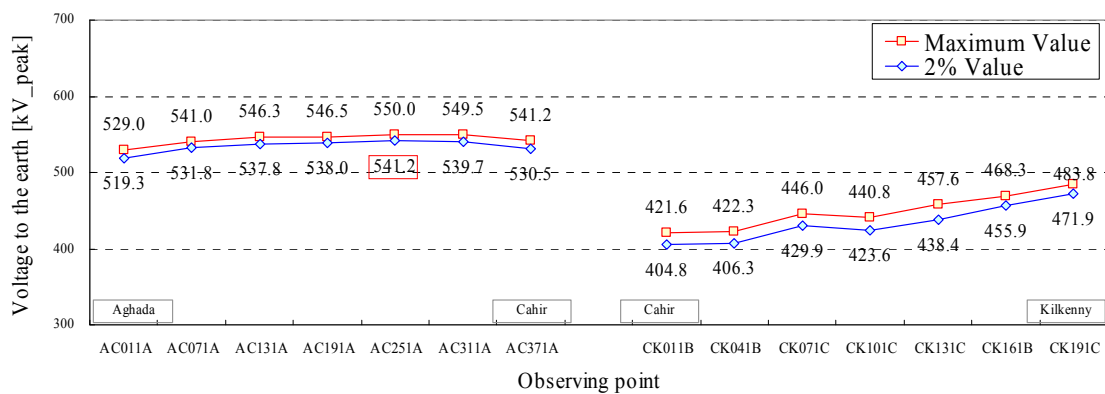
Fig. 5-32 Result of the ground fault and fault clearing analysis in Case 1
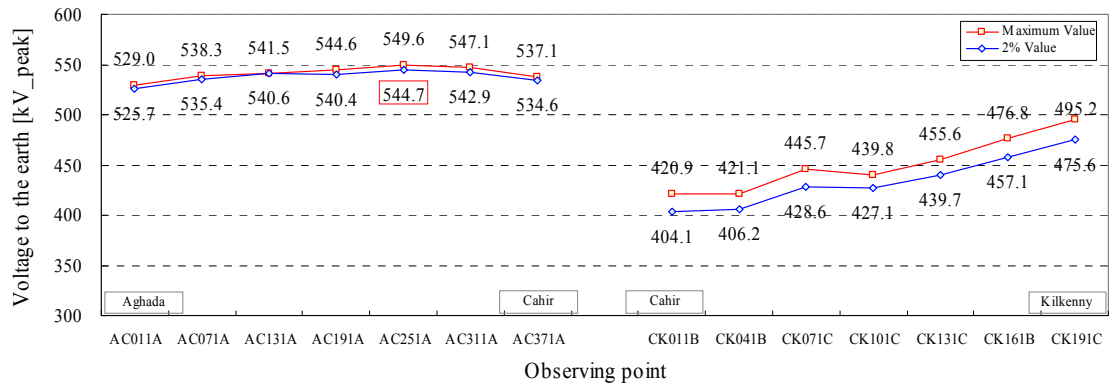
Fig. 5-33 Result of the ground fault and fault clearing analysis in Case 2
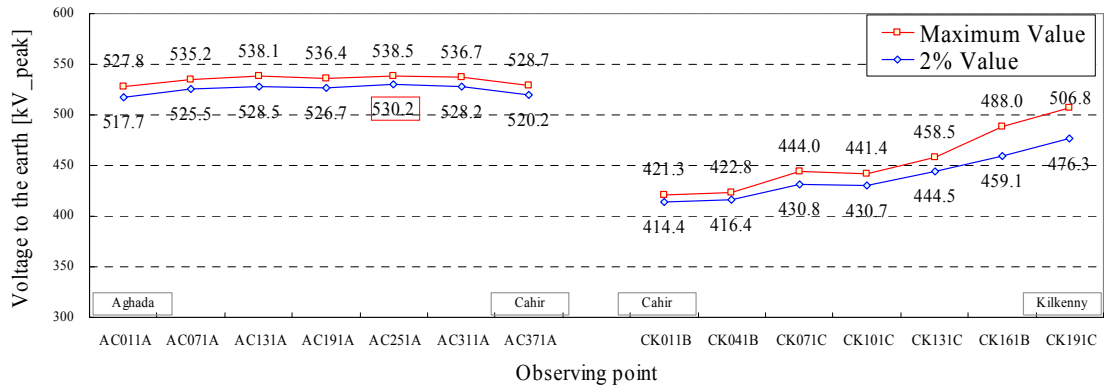
Fig. 5-34 Result of the ground fault and fault clearing analysis in Case 3

The results of the analyses are summarized in Table 5-10.

Table 5-10 Effect of Source Impedance

	Overvoltage	
	Maximum	2 %
Case 1	550.0 kV (1.68 pu)	541.2 kV (1.67 pu)
Case 2	549.6 kV (1.68 pu)	544.7 kV (1.67 pu)
Case 3	538.5 kV (1.65 pu)	530.2 kV (1.62 pu)

Fig. 5-35 – Fig. 5-37 shows the waveforms of the ground fault and fault clearing overvoltage when the 2 % values were observed in Cases 1, 2 and 3.

(file klkn-aghd_3000_ver3_gen_max_gc_obs(ac25)_max2%_lg_1_ck04_1lgs1_a--_100.pl4; x-var t) v:AC251A   v:AC251B   v:AC251C
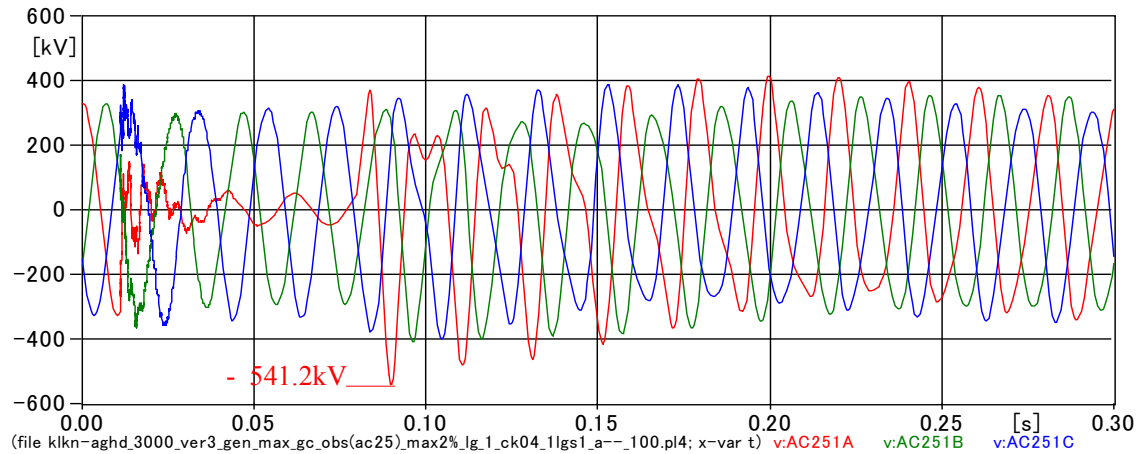
Fig. 5-35 Overvoltage in the 400 kV Aghada – Cahir line in Case 1.

(file klkn-aghd_3000_ver3_gen_middle_gc_obs(ac25)_max2%_lg_1_ck01_1lgs1_a--_040.pl4; x-var t) v:AC251A   v:AC251B   v:AC251C
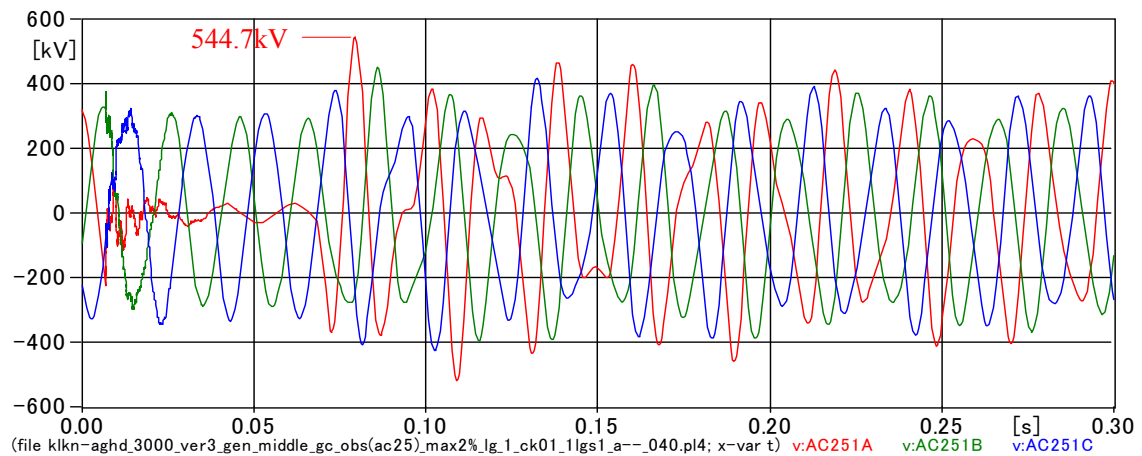
Fig. 5-36 Overvoltage in the 400 kV Aghada – Cahir line in Case 2.

(file klkn-aghd_3000_ver3_gen_min_gc_obs(ac25)_max2%_lg_1_ck04_1lgs1_a--_080.pl4; x-var t) v:AC251A   v:AC251B   v:AC251C
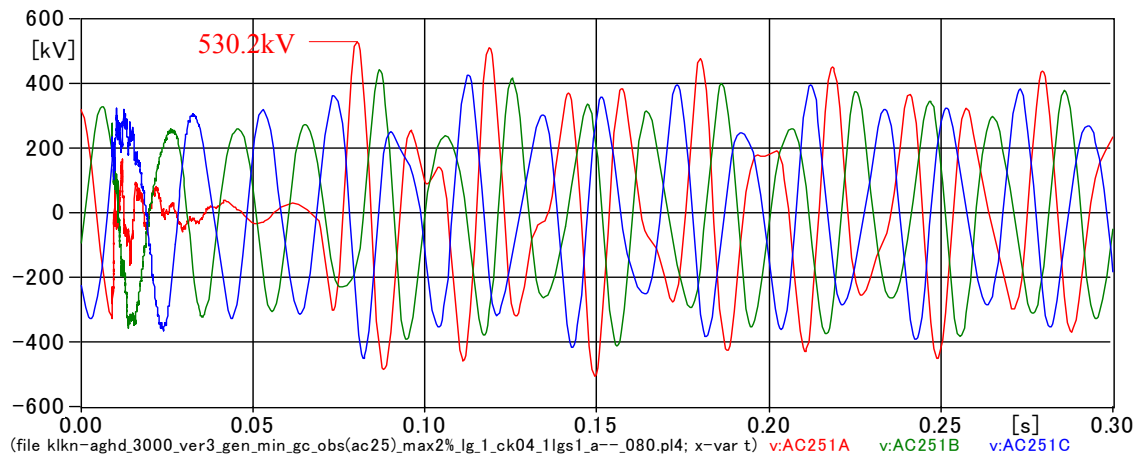
Fig. 5-37 Overvoltage in the 400 kV Aghada – Cahir line in Case 3.

In this section, the overvoltage caused by line energisation was studied with different conditions.   The observed overvoltages were much lower than SIWV in all simulated cases, which is typical for long cable systems.

5.3 Conclusion

Slow-front overvoltage caused by line energisation, ground fault, and fault clearing was studied in this chapter.   The result of the slow-front overvoltage analysis is summarized in Table 5-11.   As shown in the table, no significant overvoltage was found in the slow-front overvoltage analysis.   The observed overvoltages were much lower than SIWV in all simulated cases.

Table 5-11 Summary of the Slow-front Overvoltage Analysis

	Highest overvoltage (peak)	Withstand voltage (peak) for evaluation
Line energisation	564.2 kV (1.72 pu)	1050 kV
Ground fault and fault clearing	692.7 kV (2.12 pu)	

$$1\,\mathrm{pu} = 400\,\mathrm{kV} \times \frac{\sqrt{2}}{\sqrt{3}}\ (\mathrm{peak})$$

Chapter 6 Voltage Stability / Variation

Depending on the reactive power compensation rate of the cable, the loss of the 400 kV cable can cause large voltage variation or voltage instability.   Voltage stability and variation caused by the loss of the long 400 kV cable was studied in this chapter.

Long cables for the study of voltage stability and variation are shown in Table 6-1.   Reactive power compensation rates of the cables were varied from 70 % to 100 % in 10 % steps.

Table 6-1 List of Cables for the Study of Voltage Stability and Variation

KV	From Bus		To Bus		Charging [MVA/cct]	Length [km]
	3774	KINGSCOURT	90140	TURL	762.3	82
400	3774	KINGSCOURT	5464	WOODLAND	539.2	58
	1044	AGHADA	1724	CAHIR	1350.2	112

6.1 Voltage Variation by the Loss of the 400 kV Cable

The following voltage variation is allowed in the operation of the all-island transmission system.

Under normal operating conditions: 3 %   (11.4 kV)

Under contingencies: 10 %   (38.0 kV)

As the most severe condition, the power flow data in summer off-peak demand and in winter peak demand with maximum wind were selected for the analysis of the voltage variation.   In this power flow data, a cable and shunt reactors connected directly to the cable were switched off to find the voltage variation caused by the loss of the 400 kV cable.   Reactive power compensation rates of the cables were varied from 70 % to 100 % in 10 % steps.   Fig. 6-1 shows the voltage variation by the loss of the 400 kV Kingscourt – Turleenan line in winter peak demand with maximum wind.   In Fig. 6-1, positive values of voltage variation indicate a voltage drop.
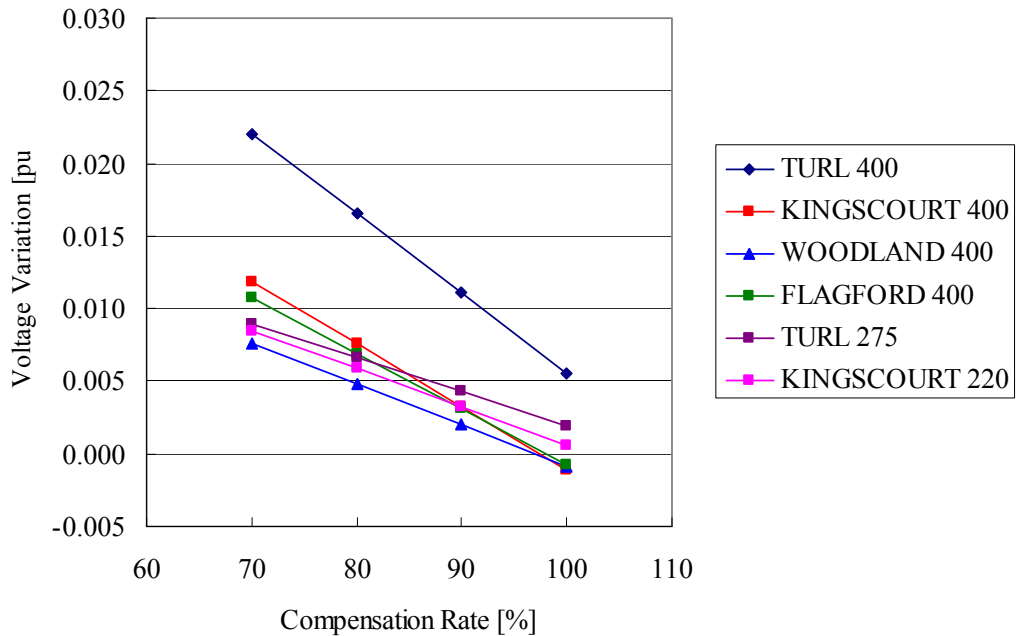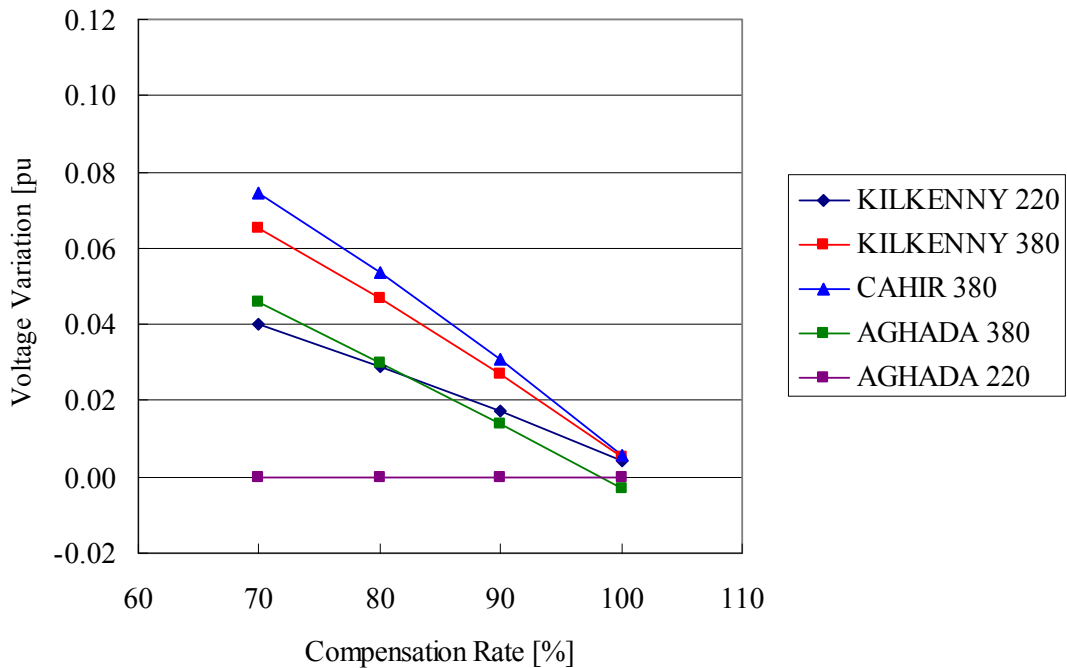
Fig. 6-1 Voltage variation by the loss of the 400 kV Kingscourt – Turleenan line in winter peak demand with maximum wind.

From Fig. 6-1, it can be seen that the voltage variation is kept within 10 %.

Next, the same analysis was performed in the summer off-peak demand.　The result of the analysis is shown in Fig. 6-2.
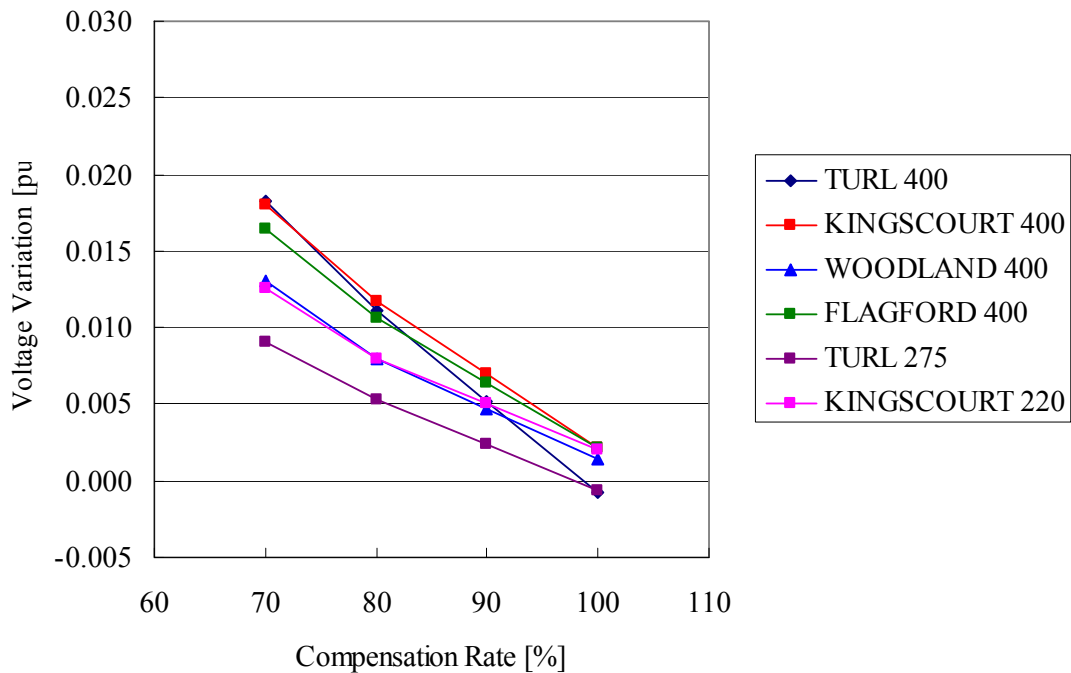
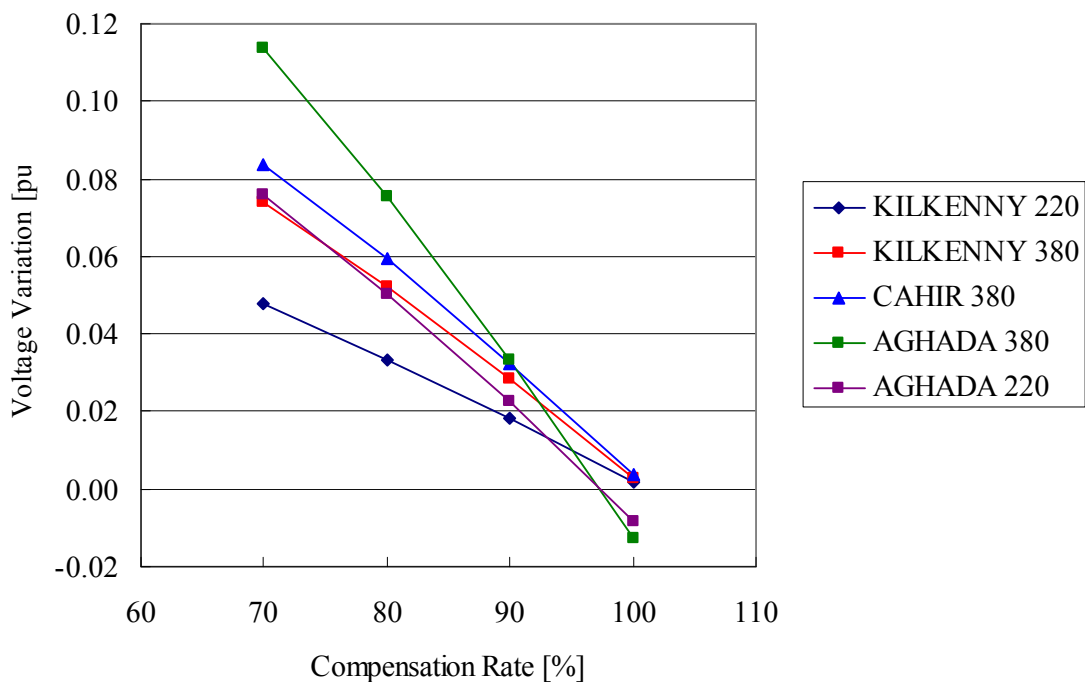**Fig. 6-2 Voltage variation with the loss of the 400 kV Kingscourt – Turleenan line in the summer off-peak demand.**

From Fig. 6-2, it can be seen that there is no problem in the voltage variation also in the summer off-peak demand.

The same analysis was performed for the 400 kV Woodland – Kingscourt line in the winter peak demand with maximum wind. The results of the analysis are shown in Fig. 6-3.
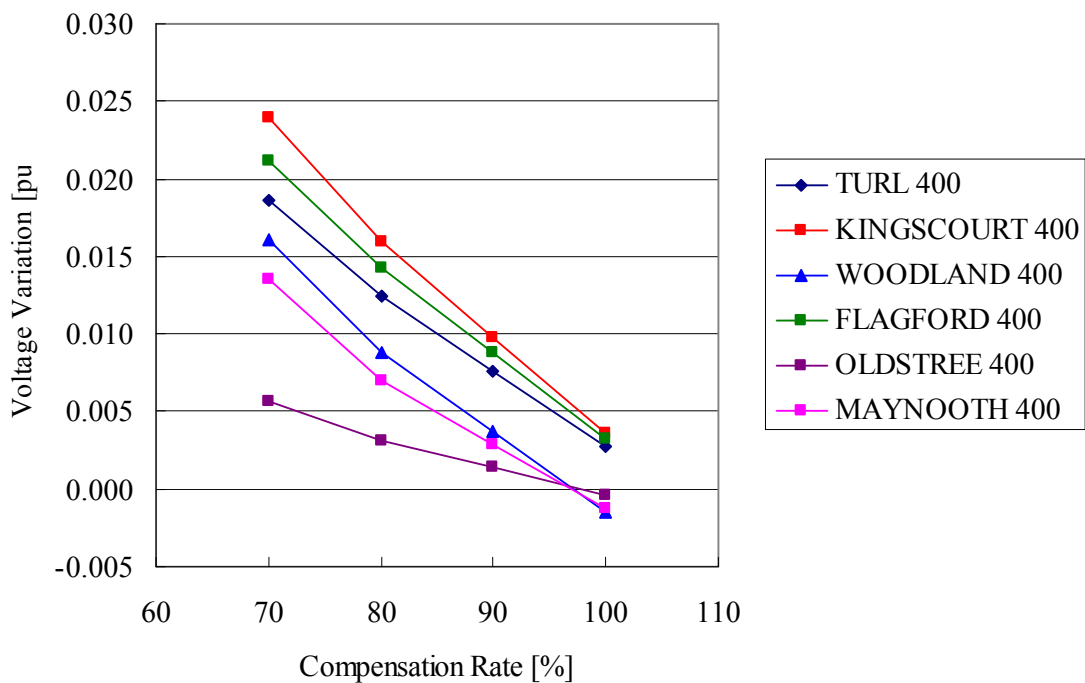
Fig. 6-3 Voltage variation by the loss of 400 kV Woodland – Kingscourt line in winter peak demand with maximum wind.

From Fig. 6-3, it can be seen that the voltage variation is maintained within 10 %.

The same analysis was performed in the summer off-peak demand. The result of the analysis is shown in Fig. 6-4.
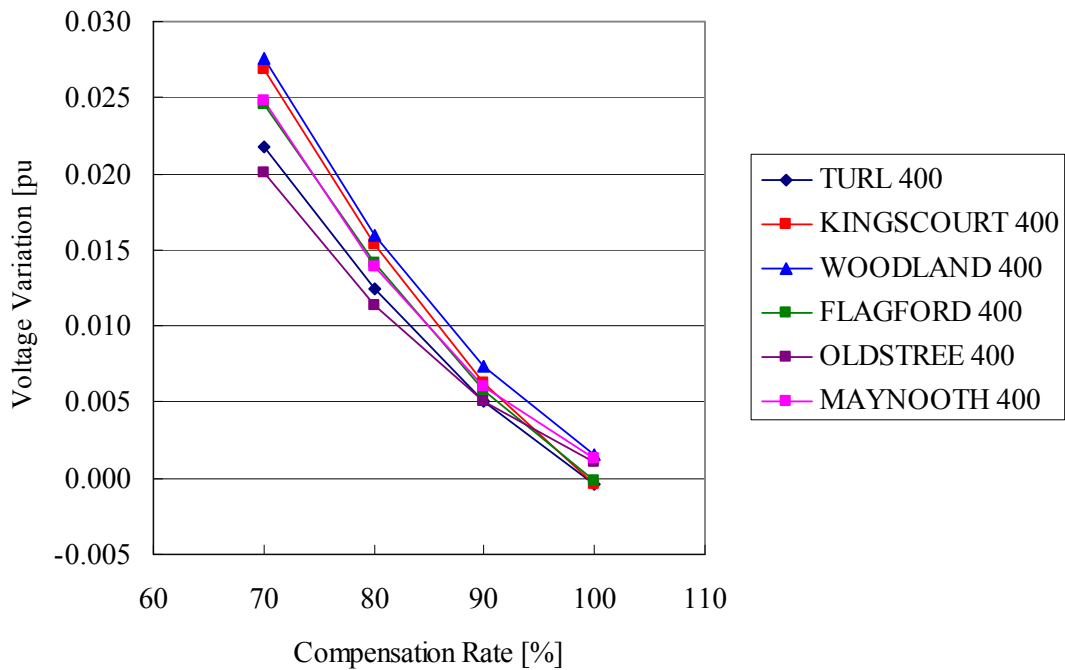
Fig. 6-4 Voltage variation with the loss of the 400 kV Woodland – Kingscourt line in summer off-peak demand.

From Fig. 6-4, it can be seen that there is no problem in the voltage variation.

The same analysis was performed for the 400 kV Cahir – Aghada line in the winter peak demand with maximum wind.   The results of the analysis are shown in Fig. 6-5.

Fig. 6-5 Voltage variation with the loss of the 400 kV Cahir – Aghada line in winter peak demand with maximum wind.

From Fig. 6-5, it can be seen that there is no problem in the voltage variation. Aghada 220 kV bus voltage is maintained at a constant voltage by reactive power supply from neighboring generators.

Next, the same analysis was performed in the summer off-peak demand. The result of the analysis is shown in Fig. 6-6.

Fig. 6-6 Voltage Variation with the Loss of Cahir – Aghada 400 kV Line in Summer Off-Peak Demand.

From Fig. 6-6, when the compensation rate is 70 %, the voltage variation of the Aghada 380 kV bus exceeds 10 %. In all other cases, it was found that there was no problem in the voltage variation.

6.2 Voltage Stability with the Loss of the 400 kV Cable

As the most severe condition, power flow data in the winter peak demand with maximum wind was selected for the analysis of the voltage stability.   In this power flow data, the 400 kV cables in Table 6-1 and shunt reactors connected directly to the cables were switched off in order to study the voltage stability of the system with the loss of the 400 kV cable.   Reactive power compensation rates of the 400 kV cables were varied from 70 % to 100 % by 10 % steps.   In order to increase the power flow of N-S interconnectors by 1500MW, generators in the power flow data were dispatched as shown Table 6-2.   In this analysis controls of tap changers and switched shunt capacitors/reactors were blocked.   Fig. 6-7 shows PV curves at the Kingscourt 400 kV bus with the loss of the 400 kV Kingscourt – Turleenan line.

Table 6-2 Generators Dispatched to Increase the Power Flow of N-S Interconnectors

Generators increased output			Generators decreased output		
Number	Name	Output	Number	Name	Output
70504	BAFDG4	0→168	39471	MNYPG1	285.2→115
70505	BAFDG5	0→168	39472	MNYPG2-P	285.2→115
70506	BAFDG6	0→168	39473	MNYPG3	285.2→115
70520	BAFD2-	0→400	50573	SEAL ROC	81.4→0
74520	CAST2-	0→400	50574	SEAL ROC	81.4→0
86225	BALLYCRO	425→500	44471	POLLG1_4	15→5
70515	BAFD_GC	189→200	44471	POLLG1_4	15→5
82001	KILRG1-	226→300	44471	POLLG1_4	4→1
82002	KILRG2-	227→300	28571	GLANAGOW	405→110.1
			35771	LONGPOIN	408→222
			31271	DUBLIN B	395.6→163
			29673	HUNTSTOW	308→257
			49474	WOP_G4	150→55
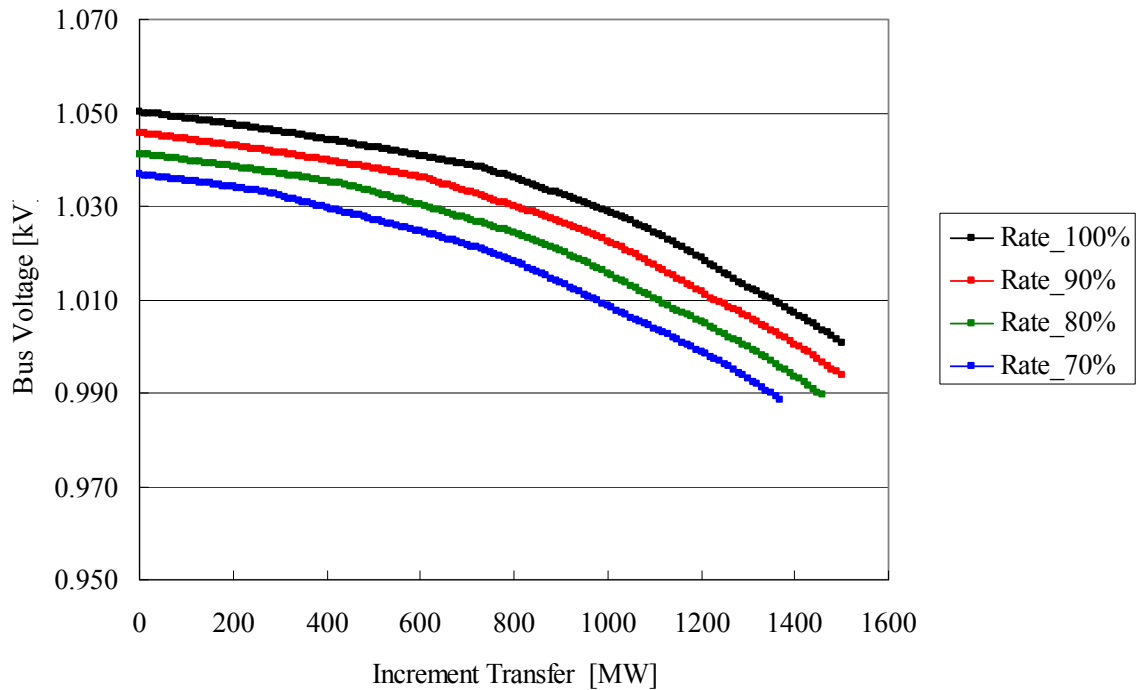
Fig. 6-7 PV-curves at the Kingscourt 400 kV bus with the loss of the 400 kV Kingscourt – Turleenan line.

The voltage stability was maintained even after the power flow in the N-S interconnectors was increased by 1500 MW as shown in Fig. 6-7.

Next, the same analysis was performed at the Woodland 400 kV bus with the loss of the 400 kV Woodland – Kingscourt line.   The result of the analysis is shown in Fig. 6-8.
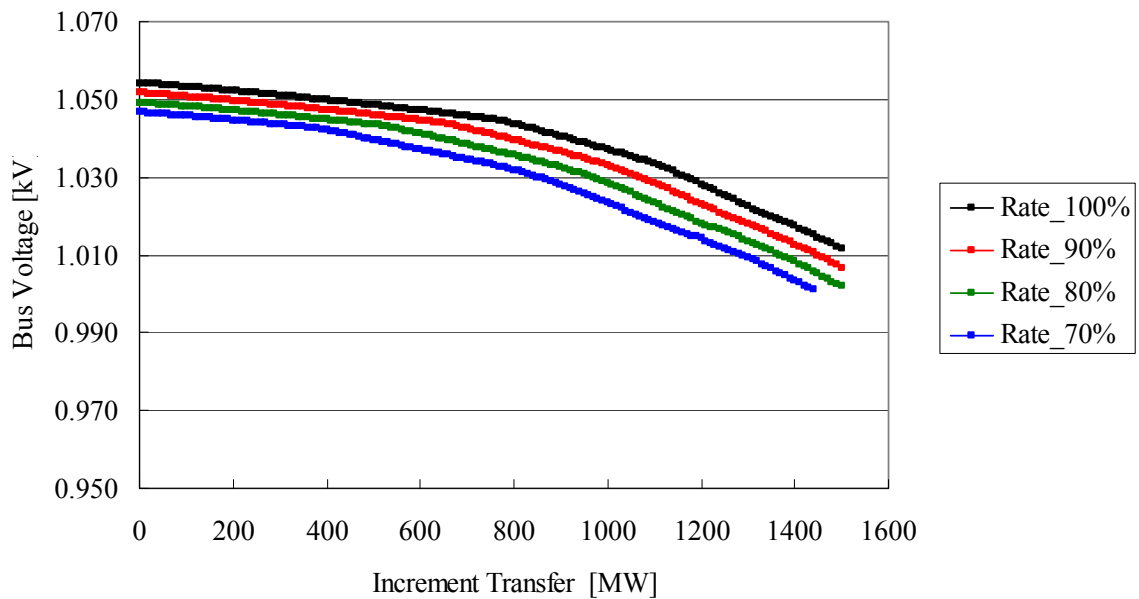
Fig. 6-8 PV-curves at the Woodland 400 kV bus with the loss of the 400 kV Woodland – Kingscourt line.

The voltage stability was maintained even after the power flow in the N-S interconnectors were increased by 1500 MW as shown in Fig. 6-8.

The loss of the 400 kV Cahir – Aghada line leads to the loss of reactive power supply to the Cahir 400 kV and 110 kV network. In order to determine the ability of a power system to maintain voltage stability at the Cahir 400 kV bus, the loads and generators in the power flow data were dispatched as shown Table 6-3.   In this analysis controls of tap changers and switched shunt capacitors/reactors were blocked.

The result of the analysis is shown in Fig. 6-9.

Table 6-3 Loads and Generators Dispatched to Increase the Power Flow of the 400 kV Kilkenny - Cahir Line

generators increased output			Increased loads		
Number	Name	Output	Area number	Area name	Total base Load (=1.0pu)
70504	BAFDG4	0→168	3	CORK KERRY	911.2MW
70505	BAFDG5	0→168	5	CAHIR NETW	554.5MW
70506	BAFDG6	0→168			
70520	BAFD2-	0→400			
74520	CAST2-	0→400			
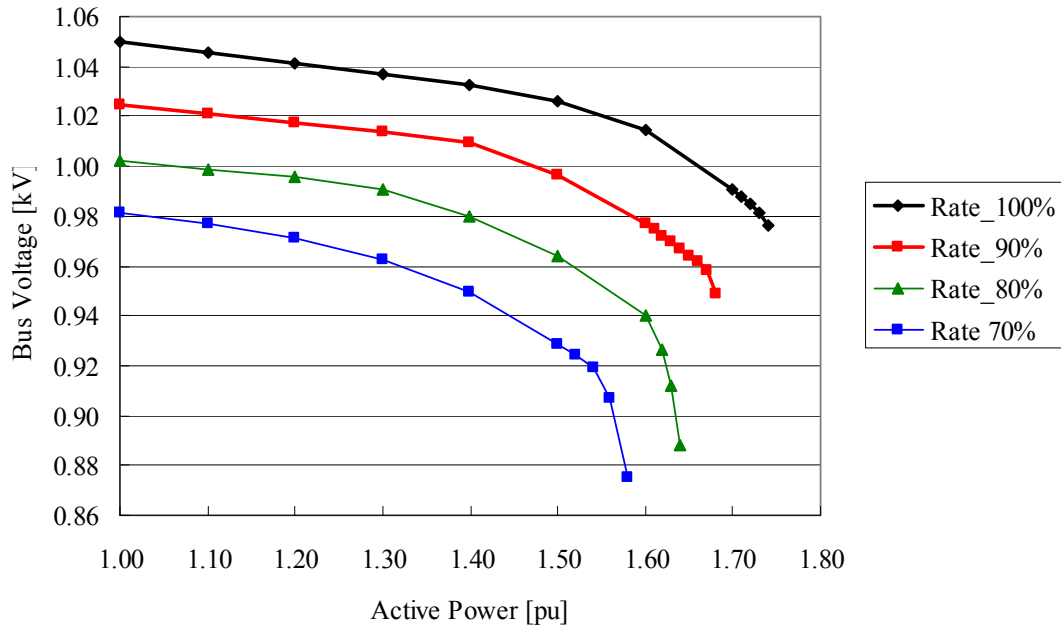
Fig. 6-9 PV-curves at the Cahir 400 kV bus with the loss of the 400 kV Cahir - Aghada line.

The voltage stability was maintained even after the winter peak demand was increased to 150% as shown in Fig. 6-9.

As the most severe condition, the same analysis was performed under outages of generators at Glanagow and Longpoint. In order to adjust the demand-supply balance, outputs of some generators in the power flow data were changed as shown in Table 6-4. The result of the analysis is shown in Fig. 6-10.

Table 6-4 Generators Dispatched to Adjust Demand-Supply

Number	Name	Output
29671	HUNT_ST	0→120
29672	HUNT_CT	0→230
39471	MNYPG1	285.2→301.5
39472	MNYPG2-P	285.2→301.5
39473	MNYPG3	285.2→301.5
44671	PBEGG1	0→115
44672	PBEGG2	0→115
44673	PBEGG3	0→255
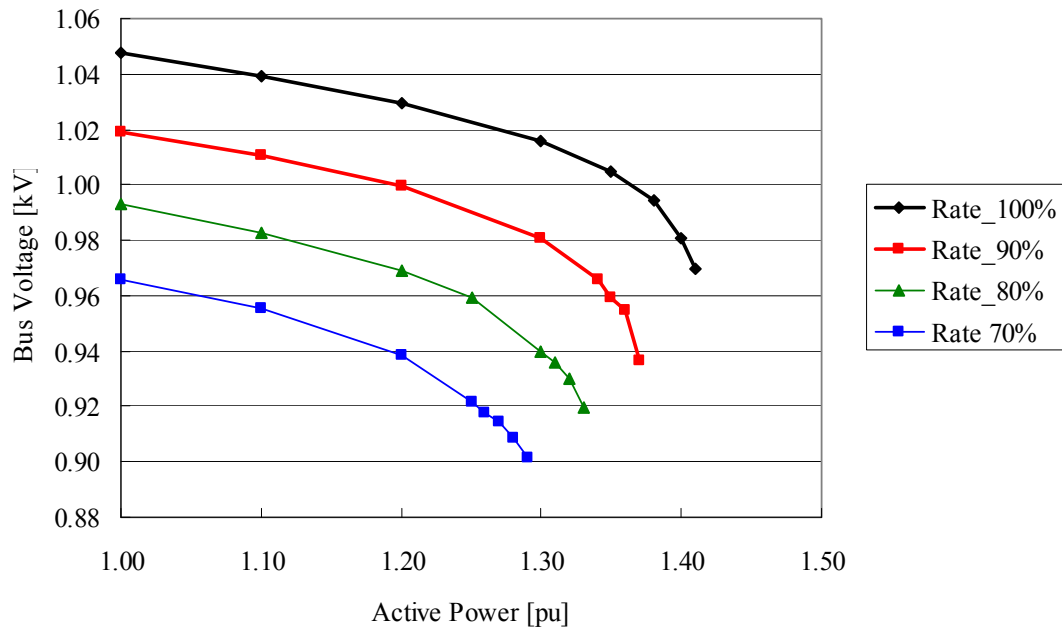
Fig. 6-10 PV-curves at the Cahir 400 kV bus with the loss of the 400 kV Cahir - Aghada line under outages of generators at Glanagow and Longpoint.

The voltage stability was maintained even after the winter peak demand was increased to 125 % as shown in Fig. 6-10.

6.3 Conclusion

Depending on the reactive power compensation rate of the cable, the loss of the 400 kV cable can cause large voltage variation or voltage instability.   Voltage stability and variation caused by the loss of the long 400 kV cable was studied in this chapter.

In the voltage variation analysis, the losses of the 400 kV Kingscourt – Turleenan line, the 400 kV Woodland – Kingscourt line, and the 400 kV Cahir – Aghada line were studied in winter peak demand with maximum wind and in summer off-peak demand.   The reactive power compensation rates were varied from 70 % to 100 % by 10 % step.   The variation above 10 % was observed in the loss of the 400 kV Cahir – Aghada line in summer off-peak demand.   Since the violation occurred when the compensation rate was 70 %, the compensation rate of the 400 kV Cahir – Aghada line has to be higher than 70 % in order to comply with the transmission planning criteria.

In the voltage stability analysis, the losses of the 400 kV Kingscourt – Turleenan line, the 400 kV Woodland – Kingscourt line, and the 400 kV Cahir – Aghada line were studied in winter peak demand with maximum wind.   As in the voltage variation analysis, the reactive power compensation rates were varied from 70 % to 100 % by 10 % step.   It was confirmed that the voltage stability was maintained after increasing the power flow in the N-S interconnectors or the winter peak demand within the reasonable range.

Chapter 7 Black-start Capability

In the restoration of the bulk power system, sustained power frequency overvoltages may be caused by charging current. When the restoration has to be realized through an EHV underground cable with significant length, black-start generators would be required to have sufficient under-excitation capability, depending on the compensation rate of the cable charging capacity.

Besides the sustained power frequency overvoltages, harmonic resonance overvoltage can be caused in the restoration of the bulk power system. The highest concern is the second harmonic current injection as in the parallel resonance overvoltage analysis. In the restoration through the network largely composed of OHTLs, it is generally possible to avoid the resonance condition by the connection of generators and loads and/or other operational measures. For the network largely composed of EHV underground cables, it requires careful assessment when establishing restoration procedures.

The analysis needs to be performed both on under-excitation capability of black-start generators and on harmonic resonance overvoltage. The blackout restoration procedures of NIE and EirGrid are evaluated after replacing some OHLs by underground cables.

7.1 Restoration in the Eirgrid Network

This section has been deleted due to the security concerns for the EirGrid Network.

7.2 Restoration in the NIE Network

The northwest area was selected for the black-start capability study because 275 kV Coolkeeragh – Strabane – Omagh line was replaced by underground cables.

7.2.1 Restoration procedure

The restoration procedure is shown in Fig. 7-1.
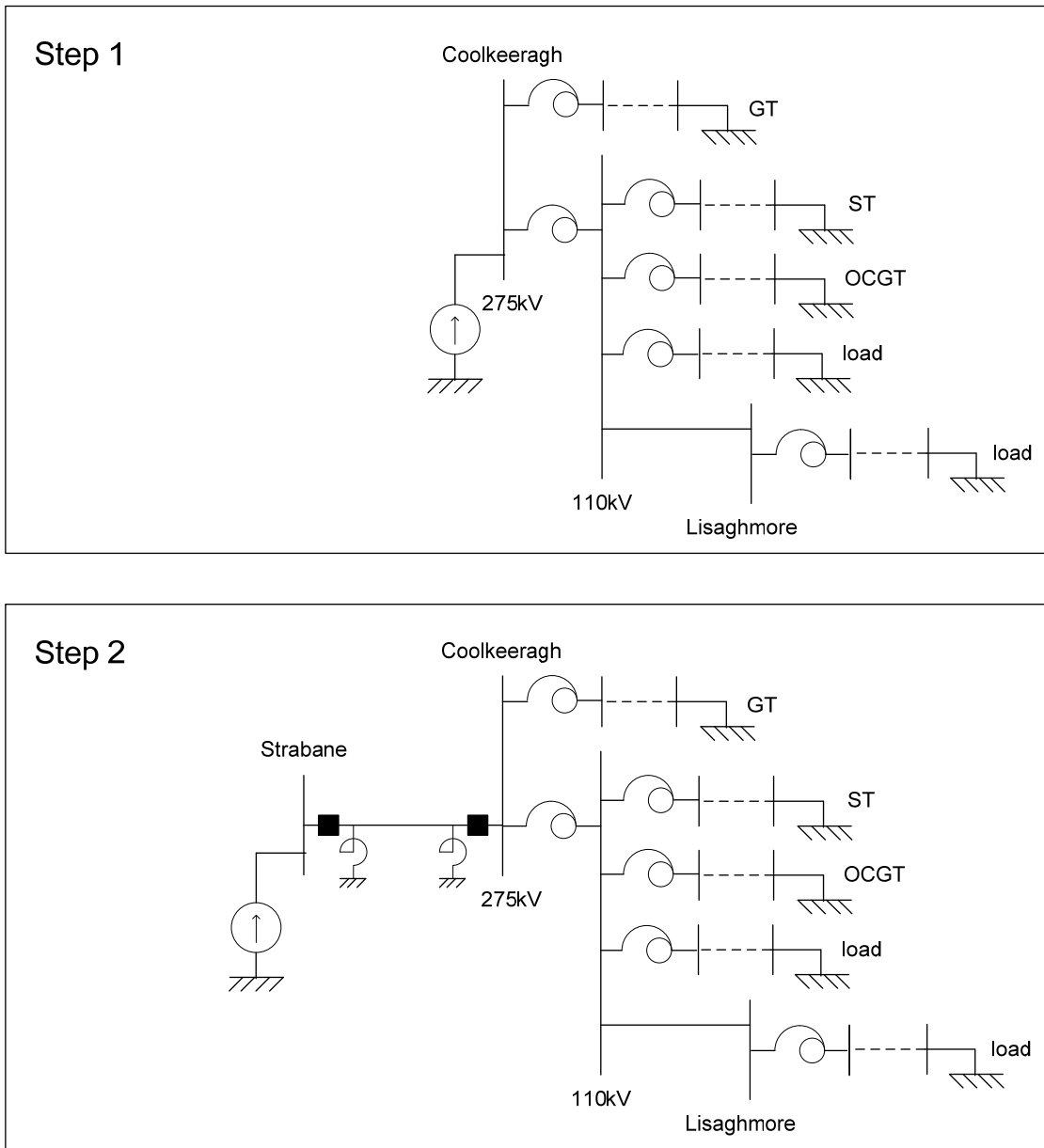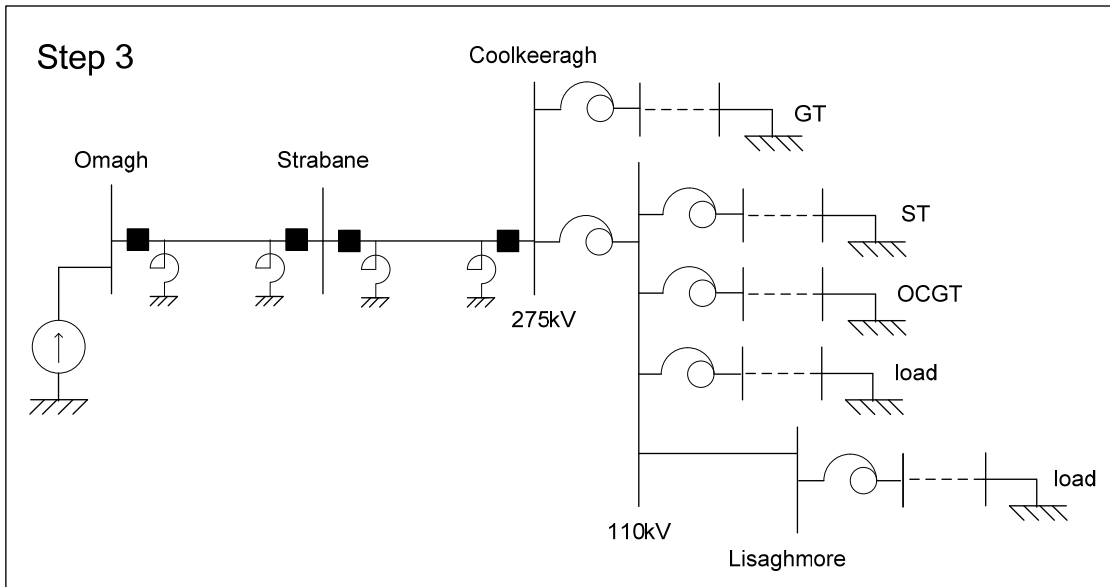
Fig. 7-1 Restoration procedure.

7.2.2 Under-excitation capability of black-start generators

In order to find the effect of the installation of cables on the ability to black-start, power flow calculations were conducted in PSS/E under both OHL and cable conditions for the lines shown in Table 7-1. Compensation rate of the Coolkeeragh – Strabane – Omagh cable was set to be 100 %.

Table 7-1 List of OHLs Replaced by Cables

KV	From Bus Name	To Bus Name	Original Impedance/Susceptance			Modified Impedance/Susceptance		
			Line R (pu)	Line X (pu)	Charging (pu)	Line R (pu)	Line X (pu)	Charging (pu)
275	COOLKEE	STRABANE	0.00126	0.01041	0.06755	0.000789	0.007978	1.3045
	OMAH	STRABANE	0.00151	0.0125	0.08106	0.001894	0.019146	3.1308

As the most severe condition, generators and loads in the power flow data were dispatched as shown Table 7-2 and Table 7-3, respectively. In this analysis, it was assumed that one transmission line and one transformer were in service, shunt capacitors were out of service, and generator terminal voltage was controlled at the rated voltage.

Table 7-2 Outputs of Generators for Black-start Analysis

Generator	Voltage[kV]	Pg[MW]	Pgmax[MW]	Pgmin[MW]
COOL_GT	16.0	20	259	20
COOL_ST	16.0	30	136	30
OCGT	11.0	13.75	55	0

Table 7-3 Loads for Black-start Analysis

Bus name	Voltage[kV]	PL[MW]	QL[MVar]
COOLG8	33.0	37.2	30.8
LSMR3	33.0	26.6	22.0

The result of the analysis is shown in Table 7-4.   It can be seen from the table that under both OHL and cable conditions, outputs of generators are kept within the generator reactive capability limitation.   In the case of OHL, output of each generator decreases; in the case of the cable, output of each generator is kept at a constant value because of 100 % compensation.   Note that the negative Qgen in the figure means the generator is absorbing reactive power.

Table 7-4 Reactive power from Coolkeeragh power staton.

Bus name	Qgen[Mvar]						Qgmax [MVar]	Qgmin [MVar]
	OHL			Cable				
	Step1	Step2	Step3	Step1	Step2	Step3		
COOL_GT	10.6	5.7	-0.3	10.6	10.6	10.6	120	-60
COOL_ST	40.5	38.5	36.2	40.5	40.5	40.5	70	-40
OCGT	13.0	12.5	11.9	13.0	13.0	13.0	50	-16

Then, in order to find the effect of the compensation rate of the Coolkeeragh – Strabane – Omagh line, the same analysis was performed with different compensation rates 70 % and 85 %.

The result of the analysis at Step 2 is shown in Fig. 7-2. The horizontal axis of the figure shows the compensation rate of the 275 kV Coolkeeragh – Strabane line. It can be seen from the figures that outputs of generators are kept within the generator reactive capability limitation in this step.

Reactive power from GT

Reactive power from ST

Qgen [MVar]
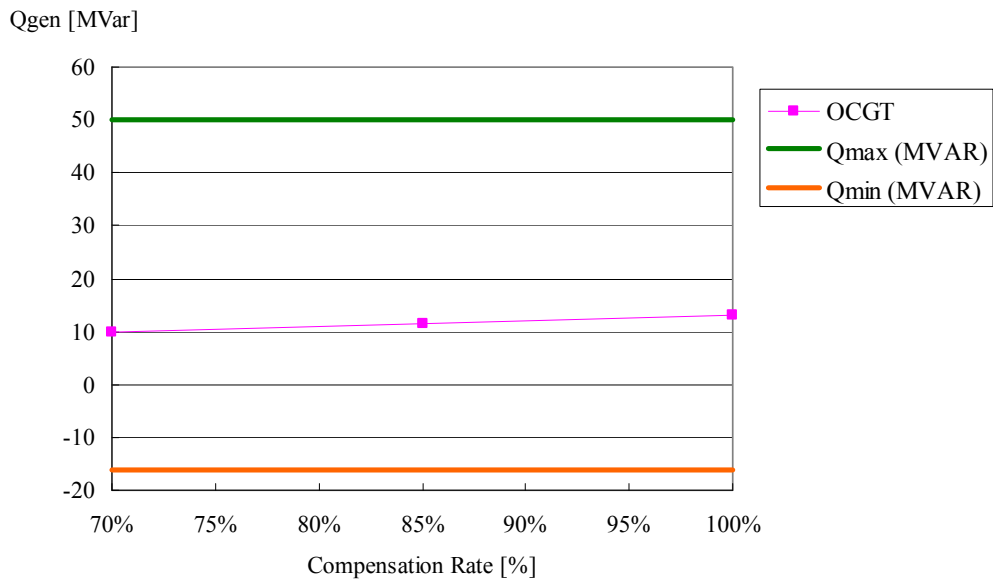
Reactive power from OCGT

Fig. 7-2 Effect of compensation rate at Step 2.

The result of the analysis at Step 3 is shown in Fig. 7-3. The horizontal axis of the figure shows the compensation rate of the 275 kV Strabane – Omagh line, and lines with different colors show the compensation rate of the 275 kV Coolkeeragh – Strabane. It can be seen from the figures that outputs of ST and OCGT are kept within the generator reactive capability limitation, but those of GT exceed the limitation with lower compensation rates. Note that negative Qgen in the figure means the generator is absorbing reactive power.
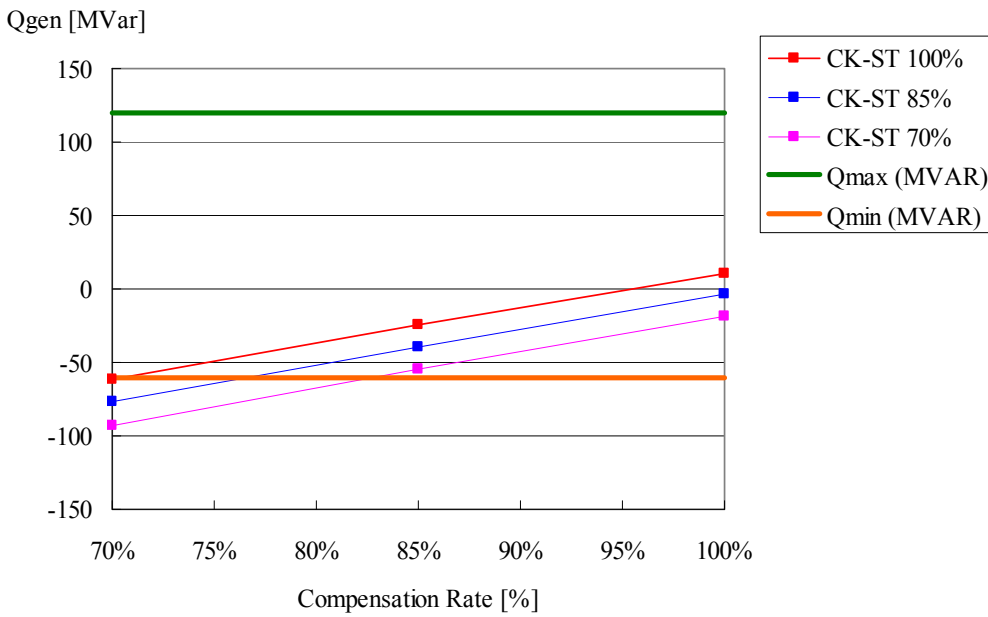
Reactive power from GT
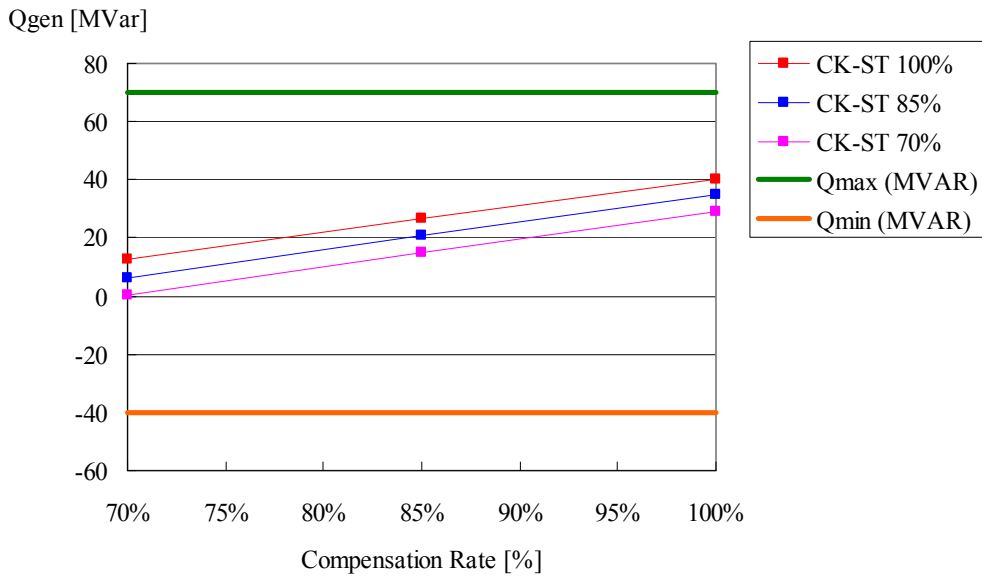
Reactive power from ST
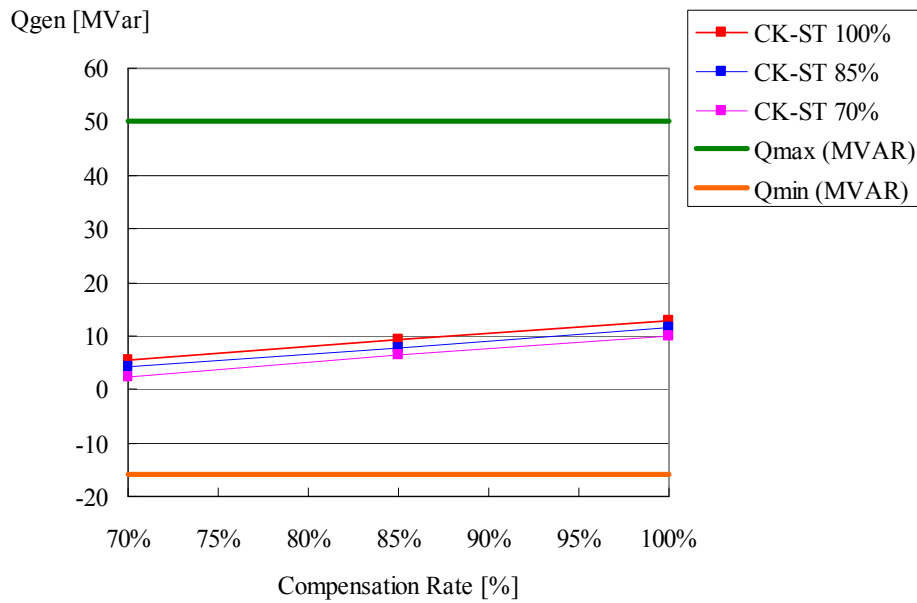
Reactive power from OCGT

Fig. 7-3 Effect of compensation rate at Step 3.

Fig. 7-4 shows the busbar voltage at the Omagh 275 kV with different compensation rates.   It can be seen from the figures that busbar voltages exceed 300 kV for lower compensation rates.
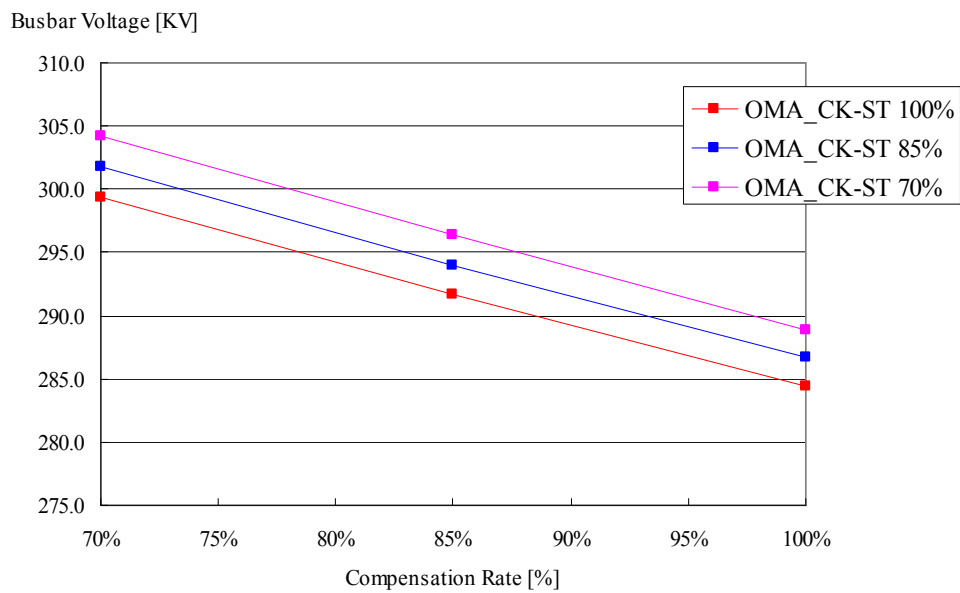
Fig. 7-4 Busbar voltage at Omagh 275kV with different compensation rates at Step 3.

7.2.3   **Parallel resonance frequency**

Parallel resonance frequency of the network was found by frequency scan using the simulation model in Fig. 7-5
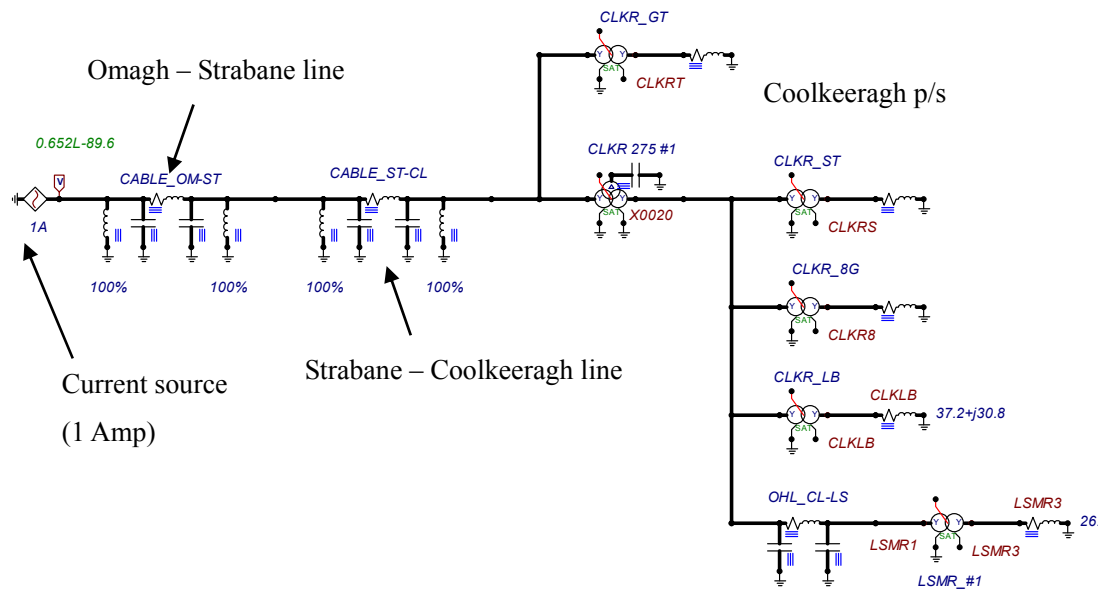
Fig. 7-5 Simulation model for frequency sweep.

First, the result of frequency scan seen from Coolkeeragh 275 kV at Step 1 is shown in Fig. 7-6.   As in the frequency scan result seen from Coolkeeragh 275 kV, the highest peak was found at 3254 Hz.
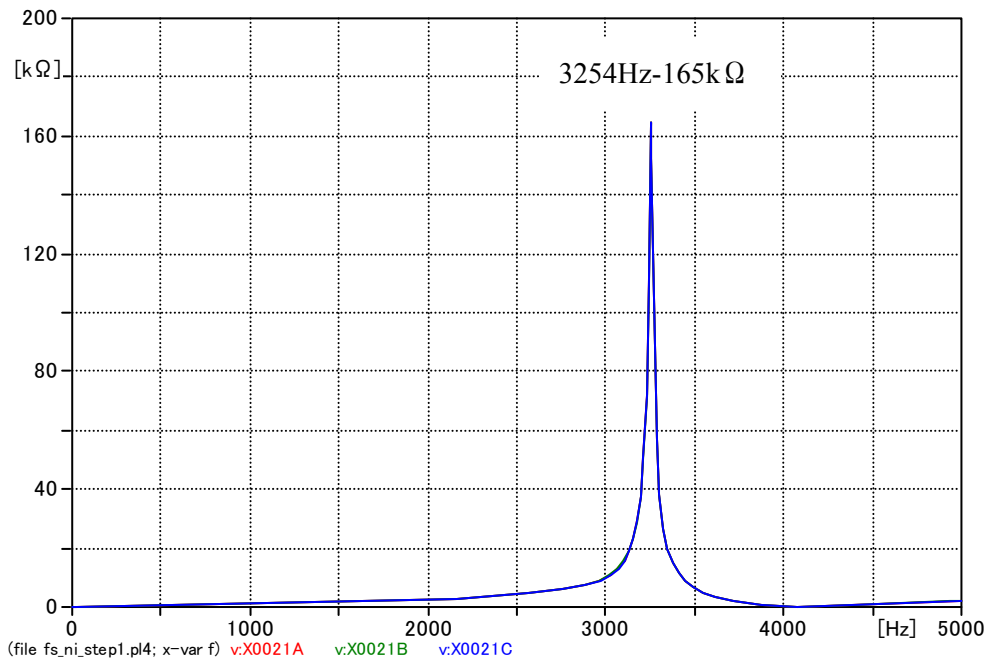
Fig. 7-6 Parallel resonance frequency of the network seen from Coolkeeragh 275 kV at Step 1.

Next, in order to find the effect of the replacement of OHLs by cables on the resonance frequency, a frequency scan was conducted under both OHL and cable conditions. In this analysis, the compensation rate of shunt reactor was set to be 100 %.

The results of frequency scan are shown in Fig. 7-7. It can be seen that parallel resonance frequency was shifted to lower frequency and the magnitude of impedance at parallel resonance decreased when 275 kV Strabane – Coolkeeragh line was replaced by cables.
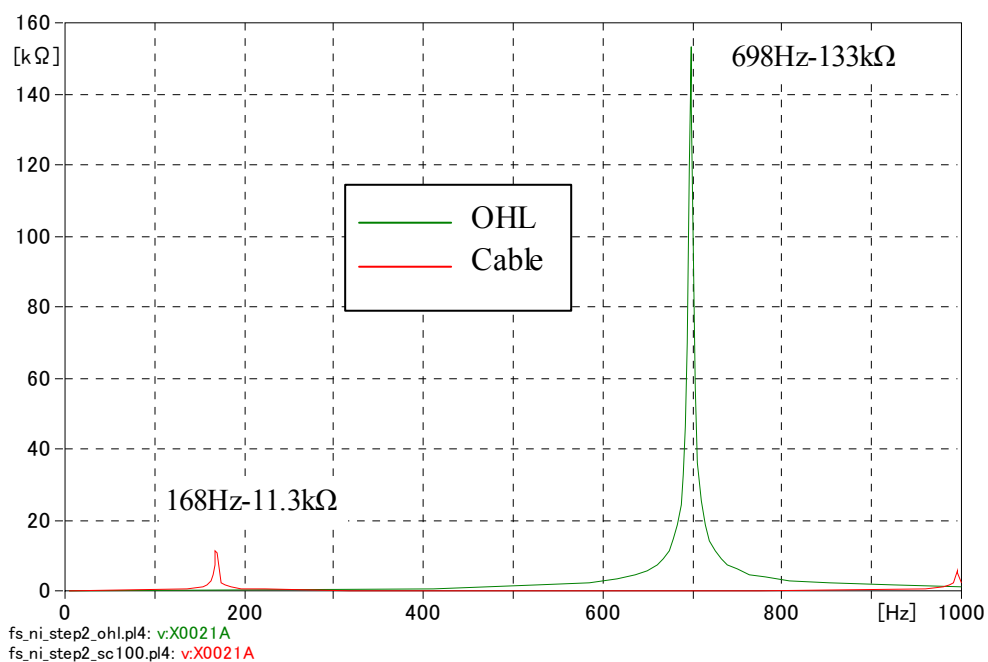
Fig. 7-7 Parallel resonance frequency of the network seen from Strabane 275 kV at Step 2.

In order to find an effect of the compensation rate of the Coolkeeragh – Strabane line, the same analysis was performed with different compensation rates 70 % and 85 %.

The result of the analysis at Step 2 is shown in Fig. 7-8. It can be seen that compensation rates of the shunt reactor have small effect to parallel resonance.
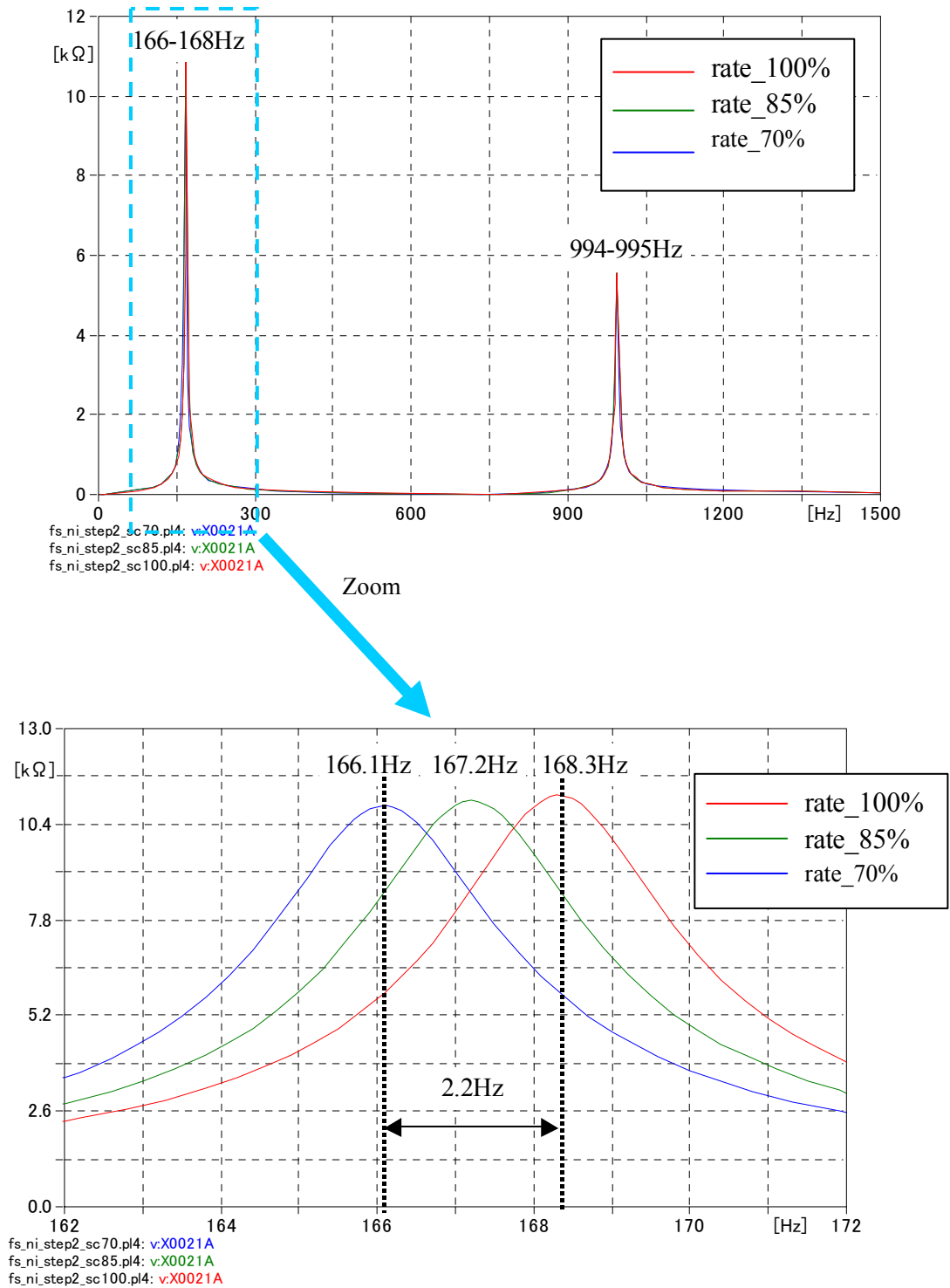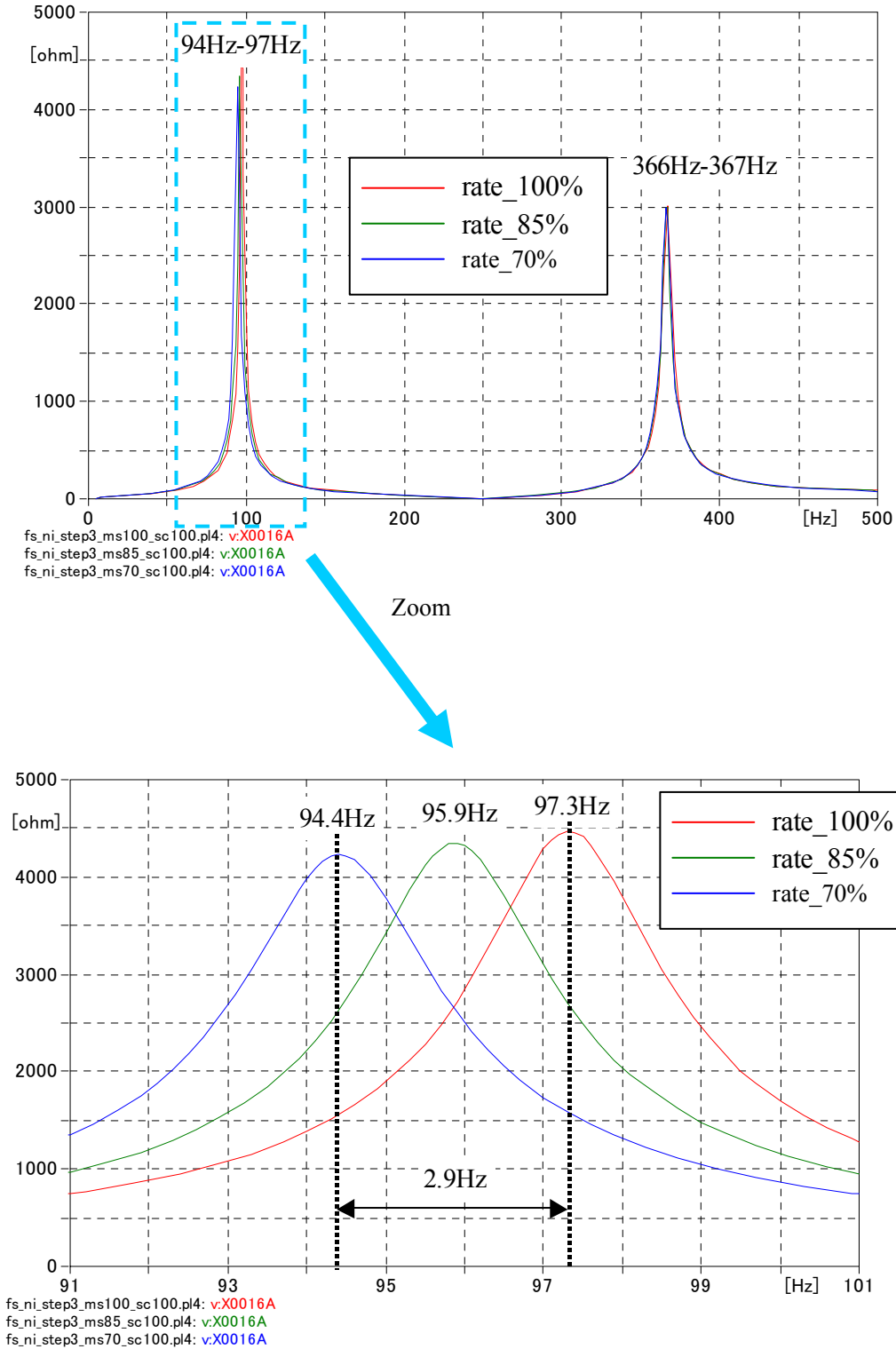

Fig. 7-8 Effect of compensation rates at Step 2.

Then, the same analysis was performed at Step 3. In this analysis, both 275 kV Omagh – Strabane line and Strabane – Coolkeeragh line were replaced by cables, and the compensation rate of shunt reactor was set to be 100%.

The results of frequency scan are shown in Fig. 7-9. It can be seen that parallel resonance frequency was shifted to lower frequency and the magnitude of impedance at parallel resonance decreased when 275 kV Omagh – Strabane – Coolkeeragh line was replaced by cables. At Step 3, parallel resonance frequency was shifted to around 100 Hz, and it is not recommended to energise a transformer at this step. The result shows that careful assessment is required when establishing restoration procedures.
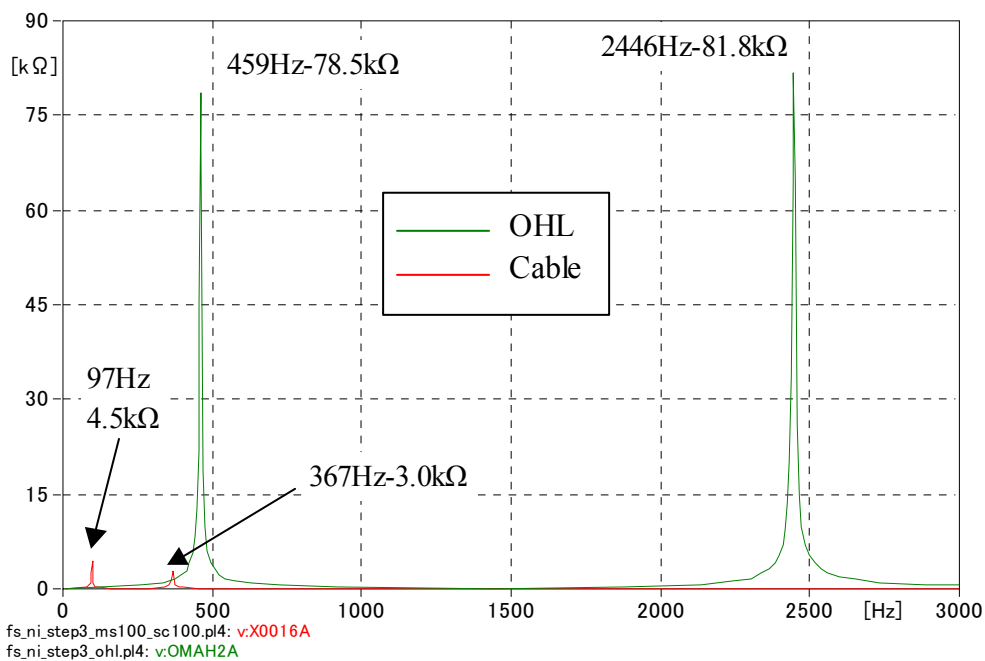
Fig. 7-9 Parallel resonance frequency of the network seen from Omahg 220 kV at Step 3.

Finally, in order to find the effect of the compensation rate of the shunt reactor, the same analysis was performed with different compensation rates for the 275 kV Omagh – Strabane line, 70 % and 85 % at Step 3. In this analysis, the compensation rate for the 275 kV Strabane – Coolkeeragh line was set to be 100 %.

The result of the analysis at Step 3 is shown in Fig. 7-10.   It can be seen that compensation rates of the shunt reactor have small effect to parallel resonance.

Fig. 7-10 Effect of compensation rates at Step 3.

7.3 Conclusion

The analysis has been performed both on under-excitation capability of black-start generators and on harmonic resonance overvoltage. The current blackout restoration procedures of NIE and EirGrid were evaluated after replacing some OHLs by underground cables.

In the assumed cable installation scenario and the restoration procedure in the EirGrid network, it was found that the black-start generator at Cathleen's Fall station had to be operated with a terminal voltage lower than 40 % in order to avoid steady-state overvoltage. It was also found that parallel resonance frequency was close to 100 Hz at some steps during the restoration process, and it is not recommended to energise a transformer at these steps. The result shows that careful assessment is required when establishing restoration procedures.

In the assumed cable installation scenario and the restoration procedure in the NIE network, it was confirmed that outputs of Coolkeeragh ST and OCGT were kept within the generator reactive capability limitation. However, outputs of Coolkeeragh GT exceeded the limitation when the cable compensation rate was low. Similar to the blackout restoration in the EirGrid network, there were some steps where parallel resonance frequency was close to 100 Hz. The result shows that careful assessment is required when establishing restoration procedures.

Part 2

Part 2:

Feasibility Study on the 400 kV Woodland – Kingscourt – Turleenan Line as AC EHV Underground Cables for the Entire Length

Table of contents

Chapter 1 Introduction

The objective of Part 2 is to conduct feasibility study on the 400 kV Woodland – Kingscourt – Turleenan line as AC EHV underground cables for the entire length.   In order to fulfill this objective, the following studies were performed:

    (1)   Transmission Capacity Calculation

    (2)   Impedance and Admittance Calculation

    (3)   Reactive Power Compensation Analysis

    (4)   Overvoltage Analysis

Here, (1) and (2) have already been conducted as a common study for Part 1, 2, and 3 and are not included in this Part 2 report.   Using cable information, such as cable size, type, layout, and impedance / admittance, found in (1) and (2), the remaining studies (3) and (4) were conducted as Part 2 studies.

The purpose of (3) is to find shunt reactors that should be installed together with the 400 kV cable.   The best combination in terms of the number of shunt reactors, shunt reactor size, and location was found from (3).

Temporary overvoltage analysis in (4) is the most important study in Part 2 that addresses the feasibility of the 400 kV Woodland – Kingscourt – Turleenan line as AC EHV underground cables for the entire length.

In addition to the studies (1) – (4), other major issues considered in the introduction of long EHV cables are described in Chapter 6.   The issues in Chapter 6 will not affect the feasibility of the 400 kV Woodland – Kingscourt – Turleenan line but will affect the specification of equipment.

It should be noted that there is a concern in the reliability of such a long EHV cable line.   If the 400 kV Woodland – Kingscourt – Turleenan line is built as EHV underground cables for the entire length, the line will be the longest 400 kV cable line in the world.   The 500 kV 40 km Shin-Toyosu line of TEPCO is the longest EHV line currently in service.   Considering its length, the 400 kV Woodland – Kingscourt – Turleenan line would require close attention in the manufacturing and installation process in order to secure required reliability.   The considerations in the manufacturing and installation process are not discussed in this report since they are not the scope of this project.

Chapter 2 Reactive Power Compensation

2.1 Considerations in Reactive Power Compensation

Shunt reactors are often installed with long cable lengths to compensate for the reactive power generated with these cables.　A compensation rate of close to 100% is preferable as the cable installation does not change the voltage profile of the network.　However it may lead to a severe zero-miss phenomenon.　The effect of the compensation rate is summarized in Table 2-1.

Table 2-1 Effect of Compensation Rate

Analyses	Close to 100%	Away from 100%
Reactive power compensation	Preferable	Generally not preferable (depends on typical operating conditions)
Zero-miss phenomenon	Not preferable (but can be avoided by a special relay)	Preferable
Oscillatory overvoltage	Preferable	Not preferable

A zero-miss phenomenon and associated equipment failure can be avoided by installing the operational countermeasure, described in Chapter 7.

Additionally, the location of shunt reactors must be taken into consideration.　Shunt reactors are connected directly to the cable, to the substation bus, or to the tertiary side of a transformer. The advantages and disadvantages of these options are described in Table 2-2.

Table 2-2 Installed Location of Shunt Reactors

Connection	Advantage	Disadvantage
Directly connected to the cable	- Can limit the overvoltage when one side of the cable is opened	- Cannot be used for voltage control when the cable is not-in-service (Some exceptions exist.)
Substation bus or tertiary side of a transformer	- Can be shared by multiple cable routes - Cheaper (tertiary side)	- May cause reactive power imbalance during　switching operations

For extended cable systems such as the 400 kV Woodland – Kingscourt – Turleenan line, shunt reactors should be directly connected to the cables to control overvoltage when one side of the cable is opened.

2.2 Maximum Unit Size of 400 kV Shunt Reactors

The maximum unit size of the 400 kV shunt reactors have been determined from a voltage variation when one unit of these shut reactors was switched.   The following voltage variation is allowed in the operation of the all-island transmission system.

Under normal operating conditions: 3 %   (11.4 kV)

Under contingencies: 10 %   (38.0 kV)

The voltage variation increases under lower load conditions.   Power flow data during summer off-peak demand was selected to allow the analysis of this voltage variation.   Shunt reactors of different sizes were switched on and off at the Turleenan 400 kV bus.   Fig. 2.1 shows the voltage variation at the buses near Turleenan 400 kV.
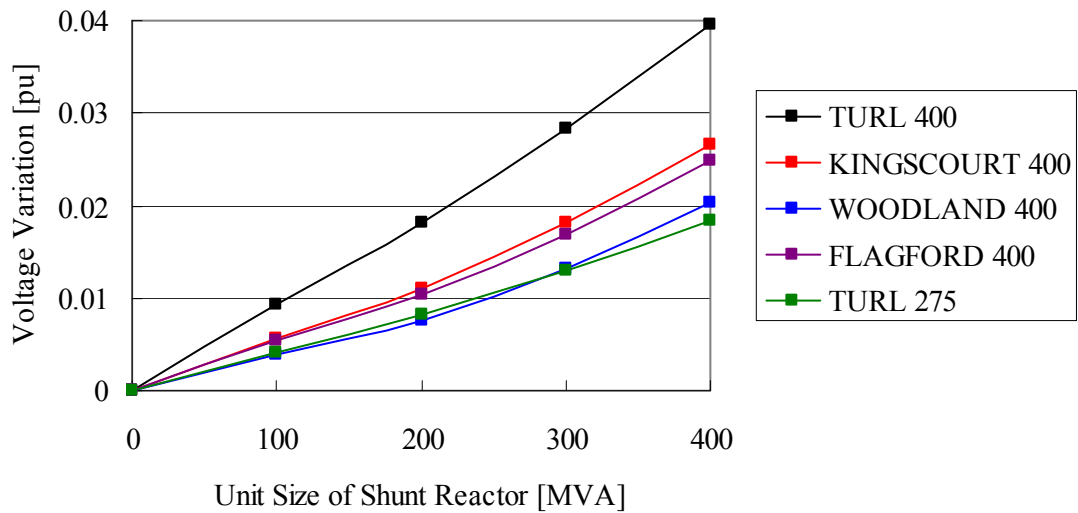
Fig. 2.1 Voltage variation with shunt reactor switchings at the Turleenan 400 kV bus.

Fig. 2.1, shows that the maximum unit size that can be installed to the Turleenan 400 kV bus is 300 MVA. The same limitation can be applied when the shunt reactor is directly connected to the cable near the Turleenan 400 kV bus.

The same analysis was performed with shunt reactors connected to the Kingscourt 400 kV bus. The result of the analysis is shown in Fig. 2.2.
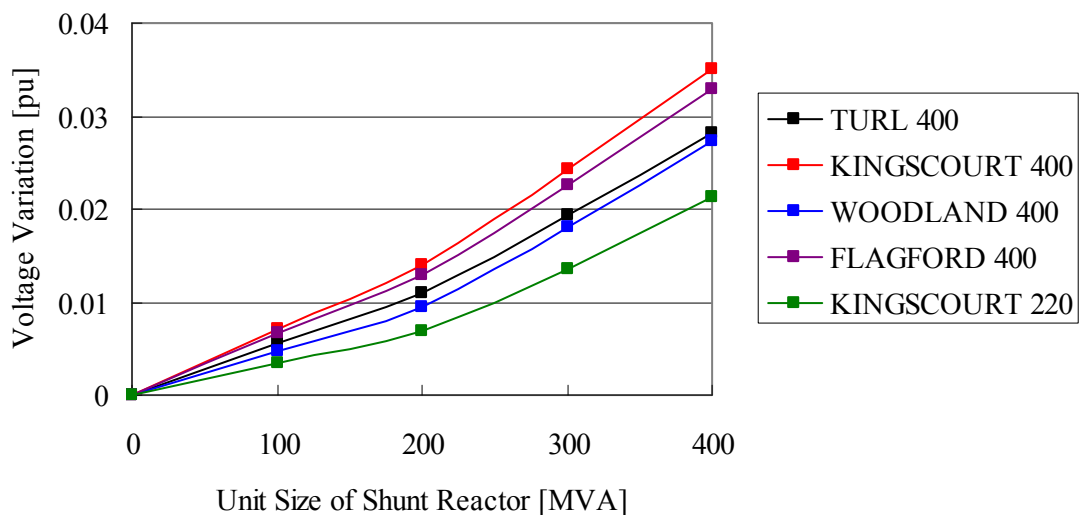
Fig. 2.2 Voltage variation with shunt reactor switchings at the Kingscourt 400 kV bus.

It can be seen that the 400 kV bus voltage of Kingscourt is more stable than that of Turleenan, however the maximum unit size that can be installed at Kingscourt 400 kV is 300 MVA.

Fig. 2.3 shows the result of the same analysis for the Woodland 400 kV bus.   The 400 kV bus voltage at Woodland is even more stable than that of Kingscourt.   For the Woodland 400 kV bus, it will be possible to install a 350 MVA shunt reactor while keeping the voltage variation limit 3 % under normal operating condition.   However, there is no benefit in installing a 350 MVA shunt reactor at Woodland 400 kV, considering charging capacity of the Woodland – Kingscourt cable 539.2 MVA/cct.
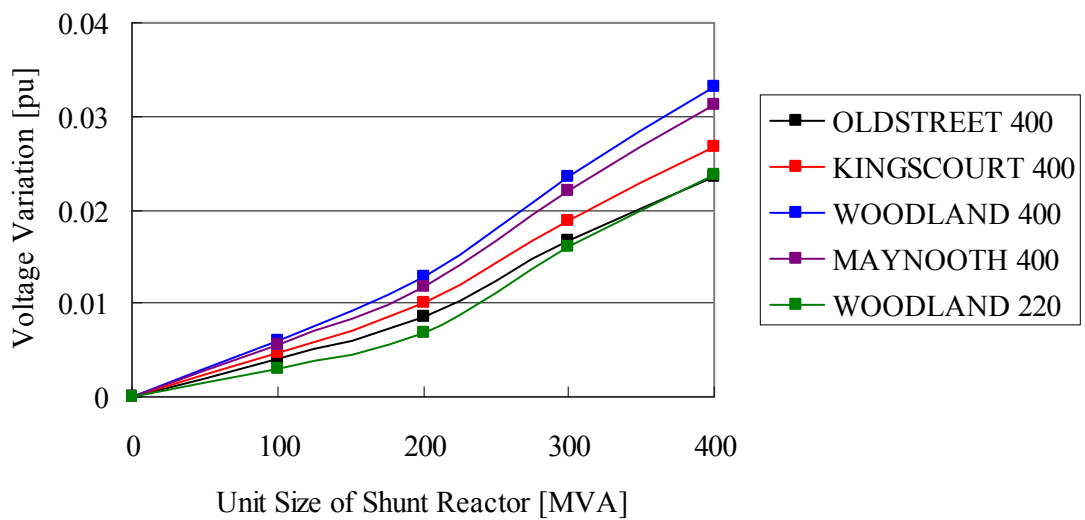
Fig. 2.3 Voltage variation with shunt reactor switchings at the Woodland 400 kV bus.

2.3 Proposed Compensation Patterns

Charging capacity of the Woodland – Kingscourt – Turleenan line (Al 1400 mm^2 – 2 cct) is:

Woodland – Kingscourt: 539.2 MVA/cct @ 400 kV

Kingscourt – Turleenan: 762.3 MVA/cct @ 400 kV

Based on the maximum unit size found in the previous section, the following reactive power compensation patterns were proposed:

Table 2-3 Proposed Compensation Patterns

For the 400 kV Woodland – Kingscourt cable:

Locations	Case A1	Case A2	Case A3	Case A4
Woodland	250 MVA × 1	150 MVA × 2	150 MVA × 1	100 MVA × 1
Station 1			120 MVA × 2	80 MVA × 2
Station 2				80 MVA × 2
Kingscourt	250 MVA × 1	120 MVA × 2	150 MVA × 1	100 MVA × 1
Compensation Rate [%]	92.7	100.1	100.1	96.4

For the 400 kV Kingscourt – Turleenan cable:

Locations	Case B1	Case B2	Case B3	Case B4
Kingscourt	300 MVA × 1	150 MVA × 2	100 MVA × 2	150 MVA × 1
Station 1			120 MVA × 3	120 MVA × 2
Station 2				120 MVA × 2
Turleenan	300 MVA × 1	200 MVA × 2	100 MVA × 2	150 MVA × 1
Compensation Rate [%]	78.7	91.8	99.7	102.3

The amount of shunt reactors in Table 2-3 are given for one circuit. Cases A3 and B3 consider the shunt reactor station at the center of the line. Similarly, Cases A4 and B4 consider the two shunt reactor stations at the location where the line is divided into three sections of equal length.

2.4 Voltage Profile under Normal Operating Conditions

From the reactive power compensation analysis, simple power flow data for the Woodland – Kingscourt – Turleenan line was constructed. In this simple model, both the Woodland – Kingscourt line and the Kingscourt – Turleenan line was divided into six sections of equal length, in order to observe the voltage profile along the line and to model the shunt reactor stations.

The following conditions were assumed in the power flow data:

- The 400 kV bus voltages of Woodland and Turleenan were maintained below 410 kV. At its severest condition, these bus voltages were fixed to 410 kV.

- An outage of the 400 kV Kingscourt – Flagford line was considered to be a severe condition, as the Kingscourt 400 kV bus voltage was not regulated from Flagford.

The power flow model created for the reactive power compensation analysis is shown in Fig. 2.4.
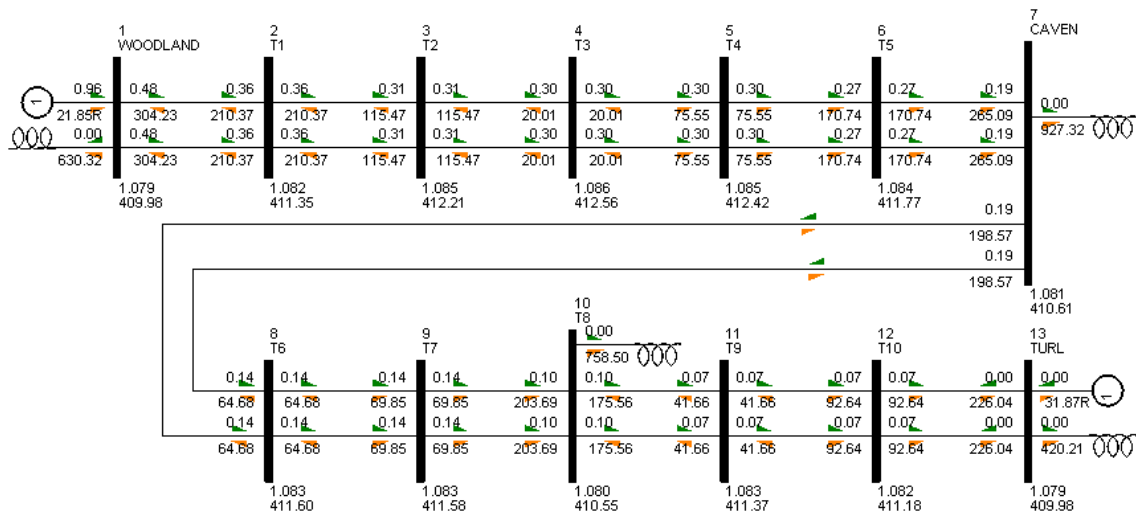
Fig. 2.4 Power flow model for the reactive power compensation analysis.

Using this power flow model, the voltage profile along the line was initially considered with all the equipment in service. The analysis was performed under a no load condition and a full load condition. In the full load condition, active power of 1500 MW was transmitted from Turleenan to Woodland.

The result of the analysis is shown in Fig. 2.5 and Fig. 2.6. In Cases A1, A2, B1, and B2, the voltage at the center of the line is comparatively high since the shunt reactors are connected only at both ends. However, even in these cases, the voltage rise at the center of the line peaks at 6 kV. Considering the highest voltage (420 kV) of the equipment, all compensation patterns have a satisfactory voltage profile.

The compensation pattern of the Kingscourt – Turleenan line was fixed to Case B3 when the voltage profile of the Woodland – Kingscourt line was studied. Similarly, the compensation pattern of the Woodland – Kingscourt line was fixed to Case A3 when the voltage profile of the Kingscourt – Turleenan line was studied.

Note that Cases B1 and B2 yielded the same result as the total amount of compensation was equal to Cases B1 and B2 except at Turleenan where the 400 kV bus voltage was fixed to 410 kV.
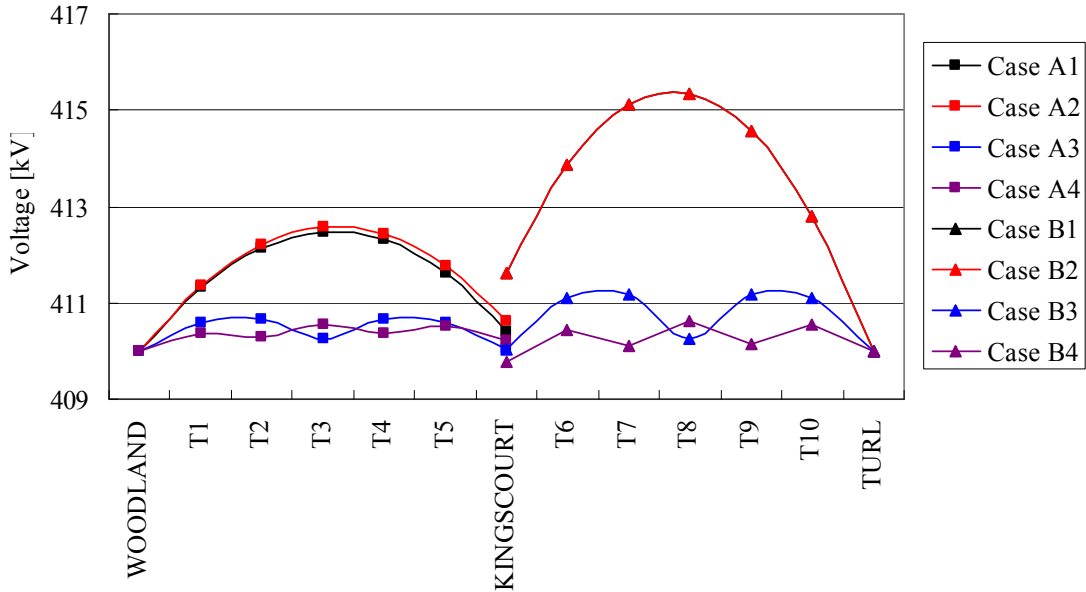
Fig. 2.5 Voltage profile in the normal operating condition (no load).
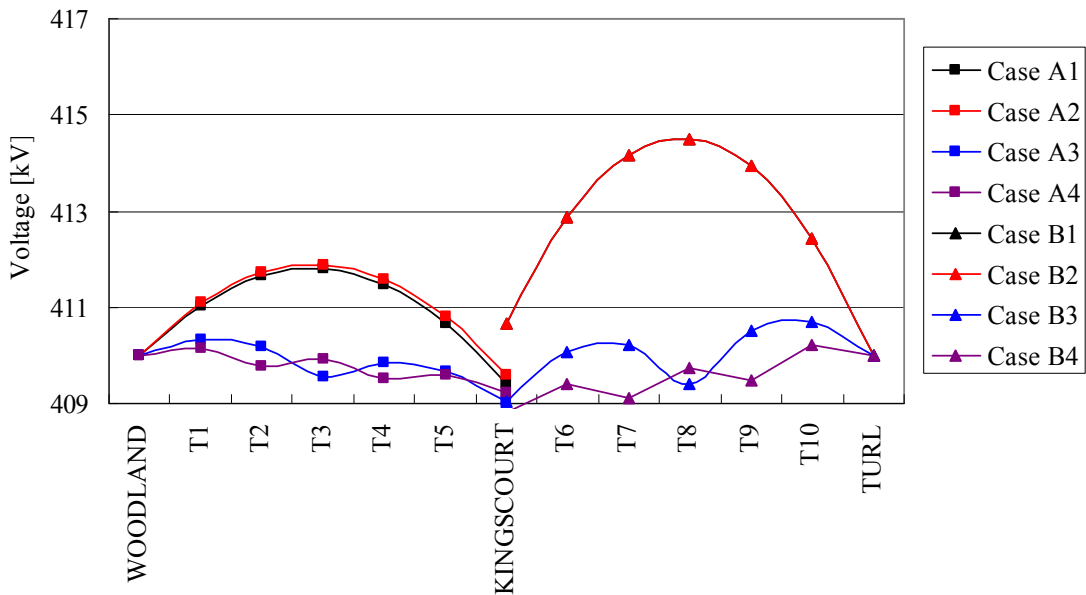
Fig. 2.6 Voltage profile in the normal operating condition (full load).

2.5 Active Power Loss

The active power loss in the line is affected by the reactive power compensation.   It is expected that Cases A3, A4, B3, and B4 have lower active power losses compared to the other compensation patterns because of the smooth voltage profile as shown in the previous section.

The power transmitted from Turleenan to Woodland was set to 750 MW (half load) and 1500 MW (full load), and active power loss in the line was calculated for the two power transmission cases.   The simple power flow model created in Section 2.4 was used for the calculation.

Table 2-4 Active Power Losses

For the Woodland – Kingscourt line:

Cases	Half load	Full load
Case A1	3.57 MW	12.60 MW
Case A2	3.57 MW	12.56 MW
Case A3	3.22 MW	12.36 MW
Case A4	3.12 MW	12.26 MW

For the Kingscourt – Turleenan line:

Cases	Half load	Full load
Case B1	6.00 MW	18.66 MW
Case B2	6.00 MW	18.66 MW
Case B3	4.70 MW	17.62 MW
Case B4	4.48 MW	17.44 MW

The result of the calculation is shown in Table 2-4.   As can be seen from the table, the difference in active power loss is at most 0.45 MW for the Woodland – Kingscourt line. Considering this small difference, it is difficult to justify the construction of a shunt reactor station from an economical standpoint.

In contrast, for the Kingscourt – Turleenan line, the difference in active power loss can be approximately 1.0 MW.   For the electricity price of 86.4 €/MWh, this difference becomes 30 M€ in 40 years (1.0 MWh × 86.4 €/MWh × 24 h × 365 days × 40 years), which may justify the construction of a shunt reactor station.   However, the construction of two shunt reactor stations as

indicated in Case B4 can not be justified from an economical standpoint, due to the small difference of active power loss between Cases B3 and B4.

Note that active power loses were calculated using a.c. resistance at the maximum operating temperature. When the conductor temperature is lower than 90 °C, the active power loss will be smaller than the values in Table 2-4.

2.6 Ferranti Phenomenon

When one end of the line is opened in a switching operation or due to a bus fault, the voltage at the open terminal may rise due to charging current. Although equipment failure caused by this overvoltage can be prevented by opening the other end of the line, this overvoltage might be overlooked since the voltage at the open terminal is not monitored. From a planning standpoint, it is recommended to maintain the voltage at the open terminal below 420 kV in order to relieve operational concerns.

2.6.1 Shunt Reactors Connected to the Line

First, the voltage profile when all shunt reactors were directly connected to the line was studied. When connected to the line, shunt reactors can be used to suppress the open terminal voltage.

Fig. 2.7 shows the voltage profile when the Woodland terminal is opened. The different compensation patterns in Cases A1 – A4 were studied for the Woodland – Kingscourt line. The compensation patterns of the Kingscourt – Turleenan line were fixed to Case B3, and the Turleenan 400 kV bus voltage was fixed at 410 kV. It can be seen that all compensation patterns have a satisfactory voltage profile.
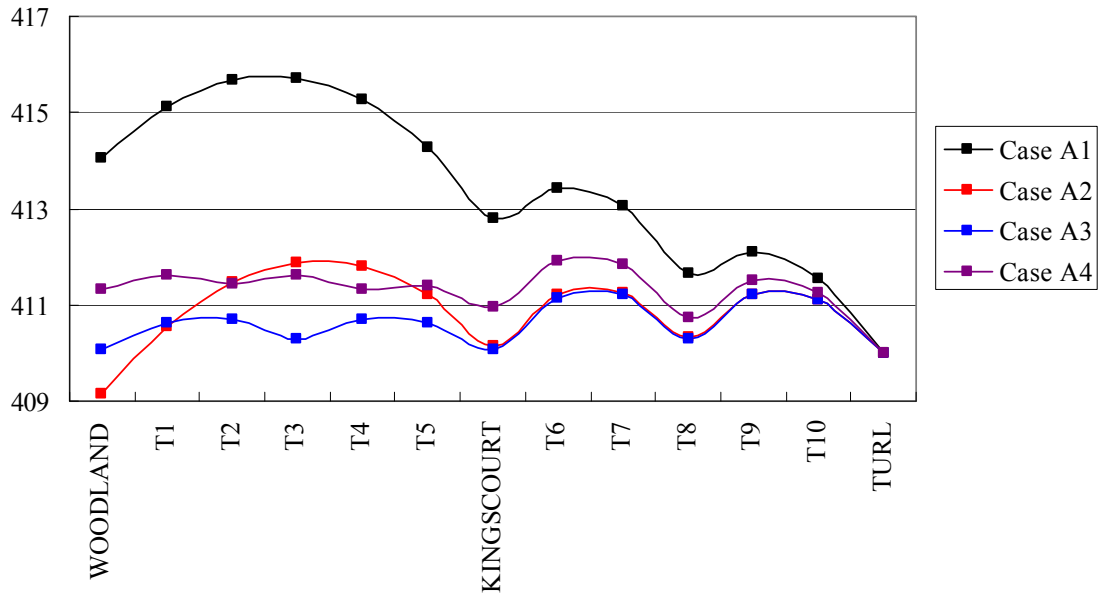
Fig. 2.7 Voltage profile when the Woodland terminal is opened.

Fig. 2.8 shows the voltage profile when the Turleenan terminal is opened.   The different compensation patterns in Cases B1 – B4 were studied for the Kingscourt – Turleenan line.   The compensation pattern of the Woodland – Kingscourt line was fixed to Case A3, and the Woodland 400 kV bus voltage was fixed at 410 kV.   Case B1 is not preferable, but other compensation patterns have a satisfactory voltage profile.
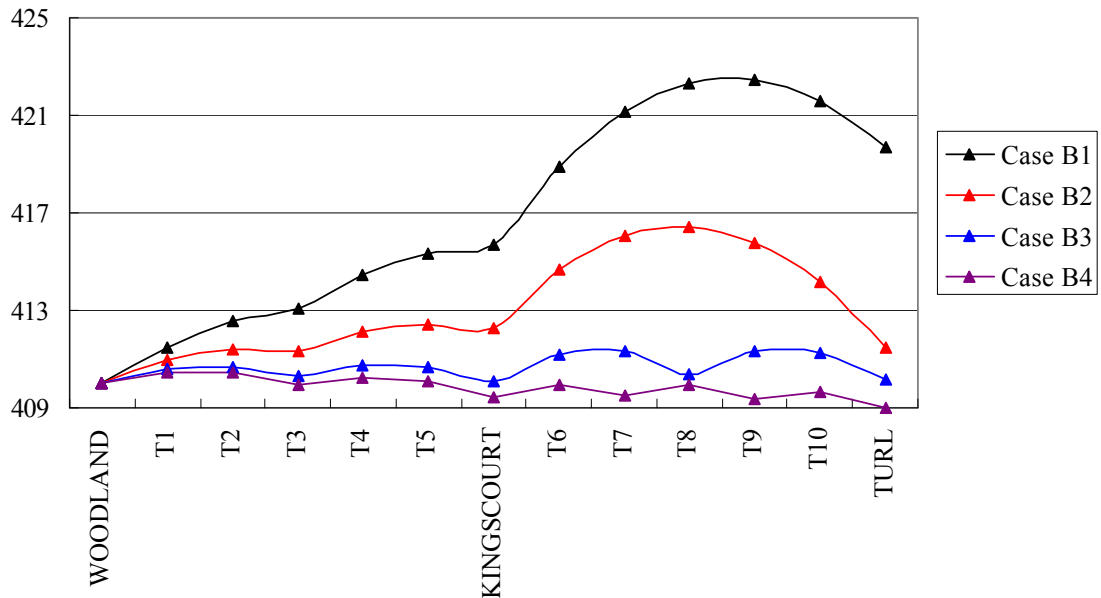
Fig. 2.8 Voltage profile when the Turleenan terminal is opened.

2.6.2 Shunt Reactors Connected to the Bus

Shunt reactors connected to the bus are often preferred, compared to those connected to the line, because of increased flexibility for wider use as voltage and reactive power control equipment. When considering the Ferranti phenomenon, bus-connected shunt reactors present more severe conditions as they can not be used to suppress the open terminal voltage.

When shunt reactors are connected to the line, they will suppress the open terminal voltage as long as they are available.　When line-connected shunt reactors are not available, for example due to maintenance outage, the condition becomes equal to bus-connected shunt reactors.

Fig. 2.9 shows the voltage profile when the Woodland terminal is opened.　All conditions are the same as in Section 2.6.1, but all shunt reactors at the Woodland open terminal are disconnected. When either Case A3 or A4 is selected, the shunt reactors at Woodland and Kingscourt can be connected to the bus.　When either Case A1 or A2 is selected, it is recommended that the shunt reactors at Woodland and Kingscourt be connected to the line.
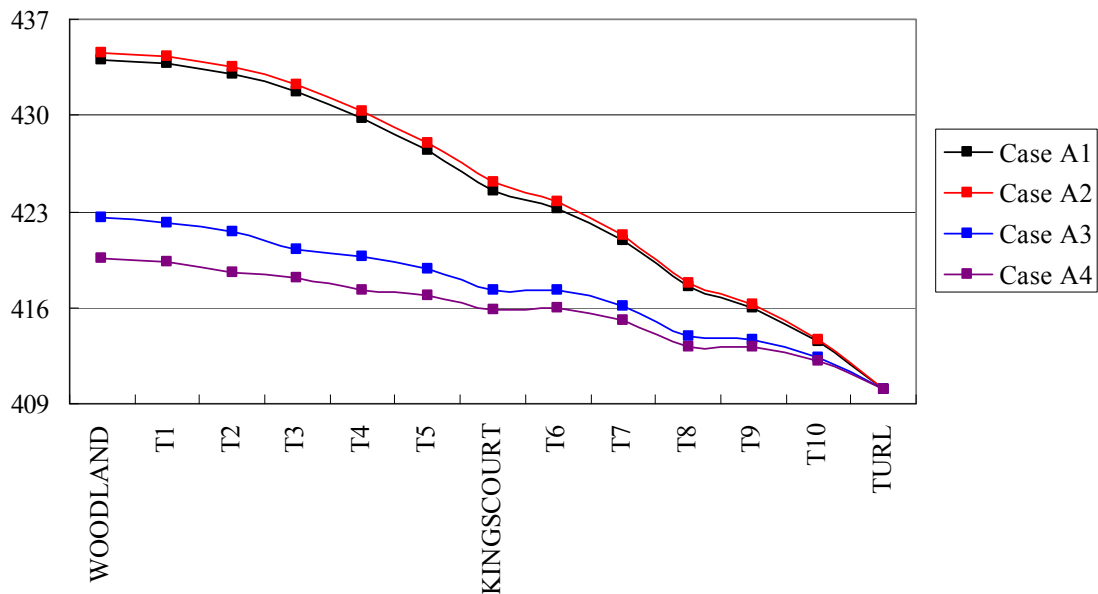
Fig. 2.9 Voltage profile when the Woodland terminal is opened without shunt reactors.

In Cases A1 and A2, the open terminal voltage can be suppressed to a satisfactory level if shunt reactors are connected to the line and are available.　In Case A1, there is one shunt reactor (250 MVA) at Woodland and one at Kingscourt.　When this shunt reactor is not available, it is important to quickly open the other end of the line when one terminal is opened.

In Case A2, there are two units of shunt reactors both at Woodland (150 MVA × 2) and Kingscourt (120 MVA × 2). In Fig. 2.10, Case A2-2 shows what occurs when one shunt reactor at Woodland is available and the other is not.
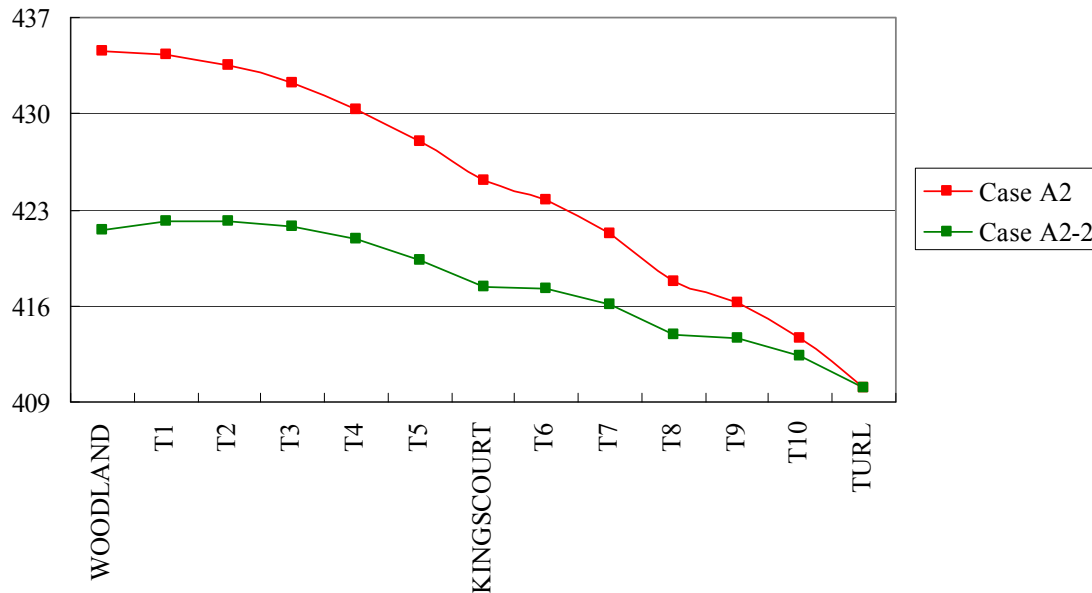
Fig. 2.10 Voltage profile when the Woodland terminal is opened in Case A2.

As can be seen from Fig. 2.10, the open terminal voltage is suppressed with one 150 MVA shunt reactor connected to the line. The open terminal voltage still exceeds 420 kV, but the voltage rise from Kingscourt is within 10 kV. If the Kingscourt 400 kV bus voltage is maintained below 410 kV, the open terminal voltage will be maintained below 420 kV.

Fig. 2.11 shows the voltage profile when the Turleenan terminal is opened. All conditions are the same as in Section 2.6.1, but all shunt reactors at the Turleenan open terminal are disconnected. When Case B4 is selected, the shunt reactors at Kingscourt and Turleenan can be connected to the bus as long as the Kingscourt 400 kV bus voltage is maintained below 410 kV. When either Case B2 or B3 is selected, it is recommended that the shunt reactors at Kingscourt and Turleenan be connected to the line. Case B1 is not preferable even with line-connected shunt reactors as found in Section 2.6.1.
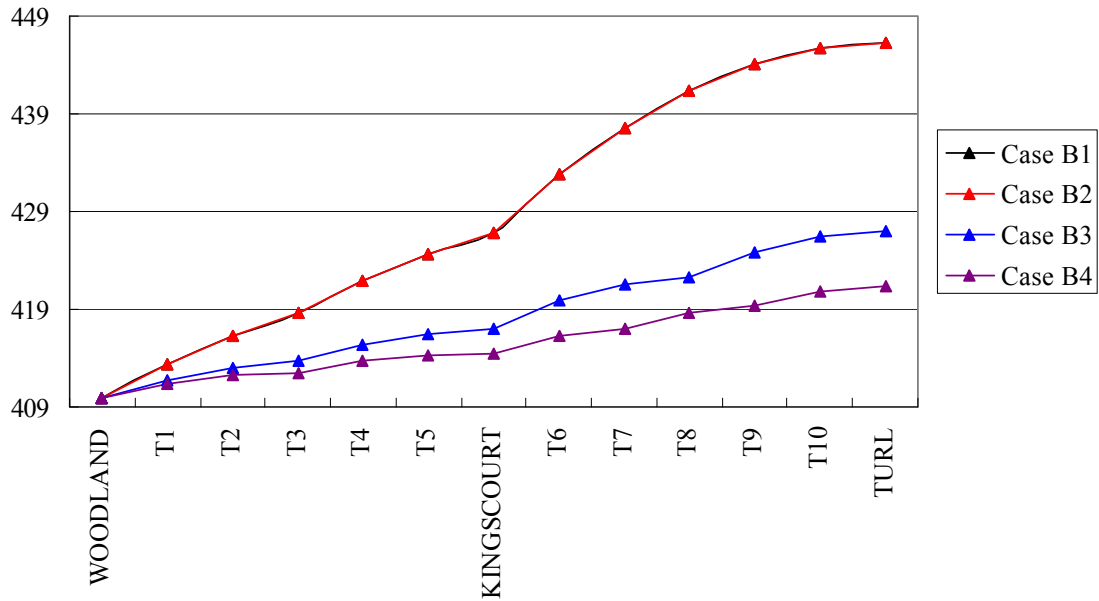
Fig. 2.11 Voltage profile when the Turleenan terminal is opened without shunt reactors.

There are two units of shunt reactors both at Kingscourt (150 MVA × 2) and Turleenan (200 MVA × 2) in Case B2.   Similarly, there are two shunt reactors (100 MVA × 2) each at Kingscourt and Turleenan in Case B3.   In Fig. 2.12, Cases B2-2 and B3-2 show the voltage profile when one of these shunt reactors at Turleenan is not available.   It can be seen from the figure that Case B3-2 has a satisfactory voltage profile.   Case B2-2 is acceptable as long as the Kingscourt 400 kV bus voltage is kept below 410 kV.
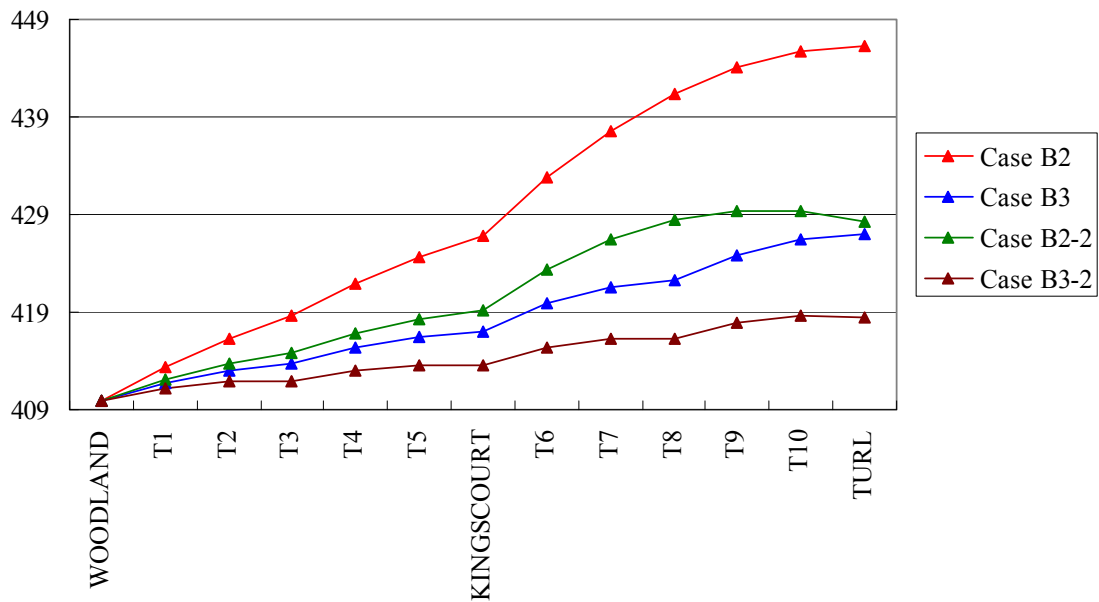
Fig. 2.12 Voltage profile when the Turleenan terminal is opened in Case B2 and B3.

2.7 Conclusion

As a result of the reactive power compensation analysis, compensation patterns A2 and B3 were selected for further analysis.

For the 400 kV Woodland – Kingscourt cable, Case A2 has a satisfactory voltage profile in all of the studied conditions.   Two shunt reactors at both ends have to be connected to the line in order to suppress the open terminal voltage even when one shunt reactor is out of service.   Since Case A2 has a satisfactory voltage profile, it is difficult to justify the selection of Cases A3 and A4 from both an electrical and economical standpoint.

Locations	Case A1	Case A2	Case A3	Case A4
Woodland	250 MVA × 1	150 MVA × 2	150 MVA × 1	100 MVA × 1
Station 1			120 MVA × 2	80 MVA × 2
Station 2				80 MVA × 2
Kingscourt	250 MVA × 1	120 MVA × 2	150 MVA × 1	100 MVA × 1
Compensation Rate [%]	92.7	100.1	100.1	96.4

For the 400 kV Kingscourt – Turleenan cable, Cases B2 and B3 have a satisfactory voltage profile when all shunt reactors are connected to the line.   Case B3 is selected because of its lower active power loss and more preferable voltage profile over Case B2.

Locations	Case B1	Case B2	Case B3	Case B4
Kingscourt	300 MVA × 1	150 MVA × 2	100 MVA × 2	150 MVA × 1
Station 1			120 MVA × 3	120 MVA × 2
Station 2				120 MVA × 2
Turleenan	300 MVA × 1	200 MVA × 2	100 MVA × 2	150 MVA × 1
Compensation Rate [%]	78.7	91.8	99.7	102.3

Note: If it is not necessary to switch these shunt reactors for the voltage and reactive power control, it is possible to choose a shunt reactor of larger unit size.   For example in Case B3, it is

possible to install one unit of 200 MVA shunt reactor in Kingscourt instead of two units of 100 MVA.   The compensation pattern in Case B3 was selected without the consideration of the requirements for the voltage and reactive power control, since it is not included in the scope of this study and the difference can have only small effects on the simulation results.

When a shunt reactor with large unit size is selected, an outage of this shunt reactor will significantly lower the compensation rate of the cable line, which may limit the use of the line during the outage.

2.8 Reactive Power Compensation for the Single Circuit Option

Charging capacity of the Woodland – Kingscourt – Turleenan line (Cu 2500 mm^2 – 1 cct) is:

Woodland – Kingscourt:　　　　　　　699.2 MVA/cct @ 400 kV

Kingscourt – Turleenan:　　　　　　　988.6 MVA/cct @ 400 kV

Based on the maximum unit size found in the previous section, the following reactive power compensation patterns were proposed:

Table 2-5 Proposed Compensation Patterns

	Woodland – Kingscourt
Woodland Station 1 Kingscourt	200 MVA × 2　　　　150 MVA × 2
Compensation Rate [%]	100.1

	Kingscourt – Turleenan
Kingscourt Station 1 Kingscourt	150 MVA × 2　150 MVA × 2　150 MVA × 2
Compensation Rate [%]	91.0

With the proposed compensation patterns, the voltage profile under the normal operating conditions (no load and full load) is shown in Fig. 2.13.　All the conditions were kept equal to the previous studies in this section.　The proposed compensation patterns yield preferable voltage profiles under the normal operating conditions.
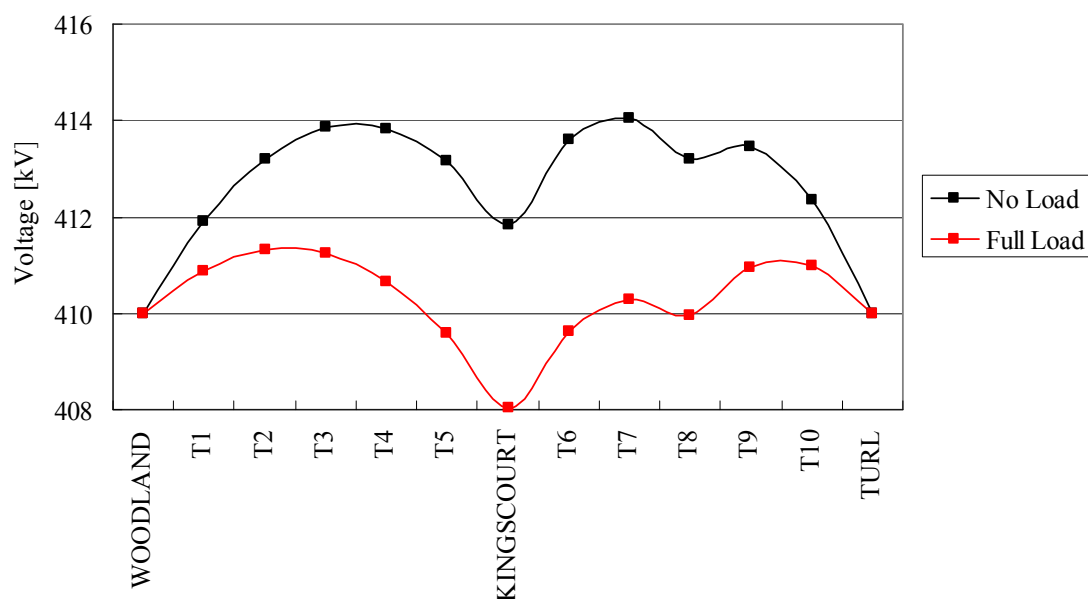
Fig. 2.13 Voltage profile in the normal operating condition.

To study the Ferranti phenomenon, the voltage profile when the Woodland terminal is opened is shown in Fig. 2.14.   When all shunt reactors (200 MVA × 2 units) are directly connected to the line, the voltage along the line does not exceed 420 kV.

When one 200 MVA shunt reactor is connected to the bus or is not in service, the voltage near the open terminal rises to 428 kV.   The voltage rise from Kingscourt is, however, only 6 kV.   The open terminal voltage is kept below 420 kV as long as the Kingscourt 400 kV bus voltage is maintained within 410 kV.   It is not acceptable to connect all shunt reactors to the bus because the open terminal voltage is too high.
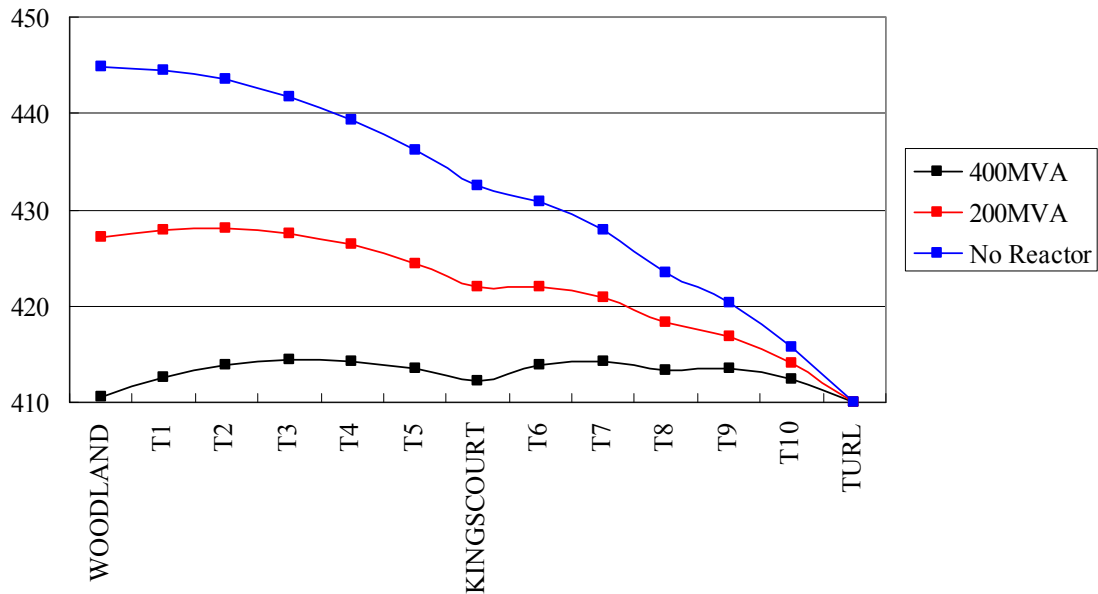
Fig. 2.14 Voltage profile when the Woodland terminal is opened.
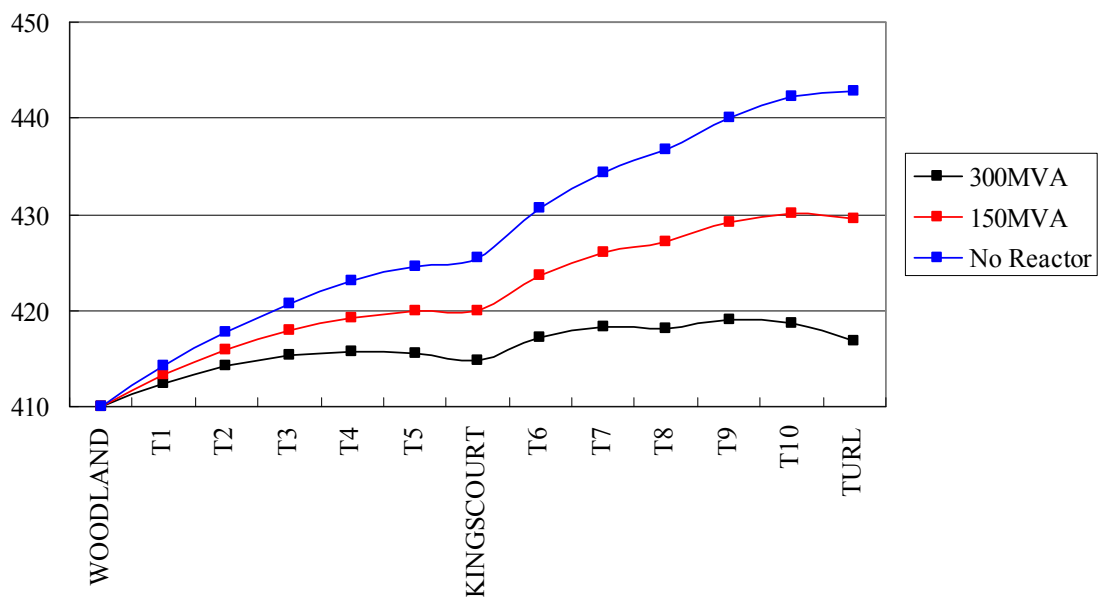
Fig. 2.15 Voltage profile when the Turleenan terminal is opened.

Finally, the voltage profile when the Turleenan terminal is opened is shown in Fig. 2.15. When all shunt reactors (150 MVA × 2 units) are directly connected to the line, the voltage along the line does not exceed 420 kV.

When one 150 MVA shunt reactor is connected to the bus or is not in service, the voltage near the open terminal rises to 430 kV, and the voltage rise from Kingscourt is 10 kV. The open terminal voltage is kept at 420 kV as long as the Kingscourt 400 kV bus voltage is maintained within 410 kV. It is not acceptable to connect all shunt reactors to the bus because the open terminal voltage is too high.

In conclusion, the proposed compensation patterns shown in Table 2-5 were considered acceptable, and the shunt reactors have to be connected directly to the lines. The proposed compensation patterns were used for further analysis.

Chapter 3 Model Setup

3.1 Modeled Area for This Project

The entire 400 kV network is included in this model for the temporary overvoltage analysis and the slow-front overvoltage analysis. The figure below shows an example of the model created by ATP-Draw. Each component in the figure is explained in this section.

Fig. 3.1 Simulation model for the temporary overvoltage and slow-front overvoltage analysis.

3.2 Overhead Transmission Lines

400 kV overhead lines were modelled using a frequency dependent model (J. Marti model). Input data for ATP-EMTP are shown in Table 3-1, and a cross-section diagram of transmission lines and ground wires are shown in Fig. 3.2.

Table 3-1 Overhead Line Data

Types	Inner Radius [mm]	Outer Radius [mm]	Resistance per conductor [ohm/km]	Number of conductors in a bundle	Separation between conductors [cm]
Transmission Line (Curlew) 54/7	5.269	15.8	0.01655	2	45
Ground Wire	5.269	10	0.18	–	–
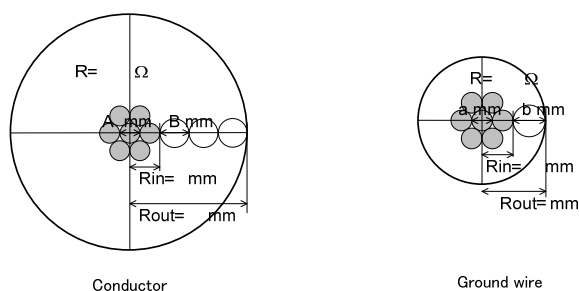
Fig. 3.2 Cross-section diagram of transmission line (left) and ground wire (right).

The layout of transmission lines and ground wires were derived from the typical tower configuration. The tower configuration (401 Configuration) applied to the existing 400 kV OHLs is shown in Fig. 3.3. The layout of the existing 400 kV OHLs was derived from the figure as shown in Table 3-2.

Table 3-2 Layout of the Existing 400 kV OHLs

Types	Horizontal position [m]	Vertical position [m]
Conductors	-10.50	21.95
	0	21.97
	+10.50	21.95
Ground wires	-6.50, +6.50	32.00
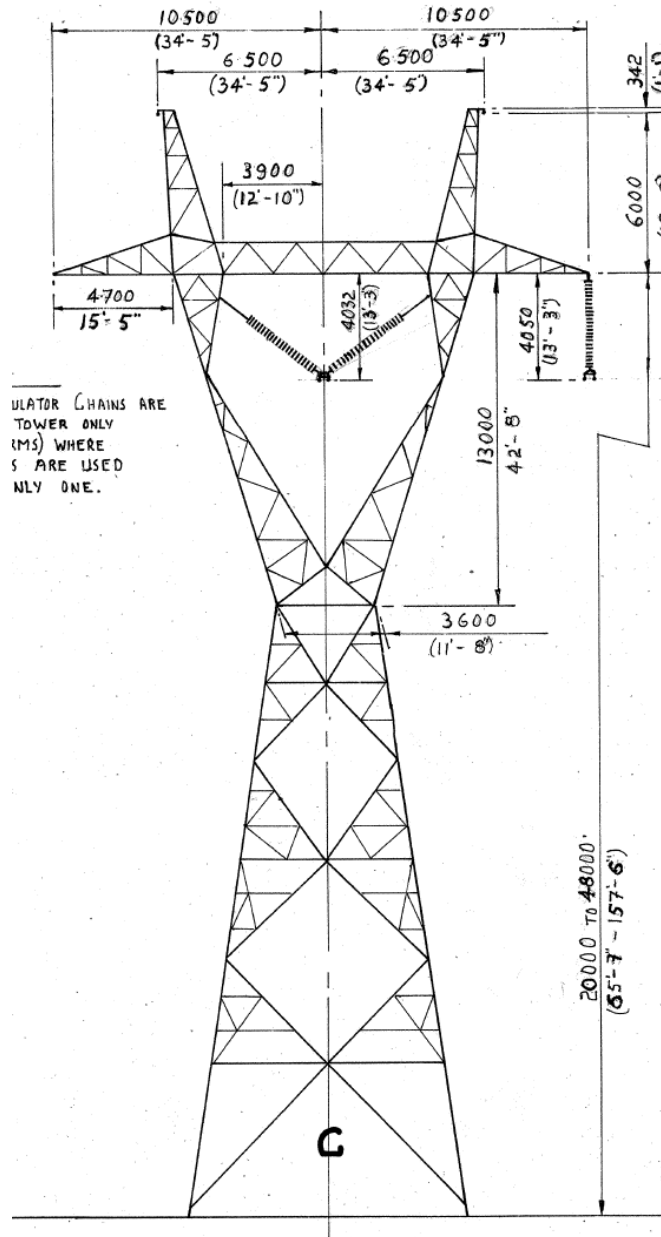
Fig. 3.3 Tower configuration of the existing 400 kV OHLs.

The tower configuration (IVI Configuration) applied to the new 400 kV OHLs is shown in Fig. 3.4. The layout of the new 400 kV OHLs was derived from the figure as shown in Table 3-3.

Table 3-3 Layout of the New 400 kV OHLs

Types	Horizontal position [m]	Vertical position [m]
Conductors	-9.50	21.70
	0	27.75
	+9.50	21.70
Ground wires	-6.75, +6.75	32.00

Fig. 3.4 Tower configuration of the new 400 kV OHLs.

3.3 Transformers

Model parameters of the Turleenan 400/275 kV transformer and the Kingscourt 400/220 kV transformer were provided by NIE/EirGrid. These parameters are shown in Table 3-4. All 400/220 kV transformers in the RoI were assumed to have the same parameters as the Kingscourt 400/220 kV transformer.

Table 3-4 Model Parameters of 400 kV Transformers

Transformer	Thurleenan 500MVA			Transformer	Kingscourt ABB 500MVA		
Voltage rating	HV	LV	TV	Voltage rating	HV	LV	TV
kV line-line	400	275	33	kV line-line	400	220	21
MVA Rating	500	500	90	MVA Rating	500	500	80
Vector Config	Y auto	Y auto	delta	Vector Config	Y auto	Y auto	delta
S/C Impedances	HV-LV	HV - TV	LV-TV	S/C Impedances	HV-LV	HV-TV	LV - TV
% on 500MVA base	15	50	44.4	% on 500MVA base	13.46	39.5	18.63
S/C Loss kW	430	43	47	S/C Loss kW	653	218	163
Core loss @ 1.0pu (kW)		360		Core loss @ 1.0pu (kW)		250	
Capacitances	pF			Capacitances	pF		
HV-LV	2500			HV-LV	2500		
LV-TV	2200			LV-TV	2200		
HV-Earth	1100			HV-Earth	1100		
LV-Earth	400			LV-Earth	400		
TV-Earth	8900			TV-Earth	8900		

For leakage inductances in Table 3-4, percent impedances were converted to mH by the following calculations.

$$(x_{\%1\text{-}2}, x_{\%1\text{-}3}, x_{\%2\text{-}3}) \rightarrow (x_{\%1}, x_{\%2}, x_{\%3})$$

$$x_{\%1} = \frac{x_{\%1-2} + x_{\%1-3} - x_{\%2-3}}{2}$$

$$x_{\%2} = \frac{x_{\%1-2} + x_{2-3} - x_{\%1-3}}{2}$$

$$x_{\%3} = \frac{x_{\%1-3} + x_{\%2-3} - x_{\%1-2}}{2}$$

$$(x_{\%1}, x_{\%2}, x_{\%3}) \rightarrow (x_1, x_2, x_3)$$

$$x_1 = \frac{x_{\%1}}{100} \times \frac{(400\text{kV})^2}{100\text{MVA}} \times \frac{1}{2\pi \times 50} \times 1000 \quad [\text{mH}]$$

$$x_2 = \frac{x_{\%2}}{100} \times \frac{(275 \text{ or } 220\text{kV})^2}{100\text{MVA}} \times \frac{1}{2\pi \times 50} \times 1000 \quad [\text{mH}]$$

$$x_3 = \frac{x_{\%3}}{100} \times \frac{(33 \text{ or } 21\text{kV})^2}{100\text{MVA}} \times \frac{1}{2\pi \times 50} \times 1000 \quad [\text{mH}]$$

Internal resistance and leakage inductance of these transformers were obtained as follows:

Substations	R1 [Ω]	X1 [mH]	R2 [Ω]	X2 [mH]	R3 [Ω]	X3 [mH]
Turleenan	0.45981	104.91	0.25113	22.628	0.062879	8.2570
Kingscourt	0.3719	137.10	0.1793	0.001	0.035430	1.8812

Saturation characteristics of a 400/275/13 kV 750 MVA transformer in National Grid was provided from NIE/EirGrid as shown in Table 3-5. The same saturation characteristics were assumed for the Woodland and Kingscourt 400/220 kV transformer.

Table 3-5 Saturation Characteristic of the 400 kV Transformer (defined in tertiary)

I [A]	Phi [Wb-T]
2.30940	51.63578
5.35781	55.07817
9.79186	58.52055
21.70836	61.96294
61.43004	65.40533
187.06140	68.84771
424.92960	72.29010
6267.24695	82.61725

For transformer inrush studies, a magnetizing branch hysteresis curve was derived from the saturation characteristic shown in Table 3-5 using the subroutine HYSDAT.   The lower half of the obtained hysteresis curve is shown in Table 3-6.

Table 3-6 Hysteresis Curve of the 400 kV Transformer (defined in primary)

I [A]	Phi [Wb-T]
-29.4000	-1424.49
-3.6750	-1349.38
2.2050	-1243.19
5.1450	-966.929
9.9225	837.430
15.4350	1105.06
26.4600	1269.09
48.8775	1381.33
117.6000	1467.66
161.7000	1476.29

Another saturation characteristic as shown in Fig. 3.5 was also provided from NIE/EirGrid.

(file EIRGRID_TX_magbranchtest.pl4; x-var c:RSWA -RSWC) t   m:FL   A peak

Knee point   =   113 Wb.t
1pu flux   =   21000/222 = 94.6Wb.t
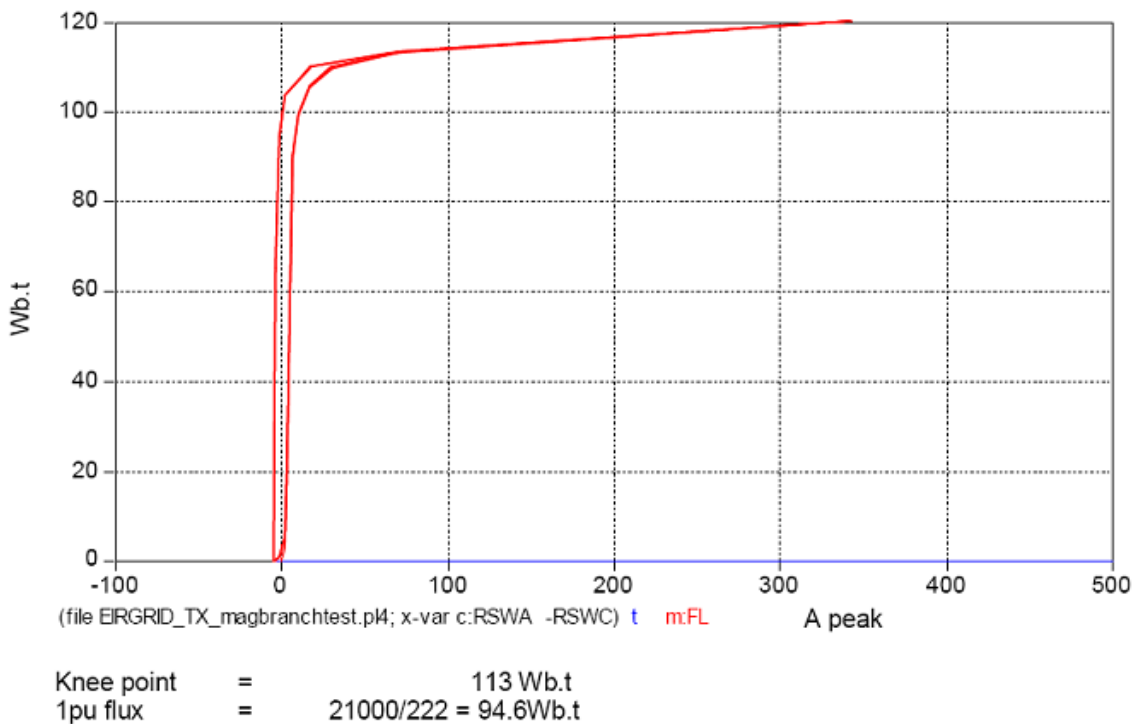
Fig. 3.5 Another saturation characteristic of the 400 kV transformers (defined in tertiary).

From this saturation characteristic, another hysteresis curve was derived by HYSDAT as shown in Table 3-7.

Table 3-7 Another Hysteresis Curve of the 400 kV Transformer (defined in primary)

I [A]	Phi [Wb-T]
-0.65168	-1206.13
-0.081459	-1142.53
0.048876	-1052.62
0.11404	-818.707
0.21994	709.059
0.34213	935.665
0.58651	1074.55
1.0834	1169.58
2.6067	1242.68
3.5842	1249.99

This hysteresis characteristic was used only in one time domain simulation since it was considered less severe compared to the one in Table 3-6.

3.4 Shunt Reactors

Shunt reactors were connected to both ends of the 400 kV cables or 400 kV buses, in order to compensate charging capacity of the cables.   Only for the 400 kV Kingscourt – Turleenan line, shunt reactors were also connected to the center of the line.   Shunt reactors for the Woodland – Kingscourt – Turleenan line were modeled based on the results of the analysis in Chapter 1.   400 kV shunt reactors in the simulation model are shown in Table 3-8.

Table 3-8 400 kV Shunt Reactors in the Simulation Model

Woodland – Kingscourt (58 km)	Woodland: 150 MVA × 2 Kingscourt: 120 MVA × 2
Kingscourt – Turleenan (82 km)	Kingscourt: 100 MVA × 2 Centre: 120 MVA × 3 Turleenan: 100 MVA × 2
Woodland – Oldstreet (125 km)	Woodland: 80 MVA × 1
Moneypoint – Tarbert (6.5 km)	Moneypoint: 50 MVA × 1 Tarbert: 50 MVA × 1

When 400 kV shunt reactors are close to *the point of interest*, they are modeled with the saturation characteristic.   Otherwise, they are modeled as linear inductances.

Note: Other sections of this chapter have been deleted.

Chapter 4 Temporary Overvoltage Analysis

For long EHV cables, temporary overvoltages are of highest concerns in terms of the safe operation after the installation. Highest temporary overvoltages are often higher than highest slow-front overvoltages.

Due to the large capacitance associated with the long EHV cable and the inductance of shunt reactors for the reactive power compensation, the following temporary overvoltages require a close attention for the network with long EHV cables. The theoretical backgrounds relating the large capacitance and the inductance to these temporary overvoltages are given in the beginning of each section:

(1) Parallel resonance overvoltage

(2) Oscillatory overvoltage caused by the system islanding

For equipment whose highest voltage is higher than 245 kV, the standard short-duration power-frequency withstand voltage is not specified in IEC, but it is specified by a utility or a manufacturer. Surge arresters are generally the weakest among different equipment. The temporary overvoltages have to be evaluated against typical withstand voltage and energy absorption capability of surge arresters. Note that the temporary overvoltages may be evaluated with SIWV depending on their decay time.

4.1 Parallel Resonance Overvoltage

4.1.1 Overview

In EHV systems, the highest concern in terms of parallel resonance is the second harmonic current injection due to transformer inrush.   Parallel resonance frequencies were found from the results of frequency scan in EMTP.

It is necessary to consider different operating configurations since it affects parallel resonance frequencies.   In order to find the most critical parallel resonance condition, a number of on/off combinations of the 400 kV lines and shunt reactors were studied as shown in blue in Fig. 4.1.

When the EHV underground cable has significant length, the switching overvoltage caused by its energisation can have very low frequency components for switching overvoltage.   For example, energisation of the EHV underground cable of the length of around 100 km may largely contain third to fifth harmonics.   Therefore, parallel resonance frequencies higher than 100 Hz (second harmonic) must be searched in frequency scan.
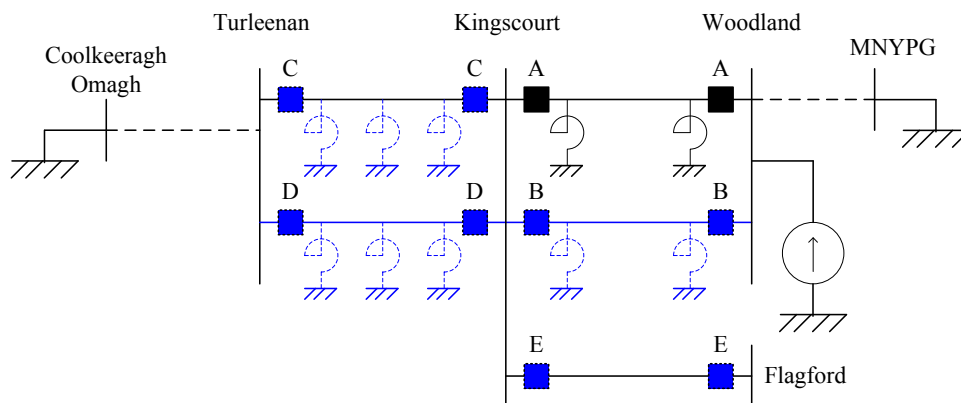
Parallel resonance frequency seen from the Woodland substation
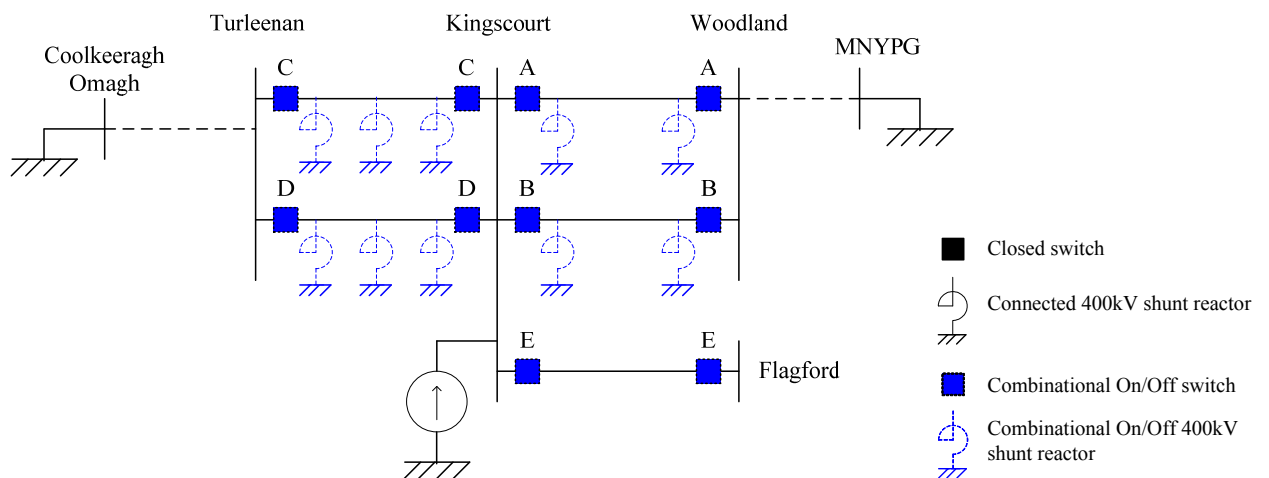
Parallel resonance frequency seen from the Kingscourt substation
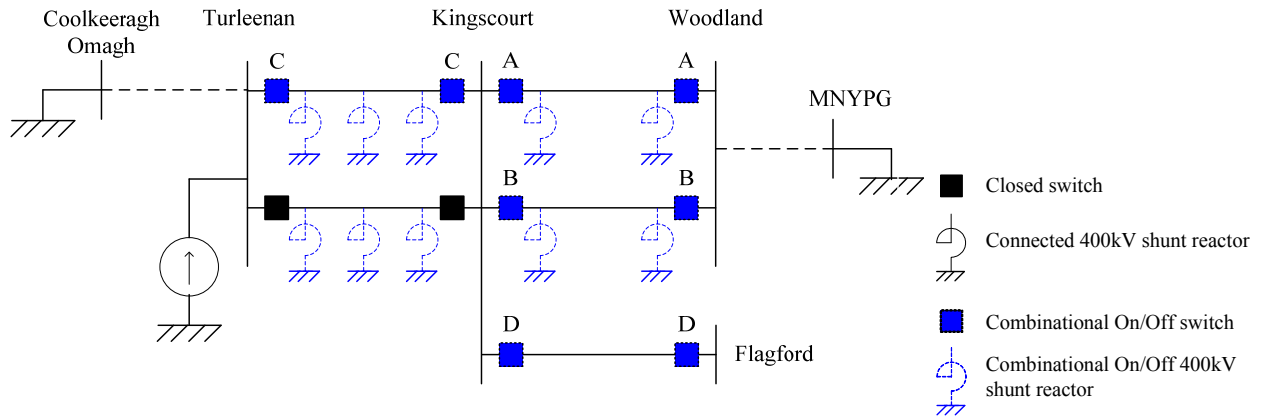
Parallel resonance frequency seen from the Turleenan substation

Fig. 4.1 Frequency sweep for the parallel resonance overvoltage analysis.

After the frequency scan, a time domain simulation under the most critical conditions was performed. If parallel resonance frequency seen from the 400 kV Woodland bus is assumed to be the severest condition with an outage of the Kingscourt – Turleenan lines, the Woodland 400/220 kV transformer energisation is studied as shown in Fig. 4.2.
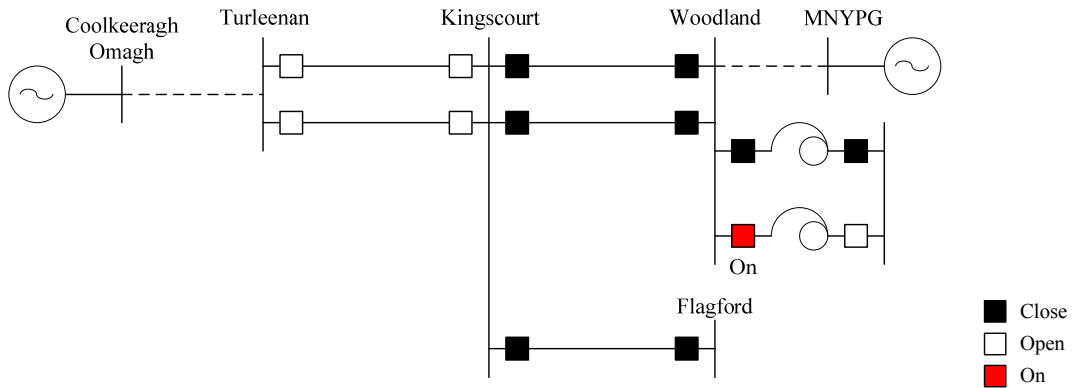
Fig. 4.2 Sample scenario of the time domain simulation for the parallel resonance overvoltage analysis.

4.1.2 Fault Current Level

In the parallel resonance analysis, an effect of the fault current level (source impedance) at Woodland 220 kV, Kingscourt 220 kV, and Turleenan 275 kV buses was studied as one of the parameters. First, the fault current calculation was performed at these buses to find a reasonable range for this parameter. Here, power flow data for the planned transmission system in 2020 were used for the calculation.

The results of the calculation are shown in Table 4-1. Since it is necessary to find the fault current level in the 275 and 220 kV network, fault current that flows from the 400 kV network is not included in the calculation result. In the table, values of source impedance that correspond to the fault current levels are shown in parentheses.

Table 4-1 Fault Current Levels at Woodland, Kingscourt, and Turleenan LV Side Buses

	Summer off-peak	Winter peak with maximum wind	Normal winter peak
Woodland 220 kV	8.673 kA (46.62 mH)	11.24 kA (35.97 mH)	14.59 kA (27.71 mH)
Kingscourt 220 kV	7.657 kA (52.80 mH)	8.623 kA (46.89 mH)	8.679 kA (46.58 mH)
Turleenan 275 kV	13.43 kA (37.62 mH)	18.91 kA (26.73 mH)	15.99 kA (31.60 mH)

Generators included in the simulation model are fewer than those in service in summer off-peak power flow data. The generators included in the simulation model caused the following fault current levels at Woodland, Kingscourt, and Turleenan LV side buses.

Table 4-2 Fault Current Levels at Woodland, Kingscourt, and Turleenan LV Side Buses

	Summer off-peak
Woodland 220 kV	1.543 kA (262.0 mH)
Kingscourt 220 kV	1.671 kA (241.9 mH)
Turleenan 275 kV	1.257 kA (402.0 mH)

An adjustment of the fault current level can be achieved by adding a dummy source at Woodland, Kingscourt, and Turleenan LV side buses with different source impedances. Based on current calculation results of the fault, the source impedance values were varied in the range shown below, considering the difference between the values in Table 4-1 and the values in Table 4-2.

Table 4-3 Assumed Range of Source Impedance Values

Woodland 220 kV	20 – 60 mH
Kingscourt 220 kV	40 – 60 mH
Turleenan 275 kV	20 – 50 mH

4.1.3 Study of the Simple Network

In this section, the characteristic of the 400 kV Woodland – Kingscourt – Turleenan line with a generator was studied. As a simple network model, only one voltage source is assumed at Turleenan behind source impedance. With the existence of this voltage source, parallel resonance frequency shifts from $f = \dfrac{1}{2\pi\sqrt{LC}}$ to $f = \dfrac{1}{2\pi}\sqrt{\dfrac{1}{LC} + \dfrac{1}{L_0 C}}$ (L_0: source impedance).

In this simple theoretical calculation, the source impedance necessary to shift parallel resonance frequency from 50.0 Hz to 100 Hz is

$$\frac{1}{2\pi}\sqrt{\frac{1}{0.1959 \times 51.80 \times 10^{-6}} + \frac{1}{L_0 \times 51.80 \times 10^{-6}}} = 100$$

$$L_0 = 65.2 \text{ mH}$$

The effect of source impedance was then confirmed by frequency scan. Fig. 4.3 shows the simulation model for frequency scan. Source impedance of 65.2 mH is connected to the Turleenan 400 kV bus.
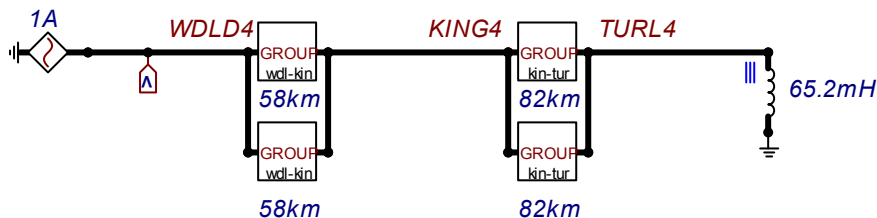
Fig. 4.3 Simulation model for frequency scan to study the simple network.

The results of frequency scan are shown in Fig. 4.4. Parallel resonance frequency was shifted from 48.3 Hz to around 90.0 Hz. It can be seen from the figure that source impedance has a small effect on the frequency response at higher frequencies. This is reasonable since the magnitude of source impedance (inductance) becomes larger at higher frequencies.

In Fig. 4.4, a frequency scan was performed with a large frequency step (10 Hz). In order to find an effect of source impedance on the magnitude of impedance at parallel resonance, frequency scan must be performed using a smaller frequency step.
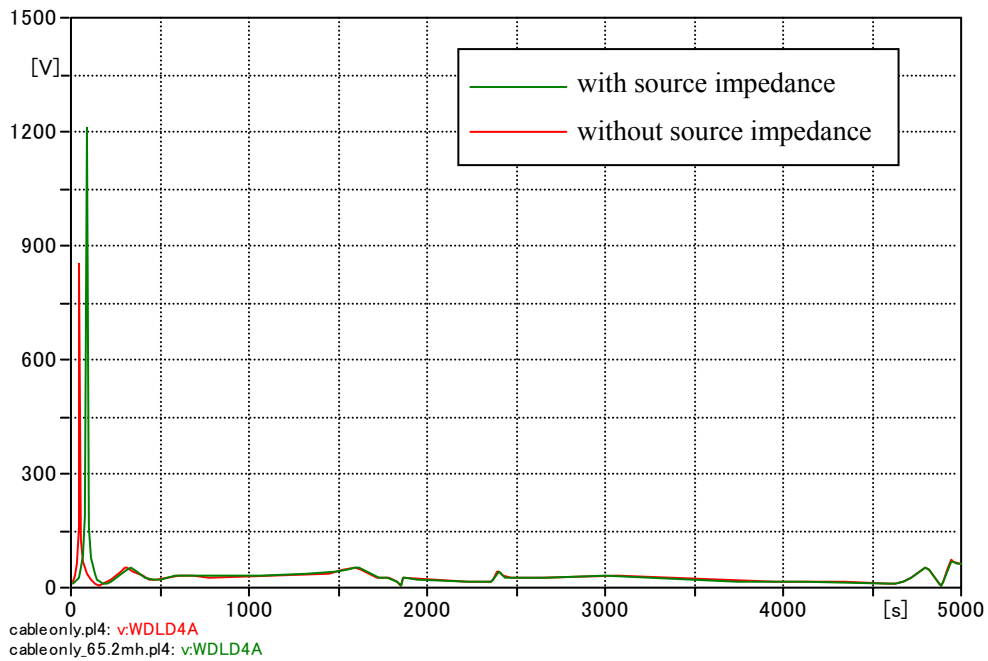
Fig. 4.4 Characteristic of the simple network.

Fig. 4.5 shows the result of a frequency scan with different source impedance values of 1000, 100, and 65.2 mH.   Here, the frequency scan was performed only near the highest peak with a small frequency step (0.1 Hz).   The vertical axis of the figure is the log scale.   It can be seen that the magnitude of impedance at parallel resonance significantly decreases for smaller source impedance, that is for a higher fault current level.
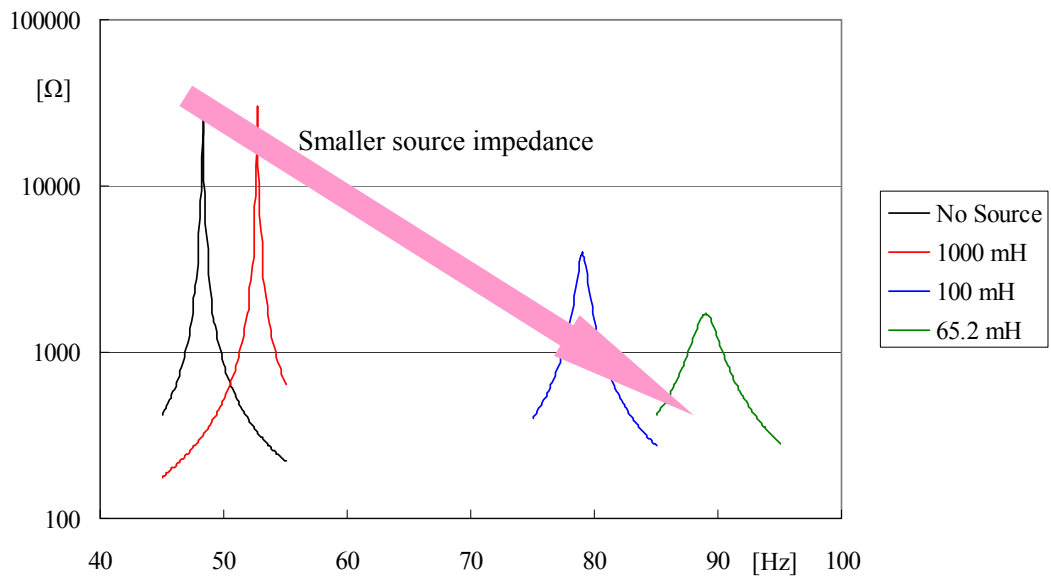
Fig. 4.5 Effect of source impedance on the characteristic of the simple network.

An outage of the shunt reactor is not assumed to have a large impact on parallel resonance, also in this simulation model with a generator. In contrast, it can be understood that an outage of a 400 kV cable has some effect on parallel resonance in this simple network. It can be seen from the theoretical equation $f = \dfrac{1}{2\pi}\sqrt{\dfrac{1}{LC} + \dfrac{1}{L_0 C}}$ that an outage of a 400 kV cable (change of C) will change the effect of source impedance.

First, an outage of the largest shunt reactor (150 MVA) was studied by a frequency scan as shown in Fig. 4.6. The source impedance was fixed to 100 mH. An outage of the largest shunt reactor shifted the parallel resonance frequency only by 0.9 Hz, as was expected based on the theoretical equation. In addition, the magnitude of impedance at parallel resonance was not changed by the shunt reactor outage.

cableonly_100mh_zoom.pl4: v:WDLD4A
cableonly_100mh_shroutage_zoom.pl4: v:WDLD4A
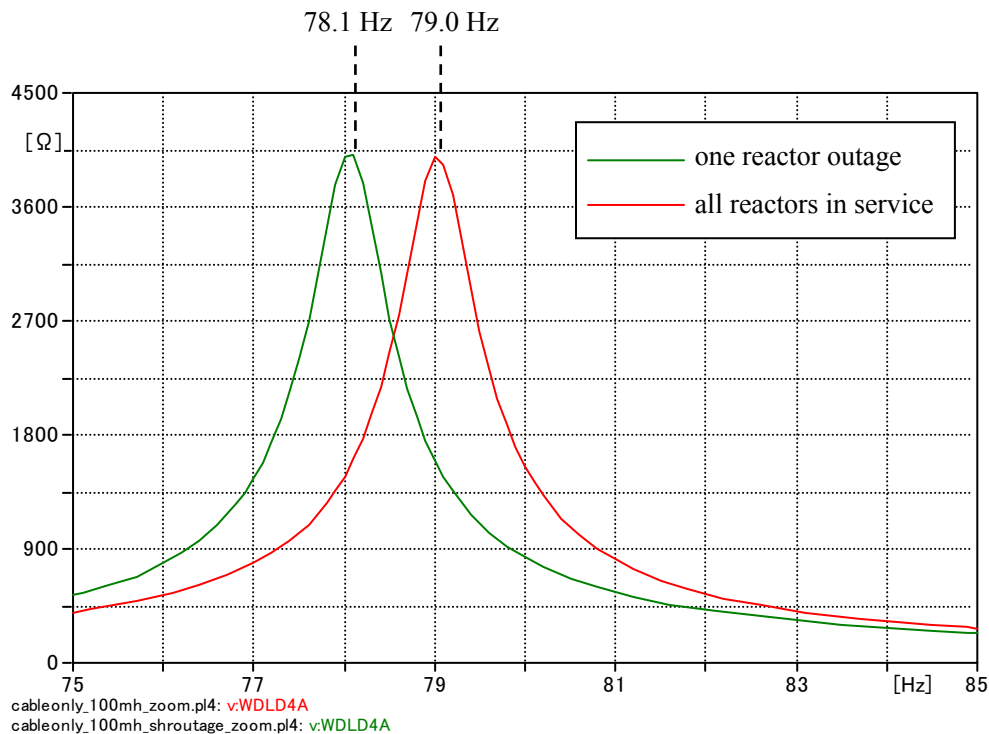
Fig. 4.6 Effect of a shunt reactor outage on the characteristic of the simple network.

Fig. 4.7 shows the effect of a 400 kV cable outage. An outage of one circuit of the Kingscourt – Turleenan lines caused parallel resonance frequency to shift by 4.4 Hz. In addition, the magnitude of impedance at parallel resonance was lowered from 3987 Ω to 2238 Ω.
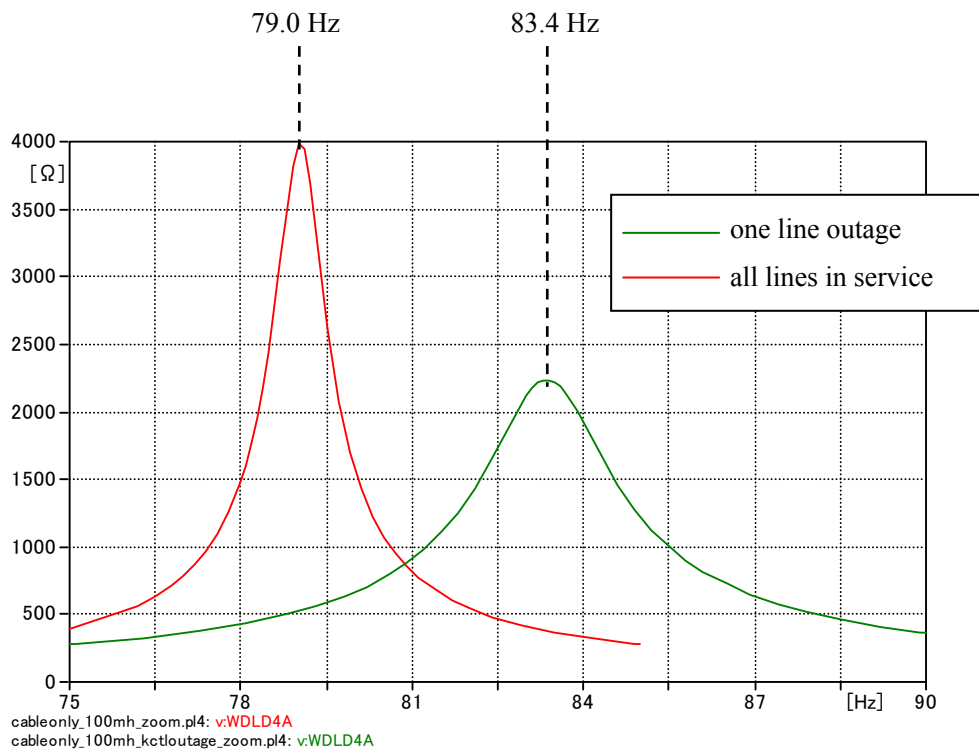
Fig. 4.7 Effect of a line outage on the characteristic of the simple network.

Then, an effect of target frequency of the Bergeron model was studied.   Target frequency of all cable models were changed from 50 Hz to 100 Hz.
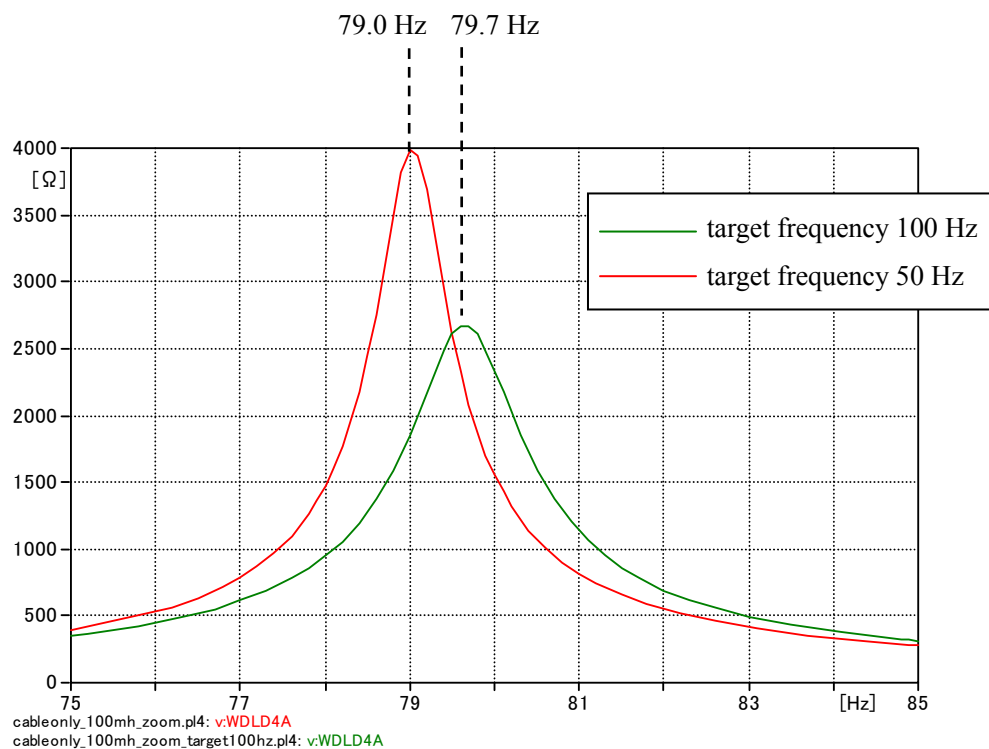
Fig. 4.8 Effect of a line outage on the characteristic of the simple network.

Fig. 4.8 shows the result of the frequency scan. Parallel resonance frequency was shifted only by 0.7 Hz by changing target frequency from 50 Hz to 100 Hz. The target frequency was set to 50 Hz for further analysis since the magnitude of impedance at parallel resonance frequency was larger when the target frequency was set to 50 Hz.

In conclusion, the effects of the parameters have been summarized in Table 4-4. Since the shunt reactor outage does not have a significant impact on parallel resonance frequency, it has to be adjusted by changing the fault current level or through line outages. Additionally, in order to yield a severe condition, some OHL outages should be considered in order to increase the magnitude of impedance at parallel resonance frequency.

Note that the result summarized in this table applies only to this study, since these effects depend on the compensation rate, the unit size of shunt reactor, and so on.

Table 4-4 Effect of a Shunt Reactor / Line Outage and Fault Current Level (Summary)

	Parallel resonance frequency	Magnitude of impedance
Target frequency	Very small	Moderate
Shunt reactor outage	Very small	No effect
Line outage	Moderate	Moderate
Fault current level	Large	Very large

4.1.4   Transformer Inrush Current

In this section, transformer energisation was studied in order to find the frequency components contained in transformer inrush current.   First, energisation of the 400/220 kV Woodland transformer was simulated.   Fig. 4.9 shows inrush current into the transformer.   The switch timing was selected so that the largest inrush current appeared in Phase A.   Residual flux in Phases A and B were set to 85 % of the rated flux.
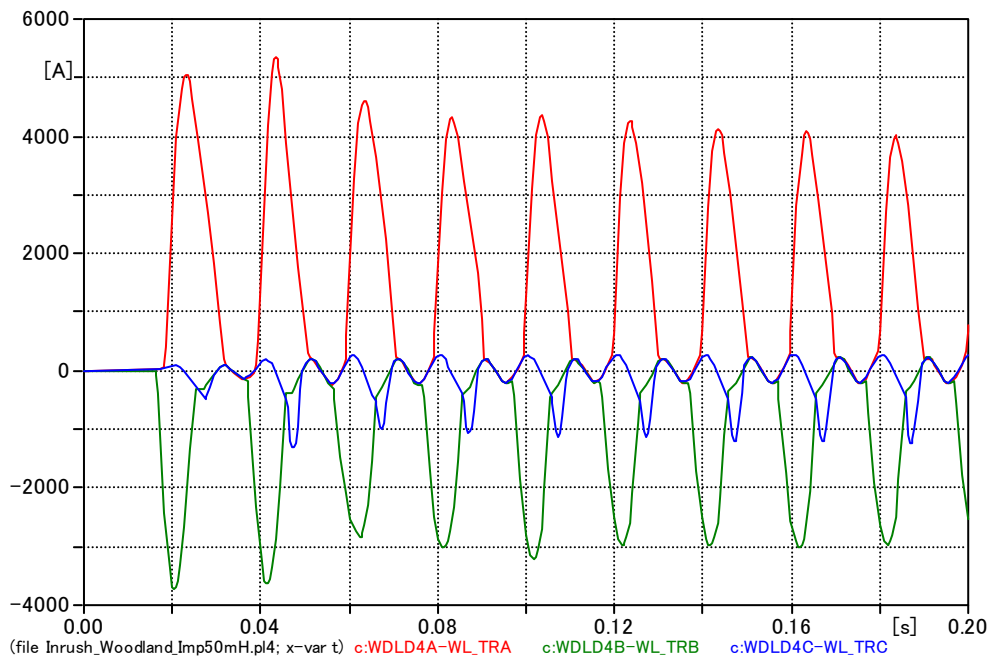
Fig. 4.9 Inrush current into the 400/220 Woodland transformer.

Inrush current largely contains second harmonic.   As shown in Fig. 4.10, Fourier transform of inrush current (Phase A) shows that second harmonic current 513.2 A is contained in inrush current.
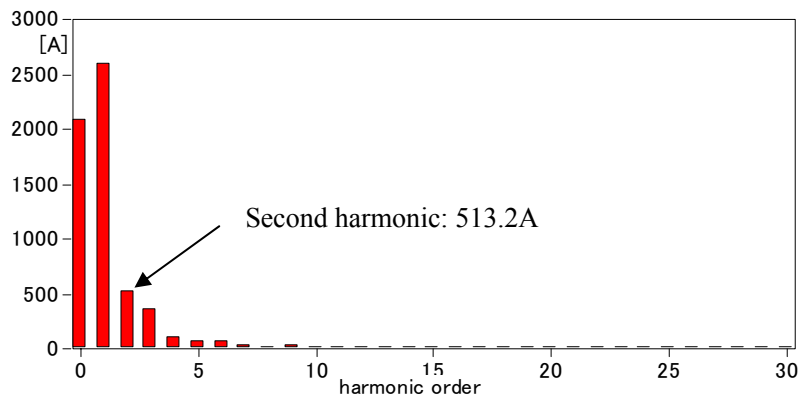
Fig. 4.10 Fourier transform of inrush current.

Fig. 4.11 shows the result of Fourier transform when it was performed with a frequency resolution of 1 Hz.
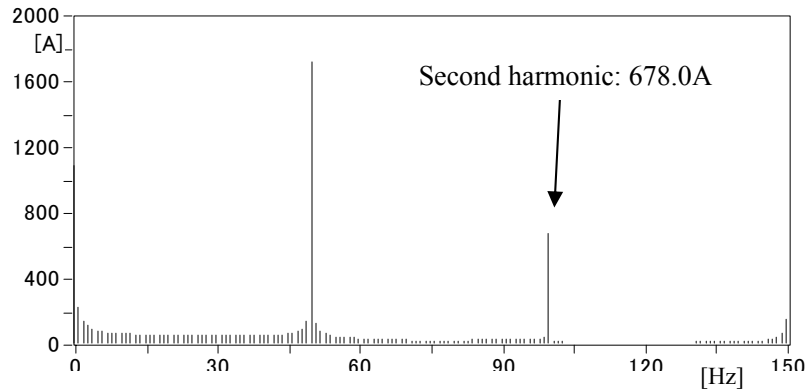
Fig. 4.11 Fourier transform of inrush current (1 Hz step).

It is known that inrush current reaches its maximum if a transformer is energised when the bus voltage crosses the zero point. In contrast, second harmonic contained in inrush current reaches its maximum at the different switch timing, which has to be found by simulations. As a result of the simulations shown in Fig. 4.12, it was determined that transformer energisation was simulated at switch timings between 10 ms and 14 ms by 1 ms step.
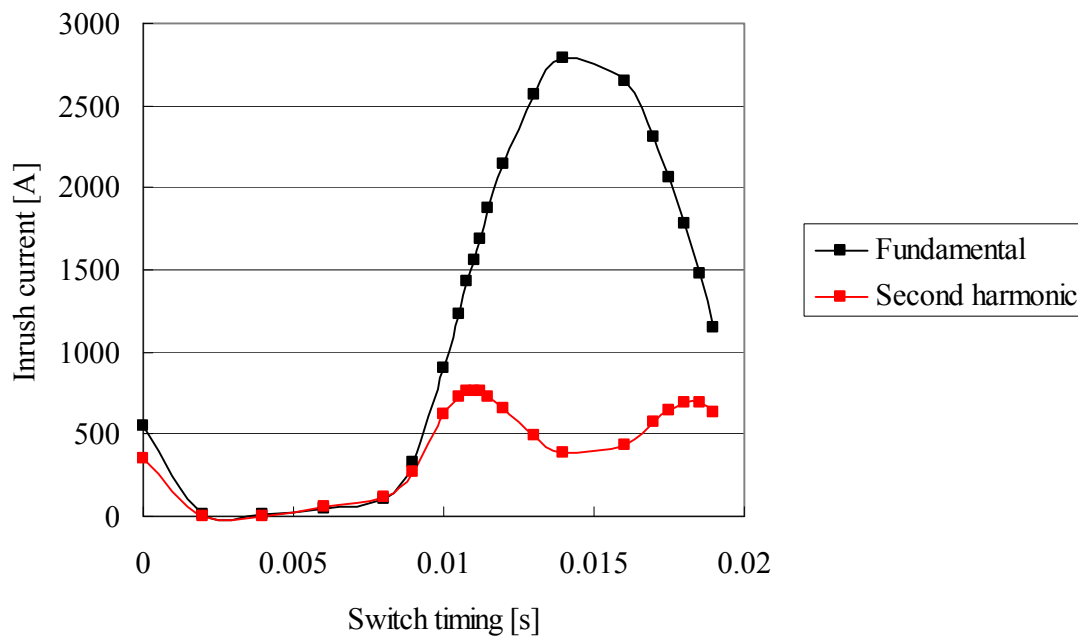
Fig. 4.12 Fundamental component and second harmonic contained in inrush current.

4.1.5 Parallel Resonance Frequency Seen from Woodland 400 kV

Parallel resonance frequency of the network seen from Woodland 400 kV was found by frequency scan using the simulation model in Fig. 4.13.
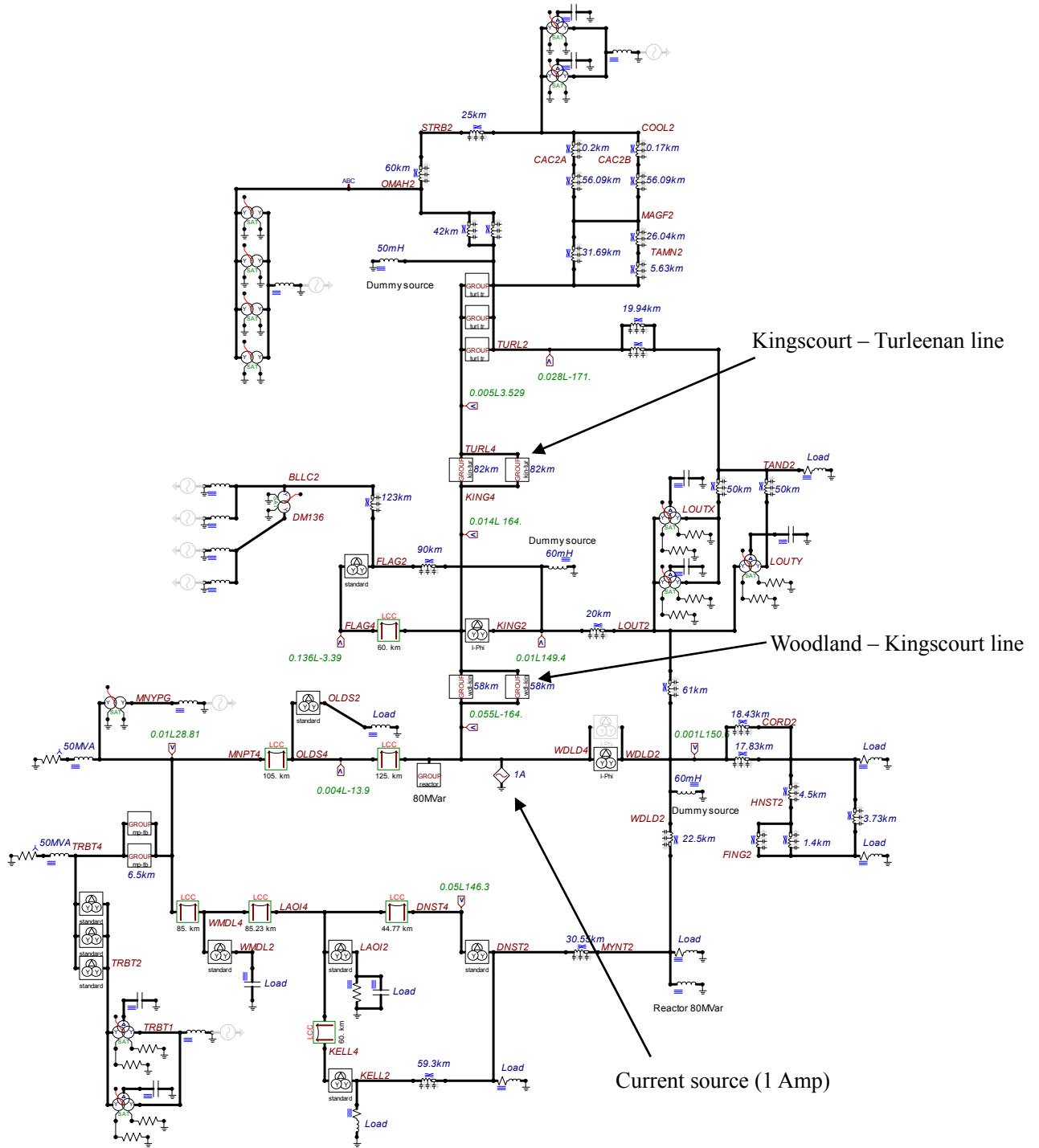
Fig. 4.13 Simulation model for frequency scan seen from Woodland 400 kV.

In the first example, the largest source impedance (lowest fault current level) in Table 4-3 was set to the Woodland 220 kV, the Kingscourt 220 kV, and the Turleenan 275 kV buses. The result of the frequency scan is shown in Fig. 4.14. The highest peak was found at 90 Hz, and other high peaks were not a level requiring careful consideration.
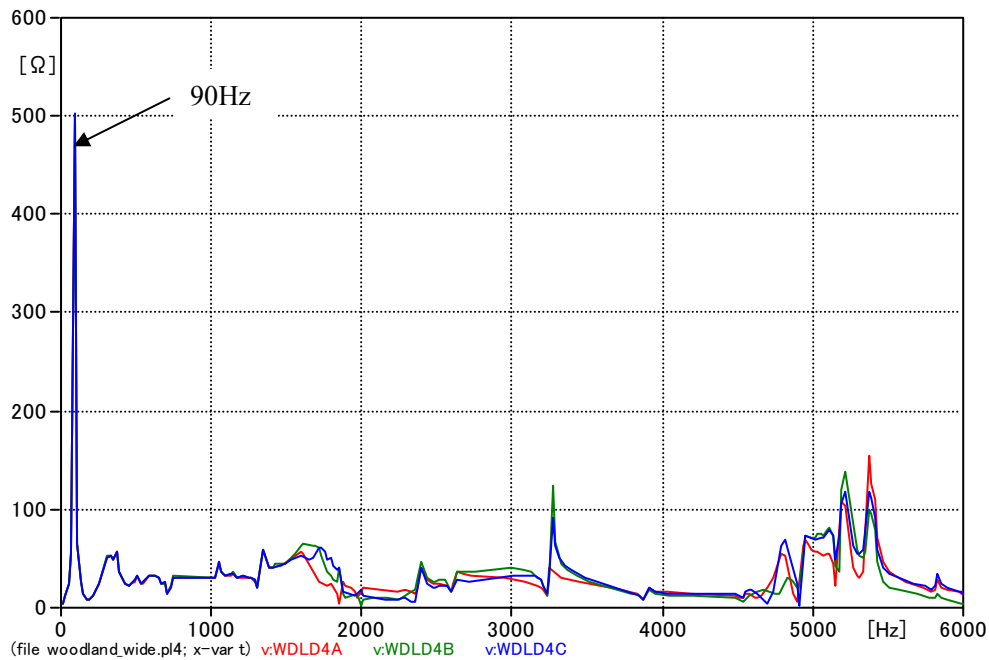
Fig. 4.14 Parallel resonance frequency of the network seen from Woodland 400 kV.

As a result, an energisation of the Woodland 400/220 kV transformer was considered as the most severe source of harmonic current injection. Since parallel resonance frequency was found to be 90 Hz, it was necessary to shift it by 10 Hz.

Next, in order to realize a higher magnitude of impedance at parallel resonance, some combinations of OHL outages were studied. The result of the analysis is shown in Fig. 4.15. As a result of the analysis, two 400 kV OHLs, Woodland – Oldstreet line and Kingscourt – Flagford line, will be considered as out of service, in order to achieve a higher magnitude of impedance.

woodland.pl4: v:WDLD4A
woodland_wlosoutage.pl4: v:WDLD4A
woodland_kcffoutage.pl4: v:WDLD4A
woodland_wlosoutage_kcffoutage.pl4: v:WDLD4A

—— all OHLs in service		—— Kingscourt-Flagford line outage
—— Woodland-Oldstreet line outage		—— both two OHLs outage
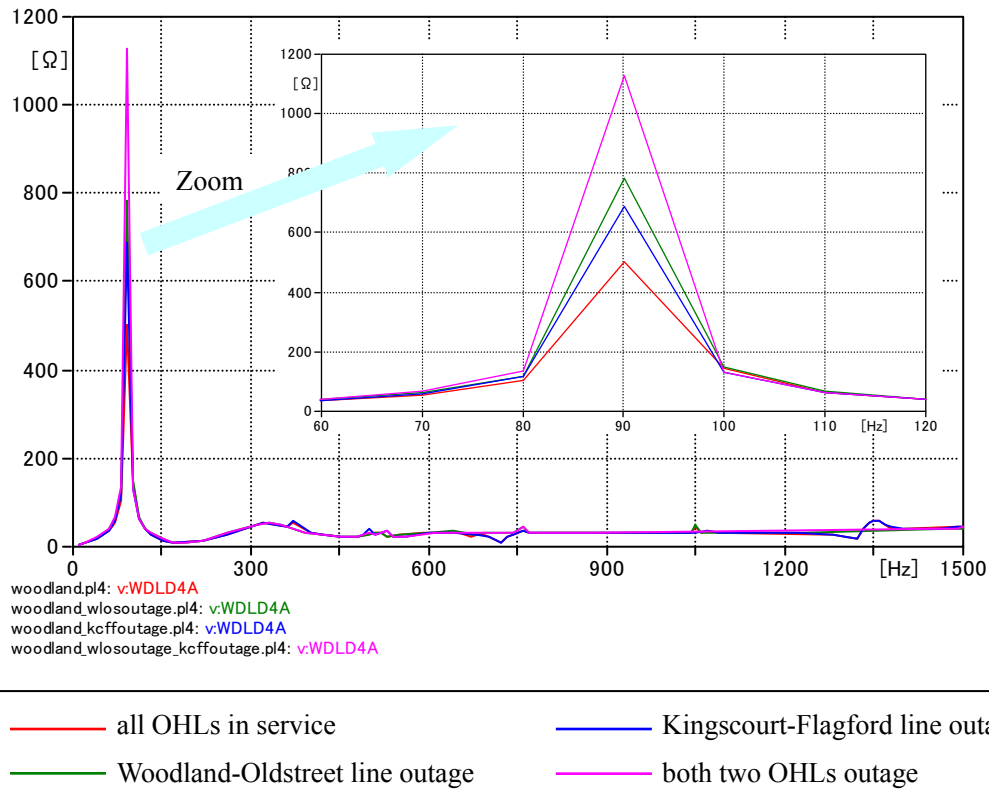
Fig. 4.15 Effect of OHL outages on parallel resonance frequency.

Considering the operating status of the Woodland – Kingscourt – Turleenan line, the four cases shown in Table 4-5 were studied.   For each case, source impedance at the Turleenan 275 kV bus was adjusted in order to yield parallel resonance frequency of 100 Hz.   The value of this source impedance and the magnitude of impedance at parallel resonance frequency are shown in Table 4-5.

Table 4-5 Magnitude of impedance at parallel resonance frequency (Woodland)

	Woodland – Kingscourt line	Kingscourt – Turleenan line	Source impedance (Turleenan)	Magnitude of impedance
Case 1	Two circuits	Two circuits	17.0 mH	1642 Ω
Case 2	Two circuits	One circuit	51.0 mH	1326 Ω
Case 3	One circuit	Two circuits	39.8 mH	1142 Ω
Case 4	One circuit	One circuit	252.0 mH	856 Ω

The reasonable range of source impedance values at Turleenan 275 kV was 20 – 50 mH. However, in order to shift parallel resonance frequency to 100 Hz in Case 4, it was necessary to set the values of source impedance at Turleenan 275 kV bus much higher than this range.

Finally, a time domain simulation was carried out under the assumed severest conditions, Case 1.   As stated in the previous section, transformer energisation was simulated at switch timings between 10 ms and 14 ms in 1 ms steps in order to find the severest switch timing.   The result of the analysis is summarized in Table 4-6.

Table 4-6 Highest Overvoltage for Different Switch Timings

Switch timing [ms]	Highest overvoltage [kV]		
	Phase A	Phase B	Phase C
10	509.8	444.4	528.5
11	484.0	465.4	532.7
12	445.1	489.8	540.7
13	420.6	509.3	534.5
14	418.0	511.4	532.9

As can be seen from Table 4-6, the highest overvoltage always occurred in Phase C, and it is not very sensitive to the switch timing.   When the switch timing is changed from 12 ms to 14 ms, the change in the overvoltage is only 7.8 kV.   The voltage of the Woodland 400 kV bus and inrush current into the Woodland 400/220 kV transformer for the switch timing 12 ms are shown in Fig. 4.16 and Fig. 4.17.
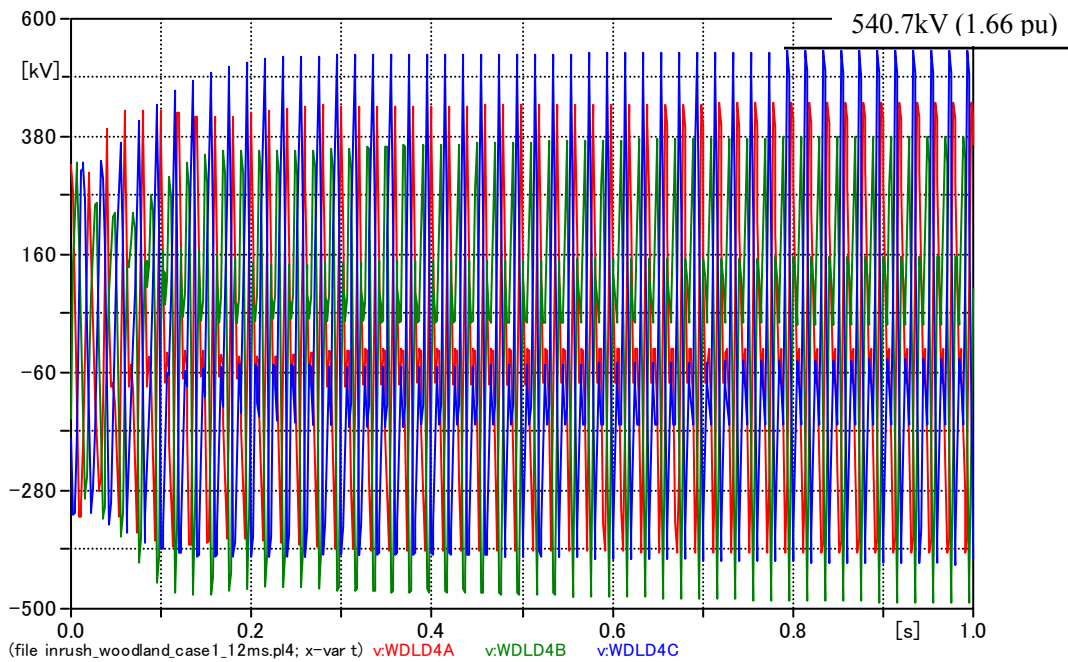
Fig. 4.16 Woodland 400 kV bus voltage in transformer inrush.
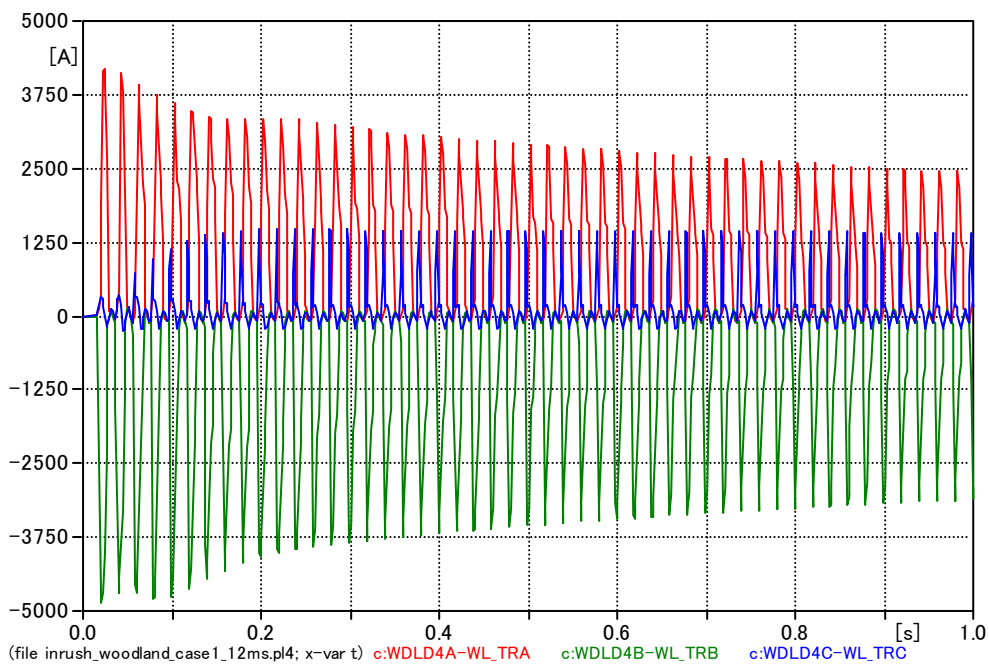
Fig. 4.17 Inrush current into the Woodland 400/220 kV transformer.

The observed highest overvoltage is high for temporary overvoltage, but it is not at the level where surge arresters operate in a low-impedance mode (537 kV – 1 A).   In the actual network, the overvoltages should have better damping due to larger resistance (temperature rise) and losses (eddy current losses and etc.).

In order to evaluate the energy absorption capability of the surge arresters, the same time domain simulation was repeated with surge arresters.   As the severest assumption, only one surge arrester was connected to the Woodland 400 kV bus.   As a result of the analysis shown in Fig. 4.18 and Fig. 4.19, it was confirmed that there was no problem in the energy absorption capability of the surge arrester.
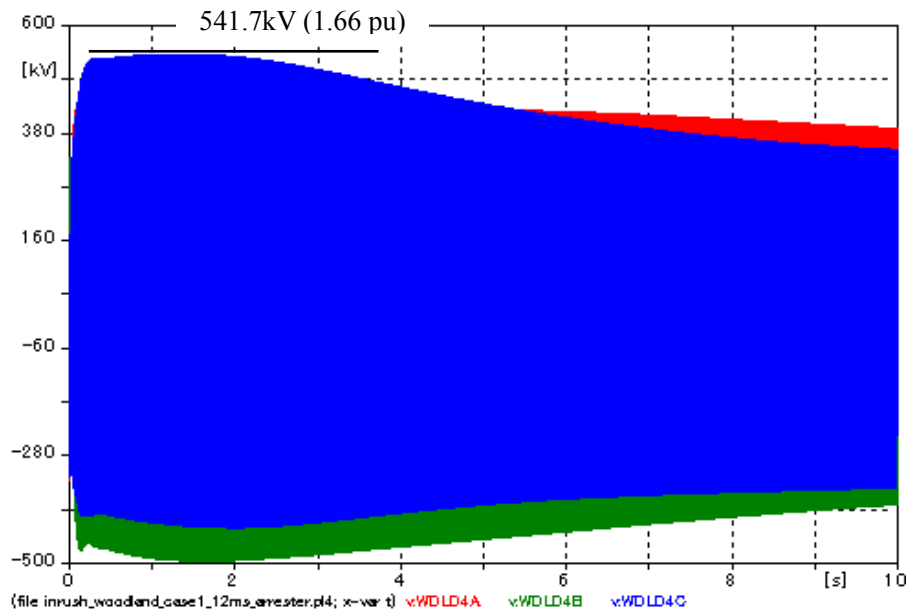
Fig. 4.18 Woodland 400 kV bus voltage in transformer inrush with a surge arrester.
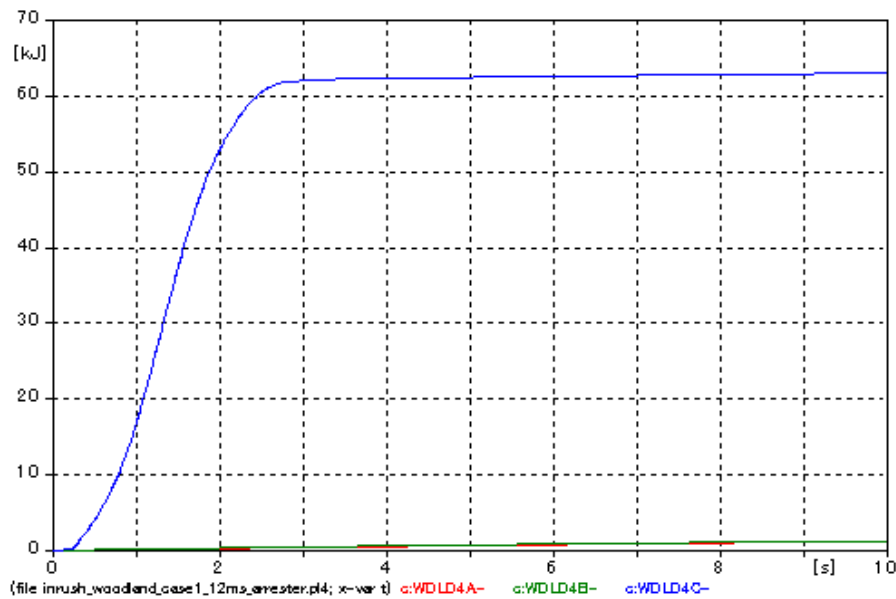
Fig. 4.19 Energy absorbed by the surge arrester.

The withstand voltages of surge arresters are often given in their specification.   For example, Siemens 3ES5 336-5PM51-1HA2-Z has the withstand voltages as shown in Table 4-7.   As can be seen from the table, the observed highest overvoltage 541.7 kV (1.66 pu, peak) was higher than the temporary overvoltage allowed for 10 seconds.

Table 4-7 Withstand Voltages of Surge Arresters (r.m.s.)

Maximum continuous operating voltage		269 kV (1.16 pu)
Power frequency withstand voltage (1 min)		364 kV (1.58 pu)
Temporary overvoltage	10 s	370 kV (1.60 pu)
	1 s	390 kV (1.69 pu)

From a manufacturer's standpoint, it is possible to develop a surge arrester with higher withstand voltages, for example 1.8 pu for 10 seconds.   With this in mind, the observed overvoltage is not at the level which affects the feasibility of the 400 kV Woodland – Kingscourt – Turleenan line.

It may, however, lead to higher protective levels ensured by the arrester, which may affect the insulation design of other equipment.   These additional costs need to be evaluated by the manufacturer.   Finally, it will of course affect the total insulation coordination studied by utilities.

The time domain simulations as shown in Fig. 4.16 – Fig. 4.19 were performed with the hysteresis curve in Table 3-6, which was derived from the saturation characteristics of the 400/275/13 kV 750 MVA transformer in the National Grid. Here, the time domain simulation was repeated with the other hysteresis curve as shown in Table 3-7. The Woodland 400/220 kV transformer was energised at 12 ms.

The waveform of the inrush current is shown in Fig. 4.20. Due to the difference between the two hysteresis curves, the magnitude of inrush current is significantly lower compared to the one in Fig. 4.17.

(file Inrush_Woodland_Case1_12ms_EirGridHysteresis.pl4; x-var t) c:WDLD4A-WL_TRA   c:WDLD4B-WL_TRB
c:WDLD4C-WL_TRC
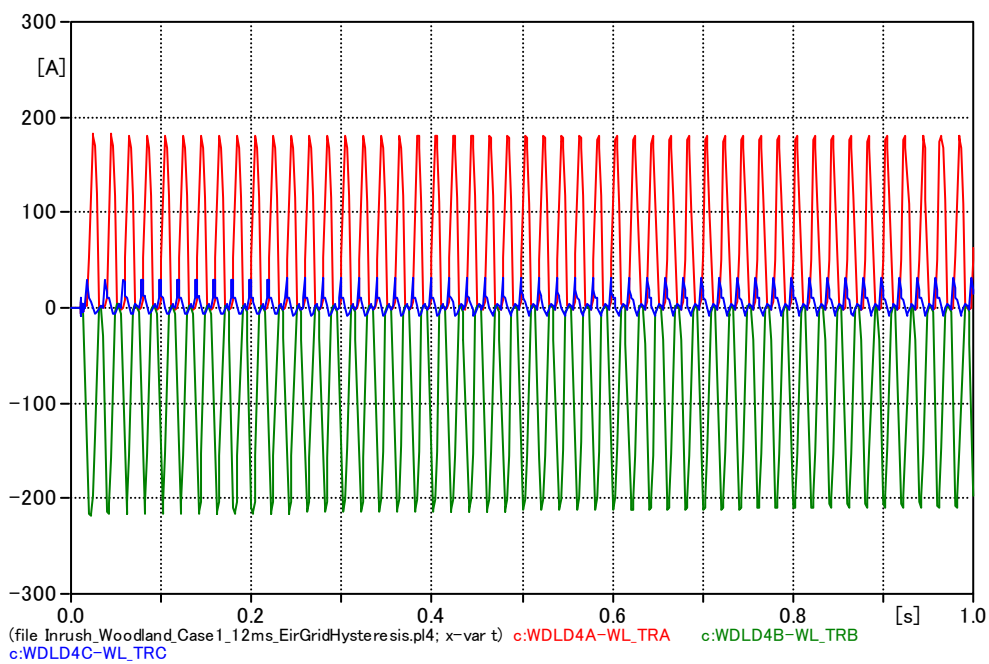
Fig. 4.20 Inrush current into the Woodland 400/220 kV transformer with the other hysteresis curve.

The voltage of the Woodland 400 kV bus is shown in Fig. 4.21.   The highest voltage of 337.8 kV (1.03 pu) was observed in Phase A.   Since inrush current is small, an overvoltage caused by parallel resonance was not observed.
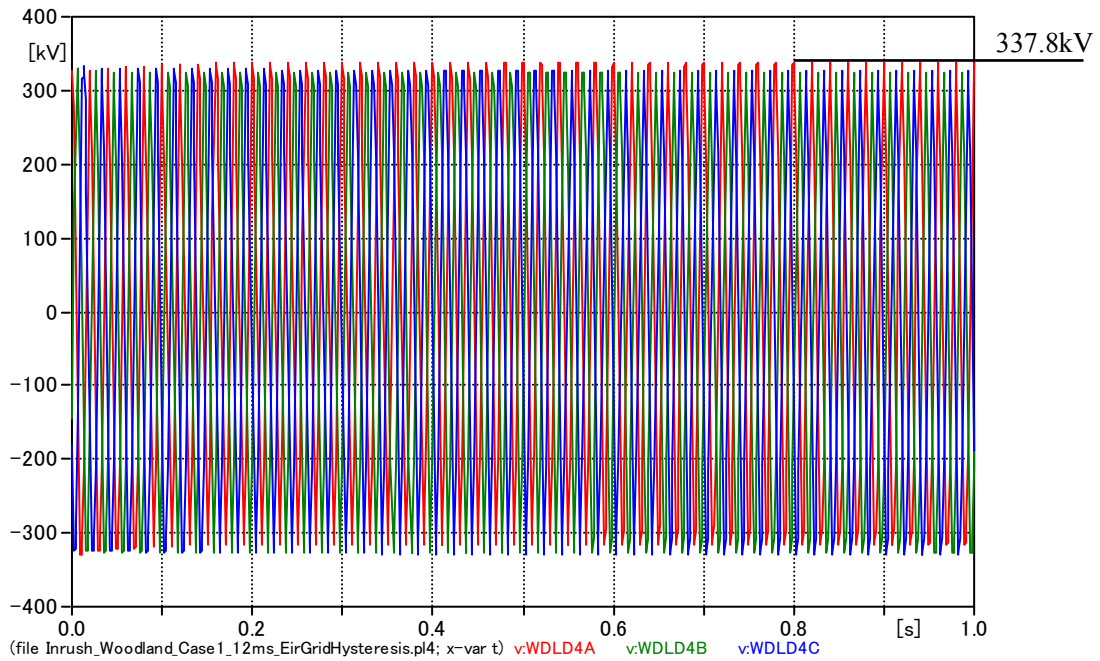
Fig. 4.21 Woodland 400 kV bus voltage in transformer inrush with the other hysteresis curve.

Considering this result, the transformer inrush studies were hereafter performed only with the hysteresis curve derived from the 400/275/13 kV 750 MVA transformer data in the National Grid.

4.1.6 Parallel Resonance Frequency Seen from Kingscourt 400 kV

In this section, parallel resonance frequency seen from the Kingscourt 400 kV bus was studied. First, the result of the frequency scan is shown in Fig. 4.22. For the analysis, the largest source impedance (lowest fault current level) in Table 4-3 was set to Woodland 220 kV, Kingscourt 220 kV, and Turleenan 275 kV buses. As in the frequency scan result seen from Kingscourt 400 kV, the highest peak was found at 90 Hz, and other high peaks were not at a level needing careful consideration.
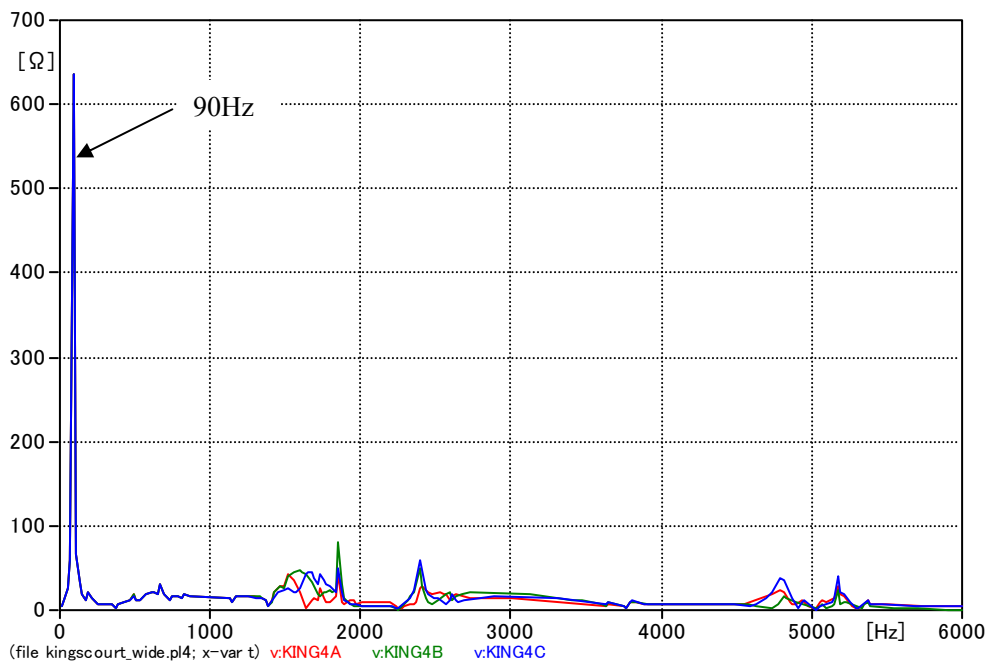
Fig. 4.22 Parallel resonance frequency of the network seen from Kingscourt 400 kV.

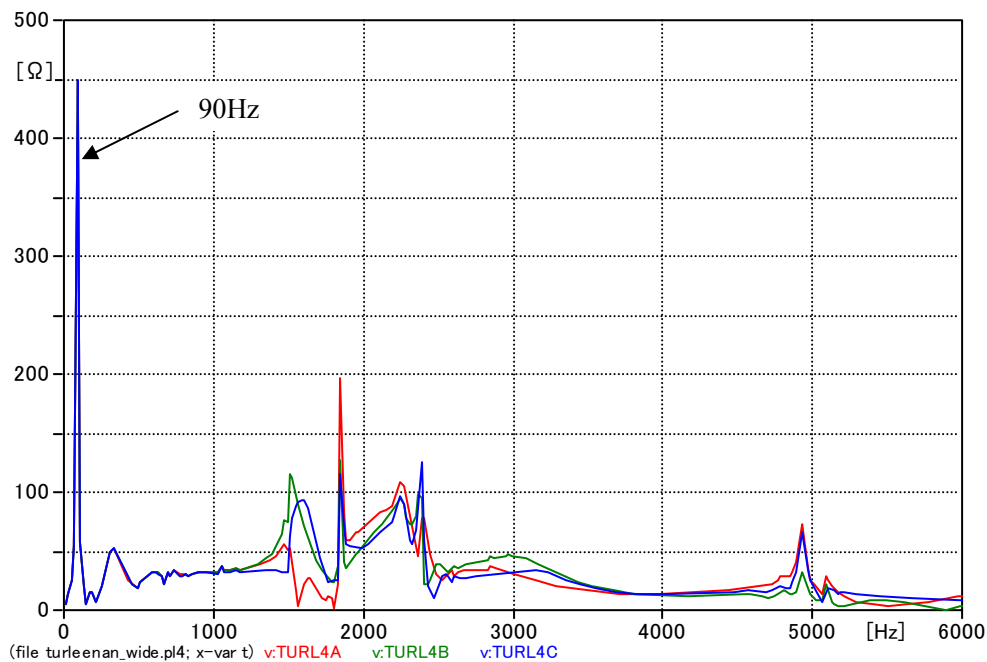As a result, an energisation of the Kingscourt 400/220 kV transformer was considered as the severest source of harmonic current injection. Since parallel resonance frequency was found to be at 90 Hz, it was necessary to shift it by 10 Hz.

The same four combinations were studied with regard to the operating status of the 400 kV Woodland – Kingscourt – Turleenan line, as shown in Table 4-8. As in the previous section, outages of the Woodland – Oldstreet line and the Kingscourt – Flagford line were assumed in order to have larger impedance at parallel resonance frequency, without shifting the parallel resonance frequency.

For each case, the source impedance at Turleenan 275 kV bus was adjusted first in order to yield a parallel resonance frequency at 100 Hz.   Source impedance at Woodland 220 kV bus was also adjusted when it was not possible to shift parallel resonance frequency to 100 Hz by only adjusting the source impedance at the Turleenan 275 kV bus.   The values of these source impedances and the magnitude of impedance at parallel resonance frequency are shown in Table 4-8.

Table 4-8 Magnitude of impedance at parallel resonance frequency (Kingscourt)

	Woodland – Kingscourt line	Kingscourt – Turleenan line	Source impedance		Magnitude of impedance
			Turleenan	Woodland	
Case 1	Two circuits	Two circuits	20.0 mH	24.8 mH	2606 Ω
Case 2	Two circuits	One circuit	31.3 mH	60.0 mH	1263 Ω
Case 3	One circuit	Two circuits	27.0 mH	60.0 mH	1247 Ω
Case 4	One circuit	One circuit	130.0 mH	60.0 mH	923 Ω

The reasonable range of source impedance value at Turleenan 275 kV was 20 – 50 mH. However, in order to shift parallel resonance frequency to 100 Hz in Case 4, it was necessary to set the value of source impedance at Turleenan 275 kV bus much higher than this range.

Finally, the time domain simulation was carried out under the assumed severest conditions, Case 1.   The voltage of the Kingscourt 400 kV bus and inrush current into the Woodland 400/220 kV transformer are shown in Fig. 4.23 and Fig. 4.24.   Since it was discovered that the switch timing does not have a large effect on the overvoltage, the transformer was energised at voltage zero.   As a result, the highest voltage observed at the Kingscourt 400 kV bus was 515.8 kV (1.58 pu) in Phase C.   This is high for a temporary overvoltage, but is not at the level where surge arresters operate in a low-impedance mode (511 kV – 0.01 A).   This is not a concern for the operation of the 400 kV Woodland – Kingscourt – Turleenan line.
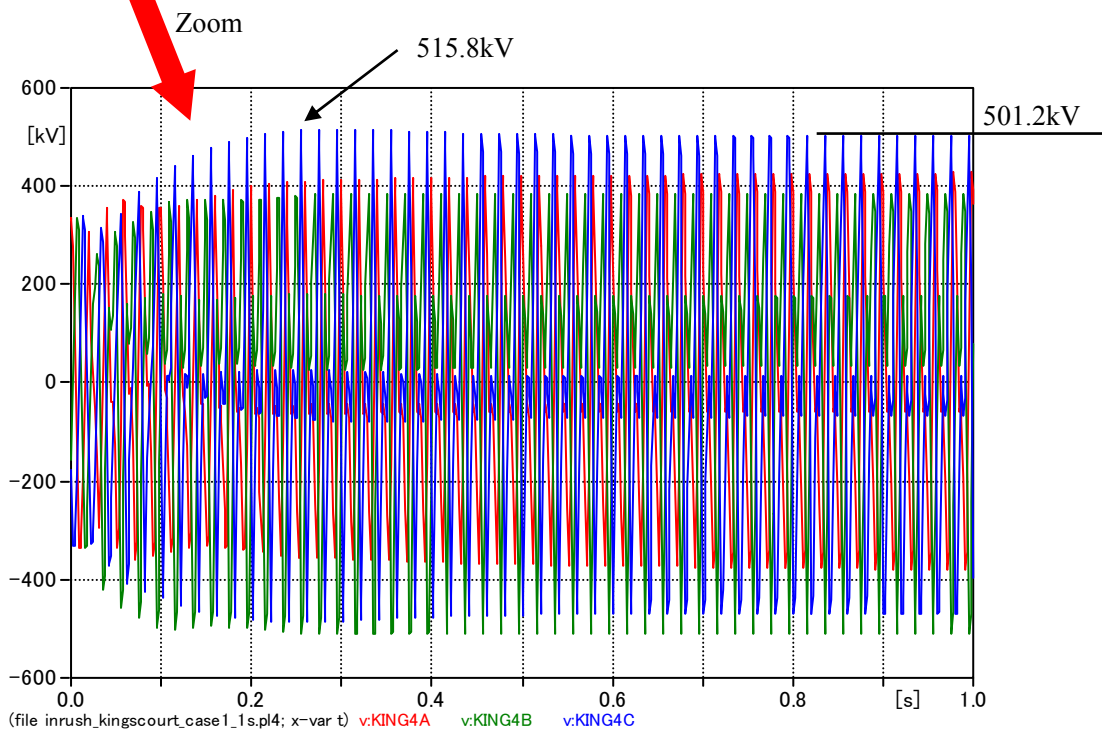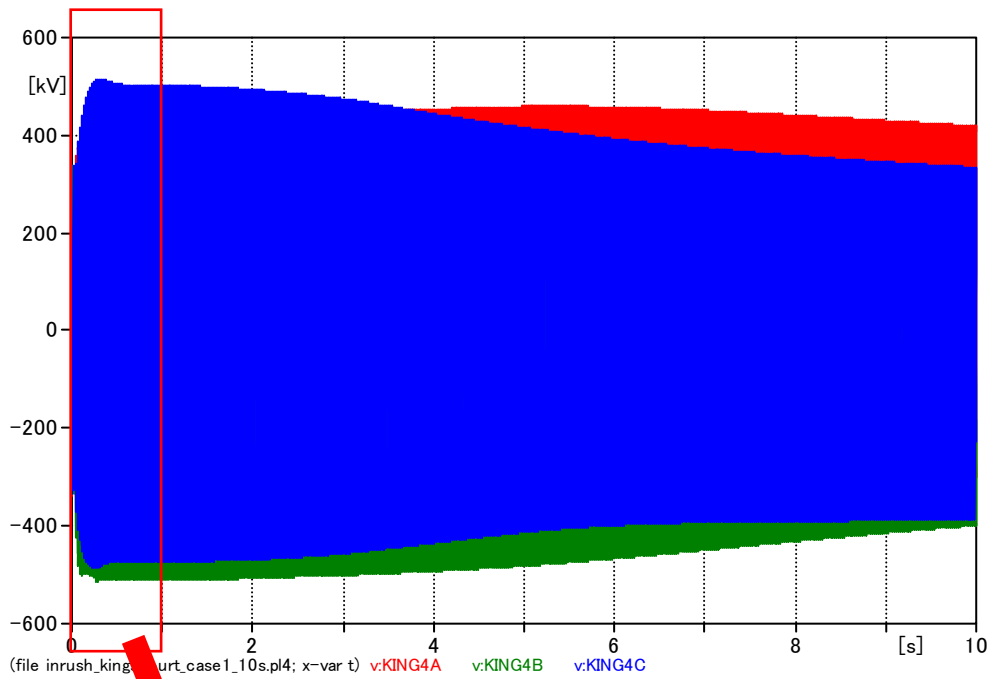
Fig. 4.23 Kingscourt 400 kV bus voltage in transformer inrush.
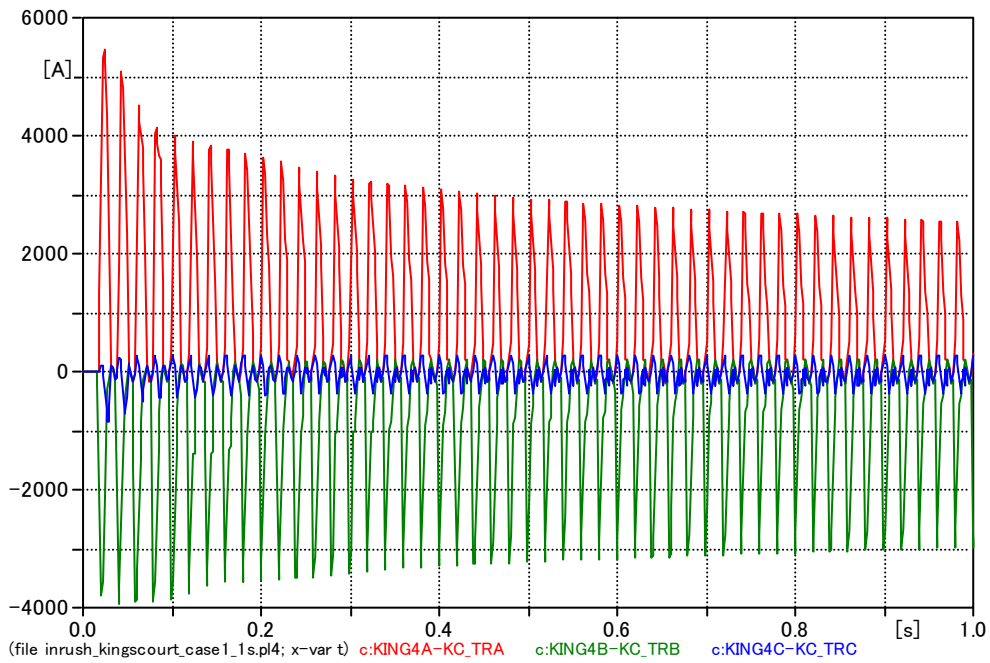
Fig. 4.24 Inrush current into the Kingscourt 400/220 kV transformer.

4.1.7   Parallel Resonance Frequency Seen from Turleenan 400 kV

In this section, parallel resonance frequency seen from the Turleenan 400 kV bus was studied. First, the result of frequency scan is shown in Fig. 4.25.   For the analysis, the largest source impedance (lowest fault current level) in Table 4-3 was set to Woodland 220 kV, Kingscourt 220 kV, and Turleenan 275 kV buses.   As in the frequency scan result seen from Turleenan 400 kV, the highest peak was found at 90 Hz, and other high peaks were not at a level requiring careful consideration.

Fig. 4.25 Parallel resonance frequency of the network seen from Turleenan 400 kV.

As a result, an energisation of the Turleenan 400/275 kV transformer was considered as the severest source of harmonic current injection.   Since parallel resonance frequency was found to be 90 Hz, it was necessary to shift it by 10 Hz.

The same four combinations were studied with regard to the operating status of the 400 kV Woodland – Kingscourt – Turleenan line, as shown in Table 4-9. As in the previous sections, outages of the Woodland – Oldstreet line and the Kingscourt – Flagford line were assumed in order to have larger impedance at parallel resonance frequency, without shifting parallel resonance frequency.

For each case, the source impedance at Woodland 220 kV bus was adjusted first in order to yield a parallel resonance frequency at 100 Hz. Source impedance at Kingscourt 220 kV bus was also adjusted when it was not possible to shift parallel resonance frequency to 100 Hz by only adjusting the source impedance at the Woodland 220 kV bus. The values of these source impedances and the magnitude of impedance at parallel resonance frequency are shown in Table 4-9.

Table 4-9 Magnitude of impedance at parallel resonance frequency (Turleenan)

	Woodland – Kingscourt line	Kingscourt – Turleenan line	Source impedance		Magnitude of impedance
			Woodland	Kingscourt	
Case 1	Two circuits	Two circuits	20.0 mH	31.0 mH	1711 Ω
Case 2	Two circuits	One circuit	70.0 mH	60.0 mH	598 Ω
Case 3	One circuit	Two circuits	39.0 mH	60.0 mH	1230 Ω
Case 4	One circuit	One circuit	250.0 mH	250.0 mH	435 Ω

In order to shift the parallel resonance frequency to 100 Hz in Case 4, it was necessary to set the value of source impedances at Woodland and Kingscourt 220 kV buses much higher than their reasonable ranges.

Finally, the time domain simulation was carried out under the assumed severest conditions, Case 1. The voltage of the Turleenan 400 kV bus and inrush current into the Turleenan 400/275 kV transformer are shown in Fig. 4.26 and Fig. 4.27. The highest voltage observed at the Turleenan 400 kV bus was 530.3 kV (1.62 pu) in Phase C. This is high for a temporary overvoltage, but is not at a level which affects the feasibility of the 400 kV Woodland – Kingscourt – Turleenan line. The conclusion of the analysis is the same as the one for the Woodland 400/220 kV transformer energisation.
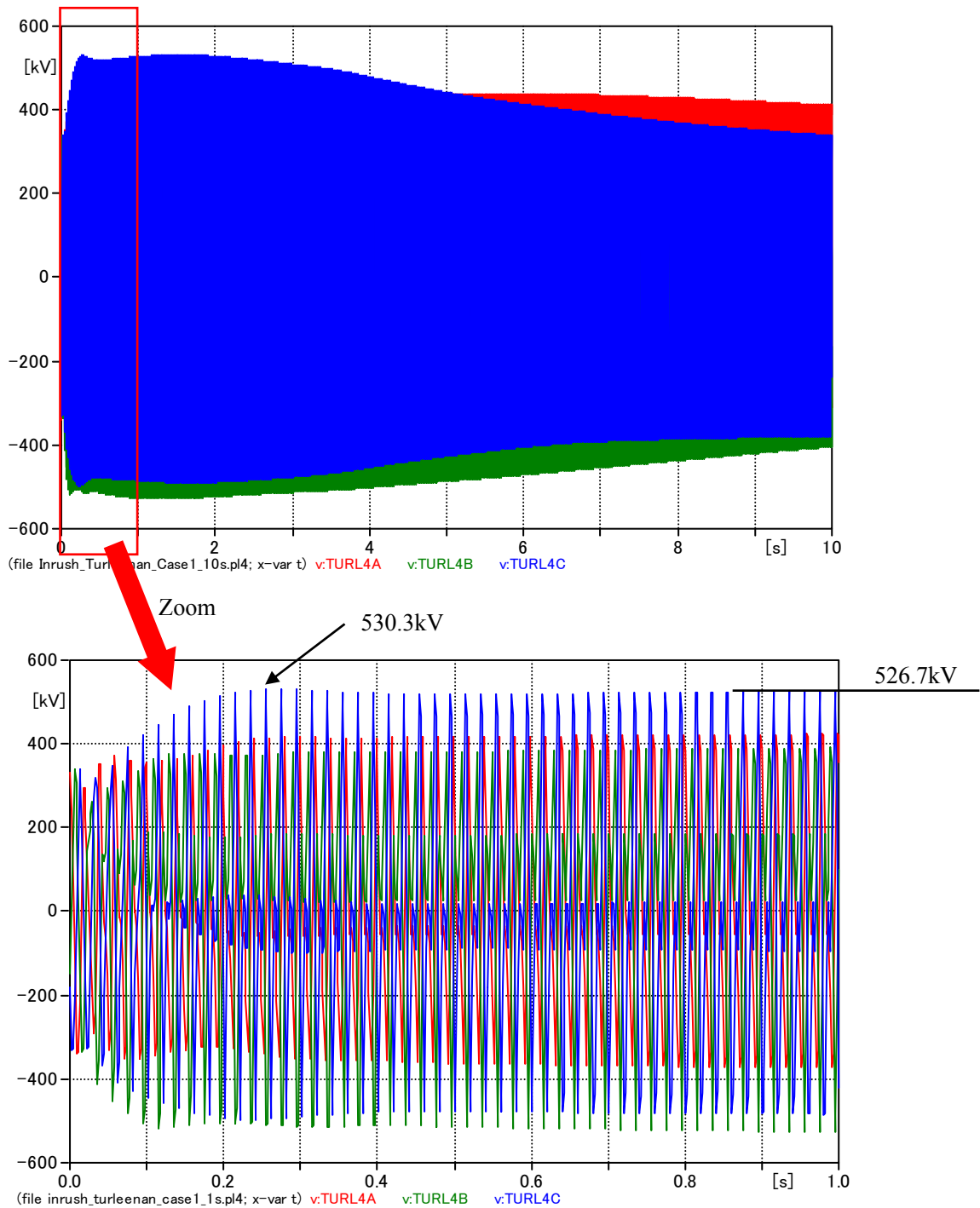
Fig. 4.26 Turleenan 400 kV bus voltage in transformer inrush.
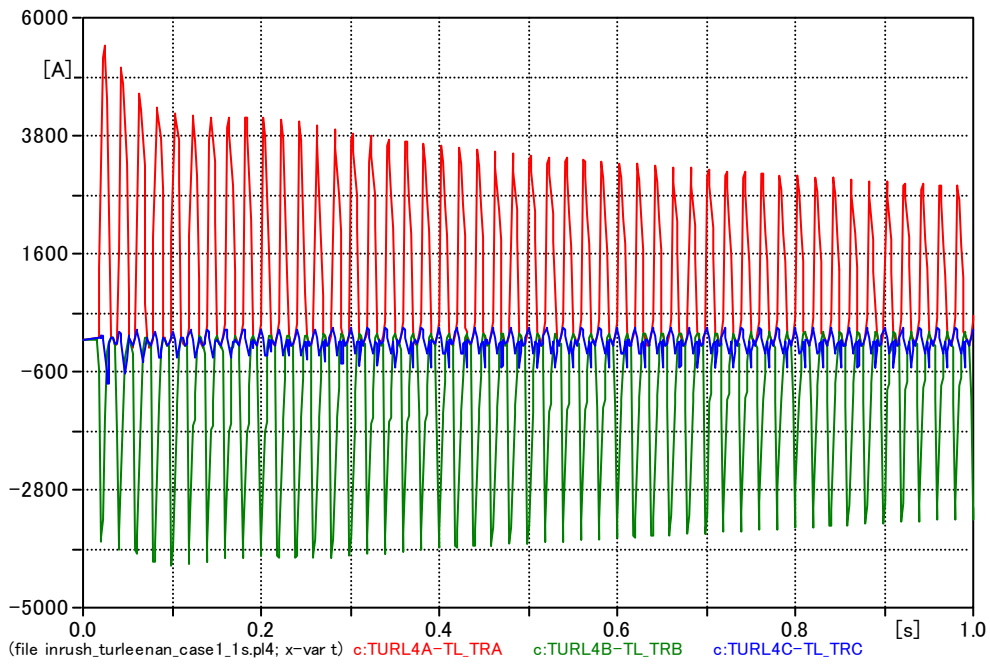
Fig. 4.27 Inrush current into the Turleenan 400/275 kV transformer.

4.1.8   Parallel Resonance Frequency for the Single Circuit Option

In this section, the parallel resonance frequency for the single circuit option was studied.   For the single circuit option, a 400 kV cable was selected to be Cu 2500 mm^2 in accordance with the transmission capacity calculation.   Reactive power compensation for the single circuit option was studied in Section 2.8.

In Sections 4.1.5 – 4.1.7, parallel resonances seen from the Woodland, Kingscourt, and Turleenan 400 kV buses were studied.   Significant differences were not observed in the time domain simulation results.   In this section, the parallel resonance seen from the Woodland 400 kV bus was studied as the transformer energisation at the Woodland 400 kV bus caused the highest overvoltage among all three of the buses in Sections 4.1.5 – 4.1.7.

First, the results of the frequency scan are shown in エラー! 参照元が見つかりません。.   For the analysis, the largest source impedance (lowest fault current level) in Table 4-3 was set to Woodland 220 kV, Kingscourt 220 kV, and Turleenan 275 kV buses.   The highest peak was found at 102.7 Hz, and other high peaks were not at a level requiring careful consideration.
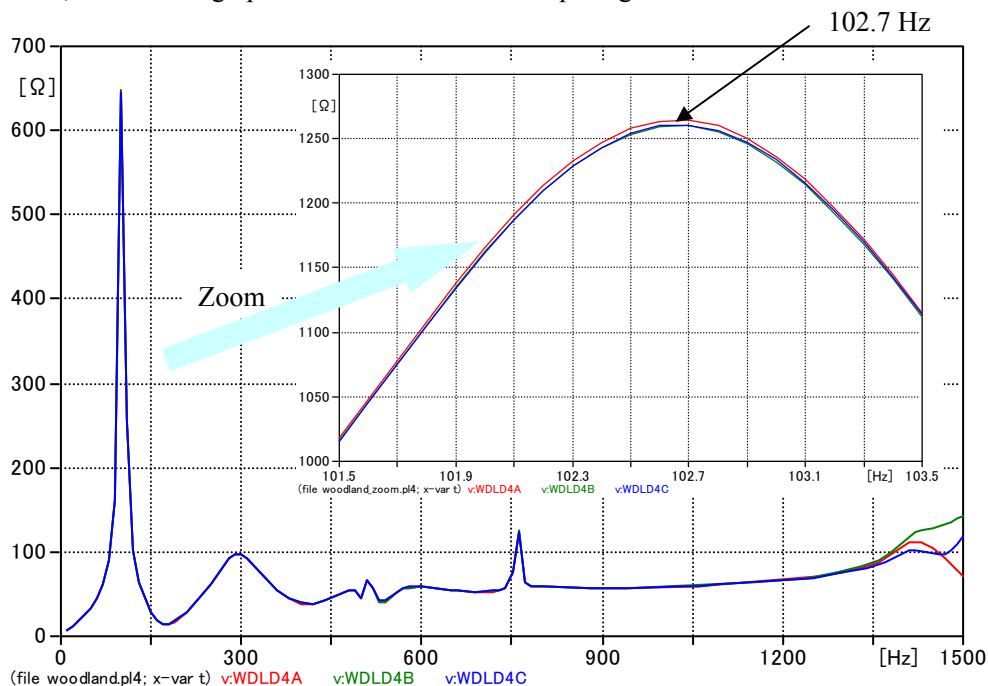
Fig. 4.28 Parallel resonance frequency of the network for the single circuit option.

Since the parallel resonance frequency was close to 100 Hz, energisation of the Woodland 400/275 kV transformer was considered as the severest source of harmonic current injection.

Tha source impedance at the Turleenan 275 kV bus was adjusted in order to yield parallel resonance frequency of 100 Hz.   Tha parallel resonance frequency was shifted to 100 Hz when source impedance at the Turleenan 275 kV bus was changed from 50 mH to 65 mH.   The impedance of the network seen from the Woodland 400 Hz bus at 100 Hz was 1173 Ω.   As in the previous sections, outages of the Woodland – Oldstreet line and the Kingscourt – Flagford line were assumed in order to yield larger impedance at parallel resonance frequency, without shifting the parallel resonance frequency.

Finally, a time domain simulation was carried out under the assumed severest conditions. The voltage of the Woodland 400 kV bus and inrush current into the Woodland 400/220 kV transformer are shown in Fig. 4.29 and Fig. 4.30.   The highest voltage observed at the Woodland 400 kV bus was 530.9 kV (1.63 pu) in Phase C.   This is high for a temporary overvoltage, but it is not at a level which affects the feasibility of the 400 kV Woodland – Kingscourt – Turleenan line. The conclusion of this analysis is the same as the one for the double circuit option (base case).
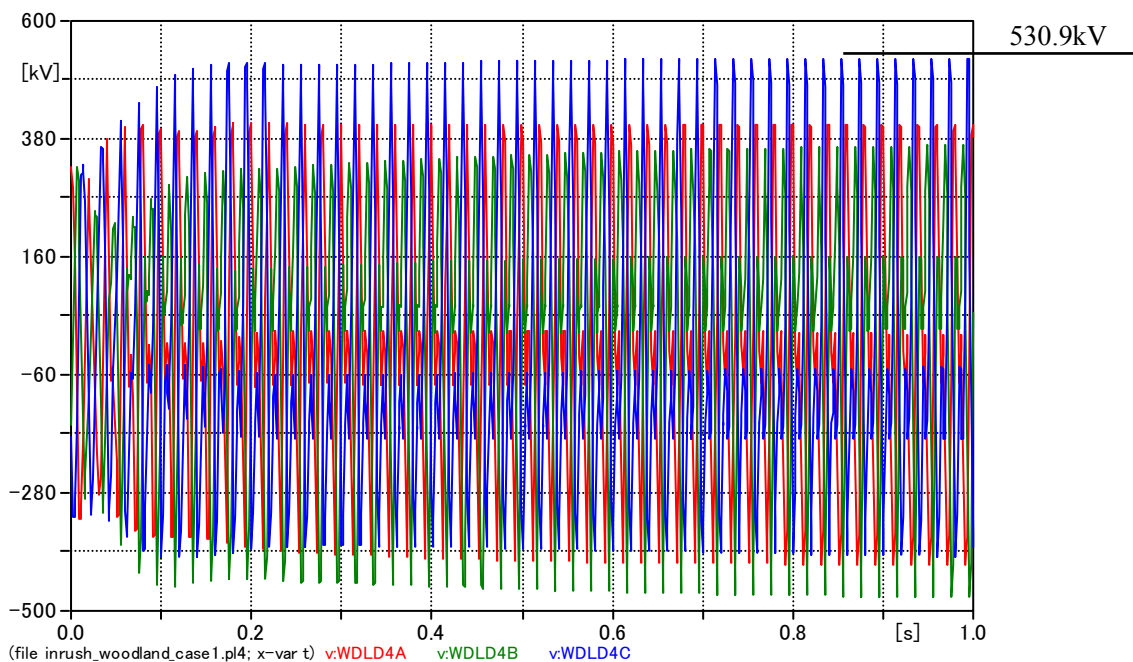
Fig. 4.29 Woodland 400 kV bus voltage in transformer inrush in the single circuit option.
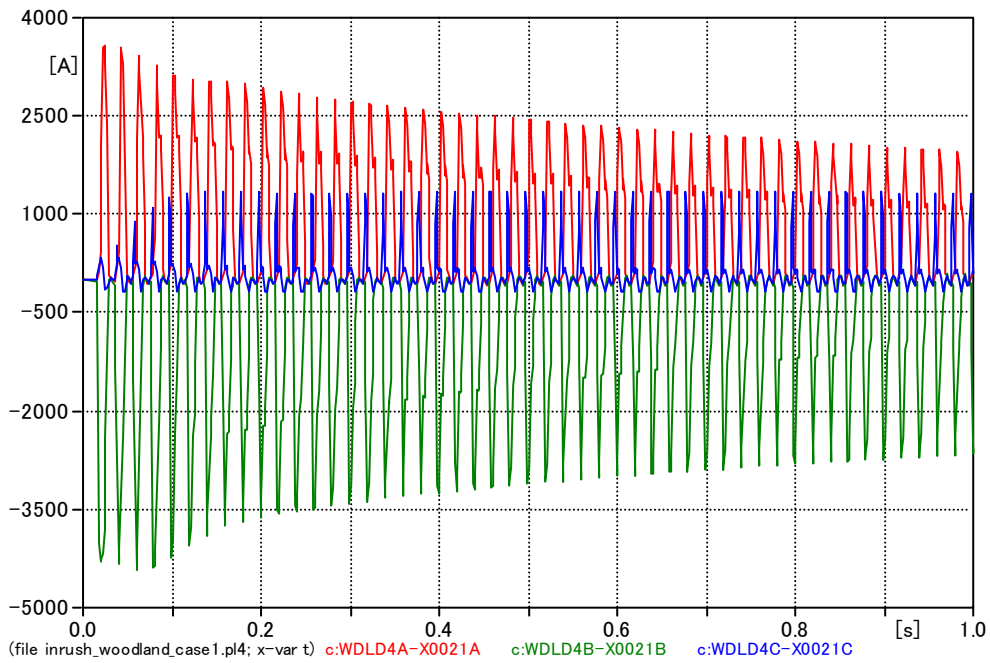
Fig. 4.30 Inrush current into the Woodland 400/220 kV transformer in the single circuit option.

4.2 Overvoltage Caused by the System Islanding

When one end of the cable is opened after a three phase fault (load shedding), the oscillatory overvoltage can be caused by the superimposition of overvoltages of two different frequencies.

Resonance frequencies can be calculated by a simple method shown below. Fig. 4.31 shows impedance and admittance data of the 400 kV Turleenan – Kingscourt line and the Turleenan 400/220 kV transformer. Impedance and admittance data in this figure is extracted from the PSS/E data set. Xb is assumed to be the source impedance and resistances are neglected in the figure.
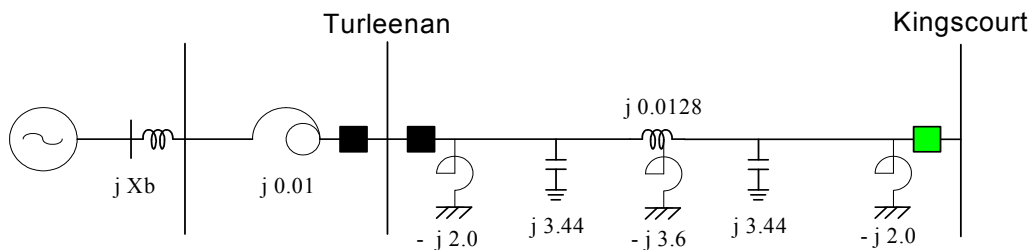
Fig. 4.31 Impedance and admittance of the 400 kV Turleenan – Kingscourt line and the Turleenan 400/220 kV transformer.

The following equations explain that X_0, Y, X can be calculated from data in Fig. 4.31.

$$X_0 = 0.01+0.0128+X_b$$
$$X = (2.0+3.6+2.0)^{-1}$$
$$Y = 6.88$$

where Xb is a source impedance behind the 220 kV Turleenan bus. Resonance frequencies were calculated with the source between 0.013 pu and 0.033 pu using the following equation, and calculated resonance frequencies are shown in.

$$\frac{\omega_0}{\omega} = \sqrt{\frac{1}{YX_0} + \frac{1}{YX}}$$

Source impedances behind the 220 kV Turleenan bus was given by short circuit calculations in

PSS/E under the summer off-peak demand and the winter peak demand with maximum wind power.
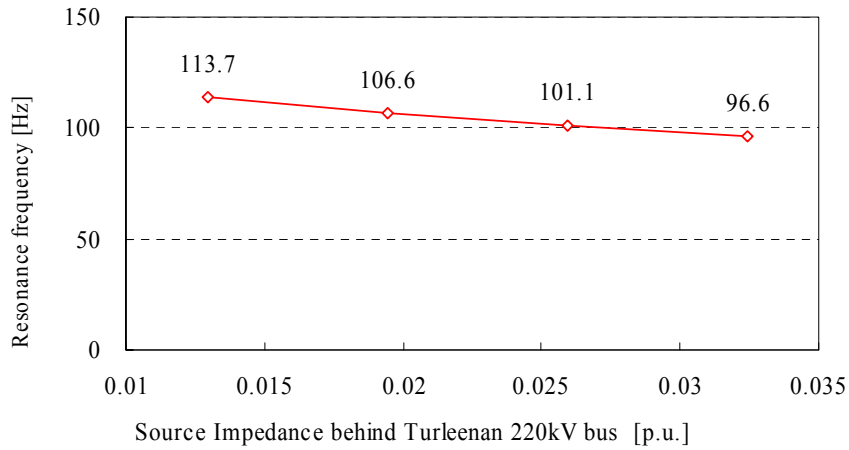
Fig. 4.32 Calculated resonance frequencies.

Fig. 4.33 and Fig. 4.34 show overvoltages in the 400 kV Turleenan – Kingscourt line caused by islanding under the assumed range of source impedance value of Turleenan as described in 4.1.2.
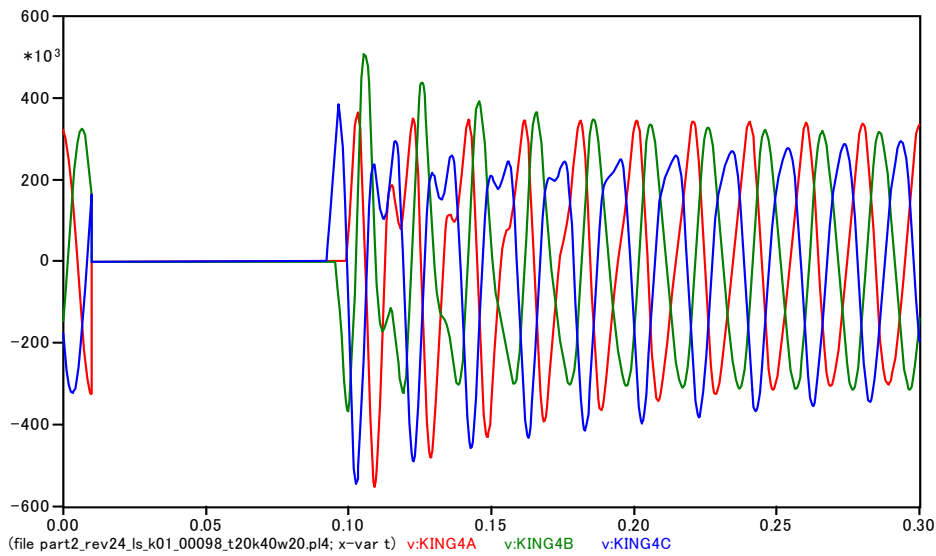
Fig. 4.33 Overvoltage caused by islanding under the smallest impedance value of Turleenan.

(dummy source impedance at Turleenan 275 kV: 20 mH)
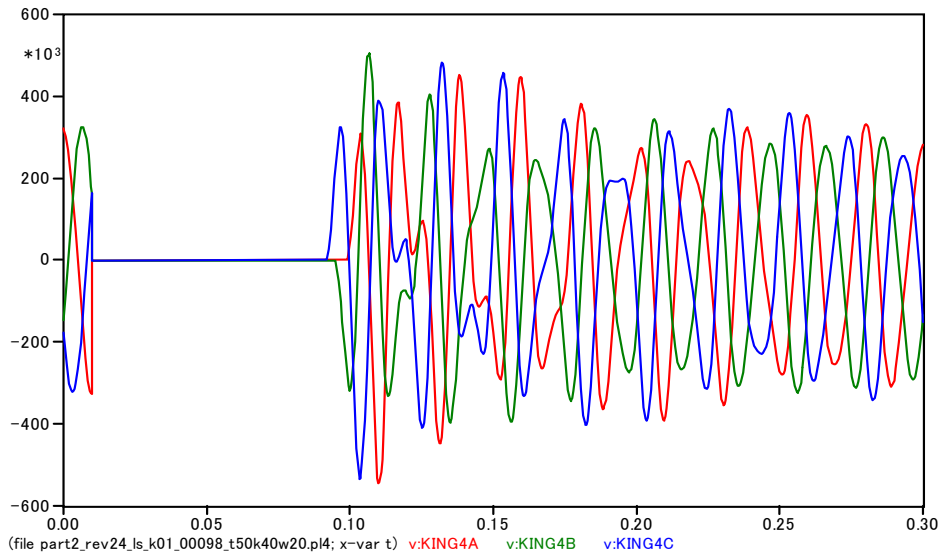
Fig. 4.34 Overvoltage caused by islanding under largest impedance value of Turleenan.

(dummy source impedance at Turleenan 275 kV: 50 mH)

Those voltage waveforms were decomposed into their frequency components as shown in Fig. 4.35. The phase in which the highest voltage was observed was chosen for each Fourier analysis.
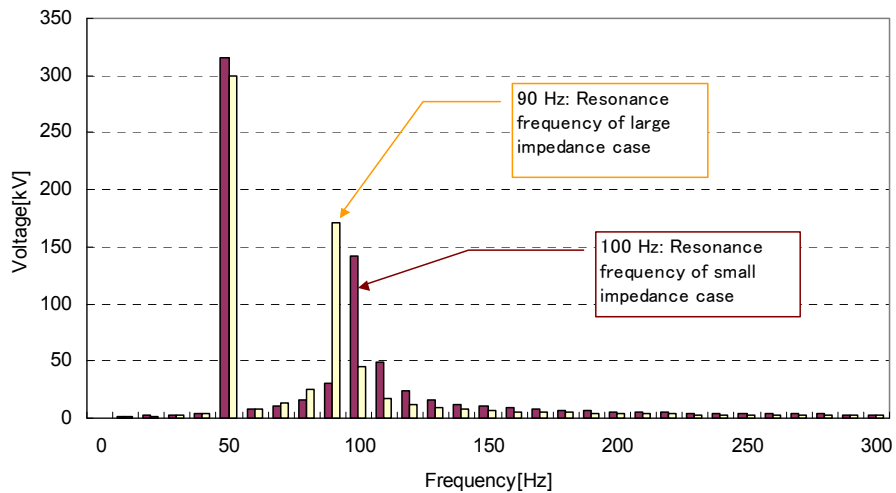
Fig. 4.35 Frequency components contained in the overvoltage.

Spectrums in the small and large additional source impedances respectively have peaks at 100 Hz and 90 Hz, as well as at 50 Hz. The results almost match with the calculated resonance frequencies shown in Fig. 4.32.

Overvoltage caused by load shedding will be studied using the switching scenario shown in Fig. 4.36.   The three phase fault in the 400 kV bus in Woodland, Kingscourt and Turleenan, and subsequent trippings of the cable lines will be assumed in the switching scenario.   A sudden trip of cable lines without loads could possibly cause a large overvoltage.   In general, larger impedance and admittance from an equivalent source will yield more severe conditions.
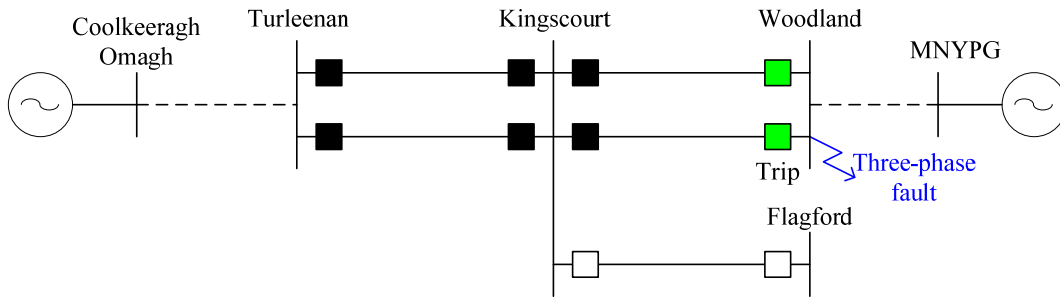
Three phase fault at Woodland 400kV bus
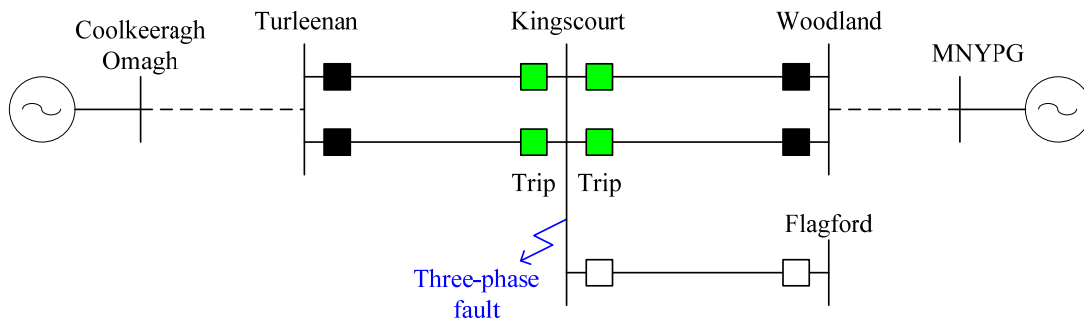
Three phase fault at Kingscourt 400kV bus
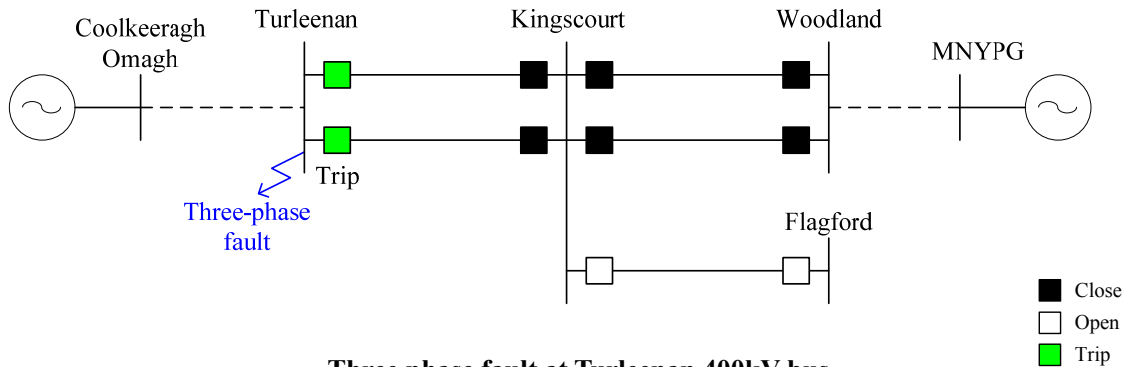
Three phase fault at Turleenan 400kV bus

Fig. 4.36 Switching scenarios for the overvoltage caused by the system islanding.

In Fig. 4.36, the 400 kV Kingscourt – Flagford line is opened in the initial condition in order to have a clear oscillatory overvoltage. When this line is in service, different frequency components will be superimposed on the two frequency components described above. With the addition of different frequency components, it will become difficult to see an oscillatory overvoltage, and the overvoltage level will generally become lower.

4.2.1 Overvoltage studies under base condition

The overvoltage caused by system islanding was studied with different network configurations. The highest observed overvoltage in each network configuration is summarized in Table 4-10. The target frequency of all Bergeron models was set to 50 Hz for the analysis.

Table 4-10 Overvoltage Caused by System Islanding

Pattern No.	Assumed Line Outage	Fault on	Overvoltage	
			At the end of the line	Highest value along the line
1 (1-1)	Turleenan – Kingscourt	Turleenan	543.6 kV (1.66 pu)	544.4 (1.67 pu)
2 (2-5)	Turleenan – Kingscourt Kingscourt – Woodland	Kingscourt	557.1 kV (1.71 pu) [Woodland side]	557.9 kV (1.71 pu) [Woodland side]
3 (3-4)	Kingscourt – Woodland	Woodland	548.4 kV (1.68 pu)	552.0 kV (1.69 pu)

$* : 1\ \text{PU} = 400\text{kV} / \sqrt{3} * \sqrt{2}$

As can be seen from the theoretical equation of this overvoltage, the magnitude of overvoltage depends on the value of the equivalent source impedance. As stated in Section 4.1.2, generators included in the simulation model are fewer than those in service in summer off-peak power flow data. An adjustment of the fault current level can be achieved by adding a dummy source with different source impedances. Based on the fault's current calculation result, the source impedance value range varied as shown in Table 4-3.

In the NIE/EirGrid network, the value of source impedance is affected by the number of distributed generators operating in the network, and it is not easy to control this source impedance to lower the oscillatory overvoltage. In order to find the sensitivity of the overvoltage to the source impedance, a time domain simulation was performed with different source impedances shown in Table 4-11.

Table 4-11 Overvoltage Caused by System Islanding (at the end of the line)

Pattern No.	Fault on	Additional Source Impedance [mH]			Overvoltage [kV] (pu) at the end of line	
		Turleenan	Kingscourt	Woodland		
1-1	Turleenan	**20**	**40**	**20**	**543.6 (1.66)**	
1-2		20	40	30	541.8 (1.66)	
1-3		20	40	60	525.1 (1.61)	
1-4		20	50	20	541.2 (1.66)	
1-5		20	60	20	539.5 (1.65)	
1-6		30	40	20	536.4 (1.64)	
1-7		40	40	20	530.8 (1.63)	
1-8		50	40	60	500.5 (1.53)	
1-9		50	60	20	521.0 (1.60)	
	Kingscourt				[Turleenan side]	[Woodland side]
2-1		20	40	20	551.9 (1.69)	548.9 (1.68)
2-2		**30**	**40**	**20**	**556.3 (1.70)**	546.8 (1.67)
2-3		40	40	20	553.4 (1.69)	544.2 (1.67)
2-4		50	40	20	546.2 (1.67)	541.3 (1.66)
2-5		**20**	**40**	**30**	549.3 (1.68)	**557.1 (1.71)**
2-6		20	40	40	547.1 (1.68)	556.6 (1.70)
2-7		20	40	50	544.9 (1.67)	554.3 (1.70)
2-8		20	40	60	543.2 (1.66)	548.8 (1.68)
2-9		20	50	20	551.0 (1.69)	547.3 (1.68)

Pattern No.	Fault on	Additional Source Impedance [mH]			Overvoltage [kV] (pu) at the end of line	
		Turleenan	Kingscourt	Woodland		
2-10	Kingscourt	20	50	30	548.5 (1.68)	555.5 (1.70)
2-11		30	50	20	552.5 (1.69)	545.1 (1.67)
2-12		20	60	20	548.5 (1.68)	546.3 (1.67)
2-13		20	60	30	546.0 (1.67)	554.0 (1.70)
2-14		30	60	20	552.2 (1.69)	544.1 (1.67)
3-1	Woodland	20	40	20	538.8 (1.65)	
3-2		30	40	20	543.7 (1.66)	
3-3		40	40	20	548.2 (1.68)	
3-4		**50**	**40**	**20**	**548.4 (1.68)**	
3-5		40	50	20	548.3 (1.68)	
3-6		50	50	20	547.4 (1.68)	
3-7		50	60	20	545.8 (1.67)	
3-8		50	40	30	540.0 (1.65)	
3-9		50	40	40	534.6 (1.64)	
3-10		50	40	50	530.8 (1.63)	
3-11		50	40	60	528.0 (1.62)	

$* : 1\ PU = 400kV / \sqrt{3} * \sqrt{2}$

The highest overvoltage at the end of the line was observed in Pattern 2-5, at the fault on Kingscourt and the assumed Woodland – Kingscourt line outage.　 Fig. 4.37 shows the result of the analysis with Pattern 2-5.　 This overvoltage is not an operational concern as it is damped in a few cycles.

Turleenan side　　　　　Woodland side
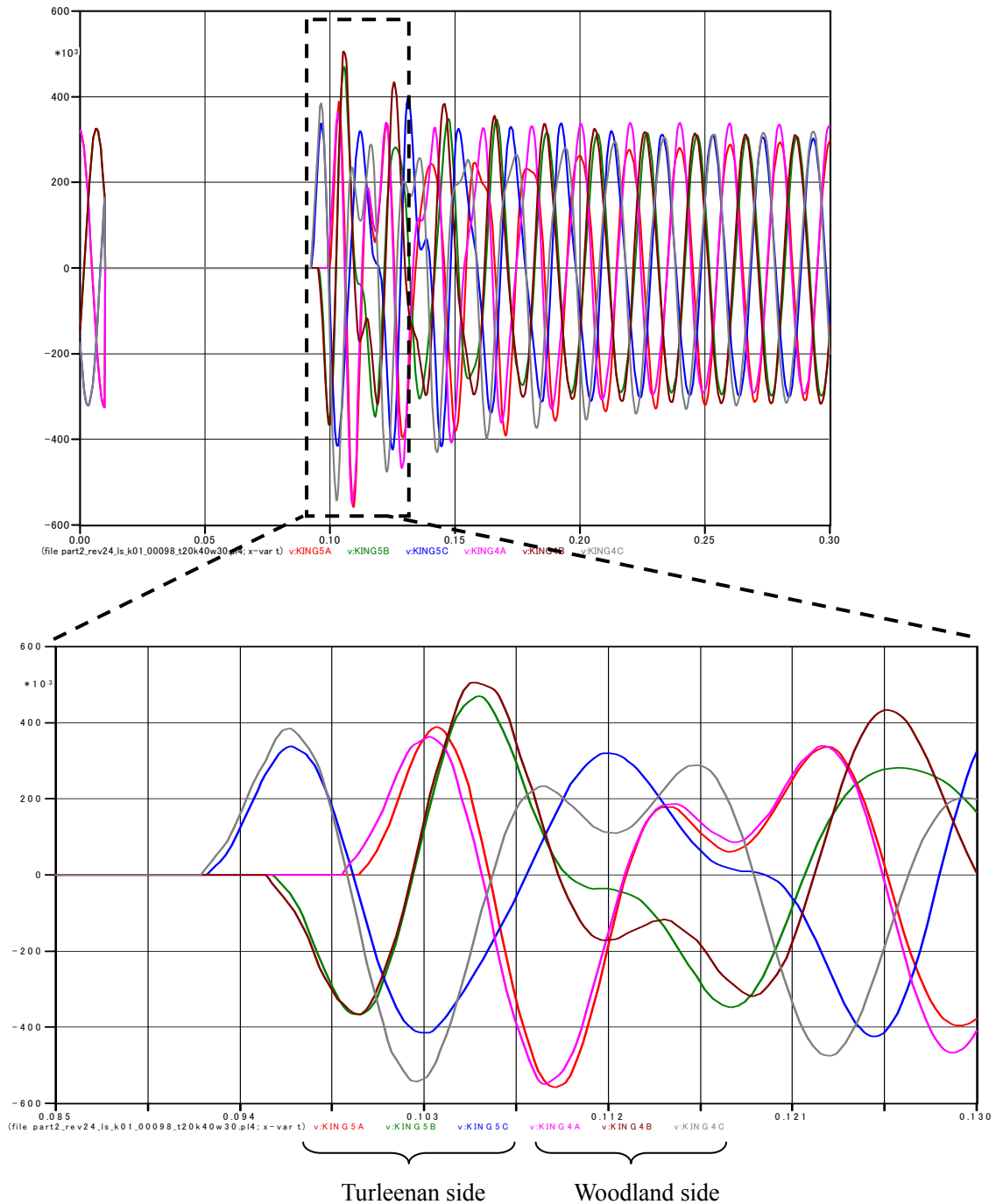
Fig. 4.37 Overvoltage caused by system islanding in Pattern 2-5.

The highest overvoltage along the Woodland – Kingscourt line in Pattern 2-5 was observed at the next point to Kingscourt. Fig. 4.38 shows the results of the maximum overvoltage of the Woodland – Kingscourt line in Pattern 2-5. The highest overvoltage along the line of the highest line end overvoltage in each switching scenario is shown in Table 4-10.
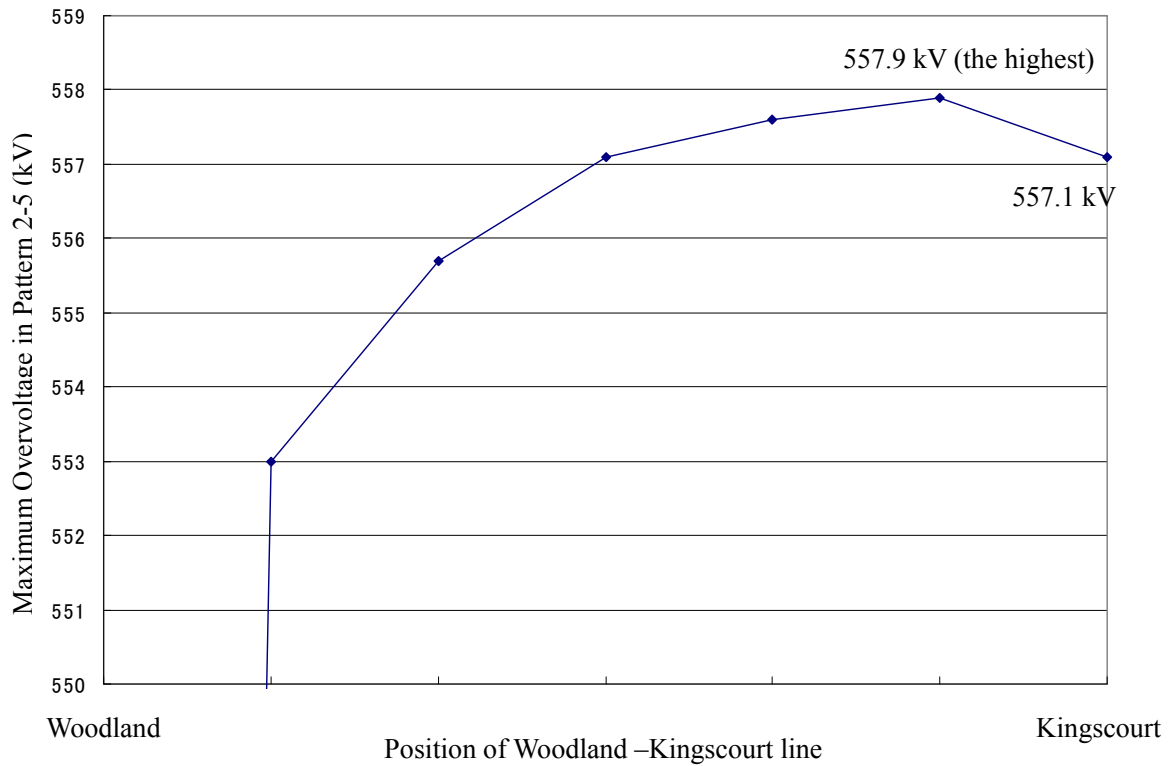
Fig. 4.38 Overvoltage caused by system islanding in Pattern 2-5 (Woodland side).

4.2.2   Overvoltage studies under additional conditions

The following additional and more severe conditions are also studied with the overvoltage caused by system islanding for reference.   These additional cases were calculated with the three patterns of additional equivalent source impedance, "low pattern", "middle pattern" and "high pattern".   Each pattern of source impedance is shown in Table 4.12.   The highest observed overvoltage at the end of the line in each network condition is summarized in Table 4.13 and Table 4.14.

a) Base condition (the detail study result was described in 4.2.1)

b) No load in Kingscourt substation (the switches of primary side of transformers are opened in the initial condition)

c) The 400 kV transformers at Woodland, Kingscourt and Turleenan are tripped together with the 400 kV cables at the same time. (shown in Fig. 4.39)

d) The 400 kV transformers at Kingscourt are disconnected from the 400 kV bus in the initial condition as in b).   In addition, the 400 kV transformers at Woodland and Turleenan are tripped together with 400 kV cables as in c).

Note: The condition c) assumes transformers are connected to the same bus (faulted bus) as the 400 kV cables.   In contrast, in the condition a) (base condition), the 400 kV transformers are not tripped, which assumes transformers are not connected to the faulted bus.

In condition d), the 400 kV transformer at Kingscourt is not tripped together with 400 kV cables since it is already opened in the initial condition.

Fig. 4.39 Additional condition of transformer trip (example of fault at the Woodland bus).

Table 4.12 Overvoltage Caused by System Islanding in Additional Conditions

Source impedance pattern	Additional impedance (mH)		
	Turleenan	Kingscourt	Woodland
low	20	40	20
middle	35	50	40
high	50	60	60

Table 4.13 Overvoltage Caused by System Islanding in Additional Conditions (Summary)

Case	Source impedance pattern	Assumed Line Outage	Fault on	Overvoltage at the end of the line
a	low	Turleenan – Kingscourt Kingscourt – Woodland	Kingscourt	551.9 kV (1.69 pu) [Turleenan side]
b	high	Turleenan – Kingscourt Kingscourt – Woodland	Kingscourt	606.6 kV (1.86 pu) [Turleenan side]
c	middle	Turleenan – Kingscourt Kingscourt – Woodland	Kingscourt	599.6 kV (1.84 pu) [Turleenan side]
d	high	Turleenan – Kingscourt Kingscourt – Woodland	Kingscourt	606.6 kV (1.86 pu) [Turleenan side]

$* : 1\ PU = \ 400kV / \sqrt{3} * \sqrt{2}$

Table 4.14 Overvoltage Caused by System Islanding in Additional Conditions

case	source impedance pattern	Assumed Line Outage	Fault on	Overvoltage [kV] (pu) at the end of line
a	low	Turleenan – Kingscourt	Turleenan	543.6 (1.66)
	middle			516.3 (1.58)
	high			485.2 (1.49)

case	source impedance pattern	Assumed Line Outage	Fault on	Overvoltage [kV] (pu) at the end of line	
		Turleenan – Kingscourt Kingscourt – Woodland	Kingscourt	[Turleenan side]	[Woodland side]
	low			551.9 (1.69)	548.9 (1.68)
	middle			543.1 (1.66)	551.8 (1.69)
	high			526.4 (1.61)	532.4 (1.63)
	low	Kingscourt – Woodland	Woodland	538.8 (1.65)	
	middle			535.1 (1.64)	
	high			522.7 (1.60)	
b	low	Turleenan – Kingscourt	Turleenan	530.7 (1.62)	
	middle			529.6 (1.62)	
	high			503.3 (1.54)	
		Turleenan – Kingscourt Kingscourt – Woodland	Kingscourt	[Turleenan side]	[Woodland side]
	low			583.8 (1.79)	569.2 (1.74)
b	middle			598.1 (1.83)	590.5 (1.81)
	high			606.6 (1.86)	585.5 (1.79)
	low	Kingscourt – Woodland	Woodland	535.1 (1.64)	
	middle			507.4 (1.55)	
	high			484.5 (1.48)	
	low	Turleenan – Kingscourt	Turleenan	582.4 (1.78)	
	middle			583.2 (1.79)	
	high			574.1 (1.76)	
		Turleenan – Kingscourt Kingscourt – Woodland	Kingscourt	[Turleenan side]	[Woodland side]
c	low			580.0 (1.78)	566.7 (1.74)
	middle			599.6 (1.84)	586.6 (1.80)
	high			595.2 (1.82)	579.7 (1.77)
	low	Kingscourt – Woodland	Woodland	574.5 (1.76)	
	middle			595.1 (1.82)	
	high			597.7 (1.83)	

case	source impedance pattern	Assumed Line Outage	Fault on	Overvoltage [kV] (pu) at the end of line	
d	low	Turleenan – Kingscourt	Turleenan	549.4 (1.68)	
	middle			575.0 (1.76)	
	high			565.1 (1.73)	
		Turleenan – Kingscourt Kingscourt – Woodland	Kingscourt	[Turleenan side]	[Woodland side]
	low			583.8 (1.79)	569.2 (1.74)
	middle			598.1 (1.83)	590.5 (1.81)
	high			606.6 (1.86)	585.1 (1.79)
	low	Kingscourt – Woodland	Woodland	570.7 (1.75)	
	middle			564.7 (1.73)	
	high			554.8 (1.70)	

The highest overvoltage at the end of the line was observed in case b (and case d) and high impedance pattern, at the fault on Kingscourt and the assumed Turleenan – Kingscourt line outage. Fig. 4.40 shows the result of the analysis with the case. This overvoltage is not an operational concern because it is damped in a few cycles and it can be evaluated by SIWV (1050 kV) due to its rapid decaying properties.
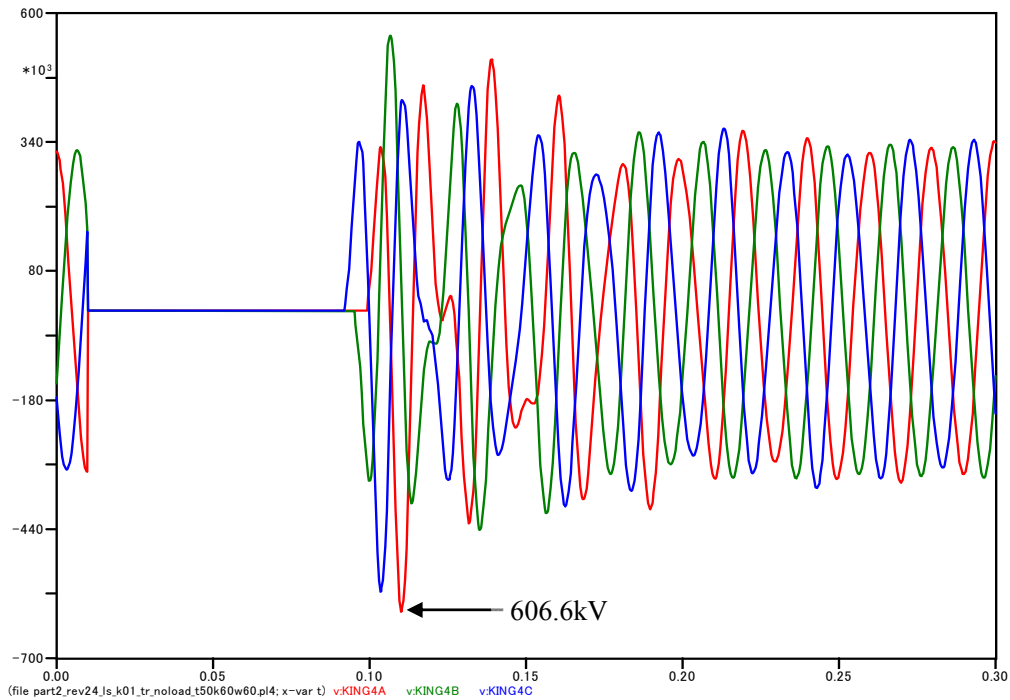
Fig. 4.40 Overvoltage caused by system islanding in case b and high impedance pattern.

4.3 Conclusion

The temporary overvoltage analysis was performed based on the compensation pattern determined by the reactive power compensation analysis. Resonance overvoltages and overvoltages caused by load shedding were studied under different network conditions.

The severest parallel resonance overvoltage was found with transformer energisation. The observed overvoltage was higher than the withstand voltage of a typical 400 kV surge arrester. From a manufacturer's standpoint, it is possible to develop a surge arrester with higher withstand voltages, for example 1.8 pu for 10 seconds. In this sense, the observed overvoltage is not at a level which would affect the feasibility of the 400 kV Woodland – Kingscourt – Turleenan line.

Load sheddings also yielded very high overvoltages. However, as observed in the Part 1 studies, in terms of the safe operation of the network, an overvoltage is not a concern because it can be evaluated by SIWV (1050 kV) due to its rapid decaying properties.

Table 4.15 Summary of the Temporary Overvoltage Analysis

	Highest overvoltage (peak)	Withstand voltage for evaluation
Parallel resonance	541.7 kV (1.66 pu)	370 kV (r.m.s.) (1.60 pu) for 10 seconds
Load shedding	606.6 kV (1.86 pu)	1050 kV (peak)

$$1\,pu = 400 \text{ or } 220\,kV \times \frac{\sqrt{2}}{\sqrt{3}}\,(peak),\, 400 \text{ or } 220\,kV \times \frac{1}{\sqrt{3}}\,(r.m.s.)$$

Chapter 5 Slow-front Overvoltage Analysis

Generally, the overvoltage caused by energisation, de-energisation, fault clearance, and other switching events is lower for longer cables due to the decay of the overvoltage along the length of the cable.   The overvoltage in the cable is caused by the superimposition of overvoltages reflected at the both ends of the cable.   When the cable has a significant length, the overvoltage would decay enough by the time it reaches at one end of the cable.

TEPCO has studied switching overvoltages of various lengths of EHV cables, including the 500 kV 39.5 km cable and the 400 kV 106 km cable.   The studies did not show any concerns on the switching overvoltage, particularly due to the significant lengths of the cables.

With this in mind, however, it is a typical practice to study slow-front overvoltages for the installation of EHV cables.   Slow-front overvoltage caused by line energisation, ground fault, and fault clearing was studied in this chapter for reference.   The results of the analysis were evaluated with SIWV (1050 kV: phase to earth, peak) of 400 kV equipment in NIE and EirGrid.

5.1 Overvoltage Caused by Line Energisation

Overvoltage caused by line energisations was studied using the switching scenarios shown in Fig. 5.1.   When one circuit is energised, other circuits are assumed to be out of service as shown in the figure.   This assumption yields the most severe condition for line energisation since the overvoltage cannot propagate into other circuits.

It was assumed that the time between line outage and line energisation is long enough to discharge each cable.   Hence, residual voltage in the cable was not assumed in line energisations.

Line energisations were simulated two hundred times using the statistical switch, in order to investigate slow-front overvoltages caused by different switching timings.
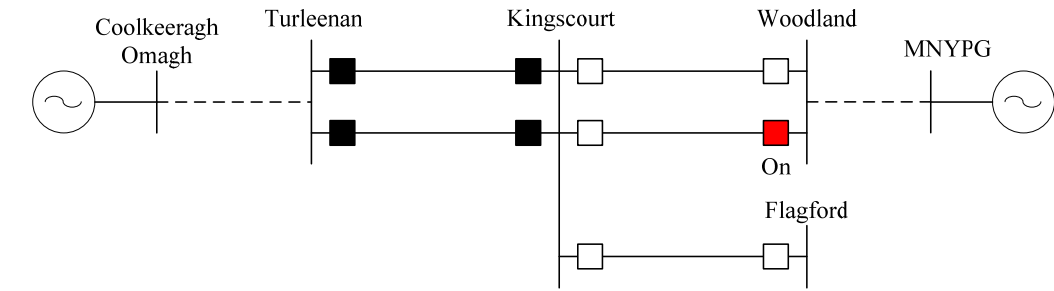
Case-1 Closing at Woodland from Moneypoint-side
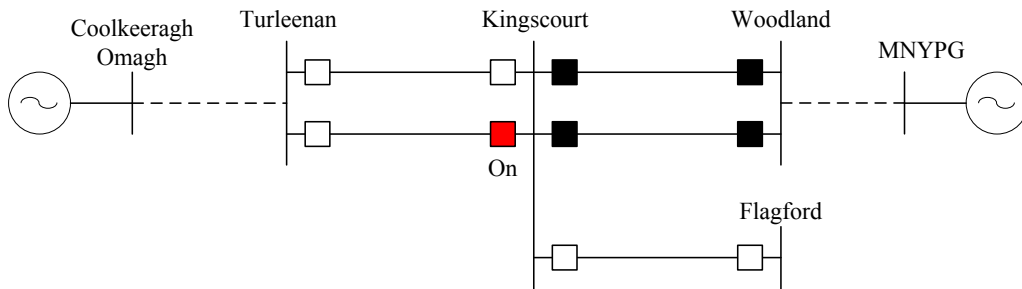
Case-2 Closing at Kingscourt from Woodland-side
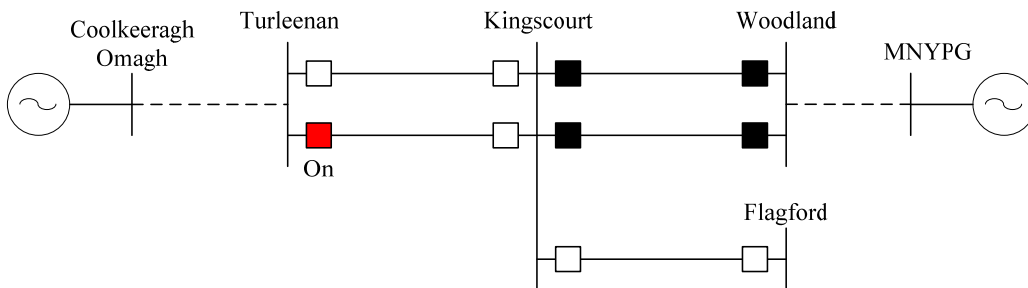
Case-3 Closing at Turleenan from Coolkeeragh Omagh-side
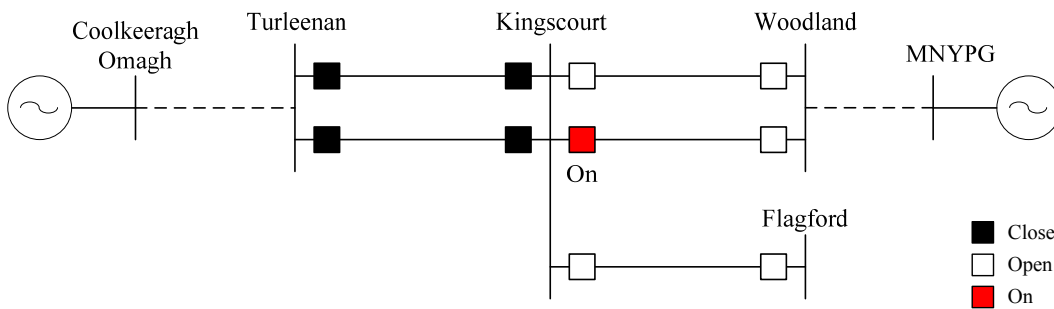
Case-4 Closing at Kingscourt from Turleenan-side

Fig. 5.1 Switching scenarios for the overvoltage caused by the line energisation.

Fig. 5.2 illustrates the node names.
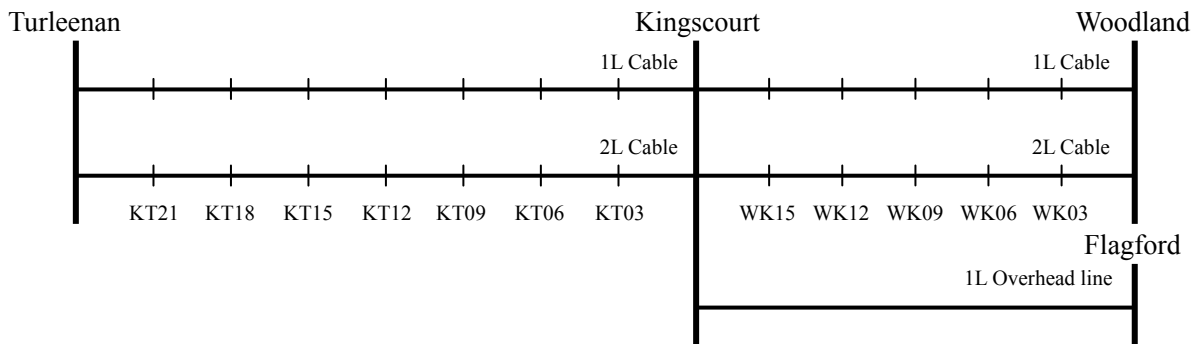
Fig. 5.2   Node names.

5.1.1   Results of simulations

The steady state bus voltages when closing the CB were set at around 400 kV in order to standardize the initial voltage profile.   In this study, 200-time simulations were conducted to realize randomness of the closing switch.   According to IEC, the overvoltage was evaluated with the maximum overvoltage at each node as well as 2 % overvoltage value.   The 2 % value is the twelfth-largest value (200 simulations × 3 phases × 2 % = 12) in the simulation at each node.

The open end terminal produced a larger overvoltage than at other locations due to its positive reflection in general.   In this analysis, the severest overvoltages were observed at the Woodland cable open end terminal in the energisation of the Kingscourt – Woodland line from Kingscourt (Case 4).   In this case, the maximum overvoltage was 1.86 pu, and the 2 % overvoltage was 1.59 pu, both of which were much lower than SIVW (1050 kV, 3.2 pu).

Table 5-1   Maximum and 2 % Value in the Line Energisation Analysis

(Unit: pu)

Cases	Case 1		Case 2		Case 3		Case 4	
Energised circuit	Kings.-Wood.		Turl. –Kings.		Turl. –Kings.		Kings.-Wood.	
Closing CB	Woodland		Kingscourt		Turleenan		Kingscourt	
Nodes	Max.	2 %	Max.	2 %	Max.	2 %	Max.	2 %
Turleenan	n/a	n/a	1.65	1.54	1.53	1.48	1.30	1.22
KT21	n/a	n/a	1.56	1.46	1.54	1.49	1.24	1.22
KT18	n/a	n/a	1.44	1.37	1.54	1.50	1.24	1.22
KT15	n/a	n/a	1.38	1.30	1.54	1.50	1.24	1.22
KT12	n/a	n/a	1.33	1.25	1.53	1.51	1.24	1.22
KT09	n/a	n/a	1.26	1.24	1.53	1.51	1.24	1.22
KT06	n/a	n/a	1.26	1.23	1.54	1.52	1.24	1.22
KT03	n/a	n/a	1.25	1.23	1.55	1.53	1.24	1.22
Kingscourt (Turl.-side)	n/a	n/a	1.24	1.22	1.55	1.53	1.26	1.22
Kingscourt (Wood.-side)	1.62	1.58	1.24	1.22	n/a	n/a	1.23	1.22
WK15	1.61	1.57	1.25	1.22	n/a	n/a	1.33	1.24
WK12	1.60	1.56	1.25	1.22	n/a	n/a	1.40	1.35
WK09	1.60	1.56	1.25	1.22	n/a	n/a	1.57	1.46
WK06	1.57	1.54	1.25	1.22	n/a	n/a	1.55	1.49
WK03	1.55	1.52	1.25	1.22	n/a	n/a	1.66	1.54
Woodland	1.53	1.47	1.28	1.21	n/a	n/a	1.86	1.59

$$(1\,\mathrm{pu} = 400 \times \frac{\sqrt{2}}{\sqrt{3}}\,\mathrm{kV})$$
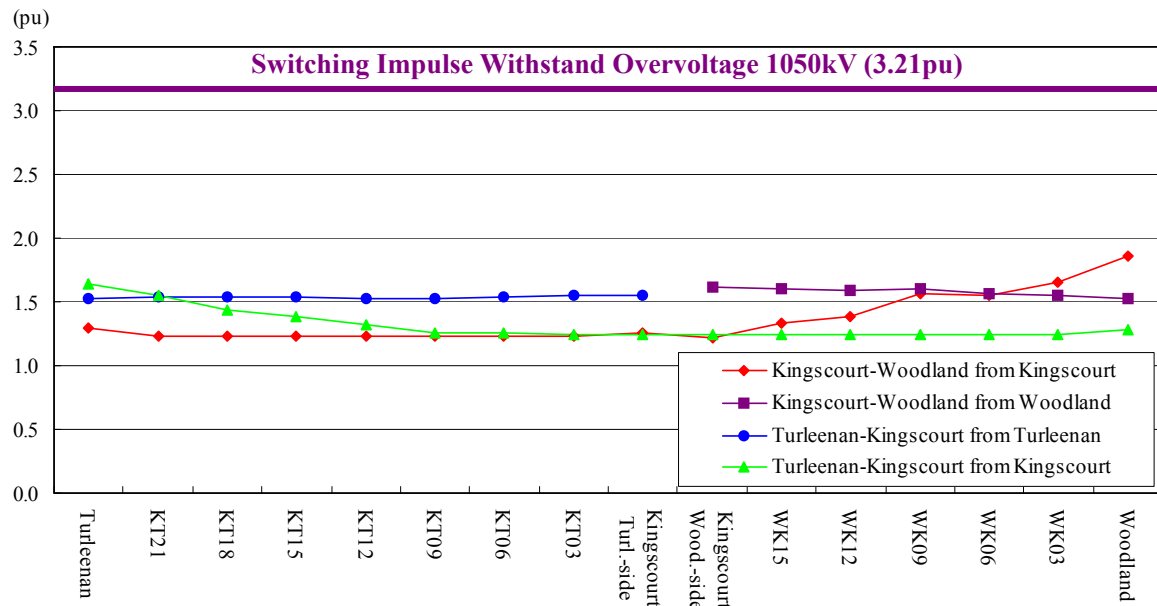
Fig. 5.3   Maximum overvoltage profile in line energisation.
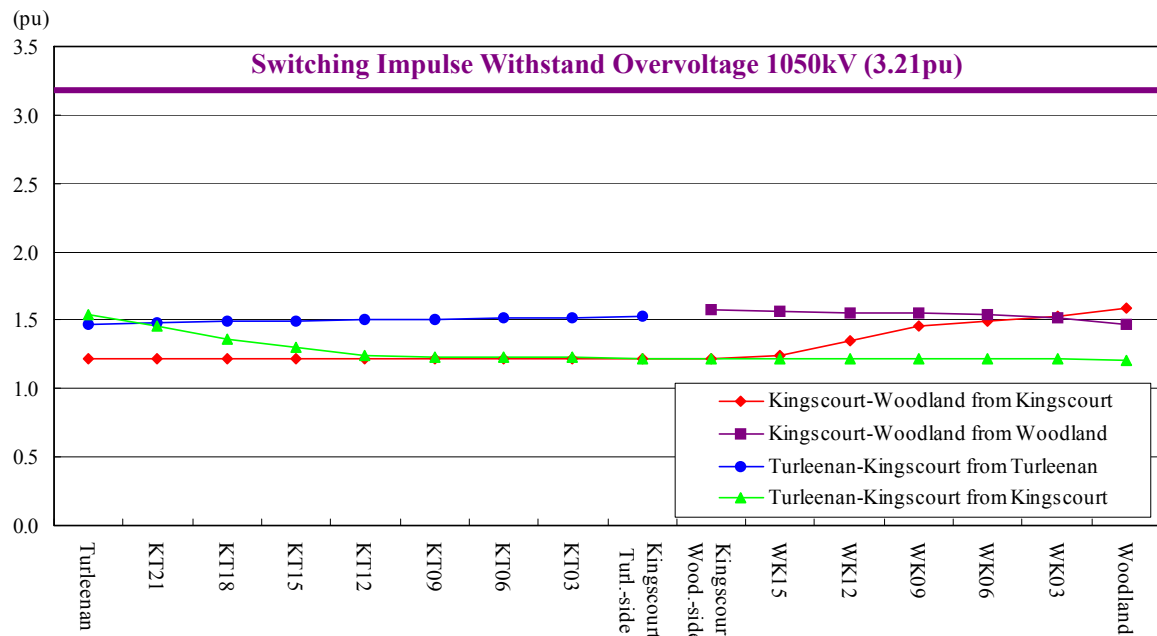
Fig. 5.4   2 % overvoltage profile in line energisation.

5.1.2   Waveform of the maximum overvoltage

The following figure shows the waveform of the maximum overvoltage. The maximum overvoltage was observed at the Woodland cable open terminal when the Woodland – Kingscourt line was energised from Kingscourt at the following timings.

Phase	Phase A	Phase B	Phase C
Close timing	18.642 ms	18.049 ms	16.702 ms
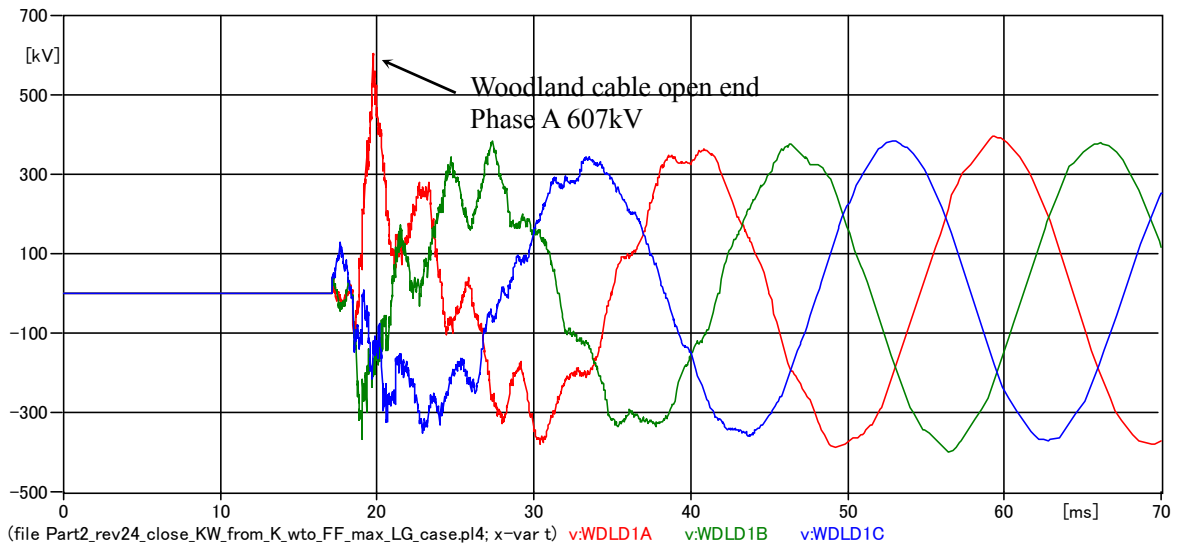
Fig. 5.5   Waveform of the maximum overvoltage at the Woodland cable end terminal.
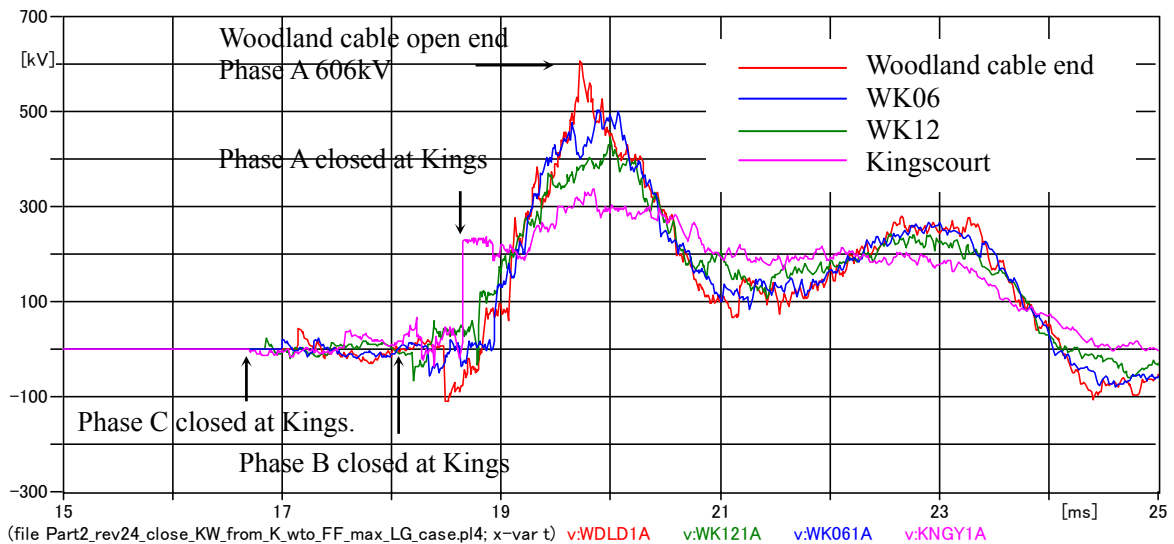
Fig. 5.6   Voltage profile along the Kingscourt-Woodland line.

5.1.3 Effect of the number of shunt reactors

The number of shunt reactors in service may affect the energisation overvoltage. Four reduced compensation cases were studied for the Woodland – Kingscourt line in addition to the original case depicted in Fig. 5.7. The following simulation analyses the effect of it with the scenario which produced the maximum overvoltage in the previous sections. In the scenario, the Woodland – Kingscourt line is energised from the Kingscourt side, and Fig. 5.7 shows the waveforms of the Phase A voltage at the Woodland cable open terminal.

As we can see from the figure, the waveforms just after the energisation are approximately equal between different compensations. This shows that the number of shunt reactors in service has small effect on the line energisation overvoltage. The voltage difference of one cycle after line energisation was caused by the difference compensations, which can also be observed in the steady-state. It is reasonable to conclude that line energisation is not sensitive to the number of shunt reactors in service.
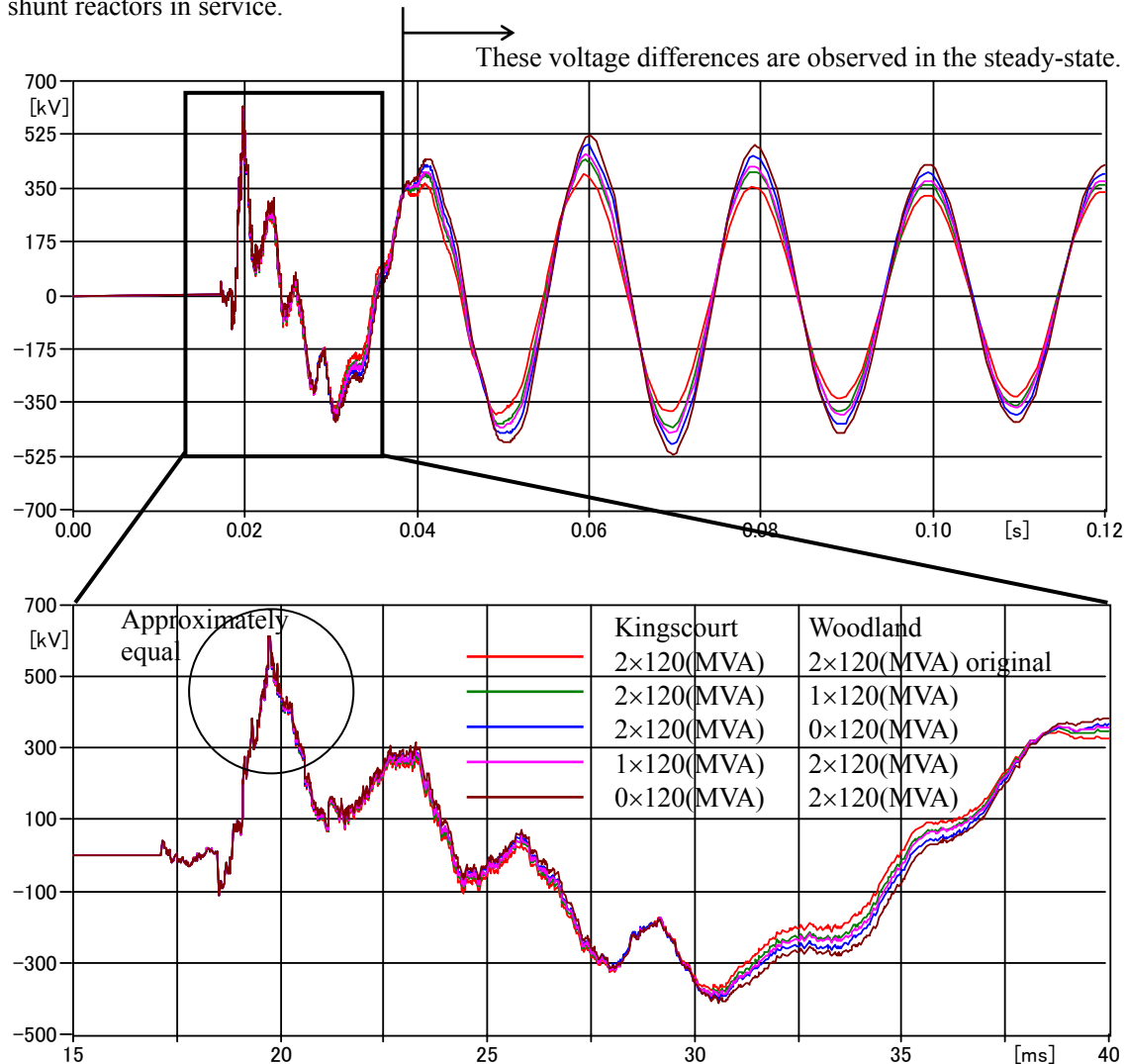
Fig. 5.7   Voltage profile along the Kingscourt-Woodland line.

5.2 Ground Fault and Fault Clearing Overvoltage

The slow-front overvoltage caused by ground faults and fault clearings was studied with different fault timings.   The conditions of the analysis are:

Fault point: Seven points in each 400 kV cable route

Fault type: Single line to ground fault (core to sheath) at Phase A

Fault timing: $0° – 170°$ ($10°$ step – 18 faults)

In this analysis, fault timing was varied because the fault angle was changed from $0° – 170°$ in $10°$ steps.   The circuit breakers clearing the fault were opened at the first current-zero, 60ms after the fault occurrence.   All three phases were opened at the same time in cable line faults, because cable lines will not be auto-reclosed.   On the other hand, only the faulted phase was opened in overhead lines.

In this analysis, the simulation was repeated 126 times for each case (= 7 fault points × 18 fault angles).   Hence, 2 % value is the seventh largest value (126 simulations × 3 phases × 0.02) in the simulation at each location.

In general, smaller system modeling yields a larger overvoltage due to its low attenuation and small number of propagation routes, in which the transient components can be dispersed.   Fig. 5.9 illustrates scenarios of the ground fault and fault clearing overvoltage analysis.

The following figure shows the observation nodes and fault nodes used in the simulation.

Turleenan   Kingscourt   Woodland

1L Cable   1L Cable

2L Cable   2L Cable

KT21 KT18 KT15 KT12 KT09 KT06 KT03   WK15 WK12 WK09 WK06 WK03

Flagford

1L Overhead line
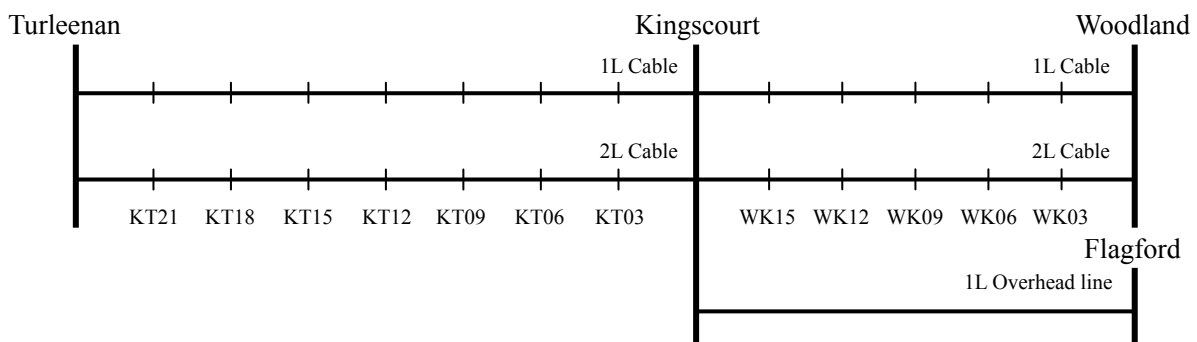
Fig. 5.8   Node names.
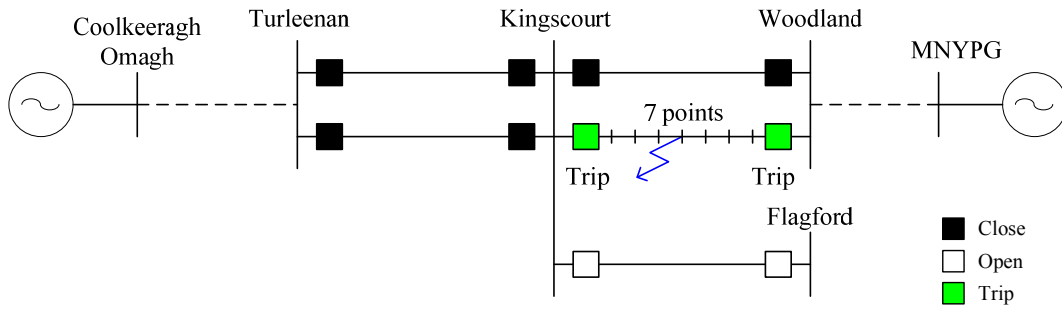
Case 1 - Tripping of Kingscourt – Woodland line after SLGF (2 circuits in service)
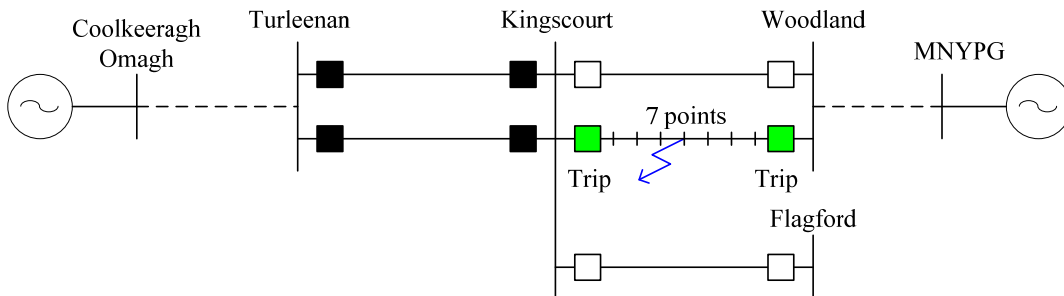
Case 2 - Tripping of Kingscourt – Woodland line after SLGF (1 circuit in service)
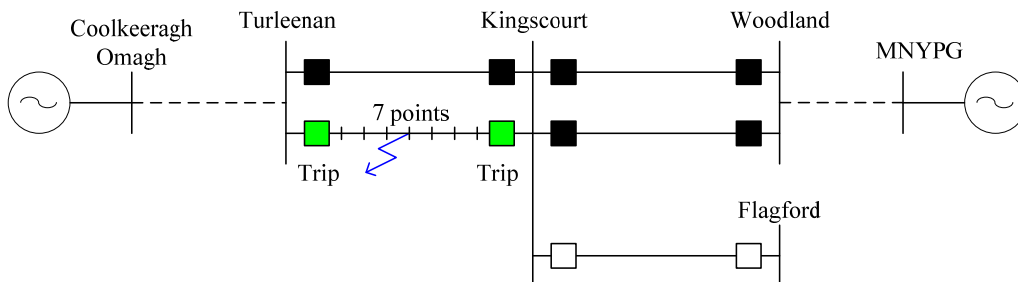
Case 3 - Tripping of Turleenan – Kingscourt line after SLGF (2 circuits in service)
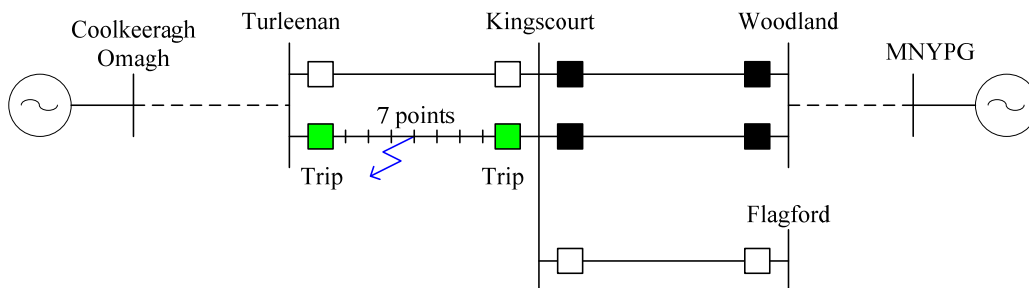
Case 4 - Tripping of Turleenan – Kingscourt line after SLGF (1 circuit in service)

Fig. 5.9 Switching scenarios for the ground fault and fault clearing overvoltage analysis.

5.2.1　　Results of simulations

According to IEC, the overvoltage was evaluated with the maximum overvoltage at each node as well as 2 % overvoltage value.　　The maximum overvoltage and 2 % overvoltage at each node are shown in Table 5-2.

Table 5-2　　Maximum Overvoltage in the Ground Fault and Fault Clearing Analysis

(Unit: pu)

Cases	Case 1	Case 2	Case 3	Case 4
# of circuits (Kings.-Wood.)	2→1	1→0	2	2
# of circuits (Turl. –Kings.)	2	2	2→1	1→0
Opening CB	Kingscourt Woodland	Kingscourt Woodland	Turleenan Kingscourt	Turleenan Kingscourt
Turleenan	1.64-B-KINGA	1.57-B-KINGA	1.66-B-KINGA	1.82-B-KINGA
KT21	1.64-B-KINGA	1.59-B-KINGA	1.64-B-KINGA	1.75-B-KINGA
KT18	1.65-B-KINGA	1.57-B-KINGA	1.67-B-KINGA	1.76-B-KINGA
KT15	1.51-B-KINGA	1.56-A-KINGA	1.53-B-KINGA	1.76-B-KINGA
KT12	1.47-B-KINGA	1.56-A-KINGA	1.48-B-KT03A	1.61-B-KINGA
KT09	1.52-B-KINGA	1.56-A-KINGA	1.53-B-KINGA	1.54-B-KINGA
KT06	1.61-B-KINGA	1.57-B-KINGA	1.62-B-KINGA	1.54-B-KINGA
KT03	1.66-B-KINGA	1.62-B-KINGA	1.65-B-KINGA	1.47-B-KINGA
Kingscourt (Turl.-side)	1.39-B-WK06A	1.56-A-KINGA	1.38-B-KT15A	1.47-B-KT09A
Kingscourt (Wood.-side)	1.39-B-WK06A	1.43-B-WK03A	1.38-B-KT15A	1.47-B-KT09A
WK15	1.40-B-WK03A	1.47-B-WK03A	1.37-B-KT09A	1.44-B-KT12A
WK12	1.45-B-WK15A	1.47-B-WDLDA	1.39-B-KINGA	1.46-B-KT09A
WK09	1.47-B-WK15A	1.53-B-WK03A	1.42-B-KINGA	1.47-B-KT09A
WK06	1.44-B-WK15A	1.50-B-WK03A	1.44-B-KINGA	1.51-B-KT09A
WK03	1.45-B-KINGA	1.51-B-WK06A	1.44-B-KINGA	1.49-B-KT09A
Woodland	1.52-B-KINGA	1.55-B-KINGA	1.52-B-KINGA	1.54-B-KINGA

Note)　　X – Y – Z　　　　X: Magnitude of overvoltage in per unit (1 pu = 326.6 kV)

　　　　　　　　　　　　　Y: Observed phase

　　　　　　　　　　　　　Z: Fault node and phase

The highest overvoltage of 1.815 pu was observed in Phase B at the Turleenan bus, when the fault occurred in Phase A at the Kingscourt-side cable terminal of the Kingscourt – Turleenan line.

Table 5-3   2 % Value in the Ground Fault and Fault Clearing Analysis

(Unit: pu)

Cases	Case 1	Case 2	Case 3	Case 4
Circuit # of Kings.-Wood.	2→1	1→0	2	2
Circuit # of Turl. –Kings.	2	2	2→1	1→0
Opening CB	Kingscourt Woodland	Kingscourt Woodland	Turleenan Kingscourt	Turleenan Kingscourt
Turleenan	1.44-B-WK15A	1.55-A-WK15A	1.44-B-TRLTA	1.65-B-KT03A
KT21	1.41-B-WK03A	1.55-A-WK15A	1.38-B-KT03A	1.55-B-KT03A
KT18	1.41-B-KINGA	1.55-A-WK15A	1.39-B-KT06A	1.55-B-KT03A
KT15	1.40-B-WK15A	1.55-A-WK12A	1.41-B-KT03A	1.55-B-KT09A
KT12	1.38-B-WK15A	1.54-A-WK12A	1.39-B-KT15A	1.51-B-KT12A
KT09	1.39-B-WK03A	1.55-A-WK12A	1.38-B-KT03A	1.47-B-KT12A
KT06	1.41-B-WDLDA	1.55-A-WK12A	1.40-B-TRLTA	1.43-B-KT12A
KT03	1.39-B-WK06A	1.55-A-KINGA	1.39-B-KT21A	1.43-B-KT09A
Kingscourt (Turl.-side)	1.36-B-WK03A	1.54-A-WK12A	1.34-B-KT09A	1.41-B-KT18A
Kingscourt (Wood.-side)	1.36-B-WK03A	1.40-B-WK06A	1.34-B-KT09A	1.41-B-KT18A
WK15	1.36-B-WK06A	1.44-B-WK03A	1.33-B-TRLTA	1.41-B-KT06A
WK12	1.39-B-WK12A	1.43-B-WK06A	1.36-B-KINGA	1.41-B-KT12A
WK09	1.40-B-WK15A	1.45-B-WK06A	1.37-B-KT09A	1.42-B-KT18A
WK06	1.40-B-KINGA	1.46-B-WK03A	1.38-B-KT12A	1.44-B-KT06A
WK03	1.41-B-KINGA	1.47-B-WK06A	1.37-B-KT12A	1.43-B-KINGA
Woodland	1.39-B-WDLDA	1.48-B-WK03A	1.38-B-KT09A	1.44-B-KT09A

Note)   X – Y – Z   X: Overvoltage value in per unit (1pu = 326.6kV)

Y: Observed phase

Z: Fault node and phase

The highest 2 % overvoltage 1.644 pu was observed in Phase B at the Turleenan bus, when the fault occurred in Phase A at the node KT03 in the Kingscourt – Turleenan line.

Fig. 5.10 shows waveforms of the highest overvoltage of 1.815 pu, and Fig. 5.11 shows current through CBs on both sides of the line when the highest overvoltage was observed.

Case 4 – Overvoltage: 1.82 pu

Fault: Phase A at the Kingscourt-side cable terminal of the Kingscourt – Turleenan line

Maximum overvoltage: Observed in Phase B at the Turleenan bus

(file Part2_rev24_clear_TK1_KW2_nonFF_gc_MAX_LG_1_KNGX_1LGS1_A--_100.pl4; x-var t) v:KNGY1A   v:KNGY1B
v:KNGY1C   v:TRLT1A   v:TRLT1B   v:TRLT1C
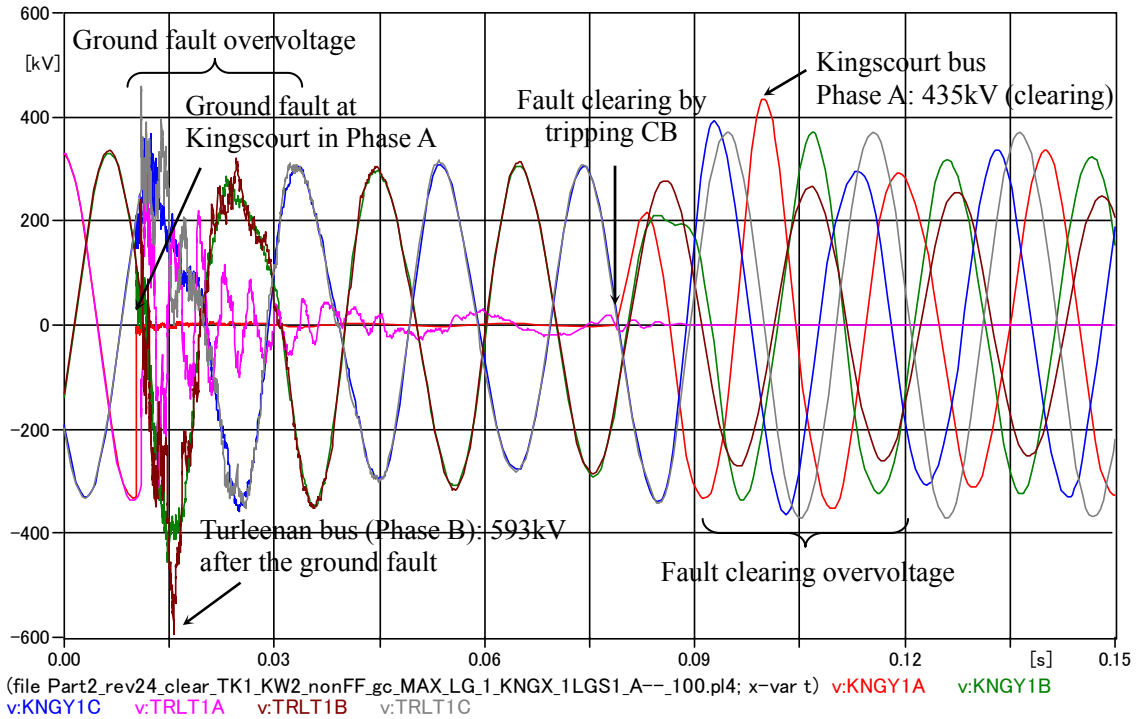
Fig. 5.10 Waveform of the maximum overvoltage.

(file Part2_rev24_clear_TK1_KW2_nonFF_gc_MAX_LG_1_KNGX_1LGS1_A--_100.pl4; x-var t) c:KNGX1A-FAULTP
c:TRLT1A-TRLBSA   c:TRLT1B-TRLBSB   c:TRLT1C-TRLBSC   c:KNG4BA-KNGX1A   c:KNG4BB-KNGX1B
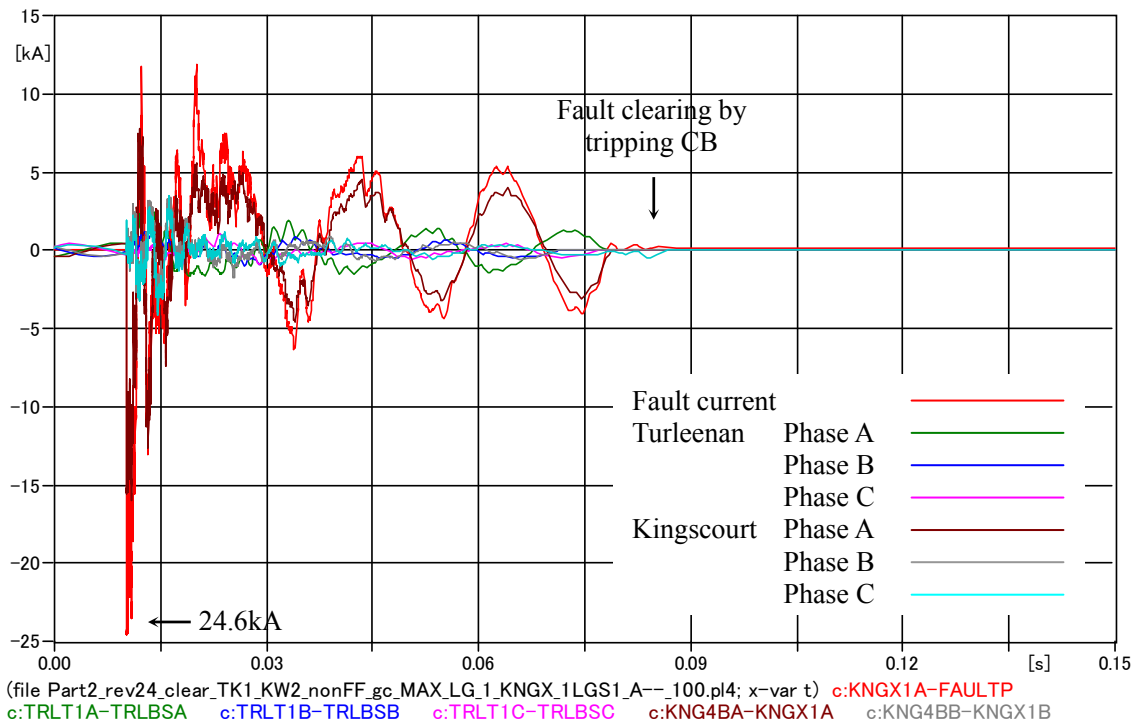
Fig. 5.11 Waveform of fault current.
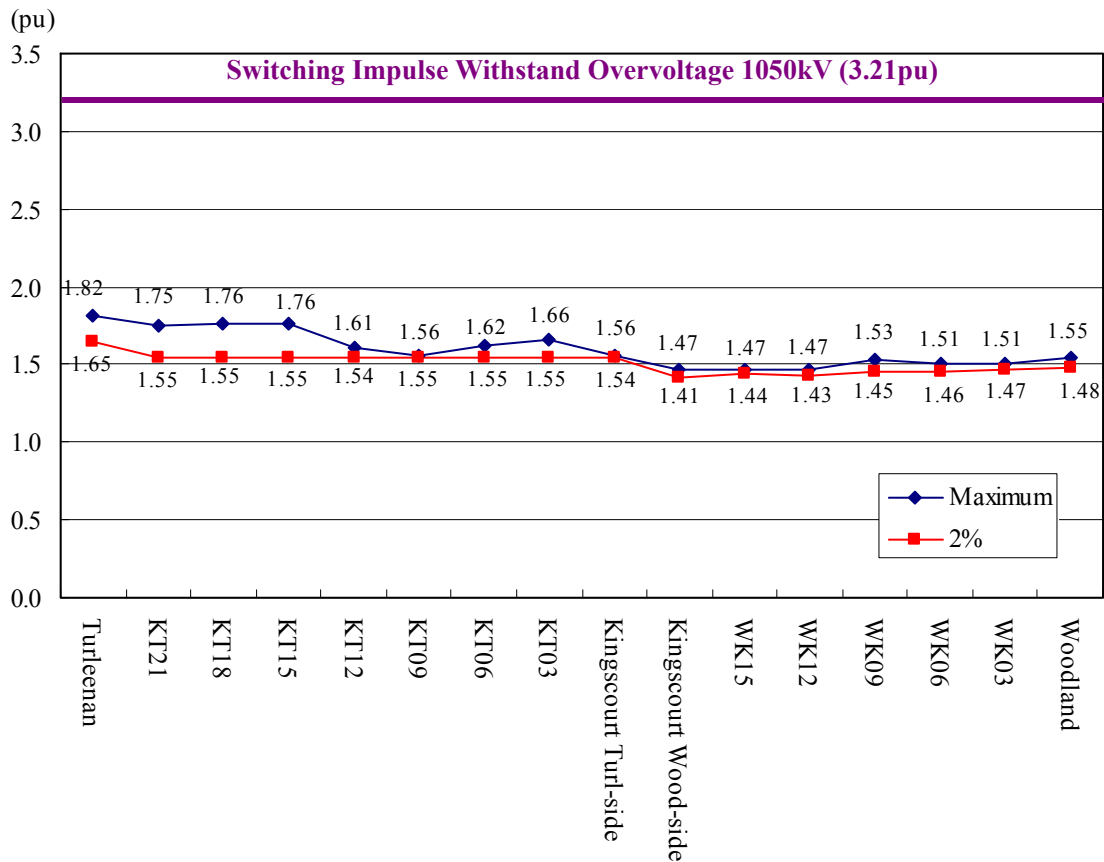
Fig. 5.12 Maximum overvoltage and 2 % overvoltage in the ground fault and fault clearing.

Fig. 5.12 shows the overall maximum and 2 % overvoltage in the ground fault and fault clearing analysis. The maximum overvoltage of 1.82 pu and the 2 % overvoltage of 1.65 pu were observed at the Turleenan bus. The single line to ground fault produced a much higher overvoltage than the fault clearing as shown in Fig. 5.10, but both of them were much lower than SIWV of 400 kV equipment.

5.3 Conclusion

Slow-front overvoltage caused by line energisation, ground fault, and fault clearing was studied in this chapter.   The result of the slow-front overvoltage analysis is summarized in Table 5-4.   As shown in the table, no significant overvoltage was found in the slow-front overvoltage analysis.   The observed overvoltages were much lower than SIWV in all simulated cases.

Table 5-4   Summary of the Slow-front Overvoltage Analysis

	Highest overvoltage (peak)	Withstand voltage (peak) for evaluation
Line energisation	607.0 kV (1.86 pu)	1050 kV
Ground fault and fault clearing	593.0 kV (1.82 pu)	

$$1\,\text{pu} = 400\,\text{kV} \times \frac{\sqrt{2}}{\sqrt{3}}\ (\text{peak})$$

Part 3

Part 3:

Feasibility Study on the 400 kV Woodland – Kingscourt – Turleenan Line as Mixed OHL / Underground Cable

Table of contents

Chapter 1 Introduction

The objective of Part 3 is to conduct feasibility study on the 400 kV Woodland – Kingscourt – Turleenan line as mixed OHL / underground cable.   In order to fulfill this objective, the following studies were performed:

(1)   Transmission Capacity Calculation

(2)   Impedance and Admittance Calculation

(3)   Reactive Power Compensation Analysis

(4)   Overvoltage Analysis

Here, (1) and (2) have already been conducted as a common study for Part 1, 2, and 3 and are not included in this Part 3 report.   Using cable information, such as cable size, type, layout, and impedance / admittance, found in (1) and (2), the remaining studies (3) and (4) were conducted as Part 3 studies.

The purpose of (3) is to find shunt reactors that should be installed together with the 400 kV cable.   The best combination in terms of the number of shunt reactors, shunt reactor size, and location was found from (3).

Temporary overvoltage analysis in (4) is the most important study in Part 3 that addresses the feasibility of the 400 kV Woodland – Kingscourt – Turleenan line as mixed OHL / underground cable.   In addition to it, overvoltage caused by autoreclose and lightning overvoltage were studied in (4).   These overvoltages are usually not studied when the line is composed of underground cables for the entire length and are thus peculiar for the mixed OHL / underground cable line.

Chapter 2 Reactive Power Compensation

2.1 Proposed Compensation Patterns

In Part 3, the 400 kV Woodland – Kingscourt line was assumed to be an overhead line, and the 400 kV Kingscourt – Turleenan line was assumed to be a mixed OHL / underground cable. In order to find effects of the ratio of the cable part, the following combinations were considered for the Kingscourt – Turleenan line:

Underground cable (Al 1400 mm^2 2 cct)	OHL (1 cct)
30 %	70 %
60 %	40 %

For each cable ratio, 30% and 60% charging capacity of the Kingscourt – Turleenan line was calculated at 400 kV as follows:

	Cable section	OHL section	Total
Cable ratio 30 %	457.4 MVA	32.1 MVA	489.5 MVA
Cable ratio 60 %	914.8 MVA	18.3 MVA	933.1 MVA

Based on the maximum unit size found in Part 2, the following reactive power compensation patterns were proposed. Shunt reactor stations were not proposed:

Table 2.1 Proposed Compensation Patterns

Locations	Cable ratio 30 %	Cable ratio 60 %
Kingscourt	100 MVA × 2	200 MVA × 2
Turleenan	100 MVA × 2	200 MVA × 2
Compensation Rate [%]	81.7	85.7

The compensation rates were lower compared to those in Part 2 in order to avoid a resonance overvoltage which occurs when one line is opened for single phase autoreclose. This will be discussed in Section 2.3.

2.2 Ferranti Phenomenon

For the reactive power compensation analysis, simple power flow data which includes only the Woodland – Kingscourt – Turleenan line was built as in Part 2. In this simple model, the Woodland – Kingscourt line and the Kingscourt – Turleenan line were respectively divided into six and ten sections, in order to observe the voltage profile along the line and to model shunt reactor stations.

The following conditions were assumed in the power flow data:

- The 400 kV bus voltages of Woodland and Turleenan are maintained below 410 kV. As a most severe condition, these bus voltages are fixed at 410 kV.

- An outage of the 400 kV Kingscourt – Flagford line is assumed as a severe condition, in which the Kingscourt 400 kV bus voltage is not regulated from Flagford.

The power flow model created for the reactive power compensation analysis is shown in Fig. 2.1.
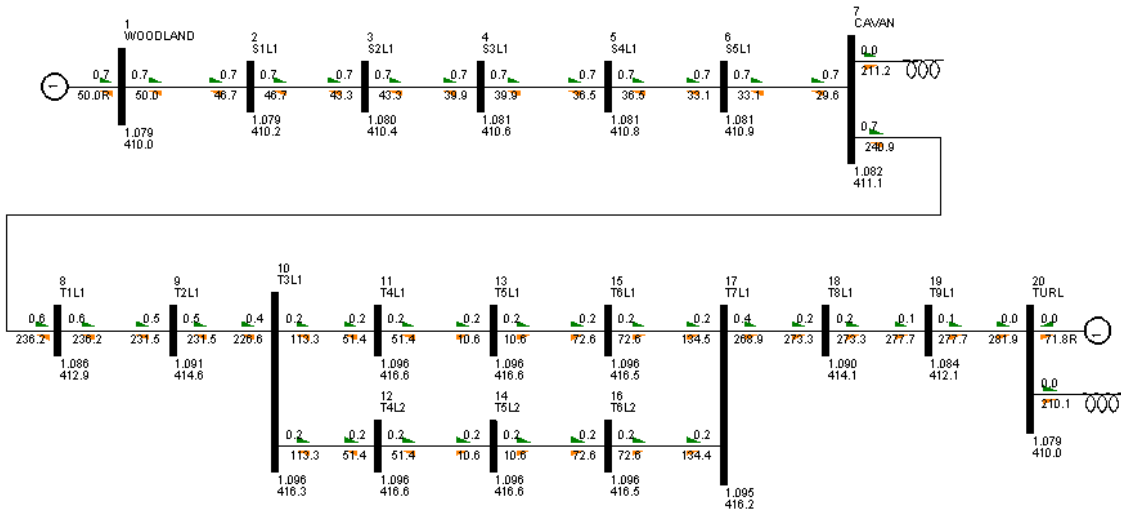
Fig. 2.1 Power flow model for the reactive power compensation analysis.

2.2.1 Cable ratio 30 %

First, the reactive power compensation for cable ratio 30 % was studied. In Fig. 2.2, the black line shows the voltage profile when all equipment is in service and the Woodland – Kingscourt – Turleenan line is carrying no load. The voltage profile in this condition is satisfactory. The voltage along the line does not exceed 420 kV.

The other lines in Fig. 2.2 shows the voltage profile when the Turleenan terminal is opened. When two 100 MVA shunt reactors are directly connected to the line at the open end (red line), the highest voltage along the line is 420.5 kV, and the voltage profile is acceptable. When only one 100 MVA shunt reactor is directly connected to the line at the open end (blue line), the highest voltage exceeds 426 kV, but the voltage rise from the Kingscourt 400 kV bus is within 10 kV. The voltage profile is still permissible as long as the Kingscourt 400 kV bus voltage is maintained below 410 kV. When no shunt reactors are connected to the line at the open end (purple line), the voltage profile is hardly acceptable.
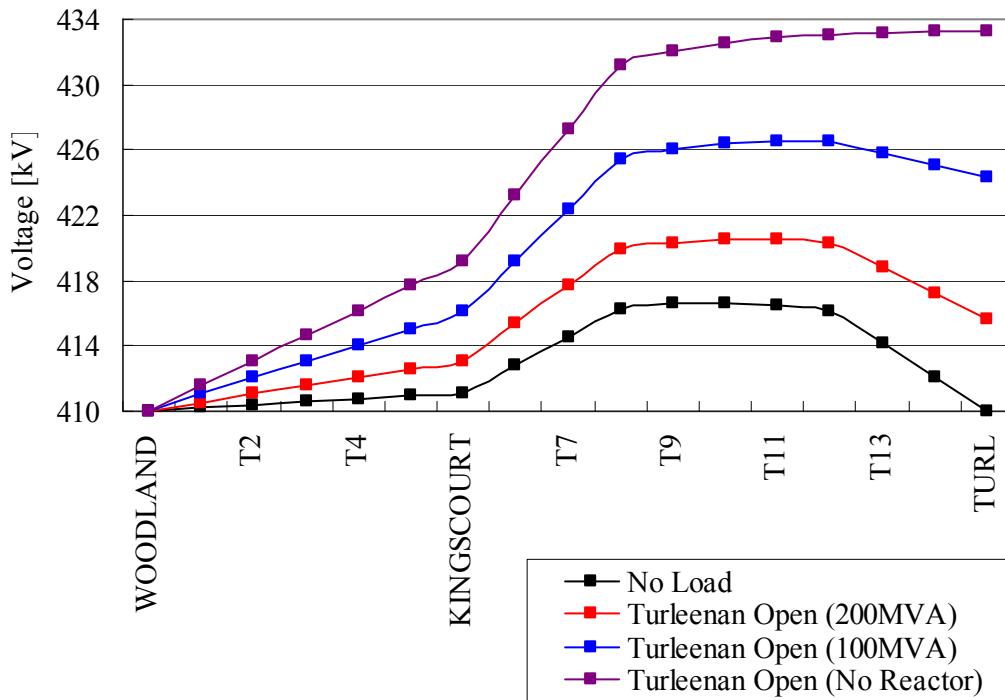
Fig. 2.2 Voltage profile when the Turleenan terminal is opened (cable ratio 30 %).

Fig. 2.3 shows the voltage profile when the Kingscourt terminal is opened. As in Fig. 2.2, the different colors (red, blue, and purple) stand for the different amount of shunt reactors connected to the line at the open end. When at least one 100 MVA shunt reactor is connected to the line at the open end, the voltage along the line is maintained below 420 kV.
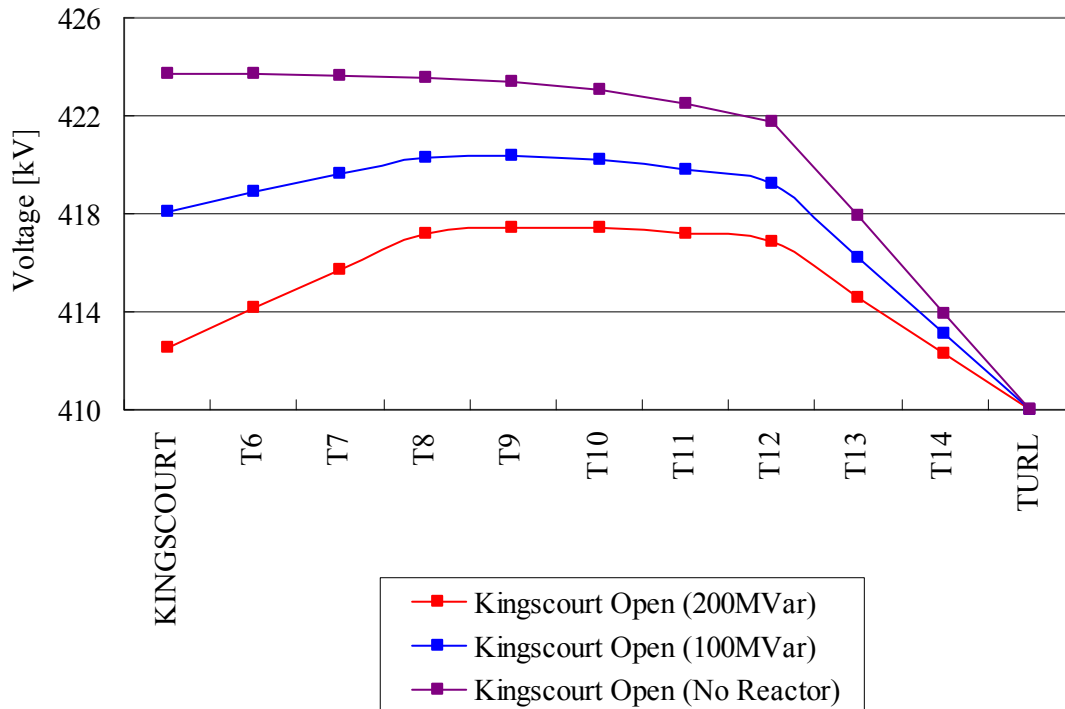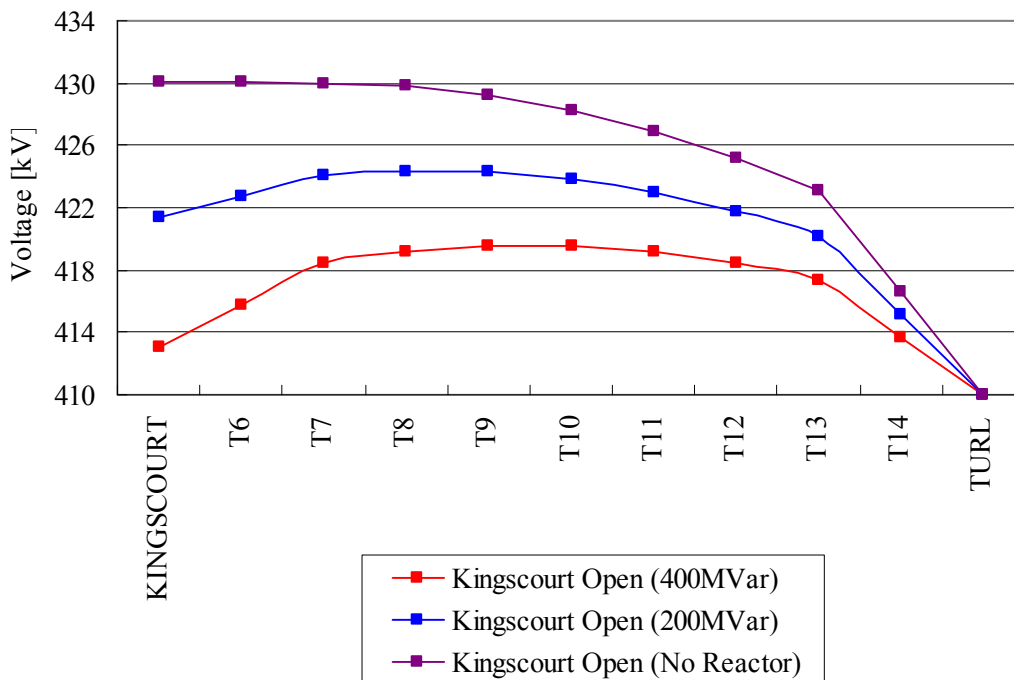

Fig. 2.3 Voltage profile when the Kingscourt terminal is opened (cable ratio 30 %).

2.2.2 Cable ratio 60 %

Next, the reactive power compensation for cable ratio 60 % was studied. In Fig. 2.4, the black line shows the voltage profile when all equipment is in service and the Woodland – Kingscourt – Turleenan line carries no load. The voltage profile in this condition is satisfactory. The voltage along the line does not exceed 420 kV.

The other lines in Fig. 2.4 shows the voltage profile when the Turleenan terminal is opened. When the two 200 MVA shunt reactors are directly connected to the line at the open end (red line), the highest voltage along the line is 424.3 kV, but the voltage rise from the Kingscourt 400 kV bus is within 10 kV. The voltage profile is still acceptable as long as the Kingscourt 400 kV bus voltage is maintained below 410 kV. When only one of the 200 MVA shunt reactors is directly connected to the line at the open end (blue line), the highest voltage is 435.6 kV. The voltage rise from the Kingscourt 400 kV bus is 15 kV. When no shunt reactors are connected to the line at the open end (purple line), the voltage profile is hardly acceptable.
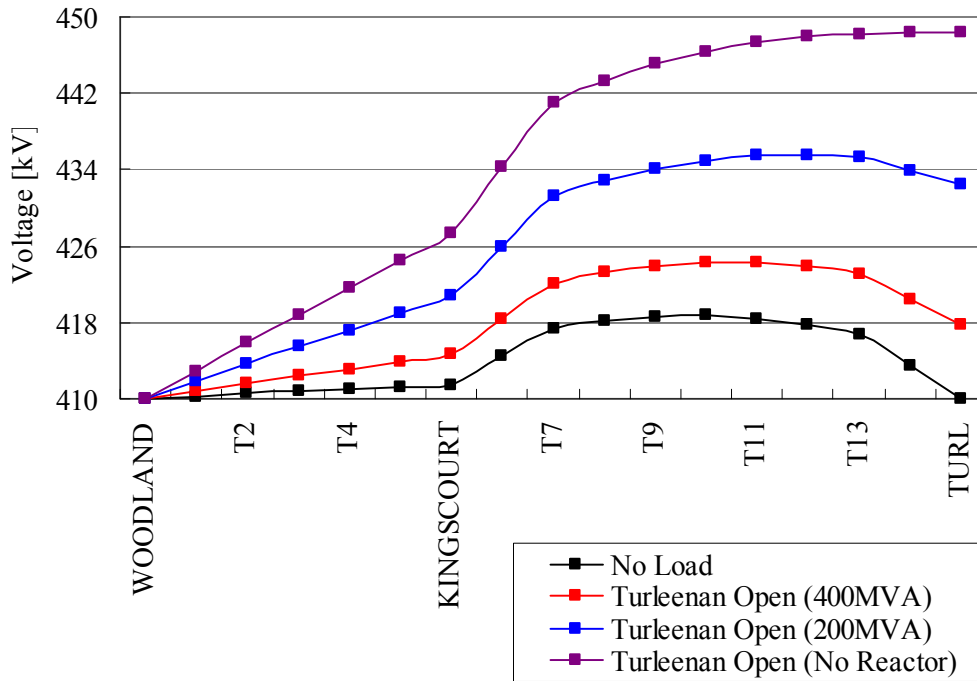
Fig. 2.4 Voltage profile when the Turleenan terminal is opened (cable ratio 60 %).

Fig. 2.5 shows the voltage profile when the Kingscourt terminal is opened. As in Fig. 2.4, the different colors (red, blue, and purple) stand for the different amount of shunt reactors connected to the line at the open end. When two 200 MVA shunt reactors are connected to the line at the open end, the voltage along the line is maintained below 420 kV.

Fig. 2.5 Voltage profile when the Kingscourt terminal is opened (cable ratio 60 %).

2.3 Resonance Overvoltage in an Opened Phase

When charging capacity of an overhead line or a mixed OHL / underground cable is compensated by line-connected shunt reactors, resonance overvoltage can occur in the faulted phase if this phase is opened for single phase autoreclose.   This resonance overvoltage often poses a limitation to the compensation rate achievable, and it is necessary to study so that the resonance overvoltage does not occur in the proposed compensation patterns.

When shunt reactors are connected to the bus (not to the line), they are disconnected from the faulted (open) line when the fault is cleared.   Thus, resonance overvoltage does not occur without inductance of shunt reactors.   Additionally, when the line is composed of the underground cable for its entire length, resonance overvoltage does not occur since mutual capacitance between faulted phase and healthy phases does not exist.

The ATP-EMTP simulation model as shown in Fig. 2.6 was built for the resonance overvoltage analysis.   The simulation model includes only the Kingscourt – Turleenan line, and both ends of the line were fixed to 400 kV by voltage sources.
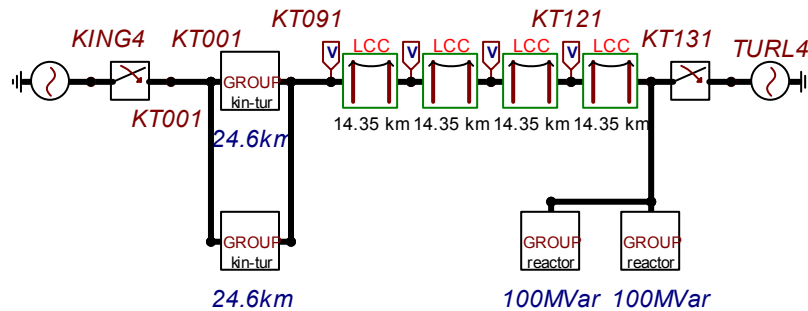
Fig. 2.6 Simulation model for the resonance overvoltage analysis.

Fig. 2.7 shows the result of the resonance overvoltage analysis for cable ratio 30 %.   For the analysis, circuit breakers of Phases A, B, and C were opened one by one.   In the figure, red, green, and blue lines are the voltages of the opened phase A, B, and C, respectively.
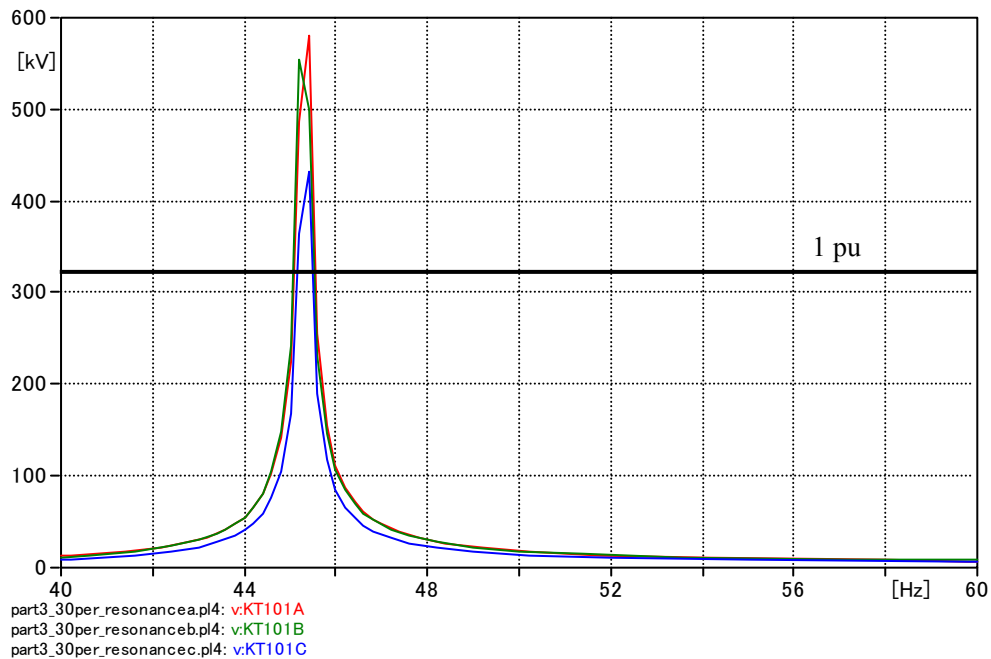
Fig. 2.7 Result of resonance overvoltage analysis (cable ratio 30 %).

Resonance frequencies were found between 45.2 Hz and 45.4 Hz, which was out of the normal operating range. The voltage of the faulted phase was reasonably low in the normal operating range.

Then, the resonance overvoltage analysis was performed for higher compensation rates. The red line in Fig. 2.8 corresponds to the proposed compensation pattern. Green and blue lines correspond to higher compensation rates as shown in the table below. It can be seen that the resonance frequency shifts closer to the normal operating range for a higher compensation rate. The proposed compensation pattern is considered safe, but the green line can be a little risky considering errors in the simulation and manufacture of equipment. The blue line is not acceptable since the resonance frequency (49.4 Hz) is too close to nominal frequency.

part3_30per_resonancea.pl4: v:KT101A
part3_30per_resonancea_120mvar.pl4: v:KT101A
part3_30per_resonancea_120mvar2.pl4: v:KT101A
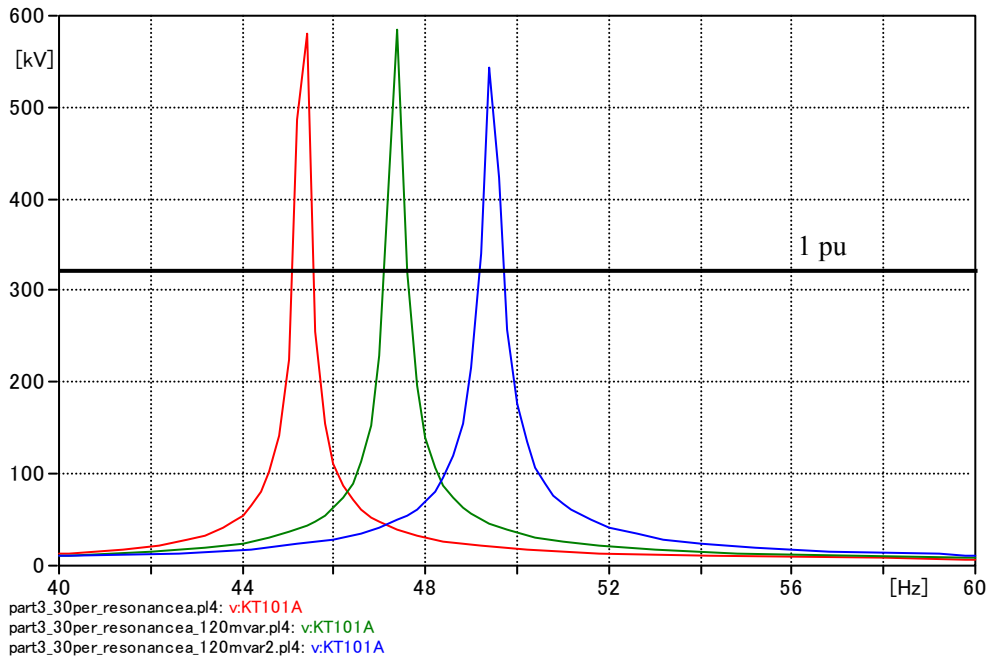
	Kingscourt	Turleenan	Compensation rate	Resonance frequency
Red line	100 MVA × 2	100 MVA × 2	81.7 %	45.4 Hz
Green line	100 MVA × 2	120 MVA × 2	89.9 %	47.4 Hz
Blue line	120 MVA × 2	120 MVA × 2	98.1 %	49.4 Hz

Fig. 2.8 Result of resonance overvoltage analysis for higher compensation rates.

There are two countermeasures that can be utilized if it is necessary to achieve a reactive power compensation rate closer to 100 % in order to control the voltage profile and reactive power flow in the network and to prevent harmful overvoltages.

One of the countermeasures is to adopt four-legged shunt reactors. By the adoption of four-legged shunt reactors, it is possible to shift the resonance frequency. Fig. 2.9 compares the result of the analysis with the four-legged shunt reactors (green line) and the normal shunt reactors (red line). Compensation rate was fixed at 98.1 % (Kingscourt: 120 MVA × 2, Turleenan: 120 MVA × 2). For the four-legged shunt reactors, impedance of the grounding reactor was set to 1000 mH.

As shown in Fig. 2.9, it was confirmed that the resonance frequency was shifted from 49.4 Hz to 46.0 Hz by adopting four-legged shunt reactors. However, the open phase voltage at the resonance frequency became very high. The normal operating range is far away from 46 Hz, but the open phase voltage is higher than 1 pu even at 49 Hz. This result implies that careful attention is necessary when adopting four-legged shunt reactors in order to shift the resonance frequency.

part3_30per_resonancea_120mvar2.pl4: v:KT101A
part3_30per_resonancea_120mvar2_4leg.pl4: v:KT101A
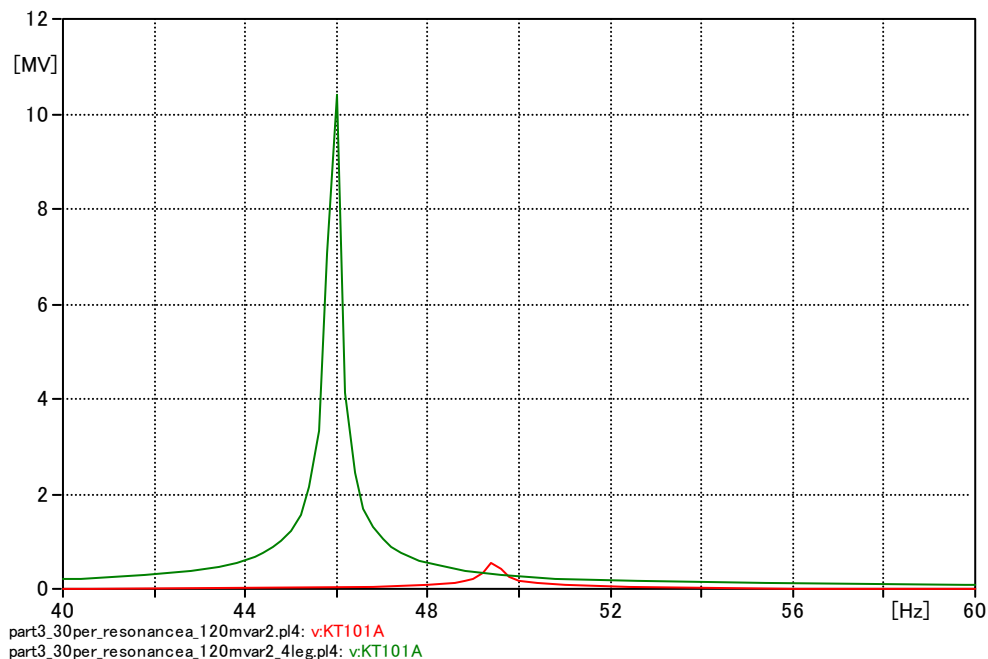
Fig. 2.9 Result of resonance overvoltage analysis with four-legged shunt reactors.

The other countermeasure is to adopt three phase autoreclose instead of single phase autoreclose. Reliability of the interconnector is undermined by this change, but open phase resonance does not occur since all three phases are opened even in single line to ground faults. Overvoltages caused by autoreclose become more severe for three phase autoreclose compared to

single phase autoreclose as explained in Chapter 4.

The resonance overvoltage analysis was also performed for cable ratio 60 %. In the proposed compensation pattern, the resonance frequency was found at 45.6 Hz for the faulted phases A, B, and C. Although resonance overvoltage was lower than 1 pu, it is not recommended to increase the compensation rate.

part3_60per_resonancea.pl4: v:KT151A
part3_60per_resonanceb.pl4: v:KT151B
part3_60per_resonancec.pl4: v:KT151C
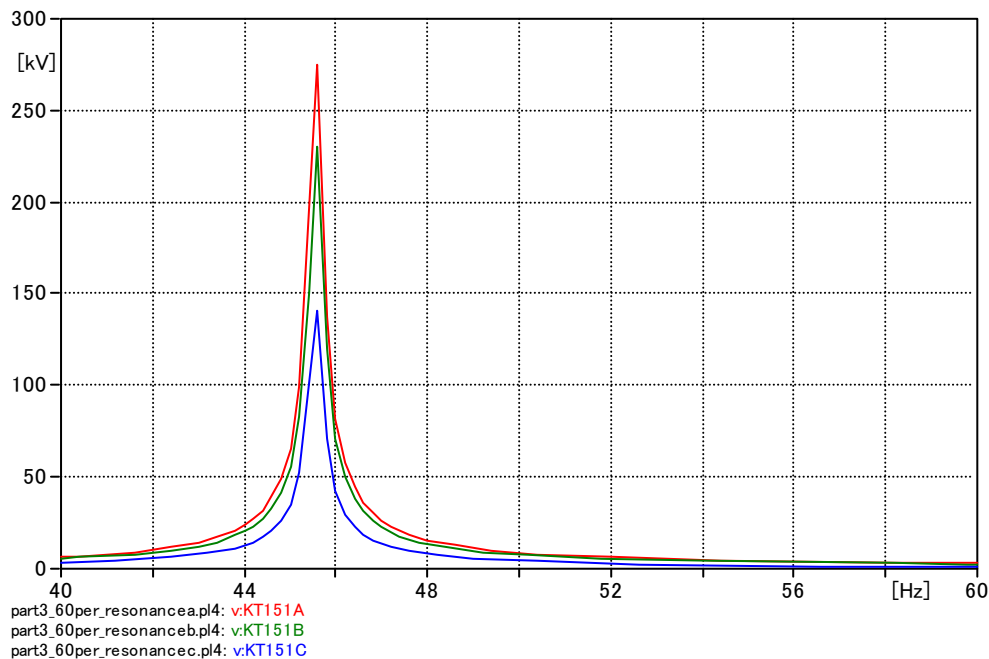
Fig. 2.10 Result of resonance overvoltage analysis (cable ratio 60 %).

2.4 Conclusion

As a result of the reactive power compensation analysis, the proposed compensation patterns were found to be satisfactory even when one terminal of the line was opened as long as all shunt reactors were connected to the line at the open terminal.

For cable ratio 30 %, one 100 MVA shunt reactor can be connected to the bus instead of the line, but it is recommended to connect both shunt reactors to the line considering a potential outage of the shunt reactor.

For cable ratio 60%, both 200 MVA shunt reactors have to be connected to the line in order to maintain the voltage below 420 kV. When one shunt reactor is not available, the voltage at the open end can be higher than the other end by 15 kV. This can be an acceptable risk, but it is preferable to conduct maintenance of the line and the shunt reactor at the same time.

Additionally, the resonance overvoltage analysis was carried out, and the proposed compensation patterns were found to be safe when any faulted phase was opened for single phase autoreclose.

In conclusion, the proposed compensation patterns shown below will be used for further analysis in Part 3.

Locations	Cable ratio 30 %	Cable ratio 60 %
Kingscourt	100 MVA × 2	200 MVA × 2
Turleenan	100 MVA × 2	200 MVA × 2
Compensation Rate [%]	81.7	85.7

Chapter 3 Model Setup

3.1 Combinations of OHLs and Underground Cables

The following combinations of OHLs and underground cables as shown in Fig. 3.1 were studied in Part 3.   The cable section was placed at the Kingscourt end or in the center of the 400 kV Kingscourt – Turleenan line.   The location and amount of shunt reactors in the figure reflect the results of the reactive power compensation analysis in Chapter 1.
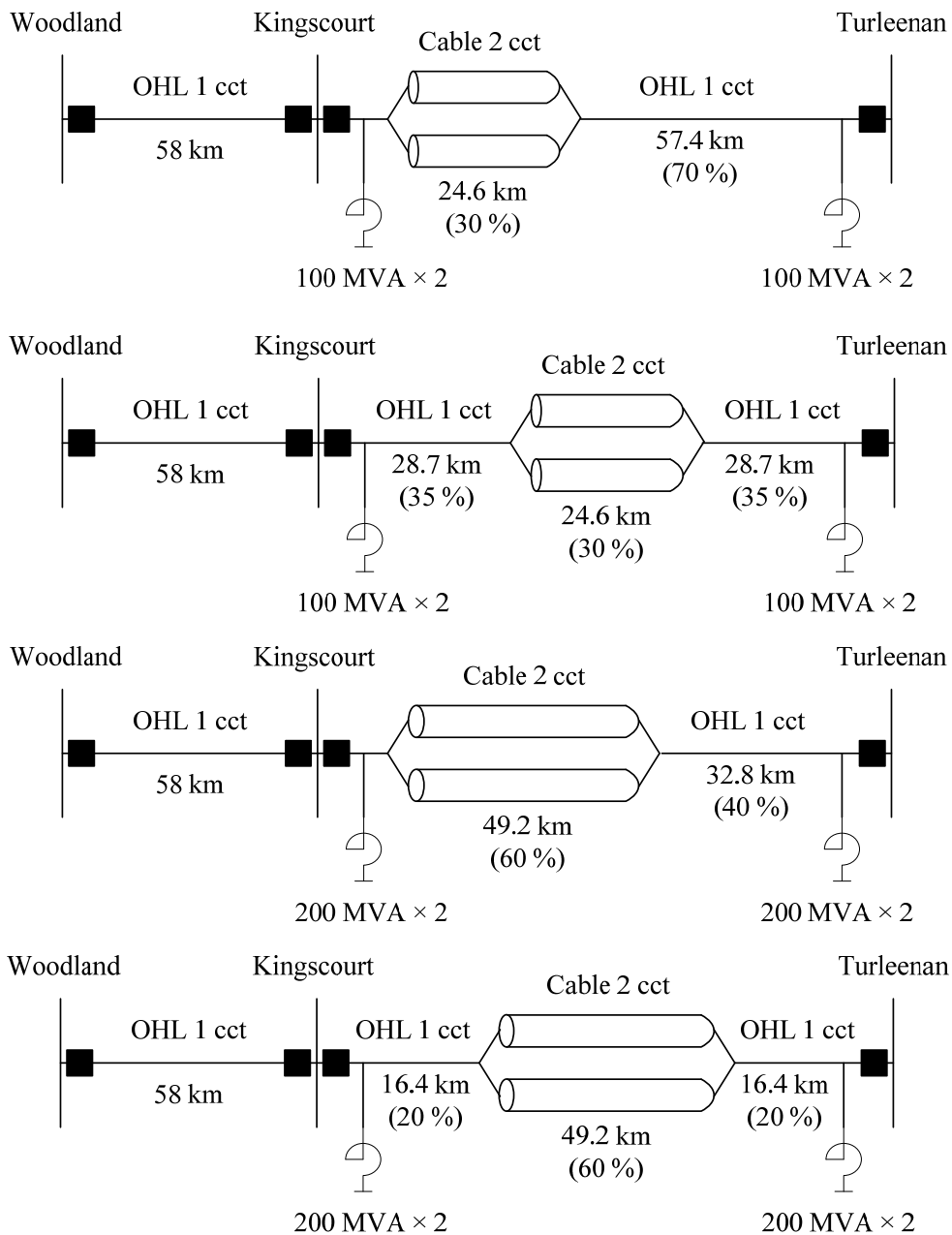
Fig. 3.1 Combinations of OHLs and underground cables for the Kingscourt – Turleenan line.

Additionally for the analysis of the overvoltage caused by autoreclose, another setup as shown in Fig. 3.2 was studied in order to determine the effect of different shunt reactor locations.
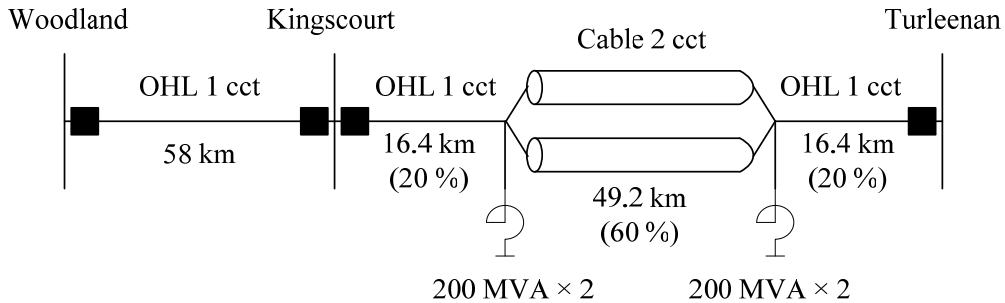
Fig. 3.2 Additional combination of OHLs and underground cables for the Kingscourt – Turleenan line.

Other models – such as OHL models, transformer models, surge arrester models, generator models, and load models – are the same as those in Part 2. Explanations of these models are given in Part 2 of the report. Since 200 MVA shunt reactors are used only in Part 3, explanations on shunt reactor models are given here.

3.2 Shunt Reactors

Shunt reactors were connected to both ends of the 400 kV cables or 400 kV buses, in order to compensate charging capacity of the cables. Shunt reactors for the Kingscourt – Turleenan line were modeled as shown in Fig. 3.1 and Fig. 3.2. 400 kV shunt reactors in the simulation model are shown in Table 3.1.

Table 3.1 400 kV Shunt Reactors in the Simulation Model

Kingscourt – Turleenan (82 km)	Kingscourt: 100 or 200 MVA × 2 Turleenan: 100 or 200 MVA × 2
Woodland – Oldstreet (125 km)	Woodland: 80 MVA × 1
Moneypoint – Tarbert (6.5 km)	Moneypoint: 50 MVA × 1 Tarbert: 50 MVA × 1

When 400 kV shunt reactors are close to *the point of interest*, they are modeled with the saturation characteristics. Otherwise they are modeled as linear inductances.

Chapter 4 Temporary Overvoltage Analysis

For long EHV cables, temporary overvoltages are of highest concerns in terms of the safe operation after the installation. Highest temporary overvoltages are often higher than highest slow-front overvoltages.

Due to the large capacitance associated with the long EHV cable and the inductance of shunt reactors for the reactive power compensation, the following temporary overvoltages require a close attention for the network with long EHV cables:

(1) Parallel resonance overvoltage

(2) Oscillatory overvoltage caused by the system islanding

For equipment whose highest voltage is higher than 245 kV, the standard short-duration power-frequency withstand voltage is not specified in IEC, but it is specified by a utility or a manufacturer. Surge arresters are generally the weakest among different equipment. The temporary overvoltages have to be evaluated against typical withstand voltage and energy absorption capability of surge arresters. Note that the temporary overvoltages may be evaluated with SIWV depending on their decay time.

4.1 Conditions for the Parallel Resonance Overvoltage Analysis

Parallel resonance frequencies were found from the results of a frequency scan in EMTP as shown in Fig. 4.1.
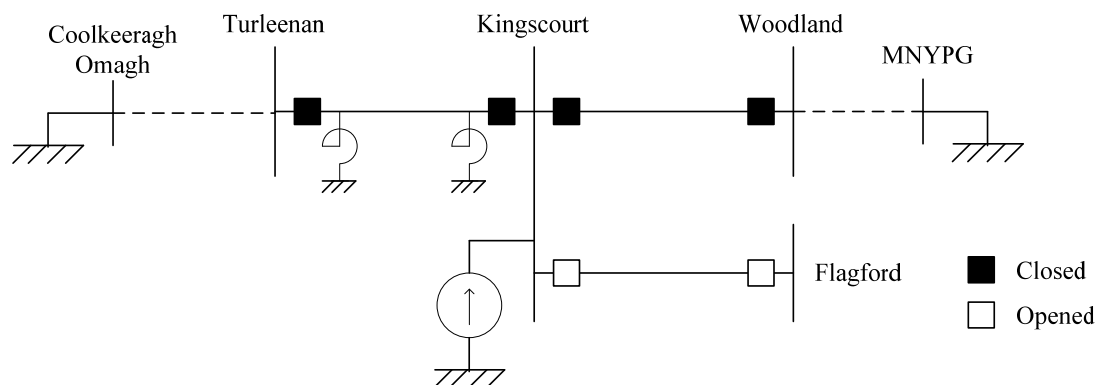
Parallel resonance frequency seen from the Kingscourt substation

Fig. 4.1 Frequency sweep for the parallel resonance overvoltage analysis.

Since the focus of the parallel resonance overvoltage analysis in Part 3 is to find the effect of the partial cabling on parallel resonance, the following conditions were fixed in Part 3 in consideration of the result of the parallel resonance overvoltage analysis conducted in Part 2:

- Since impedance of the network seen from the Woodland, Kingscourt, and Turleenan 400 kV were similar, the analysis in Part 3 focused on impedance seen from Kingscourt 400 kV.

- The 400 kV Kingscourt – Flagford line and the 400 kV Woodland – Oldstreet line were assumed to be out of service in order to yield a larger magnitude of impedance at the parallel resonance frequency.

Source impedances of dummy generators connected to the Woodland 220 kV, the Kingscourt 220 kV, and the Turleenan 275 kV buses were adjusted to shift the parallel resonance frequency to 100 Hz. After the frequency scan, the time domain simulation was conducted under the most severe conditions as shown in Fig. 4.2.
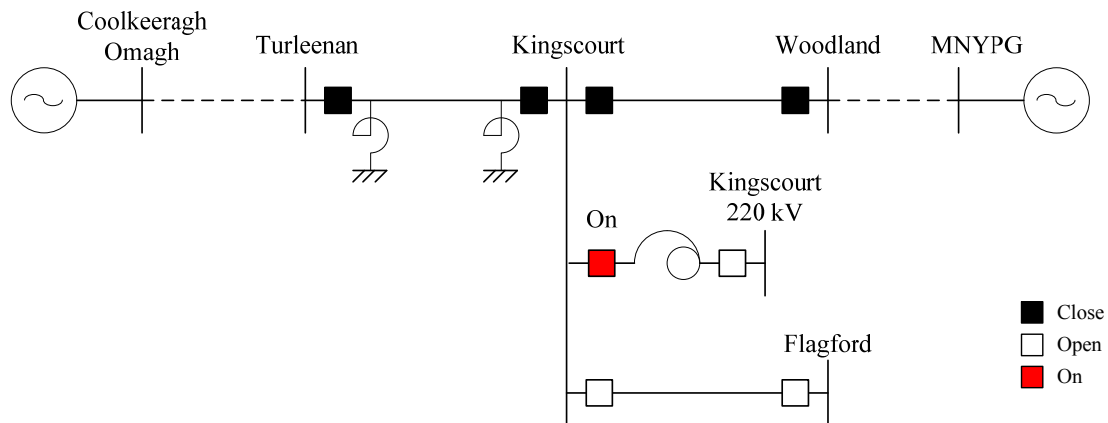
Fig. 4.2 Sample scenario of the time domain simulation for the parallel resonance overvoltage analysis.

In the parallel resonance overvoltage analysis, an effect of the fault current level (source impedance) at the Woodland 220 kV, the Kingscourt 220 kV, and the Turleenan 275 kV buses was studied as one of parameters.   In order to find the reasonable range for this parameter, the fault current calculation was performed at these buses in Part 2.

Generators included in the simulation model are fewer than those in service in summer off-peak power flow data.   An adjustment of the fault current level can be achieved by adding a dummy source with different source impedances.   Based on the fault current calculation result in Part 2, the source impedance values were varied in the range shown below.

Table 4.1 Assumed Range of Source Impedance Values

Woodland 220 kV	20 – 60 mH
Kingscourt 220 kV	40 – 60 mH
Turleenan 275 kV	20 – 50 mH

4.2 Parallel Resonance Frequency Seen from Kingscourt 400 kV

Parallel resonance frequency of the network seen from Kingscourt 400 kV was found by a frequency scan based on the simulation model in Fig. 4.3.
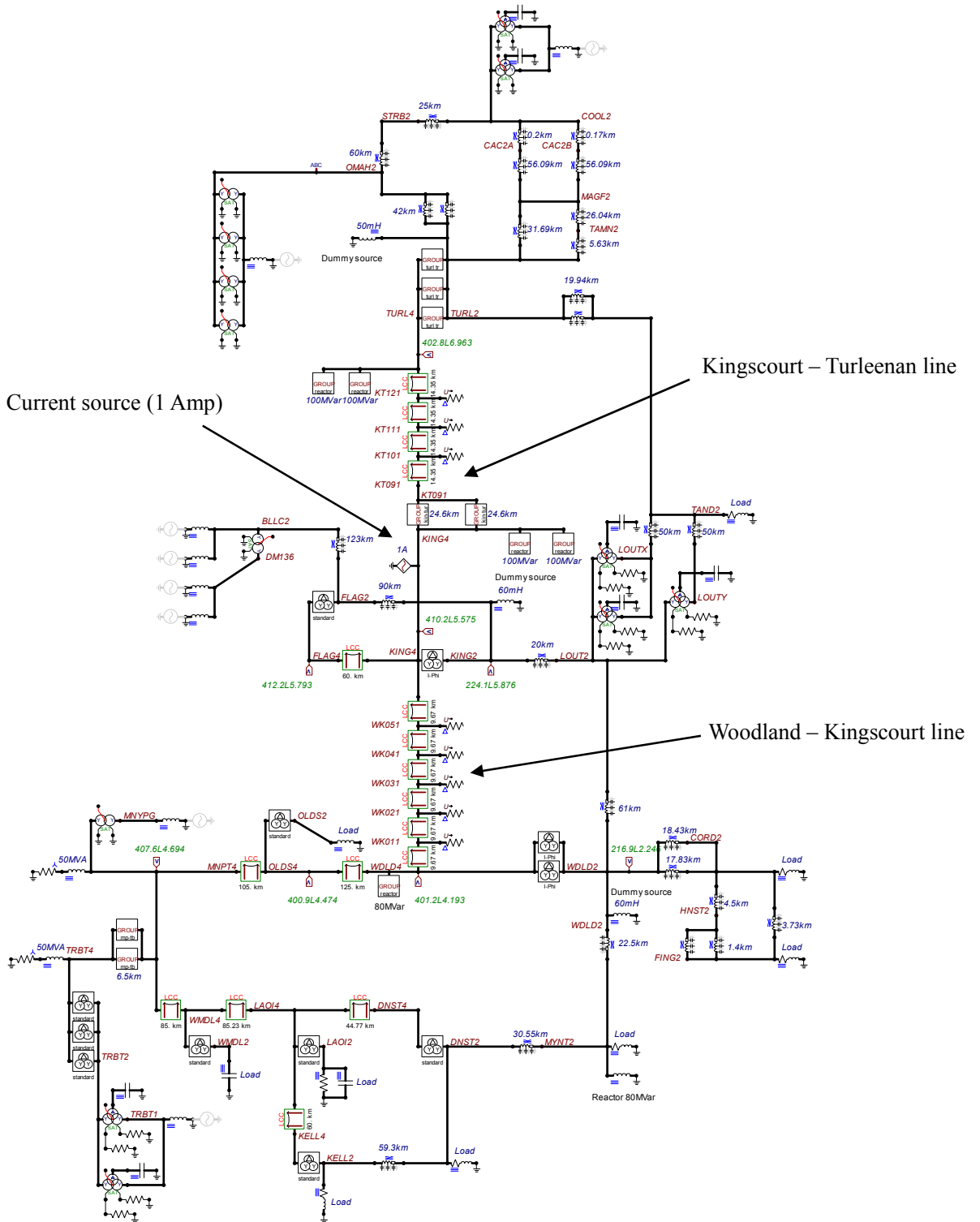
Fig. 4.3 Simulation model for a frequency scan seen from Kingscourt 400 kV.

In the first example, the largest source impedance (lowest fault current level) in Table 4.1 was set to the Woodland 220 kV, the Kingscourt 220 kV, and the Turleenan 275 kV buses. The results of a frequency scan for cable ratio 60 % and 30 % are respectively shown in Fig. 4.4 and Fig. 4.5. For cable ratio 60 % and 30 %, the highest peak was found at 113 Hz and 155 Hz, respectively, and other high peaks were not at a level requiring careful consideration.
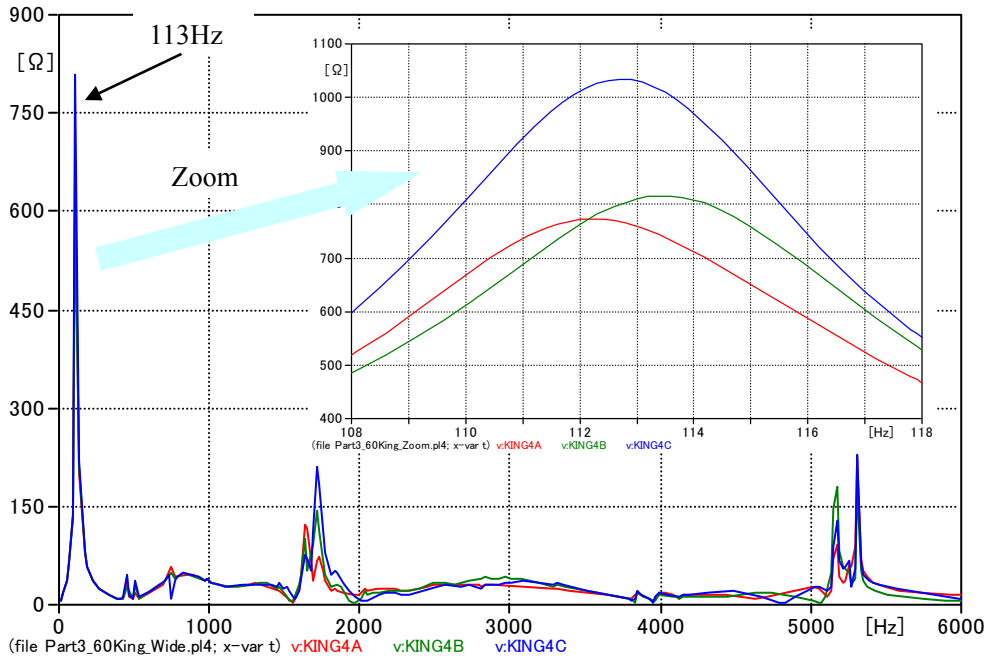
Fig. 4.4 Parallel resonance frequency for cable ratio 60 %.
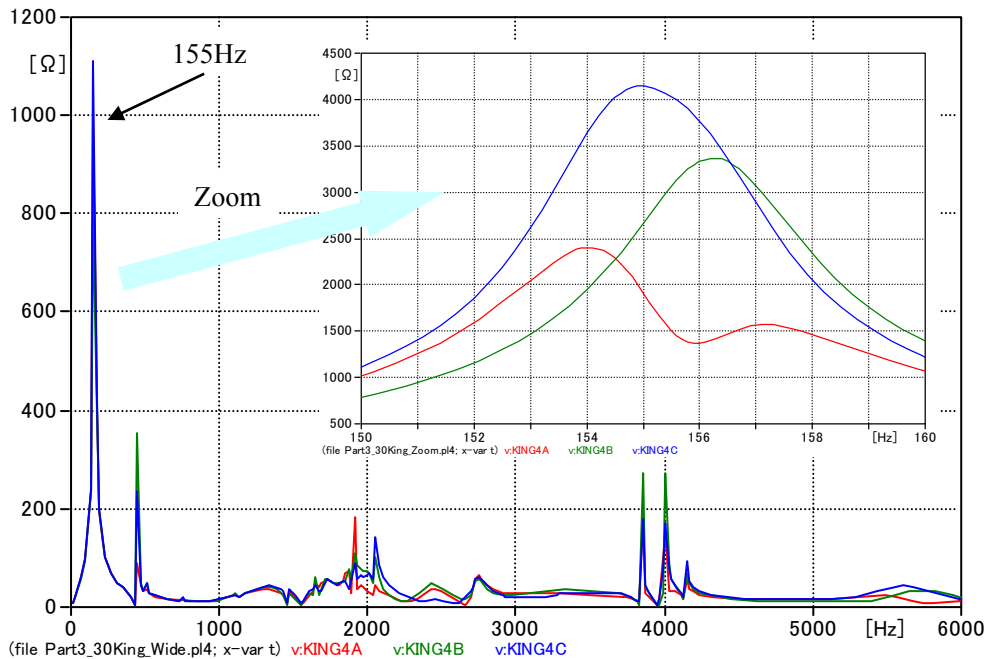
Fig. 4.5 Parallel resonance frequency for cable ratio 30 %.

With the largest source impedance (lowest fault current level), the parallel resonance frequency and the magnitude of impedance changed with the cable ratio as shown in Table 4.2.

Table 4.2 Magnitude of Impedance at the Parallel Resonance Frequency

	Parallel resonance frequency	Magnitude of impedance
Cable ratio 100% (from Part 2 for reference)	86.9 Hz	933 Ω
Cable ratio 60 %	113 Hz	1034 Ω
Cable ratio 30%	155 Hz	4145 Ω

As a result, an energisation of the Kingscourt 400/220 kV transformer was considered to be the most critical source of harmonic current injection.   For each cable ratio, the source impedance at the Woodland 220 kV and Turleenan 275 kV buses were adjusted in order to yield the parallel resonance frequency at 100 Hz for cable ratio 60%.   For cable ratio 30 %, it seems more reasonable to shift the parallel resonance frequency to 150 Hz since third harmonic is also contained in transformer inrush current.   The value of this source impedance and the magnitude of impedance at the parallel resonance frequency are shown in Table 4.3.

Table 4.3 Magnitude of Impedance at the Parallel Resonance Frequency

	Source impedance		Parallel resonance frequency	Magnitude of impedance
	Turleenan	Woodland		
Cable ratio 100% (from Part 2 for reference)	20.0 mH	24.8 mH	100 Hz	2606 Ω
Cable ratio 60 %	120 mH	112 mH	100 Hz	849 Ω
Cable ratio 30%	77 mH	70 mH	150 Hz	2692 Ω

In order to shift the parallel resonance frequency to 100 Hz or 150 Hz, it was necessary to set the values of the source impedance at the Kingscourt 220 kV and the Turleenan 275 kV buses much higher than their designated reasonable range.

Finally, a time domain simulation was carried out for both cable ratio 60 % and 30 %.   For cable ratio 60 %, the voltage of the Kingscourt 400 kV bus and inrush current into the Kingscourt 400/220 kV transformer are shown in Fig. 4.6 and Fig. 4.7.   The highest voltage observed at the Kingscourt 400 kV bus was 436.3 kV (1.34 pu) in Phase C.   This is not a concern in terms of the operation of the 400 kV Woodland – Kingscourt – Turleenan line.

(file Inrush_Part3_60King_100Hz.pl4; x-var t) v:KING4A   v:KING4B   v:KING4C
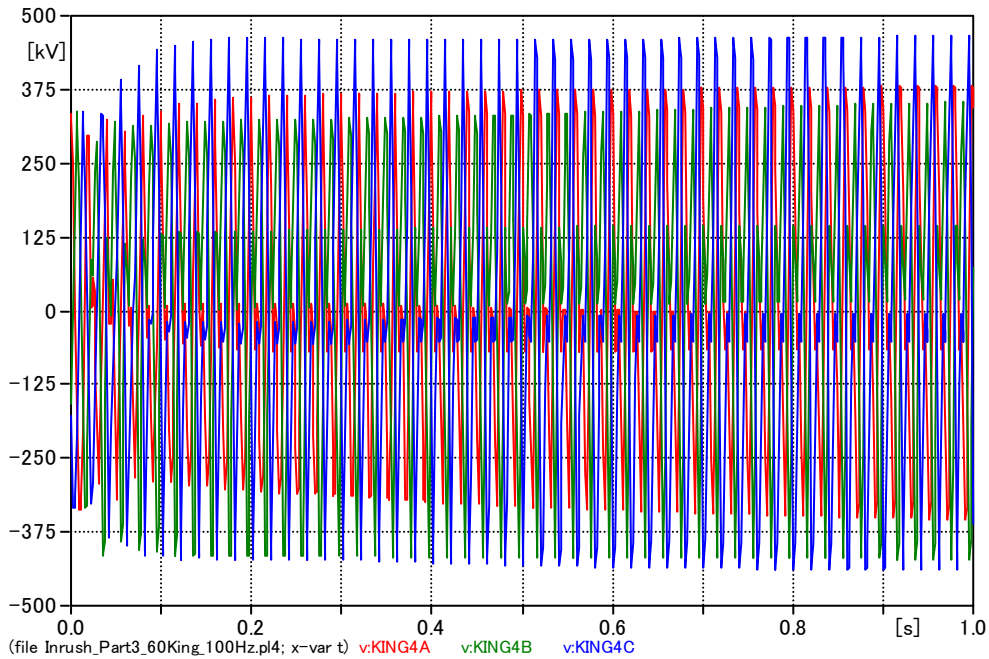
Fig. 4.6 Kingscourt 400 kV bus voltage in transformer inrush for cable ratio 60 %.

(file Inrush_Part3_60King_100Hz.pl4; x-var t) c:KING4A–KC_TRA   c:KING4B–KC_TRB   c:KING4C–KC_TRC
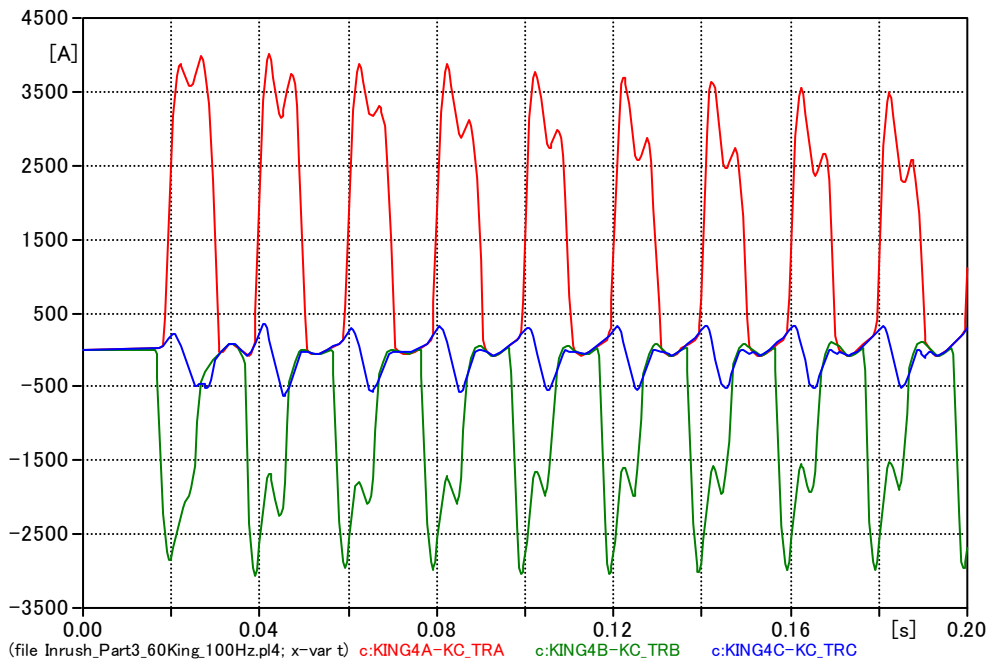
Fig. 4.7 Inrush current into the Kingscourt 400/220 kV transformer for cable ratio 60 %.

For cable ratio 30 %, the voltage of the Kingscourt 400 kV bus and inrush current into the Kingscourt 400/220 kV transformer are shown in Fig. 4.8 and Fig. 4.9. The highest voltage observed at the Kingscourt 400 kV bus was 604.2 kV (1.85 pu) in Phase C. Since the resonance frequency was set to 150 Hz, the initial overvoltage is very high for a temporary overvoltage. However, the resonance level is not high, and the overvoltage decays in several cycles to a level similar to that in Part 2.
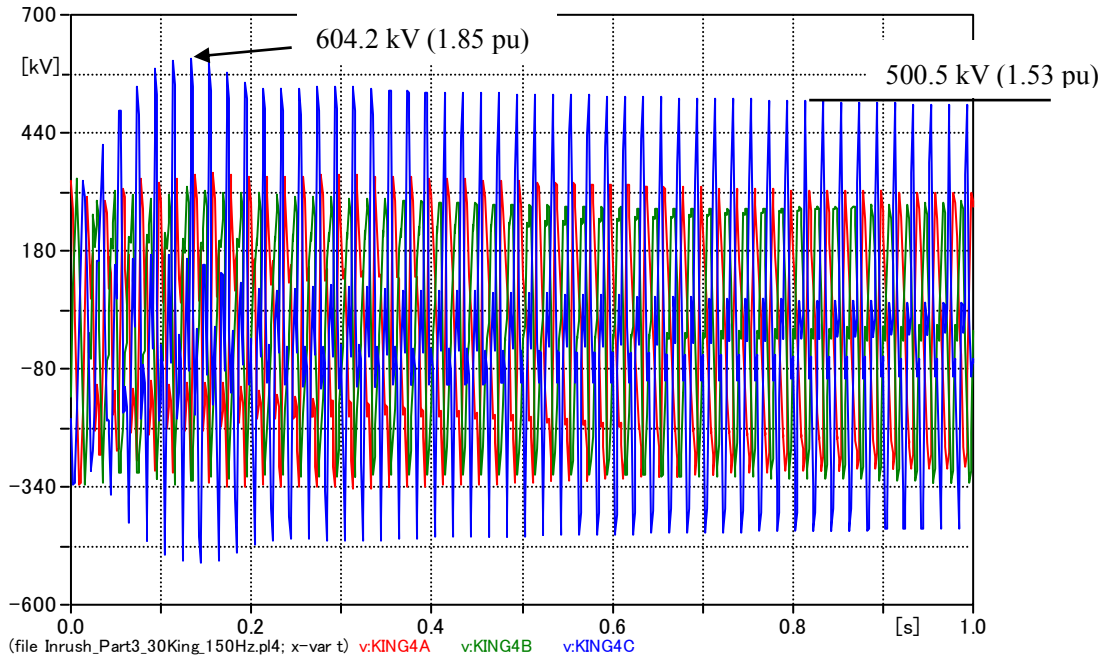
Fig. 4.8 Kingscourt 400 kV bus voltage in transformer inrush for cable ratio 30 %.
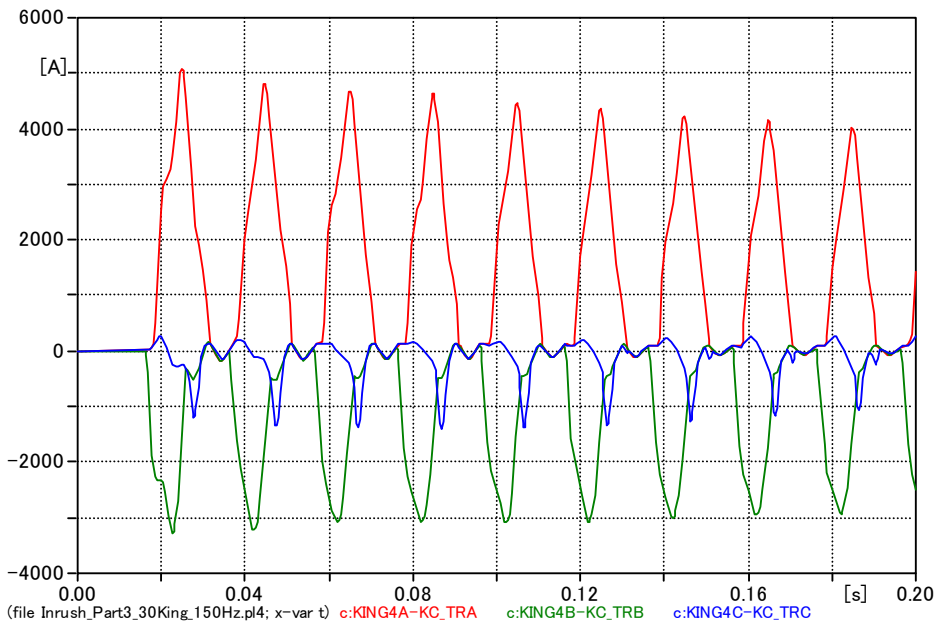
Fig. 4.9 Inrush current into the Kingscourt 400/220 kV transformer for cable ratio 30 %.

Since the observed overvoltage was high for a temporary overvoltage, the energy absorption capability of the surge arrester was tested.   As the most severe assumption, only one surge arrester was connected to the Kingscourt 400 kV bus.   As a result of the analysis, it was confirmed that there was no problem in the energy absorption capability of the surge arrester.
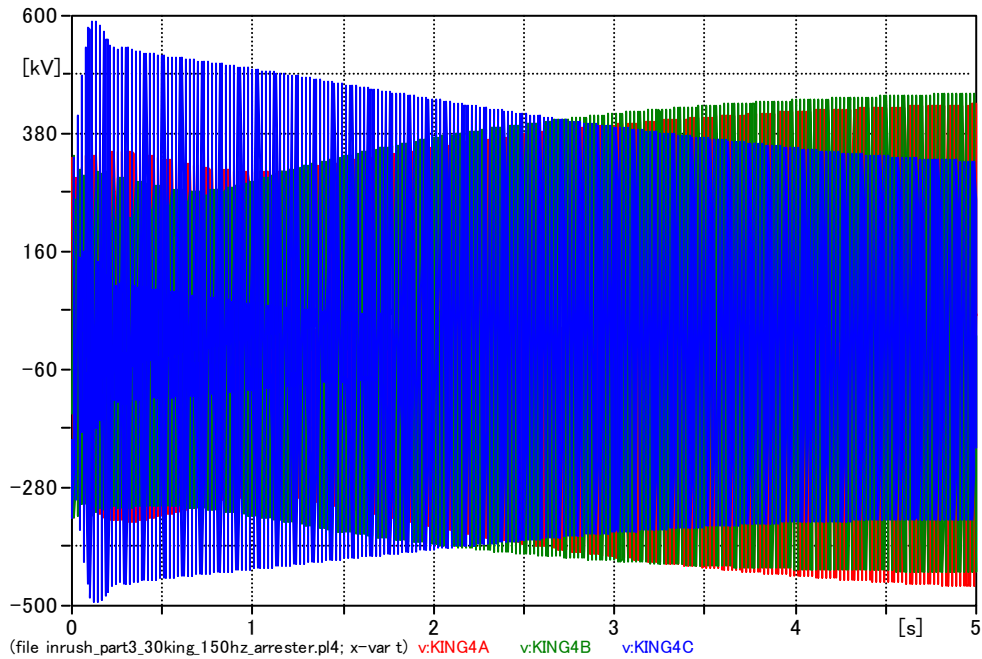
Fig. 4.10 Kingscourt 400 kV bus voltage in transformer inrush for cable ratio 30 % with a surge arrester.
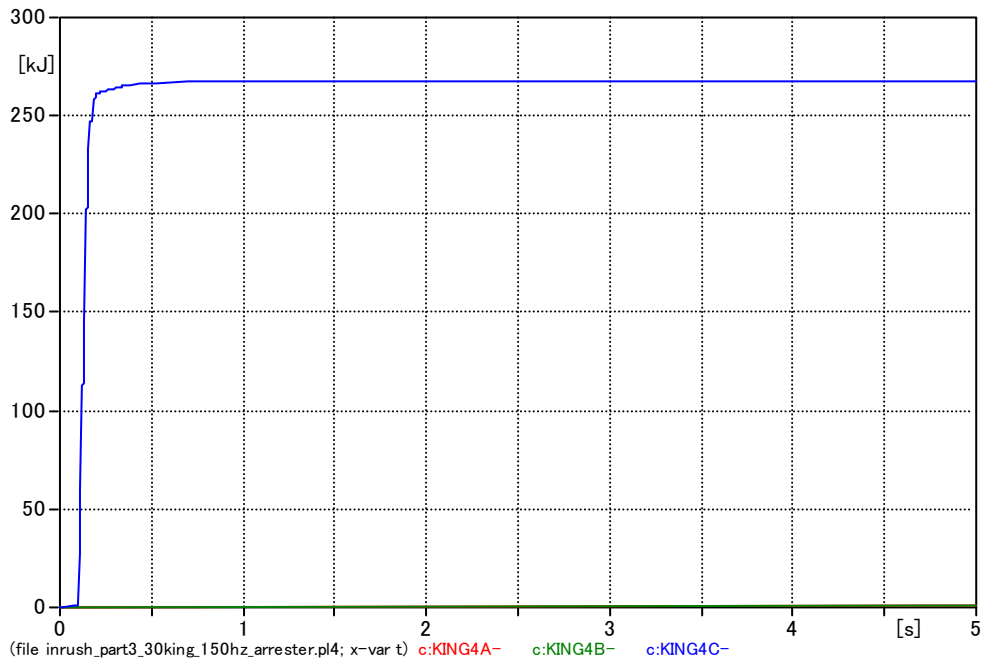
Fig. 4.11 Energy absorbed by the surge arrester.

In Fig. 4.10, it was observed that the overvoltages in Phase A and B were increasing and the overvoltage in Phase C was decreasing.   From this result, it is expected that non-fundamental frequency components are increasing in Phase A and B transformer inrush current.

First, Fig. 4.12 shows transformer inrush current in Phase A – C.   We can see inrush current in each phase monotonically decays with time.   Note that the decay of inrush current should be much faster in the actual network due to due to larger resistance (temperature rise) and losses (eddy current losses and etc.).
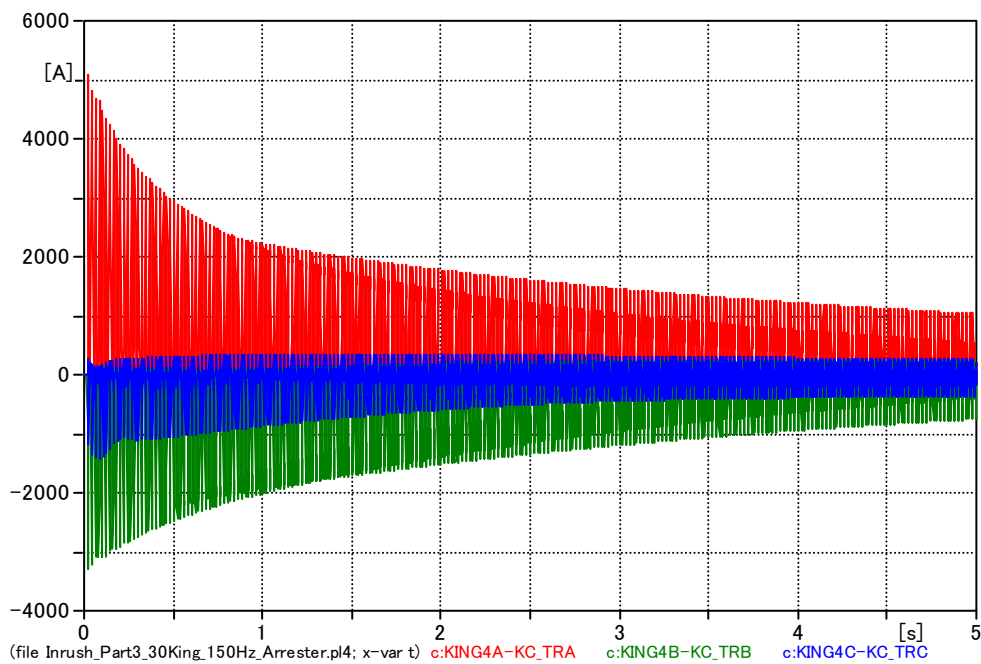
Fig. 4.12 Transformer inrush current for cable ratio 30 % with a surge arrester.

When we perform Fourier transform to the waveform of inrush current for the duration 0.98 – 1.00 sec and 4.98 – 5.00 sec, we can see the following change in frequency components.

(a) Phase A

Third harmonic current is increased at around 5 sec, which causes the higher parallel resonance overvoltage at the end of simulation time.
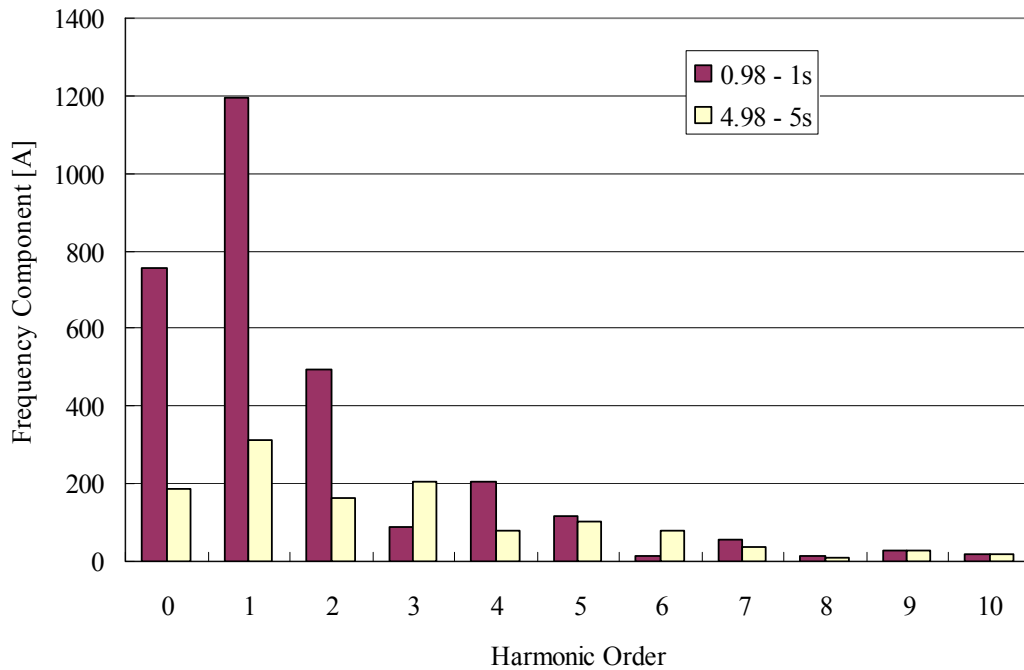
Fig. 4.13 Frequency components in transformer inrush current in Phase A.

(b) Phase C

Third harmonic current is at a comparable level for 5 seconds. It is assumed that in Phase C the transient overvoltage caused by the initial inrush is damped with time.
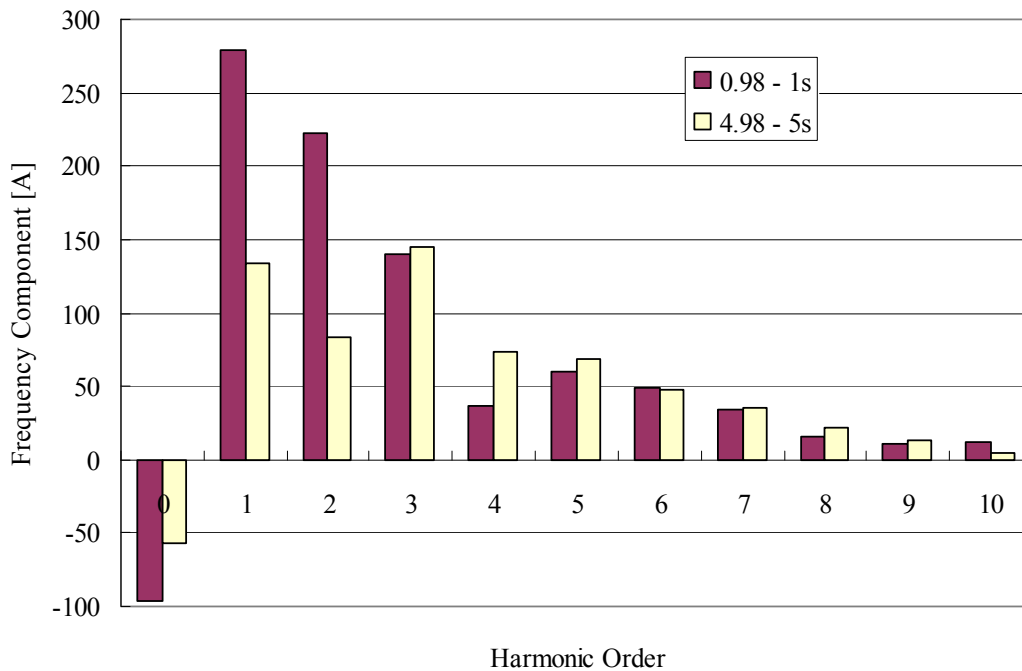
Fig. 4.14 Frequency components in transformer inrush current in Phase C.

Since the parallel resonance frequency of the network was set to 150 Hz, it was expected that third harmonic current contained in transformer inrush current circulated in the tertiary winding of the Kingscourt 400/220 kV transformer.

Fig. 4.15 shows circulating current in the tertiary delta winding. The magnitude of circulating current is not large as inrush current, considering the rated capacity and voltage of the tertiary winding, 80 MVA and 21 kV.

(file inrush_part3_30king_150hz_tertiaryiout.pl4; x-var t) c:X021DA-X0212A
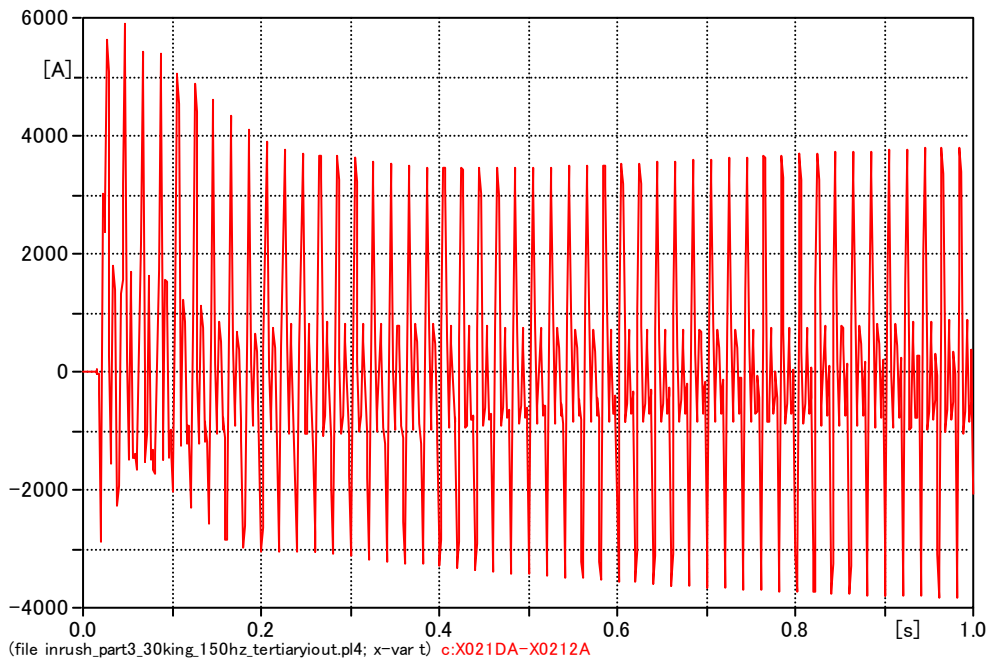
Fig. 4.15 Current in the tertiary winding.

Fig. 4.16 shows the result of Fourier transform of current in the tertiary winding. Third harmonic current is smaller than fundamental or second harmonic current in the primary side, but it is larger than fundamental or second harmonic current in the tertiary side.
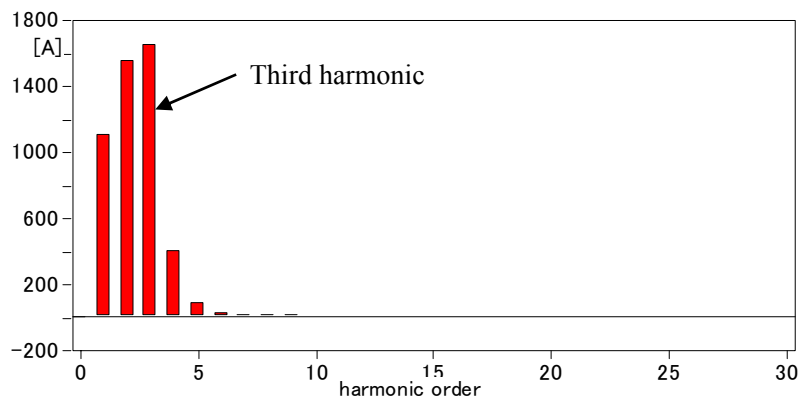
Fig. 4.16 Fourier transform of current in the tertiary winding.

4-12

4.3 Overvoltage Caused by the System Islanding

When one end of the cable is opened after a three phase fault (load shedding), an oscillatory overvoltage can be caused by the superimposition of overvoltages having two different frequencies.

Overvoltage caused by load shedding was studied using the switching scenario shown in Fig. 4.22. A three phase fault in the 400 kV bus in Woodland, Kingscourt and Turleenan, and subsequent trippings of cable lines were assumed in the switching scenario. A sudden trip of cable lines without loads could possibly produce a large overvoltage. In general, a larger impedance and admittance from an equivalent source yields a more severe condition.

Resonance frequencies can be calculated by a simple method shown below. Fig. 4.17 shows impedance and admittance data of the 400 kV Turleenan – Kingscourt line and the Turleenan 400/220 kV transformer. Impedance and admittance data in this figure is extracted from the PSS/E data set. Xb is assumed to be the source impedance and resistances are neglected in the figure.
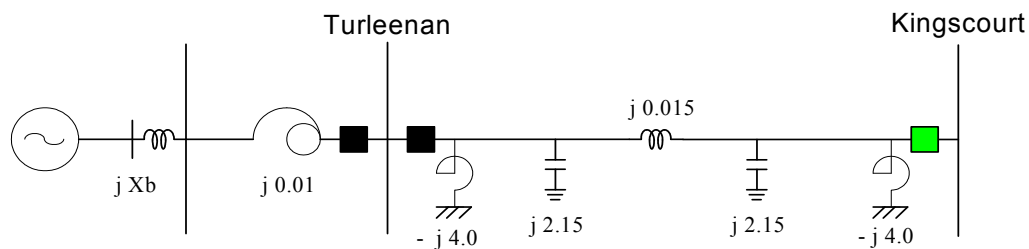
Fig. 4.17 Impedance and admittance of the 400 kV Turleenan – Kingscourt line and the Turleenan 400/220 kV transformer. (60%-ratio cable at Kingscourt end)

The following equations explain that X_0, Y, X can be calculated from data in Fig. 4.17.

$$X_0 = 0.01 + 0.015 + X_b$$
$$X = (4.0 + 4.0)^{-1}$$
$$Y = 4.3$$

where Xb is a source impedance behind the 220 kV Turleenan bus. Resonance frequencies were calculated with the source between 0.013 pu and 0.033 pu using the following equation, and calculated resonance frequencies are shown in Fig. 4.18.

$$\frac{\omega_0}{\omega} = \sqrt{\frac{1}{YX_0} + \frac{1}{YX}}$$

Source impedances behind the 220 kV Turleenan bus was given by short circuit calculations in PSS/E under the summer off-peak demand and the winter peak demand with maximum windpower.
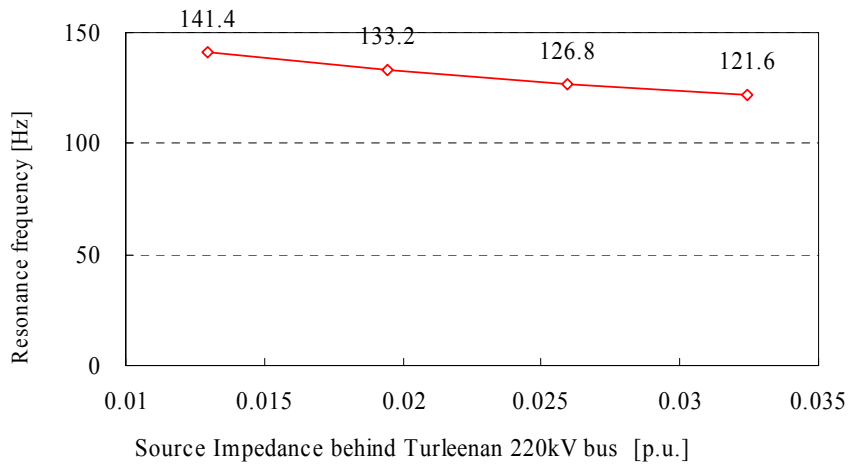
Fig. 4.18 Calculated resonance frequencies.

Fig. 4.19 and Fig. 4.20 show overvoltages in the 400 kV Turleenan – Kingscourt line caused by islanding in the case of cable ratio 60 % at Kingscourt end under the assumed range of the source impedance value of Turleenan as described in Section 4.1.
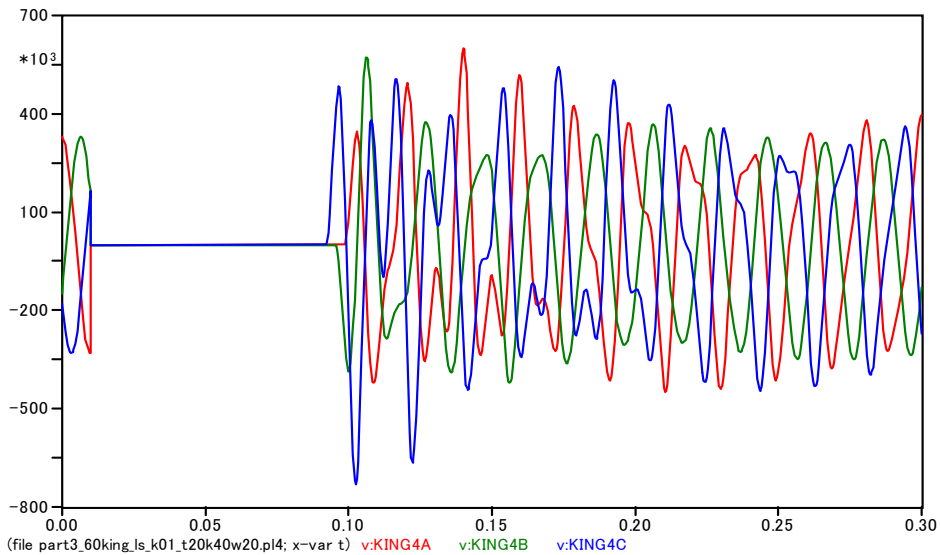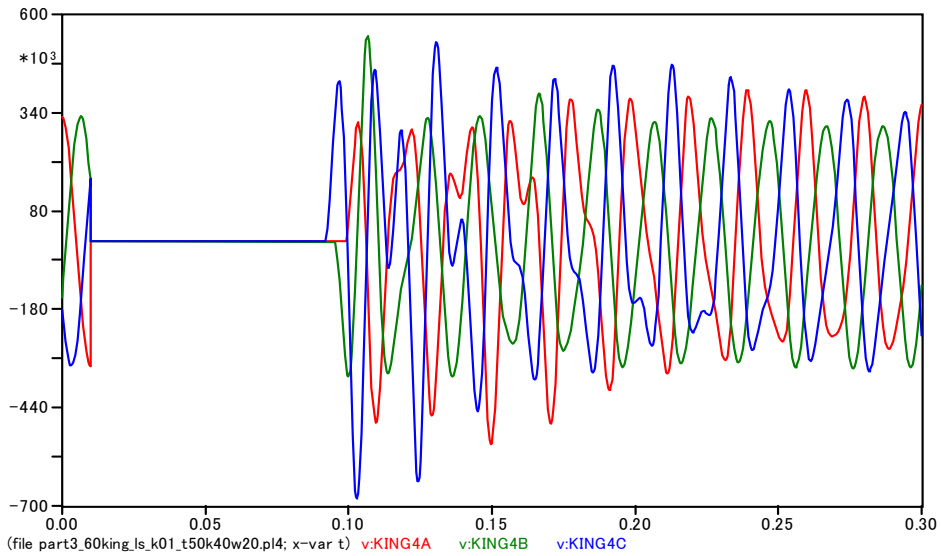

Fig. 4.19 Overvoltage caused by islanding under the smallest impedance value of Turleenan.

(Dummy source impedance at Turleenan 275 kV: 20 mH)

Fig. 4.20 Overvoltage caused by islanding under largest impedance value of Turleenan.

(Dummy source impedance at Turleenan 275 kV: 50 mH)

Those voltage waveforms were decomposed into their frequency components as shown in Fig. 4.21. The phase in which the highest voltage was observed was chosen for each Fourier analysis.
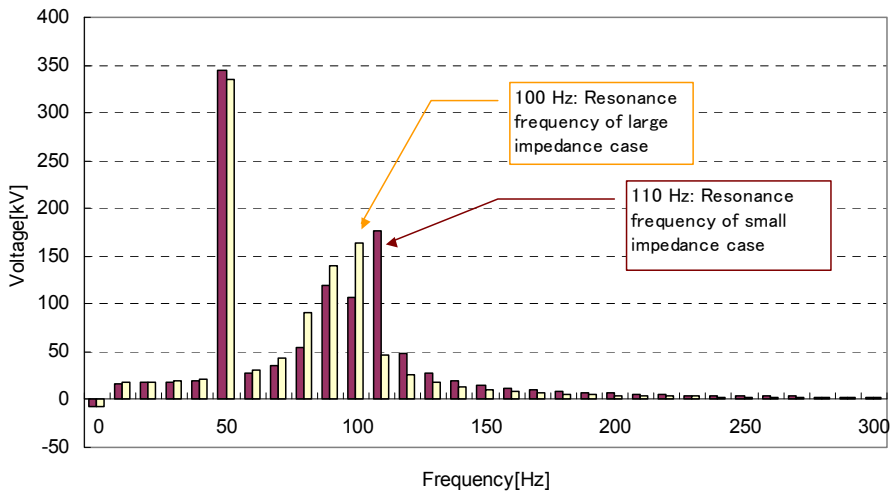
Fig. 4.21 Frequency components contained in the overvoltage.

Spectrums in the summer off-peak demand and the winter peak demand with maximum wind power respectively have peaks at 110 Hz and 100 Hz, as well as at 50 Hz. The results almost match with the calculated resonance frequencies shown in Fig. 4.18.
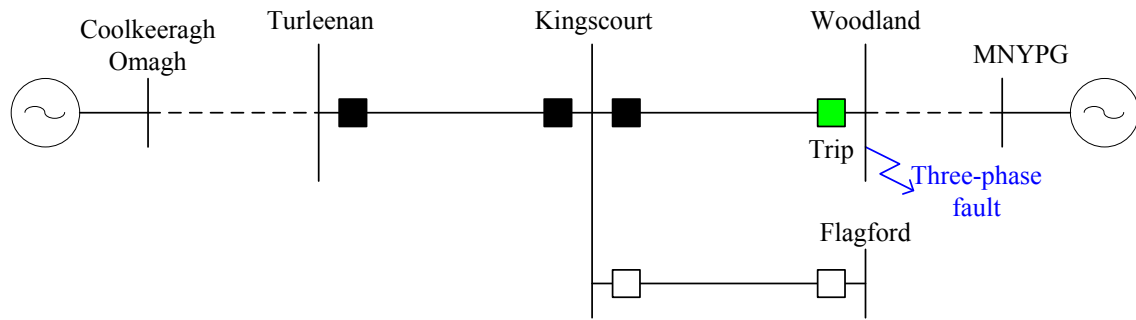
Three phase fault at Woodland 400kV bus
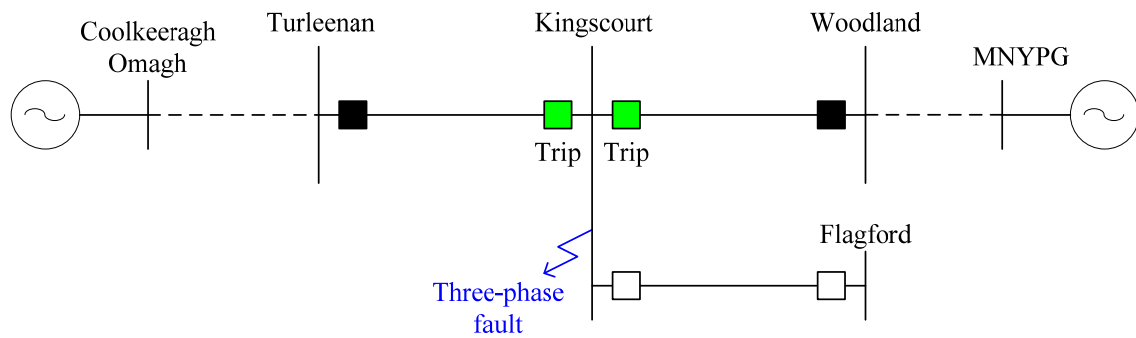
Three phase fault at Kingscourt 400kV bus
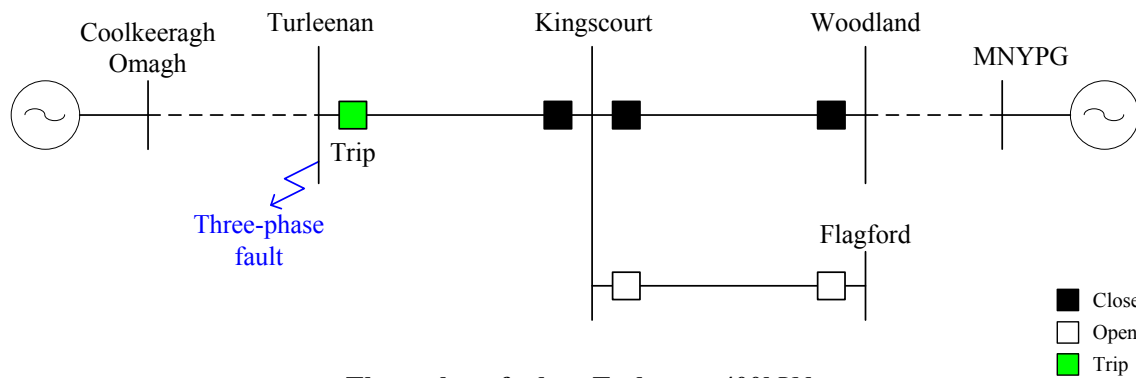
Three phase fault at Turleenan 400kV bus

Fig. 4.22 Switching scenarios for the overvoltage caused by the system islanding.

In Fig. 4.22, the 400 kV Kingscourt – Flagford line is opened in the initial condition to have a clear oscillatory overvoltage.　When this line is in service, different frequency components will be superimposed on the two frequency components described above.　By adding different frequency components, it will become difficult to see the oscillatory overvoltage, and the overvoltage level will generally decrease.

4.3.1　Overvoltage studies under base condition

The overvoltage caused by system islanding was studied using different network configurations including a combination of the cable ratio and cable position as shown in Fig. 3.1. The highest observed overvoltage in each network configuration is summarized in Table 4.4. Target frequencies of all Bergeron models were set to 50 Hz for the analysis.　"K-end" in the table means that the cable section is placed at the Kingscourt end, and "Center" means at the center of the Kingscourt – Turleenan line.

Table 4.4 Overvoltage Caused by System Islanding

Pattern No.	Assumed Line Outage	Fault on	Overvoltage	
			At the end of the line	Highest value along the line
Ratio 60% (K-end)	Turleenan – Kingscourt	Turleenan	499.2kV (1.53 pu)	499.2kV (1.53 pu)
	Turleenan – Kingscourt Kingscourt – Woodland	Kingscourt	731.9kV (2.24 pu) [Turleenan side]	734.0 kV (2.25 pu) [Turleenan side]
	Kingscourt – Woodland	Woodland	458.3kV (1.40 pu)	458.3kV (1.40 pu)
Ratio 60% (Center)	Turleenan – Kingscourt	Turleenan	580.7 kV (1.78 pu)	582.8kV (1.78 pu)
	Turleenan – Kingscourt Kingscourt – Woodland	Kingscourt	621.3 kV (1.90 pu) [Turleenan side]	629.6 kV (1.93 pu) [Turleenan side]
	Kingscourt – Woodland	Woodland	471.6 kV (1.44 pu)	471.6 kV (1.44 pu)
Ratio 30% (K-end)	Turleenan – Kingscourt	Turleenan	494.4 kV (1.51 pu)	494.4 kV (1.51 pu)
	Turleenan – Kingscourt Kingscourt – Woodland	Kingscourt	637.4 kV (1.95 pu) [Turleenan side]	637.4 kV (1.95 pu) [Turleenan side]
	Kingscourt – Woodland	Woodland	495.9 kV (1.52 pu)	495.9 kV (1.52 pu)

Pattern No.	Assumed Line Outage	Fault on	Overvoltage	
			At the end of the line	Highest value along the line
Ratio 30% (Center)	Turleenan – Kingscourt	Turleenan	477.1 kV (1.46 pu)	487.3kV (1.49 pu)
	Turleenan – Kingscourt Kingscourt – Woodland	Kingscourt	591.9 kV (1.81 pu) [Turleenan side]	592.4 kV (1.81 pu) [Turleenan side]
	Kingscourt – Woodland	Woodland	474.0 kV (1.45 pu)	474.0 kV (1.45 pu)

$$* : 1\ PU = \ 400kV\ /\ \sqrt{3}\ *\ \sqrt{2}$$

As can be seen from the theoretical overvoltage equation, the magnitude depends on the value of the equivalent source impedance.   As stated in 4.1, the generators included in the simulation model are fewer than those in service in summer off-peak power flow data.   An adjustment of the fault current level can be achieved by adding a dummy source with different source impedances. Based on the fault current calculation result, the source impedance value was varied as shown in Table 4.1.

In the NIE/EirGrid network, the value of the source impedance is affected by the number of distributed generators operating in the network, and it is not easy to control this source impedance to lower the oscillatory overvoltage.   In order to find the sensitivity of the overvoltage to the source impedance, the time domain simulation was performed with different source impedances shown in Table 4.5 to Table 4.8.

Table 4.5 Overvoltage Caused by System Islanding (at the end of the line)
(cable ratio 60 % at Kingscourt end)

Pattern No.	Fault on	Additional Source Impedance [mH]			Overvoltage [kV] (PU) at the end of line
		Turleenan	Kingscourt	Woodland	
K-60-1-1		20	40	20	459.3 (1.41)
K-60-1-2	Turleenan	**30**	**40**	**20**	**499.2 (1.53)**
K-60-1-3		40	40	20	495.5 (1.52)

Pattern No.	Fault on	Additional Source Impedance [mH]			Overvoltage [kV] (PU) at the end of line	
		Turleenan	Kingscourt	Woodland		
K-60-1-4	Turleenan	50	40	20	492.9 (1.51)	
K-60-1-5		30	50	20	453.0 (1.39)	
K-60-1-6		30	60	20	447.5 (1.37)	
K-60-1-7		30	40	30	446.0 (1.37)	
K-60-1-8		30	40	40	430.9 (1.32)	
K-60-1-9		30	40	50	425.8 (1.30)	
K-60-1-10		30	40	60	428.8 (1.31)	
	Kingscourt				[Turleenan side]	[Woodland side]
K-60-2-1		**20**	**40**	**20**	**731.9 (2.24)**	**403.2 (1.23)**
K-60-2-2		30	40	20	711.1 (2.18)	393.0 (1.20)
K-60-2-3		40	40	20	698.7 (2.14)	389.0 (1.19)
K-60-2-4		50	40	20	680.7 (2.08)	384.5 (1.18)
K-60-2-5		20	50	20	728.0 (2.23)	400.3 (1.23)
K-60-2-6		20	60	20	724.5 (2.22)	398.8 (1.22)
K-60-2-7		20	40	30	730.5 (2.24)	365.6 (1.12)
K-60-2-8		20	40	40	730.0 (2.24)	368.3 (1.13)
K-60-2-9		20	40	50	728.8 (2.23)	356.9 (1.09)
K-60-2-10		20	40	60	727.9 (2.23)	348.5 (1.07)
K-60-3-1	Woodland	20	40	20	392.0 (1.20)	
K-60-3-2		30	40	20	438.5 (1.34)	
K-60-3-3		**40**	**40**	**20**	**458.3 (1.40)**	

Pattern No.	Fault on	Additional Source Impedance [mH]			Overvoltage [kV] (PU) at the end of line
		Turleenan	Kingscourt	Woodland	
K-60-3-4	Woodland	50	40	20	409.9 (1.26)
K-60-3-5		40	50	20	440.6 (1.35)
K-60-3-6		40	60	20	419.0 (1.28)
K-60-3-7		40	40	30	452.3 (1.38)
K-60-3-8		40	40	40	447.0 (1.37)
K-60-3-9		40	40	50	442.5 (1.35)
K-60-3-10		40	40	60	438.9 (1.34)

$* : 1\ PU = \ 400kV / \sqrt{3} * \sqrt{2}$

Table 4.6 Overvoltage Caused by System Islanding (at the end of the line)

(cable ratio 60 % at Center)

Pattern No.	Fault on	Additional Source Impedance [mH]			Overvoltage [kV] (PU) at the end of line
		Turleenan	Kingscourt	Woodland	
C-60-1-1	Turleenan	**20**	**40**	**20**	**580.7 (1.78)**
C-60-1-2		30	40	20	569.2 (1.74)
C-60-1-3		40	40	20	563.1 (1.72)
C-60-1-4		50	40	20	559.0 (1.71)
C-60-1-5		20	50	20	578.5 (1.77)
C-60-1-6		20	60	20	579.4 (1.77)

Pattern No.	Fault on	Additional Source Impedance [mH]			Overvoltage [kV] (PU) at the end of line	
		Turleenan	Kingscourt	Woodland		
C-60-1-7	Turleenan	20	40	30	565.7 (1.73)	
C-60-1-8		20	40	40	552.1 (1.69)	
C-60-1-9		20	40	50	543.6 (1.66)	
C-60-1-10		20	40	60	535.6 (1.64)	
	Kingscourt				[Turleenan side]	[Woodland side]
C-60-2-1		**20**	**40**	**20**	**621.3 (1.90)**	**407.4 (1.25)**
C-60-2-2		30	40	20	585.6 (1.79)	399.5 (1.22)
C-60-2-3		40	40	20	580.3 (1.78)	394.8 (1.21)
C-60-2-4		50	40	20	601.6 (1.84)	387.2 (1.19)
C-60-2-5		60	40	20	599.2 (1.83)	389.1 (1.19)
C-60-2-6		20	50	20	617.6 (1.89)	403.7 (1.24)
C-60-2-7		20	60	20	615.1 (1.88)	402.7 (1.23)
C-60-2-8		20	40	30	619.6 (1.90)	371.0(1.14)
C-60-2-9		20	40	40	619.1 (1.90)	374.3 (1.15)
C-60-2-10		20	40	50	617.9 (1.89)	365.7 (1.12)
C-60-2-11		20	40	60	617.1 (1.89)	358.8 (1.10)
C-60-3-1	Woodland	20	40	20	410.1 (1.26)	
C-60-3-2		**30**	**40**	**20**	**471.6 (1.44)**	
C-60-3-3		40	40	20	428.7 (1.31)	
C-60-3-4		50	40	20	430.1 (1.32)	
C-60-3-5		30	50	20	464.5 (1.42)	

Pattern No.	Fault on	Additional Source Impedance [mH]			Overvoltage [kV] (PU) at the end of line
		Turleenan	Kingscourt	Woodland	
C-60-3-6	Woodland	30	60	20	450.1 (1.38)
C-60-3-7		30	40	30	466.6 (1.43)
C-60-3-8		30	40	40	462.5 (1.42)
C-60-3-9		30	40	50	460.1 (1.41)
C-60-3-10		30	40	60	458.3 (1.40)

* : 1 PU = 400kV / $\sqrt{3}$ * $\sqrt{2}$

Table 4.7 Overvoltage Caused by System Islanding (at the end of the line)

(cable ratio 30 % at Kingscourt end)

Pattern No.	Fault on	Additional Source Impedance [mH]			Overvoltage [kV] (PU) at the end of line	
		Turleenan	Kingscourt	Woodland		
K-30-1-1	Turleenan	20	40	20	479.2 (1.47)	
K-30-1-2		20	50	20	476.4 (1.46)	
K-30-1-3		20	60	20	476.1 (1.46)	
K-30-1-4		20	60	30	473.4 (1.45)	
K-30-1-5		**20**	**60**	**40**	**494.4 (1.51)**	
K-30-1-6		20	60	50	484.3 (1.48)	
K-30-1-7		20	60	60	472.4 (1.45)	
K-30-1-8		30	60	40	482.7 (1.48)	
K-30-1-9		40	60	40	480.2 (1.47)	
K-30-1-10		50	60	40	474.9 (1.45)	
K-30-1-11		20	40	40		
K-30-1-12		20	50	40	481.0 (1.47)	
					[Turleenan side]	[Woodland side]
K-30-2-1	Kingscourt	**20**	**40**	**20**	636.6 (1.95)	**411.8 (1.26)**
K-30-2-2		**30**	**40**	**20**	**637.4 (1.95)**	387.4 (1.19)
K-30-2-3		40	40	20	631.4 (1.93)	393.3 (1.20)
K-30-2-4		50	40	20	612.2 (1.87)	385.7 (1.18)
K-30-2-5		20	50	20	633.9 (1.94)	409.1 (1.25)
K-30-2-6		20	60	20	630.8 (1.93)	408.4 (1.25)

Pattern No.	Fault on	Additional Source Impedance [mH]			Overvoltage [kV] (PU) at the end of line	
		Turleenan	Kingscourt	Woodland		
K-30-2-6	Kingscourt	30	50	20	629.8 (1.93)	392.8 (1.20)
K-30-2-7		30	60	20	622.4 (1.91)	392.6 (1.20)
K-30-2-8		30	40	30	634.5 (1.94)	374.8 (1.15)
K-30-2-9		30	40	40	631.8 (1.93)	369.0 (1.13)
K-30-2-10		30	40	50	629.5 (1.93)	368.3 (1.13)
K-30-2-11		20	40	60	632.9 (1.94)	372.8 (1.14)
K-30-3-1	Woodland	20	40	20	454.8 (1.39)	
K-30-3-2		30	40	20	487.5 (1.49)	
K-30-3-3		40	40	20	480.8 (1.47)	
K-30-3-4		50	40	20	467.2 (1.43)	
K-30-3-5		20	50	20	450.8 (1.38)	
K-30-3-6		**30**	**50**	**20**	**495.9 (1.52)**	
K-30-3-7		40	50	20	475.6 (1.46)	
K-30-3-8		50	50	20	430.8 (1.32)	
K-30-3-9		30	60	20	487.7 (1.49)	
K-30-3-10		30	50	30	487.2 (1.49)	
K-30-3-11		30	50	40	481.8 (1.48)	
K-30-3-12		30	50	50	477.9 (1.46)	

$* : 1 \text{ PU} = 400\text{kV} / \sqrt{3} * \sqrt{2}$

Table 4.8 Overvoltage Caused by System Islanding (at the end of the line)
(cable ratio 30 % at Center)

Pattern No.	Fault on	Additional Source Impedance [mH]			Overvoltage [kV] (PU) at the end of line	
		Turleenan	Kingscourt	Woodland		
C-30-1-1		20	40	20	458.6 (1.40)	
C-30-1-2		20	40	30	458.8 (1.40)	
C-30-1-3		20	40	40	465.3 (1.42)	
C-30-1-4		20	40	50	465.2 (1.42)	
C-30-1-5		20	40	60	473.9 (1.45)	
C-30-1-6		30	40	60	462.7 (1.42)	
C-30-1-7		**40**	**40**	**60**	**477.1 (1.46)**	
C-30-1-8	Turleenan	50	40	60	471.8 (1.44)	
C-30-1-9		40	50	60	435.7 (1.33)	
C-30-1-10		40	60	60	415.2 (1.27)	
C-30-1-11		40	40	20	446.6 (1.37)	
C-30-1-12		40	40	30	452.0 (1.38)	
C-30-1-13		40	40	40	455.1 (1.39)	
C-30-1-14		40	40	50	459.1 (1.41)	
					[Turleenan side]	[Woodland side]
C-30-2-1		**20**	**40**	**20**	482.5 (1.48)	**414.4 (1.27)**
C-30-2-2	Kingscourt	20	40	30	481.6 (1.47)	378.9 (1.16)
C-30-2-3		20	40	40	481.3 (1.47)	382.5 (1.17)
C-30-2-4		20	40	50	481.4 (1.47)	375.8 (1.15)

Pattern No.	Fault on	Additional Source Impedance [mH]			Overvoltage [kV] (PU) at the end of line	
		Turleenan	Kingscourt	Woodland		
C-30-2-5		20	40	60	481.5 (1.47)	368.9 (1.13)
C-30-2-6		20	50	20	480.1 (1.47)	412.1 (1.26)
C-30-2-7		20	60	20	479.4 (1.47)	410.5 (1.26)
C-30-2-8		30	60	20	562.3 (1.72)	402.6 (1.23)
C-30-2-9		**30**	**60**	**30**	**591.9 (1.81)**	373.7 (1.14)
C-30-2-10		30	60	40	587.4 (1.80)	378.4 (1.16)
C-30-2-11	Kingscourt	30	60	50	583.2 (1.79)	369.5 (1.13)
C-30-2-12		30	60	60	579.9 (1.78)	364.0 (1.11)
C-30-2-13		30	40	30	571.5 (1.75)	371.9 (1.14)
C-30-2-14		30	50	30	564.4 (1.73)	368.9 (1.13)
C-30-2-15		20	60	30	478.3 (1.46)	373.8 (1.14)
C-30-2-16		40	60	30	500.3 (1.53)	376.8 (1.15)
C-30-2-17		50	60	30	488.0 (1.49)	373.6 (1.14)
C-30-3-1		20	40	20	464.2 (1.42)	
C-30-3-2		20	50	20	469.5 (1.44)	
C-30-3-3		**20**	**60**	**20**	**474.0 (1.45)**	
C-30-3-4	Woodland	20	60	30	467.3 (1.43)	
C-30-3-5		20	60	40	462.7 (1.42)	
C-30-3-6		20	60	50	459.4 (1.41)	
C-30-3-7		20	60	60	457.0 (1.40)	
C-30-3-8		30	60	20	467.1 (1.43)	

Pattern No.	Fault on	Additional Source Impedance [mH]			Overvoltage [kV] (PU) at the end of line
		Turleenan	Kingscourt	Woodland	
C-30-3-9	Woodland	40	60	20	445.7 (1.36)
C-30-3-10		50	60	20	459.9 (1.41)

* : 1 PU = 400kV / $\sqrt{3}$ * $\sqrt{2}$

The highest overvoltage at the end of the line was observed in Pattern K-60-2-1, with the fault on Kingscourt. Fig. 4.23 shows the result of the analysis with Pattern K-60-2-1. This overvoltage is not a concern in operation as it is damped in a few cycles.
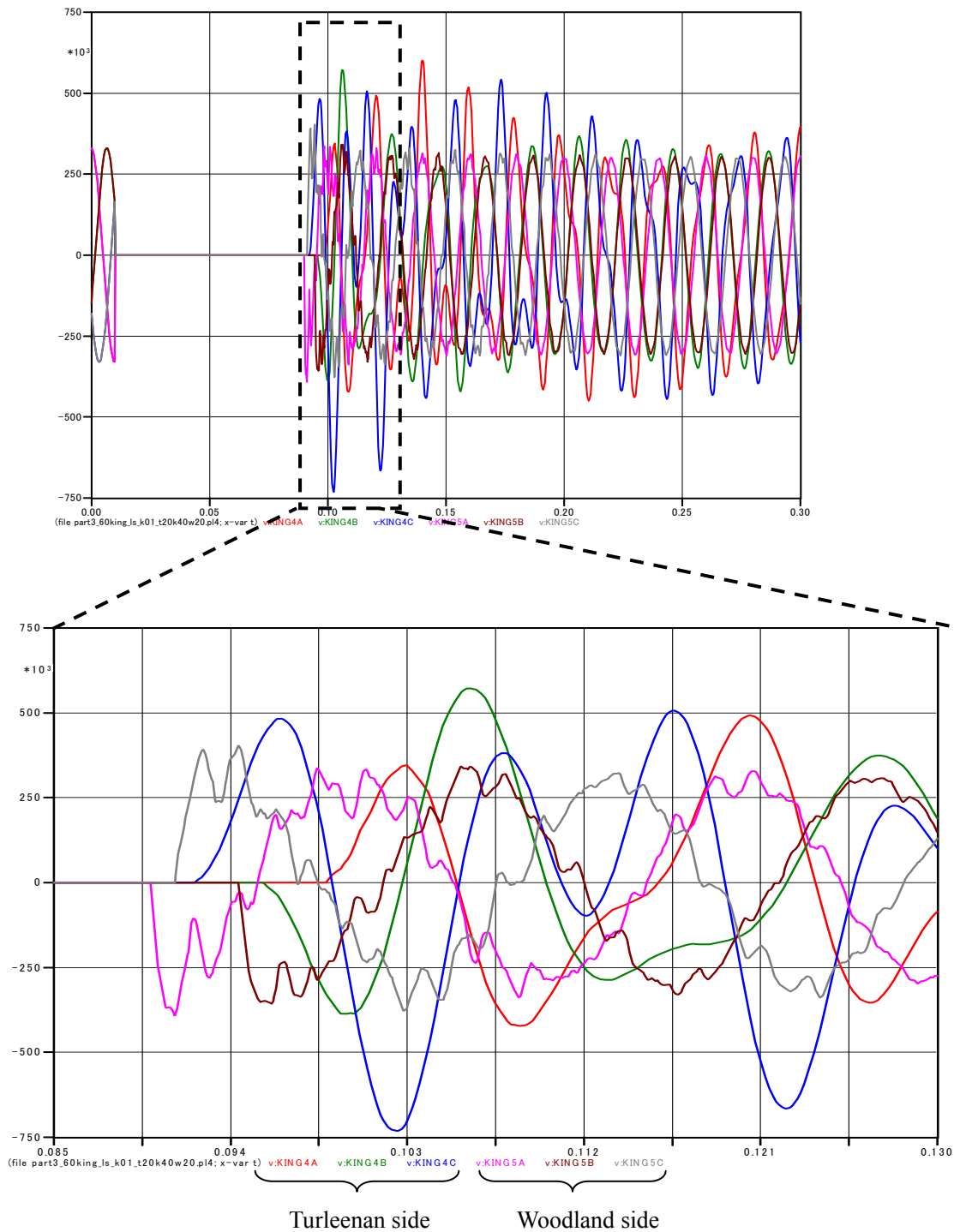
Fig. 4.23 Overvoltage caused by system islanding in Pattern K-60-2-1.

The highest overvoltage along the Turleenan – Kingscourt line in Pattern K-60-2-1 was observed at the next point to Kingscourt.　Fig. 4.24 shows the result of the maximum overvoltage in the Turleenan – Kingscourt line in Pattern K-60-2-1.
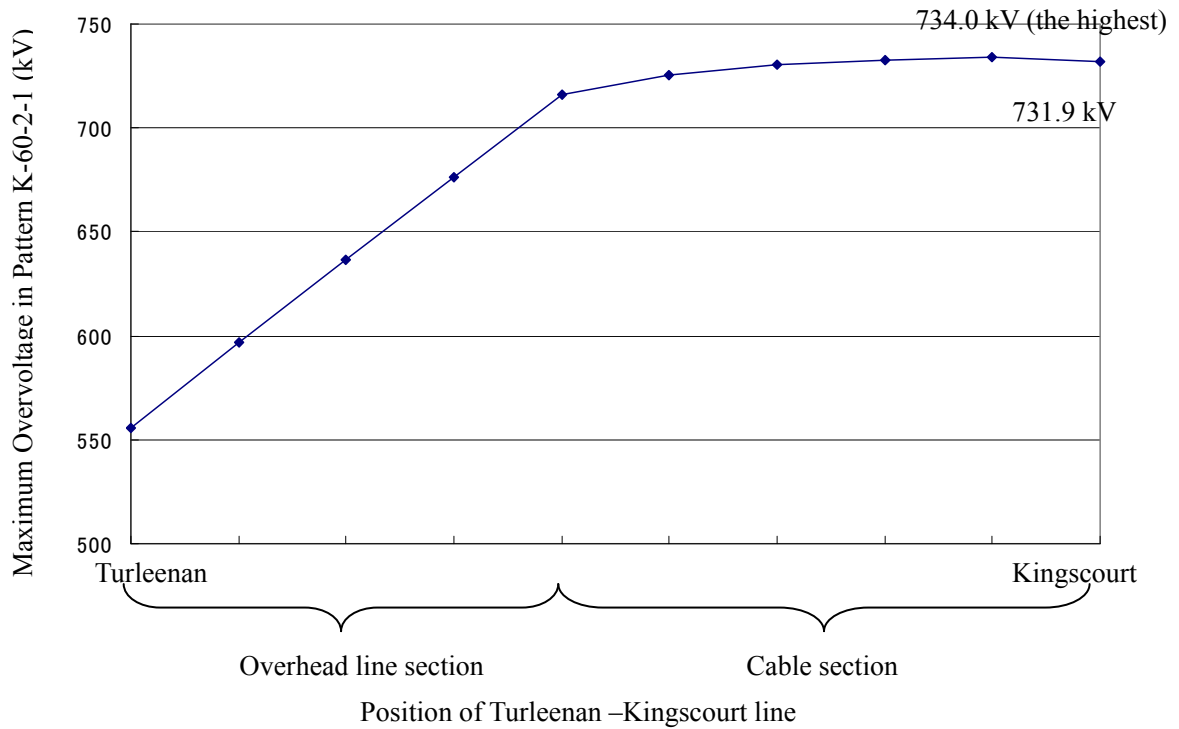
Fig. 4.24 Overvoltage caused by system islanding in Pattern K-60-2-1 (Turleenan side).

4.3.2   Overvoltage studies under additional conditions

The following more severe additional conditions are also studied with the overvoltage caused by system islanding for reference.   These additional cases were calculated with the three pattern of additional equivalent source impedance, "low pattern", "middle pattern" and "high pattern".   The each pattern of the source impedance is shown in Table 4.9.   The highest observed overvoltage at the end of the line in each network condition is summarized from Table 4.10 to Table 4.17.

a) Base condition (the detail study result was described in 4.3.1)

b) No load in Kingscourt substation (the switches of primary side of transformers are opened in the initial condition)

c) The 400 kV transformers at Woodland, Kingscourt and Turleenan are tripped together with the 400 kV cables at the same time. (shown in Fig. 4.25)

d) The 400 kV transformers at Kingscourt are disconnected from the 400 kV bus in the initial condition as in b).   In addition, the 400 kV transformers at Woodland and Turleenan are tripped together with 400 kV cables as in c).

Note: The condition c) assumes transformers are connected to the same bus (faulted bus) as the 400 kV cables.   In contrast, in the condition a) (base condition), the 400 kV transformers are not tripped, which assumes transformers are not connected to the faulted bus.

In condition d), the 400 kV transformer at Kingscourt is not tripped together with 400 kV cables since it is already opened in the initial condition.

Fig. 4.25 Additional condition of transformer trip (example of a fault at the Woodland bus).

Table 4.9 Overvoltage Caused by System Islanding under Additional Conditions

source impedance pattern	additional impedance (mH)		
	Turleenan	Kingscourt	Woodland
low	20	40	20
middle	35	50	40
high	50	60	60

Table 4.10 Overvoltage Caused by System Islanding under Additional Conditions (Summary)

(cable ratio 60 % at Kingscourt end)

Case	Source impedance pattern	Assumed Line Outage	Fault on	Overvoltage at the end of the line
K-60-a	low	Turleenan – Kingscourt Kingscourt – Woodland	Kingscourt	731.9 kV (2.24 pu) [Turleenan side]
K-60-b	low	Turleenan – Kingscourt Kingscourt – Woodland	Kingscourt	771.0 kV (2.36 pu) [Turleenan side]
K-60-c	low	Turleenan – Kingscourt Kingscourt – Woodland	Kingscourt	768.3 kV (2.35 pu) [Turleenan side]
K-60-d	low	Turleenan – Kingscourt Kingscourt – Woodland	Kingscourt	771.0 kV (2.36 pu) [Turleenan side]

＊ : 1 PU = 400kV / $\sqrt{3}$ ＊ $\sqrt{2}$

Table 4.11 Overvoltage Caused by System Islanding under Additional Conditions (Summary)

(cable ratio 60 % at Center)

Case	Source impedance pattern	Assumed Line Outage	Fault on	Overvoltage at the end of the line
C-60-a	low	Turleenan – Kingscourt Kingscourt – Woodland	Kingscourt	621.3 kV (1.90 pu) [Turleenan side]
C-60-b	high	Turleenan – Kingscourt Kingscourt – Woodland	Kingscourt	674.0 kV (2.06 pu) [Turleenan side]
C-60-c	high	Turleenan – Kingscourt Kingscourt – Woodland	Kingscourt	657.3 kV (2.01 pu) [Turleenan side]
C-60-d	low	Turleenan – Kingscourt	Turleenan	702.7 kV (2.15 pu)

$* : 1\ PU = 400kV / \sqrt{3} * \sqrt{2}$

Table 4.12 Overvoltage Caused by System Islanding under Additional Conditions (Summary)

(cable ratio 30 % at Kingscourt end)

Case	Source impedance pattern	Assumed Line Outage	Fault on	Overvoltage at the end of the line
K-30-a	low	Turleenan – Kingscourt Kingscourt – Woodland	Kingscourt	636.6 kV (1.95 pu) [Turleenan side]
K-30-b	middle	Turleenan – Kingscourt Kingscourt – Woodland	Kingscourt	683.9 kV (2.09 pu) [Turleenan side]
K-30-c	high	Turleenan – Kingscourt Kingscourt – Woodland	Kingscourt	664.5 kV (2.03 pu) [Turleenan side]
K-30-d	middle	Turleenan – Kingscourt Kingscourt – Woodland	Kingscourt	683.9 kV (2.09 pu) [Turleenan side]

$* : 1\ PU = 400kV / \sqrt{3} * \sqrt{2}$

Table 4.13 Overvoltage Caused by System Islanding under Additional Conditions (Summary)

(cable ratio 30 % at Center)

Case	Source impedance pattern	Assumed Line Outage	Fault on	Overvoltage at the end of the line
C-30-a	middle	Turleenan – Kingscourt Kingscourt – Woodland	Kingscourt	581.5 kV (1.78 pu) [Turleenan side]
C-30-b	middle	Turleenan – Kingscourt	Turleenan	604.1 kV (1.85 pu) [Turleenan side]
C-30-c	high	Turleenan – Kingscourt Kingscourt – Woodland	Kingscourt	644.1 kV (1.97 pu) [Turleenan side]
C-30-d	middle	Turleenan – Kingscourt	Turleenan	647.9 kV (1.98 pu)

$$* : 1\ PU = 400kV / \sqrt{3} * \sqrt{2}$$

Table 4.14 Overvoltage Caused by System Islanding under Additional Conditions

(cable ratio 60 % at Kingscourt end)

Case	Source impedance pattern	Assumed Line Outage	Fault on	Overvoltage [kV] (pu) at the end of line	
K-60-a	low	Turleenan – Kingscourt	Turleenan	459.3 (1.41)	
	middle			425.2 (1.30)	
	high			425.0 (1.30)	
		Turleenan – Kingscourt Kingscourt – Woodland	Kingscourt	[Turleenan side]	[Woodland side]
	low			731.9 (2.24)	403.2 (1.23)
	middle			696.2 (2.13)	353.3 (1.08)
	high			658.9 (2.02)	347.5 (1.06)
	low	Kingscourt – Woodland	Woodland	392.0 (1.20)	
	middle			448.0 (1.37)	
	high			448.7 (1.37)	

Case	Source impedance pattern	Assumed Line Outage	Fault on	Overvoltage [kV] (pu) at the end of line	
K-60-b	low	Turleenan – Kingscourt	Turleenan	595.2 (1.82)	
	middle			535.5 (1.64)	
	high			497.1 (1.52)	
		Turleenan – Kingscourt Kingscourt – Woodland	Kingscourt	[Turleenan side]	[Woodland side]
	low			771.0 (2.36)	426.3 (1.31)
	middle			765.0 (2.34)	389.6 (1.19)
	high			744.9 (2.28)	392.1 (1.20)
	low	Kingscourt – Woodland	Woodland	514.7 (1.58)	
	middle			473.3 (1.45)	
	high			478.1 (1.46)	
K-60-c	low	Turleenan – Kingscourt	Turleenan	483.2 (1.48)	
	middle			493.0 (1.51)	
	high			513.5 (1.57)	
		Turleenan – Kingscourt Kingscourt – Woodland	Kingscourt	[Turleenan side]	[Woodland side]
	low			768.3 (2.35)	412.8 (1.26)
	middle			759.5 (2.33)	399.0 (1.22)
	high			736.0 (2.25)	383.2 (1.17)
	low	Kingscourt – Woodland	Woodland	421.0 (1.29)	
	middle			489.9 (1.50)	
	high			520.5 (1.59)	
K-60-d	low	Turleenan – Kingscourt	Turleenan	616.4 (1.89)	
	middle			582.7 (1.78)	
	high			559.8 (1.71)	
		Turleenan – Kingscourt Kingscourt – Woodland	Kingscourt	[Turleenan side]	[Woodland side]
	low			771.0 (2.36)	426.3 (1.31)
	middle			765.0 (2.34)	389.6 (1.19)
	high			744.9 (2.28)	392.1 (1.20)

Case	Source impedance pattern	Assumed Line Outage	Fault on	Overvoltage [kV] (pu) at the end of line	
	low	Kingscourt – Woodland	Woodland	551.7 (1.69)	
	middle			526.7 (1.61)	
	high			565.4 (1.73)	

Table 4.15 Overvoltage Caused by System Islanding under Additional Conditions

(cable ratio 60 % at Center)

Case	Source impedance pattern	Assumed Line Outage	Fault on	Overvoltage [kV] (pu) at the end of line	
	low	Turleenan – Kingscourt	Turleenan	580.7 (1.78)	
	middle			532.2 (1.63)	
	high			495.3 (1.52)	
		Turleenan – Kingscourt Kingscourt – Woodland	Kingscourt	[Turleenan side]	[Woodland side]
	low			621.3 (1.90)	407.4 (1.25)
C-60-a	middle			570.7 (1.75)	360.9 (1.11)
	high			587.4 (1.80)	346.6 (1.06)
	low	Kingscourt – Woodland	Woodland	410.1 (1.26)	
	middle			426.5 (1.31)	
	high			424.5 (1.30)	
C-60-b	low	Turleenan – Kingscourt	Turleenan	666.8 (2.04)	
	middle			607.5 (1.86)	
	high			560.6 (1.72)	
		Turleenan – Kingscourt Kingscourt – Woodland	Kingscourt	[Turleenan side]	[Woodland side]
	low			658.1 (2.02)	431.3 (1.32)
	middle			628.4 (1.92)	396.9 (1.22)
	high			674.0 (2.06)	376.6 (1.15)

Case	Source impedance pattern	Assumed Line Outage	Fault on	Overvoltage [kV] (pu) at the end of line	
	low	Kingscourt – Woodland	Woodland	455.0 (1.39)	
	middle			483.7 (1.48)	
	high			433.7 (1.33)	
C-60-c	low	Turleenan – Kingscourt	Turleenan	631.6 (1.93)	
	middle			615.3 (1.88)	
	high			609.0 (1.86)	
		Turleenan – Kingscourt Kingscourt – Woodland	Kingscourt	[Turleenan side]	[Woodland side]
	low			653.4 (2.00)	416.3 (1.27)
	middle			614.9 (1.88)	401.4 (1.23)
	high			657.3 (2.01)	384.6 (1.18)
	low	Kingscourt – Woodland	Woodland	425.7 (1.30)	
	middle			471.1 (1.44)	
	high			504.7 (1.55)	
C-60-d	low	Turleenan – Kingscourt	Turleenan	702.7 (2.15)	
	middle			662.8 (2.03)	
	high			623.4 (1.91)	
		Turleenan – Kingscourt Kingscourt – Woodland	Kingscourt	[Turleenan side]	[Woodland side]
	low			658.1 (2.02)	431.3 (1.32)
	middle			628.4 (1.92)	396.9 (1.22)
	high			674.0 (2.06)	376.6 (1.15)
	low	Kingscourt – Woodland	Woodland	490.1 (1.50)	
	middle			539.5 (1.65)	
	high			497.9 (1.52)	

Table 4.16 Overvoltage Caused by System Islanding under Additional Conditions

(cable ratio 30 % at Kingscourt end)

Case	Source impedance pattern	Assumed Line Outage	Fault on	Overvoltage [kV] (pu) at the end of line	
K-30-a	low	Turleenan – Kingscourt	Turleenan	479.2 (1.47)	
	middle			480.2 (1.47)	
	high			442.4 (1.35)	
		Turleenan – Kingscourt Kingscourt – Woodland	Kingscourt	[Turleenan side]	[Woodland side]
	low			636.6 (1.95)	411.8 (1.26)
	middle			618.3 (1.89)	373.2 (1.14)
	high			589.5 (1.80)	352.8 (1.08)
	low	Kingscourt – Woodland	Woodland	454.8 (1.39)	
	middle			470.3 (1.44)	
	high			421.9 (1.29)	
K-30-b	low	Turleenan – Kingscourt	Turleenan	537.6 (1.65)	
	middle			498.9 (1.53)	
	high			414.5 (1.27)	
		Turleenan – Kingscourt Kingscourt – Woodland	Kingscourt	[Turleenan side]	[Woodland side]
	low			677.2 (2.07)	445.6 (1.36)
	middle			683.9 (2.09)	401.8 (1.23)
	high			675.8 (2.07)	417.1 (1.28)
	low	Kingscourt – Woodland	Woodland	469.8 (1.44)	
	middle			477.7 (1.46)	
	high			469.7 (1.44)	
K-30-c	low	Turleenan – Kingscourt	Turleenan	507.0 (1.55)	
	middle			522.4 (1.60)	
	high			513.9 (1.57)	

Case	Source impedance pattern	Assumed Line Outage	Fault on	Overvoltage [kV] (pu) at the end of line	
				[Turleenan side]	[Woodland side]
	low	Turleenan – Kingscourt Kingscourt – Woodland	Kingscourt	664.4 (2.03)	419.0 (1.28)
	middle			664.2 (2.03)	423.5 (1.30)
	high			664.5 (2.03)	394.8 (1.21)
	low	Kingscourt – Woodland	Woodland	491.1 (1.50)	
	middle			526.4 (1.61)	
	high			489.9 (1.50)	
K-30-d	low	Turleenan – Kingscourt	Turleenan	555.0 (1.70)	
	middle			479.1 (1.47)	
	high			488.1 (1.49)	
				[Turleenan side]	[Woodland side]
	low	Turleenan – Kingscourt Kingscourt – Woodland	Kingscourt	677.2 (2.07)	445.6 (1.36)
	middle			683.9 (2.09)	401.8 (1.23)
	high			675.8 (2.07)	417.1 (1.28)
	low	Kingscourt – Woodland	Woodland	503.0 (1.54)	
	middle			530.7 (1.62)	
	high			552.9 (1.69)	

Table 4.17 Overvoltage Caused by System Islanding under Additional Conditions

(cable ratio 30 % at Center)

Case	Source impedance pattern	Assumed Line Outage	Fault on	Overvoltage [kV] (pu) at the end of line
C-30-a	low	Turleenan – Kingscourt	Turleenan	458.6 (1.40)
	middle			464.3 (1.42)
	high			409.7 (1.25)

Case	Source impedance pattern	Assumed Line Outage	Fault on	Overvoltage [kV] (pu) at the end of line	
		Turleenan – Kingscourt Kingscourt – Woodland	Kingscourt	[Turleenan side]	[Woodland side]
	low			482.5 (1.48)	414.4 (1.27)
	middle			581.5 (1.78)	375.6 (1.15)
	high			574.7 (1.76)	358.6 (1.10)
	low	Kingscourt – Woodland	Woodland	464.2 (1.42)	
	middle			408.3 (1.25)	
	high			428.2 (1.31)	
C-30-b	low	Turleenan – Kingscourt	Turleenan	569.3 (1.74)	
	middle			604.1 (1.85)	
	high			530.3 (1.62)	
		Turleenan – Kingscourt Kingscourt – Woodland	Kingscourt	[Turleenan side]	[Woodland side]
	low			506.2 (1.55)	439.9 (1.35)
	middle			557.6 (1.71)	401.3 (1.23)
	high			558.5 (1.71)	387.3 (1.19)
	low	Kingscourt – Woodland	Woodland	470.6 (1.44)	
	middle			466.1 (1.43)	
	high			426.8 (1.31)	
C-30-c	low	Turleenan – Kingscourt	Turleenan	504.8 (1.55)	
	middle			530.7 (1.62)	
	high			520.6 (1.59)	
		Turleenan – Kingscourt Kingscourt – Woodland	Kingscourt	[Turleenan side]	[Woodland side]
	low			508.3 (1.56)	422.9 (1.29)
	middle			641.4 (1.96)	418.7 (1.28)
	high			644.1 (1.97)	407.0 (1.25)
	low	Kingscourt – Woodland	Woodland	506.1 (1.55)	
	middle			459.1 (1.41)	
	high			488.5 (1.50)	

Case	Source impedance pattern	Assumed Line Outage	Fault on	Overvoltage [kV] (pu) at the end of line	
C-30-d	low	Turleenan – Kingscourt	Turleenan	581.3 (1.78)	
	middle			647.9 (1.98)	
	high			589.0 (1.80)	
		Turleenan – Kingscourt Kingscourt – Woodland	Kingscourt	[Turleenan side]	[Woodland side]
	low			506.2 (1.55)	439.9 (1.35)
	middle			557.6 (1.71)	401.3 (1.23)
	high			558.5 (1.71)	387.3 (1.19)
	low	Kingscourt – Woodland	Woodland	501.4 (1.54)	
	middle			518.1 (1.59)	
	high			488.5 (1.50)	

The highest overvoltage at the end of the line was observed in case K-60-b (and K-60-d) and low impedance pattern, with the fault on Kingscourt.   Fig. 4.26 shows the result of the analysis in this case.   This overvoltage is not a concern in operation because it is damped in a few cycles and it can be evaluated by SIWV (1050 kV) due to its rapid decaying properties.
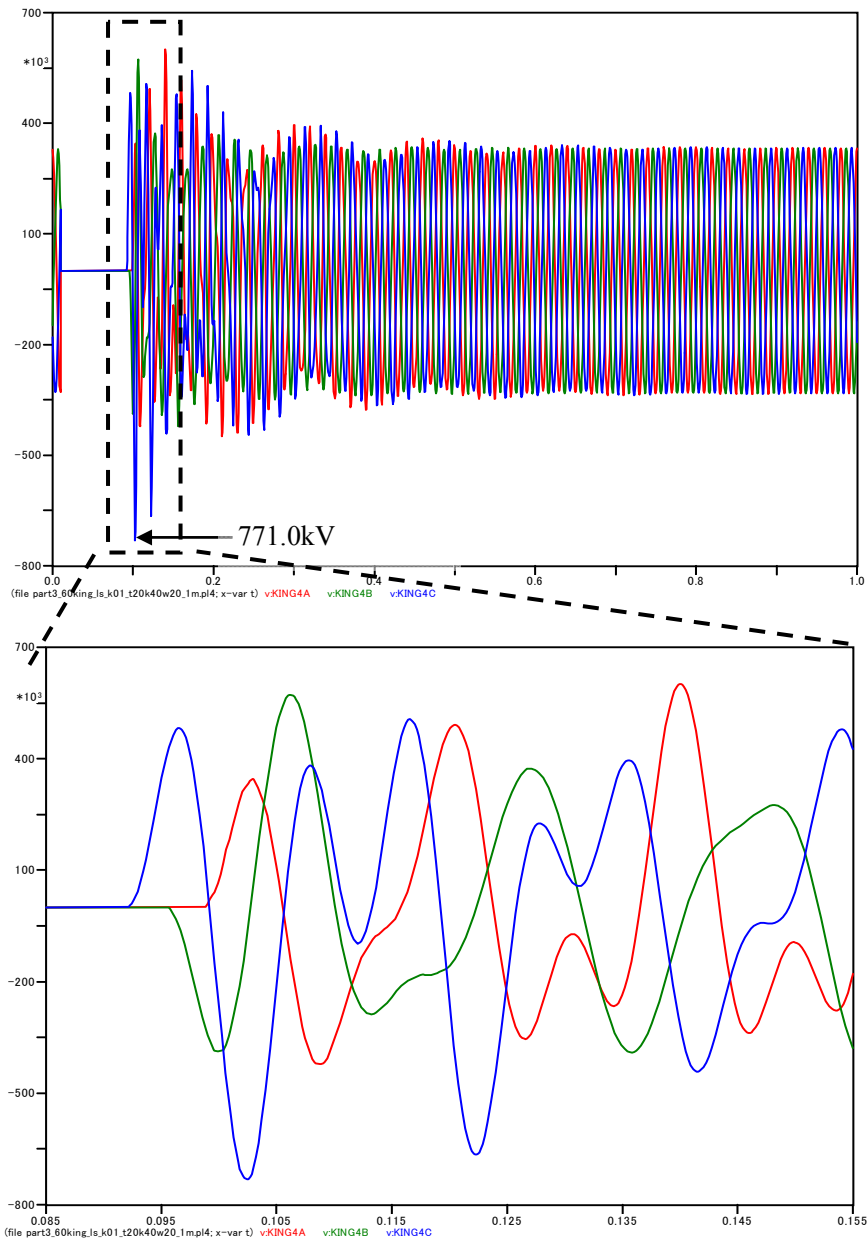
Fig. 4.26 Overvoltage caused by system islanding in case K-60-b and low impedance pattern.

4.4 Conclusion

The temporary overvoltage analysis was performed based on the compensation pattern determined by the reactive power compensation analysis. Resonance overvoltage and overvoltage caused by load shedding were studied under different network conditions.

No significant overvoltage was found in the parallel resonance overvoltage analysis. As in Part 1 and 2 studies, load sheddings yielded very high overvoltages, but this is not a concern for the safe operation of the network as it can be evaluated by SIWV (1050 kV) due to its rapid decaying properties.

Table 4-18   Summary of the Temporary Overvoltage Analysis

	Highest overvoltage (peak)	Withstand voltage for evaluation
Parallel resonance	500.5 kV (1.53 pu)	370 kV (r.m.s.) (1.60 pu) for 10 seconds
Load shedding	771.0 kV (2.36 pu)	1050 kV (peak)

$$1\,\mathrm{pu} = 400 \text{ or } 220\,\mathrm{kV} \times \frac{\sqrt{2}}{\sqrt{3}} \text{ (peak)}, 400 \text{ or } 220\,\mathrm{kV} \times \frac{1}{\sqrt{3}} \text{ (r.m.s.)}$$

Chapter 5 Overvoltage Caused by Autoreclose

When single phase autoreclose is applied to a mixed OHL / underground cable, it is necessary to study the overvoltage caused by autoreclose.   The conditions for single phase autoreclose are different from line energisation at the following points:

(1)   The cable is re-energised before the cable is discharged, and

(2)   Only the faulted phase is opened and re-energised.

Here, the condition (1) is true when a shunt reactor is directly connected to the line.   When a shunt reactor is not connected to the line, the cable will be discharged through the VTs, not through the shunt reactors.   In such a case, cable discharge is completed before the line is re-energised.

The overvoltage caused by single phase autoreclose can be higher than the overvoltage caused by line energisation because of condition (1).   For example, if the faulted phase has a negative residual voltage of -1.0 pu, a sudden voltage rise of 2.0 pu (from -1.0 pu to 1.0 pu) can be caused in the faulted phase when the cable is re-energised from the bus whose voltage is 1.0 pu.   In order to yield a severe condition:

- Timing of re-energisation has to be adjusted so that re-energisation occurs at the most severe timing, and

- Resistance of shunt reactors has to be small enough to have large residual voltage

However, at the same time, the overvoltage caused by autoreclose may be lower than the overvoltage caused by line energisation.   This is because circuit breakers on both sides of the line are reclosed simultaneously.   There is no open end terminal (total positive reflection point) after autoreclose even though there can be a few milliseconds time difference.

5.1 Simulation conditions

Overvoltage caused by single phase autoreclose was studied by switching scenarios shown in Fig. 5-1.   Statistical analysis was not applied since the timing of re-energisation was adjusted to the most severe timing.   In addition, it is not necessary to consider the close timing difference between these phases since only one faulted phase will be re-energised.   Note that the surge arrester is not considered in the simulations.
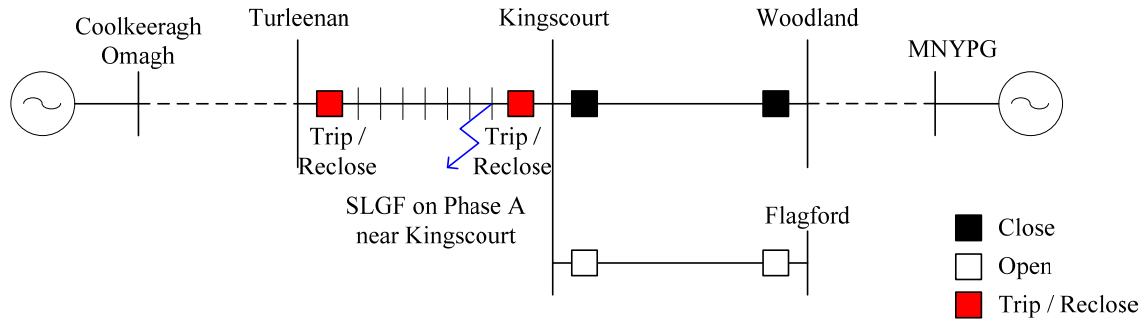
Fig. 5-1 Switching scenario for the overvoltage caused by autoreclose.

The simulations were performed under conditions in which 30 % or 60 % 400 kV 2 cct cables existed in the centre of the Turleenan – Kingscourt line. For the 60 % cable case, different locations of for the 400 kV shut reactors were also considered.
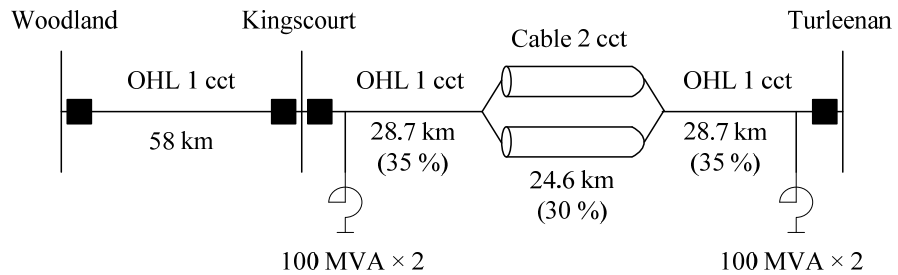
Case 1 - 30% 400kV cable in centre
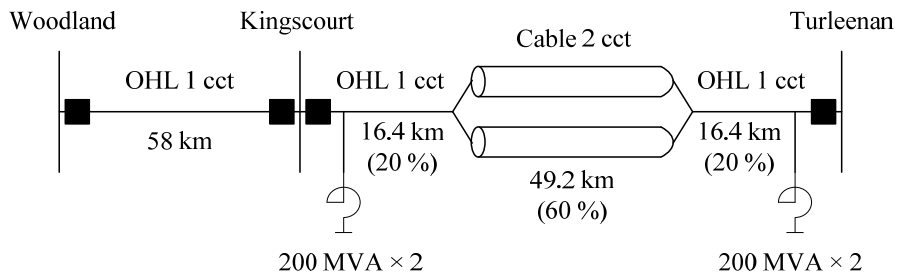
Case 2 - 60% 400kV cable in centre and 400 kV reactors at the line ends
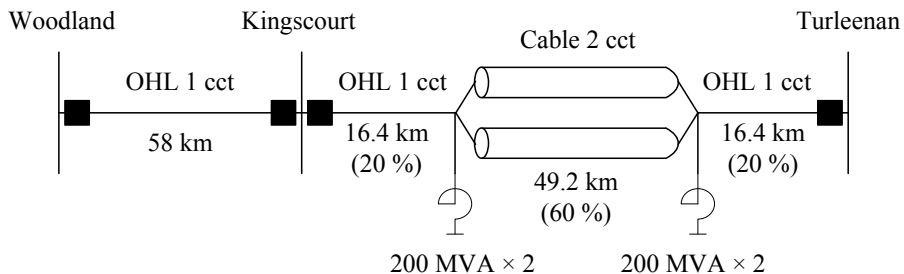
Case 3 - 60% 400kV cable in centre and 400 kV reactors at the cable ends

Fig. 5-2   System configuration of the simulations.

Table 5-1   Standard auto-reclose sequence

Step	Time	Description
Step 0	0 (ms)	Single phase fault (Phase A) on overhead line section near Kingscourt
Step 1	60 (ms)	Tripping CB (Phase A) of both sides
Step 2	60 + α (ms)	Fault clearing after tripping CB
Step 3	960 (ms)	Reclosing CB (Phase A) of both ends

Table 5-1 shows the standard sequence of autoreclose.   As described in the Part 2 study, the ground fault near Kingscourt yielded the largest overvoltage due to its large current through circuit breaker.   Hence, a ground fault in the overhead line section near Kingscourt was assumed in this study.

5.2 Residual Voltage in Typical Operation

Fig. 5-3 illustrates the residual voltage in Phase A (faulted phase) which was observed at Kingscourt in each case using the standard autoreclose sequence mentioned above.   As the line was fully compensated by shunt reactors directly connected to the cable, the waveform of voltage at the Turleenan side was almost equal to the Kingscourt side, and it contained two frequency components.

The peak residual voltages were observed during the first or second oscillatory voltage after the fault clearing.   The residual voltages decayed gradually through the shunt reactors on the cable, and the voltage at the reclosing timing became 2/3 of the one at the fault clearing.   The maximum and minimum residual voltages were recorded in Cases 1 and 3 respectively, but the difference between them was minute as shown in Fig. 5-3.
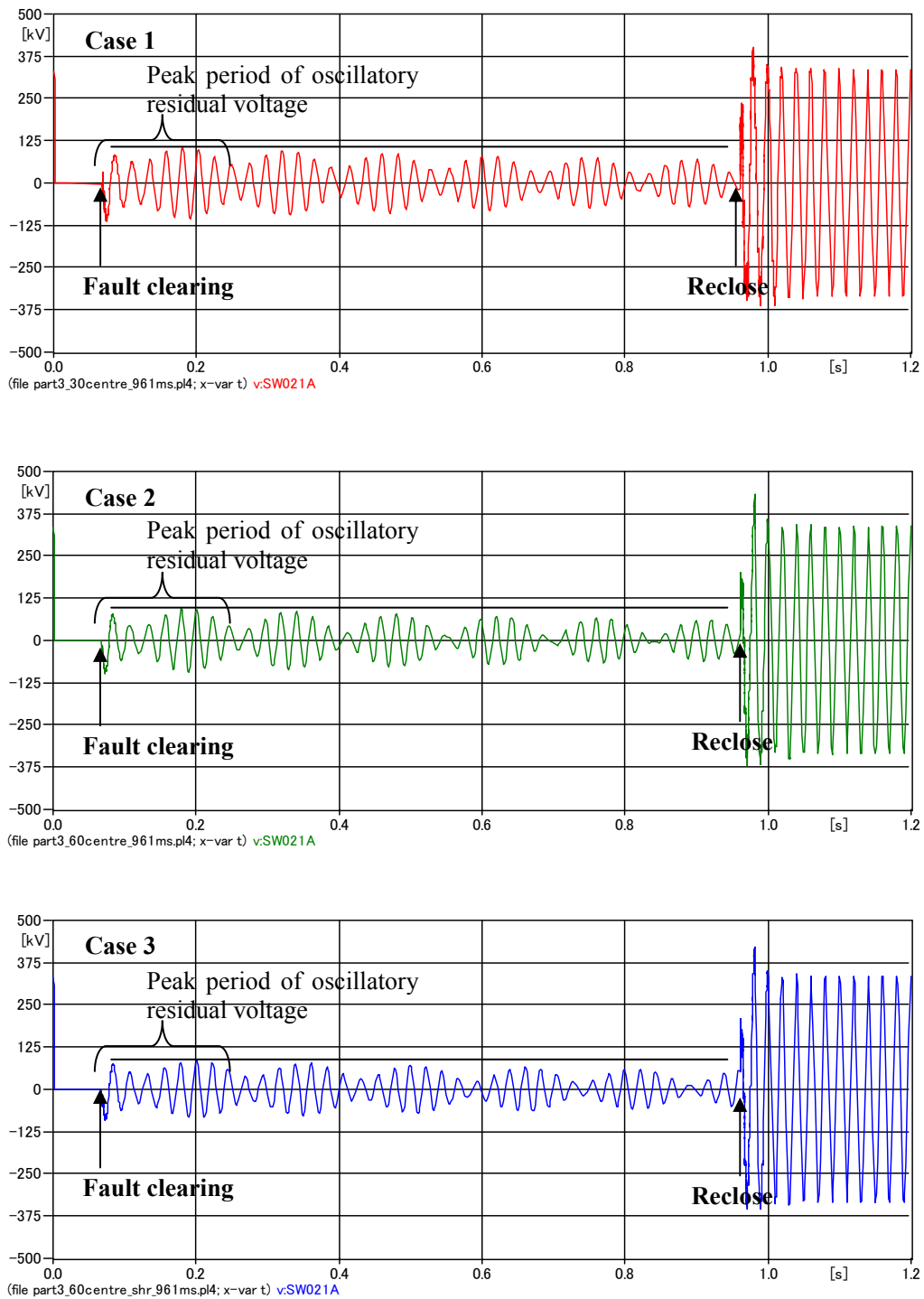
Fig. 5-3   Residual voltage in Phase A at Kingscourt in the standard operation.

5.3 Effect of Fault Clearing Timing on Residual Voltage

According to the NIE/EirGrid standard, the fault is cleared within 60 ms as shown in Table 5-1. During the actual power system operation, the fault is sometimes cleared earlier than 60 ms. Fig. 5-4 shows the current through circuit breakers of Kingscourt and Turleenan in Case 1. As can be seen from the figure, both circuits have 6-times of zero crossing points within 60 ms.
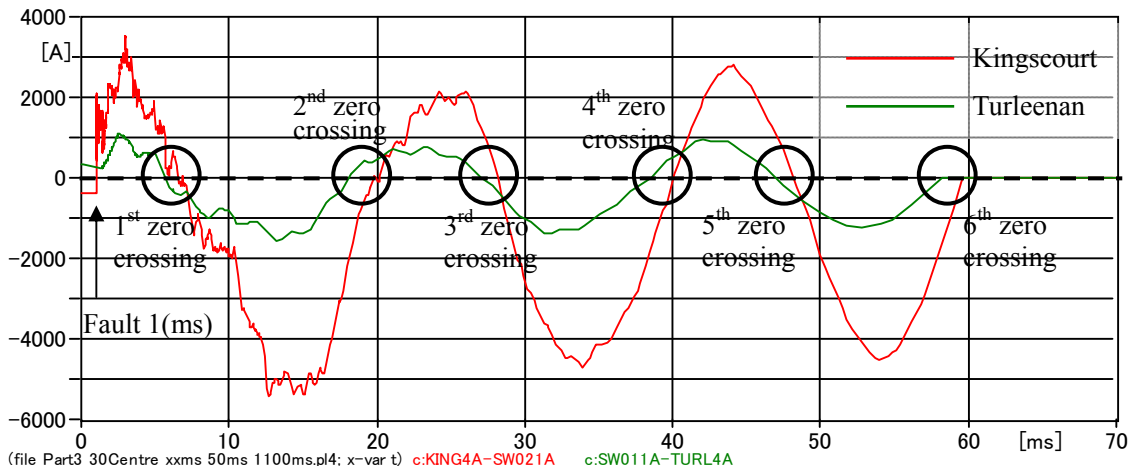
Fig. 5-4   Current through circuit breakers of Kingscourt and Turleenan.

In order to understand the effect of fault clearing timing on residual voltage, different fault clearing timings were studied as shown in Fig. 5-5 and Table 5-2. The figure shows the waveforms of residual voltage on the cable with different fault clearing timings.

It can be seen that the maximum residual voltage was observed when the fault was cleared at the first zero crossing. This is a typical result since a large amount of the surge components of the ground fault are included at the 1st and/or 2nd zero crossing periods and it decays fast. In order to consider severe overvoltage, this study assumed the fault clearing at the first zero crossing on the faulted phase and then the reclosing at the most severe timing before 900 ms.
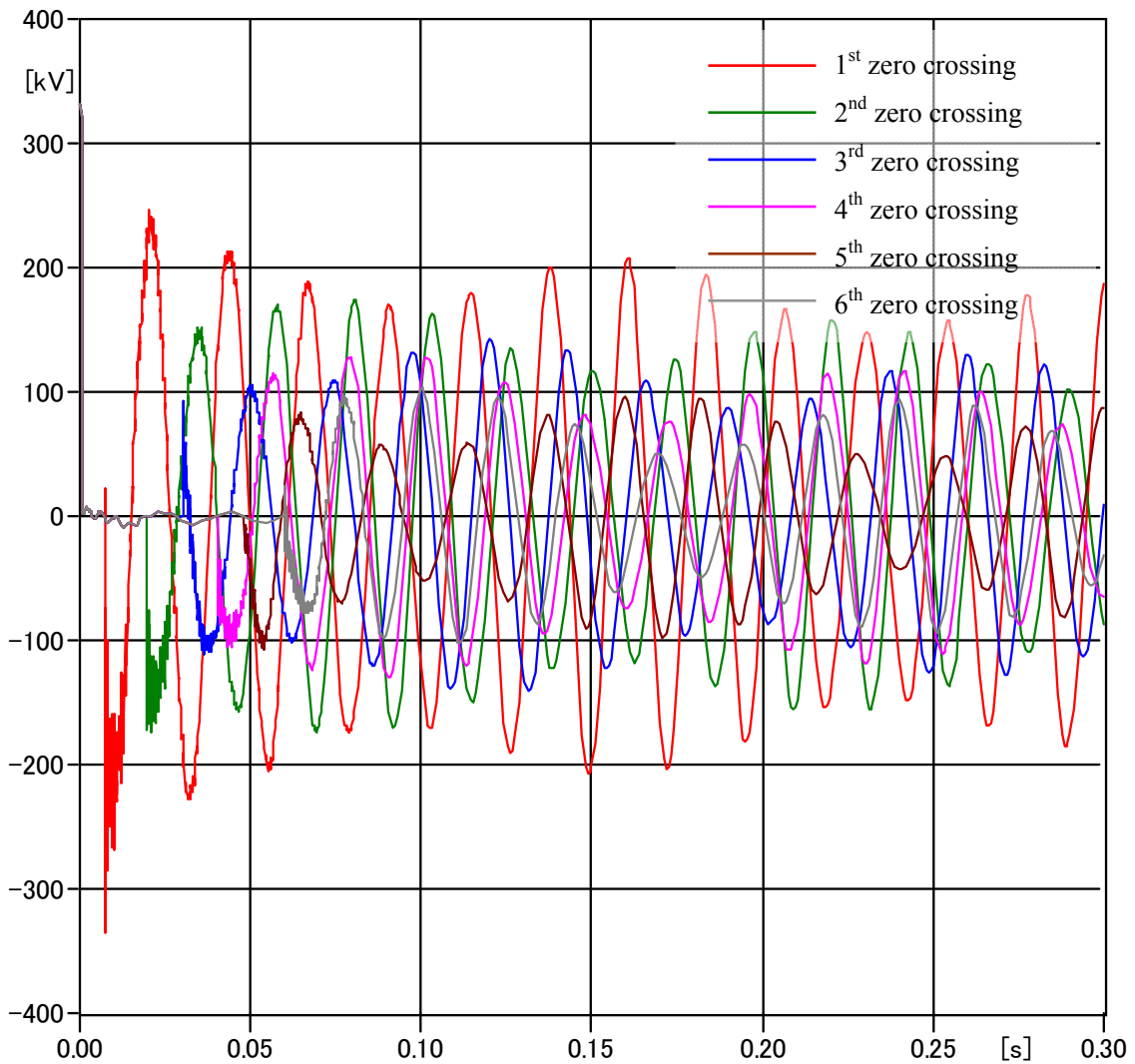
Fig. 5-5   Residual voltages by different fault clearing timings.

Table 5-2   Peak residual voltage for each fault clearing timing.

Fault clearing timings	Peak residual voltage
1st zero crossing	335 (kV)
2nd zero crossing	175 (kV)
3rd zero crossing	143 (kV)
4th zero crossing	131 (kV)
5th zero crossing	107 (kV)
6th zero crossing	104 (kV)

5.4 Reclosing Timing

In general, the switching overvoltage becomes large when the voltage difference between the two contacts of the circuit breaker (the system voltage at the bus against the residual voltage on the cable) is large.   As shown in Fig. 5-3, the residual voltage becomes oscillatory waveform by combination of cable capacitance and inductance of shut reactor, and it decays with time.

Fig. 5-6 illustrates the voltage between the circuit breaker contacts after the fault clearing. The peak voltage between the circuit breaker contacts appears periodically.   In this study, it was assumed that the line was reclosed at the second peak voltage between the circuit breaker contacts. This assumption was made in order to cause higher overvoltage, but it is not a realistic assumption since the line is reclosed 900 ms after the fault clearing in the actual operation according to the standard sequence.
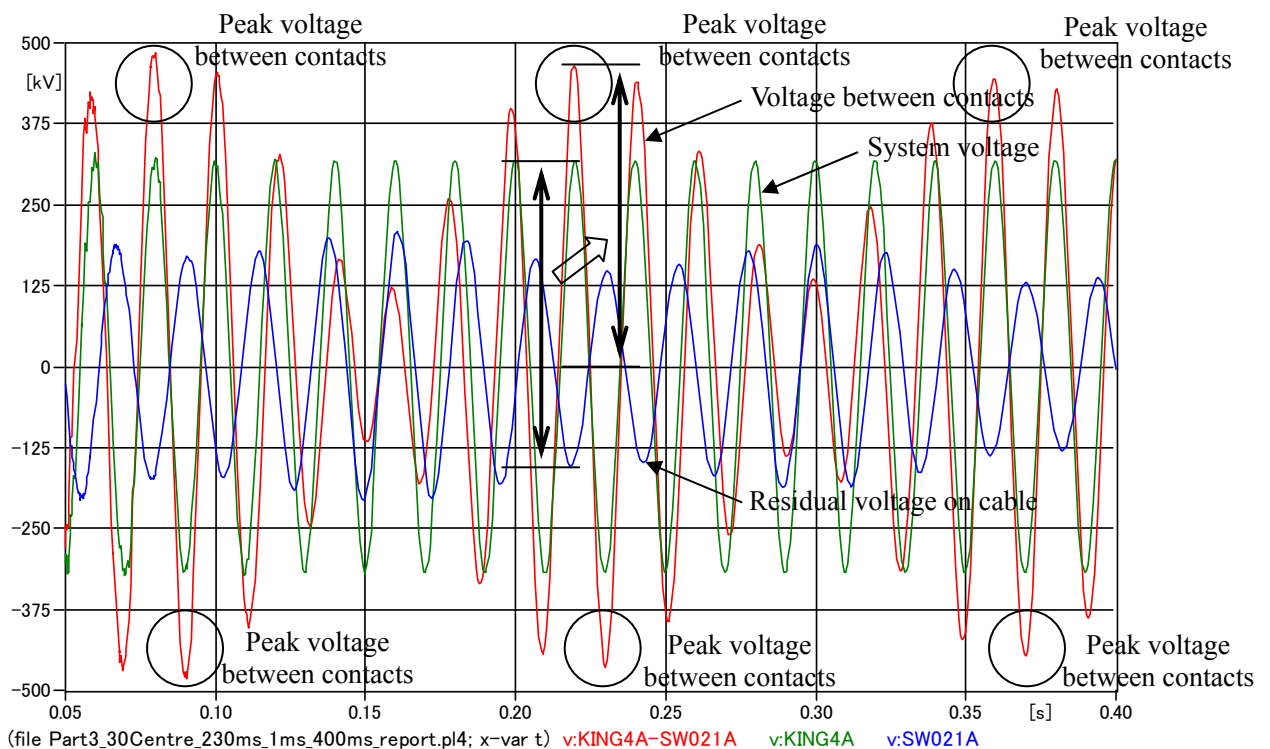
Fig. 5-6   Voltage between circuit breaker contacts

5.5 Simulation Results

The following table and figures show the simulation results.   The maximum overvoltage at each case was observed at Turleenan, but the waveforms of all the nodes along the cable line were approximately equal, as the 400 kV cables were compensated to around 100 %.

The maximum reclosing overvoltage was 523 kV in Case 3.   The overvoltage of 1.61 pu (= 523 kV) is far below SIWV of the 400 kV cable even without surge arresters.   The amount of the cable and the location of the shunt reactors did not significantly impact the overvoltage.

<div align="center">

Table 5-3   Simulated results

</div>

Items	Case 1	Case 2	Case 3
Cable amount	30% (centre)	60% (centre)	60% (centre)
Shut reactor location	Line ends	Line ends	Cable ends
Difference between circuit breaker contacts at reclosing (Kingscourt bus voltage and cable residual voltage)	463 (kV)	418 (kV)	445 (kV)
Maximum reclosing overvoltage	467 (kV)	505 (kV)	523 (kV)
Observed at	Turleenan	Turleenan	Turleenan

Waveform of the cable end at Turleenan

Fig. 5-7   Reclosing waveform at Turleenan – 30 % cable.
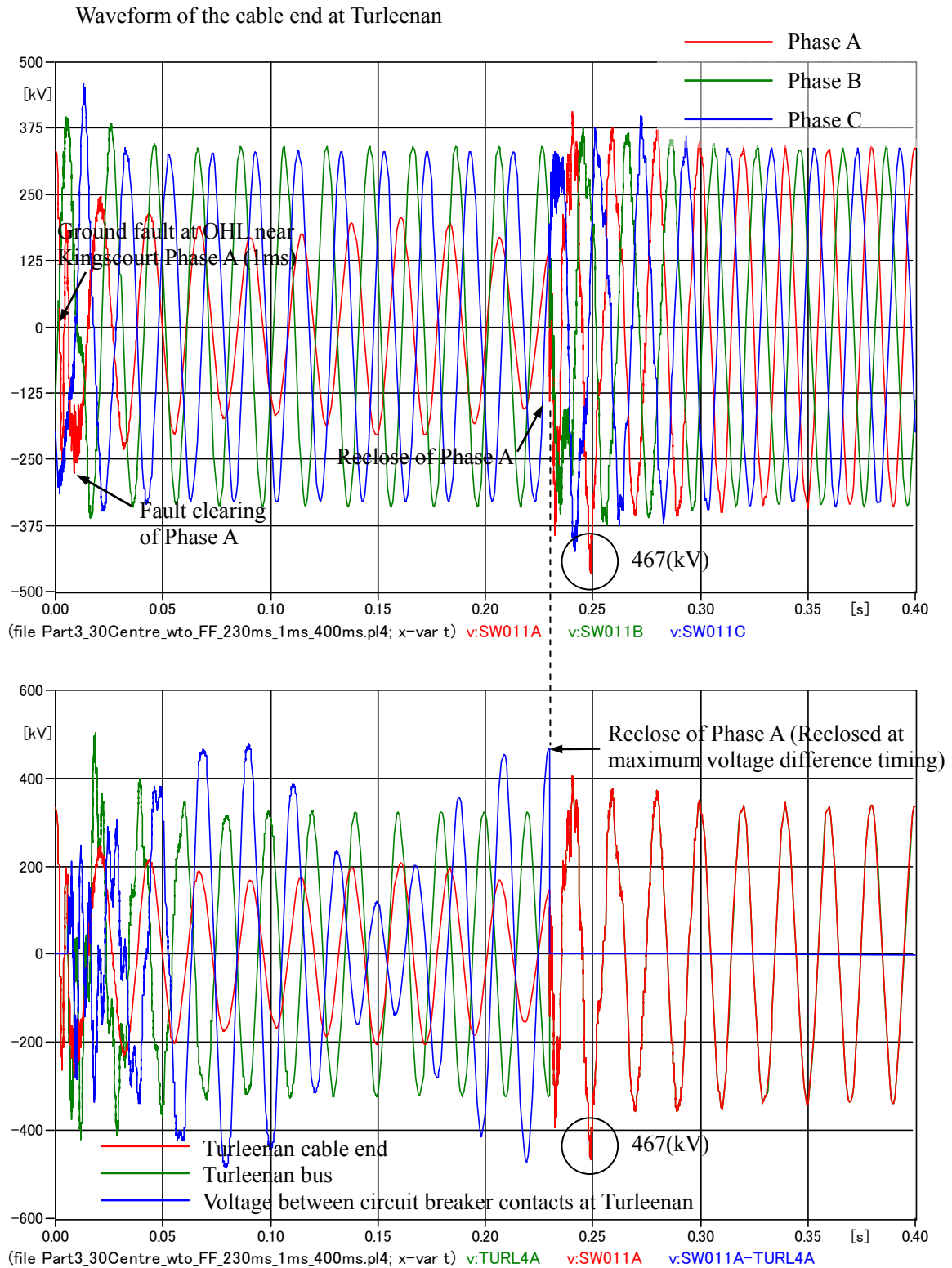
Waveform of the cable end at Turleenan
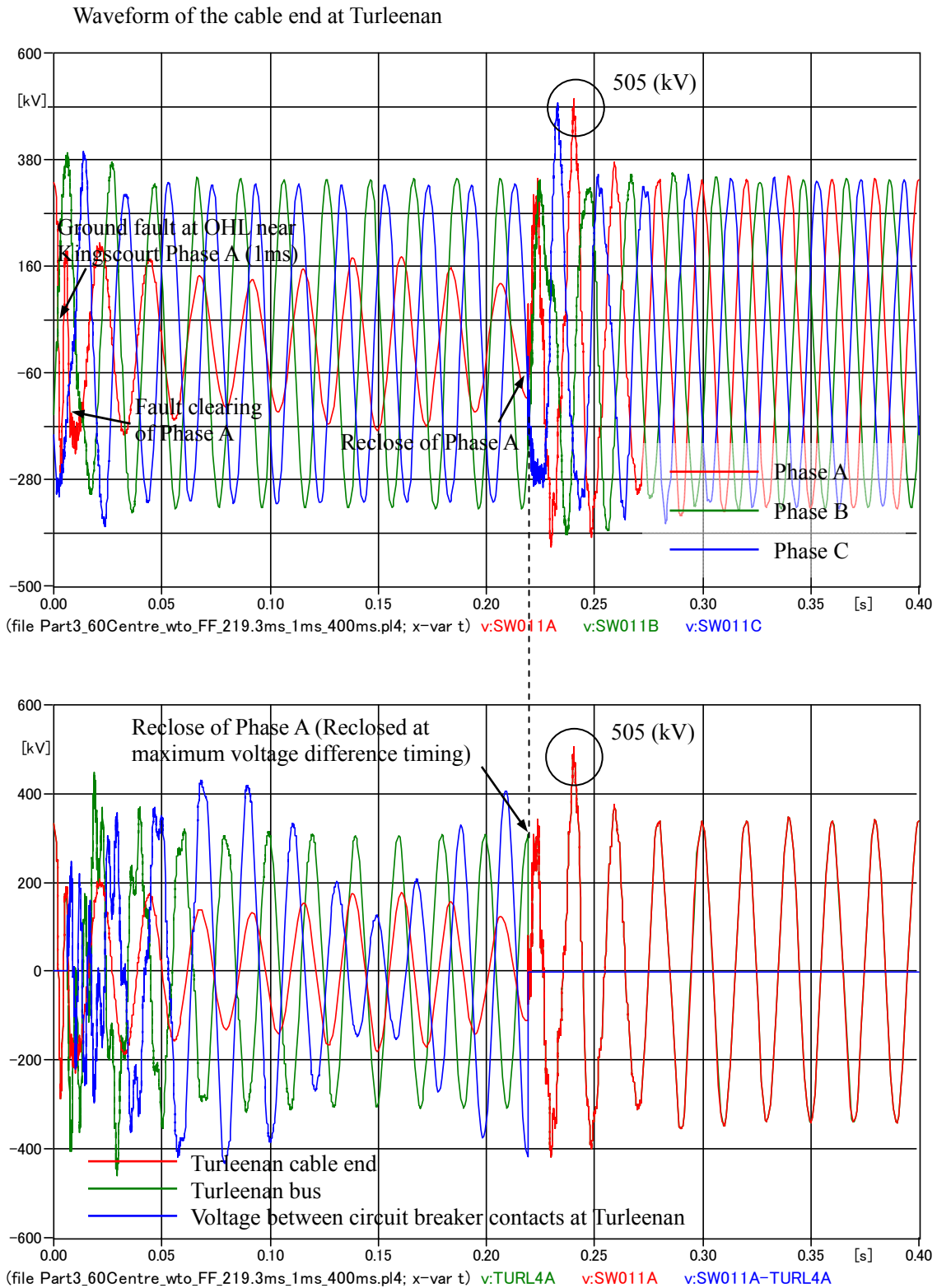
Fig. 5-8   Reclosing waveform at Turleenan - 30% cable, reactors at line ends.

Waveform of the cable end at Turleenan
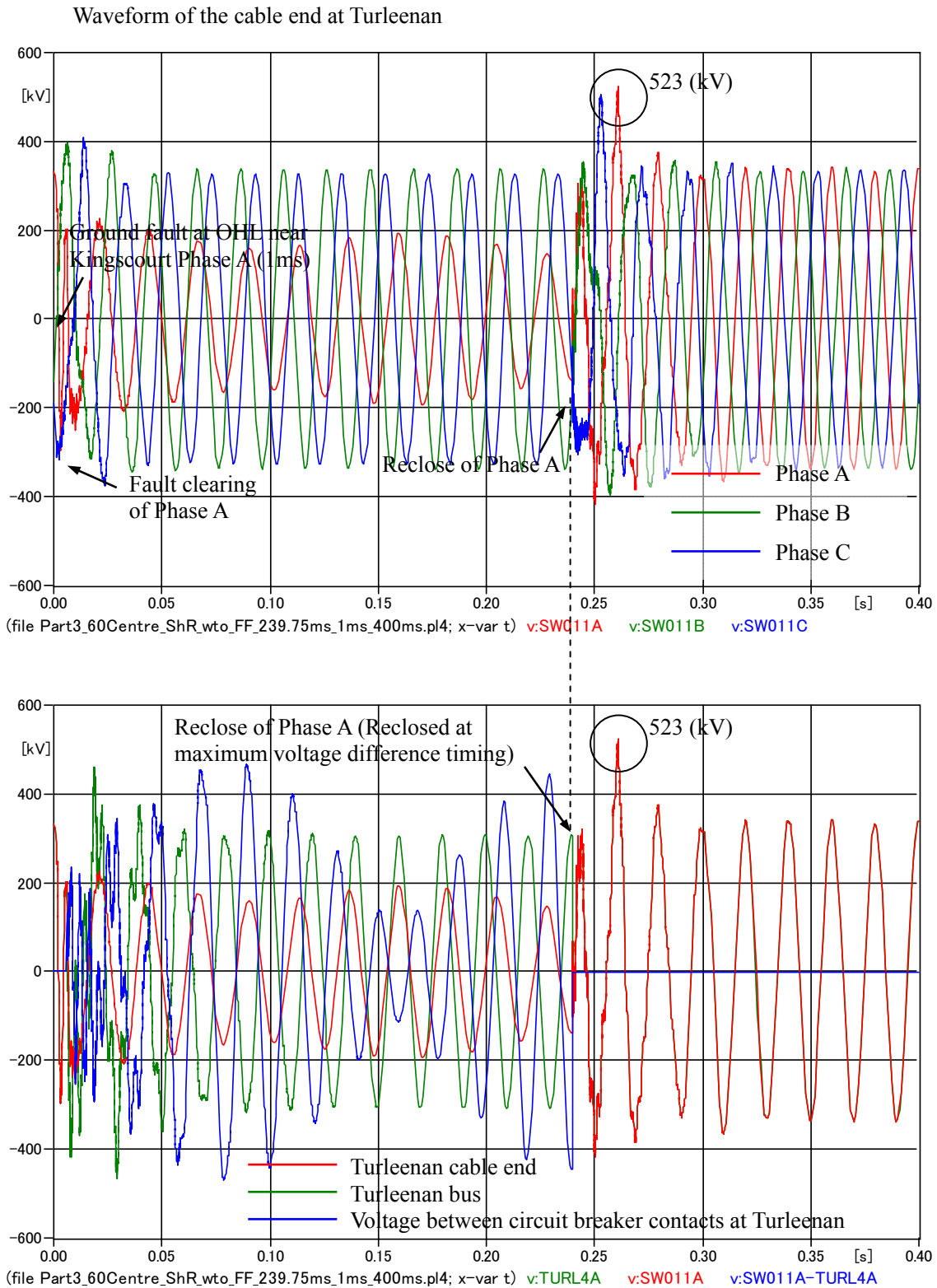
Fig. 5-10   Reclosing waveform at Turleenan - 30% cable, reactors at cable ends.

5.6 Three Phase Autoreclose

It may be necessary for the NIE/EirGrid to achieve a reactive power compensation rate closer to 100 % in order to control the voltage profile and reactive power flow in the network and to prevent harmful overvoltages.   It was discussed in Section 2.3 that one of the following two countermeasures had to be taken in order to achieve compensation rate of 100 %:

- Adoption of four-legged reactors

- Adoption of three phase autoreclose

The reliability of the interconnector is undermined by the adoption of three phase autoreclose, but open phase resonance does not occur since all three phases are opened even in single line to ground faults.

The overvoltage caused by three phase autoreclose was studied in this section since the condition becomes more severe compared to single phase autoreclose.   Statistical analysis should be considered in the three phase autoreclose analysis, as six phases of the circuit breakers at both ends are closed all together with only a few seconds time difference in between.   The same fault conditions and randomness as the Part 2 study was adopted.

Fig. 5-11 shows the system condition of the simulation, which is the same as the one in Case 3 shown in Fig. 5-2 which produced the maximum overvoltage in the single phase autoreclose analysis discussed in previous sections.   In this scenario, the fault occurred at the Kingscourt – Turleenan line near Kingscourt, and it was cleared by opening CBs (three phases) at Kingscourt and Turleenan.
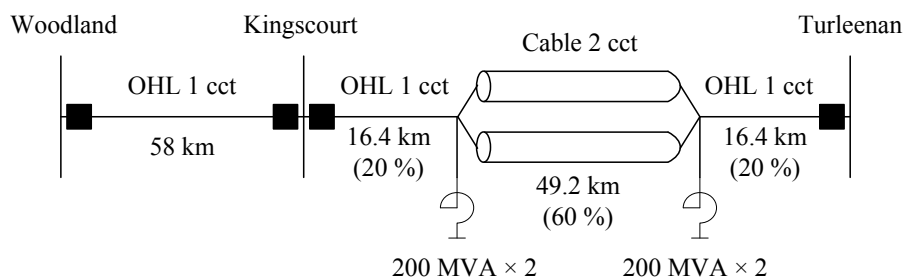
Case 3 - 60% 400kV cable in center position and 400kV ShR at the cable ends

Fig. 5-11   System configuration of three phase autoreclose simulation.

The simulation results are shown in Fig. 5-12 and Fig. 5-13.   The maximum overvoltage, 631 kV, was observed at Turleenan, which is higher than the single phase autoreclose (523 kV) due to consideration of switch timing difference between each phase of both circuit breakers.   However, even after taking into consideration the switch timing difference between the phases, the maximum overvoltage is still far below SIWV even without surge arrestors.   The simulation did not identify

the obvious overvoltage difference between the nodes of overhead line sections and the cable section.
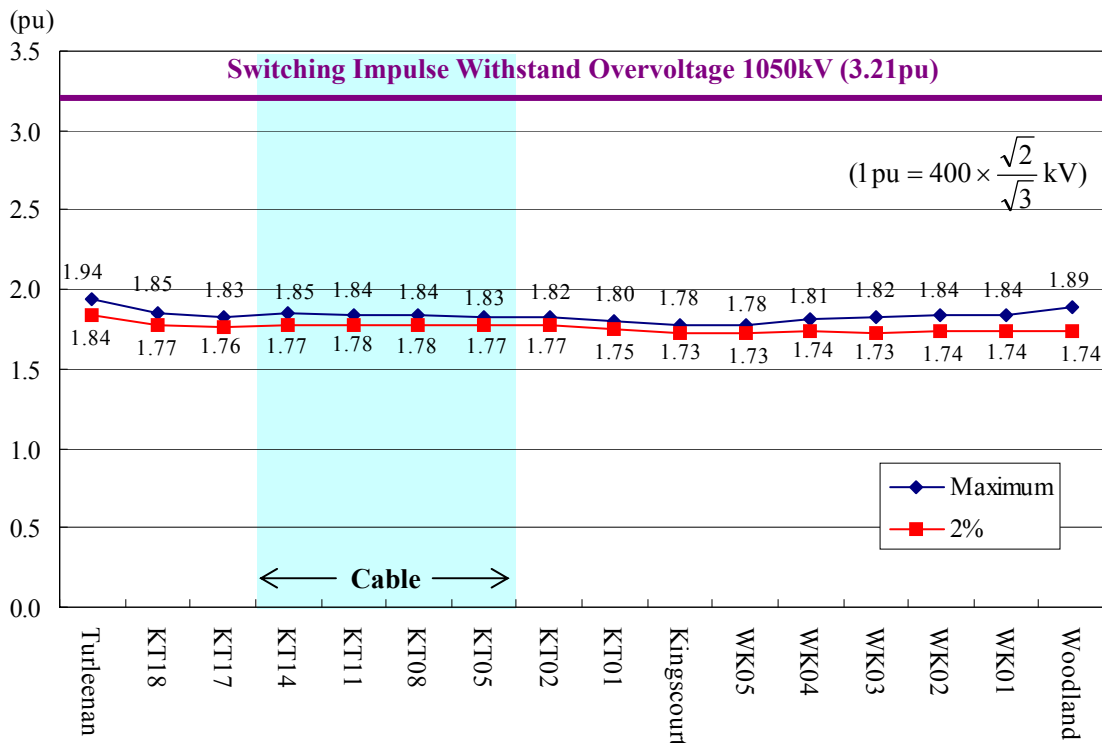
Fig. 5-12   Voltage profile in three phase auto-reclose analysis.

Reclose timing	Phase A	Phase B	Phase C
Turleenan	248.032 ms	245.822 ms	246.606 ms
Kingscourt	247.090 ms	245.735 ms	245.914 ms

(file Part3_60Centre_ShR_wto_FF_240_1ms_400ms_3phase_max.pl4; x-var t)   v:TURL1A   v:TURL1B   v:TURL1C
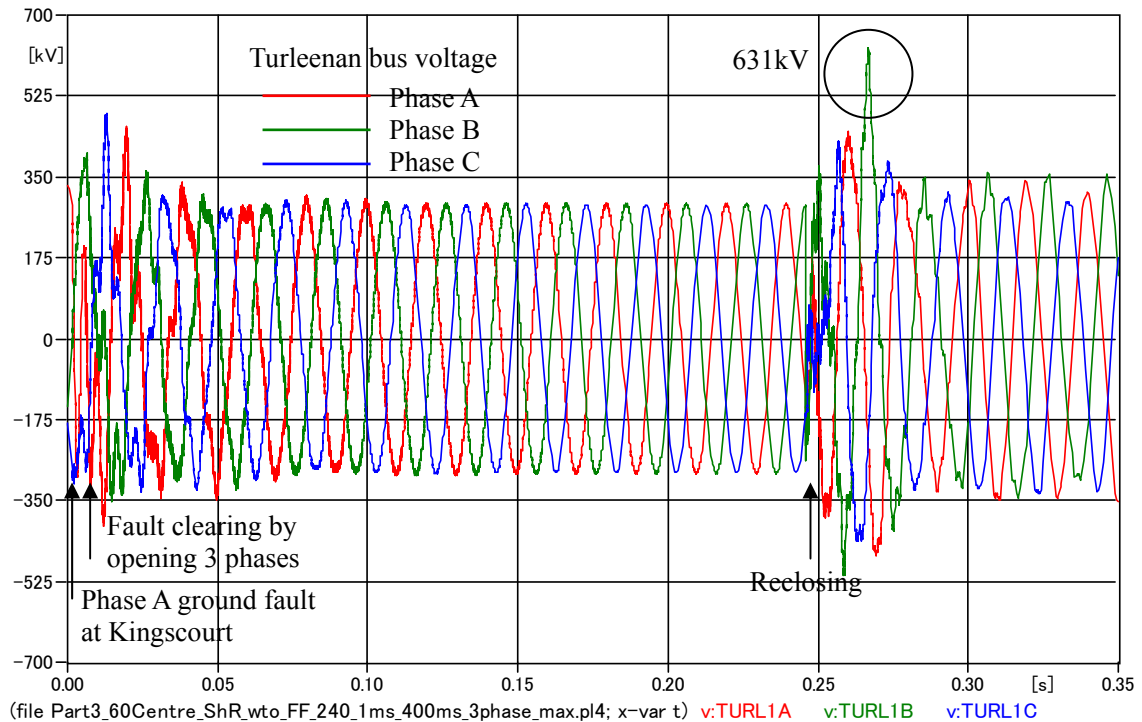
Fig. 5-13   Waveform of maximum overvoltage (Turleenan bus).

5.7 Conclusion

The analysis did not find significant overvoltage caused by autorelose. The observed overvoltages were much lower than SIWV in all simulated cases.

Table 5-4   Summary of the Overvoltage Caused by Autoreclose

	Highest overvoltage (peak)	Withstand voltage (peak) for evaluation
Single phase autoreclose	523.0 kV (1.60 pu)	1050 kV
Three phase autoreclose	631.0 kV (1.93 pu)	

$$1\,\text{pu} = 400\,\text{kV} \times \frac{\sqrt{2}}{\sqrt{3}}\ (\text{peak})$$

Chapter 6 Lightning Overvoltage

6.1 Overview

In Chapter 6, the lightning overvoltage analysis was performed in order to evaluate the overvoltage in the metallic sheath.   When a lightning strikes the ground wire near the connection between OHL and the underground cable as shown in Fig. 6.1, lightning current that flows into earth through the gantry may cause a very high overvoltage in the metallic sheath.
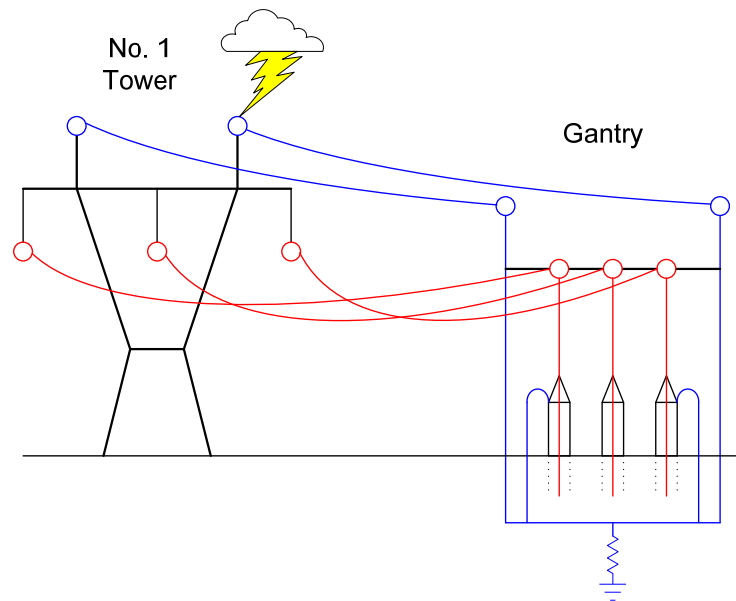
Fig. 6.1 Lightning overvoltage in metallic sheath.

As can be seen from Fig. 6.1, the level of the overvoltage highly depends on footing resistance of the gantry.   When a very high overvoltage is observed in the metallic sheath, it is necessary to evaluate the energy absorption capability of the SVLs.

6.2 Model Setup

The main focus of the lightning overvoltage analysis is the connection between the OHL and the underground cable.   Hence, the simulation model near *the point of interest* has to be more detailed compared to other analyses.   On the other hand, equipment far from *the point of interest* can be excluded from the simulation model.   This section discusses only the differences of the simulation model used for the lightning overvoltage analysis from the model for other analyses.
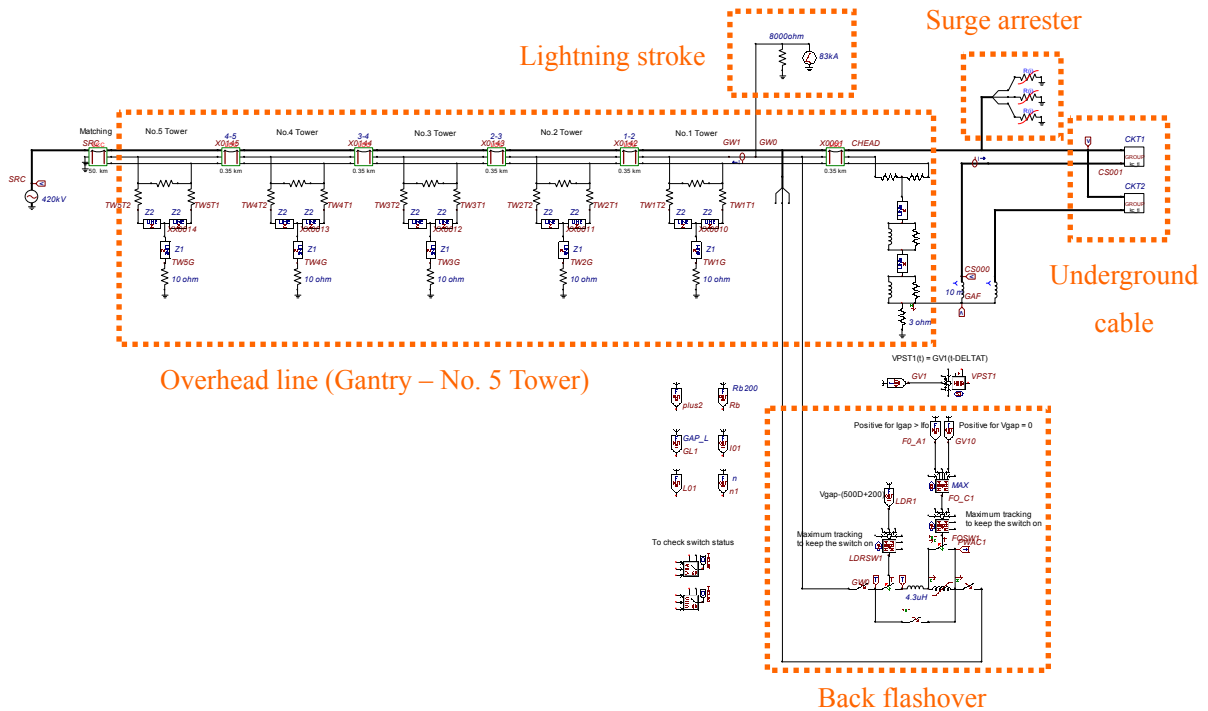
Fig. 6.2 Simulation model for the lightning overvoltage analysis.

6.2.1 Overhead line

Overhead lines near the connection are included in the model.   Spans between towers and the gantry were assumed to be 350 m as shown in Table 6.1.   The overhead lines beyond No. 5 Tower were not included in the model.   In order to avoid the reflection of the lightning overvoltage at No. 5 Tower, the overhead line model with a length of 100 km was connected to No. 5 Tower as matching impedance.

Table 6.1 Spans between towers and the gantry

Gantry – No. 1 Tower	350 m
No. 1 Tower – No. 2 Tower	350 m
No. 2 Tower – No. 3 Tower	350 m
No. 3 Tower – No. 4 Tower	350 m
No. 4 Tower – No. 5 Tower	350 m

6.2.2 Grounding resistance

The values of grounding resistance were provided from NIE / EirGrid as follows:

Gantry: 3 Ω

Cable head: 3 Ω

No. 1 – No. 5 Towers: 10 Ω

Cable joints (NJ, neutral point of IJ):   10 Ω

It was assumed that the gantry and cable head share the grounding system (earth electrodes or mesh).

6.2.3   Lightning stroke

The lightning stroke waveform was provided from NIE / EirGrid as follows.   It was modeled as the ramp wave as a more severe lightning stroke due to its sharp shape as shown below.

Stroke current:	83 kA
Ramp waveform:	1.83 / 70 µs
Lightning path impedance:	8000 Ω
Stroke point:	Top of No.1 Tower
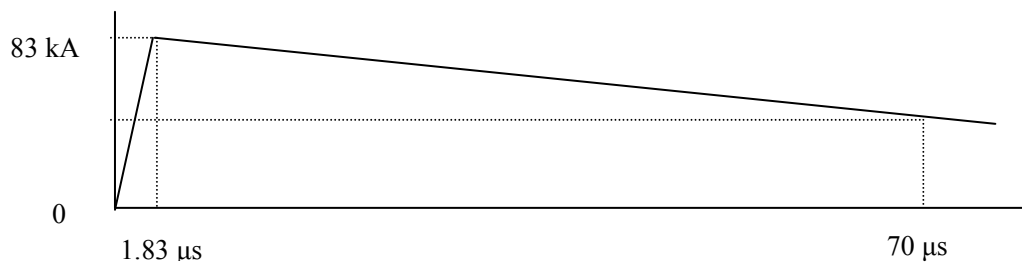
Fig. 6.3 Lightning stroke waveform (83 kA, 1.83 / 70µs).

DATA	UNIT	VALUE
Amplitude	Ampere	83000
T0	s	1.83E-6
A1	Ampere	41500
T1	s	7E-5
TStart	s	0
TStop	s	0.00013817
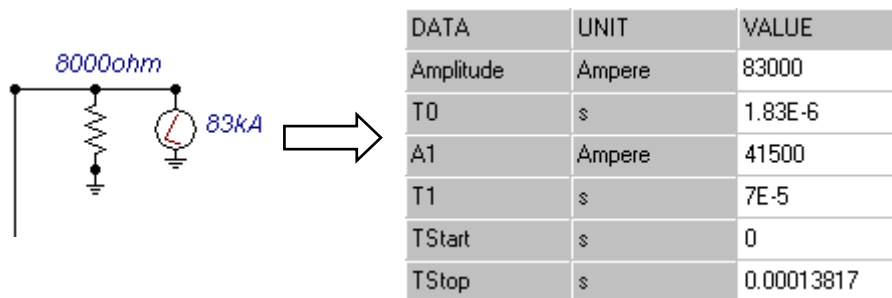
Fig. 6.4 Lightning stroke model.

As described in Section 6.1, the lightning strike was assumed to have occurred in No. 1 Tower. Direct lightning to power lines was not studied since it did not cause a severe overvoltage in the metallic sheath.

6.2.4 Back flashover model

This study applied the flashover model using leader development proposed by N. Nagaoka in 1991.   It consists of two switches, the "leader development switch" and the "flashover switch" which are controlled by the arcing horn voltage and current or zero-cross of the clearance voltage respectively, as shown in the following figure.   This model is derived from the leader model proposed by T. Shindo and T. Suzuki.   It needs to undergo some processing, such as EMTP calculations in twice and constants calculation, in order to obtain an arcing horn voltage and to make a leader model.   To improve this complication, the model applies approximate expressions to the time-dependent leader development.   It contributes to reducing computational efforts.

SW1: Start switch of leader progression

SW2: Start switch of flashover

L_f: Arc impedance (μH) (clearance × 1μH/m)

L_n: Nonlinear inductance for leader development

D: Gap / Clearance (m)

R_b: Equivalent impedance 200 (Ω)*

(The standard value of R_b is used. This model is not sensitive to R_b.)
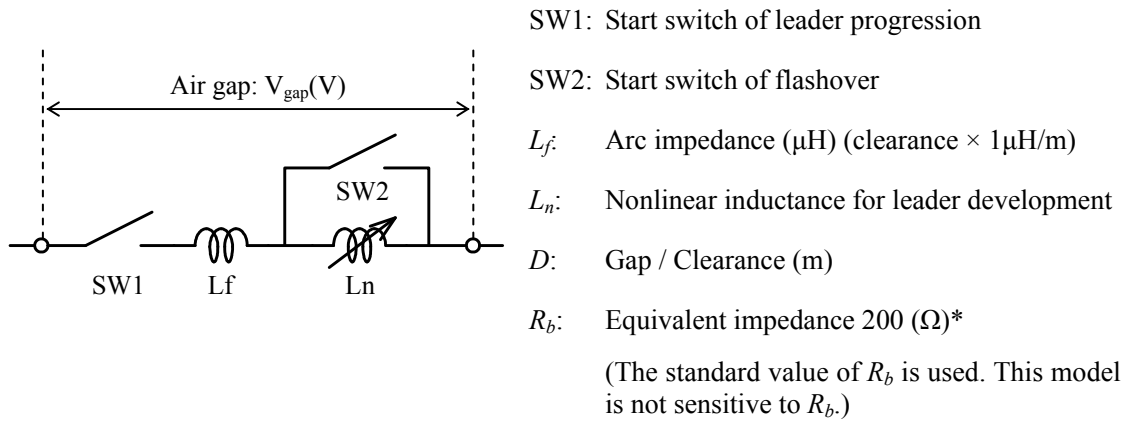
Fig. 6.5 Flashover model with non-linear inductance.

$L_0 = 1.23D - 0.432$ (mH)

$I_0 = 10^{(-0.0343D-0.00025Rb+2.85)}$ (A)

$n = -0.0743D - 0.000734Rb + 2.18$

$$\Phi_n(i) = \frac{L_0 I_0 \left\{ 1 - \dfrac{1}{(1 + i/I_0)^{n-1}} \right\}}{(n-1)} - L_f i$$

Switching conditions

SW1 ON: $V_{\text{gap}} > 500D + 200$ (kV)

SW2 ON: $V_{\text{gap}} = 0$ or $I_{\text{gap}} > I_{\text{FO}}$ where, $I_{\text{FO}} = I_0 \{(L_0\, 10^6 / D)^{1/n} - 1\}$

Table 6.2 I-Φ characteristics of non linear inductance *Ln*

Current (A)	$L_n = \Phi - L_f i$ (Wb-T)	Φ (Wb-T)
1	0.004843	0.0048
10	0.047619	0.0477
50	0.221590	0.2218
100	0.408101	0.4085
150	0.567577	0.5682
200	0.705735	0.7066
250	0.826756	0.8278
300	0.933774	0.9351
400	1.114872	1.1166
500	1.262670	1.2648
750	1.537067	1.5403
1000	1.727766	1.7321
2000	2.137469	2.1461
4000	2.445034	2.4622
8000	2.646438	2.6808
15000	2.748127	2.8126
25000	2.778492	2.8860

References

(a) T. Shindo and T. Tsuzuki: "A new calculation method breakdown voltage-time characteristics of long gaps", *IEEE Trans. on PAS*, 104, 1556, 1985

(b) N. Nagaoka: "A flashover model using a nonlinear inductance", *IEEJ*, Vol. 111-B, No. 5, p.529-534, 1991

Note: Other sections in Section 6.2 have been deleted.

6.3 Result of the Analysis

6.3.1 Sheath overvoltage

The lightning overvoltage analysis was conducted under the default conditions described in the last section.   As a result of the analysis, it was confirmed that back flashover from No.1 Tower to the power lines did not occur for the given lightning stroke model.   This is considered to be a severe condition because lightning current can propagate only into the ground wire, gantry, and metallic sheath of the cable, not into power lines.

Fig. 6.6 shows the direction of lightning current.   Since large lightning current flows into grounding resistance of the gantry and the cable head, it is expected that the metallic sheath near the cable head experience a high lightning overvoltage.
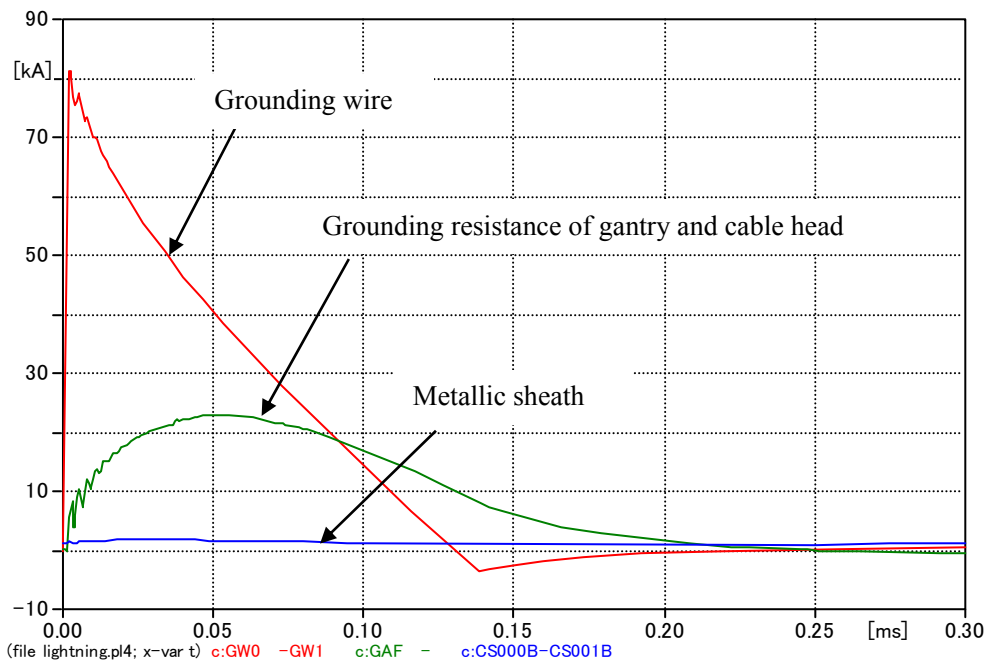
Fig. 6.6 Propagation of lightning current.

Overvoltage in the metallic sheath is shown in Fig. 6.7.   It can be seen that the sheath to earth overvoltage at the cable head (CH) is very high.   Utilities in the world typically allow sheath to earth overvoltage up to 60 kV for 400 kV cables, considering the insulation strength of the sheath. Some countermeasures have to be taken in order to suppress the sheath to earth overvoltage below 60 kV.

Sheath overvoltage travels slow for the lightning overvoltage and has good damping. When it travels to the first IJ, the overvoltage level is damped to 13 kV. When the neutral point of the first IJ is earthed, it is recommended that a voltage rating of SVLs is higher than $15\sqrt{2}$ kVrms. Sheath to sheath overvoltage at the first IJ was confirmed to be no problem because of good damping.
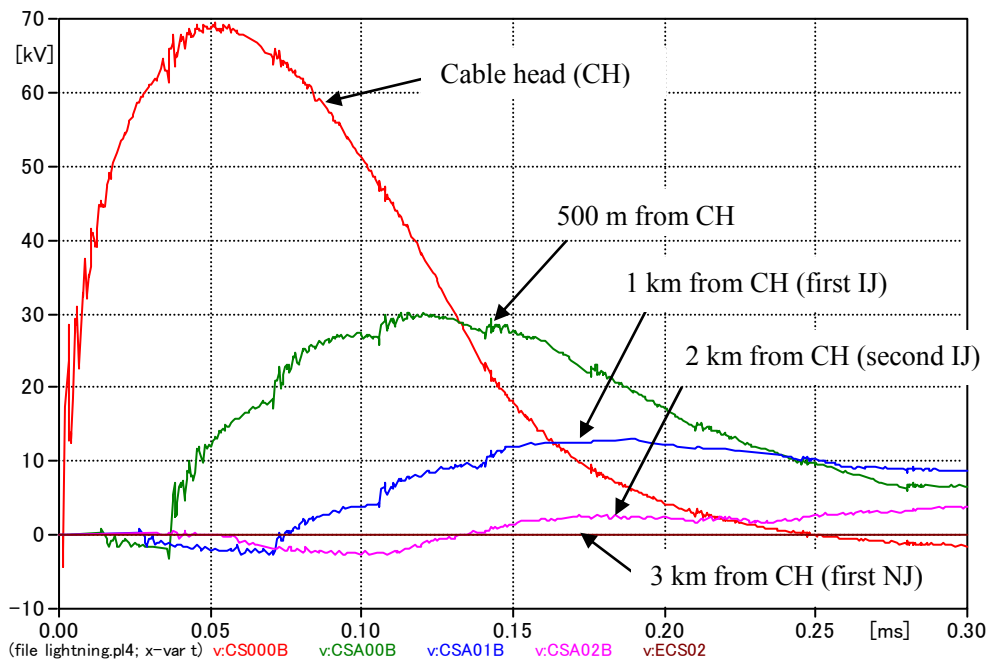
Fig. 6.7 Sheath to earth overvoltage.

If the first span from the cable head can be shorter than 1 km, it is necessary to confirm the sheath to earth overvoltage as well as the sheath to sheath overvoltage at the first IJ. Although it is preferable to earth neutral point of IJs in terms of safety considerations (sheath to earth overvoltage), neutral point of the first IJ cannot be grounded, depending on the length of the first span, in order to avoid a failure of SVLs.

6.3.2 Effect of grounding resistance

In order to determine the effect of grounding resistance on sheath to earth overvoltages, the grounding resistance at the gantry and the cable head is reduced from 3 Ω to 2 Ω or 1 Ω. As shown in Fig. 6.8, the highest sheath to earth overvoltage was reduced from 69 kV (3 Ω) to 28 kV (1 Ω). Since the effect of grounding resistance is large, it is necessary to keep the resistance as low as possible.
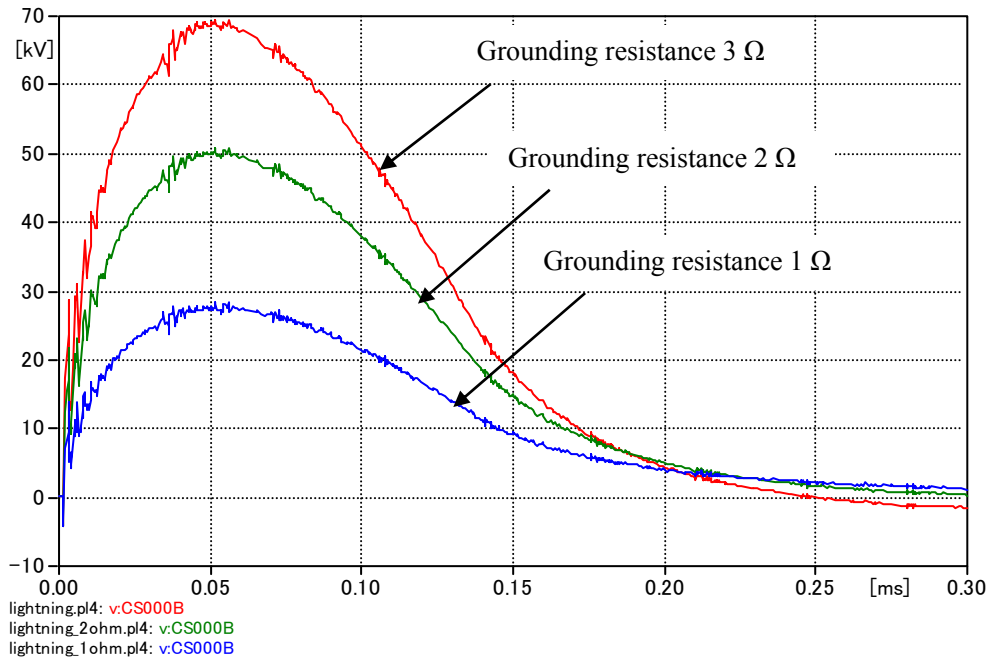
Fig. 6.8 Sheath to earth overvoltage at the cable head with different grounding resistance.

6.3.3 Effect of the length of grounding/cross-bonding wire

In order to determine the effect of the length of grounding wire and cross-bonding wire on an sheath to earth overvoltage, the length of the grounding wire at the cable head was reduced from 10 m to 5 m or 1 m (10 μH to 5 μH or 1 μH).   For cross-bonding wire, only bonding leads of the first IJ was modified.   Since sheath to earth overvoltage at the cable head was largely determined by the lightning current that flows into grounding resistance, no significant effect was observed as shown in Fig. 6.9.

lightning.pl4: v:CS000B
lightning_5m.pl4: v:CS000B
lightning_1m.pl4: v:CS000B
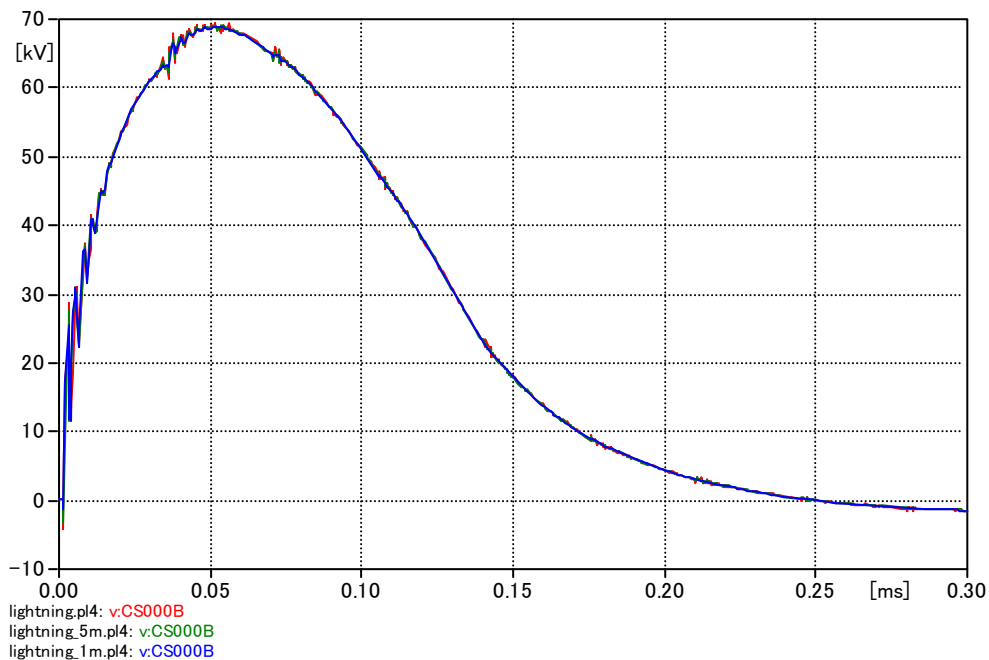
Fig. 6.9 Sheath to earth overvoltage at the cable head with different grounding wire lengths.

6.4 Conclusion

The lightning overvoltage analysis was conducted in Part 3 in order to evaluate the overvoltage in the metallic sheath.   It was found that grounding resistance at the gantry must be lower than 2 Ω in order to maintain the sheath overvoltage lower than 60 kV at the connection between the OHL and the cable.

Appendix

Table of contents

Appendix 1 Results of the Parametric Study on the 220 kV Woodland – Louth Cable Length

Frequency scans and time domain simulations of the 400 kV Woodland – Kingscourt line energisation were performed with different length of the 220 kV Woodland – Louth cable. The result of the parametric study is summarized in Section 3.1.1 of the Part 1 report. All the figures obtained in the parametric study are shown in Appendix 1.

List of the 220 kV Woodland – Louth cable length assumed in the study is shown in Table A1-1.

Table A1-1 List of the 220 kV Woodland – Louth Cable Length

	220 kV Woodland – Louth cable length		Notes
	Length	Number of circuits	
Case (4)-0	61.0 km	1	Base case
Case (4)-1	7.625 km	1	(Length of the base case) /8
Case (4)-2	12 km	1	
Case (4)-3	15.25 km	1	(Length of the base case) /4
Case (4)-4	30.5 km	1	(Length of the base case) /2
Case (4)-5	91.5 km	1	(Length of the base case) * 1.5
Case (4)-6	122.0 km	1	(Length of the base case) * 2
Case (4)-7	183.0 km	1	(Length of the base case) * 3
Case (4)-8	244.0 km	1	(Length of the base case) * 4

[Case (4)-0] Length of 220 kV cable: 61 km

The results of time domain simulations are shown in Fig. A1-1 and Fig. A1-2. The energisation timing of the 400 kV Woodland – Kingscourt line at the Woodland S/S was set to Phase A voltage peak at the Woodland 400 kV bus.
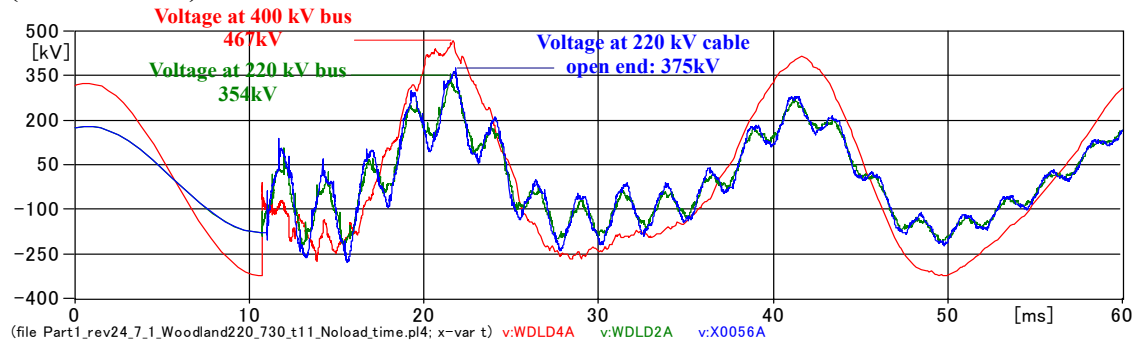
(Phase to earth)
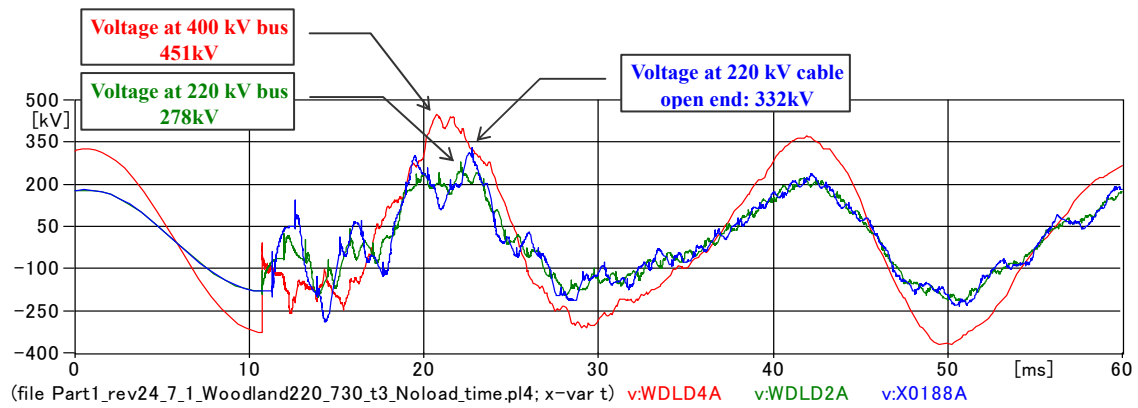
Fig. A1-1 Switching waveforms at the Woodland 400 kV and 220 kV buses and 220 kV cable open end (phase to earth).
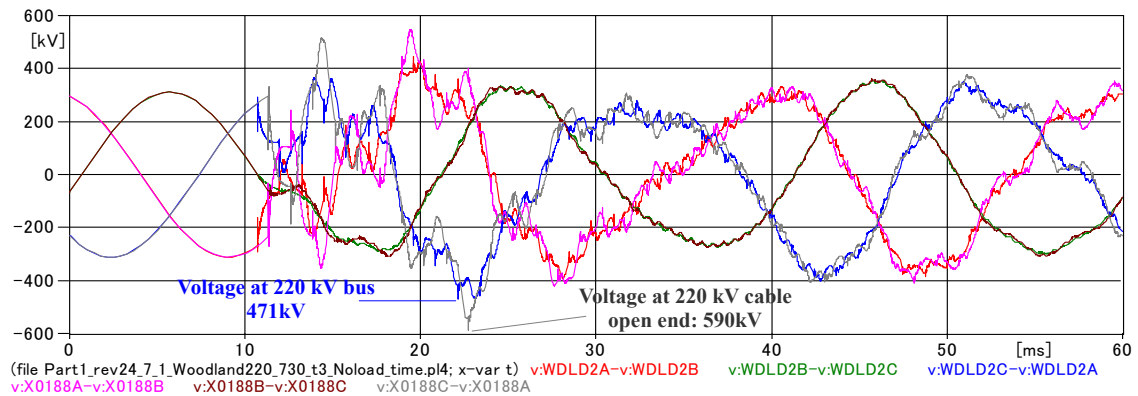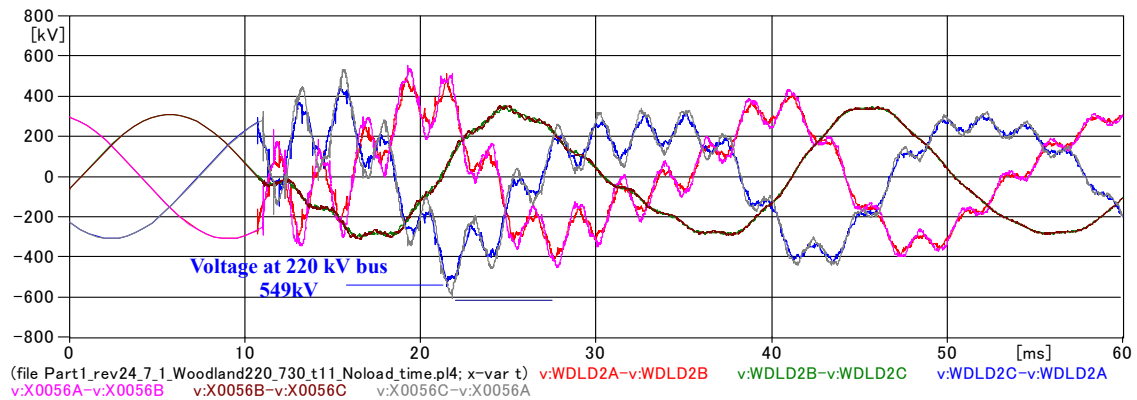
(Phase to Phase)

Fig. A1-2 Switching waveforms at the Woodland 220 kV bus and 220 kV cable open end (phase to phase).

The following figures reflect frequency component spectrums derived from the voltage waveforms at the Woodland 220 kV bus and the 220 kV cable open end respectively. The frequency components were calculated for one cycle immediately after the line closing.

MC's PlotXY – Fourier chart(s). Copying date: 2009/02/20
File part1_rev24_7_1_woodland220_730_t3_noload_time.pl4   Variable v:WDLD2A [|pu of harm. 1|]
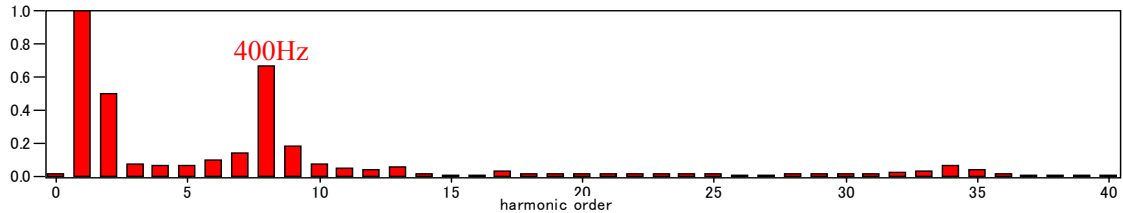Initial Time: 0.01069   Final Time: 0.03069
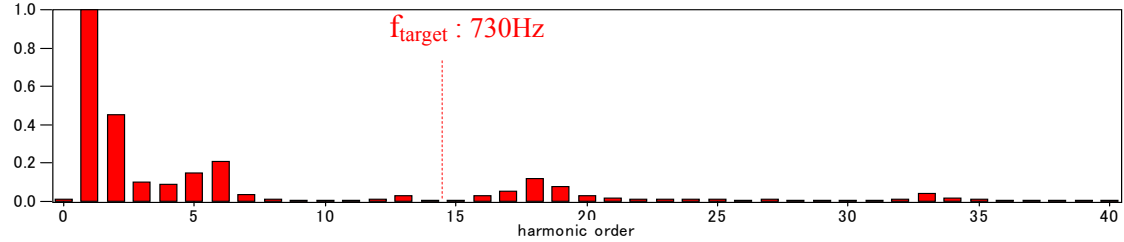
Fig. A1-3 Frequency component spectrum of the switching waveform at Woodland 220 kV bus (phase to earth).

MC's PlotXY – Fourier chart(s). Copying date: 2009/03/10
File Part1_rev24_7_1_Woodland220_730_t3_Noload_time.pl4   Variable v:X0188A [|pu of harm. 1|]
Initial Time: 0.01069   Final Time: 0.03069
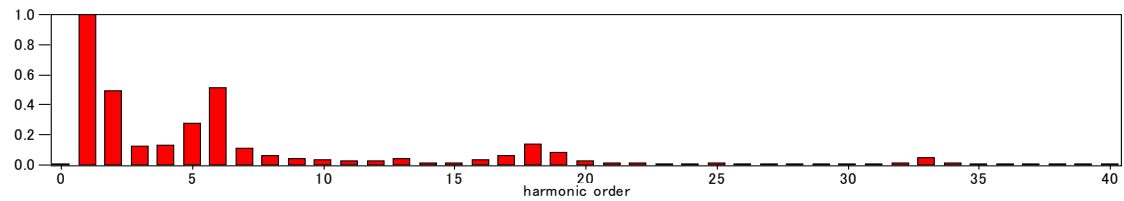
Fig. A1-4 Frequency component spectrum of the switching waveform at the 220 kV cable open end (phase to earth).
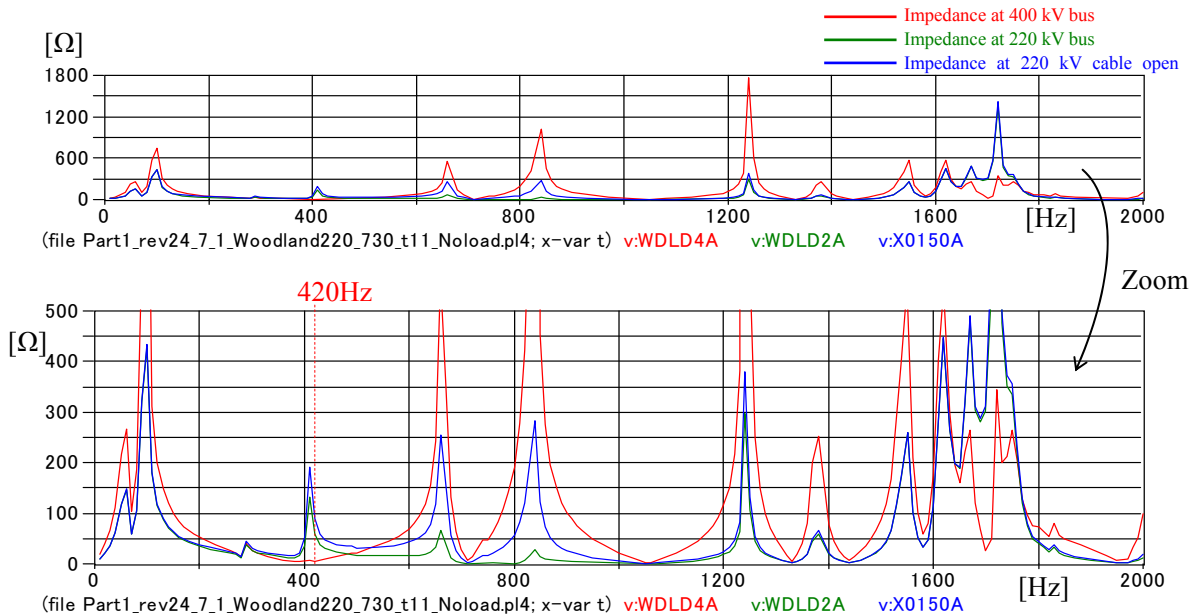
Frequency scans were conducted from 10 Hz to 2000 Hz by 10 Hz step.
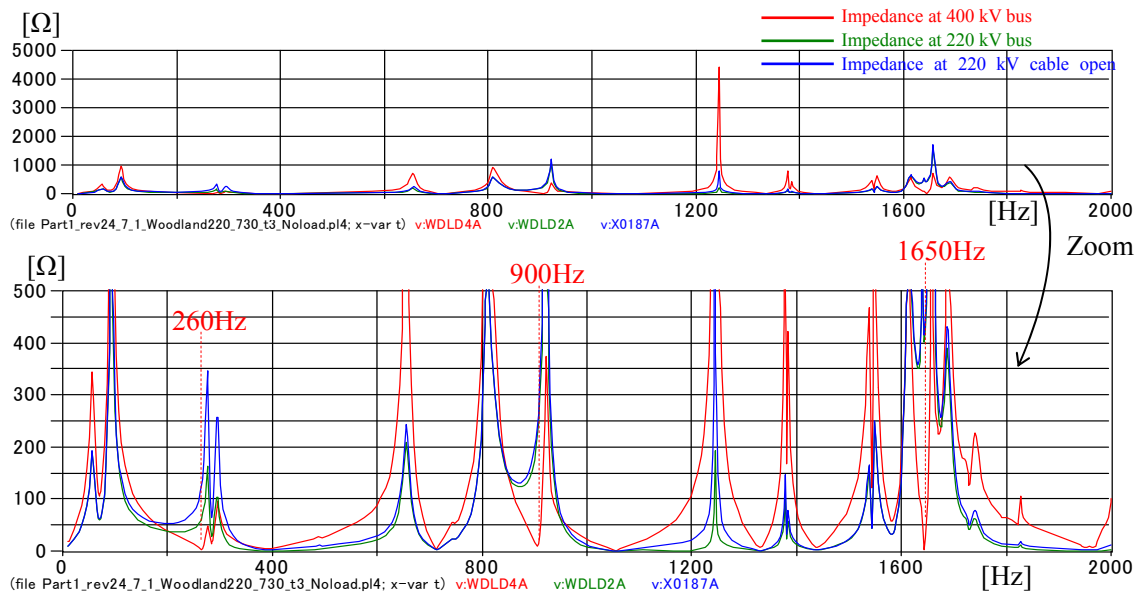
Fig. A 1-5 Frequency scan at the Woodland 400 kV and 220 kV buses and 220 kV cable open end (phase to earth).

[Case (4)-1] Length of 220 kV cable: 7.625 km

(Phase to earth)
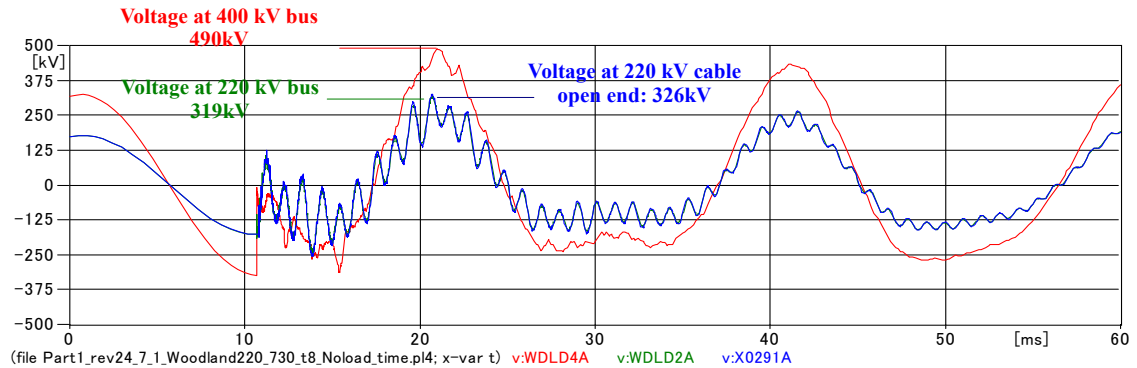
Fig. A1-6 Switching waveforms at the Woodland 400 kV and 220 kV buses and 220 kV cable open end (phase to earth).
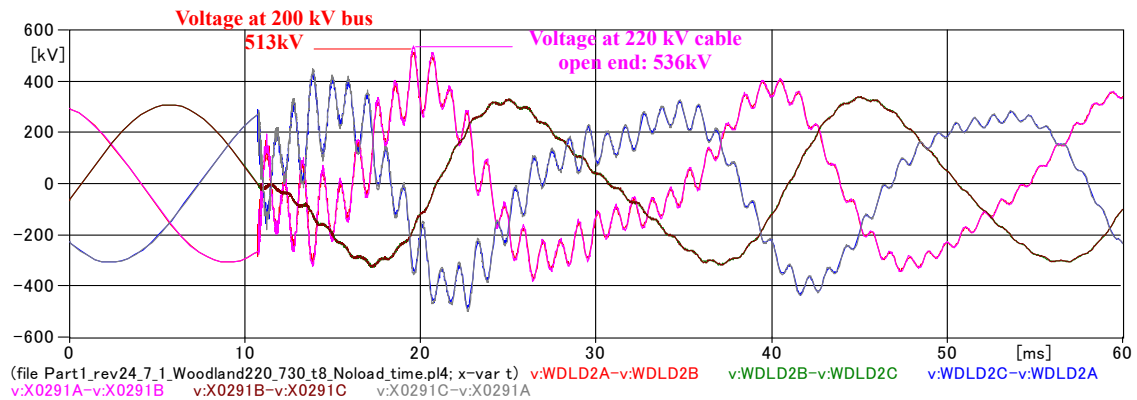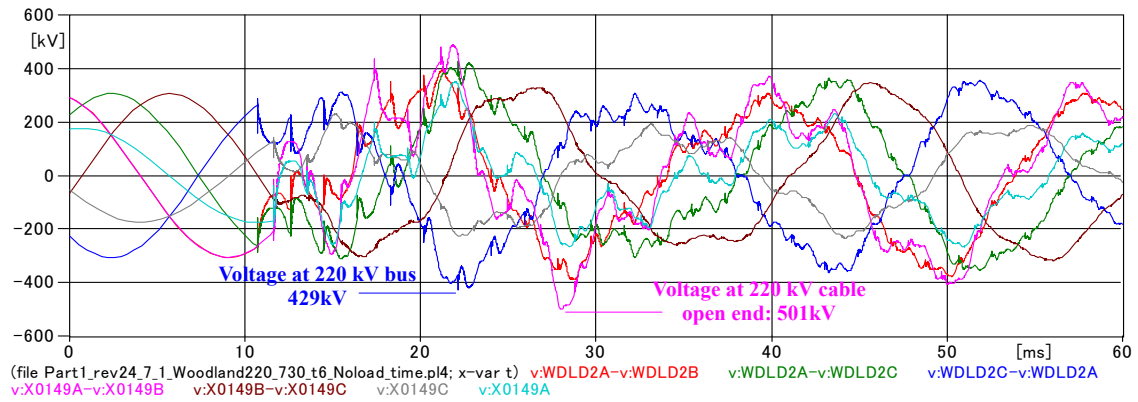
(Phase to Phase)

Zoom
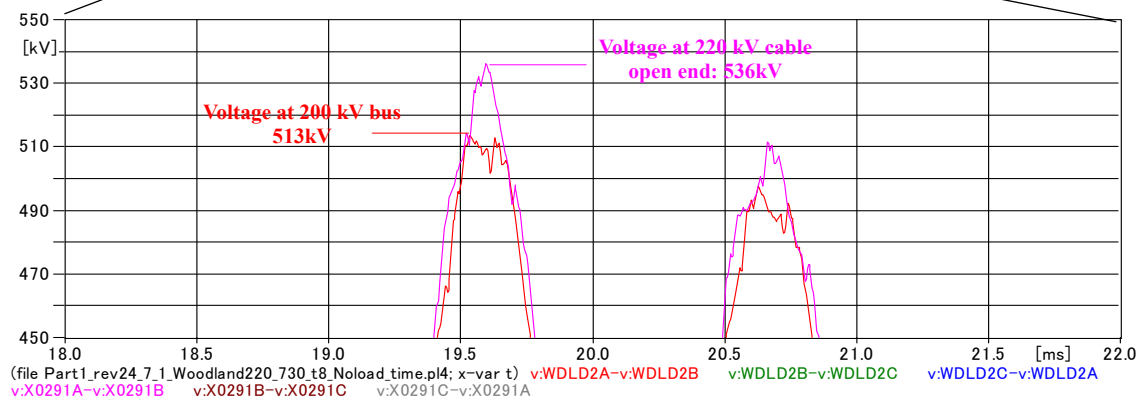
Fig. A1-7 Switching waveforms at the Woodland 220 kV bus and 220 kV cable open end (phase to phase).

The following figures show frequency component spectrums derived from the voltage waveforms at the Woodland 220 kV bus and the 220 kV cable open end respectively. The frequency components were calculated for one cycle immediately after the line closing.

MC's PlotXY – Fourier chart(s). Copying date: 2009/02/23
File Part1_rev24_7_1_Woodland220_730_t8_Noload_time.pl4   Variable v:WDLD2A [peak]
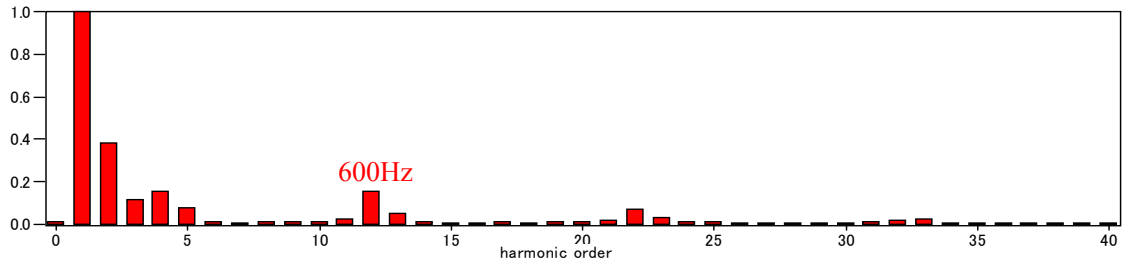Initial Time: 0.0107   Final Time: 0.0307
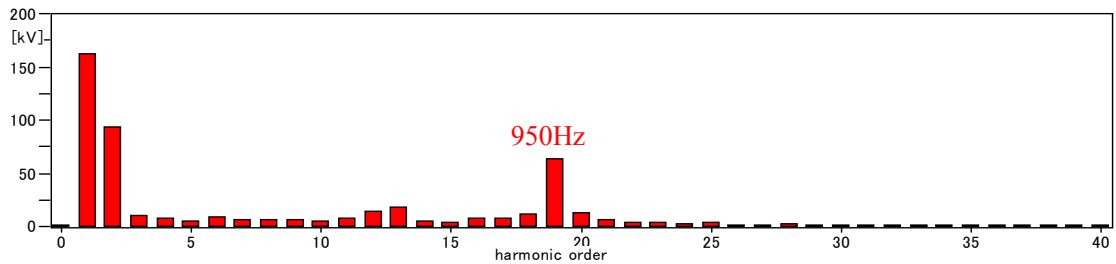
Fig. A1-8 Frequency component spectrum of the switching waveform at Woodland 220 kV bus (phase to earth).

MC's PlotXY – Fourier chart(s). Copying date: 2009/02/26
File Part1_rev24_7_1_Woodland220_730_t8_Noload_time.pl4   Variable v:X0291A [|pu of harm. 1|]
Initial Time: 0.0107   Final Time: 0.0307
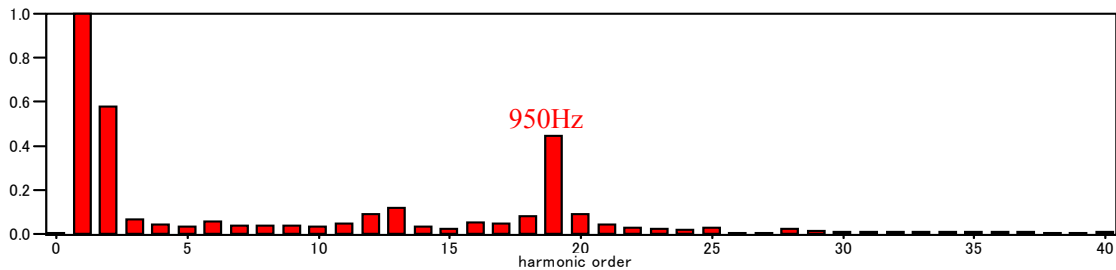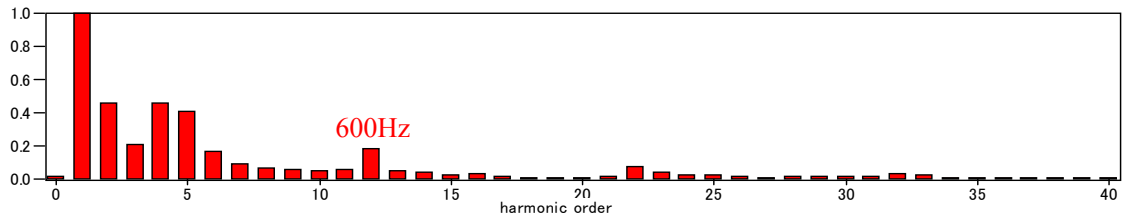

**Fig. A1-9 Frequency component spectrum of the switching waveform at the 220 kV cable open end (phase to earth).**

Frequency scans were conducted from 10 Hz to 2000 Hz by 10 Hz step.
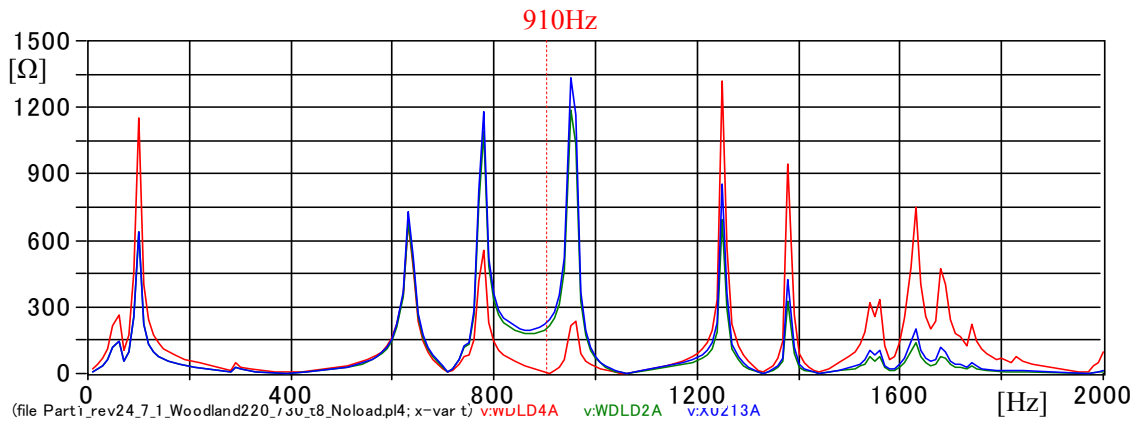
Fig. A1-10 Frequency scan at the Woodland 400 kV and 220 kV buses and 220 kV cable open end (phase to earth).

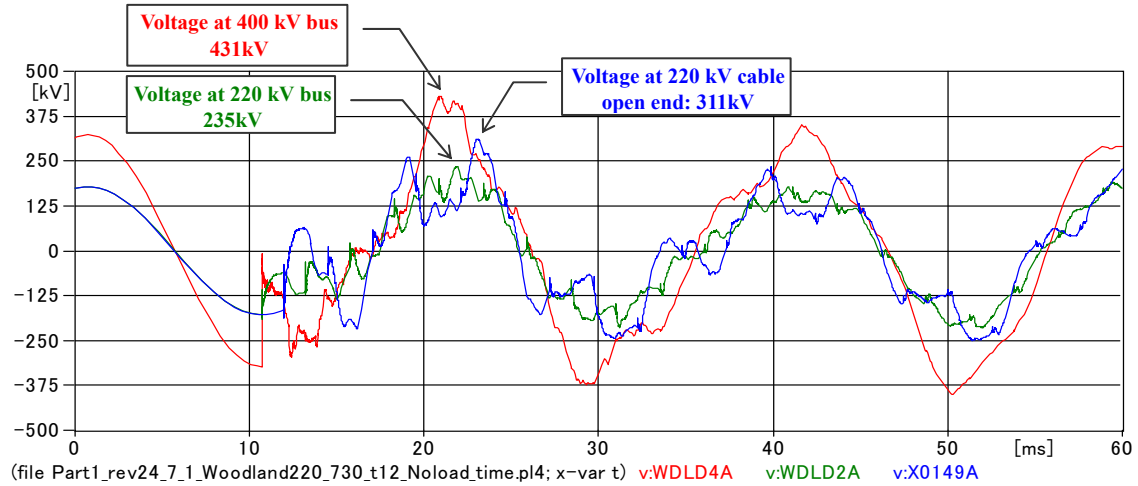[Case (4)-2] Length of 220 kV cable: 12 km

(Phase to earth)
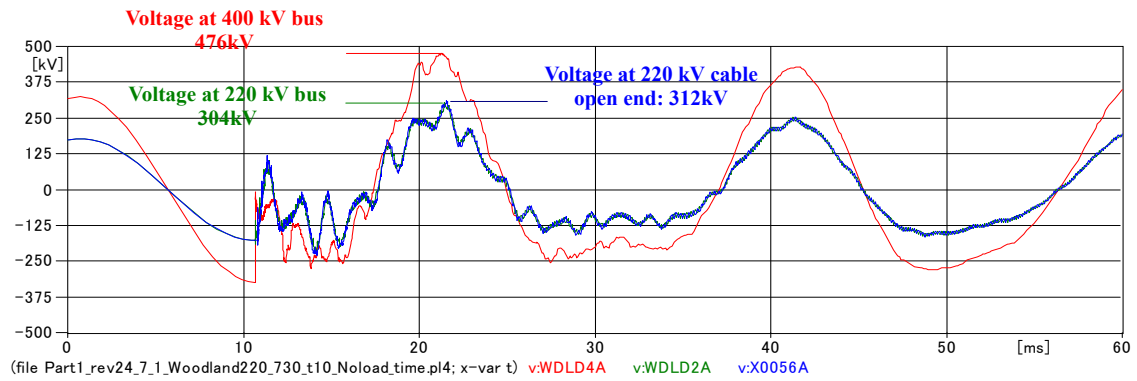
Fig. A1-11 Switching waveforms at the Woodland 400 kV and 220 kV buses and 220 kV cable open end (phase to earth).
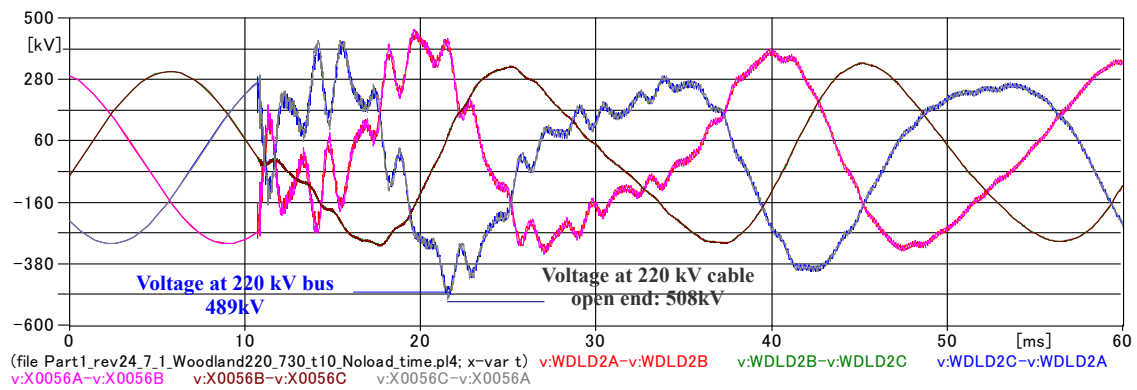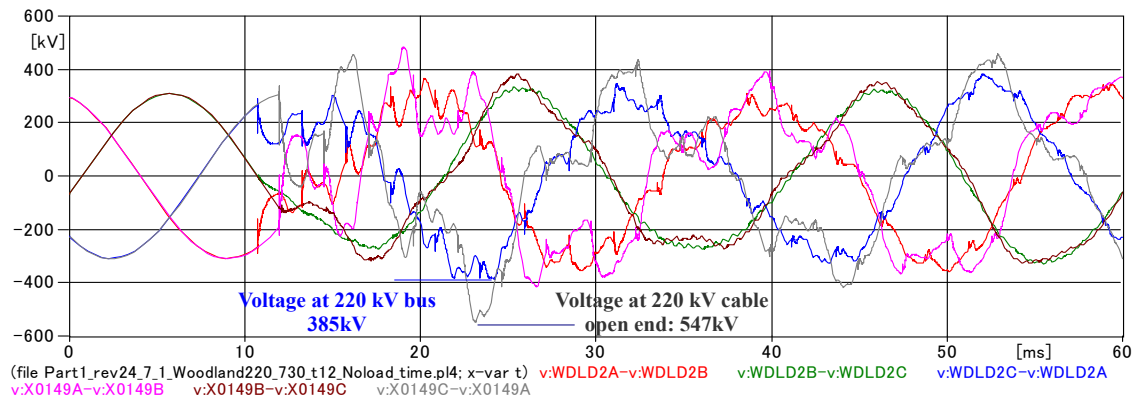
(Phase to phase)

Fig. A1-12 Switching waveforms at the and 220 kV bus and 220 kV cable open end (phase to phase).

MC's PlotXY – Fourier chart(s). Copying date: 2009/02/23
File Part1_rev24_7_1_Woodland220_730_t10_Noload_time.pl4   Variable v:WDLD2A [|pu of harm. 1|]
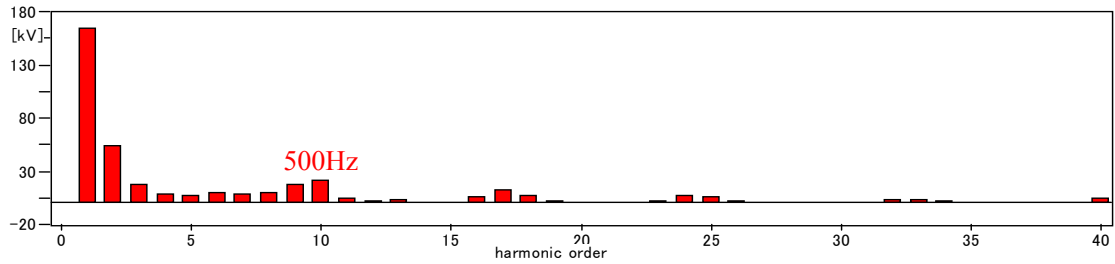Initial Time: 0.0107   Final Time: 0.0307
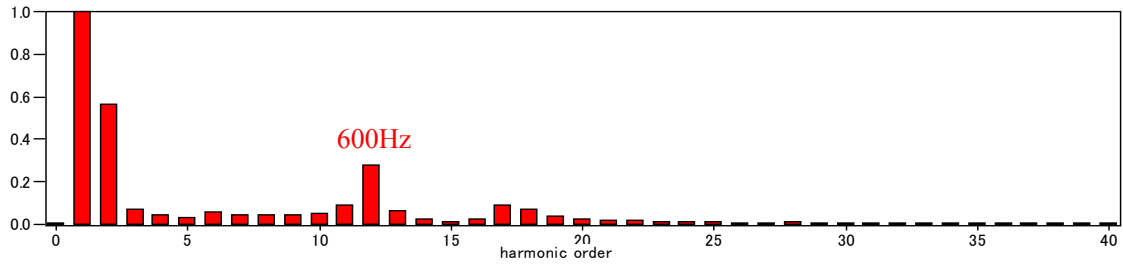
Fig. A1-13 Frequency component spectrum of the switching waveform at Woodland 220 kV bus (phase to earth).

MC's PlotXY – Fourier chart(s). Copying date: 2009/02/26
File Part1_rev24_7_1_Woodland220_730_t10_Noload_time.pl4   Variable v:X0056A [|pu of harm. 1|]
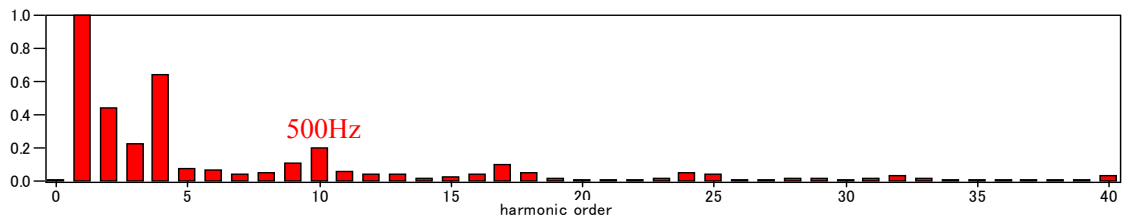Initial Time: 0.0107   Final Time: 0.0307
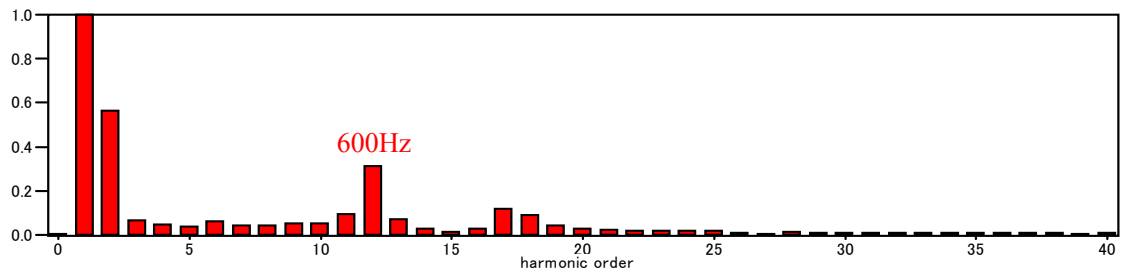
Fig. A1-14 Frequency component spectrum of the switching waveform at the 220 kV cable open end (phase to earth).
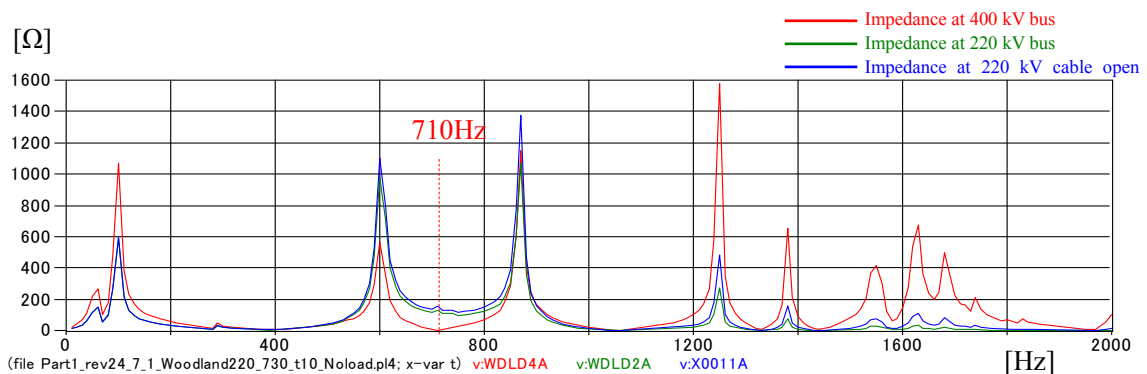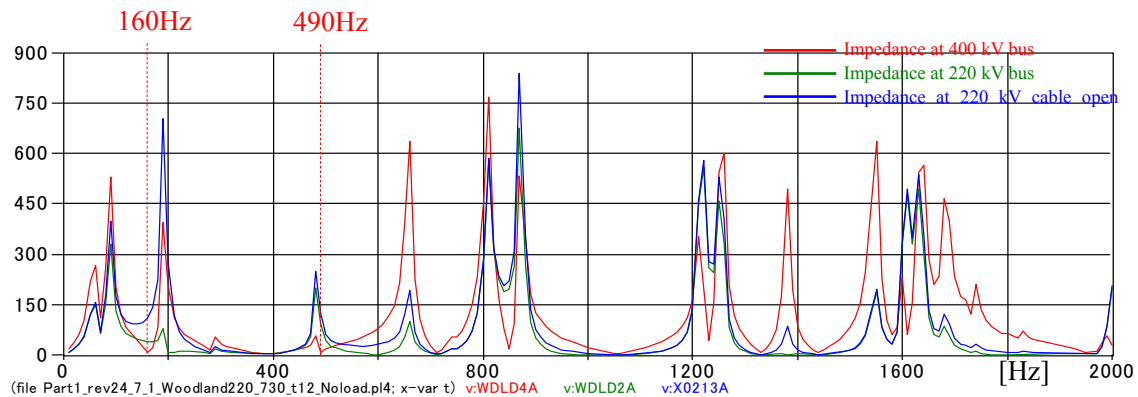

Fig. A1-15 Frequency scan at the Woodland 400 kV and 220 kV buses and 220 kV cable open end (phase to earth).

[Case (4)-3] Length of 220 kV cable: 15.25 km
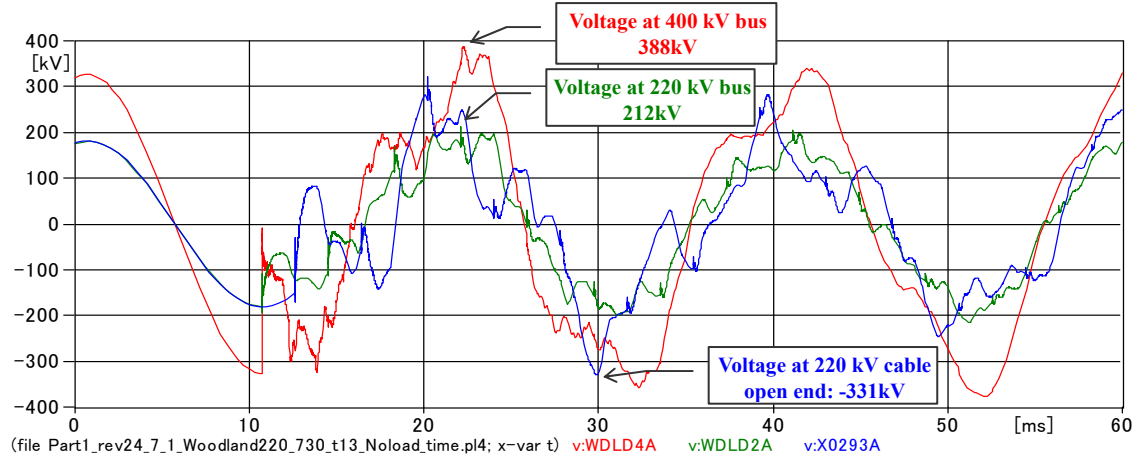
(Phase to earth)
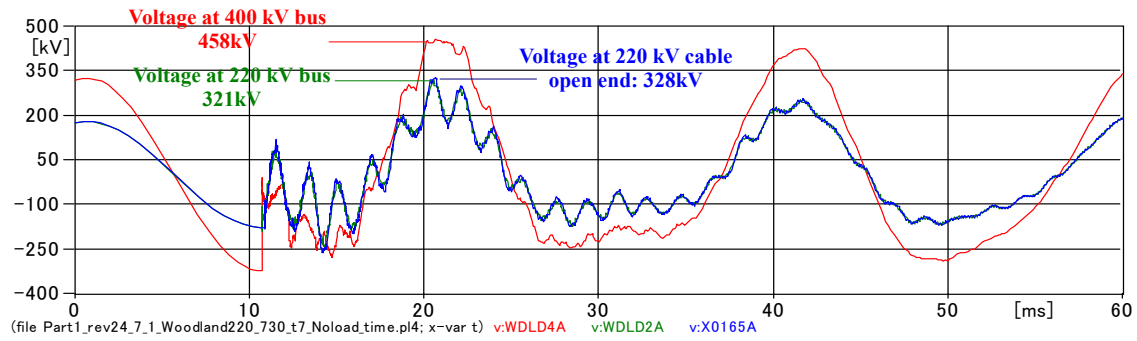
Fig. A1-16 Switching waveforms at the Woodland 400 kV and 220 kV buses and 220 kV cable open end (phase to earth)..
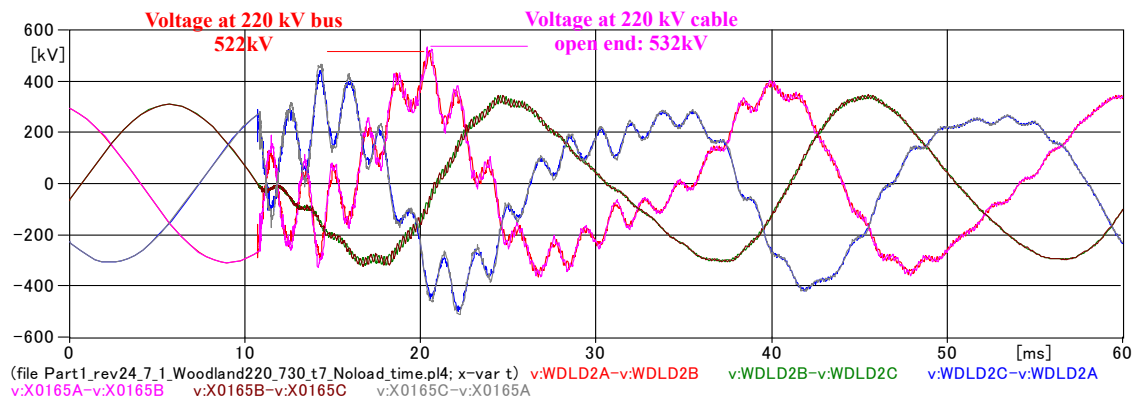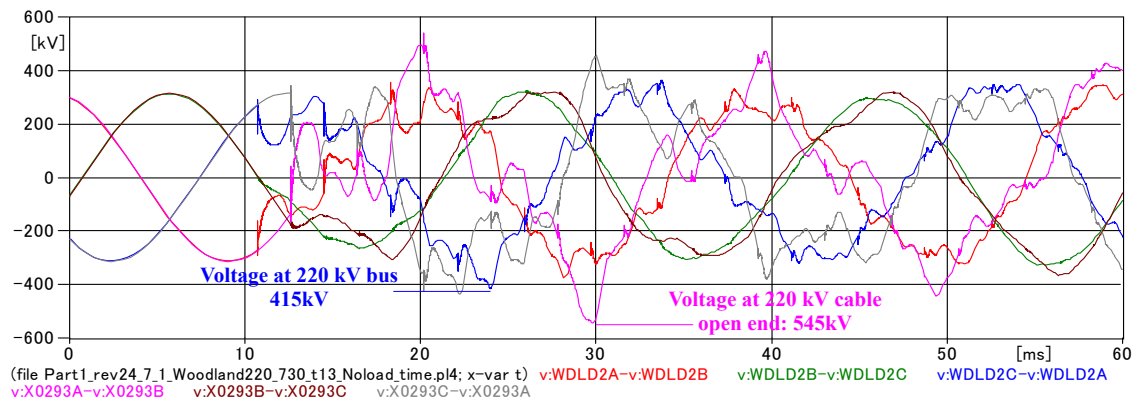
(Phase to phase)

Fig. A1-17 Switching waveforms at the Woodland 220 kV bus and 220 kV cable open end (phase to phase).

MC's PlotXY - Fourier chart(s). Copying date: 2009/02/23
File Part1_rev24_7_1_Woodland220_730_t7_Noload_time.pl4 Variable v:WDLD2A [|pu of harm. 1|]
Initial Time: 0.0107   Final Time: 0.0307
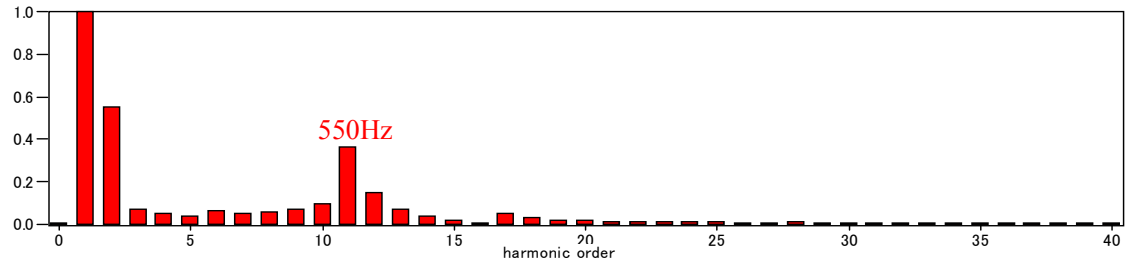
Fig. A1-18 Frequency component spectrum of the switching waveform at Woodland 220 kV bus (phase to earth).

MC's PlotXY - Fourier chart(s). Copying date: 2009/02/25
File Part1_rev24_7_1_Woodland220_730_t7_Noload_time.pl4 Variable v:X0165A [|pu of harm. 1|]
Initial Time: 0.0107   Final Time: 0.0307
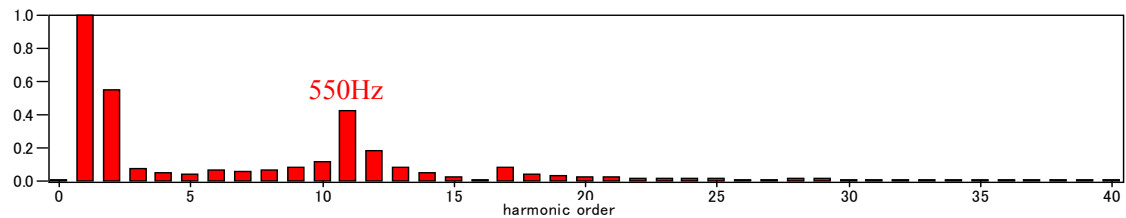
Fig. A1-19 Frequency component spectrum of the switching waveform at the 220 kV cable open end (phase to earth).
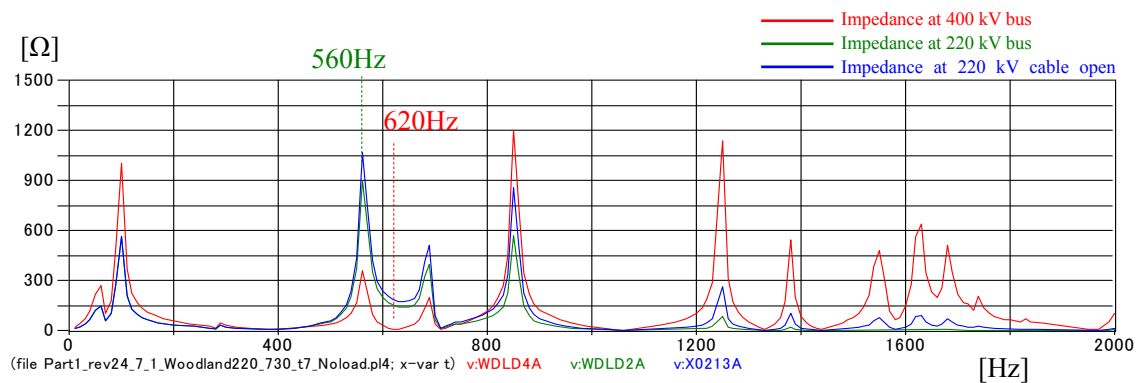
Fig. A1-20 Frequency scan at the Woodland 400 kV and 220 kV buses and 220 kV cable open end (phase to earth).

[Case (4)-4] Length of 220 kV cable: 30.5km

(Phase to earth)

Fig. A1-21 Switching waveforms at the Woodland 400 kV and 220 kV buses and 220 kV cable open end (phase to earth).

(Phase to phase)

Fig. A1-22 Switching waveforms at the Woodland 220 kV bus and 220 kV cable open end (phase to phase).

MC's PlotXY — Fourier chart(s). Copying date: 2009/02/23
File Part1_rev24_7_1_Woodland220_730_t11_Noload_time.pl4   Variable v:WDLD2A [|pu of harm. 1|]
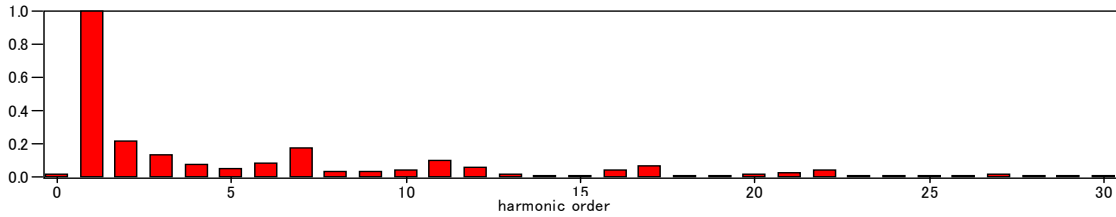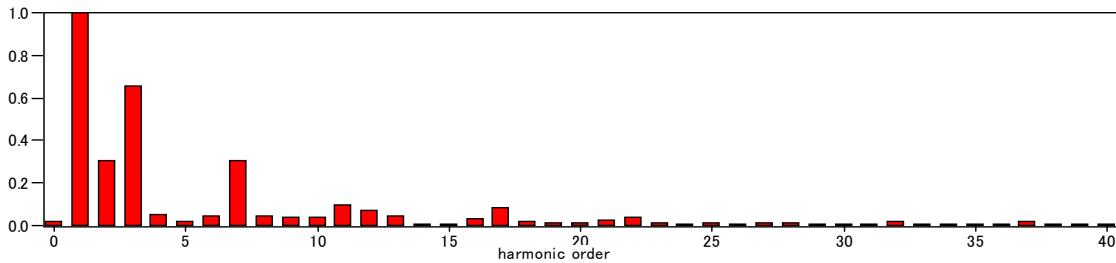Initial Time: 0.0107   Final Time: 0.0307

400Hz
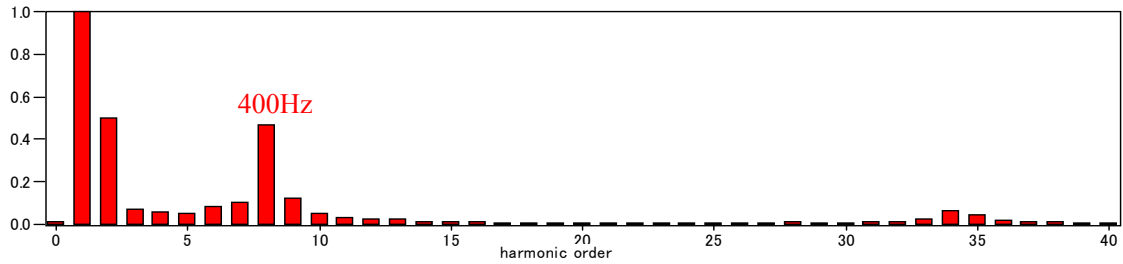
Fig. A1-23 Frequency component spectrum of the switching waveform at Woodland 220 kV bus (phase to earth).

MC's PlotXY — Fourier chart(s). Copying date: 2009/02/25
File Part1_rev24_7_1_Woodland220_730_t11_Noload_time.pl4   Variable v:X0056A [|pu of harm. 1|]
Initial Time: 0.0107   Final Time: 0.0307

400Hz

Fig. A1-24 Frequency component spectrum of the switching waveform at the 220 kV cable open end (phase to earth).

Impedance at 400 kV bus
Impedance at 220 kV bus
Impedance at 220 kV cable open

(file Part1_rev24_7_1_Woodland220_730_t11_Noload.pl4; x-var t)   v:WDLD4A   v:WDLD2A   v:X0150A

Zoom

420Hz

(file Part1_rev24_7_1_Woodland220_730_t11_Noload.pl4; x-var t)   v:WDLD4A   v:WDLD2A   v:X0150A
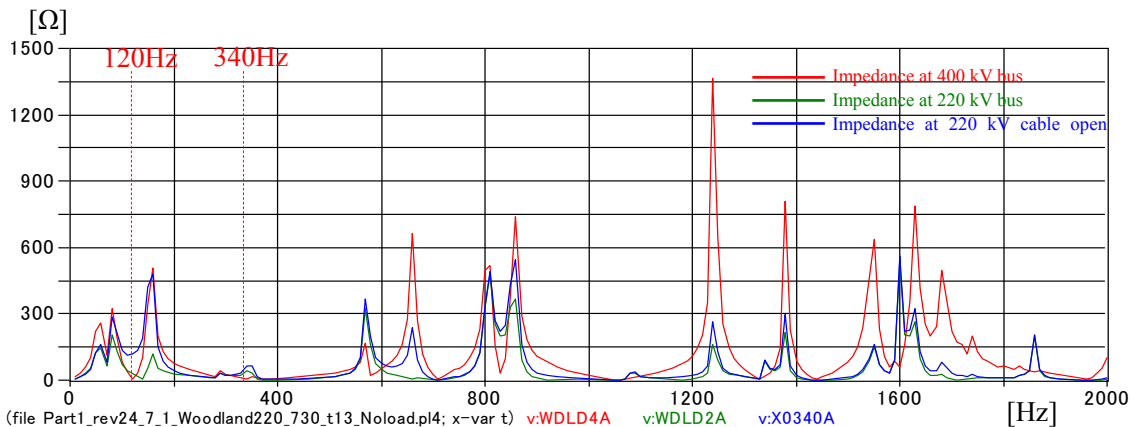
Fig. A1-25 Frequency scan at the Woodland 400 kV and 220 kV buses and 220 kV cable open end (phase to earth).

V4

[Case (4)-5] Cable length: (Length of the base case) * 1.5 = 91.5 km
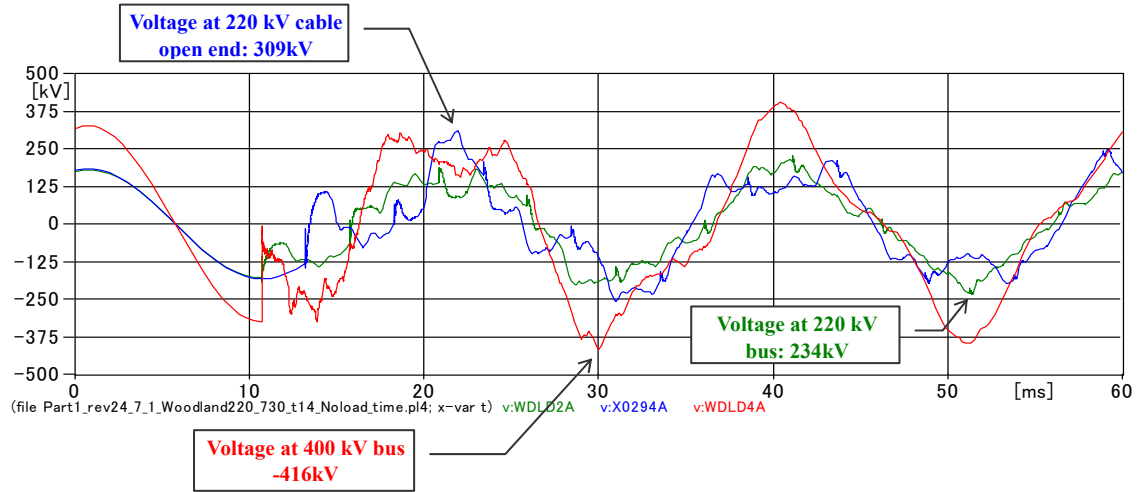
(Phase to earth)
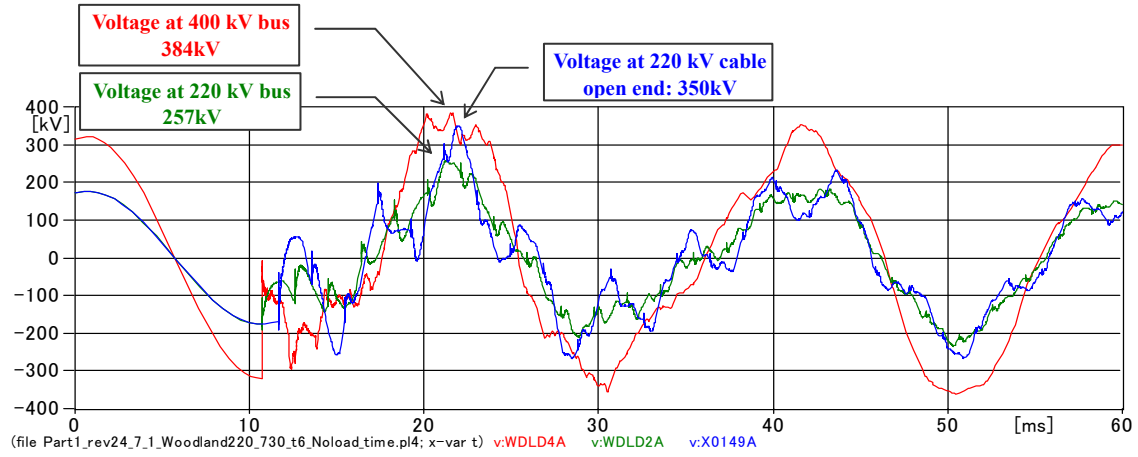
Fig. A1-26 Switching waveforms at the Woodland 400 kV and 220 kV buses and 220 kV cable open end (phase to earth).

(Phase to phase)

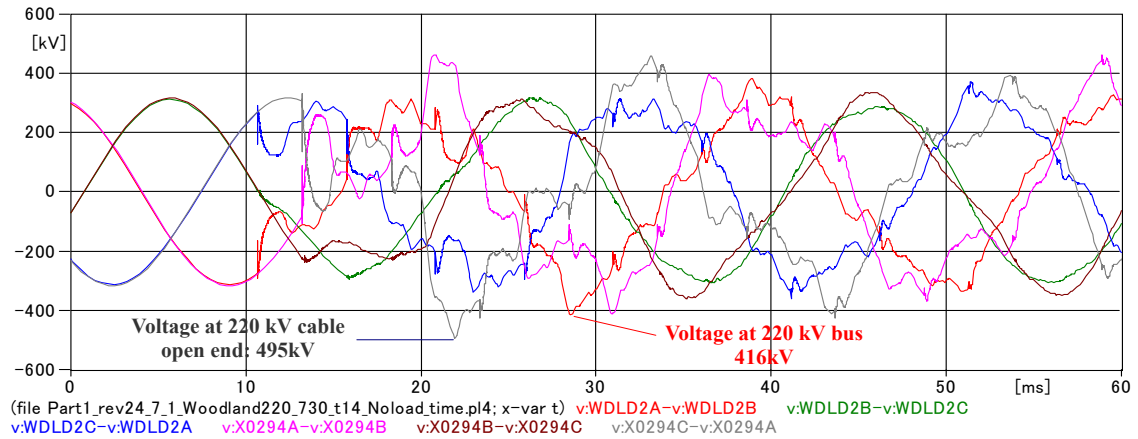**Fig. A1-27 Switching waveforms at the Woodland 220 kV bus and 220 kV cable open end (phase to phase).**

MC's PlotXY – Fourier chart(s). Copying date: 2009/02/20
File Part1_rev24_7_1_Woodland220_730_t6_Noload_time.pl4   Variable v:WDLD2A [|pu of harm. 1|]
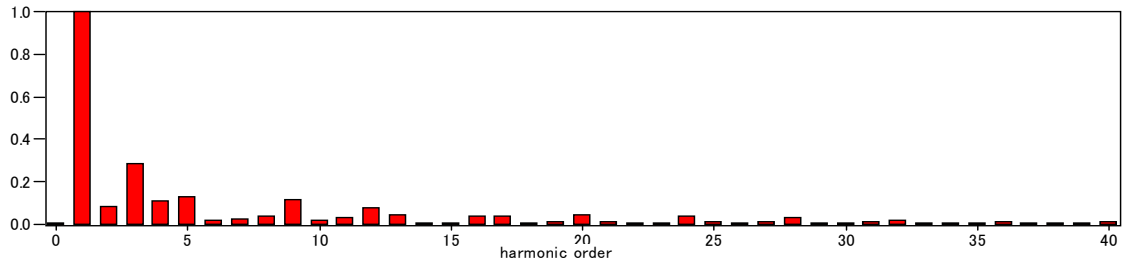Initial Time: 0.01069   Final Time: 0.03069

Fig. A1-28 Frequency component spectrum of the switching waveform at Woodland 220 kV bus (phase to earth).

MC's PlotXY – Fourier chart(s). Copying date: 2009/02/25
File Part1_rev24_7_1_Woodland220_730_t6_Noload_time.pl4   Variable v:X0149A [|pu of harm. 1|]
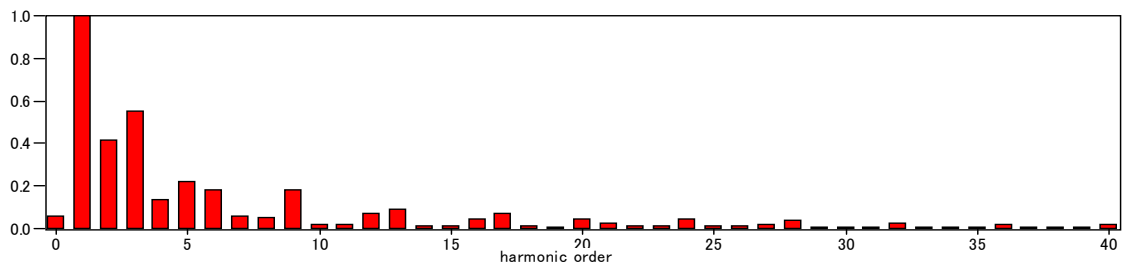Initial Time: 0.01069   Final Time: 0.03069

**Fig. A1-29 Frequency component spectrum of the switching waveform at the 220 kV cable open end (phase to earth).**

(file Part1_rev24_7_1_Woodland220_730_t6_Noload.pl4; x-var t)   v:WDLD2A   v:X0226A   v:WDLD4A
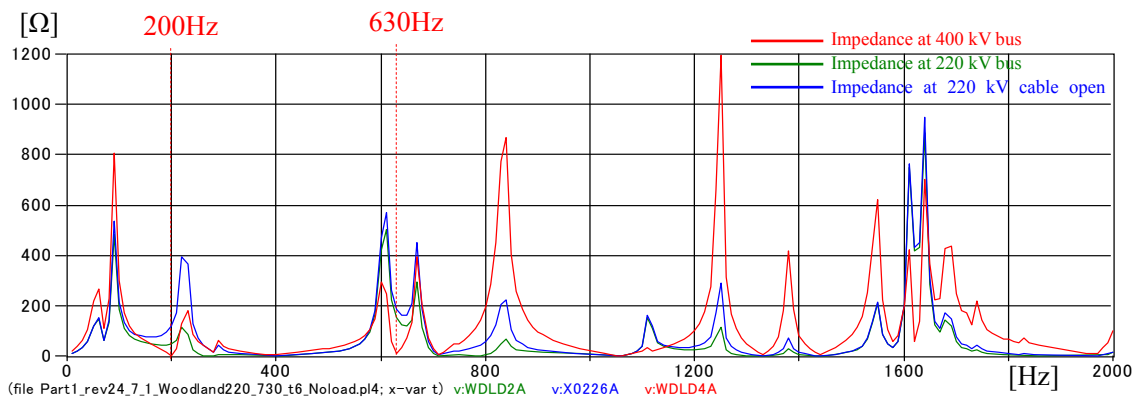
Fig. A1-30 Frequency scan at the Woodland 400 kV and 220 kV buses and 220 kV cable open end (phase to earth).

[Case (4)-6] Cable length: (Length of the base case) * 2 = 122 km

(Phase to earth)

(file Part1_rev24_7_1_Woodland220_730_t12_Noload_time.pl4; x-var t)   v:WDLD4A   v:WDLD2A   v:X0149A

Fig. A1-31 The switching waveforms at the Woodland 400 kV and 220 kV buses and 220 kV cable open end (phase to earth).

(Phase to phase)

(file Part1_rev24_7_1_Woodland220_730_t12_Noload_time.pl4; x-var t)   v:WDLD2A-v:WDLD2B   v:WDLD2B-v:WDLD2C   v:WDLD2C-v:WDLD2A
v:X0149A-v:X0149B   v:X0149B-v:X0149C   v:X0149C-v:X0149A

Fig. A1-32 The switching waveforms at the Woodland 220 kV bus and 220 kV cable open end (phase to phase).

MC's PlotXY – Fourier chart(s). Copying date: 2009/02/25
File Part1_rev24_7_1_Woodland220_730_t12_Noload_time.pl4   Variable v:WDLD2A [peak]
Initial Time: 0.01069   Final Time: 0.03069

Fig. A1-33 Frequency component spectrum of the switching waveform at Woodland 220 kV bus (phase to earth).

MC's PlotXY – Fourier chart(s). Copying date: 2009/02/25
File Part1_rev24_7_1_Woodland220_730_t12_Noload_time.pl4   Variable v:X0149A [|pu of harm. 1|]
Initial Time: 0.01069   Final Time: 0.03069

Fig. A1-34 Frequency component spectrum of the switching waveform at the 220 kV cable open end (phase to earth).

Fig. A1-35 Frequency scan at the Woodland 400 kV and 220 kV buses and 220 kV cable open end (phase to earth).

[Case (4)-7] Cable length: (Length of the base case) * 3 = 183 km

(Phase to earth)

(file Part1_rev24_7_1_Woodland220_730_t13_Noload_time.pl4; x-var t)   v:WDLD4A   v:WDLD2A   v:X0293A

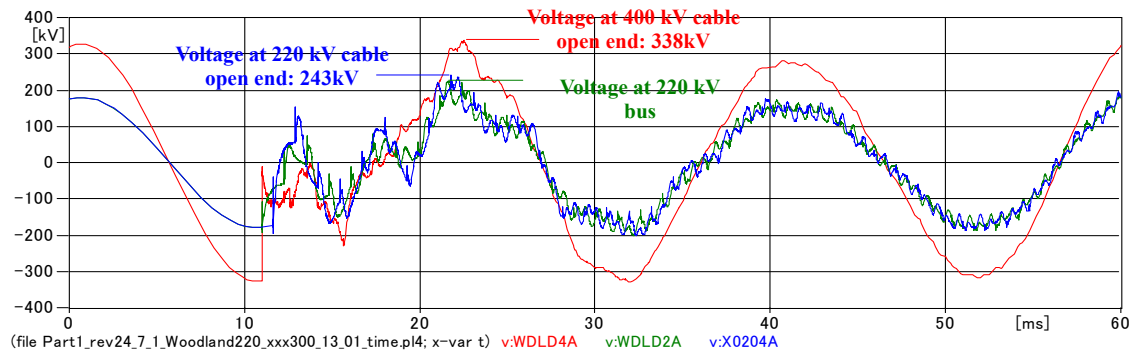**Fig. A1-36 Switching waveforms at the Woodland 400 kV and 220 kV buses and 220 kV cable open end (phase to earth).**

(Phase to Phase)

(file Part1_rev24_7_1_Woodland220_730_t13_Noload_time.pl4; x-var t)   v:WDLD2A-v:WDLD2B   v:WDLD2B-v:WDLD2C   v:WDLD2C-v:WDLD2A
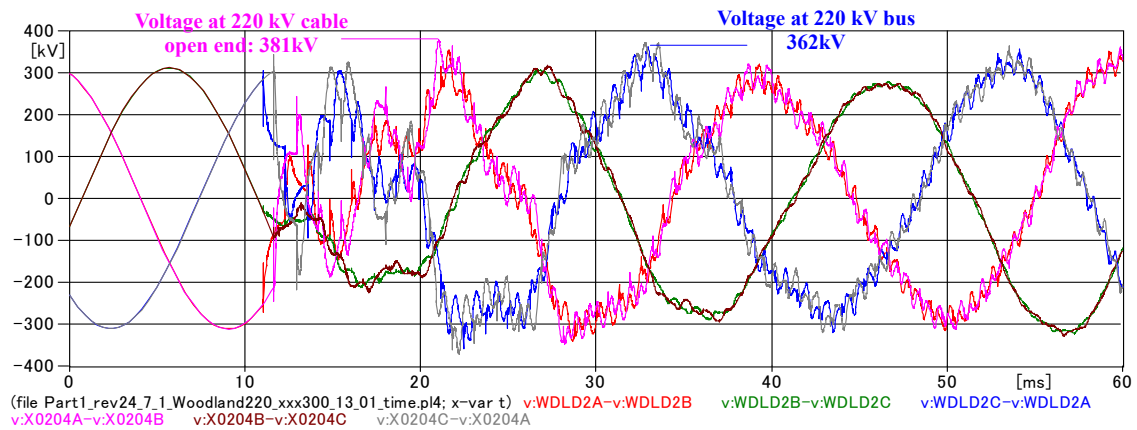v:X0293A-v:X0293B   v:X0293B-v:X0293C   v:X0293C-v:X0293A

Fig. A1-37 Switching waveforms at the Woodland 220 kV bus and 220 kV cable open end (phase to earth).

MC's PlotXY - Fourier chart(s). Copying date: 2009/02/25
File Part1_rev24_7_1_Woodland220_730_t13_Noload_time.pl4   Variable v:WDLD2A [|pu of harm. 1|]
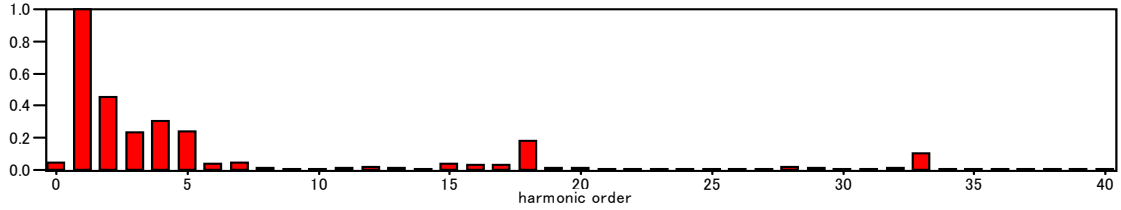Initial Time: 0.01069   Final Time: 0.03069

Fig. A1-38 Frequency component spectrum of the switching waveform at Woodland 220 kV bus (phase to earth).

MC's PlotXY - Fourier chart(s). Copying date: 2009/02/25
File Part1_rev24_7_1_Woodland220_730_t13_Noload_time.pl4   Variable v:X0293A [|pu of harm. 1|]
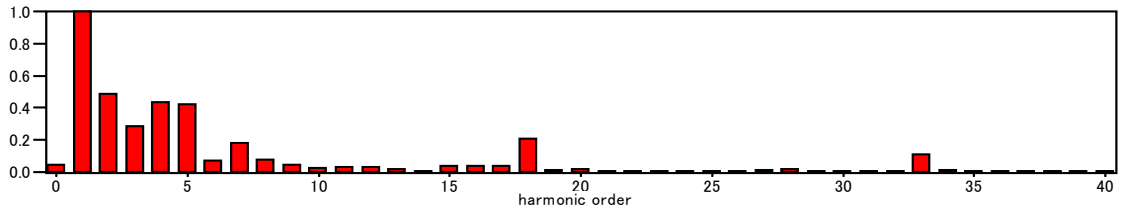Initial Time: 0.01069   Final Time: 0.03069

Fig. A1-39 Frequency component spectrum of the switching waveform at the 220 kV cable open end (phase to earth).
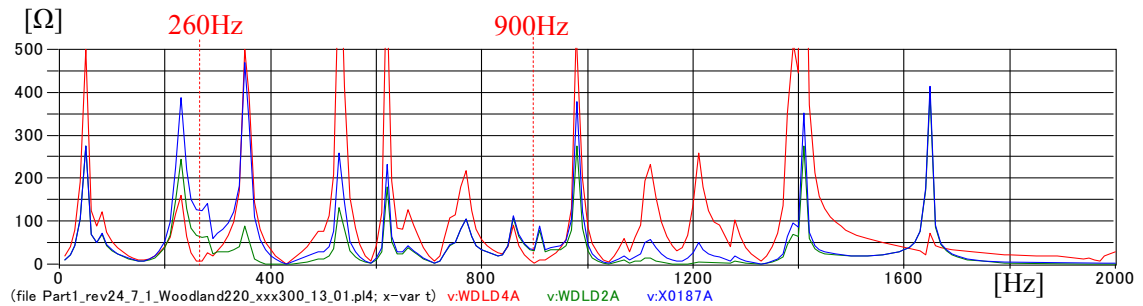

Fig. A1-40 Frequency scan at the Woodland 400 kV and 220 kV buses and 220 kV cable open end (phase to earth).

[Case (4)-8] Cable length: (Length of the base case) * 4 = 244 km

(Phase to earth)

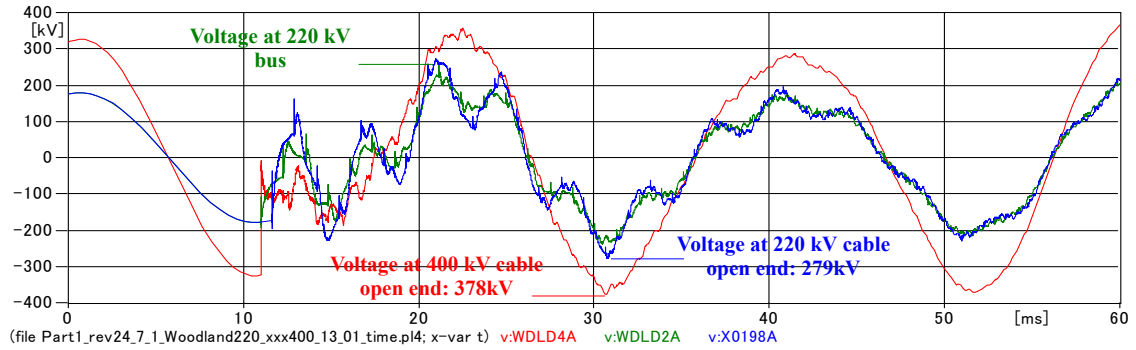(file Part1_rev24_7_1_Woodland220_730_t14_Noload_time.pl4; x-var t) v:WDLD2A   v:X0294A   v:WDLD4A

Fig. A1-41 Switching waveforms at the Woodland 400 kV and 220 kV buses and the 220 kV cable open end (phase to earth).

(Phase to phase)

(file Part1_rev24_7_1_Woodland220_730_t14_Noload_time.pl4; x-var t) v:WDLD2A-v:WDLD2B   v:WDLD2B-v:WDLD2C
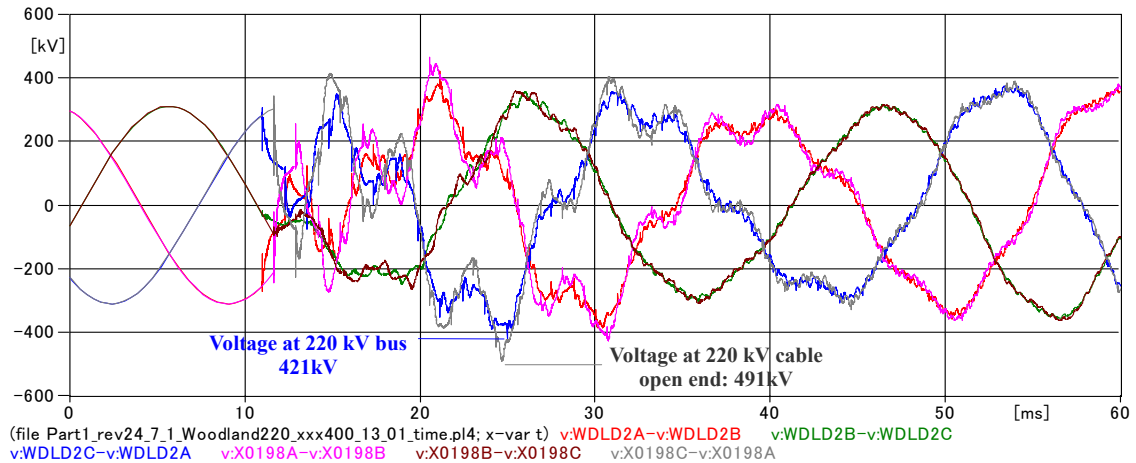v:WDLD2C-v:WDLD2A   v:X0294A-v:X0294B   v:X0294B-v:X0294C   v:X0294C-v:X0294A

Fig. A1-42 Switching waveforms at the Woodland 220 kV bus and the 220 kV cable open end (phase to phase).

MC's PlotXY – Fourier chart(s). Copying date: 2009/02/25
File Part1_rev24_7_1_Woodland220_730_t14_Noload_time.pl4   Variable v:WDLD2A [|pu of harm. 1|]
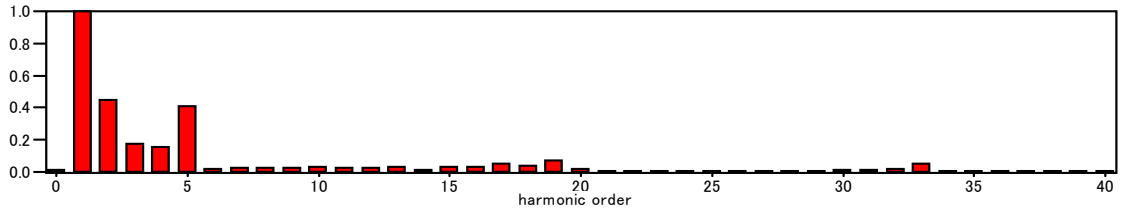Initial Time: 0.01069   Final Time: 0.03069

Fig. A1-43 Frequency component spectrum of the switching waveform at Woodland 220 kV bus (phase to earth).

MC's PlotXY – Fourier chart(s). Copying date: 2009/02/25
File Part1_rev24_7_1_Woodland220_730_t14_Noload_time.pl4   Variable v:X0294A [|pu of harm. 1|]
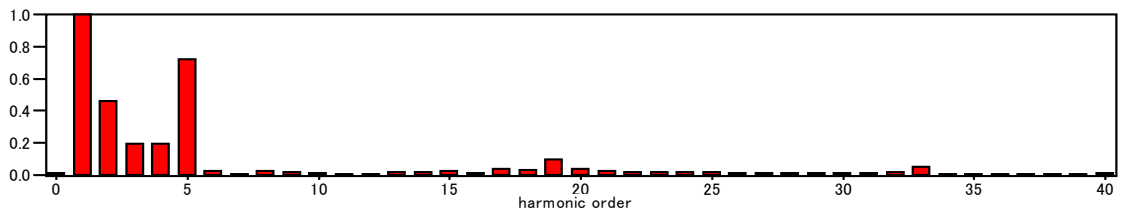Initial Time: 0.01069   Final Time: 0.03069

Fig. A1-44 Frequency component spectrum of the switching waveform at the 220 kV cable open end (phase to earth).
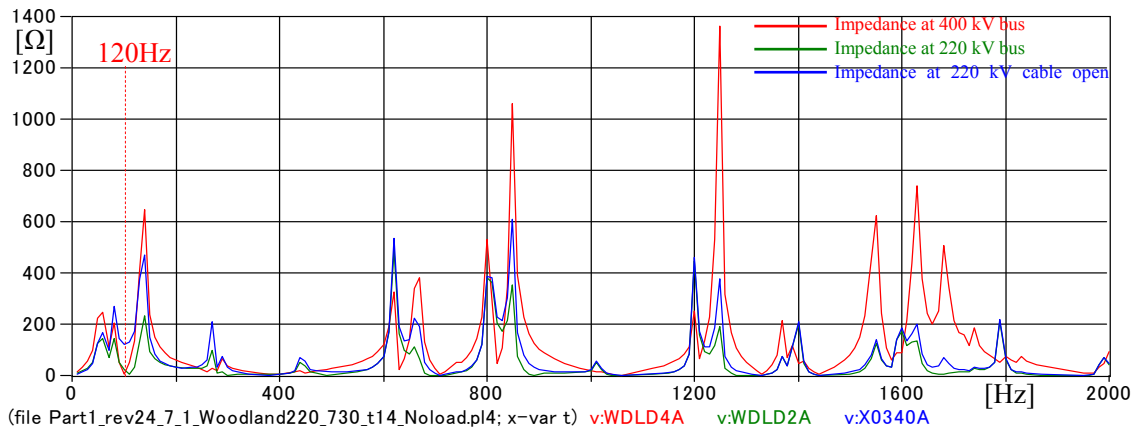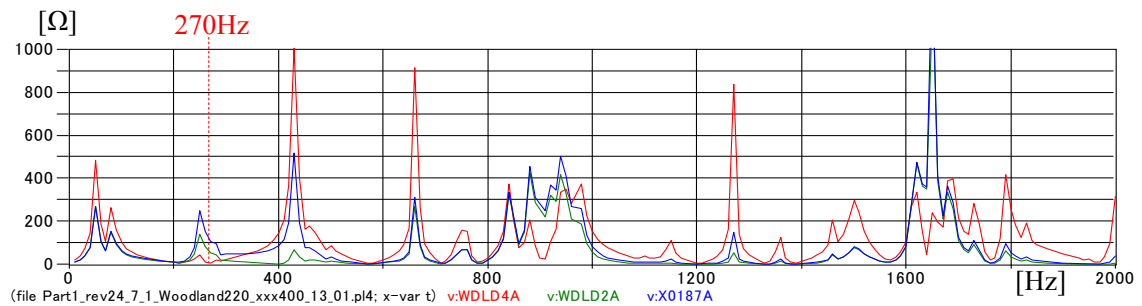
Fig. A1-45 Frequency scan at the Woodland 400 kV and 220 kV buses and the 220 kV cable open end (phase to earth).

Appendix 2 Results of the Parametric Study on the 400 kV Woodland – Kingscourt Cable Length

Frequency scans and time domain simulations of the 400 kV Woodland – Kingscourt line energisation were performed with different lengths of the 400 kV Woodland – Kingscourt cable. The results of the parametric study have been summarized in Section 3.1.1 of the Part 1 report. All the figures obtained in the parametric study are shown in Appendix 2.

List of the 220 kV Woodland – Louth cable length assumed in the study is shown in Table A2-1.

Table A2-1 List of the 400 kV Woodland – Kingscourt Cable Length

	400kV cable	Target frequency	Charging capacity	Reactor for 400kV cable		Compensation rate
				Woodland	Kingscourt	
(5)- 1	141.7 km	300 Hz	1,317 MVA	750 MVA	600 MVA	102.5%
(5)- 2	106.3 km	400 Hz	988 MVA	600 MVA	360 MVA	97.2%
(5)- 3	85.0 km	500 Hz	790 MVA	450 MVA	360 MVA	102.5%
(5)- 4	70.8 km	600 Hz	659 MVA	300 MVA	360 MVA	100.2%
(5)- 5	60.7 km	700 Hz	564 MVA	300 MVA	300 MVA	106.3%
(5)- 6	47.2 km	900 Hz	439 MVA	300 MVA	120 MVA	95.7%
(5)- 7	38.6 km	1100 Hz	359 MVA	240 MVA	120 MVA	100.2%
(5)- 8	26.6 km	1600 Hz	247 MVA	120 MVA	120 MVA	97.2%
(5)- 9	22.4 km	1900 Hz	208 MVA	120 MVA	120 MVA	115.4%

Charging capacity: 9.3 MVA/cct/km

[Case (5)-1] Total 400 kV cable length: 141.7 km, Target frequency: 300 Hz

(Phase to earth)

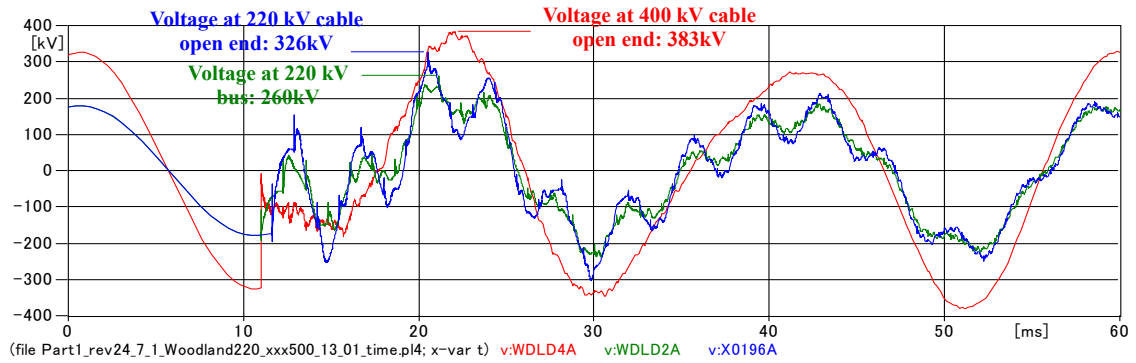(file Part1_rev24_7_1_Woodland220_xxx300_13_01_time.pl4; x-var t)   v:WDLD4A   v:WDLD2A   v:X0204A

Fig. A2-1 Switching waveforms at the Woodland 400 kV and 220 kV buses and the 220 kV cable open end (Phase to earth).
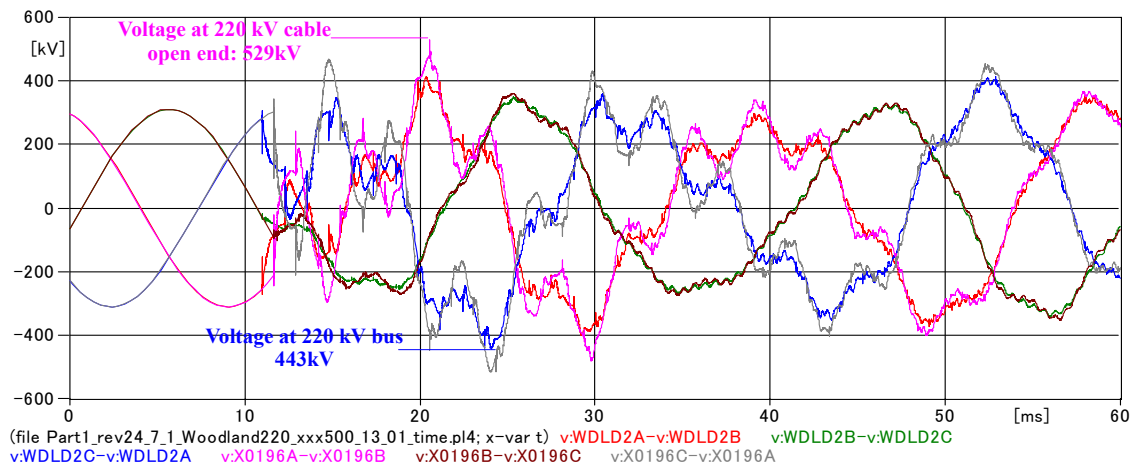
(Phase to phase)

(file Part1_rev24_7_1_Woodland220_xxx300_13_01_time.pl4; x-var t)   v:WDLD2A-v:WDLD2B   v:WDLD2B-v:WDLD2C   v:WDLD2C-v:WDLD2A
v:X0204A-v:X0204B   v:X0204B-v:X0204C   v:X0204C-v:X0204A

Fig. A2-2 Switching waveforms at the Woodland 220 kV bus and the 220 kV cable open end (phase to phase).

MC's PlotXY – Fourier chart(s). Copying date: 2009/02/27
File Part1_rev24_7_1_Woodland220_xxx300_13_01_time.pl4   Variable v:WDLD2A [|pu of harm. 1|]
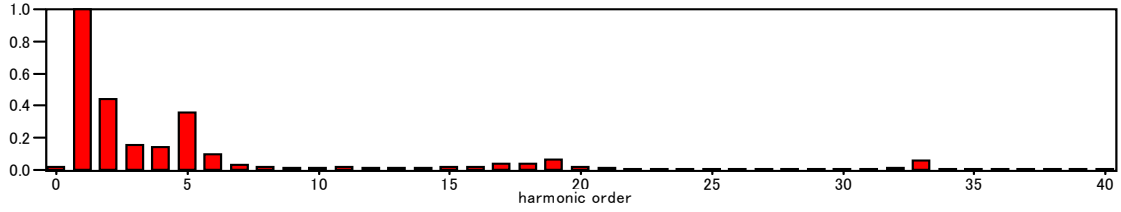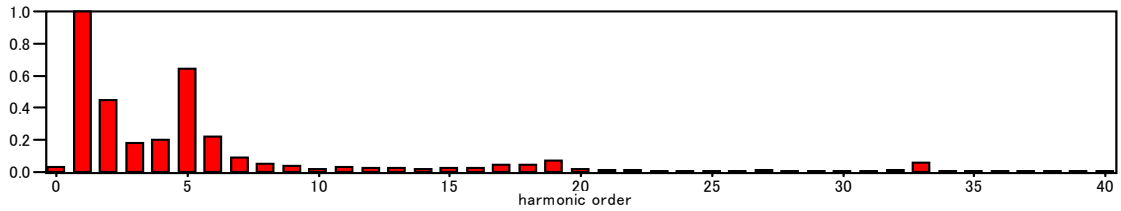Initial Time: 0.011   Final Time: 0.031

Fig. A2-3 Frequency component spectrum of the switching waveform at Woodland 220 kV bus (phase to earth).

MC's PlotXY – Fourier chart(s). Copying date: 2009/02/27
File Part1_rev24_7_1_Woodland220_xxx300_13_01_time.pl4   Variable v:X0204A [|pu of harm. 1|]
Initial Time: 0.011   Final Time: 0.031

Fig. A2-4 Frequency component spectrum of the switching waveform at the 220 kV cable open end (phase to earth).
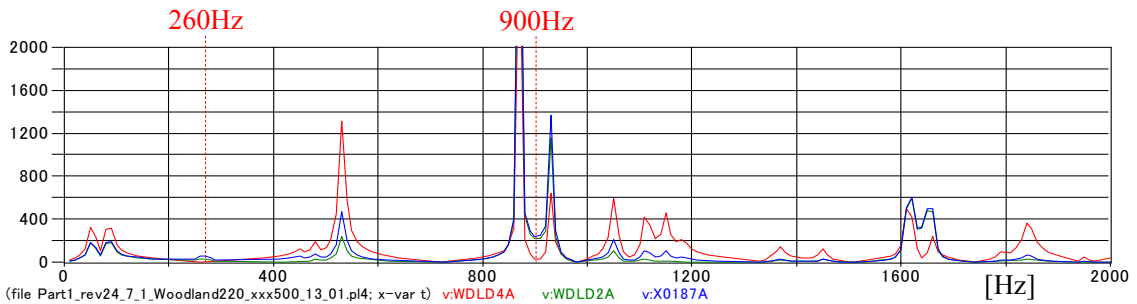

(file Part1_rev24_7_1_Woodland220_xxx300_13_01.pl4; x-var t)   v:WDLD4A   v:WDLD2A   v:X0187A

Fig. A2-5 Frequency scan at the Woodland 400 kV and 220 kV buses and 220 kV cable open end (phase to earth).

[Case (5)-2] Total 400 kV cable length: 106.3 km, Target frequency: 400 Hz
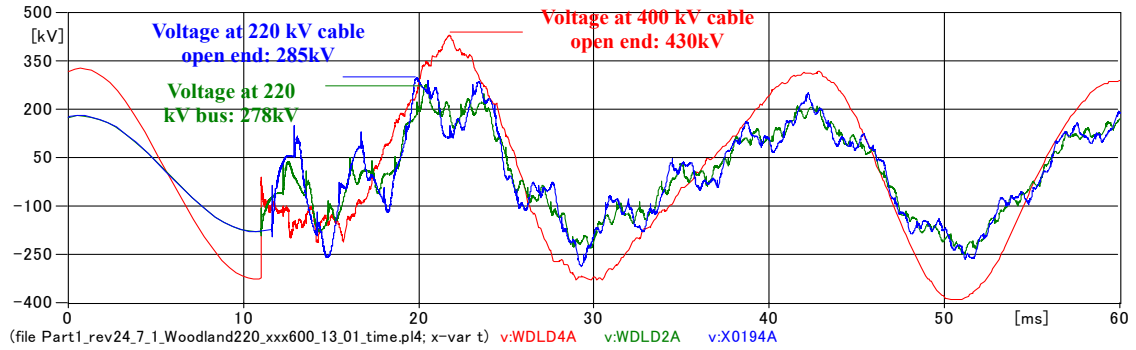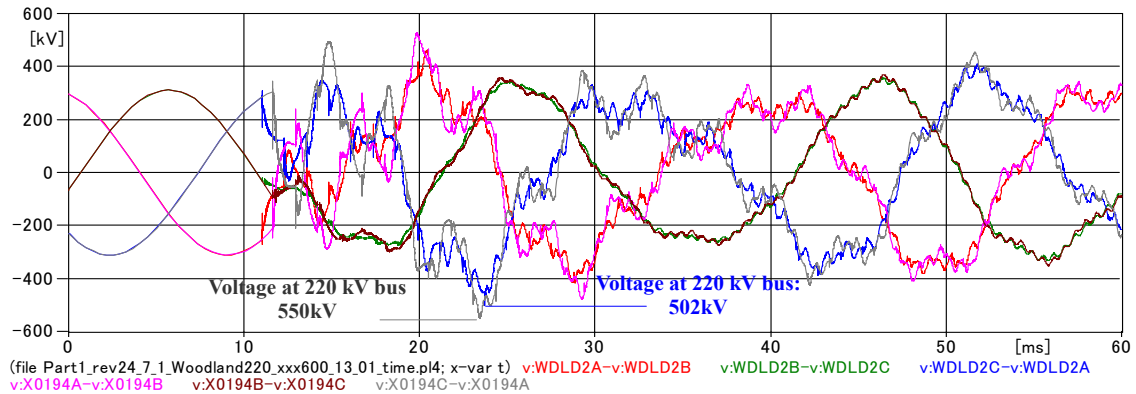
(Phase to earth)

(file Part1_rev24_7_1_Woodland220_xxx400_13_01_time.pl4; x-var t)　v:WDLD4A　　v:WDLD2A　　v:X0198A

Fig. A2-6 Switching waveforms at the Woodland 400 kV and 220 kV buses and the 220 kV cable open end (phase to earth).

(Phase to phase)

(file Part1_rev24_7_1_Woodland220_xxx400_13_01_time.pl4; x-var t)　v:WDLD2A-v:WDLD2B　　v:WDLD2B-v:WDLD2C
v:WDLD2C-v:WDLD2A　　v:X0198A-v:X0198B　　v:X0198B-v:X0198C　　v:X0198C-v:X0198A

Fig. A2-7 Switching waveforms at the Woodland 220 kV buses and the 220 kV cable open end (phase to phase).

MC's PlotXY - Fourier chart(s). Copying date: 2009/02/27
File Part1_rev24_7_1_Woodland220_xxx400_13_01_time.pl4   Variable v:WDLD2A [|pu of harm. 1|]
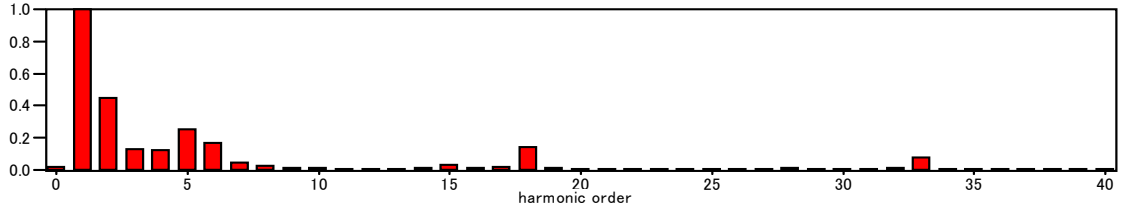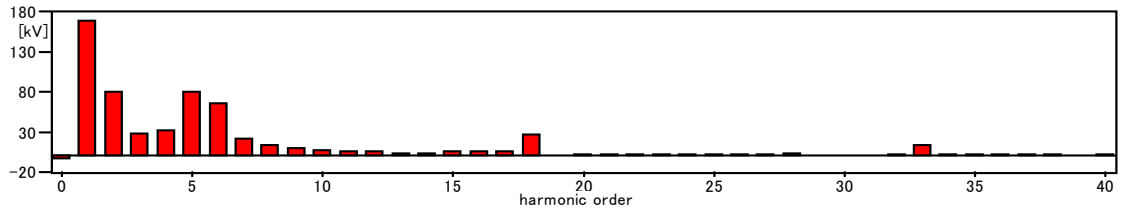Initial Time: 0.011   Final Time: 0.031

Fig. A2-8 Frequency component spectrum of the switching waveform at Woodland 220 kV bus (phase to earth).

MC's PlotXY - Fourier chart(s). Copying date: 2009/02/27
File Part1_rev24_7_1_Woodland220_xxx400_13_01_time.pl4   Variable v:X0198A [|pu of harm. 1|]
Initial Time: 0.011   Final Time: 0.031

Fig. A2-9 Frequency component spectrum of the switching waveform at the 220 kV cable open end (phase to earth).
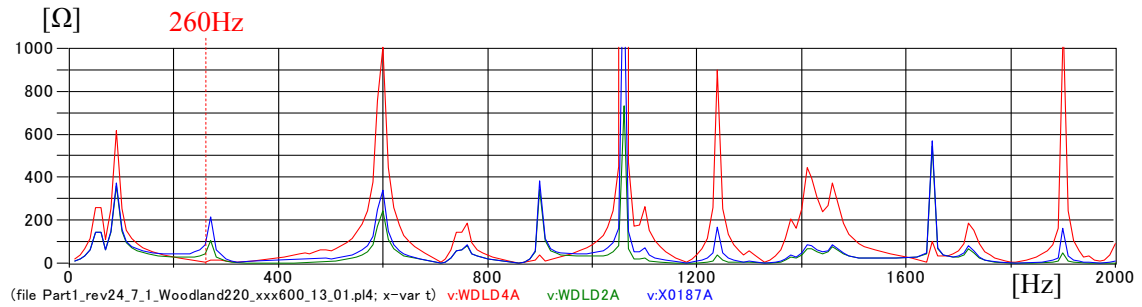
(file Part1_rev24_7_1_Woodland220_xxx400_13_01.pl4; x-var t)   v:WDLD4A   v:WDLD2A   v:X0187A

Fig. A2-10 Frequency scan at the Woodland 400 kV and 220 kV buses and 220 kV cable open end (phase to earth).

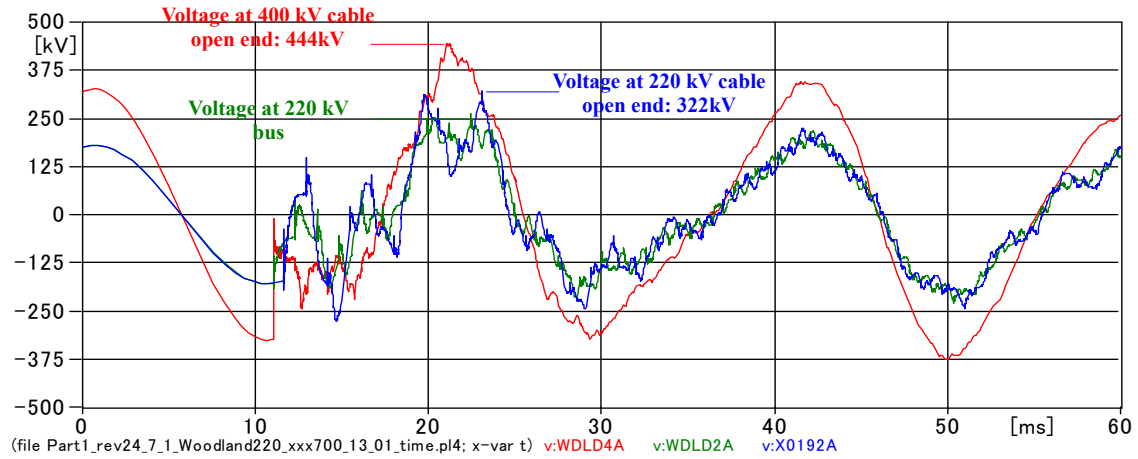[Case (5)-3] Total 400 kV cable length: 85 km, Target frequency: 500 Hz

(Phase to earth)

Fig. A2-11 Switching waveforms at the Woodland 400 kV and 220 kV buses and the 220 kV cable open end (phase to earth).
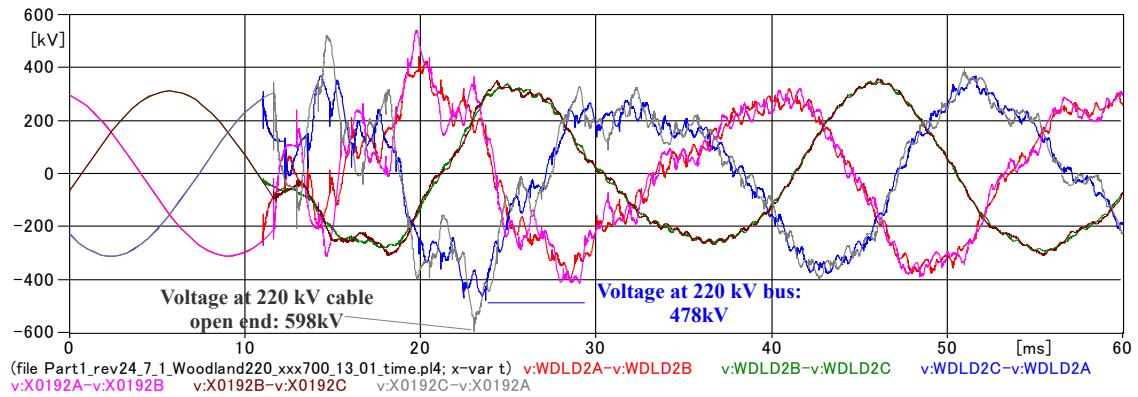
(Phase to phase)

Fig. A2-12 Switching waveforms at the Woodland 220 kV bus and the 220 kV cable open end (phase to phase).

MC's PlotXY - Fourier chart(s). Copying date: 2009/02/27
File Part1_rev24_7_1_Woodland220_xxx500_13_01_time.pl4 Variable v:WDLD2A [|pu of harm. 1|]
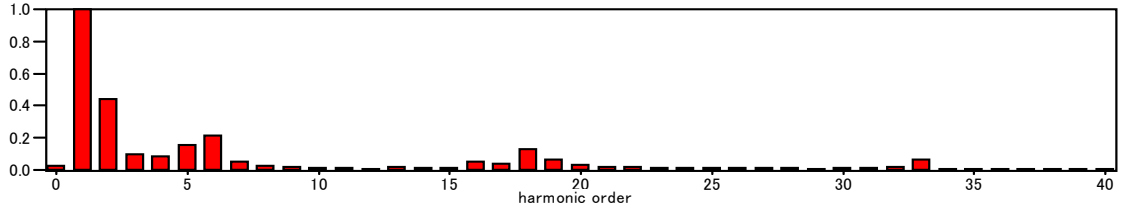Initial Time: 0.011   Final Time: 0.031

Fig. A2-13 Frequency component spectrum of the switching waveform at Woodland 220 kV bus (phase to earth).

MC's PlotXY - Fourier chart(s). Copying date: 2009/02/27
File Part1_rev24_7_1_Woodland220_xxx500_13_01_time.pl4 Variable v:X0196A [|pu of harm. 1|]
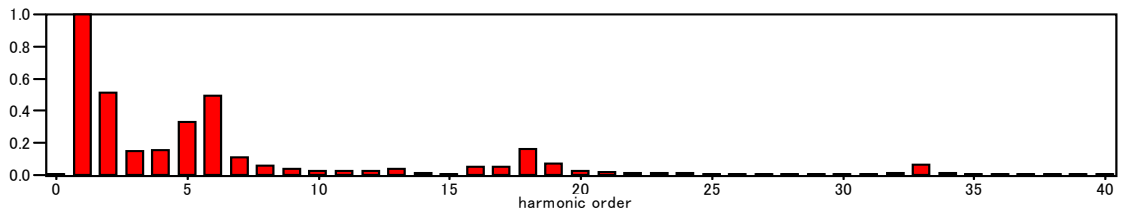Initial Time: 0.011   Final Time: 0.031

Fig. A2-14 Frequency component spectrum of the switching waveform at the 220 kV cable open end (phase to earth).
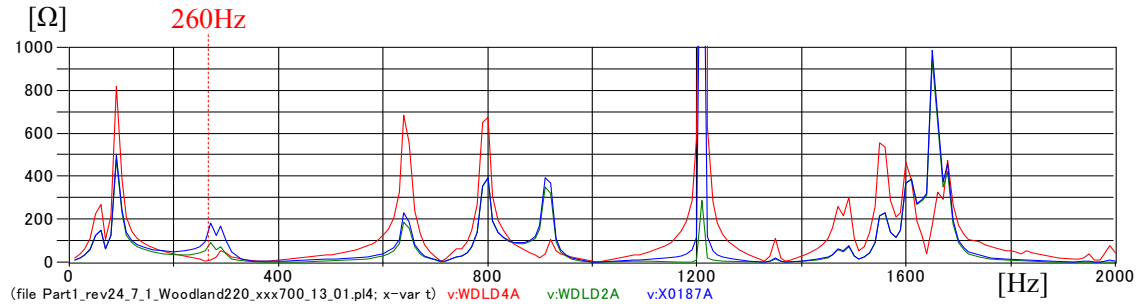
(file Part1_rev24_7_1_Woodland220_xxx500_13_01.pl4; x-var t) v:WDLD4A v:WDLD2A v:X0187A

Fig. A2-15 Frequency scan at the Woodland 400 kV and 220 kV buses and 220 kV cable open end (phase to earth).

[Case (5)-4] Total 400 kV cable length: 70.8 km, Target frequency: 600 Hz
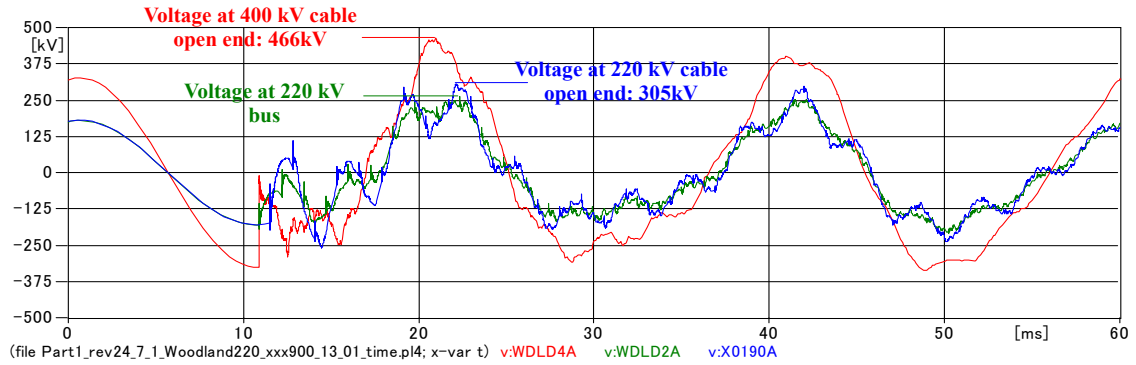
(Phase to earth)

(file Part1_rev24_7_1_Woodland220_xxx600_13_01_time.pl4; x-var t) v:WDLD4A v:WDLD2A v:X0194A

Fig. A2-16 Switching waveforms at the Woodland 400 kV and 220 kV buses and the 220 kV cable open end (phase to earth).

(Phase to Phase)

(file Part1_rev24_7_1_Woodland220_xxx600_13_01_time.pl4; x-var t) v:WDLD2A-v:WDLD2B v:WDLD2B-v:WDLD2C v:WDLD2C-v:WDLD2A
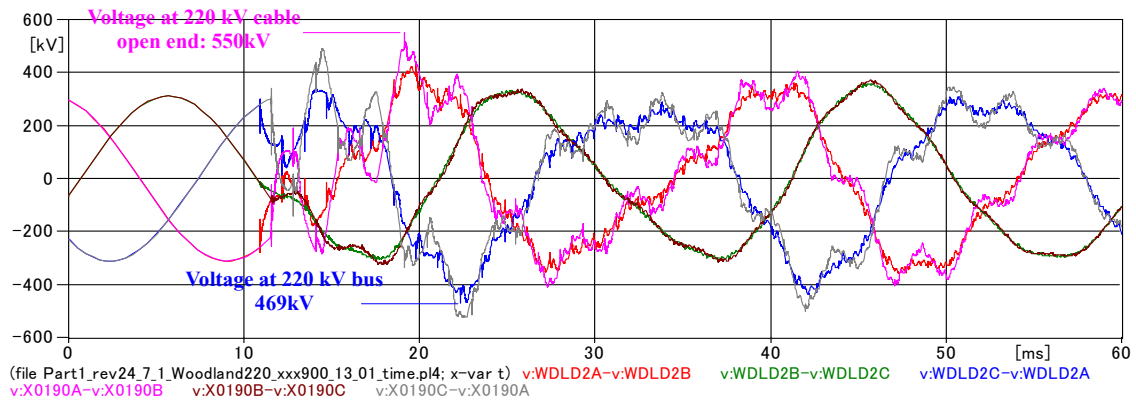v:X0194A-v:X0194B v:X0194B-v:X0194C v:X0194C-v:X0194A

Fig. A2-17 Switching waveforms at the Woodland 220 kV bus and the 220 kV cable open end (phase to phase).

MC's PlotXY - Fourier chart(s). Copying date: 2009/02/27
File Part1_rev24_7_1_Woodland220_xxx600_13_01_time.pl4   Variable v:WDLD2A [|pu of harm. 1|]
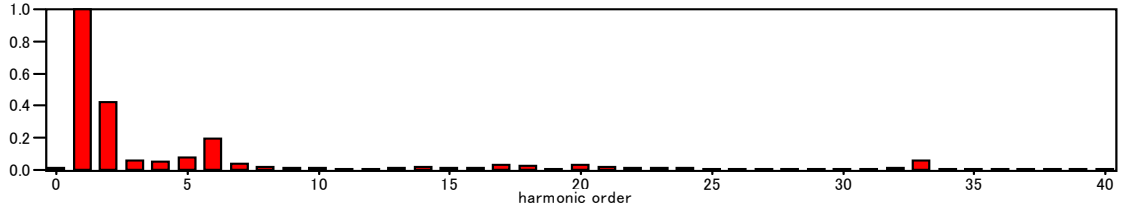Initial Time: 0.011   Final Time: 0.031

Fig. A2-18 Frequency component spectrum of the switching waveform at Woodland 220 kV bus (phase to earth).

MC's PlotXY - Fourier chart(s). Copying date: 2009/02/27
File Part1_rev24_7_1_Woodland220_xxx600_13_01_time.pl4   Variable v:X0194A [peak]
Initial Time: 0.011   Final Time: 0.031

Fig. A2-19 Frequency component spectrum of the switching waveform at the 220 kV cable open end (phase to earth).

(file Part1_rev24_7_1_Woodland220_xxx600_13_01.pl4; x-var t)   v:WDLD4A   v:WDLD2A   v:X0187A

Fig. A2-20 Frequency scan at the Woodland 400 kV and 220 kV buses and 220 kV cable open end (phase to earth).

[Case (5)-5] Total 400 kV cable length: 60.7 km, Target frequency: 700 Hz

(Phase to earth)

Fig. A2-21 Switching waveforms at the Woodland 400 kV and 220 kV buses and the 220 kV cable open end (phase to earth).

(Phase to phase)

Fig. A2-22 Switching waveforms at the Woodland 220 kV bus and the 220 kV cable open end (phase to phase).

MC's PlotXY - Fourier chart(s). Copying date: 2009/02/27
File Part1_rev24_7_1_Woodland220_xxx700_13_01_time.pl4   Variable v:WDLD2A [|pu of harm. 1|]
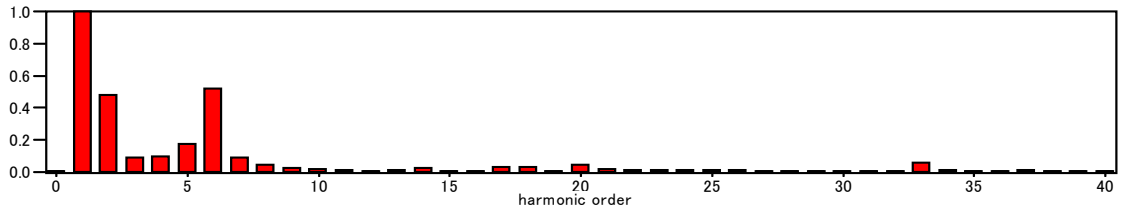Initial Time: 0.0117   Final Time: 0.0317

Fig. A2-23 Frequency component spectrum of the switching waveform at Woodland 220 kV bus (phase to earth).

MC's PlotXY - Fourier chart(s). Copying date: 2009/02/27
File Part1_rev24_7_1_Woodland220_xxx700_13_01_time.pl4   Variable v:X0192A [|pu of harm. 1|]
Initial Time: 0.0117   Final Time: 0.0317

Fig. A2-24 Frequency component spectrum of the switching waveform at the 220 kV cable open end (phase to earth).
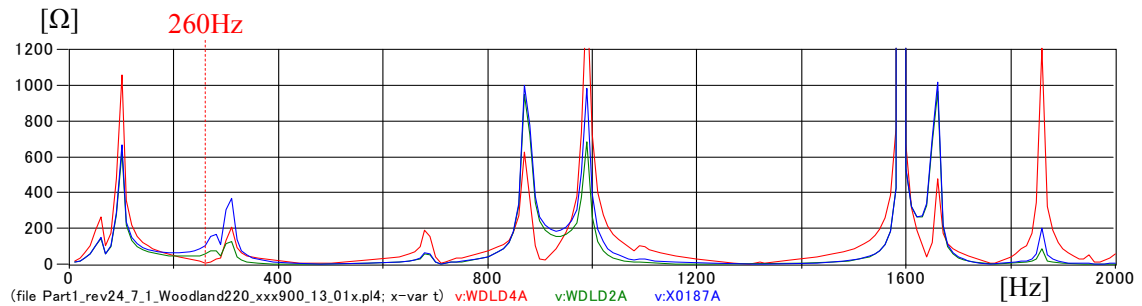

(file Part1_rev24_7_1_Woodland220_xxx700_13_01.pl4; x-var t)   v:WDLD4A   v:WDLD2A   v:X0187A

Fig. A2-25 Frequency scan at the Woodland 400 kV and 220 kV buses and 220 kV cable open end (phase to earth).

[Case (5)-6] Total 400 kV cable length: 47.2 km, Target frequency: 900 Hz
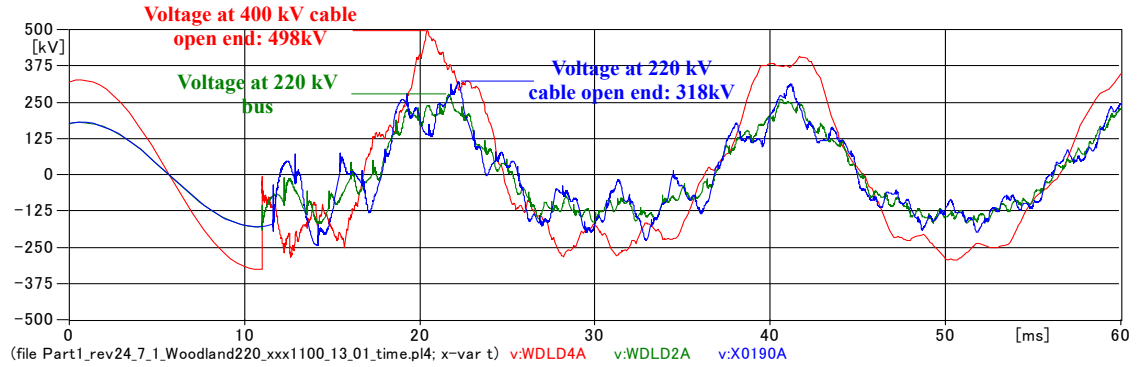
(Phase to earth)

Fig. A2-26 Switching waveforms at the Woodland 400 kV and 220 kV buses and the 220 kV cable open end (phase to earth).
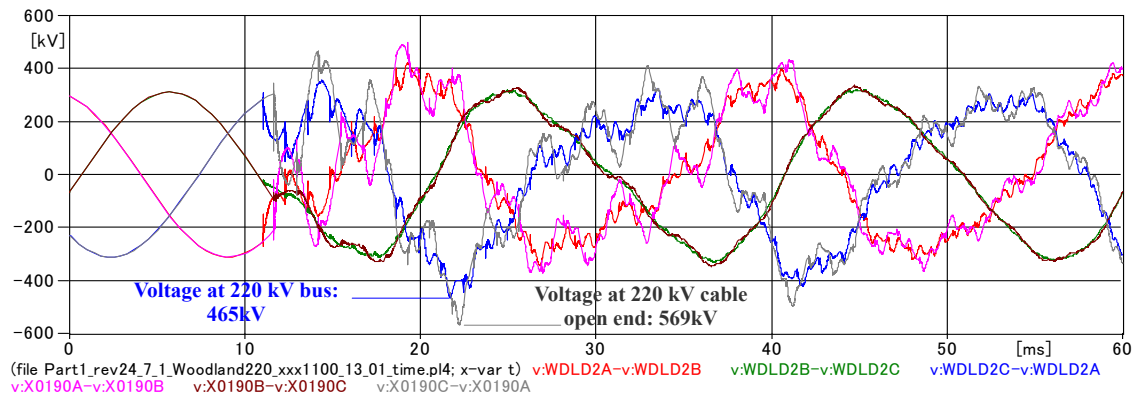
(Phase to phase)

Fig. A2-27 Switching waveforms at the Woodland 220 kV buses and the 220 kV cable open end (phase to phase).

MC's PlotXY – Fourier chart(s). Copying date: 2009/02/27
File Part1_rev24_7_1_Woodland220_xxx900_13_01_time.pl4   Variable v:WDLD2A [|pu of harm. 1|]
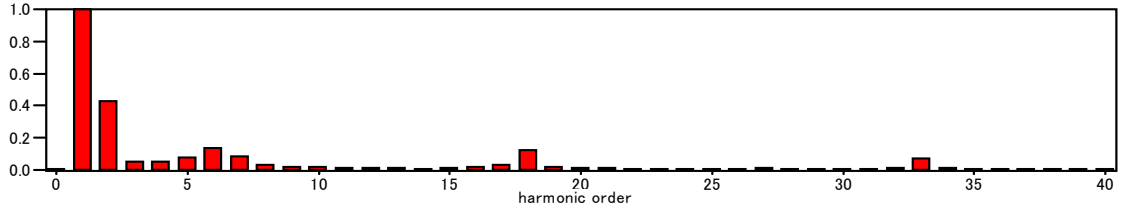Initial Time: 0.01155   Final Time: 0.03155

Fig. A2-28 Frequency component spectrum of the switching waveform at Woodland 220 kV bus (phase to earth).

MC's PlotXY – Fourier chart(s). Copying date: 2009/02/27
File Part1_rev24_7_1_Woodland220_xxx900_13_01_time.pl4   Variable v:X0190A [|pu of harm. 1|]
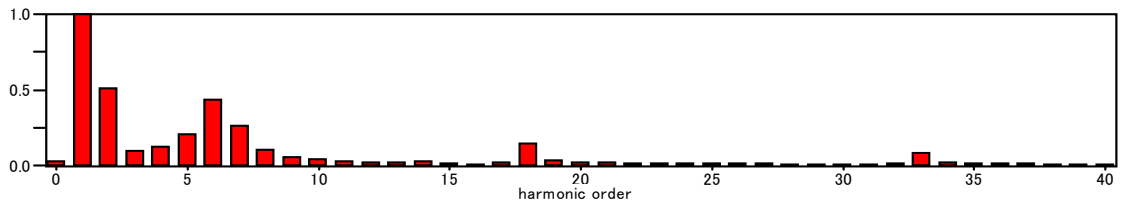Initial Time: 0.01155   Final Time: 0.03155

Fig. A2-29 Frequency component spectrum of the switching waveform at the 220 kV cable open end (phase to earth).

(file Part1_rev24_7_1_Woodland220_xxx900_13_01x.pl4; x-var t)   v:WDLD4A   v:WDLD2A   v:X0187A
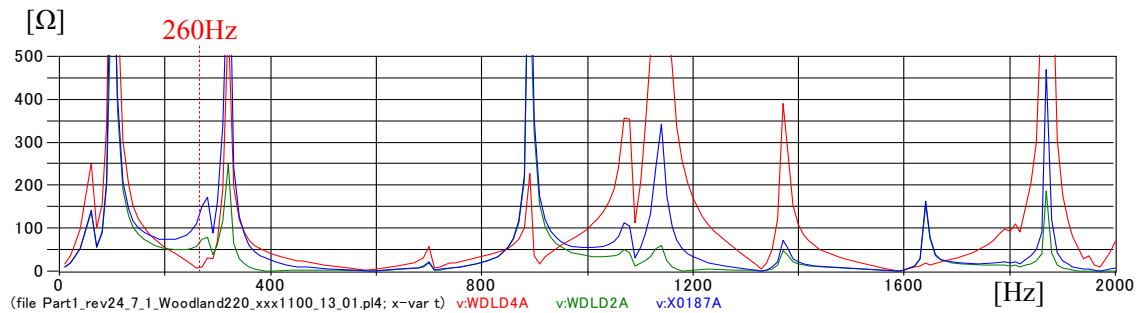
Fig. A2-30 Frequency scan at the Woodland 400 kV and 220 kV buses and 220 kV cable open end (phase to earth).

[Case (5)-7] Total 400 kV cable length: 38.6 km, Target frequency: 1100 Hz
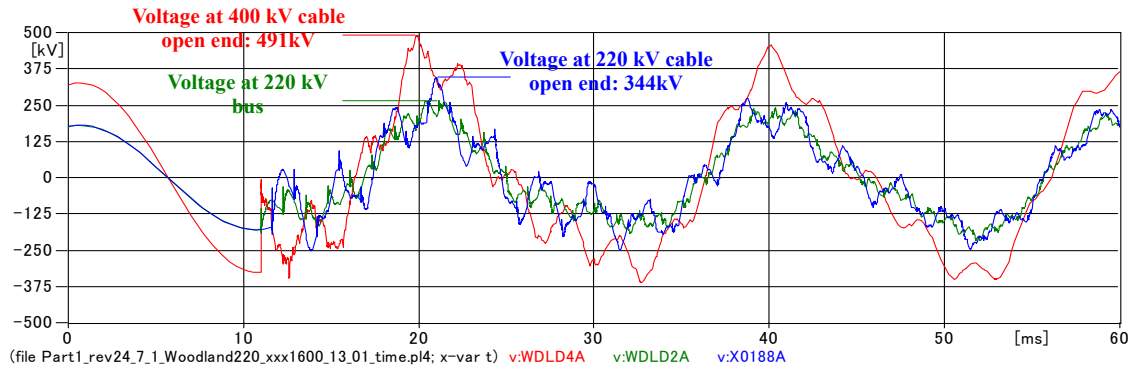
(Phase to earth)

Fig. A2-31 Switching waveforms at the Woodland 400 kV and 220 kV buses and the 220 kV cable open end (phase to earth).
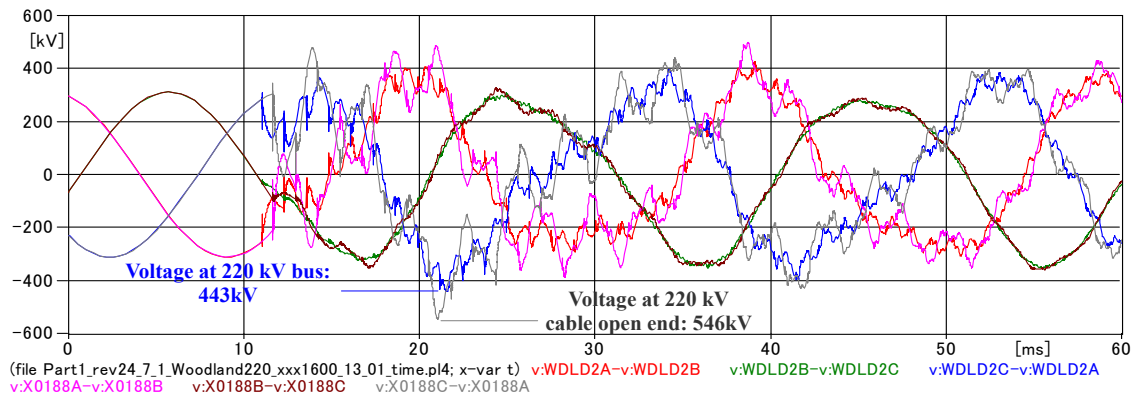
(Phase to phase)

Fig. A2-32 Switching waveforms at the Woodland 220 kV bus and the 220 kV cable open end (phase to phase).

MC's PlotXY - Fourier chart(s). Copying date: 2009/02/27
File Part1_rev24_7_1_Woodland220_xxx1100_13_01_time.pl4 Variable v:WDLD2A [|pu of harm. 1|]
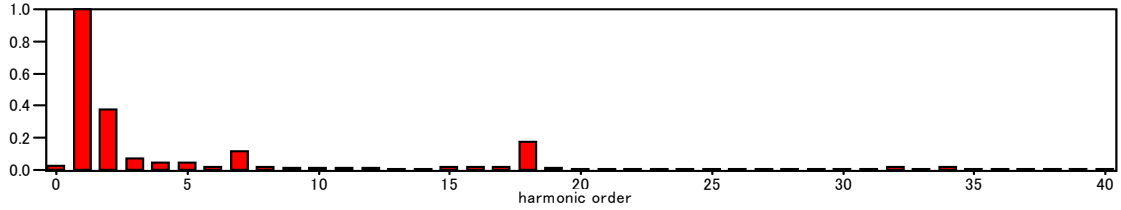Initial Time: 0.01165   Final Time: 0.03165

Fig. A2-33 Frequency component spectrum of the switching waveform at Woodland 220 kV bus (phase to earth).

MC's PlotXY - Fourier chart(s). Copying date: 2009/02/27
File Part1_rev24_7_1_Woodland220_xxx1100_13_01_time.pl4 Variable v:X0190A [|pu of harm. 1|]
Initial Time: 0.01165   Final Time: 0.03165

Fig. A2-34 Frequency component spectrum of the switching waveform at the 220 kV cable open end (phase to earth).

(file Part1_rev24_7_1_Woodland220_xxx1100_13_01.pl4; x-var t) v:WDLD4A   v:WDLD2A   v:X0187A

Fig. A2-35 Frequency scan at the Woodland 400 kV and 220 kV buses and 220 kV cable open end (phase to earth).

[Case (5)-8] Total 400 kV cable length: 26.6 km, Target frequency: 1600 Hz

(Phase to earth)

(file Part1_rev24_7_1_Woodland220_xxx1600_13_01_time.pl4; x-var t)   v:WDLD4A   v:WDLD2A   v:X0188A

Fig. A2-36 Switching waveforms at the Woodland 400 kV and 220 kV buses and the 220 kV cable open end (phase to earth).

(Phase to phase)

(file Part1_rev24_7_1_Woodland220_xxx1600_13_01_time.pl4; x-var t)   v:WDLD2A−v:WDLD2B   v:WDLD2B−v:WDLD2C   v:WDLD2C−v:WDLD2A
v:X0188A−v:X0188B   v:X0188B−v:X0188C   v:X0188C−v:X0188A

Fig. A2-37 Switching waveforms at the Woodland 220 kV bus and the 220 kV cable open end (phase to phase).

MC's PlotXY - Fourier chart(s). Copying date: 2009/02/27
File Part1_rev24_7_1_Woodland220_xxx1600_13_01_time.pl4   Variable v:WDLD2A [|pu of harm. 1|]
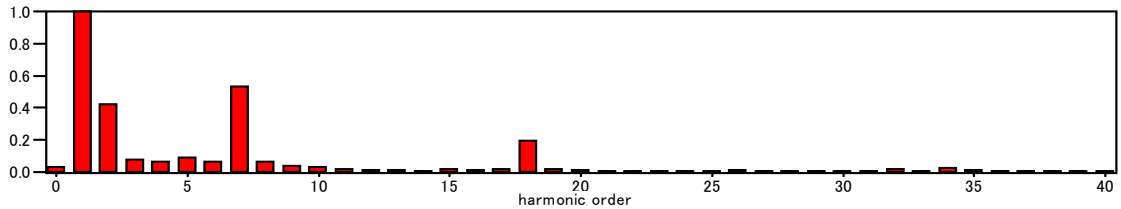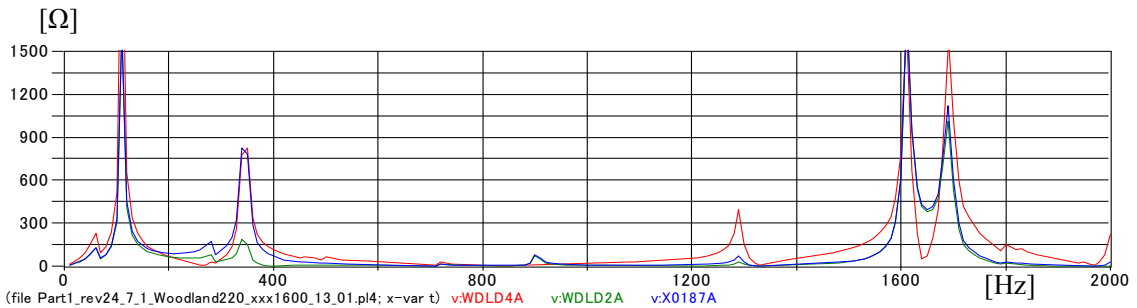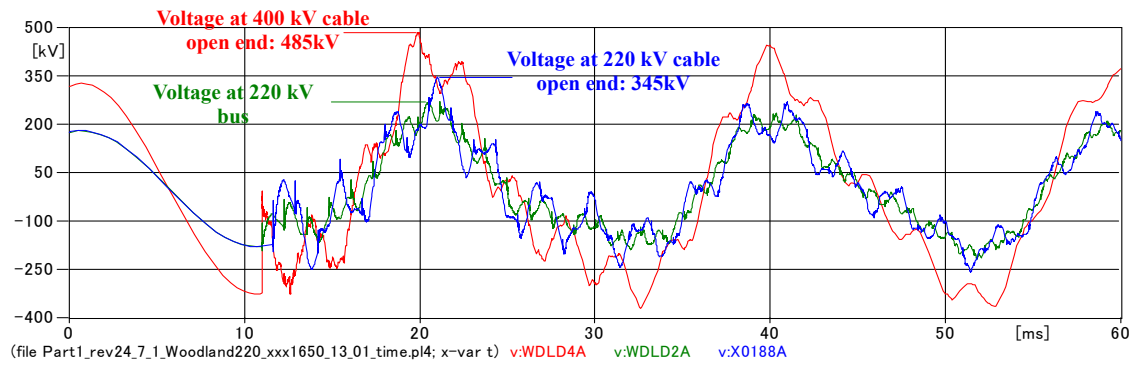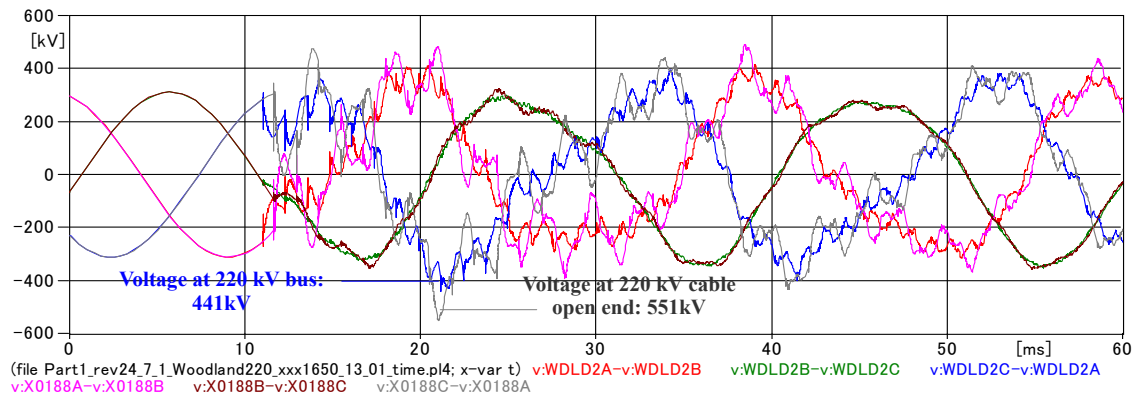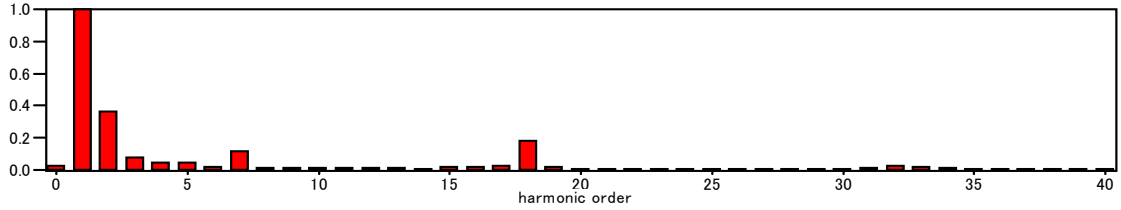Initial Time: 0.0111   Final Time: 0.0311

Fig. A2-38 Frequency component spectrum of the switching waveform at Woodland 220 kV bus (phase to earth).

MC's PlotXY - Fourier chart(s). Copying date: 2009/02/27
File Part1_rev24_7_1_Woodland220_xxx1600_13_01_time.pl4   Variable v:X0188A [|pu of harm. 1|]
Initial Time: 0.0111   Final Time: 0.0311

Fig. A2-39 Frequency component spectrum of the switching waveform at the 220 kV cable open end (phase to earth).

(file Part1_rev24_7_1_Woodland220_xxx1600_13_01.pl4; x-var t)   v:WDLD4A   v:WDLD2A   v:X0187A

Fig. A2-40 Frequency scan at the Woodland 400 kV and 220 kV buses and 220 kV cable open end (phase to earth).

[Case (5)-8'] Total 400 kV cable length: 25.8 km, Target frequency: 1650 Hz

(Phase to earth)

Fig. A2-41 Switching waveforms at the Woodland 400 kV and 220 kV buses and the 220 kV cable open end (phase to earth).

(Phase to phase)

Fig. A2-42 Switching waveforms at the Woodland 220 kV bus and the 220 kV cable open end (phase to phase).

MC's PlotXY - Fourier chart(s). Copying date: 2009/02/27
File Part1_rev24_7_1_Woodland220_xxx1650_13_01_time.pl4   Variable v:WDLD2A [|pu of harm. 1|]
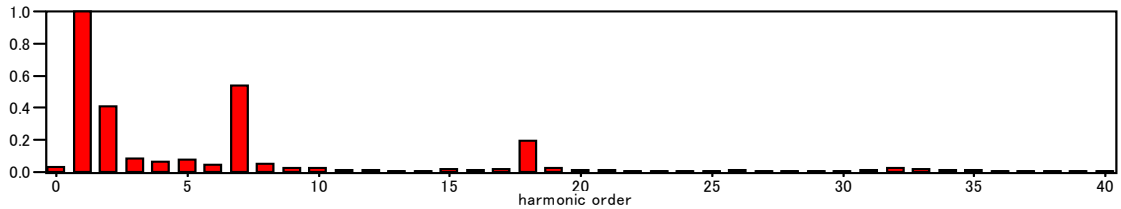Initial Time: 0.0111   Final Time: 0.0311

Fig. A2-43 Frequency component spectrum of the switching waveform at Woodland 220 kV bus (phase to earth).

MC's PlotXY - Fourier chart(s). Copying date: 2009/02/27
File Part1_rev24_7_1_Woodland220_xxx1650_13_01_time.pl4   Variable v:X0188A [|pu of harm. 1|]
Initial Time: 0.0111   Final Time: 0.0311

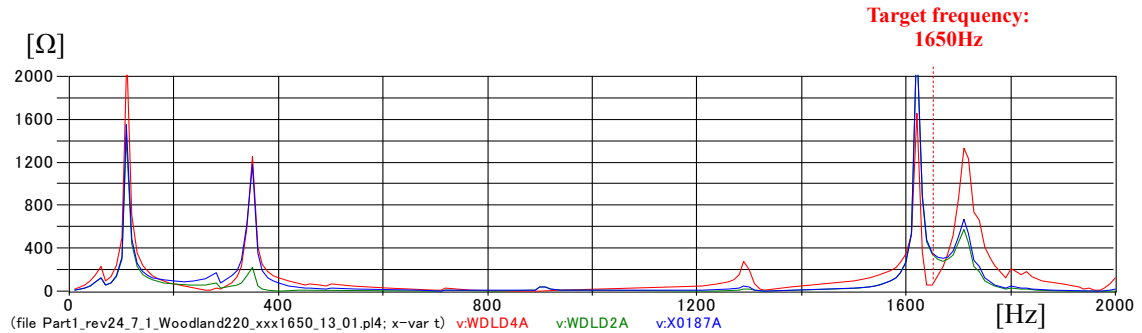**Fig. A2-44 Frequency component spectrum of the switching waveform at the 220 kV cable open end (phase to earth).**

Fig. A2-45 Frequency scan at the Woodland 400 kV and 220 kV buses and 220 kV cable open end (phase to earth).

[Case (5)-9] Total 400 kV cable length: 22.4 km, Target frequency: 1900 Hz
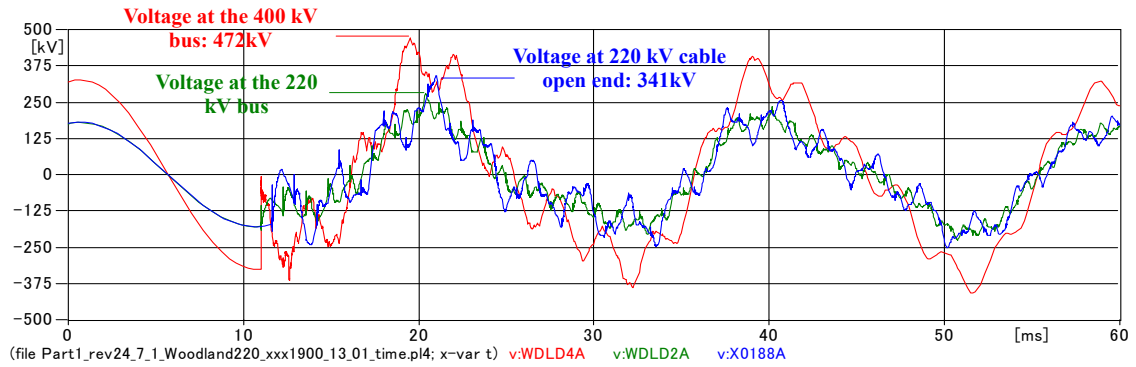
(Phase to earth)

(file Part1_rev24_7_1_Woodland220_xxx1900_13_01_time.pl4; x-var t)   v:WDLD4A   v:WDLD2A   v:X0188A

Fig. A2-46 Switching waveforms at the Woodland 400 kV and 220 kV buses and the 220 kV cable open end (phase to earth).

(Phase to phase)

(file Part1_rev24_7_1_Woodland220_xxx1900_13_01_time.pl4; x-var t)   v:WDLD2A-v:WDLD2B   v:WDLD2B-v:WDLD2C   v:WDLD2C-v:WDLD2A
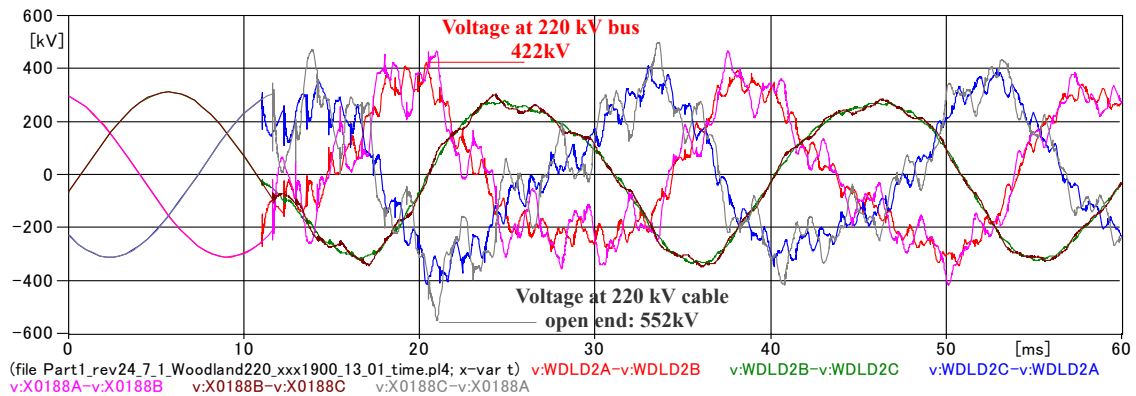v:X0188A-v:X0188B   v:X0188B-v:X0188C   v:X0188C-v:X0188A

Fig. A2-47 Switching waveforms at the Woodland 220 kV bus and the 220 kV cable open end (phase to the phase).

MC's PlotXY - Fourier chart(s). Copying date: 2009/02/27
File Part1_rev24_7_1_Woodland220_xxx1900_13_01_time.pl4   Variable v:WDLD2A [|pu of harm. 1|]
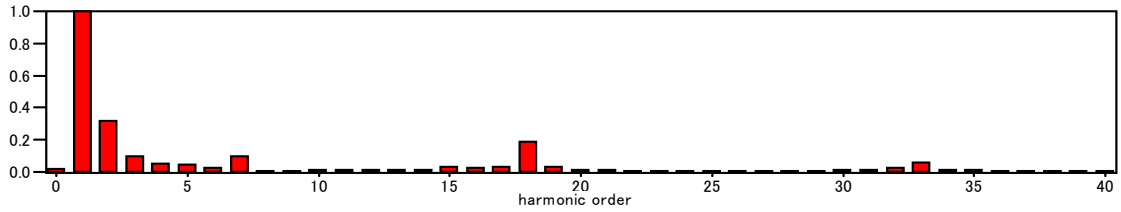Initial Time: 0.0111   Final Time: 0.0311

Fig. A2-48 Frequency component spectrum of the switching waveform at Woodland 220 kV bus (phase to earth).

MC's PlotXY - Fourier chart(s). Copying date: 2009/02/27
File Part1_rev24_7_1_Woodland220_xxx1900_13_01_time.pl4   Variable v:X0188A [|pu of harm. 1|]
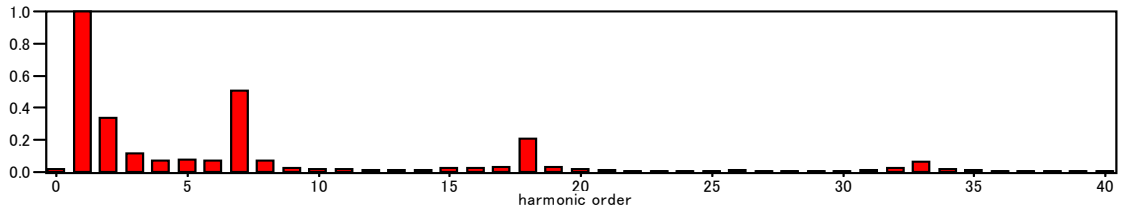Initial Time: 0.0111   Final Time: 0.0311

Fig. A2-49 Frequency component spectrum of the switching waveform at the 220 kV cable open end (phase to earth).

(file Part1_rev24_7_1_Woodland220_xxx1900_13_01.pl4; x-var t)   v:WDLD4A   v:WDLD2A   v:X0187A
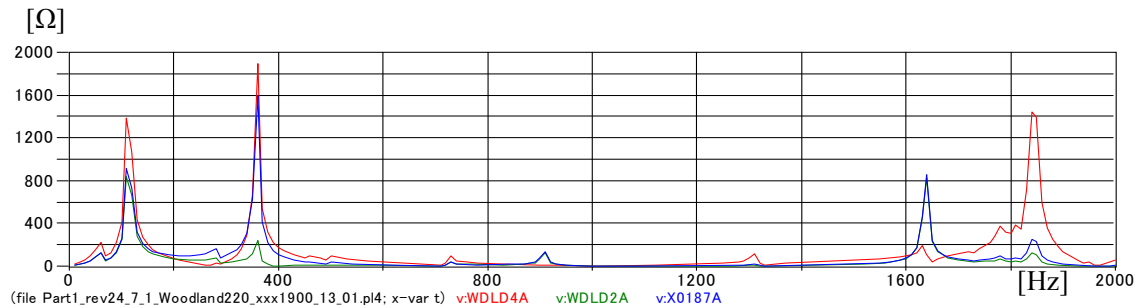
Fig. A2-50 Frequency scan at the Woodland 400 kV and 220 kV buses and 220 kV cable open end (phase to earth).